Southwest Regional Partnership on Carbon Sequestration

Phase II Final Scientific/Technical Report

Reporting Period: October 1, 2005–December 31, 2010

by Reid Grigg, Brian McPherson, and Robert Lee

DE- FC26-05NT42591

Submitting Organization: New Mexico Institute of Mining and Technology
801 Leroy Place
Socorro, New Mexico 87801

January 23, 2012

Disclaimer

Abstract

The Southwest Regional Partnership on Carbon Sequestration (SWP) one of seven regional partnerships sponsored by the U.S. Department of Energy (USDOE) carried out five field pilot tests in its Phase II Carbon Sequestration Demonstration effort, to validate the most promising sequestration technologies and infrastructure concepts, including three geologic pilot tests and two terrestrial pilot programs. This field testing demonstrated the efficacy of proposed sequestration technologies to reduce or offset greenhouse gas emissions in the region. Risk mitigation, optimization of monitoring, verification, and accounting (MVA) protocols, and effective outreach and communication were additional critical goals of these field validation tests. The program included geologic pilot tests located in Utah, New Mexico, Texas, and a region-wide terrestrial analysis. Each geologic sequestration test site was intended to include injection of a minimum of ~75,000 tons/year CO_2, with minimum injection duration of one year. These pilots represent medium-scale validation tests in sinks that host capacity for possible larger-scale sequestration operations in the future. These validation tests also demonstrated a broad variety of carbon sink targets and multiple value-added benefits, including testing of enhanced oil recovery and sequestration, enhanced coalbed methane production and a geologic sequestration test combined with a local terrestrial sequestration pilot. A regional terrestrial sequestration demonstration was also carried out, with a focus on improved terrestrial MVA methods and reporting approaches specific for the Southwest region.

Table of Contents

List of Figures

List of Tables

Executive Summary

The Southwest Regional Partnership on Carbon Sequestration (SWP) is one of seven regional partnerships sponsored by the U.S. Department of Energy (US DOE) (Figure 1).

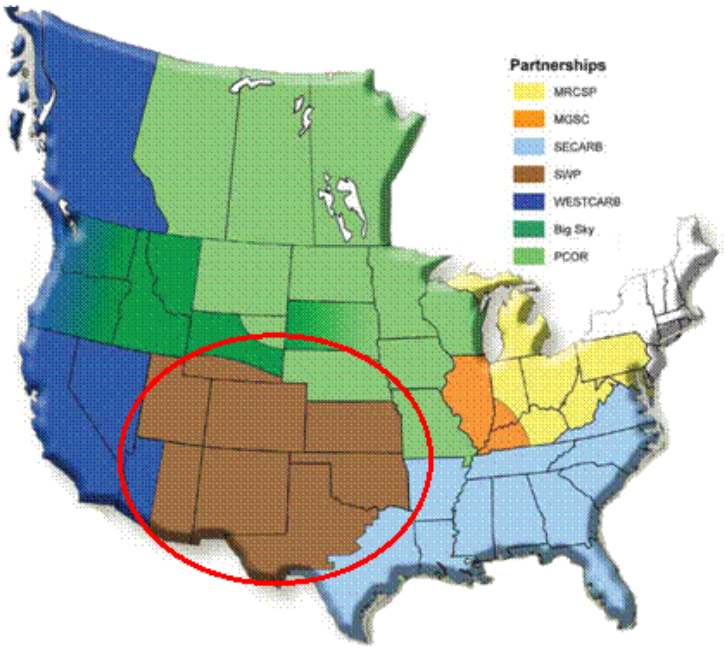

Figure 1. U.S. DOE Regional Partnerships map.

As part of the DOE/NETL Regional Carbon Sequestration Partnerships Demonstration Projects or Phase II the SWP carried out five field pilot tests to validate the most promising sequestration technologies and infrastructure concepts, including three geologic pilot tests and two terrestrial pilot projects. This field testing demonstrated the efficacy of proposed sequestration technologies to reduce or offset greenhouse gas emissions in the region. Risk mitigation, optimization of monitoring, verification, and accounting (MVA) protocols, and effective outreach and communication were additional critical goals of these field validation tests. The project included geologic pilot tests located in Utah, New Mexico, Texas, and a region-wide terrestrial analysis. Each geologic sequestration test site was intended to include injection of a minimum of ~75,000 tons/year CO_2, with minimum injection duration of one year. These pilots represent medium-scale validation tests in sinks that host capacity for possible larger-scale sequestration operations in the future. These validation tests also demonstrated a broad variety of carbon sink targets and multiple value-added benefits, including testing of enhanced oil recovery and sequestration, enhanced coalbed methane production and a geologic sequestration test combined with a local terrestrial sequestration pilot. A regional terrestrial sequestration demonstration was also carried out, with a focus on improved terrestrial MVA methods and reporting approaches specific for the Southwest region. The initial pilot test portfolio is summarized in Table 1.

Five of the initial six projects were completed but the deep saline formation injection in the Aneth field was not performed due to technical problems. The amount of injection that was

Table 1. Pilot Test Summary

Pilot Test Location	Type of Pilot(s)	Amount/Duration of CO_2 Injection	Key Industry / Govt. Partner(s)
Aneth Field, Paradox basin, Utah	-Deep Saline Reservoir -EOR with sequestration	~140,000 tons per year for the two year Phae II observation period*	-Navajo Nation Oil and Gas Co. – Resolute
San Juan Basin Coal Fairway, near Navajo City, NM	-ECBM and sequestration - local-scale terrestrial seques-tration via riparian restoration	~18,400 in 378 days	-ConocoPhillips -BLM-USDA
SACROC Unit, Permi-an basin, near Snyder, TX	EOR with Sequestration	>170,000 tons/yr into the pilot area, a 40 acre 5-spot pattern.**	-Kinder Morgan CO_2 Company, L.P.
Entire Southwest Re-gion	Regional Terrestrial Analysis	N/A	-USDA

* Injection continue as an ongoing EOR project

** Injection continues as an ongoing EOR project, this is ~25% of the injection into the four corner wells into the pattern. Total injection into the four corner wells was ~680,000 tons during the first year or up to 1,360,000 tons during the first two years of injection.

going to be allowed (<<1,000 tons total) was too small for a meaningful test. The EOR portion of Aneth, in a field that had not previously seen any CO_2 injection, has proven to be very successful. The SWP partnership set up an MVA protocol before CO_2 injection started in the geological field tests. Varying levels of success were found from these tests, which included: repeat VSP, tracer tests in the brine and CO_2, passive seismic, repeat surface gas flux, and surface potential. CO_2 injection continued through the two year observation period and is planned to continue at the Aneth field for the foreseeable future.

The San Juan Basin test in a methane producing coalbed methane has been successful in a number of areas. Injection lasted for just over a year. The injection rate had initial rates of over 200 tons/day but the injectivity soon decreased and after about six months stabilized near 30 tons/day. Thus the total injected was less than expected but is still, to date, the largest injection of CO_2 into a coalbed. The associated San Juan Basin riparian restoration project comparing treated and untreated produced water has also shown promise. The MVA tests for the San Juan Basin included: repeat VSP, repeat logging, tiltmeters/GPS, tracer test, water analysis, CO_2 sensors, gas sampling, and CO_2 surface flux.

The third geological storage project was in the Permian Basin of Texas. Initially it was going to concentrate on a new CO_2-EOR project in the Claytonville field with analysis of the SACROC project that has had CO_2 injection ongoing since 1972. Because CO_2 injection was postponed in Claytonville and was not expected to be initiated before the scheduled end of Phase II, the total emphasis was shifted to SACROC in a pattern that had had some CO_2 injection earli-

er and was being recompleted for new and increased CO_2 injection. The MVA program in the SACROC proved to be very instructive. It included: repeat VSP, repeat logging, repeat 3D, extensive water sampling and analysis, and produced fluid sampling.

The final project was a terrestrial CO_2-sequestration project, which examined the entire southwest region for terrestrial analysis. This research has identified a number of approaches to have either been proven or show great potential.

Experimental Methods

This project entailed a multidisciplinary, multifaceted effort from many research organizations. Geological characterization and MVA (monitoring, verification, and accounting) were the principal means of gathering data along with extensive laboratory analysis was employed for the results. A significant modeling effort was also undertaken in both characterization and MVA to verify mechanisms and provide predictions. These methods are detailed at length in the Topical Reports from the project and in following sections of this Final Technical Report.

Geological characterization methods included (1) mapping surface geology, (2) describing the local stratigraphy, (3) mapping the reservoir, seals, and overlying aquifers, (4) characterizing the geology of the reservoir, (5) describing the geochemical, petrographic, and geomechanical properties of the seals, and (6) evaluating the production history. For some of the project sites, located in areas of long-term hydrocarbon production, extensive characterization had already been done, while others needed more research.

The MVA plans for each field pilot were designed to track the movement and fate of CO_2 injected into deep saline aquifers and coalbeds, and oil and gas reservoirs. Additional MVA goals were to monitor CO_2 well injectivity, verify abandoned well veracity, and to assist with risk assessment and mitigation. Baseline MVA activities elucidated the geologic, hydrogeochemical, isotopic and other physical conditions prior to injection. These baseline data were compared to results of repeat and continuous MVA surveys conducted after injection to forecast ultimate fate of CO_2 in the subsurface for different conditions.

Direct MVA

- Injection well monitoring (surface pressure, temperature, and flow measurements)
- In situ pressure/temperature sensors
- Flowmeter surveys
- Production well monitoring of produced gas CO_2 content (continuous for San Juan Basin)
- Surface CO_2 flux measurements

- Isotopic and composition measurements
- Both brine (Aneth) and gas, CO_2 (SJB and Aneth) tracers.

Indirect MVA

- 2-D (all) and 3-D (SACROC) seismic surveys
- Vertical seismic profiles (VSP)
- Passive seismic (Aneth)
- Seismic modeling
- Tiltmeters and GPS(for the SJB pilot only)
- High resolution resistivity method for borehole integrity (Aneth)

Results and Discussion

Aneth Field Pilot Test, Aneth Field, Paradox Basin, Utah

Introduction and Overview

The Southwest Regional Partnership on Carbon Sequestration (SWP) designed and deployed a medium-scale field pilot test of geologic carbon dioxide (CO_2) sequestration in the Aneth oil field. Greater Aneth oil field, Utah's largest oil producer, discovered in 1956, has produced over 455 million barrels of oil (72 million m^3). Located in the Paradox Basin of southeastern Utah, Greater Aneth is a stratigraphic trap producing from the Pennsylvanian Paradox Formation, Fig. 2. Because it represents an archetypal oil field of the western U.S., Greater Aneth was selected as one of three geologic pilots to demonstrate combined enhanced oil recovery (EOR) and CO_2 sequestration under the auspices of the SWP on Carbon Sequestration, sponsored by the National Energy Technology Laboratory (NETL) of the United States Department of Energy (DOE). The pilot demonstration focused on the western portion of the Aneth Unit as this area of the field was converted from waterflood production to CO_2 EOR starting in late 2007. The Aneth Unit in the northwestern part of the field has produced 149 million barrels (24 million m^3) of the estimated 450 million barrels (71.5 million m^3) of the original oil in place – a 33% recovery rate. The large amount of remaining oil made the Aneth Unit ideal to demonstrate both CO_2 storage capacity and EOR by CO_2 flooding. CO_2 injection was started in what Resolute Natural Resources, Inc. calls their Phase I area. This project was in their Phase II injection area, where CO_2 had never been injected before the initiation of the project. Injection started on February 2008 and continued through the Phase II observation period until present. CO2 is being injected at ~140,000 ton/yr per section

This chapter summarizes the geologic characterization research, the various field monitoring tests, and the development of a geologic model and numerical simulations conducted for the Aneth demonstration project. The Utah Geological Survey (UGS), with contributions from other Partners, evaluated how the surface and subsurface geology of the Aneth Unit demonstration site will affect sequestration operations and engineering strategies. The UGS' research for the project is described in the Geological Topical Report, "Surface and Subsurface Geological Characteriza-

tion of the Aneth Unit, Greater Aneth Field, Paradox Basin, Utah." (Chidsey, 2009) and is also summarized in Chapters 1 through 7 of the Aneth Field Topical Report, "Geologic Demonstration at the Aneth Oil Field, Paradox Basin, Utah." (Rutledge, 2010).

These reports include: (1) mapping the surface geology including stratigraphy, faulting, fractures, and deformation bands, (2) describing the local Jurassic and Cretaceous stratigraphy, (3) mapping the Desert Creek zone reservoir, Gothic seal, and overlying aquifers, (4) characterizing the depositional environments and diagenetic events that produced significant reservoir heterogeneity, (5) describing the geochemical, petrographic, and geomechanical properties of the seal to determine the CO_2 or hydrocarbon column it could support, and (6) evaluating the production history to compare primary production from vertical and horizontal wells, and the effects of waterflood and water-alternating-gas (WAG) flooding.

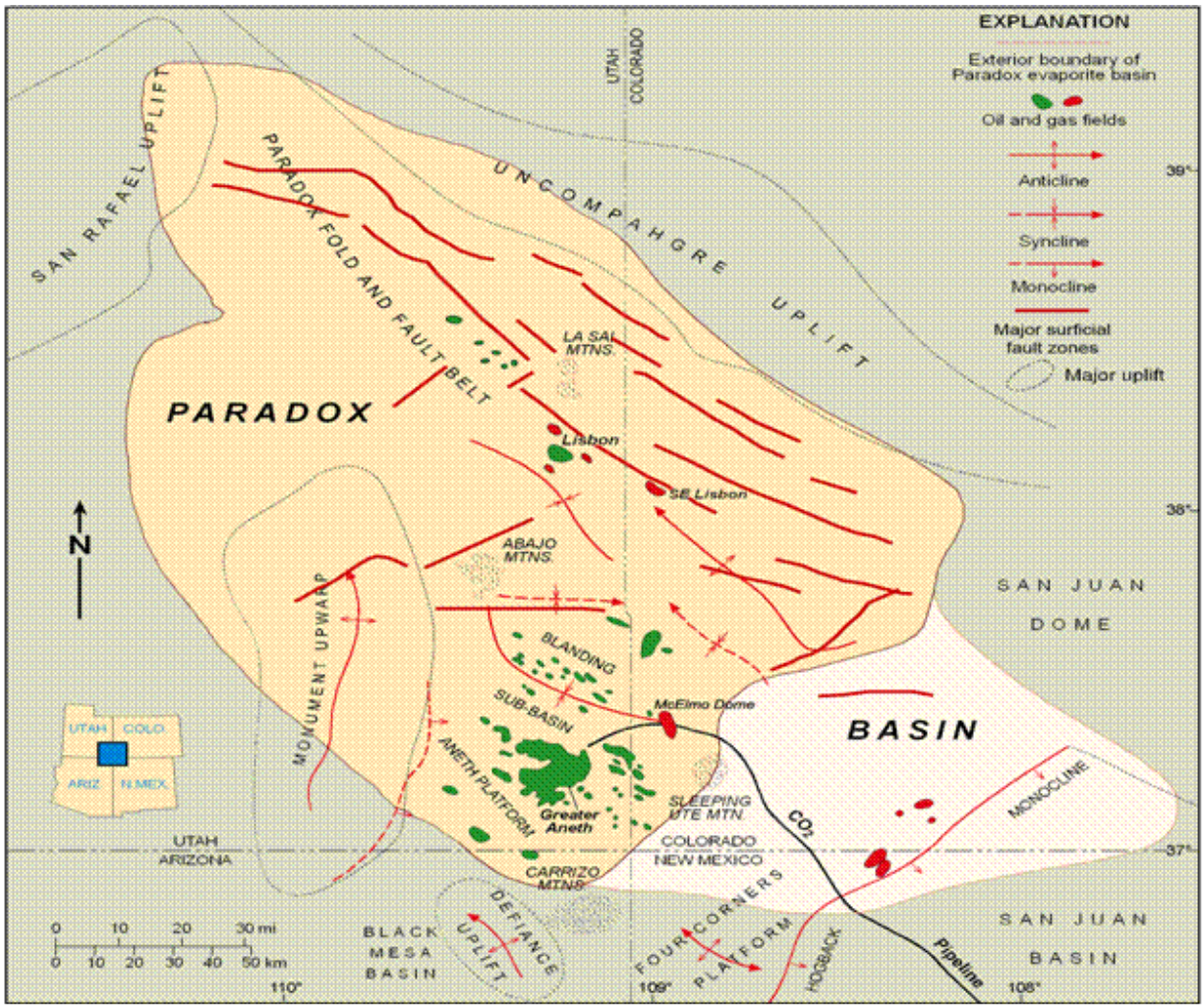

Figure 2. Oil and gas fields in the Paradox Basin of Utah, Colorado and Arizona.

The field monitoring demonstrations were conducted by various Partners including New Mexico Institute of Mining and Technology (NMT), University of Utah (UU), National Institute of Advanced Industrial Science and Technology (AIST) of Japan, and Los Alamos National Laboratory (LANL). The monitoring tests are summarized in Chapters 8 through 12 in the Aneth Field Topical Report (Rutledge, 2010). The report includes (1) interwell tracer studies during water-and CO_2-flood operations to characterize tracer behaviors in anticipation of CO_2-sequestration applications, (2) CO_2 soil flux monitoring to measure background levels and variance and assess the sensitivity levels for CO_2 surface monitoring, (3) testing the continuous monitoring of self potential as a means to detect pressure anomalies and electrochemical reaction due to CO_2 injection, (4) conducting time-lapse vertical seismic profiling to image change near a CO_2 injection well, and (5) monitoring microseismicity using a downhole string of seismic receivers to detect fracture slip and deformation associated with stress changes.

Finally, the geologic modeling and numerical simulation study were reported in Chapter 13 of the Aneth Topical Report (Rutledge, 2010). This summarizes this effort, which focused on developing a site-specific geologic model for Aneth to better understand and design CO_2 storage specifically tailored to oil reservoirs.

Surface and Subsurface Geological Characterization

Introduction

Greater Aneth oil field, Utah's largest oil producer, represents an archetype of a mature western U.S. oil field located in the Paradox Basin of southeastern Utah, Fig. 2. Greater Aneth (Figure 3) is a stratigraphic trap, with fractures and small faults. The field produces oil and gas from the Pennsylvanian (Desmoinesian) Paradox Formation. The Paradox forms a complex reservoir representing a variety of depositional environments (open-marine shelf, shallow-marine beach and shoals, algal mounds, and low-energy restricted shelf) that produce significant heterogeneity. There is evidence of hydrothermal dolomite, brecciation, and minor faults that may affect fluid flow..

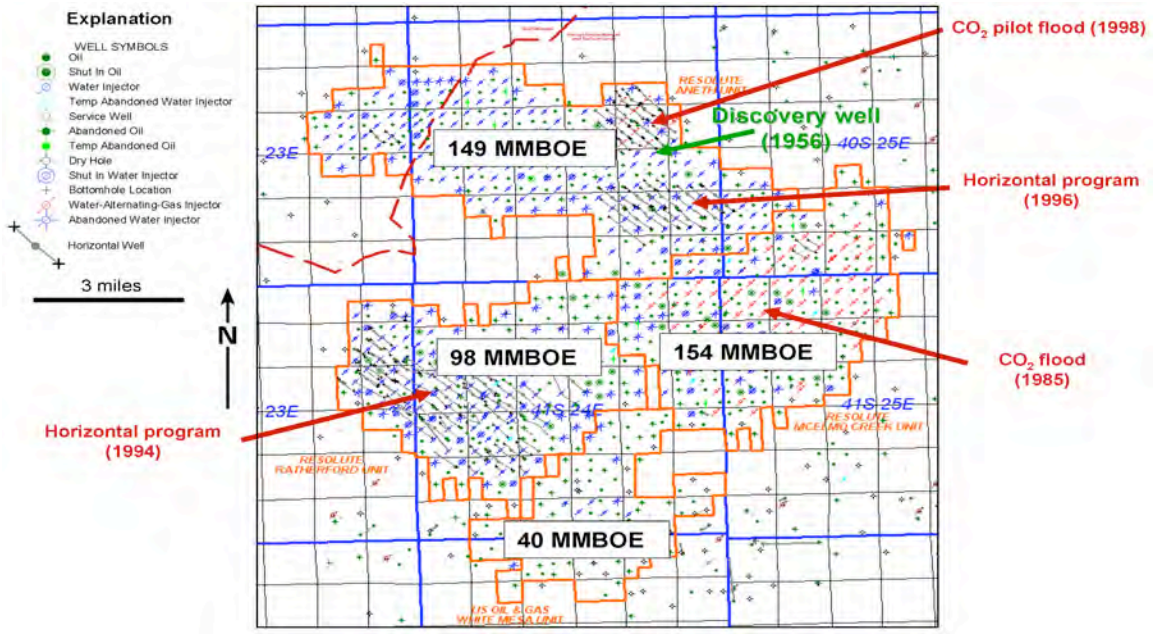

Figure 3. Units, best practices, and cumulative production, Greater Aneth field, Utah. After Resolute Natural Resources unpublished map (2007).

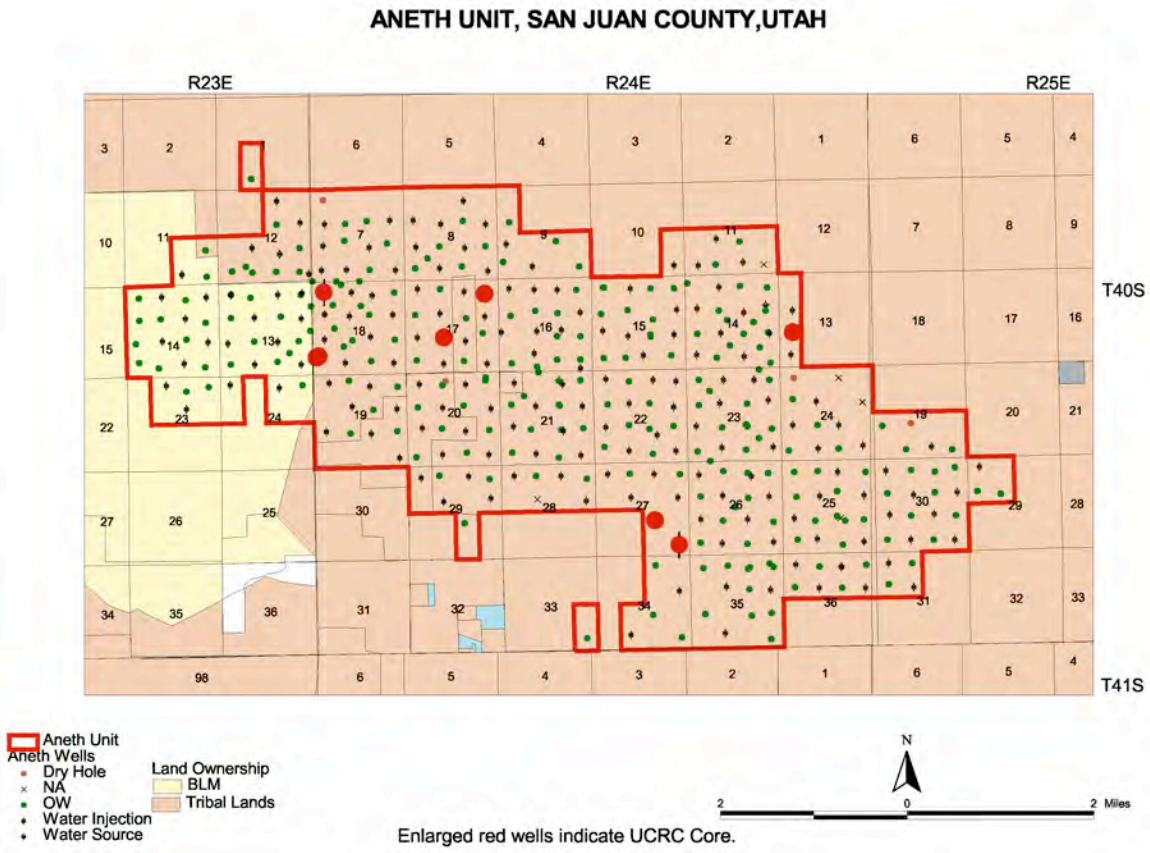

Figure 4. Land ownership and base map of wells in the Aneth Unit. Also displayed are wells from which cores were described as part of this study.

The Aneth Unit in the northwestern part of the field had no significant CO_2 injection (Figs. 3 and 4). Production had declined by 50% over the past 20 years in spite of waterflood and horizontal drilling projects. However, the unit has produced 149 million barrels of the estimated 450 million barrels of oil in place - a 33% recovery rate (Babcock, 1978a; Utah Division of Oil, Gas and Mining, 2009). The large amount of remaining oil, combined with a nearby CO_2 pipeline, made the Aneth Unit ideal to (1) demonstrate both CO_2 storage capability and EOR by flooding the reservoir with the CO_2, and (2) extensively monitor the effects of injection from reservoir to surface. Therefore, the Aneth Unit was selected as a demonstration site for the Southwest Regional Partnership on Carbon Sequestration – Phase II: Field Demonstrations project.

The Utah Geological Survey evaluated the surface and subsurface geology of the Aneth Unit demonstration site and how it would affect sequestration operations and engineering strategies. The research for the project includes (1) mapping the surface geology, (2) description of the local stratigraphy, (3) mapping the reservoir, seals, and overlying aquifers, (4) geological characterization of the reservoir, (5) geochemical, petrographic, and geomechanical description of the seals, and (6) evaluation of production history.

Geologic Map of the Aneth Area

The bedrock geology of the Montezuma Creek and Navajo Canyon quadrangles was mapped using air photos, previous mapping, and field checking. The Quaternary geology was not mapped in detail. The primary focus was to evaluate the fractures and potential pathways for leakage of injected CO_2 from the deep Pennsylvanian Paradox Formation. Due to limited access the formation contacts through much of the area were mapped using air photos and previously mapped data. Most of the fieldwork time was spent mapping deformation bands and potential faults (Fig. 5).

The exposed bedrock geology consists of strata of the Jurassic Recapture Shale Member of the Morrison Formation through the Cretaceous Dakota Sandstone, which dip gently (<5 degrees) to the northeast.

The majority of fractures in the sandstone beds appear to be related to gravity as a result of uplift and erosion of the soft underlying and overlying shale, reflecting the direction of cliff retreat and may not be a reliable indicator of deeper fracture patterns.

No significant faulting was mapped in the area. The only faults found in the area are small, with <3 feet (1 m) of slip. These faults do not appear to penetrate into the subsurface beyond shallow depths and were likely caused by gravity-driven, surficial deformation.

Stratigraphic Measured Section in the Aneth Unit Area

Figure 6 is a general stratigraphic column of the area. There were 878.5 feet (267.8 m) of exposed section measured in the Aneth area, San Juan County, Utah. The section consists of Jurassic Morrison Formation (incomplete section) through the Cretaceous Dakota Sandstone (incomplete Dakota section), covering a time span of about 65 million years.

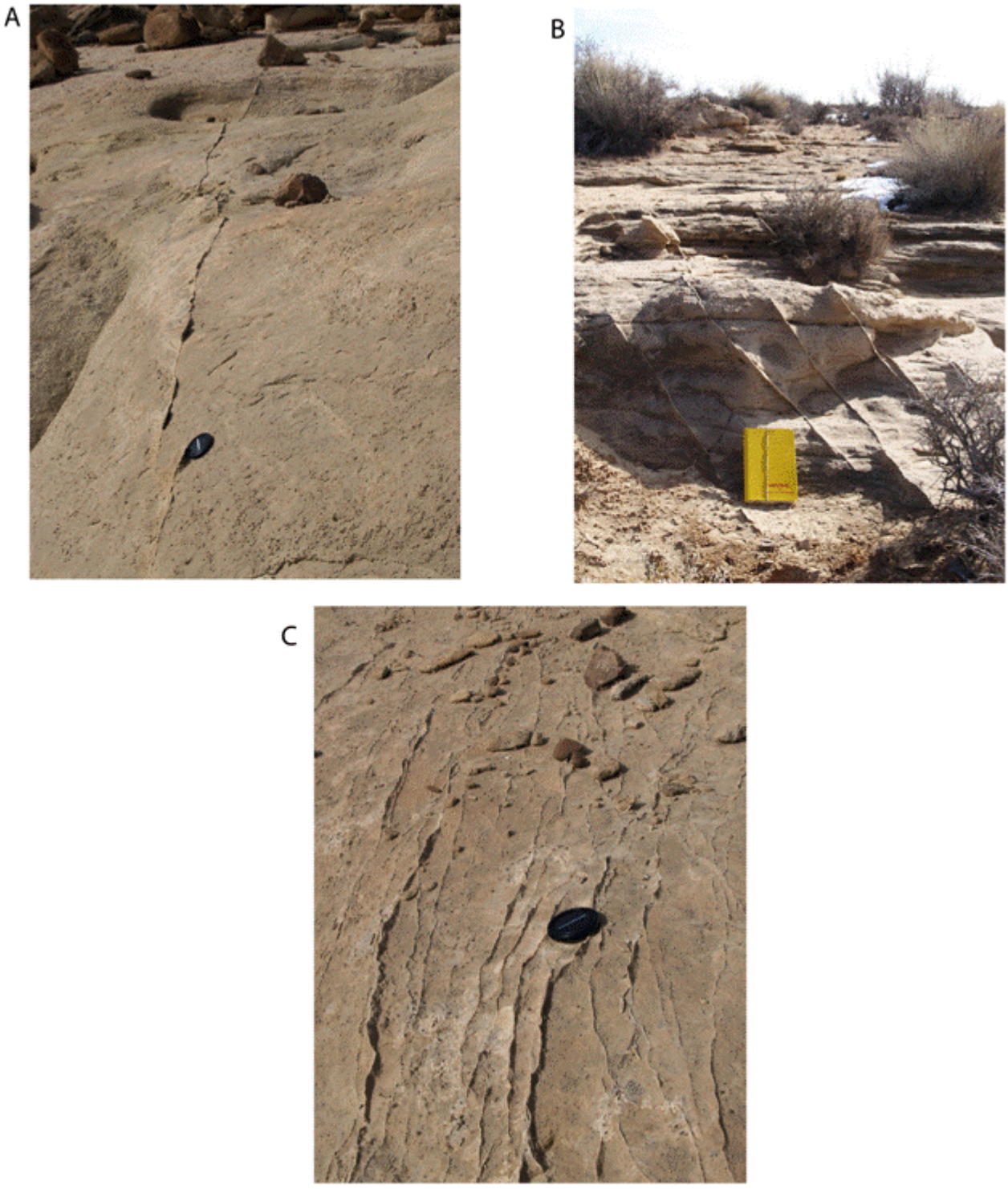

Figure 5. Photographs showing deformation bands in porous sandstone of the Morrison Formation. (A) A single band several tens of feet long. Camera lens cap for scale. (B) Parallel set of bands. (C) Set of closely spaced, mostly parallel bands.

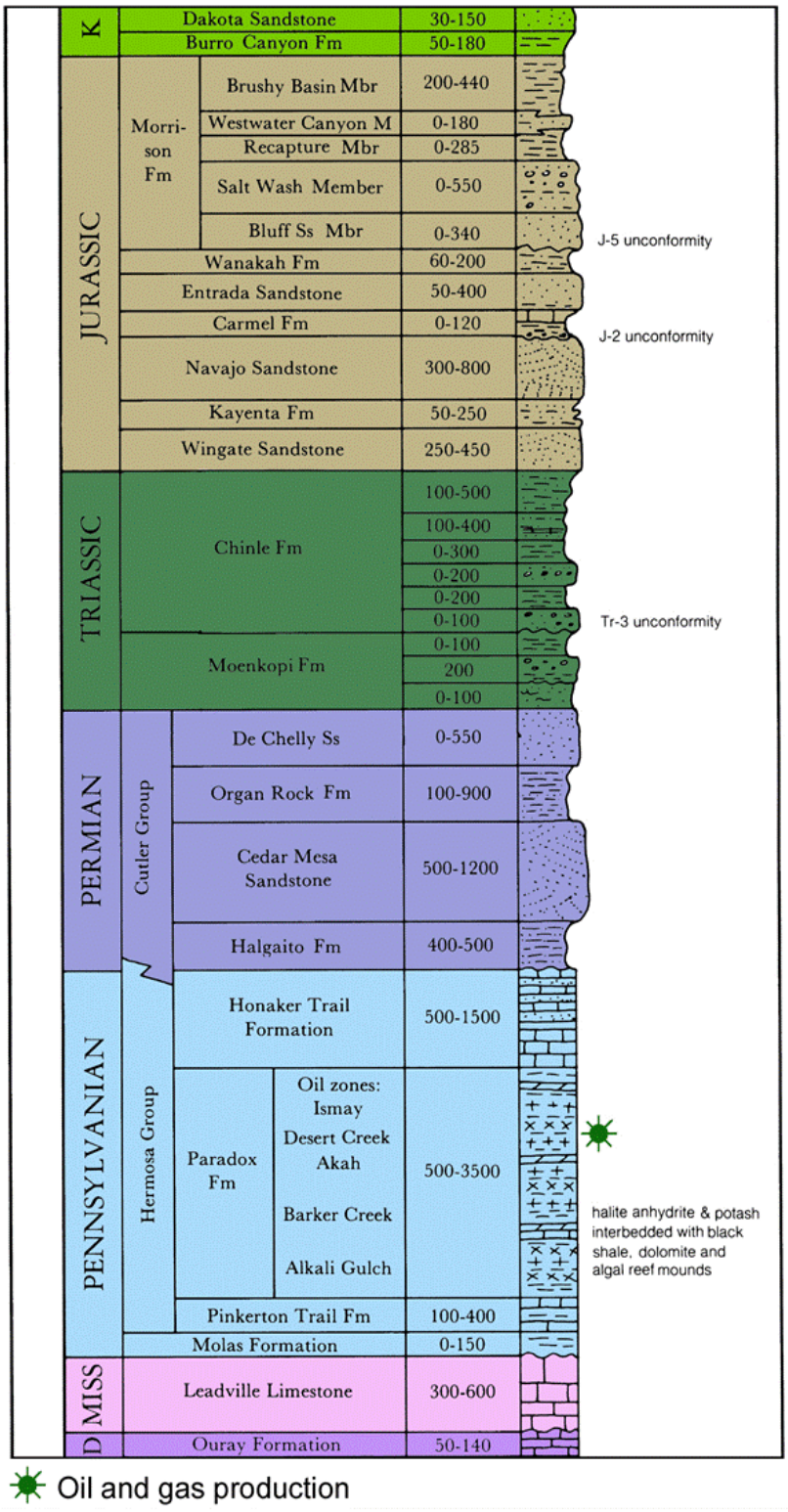

Figure 6. Stratigraphic column for the Aneth Unit and surrounding areas. Modified from Hintze and Kowallis, 2009.

The Morrison Formation consists of the Recapture Shale, Salt Wash, and Brushy Basin members; the basal Bluff Sandstone is not exposed in the Aneth area. The Recapture Shale is dominantly red shale with interbedded channel sandstone beds grading into the overlying Salt Wash, which consists of thicker, stacked channel sandstone beds and decreasing red shale. The Brushy Basin consists of brightly colored, banded, variegated shale, typical of the Brushy Basin throughout most of the Colorado Plateau.

The Cretaceous Burro Canyon Formation is bounded above and below by unconformities. In the Aneth area, the Burro Canyon consists of a basal pebble conglomerate overlain by variegated shale that can be difficult to distinguish from the underlying Brushy Basin Member shale when the conglomerate is absent. Large blocks of dark brown conglomerate often occur where the underlying Brushy Basin shale has partially been eroded.

The Cretaceous Dakota Sandstone caps the mesas in the northern portion of the Aneth area. The Dakota is typically a series of stacked channel deposits of medium- to coarsegrained sandstone with some conglomerate layers. In the Aneth area the Dakota is typically overlain by a thin soil.

Deformation Bands in the Aneth Unit Area

This study identified and documented structural linkages between the proposed subsurface CO_2 reservoir and the surface of the pilot study area that could potentially serve as pathways of CO_2 leakage. Based on the data collected and analyzed, there appear to be no major structural damage zones or faults that are likely to act as migration pathways for CO_2 from the reservoir to the surface.

The deformation bands are confined within porous sandstones at the surface and are not coincident with any major faults or damage zones that extend into the subsurface. Deformation bands observed in the study area generally have a strong northwest-southeast orientation.

These features would likely create barriers to lateral fluid flow in a reservoir confined to a single sandstone body and would not likely act as conduits for fluid flow. The bands likely formed in response to either compaction of the sediment after burial or from tectonic stresses associated with the Laramide orogeny.

Subsurface Structural and Thickness Mapping

The paleogeographic geometry and extent of the Pennsylvanian carbonate buildup complex is evident in the structure contour maps of all three zones of the Paradox Formation studied. The general shapes of subsidiary buildups are also reflected, to a lesser extent, in the overlying strata of the Permian DeChelly and Jurassic Navajo Sandstones.

Structures such as faults and folds are virtually absent from the Aneth Unit. One notable exception is a possible northeast-southwest-striking fault seen in the Ismay, Gothic, and Desert Creek structure contour maps in the location of section 18, T. 40 S., R. 24 E., SLBL&M. This potential fault, however, does not appear in the overlying DeChelly or Navajo Sandstone structure contour maps, and therefore is believed to be a small fault having minimal displacement that is localized in the Paradox Formation.

The sequestration reservoirs, Desert Creek oil reservoir and Leadville aquifer in Fig. 6, are likely sound and the risk of contaminating overlying aquifers from geologic structures or CO_2 migration to the surface is small.

Reservoir Characterization of the Desert Creek Zone of the Paradox Formation, Aneth Unit: Core Descriptions, Lithofacies, Lithologies, Pore Types, and Diagenesis

Determining the nature, location, and extent of reservoir heterogeneity is the key to determining CO_2 storage potential in the Aneth Unit. Three factors create reservoir heterogeneity: (1) variations in lihtofacies and lithology, (2) mound relief and flooding surfaces, and (3) diagenesis. The extent of these factors and how they are combined affect the degree to which they create CO_2 storage capacity and barriers to CO_2 flow.

Cores from Aneth Unit wells reveal a complex reservoir consisting of limestone (oolitic, peloidal, and skeletal grainstone and packstone, and algal boundstone/bafflestone, see Fig. 7) and finely crystalline dolomite. These lithotypes represent a variety of depositional environments (open-marine shelf, shallow-marine beach and shoals, algal mounds, low-energy restricted shelf) that produce reservoir heterogeneity beyond what can be determined from well logs.

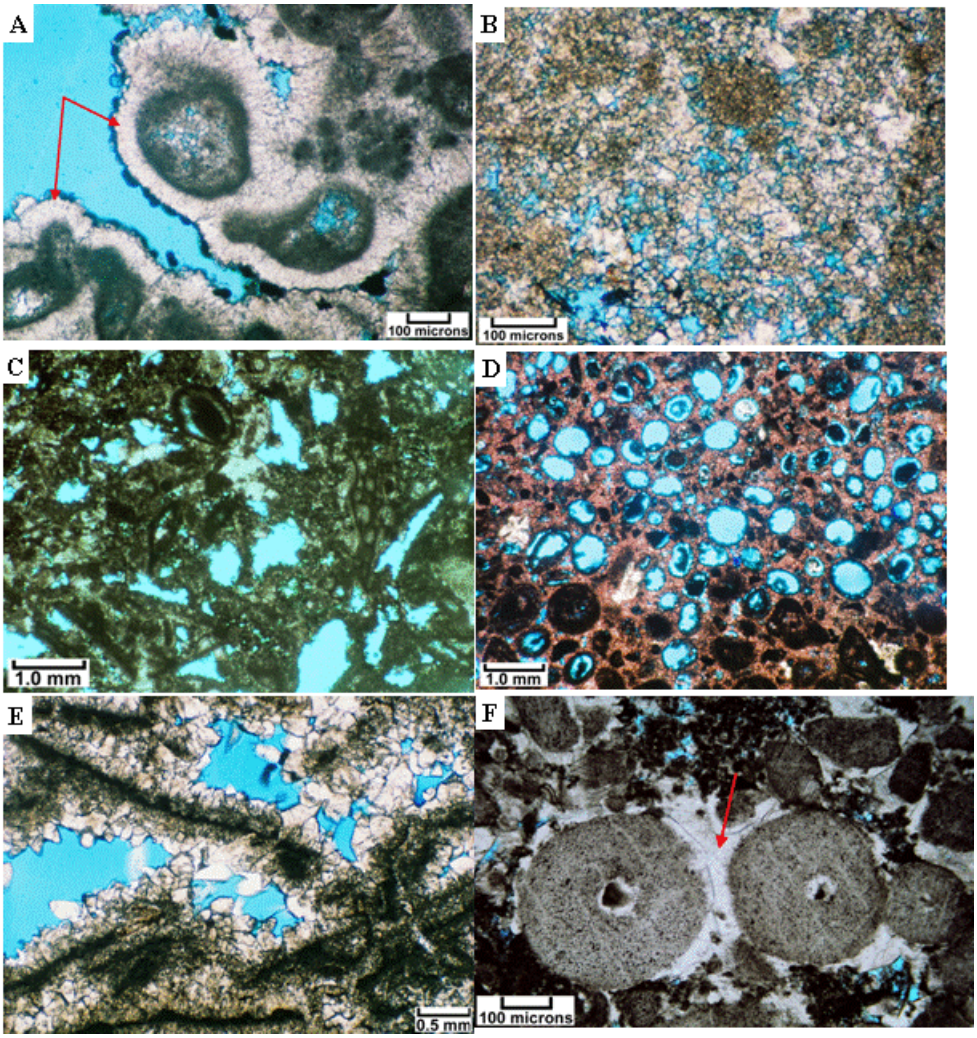

Figure 7. Photomicrographs (plane light) of early diagenesis. A – Rinds of early marine isopachous cement (red arrows) on ooids and skeletal grains, thus filling interparticle pores (blue) of an oolitic/skeletal grainstone fabric. Aneth Unit No. H-117 well, 5441 feet. B – Extensive dolomitization and microintercrystalline porosity (blue) in an original peloidal packstone/wackestone fabric. Note brown rounded areas representing "ghosts" of peloids. Aneth Unit No. F-317 well, 5395 feet. C – Moldic and vuggy porosity (blue) in a skeletal/peloidal packstone/wackestone fabric with skeletal fragments including crinoid, phylloid-algal plates, small benthic forams, and fusilinids; peloids include both hard and soft varieties. Aneth Unit No. 27-C-3 well, 5738 feet. D – Oomoldic porosity (blue) in an oolitic grainstone fabric. Sparry mosaic calcite cement between ooid molds and grains results in an isolated "heartbreak" porosity system. Aneth Unit No. 27-D-4 well, 5621 feet. E – "Dogtooth" spar filling shelter pores (blue) between phylloid-algal plates in a phylloid-algal bafflestone fabric. Aneth Unit No. F-317 well, 5472 feet. F – white syntaxial calcite cement (red arrow) overgrowths surrounding two discrete ossicles within a crinoidal grainstone fabric. Aneth Unit No. 27-C-3 well, 5806 feet.

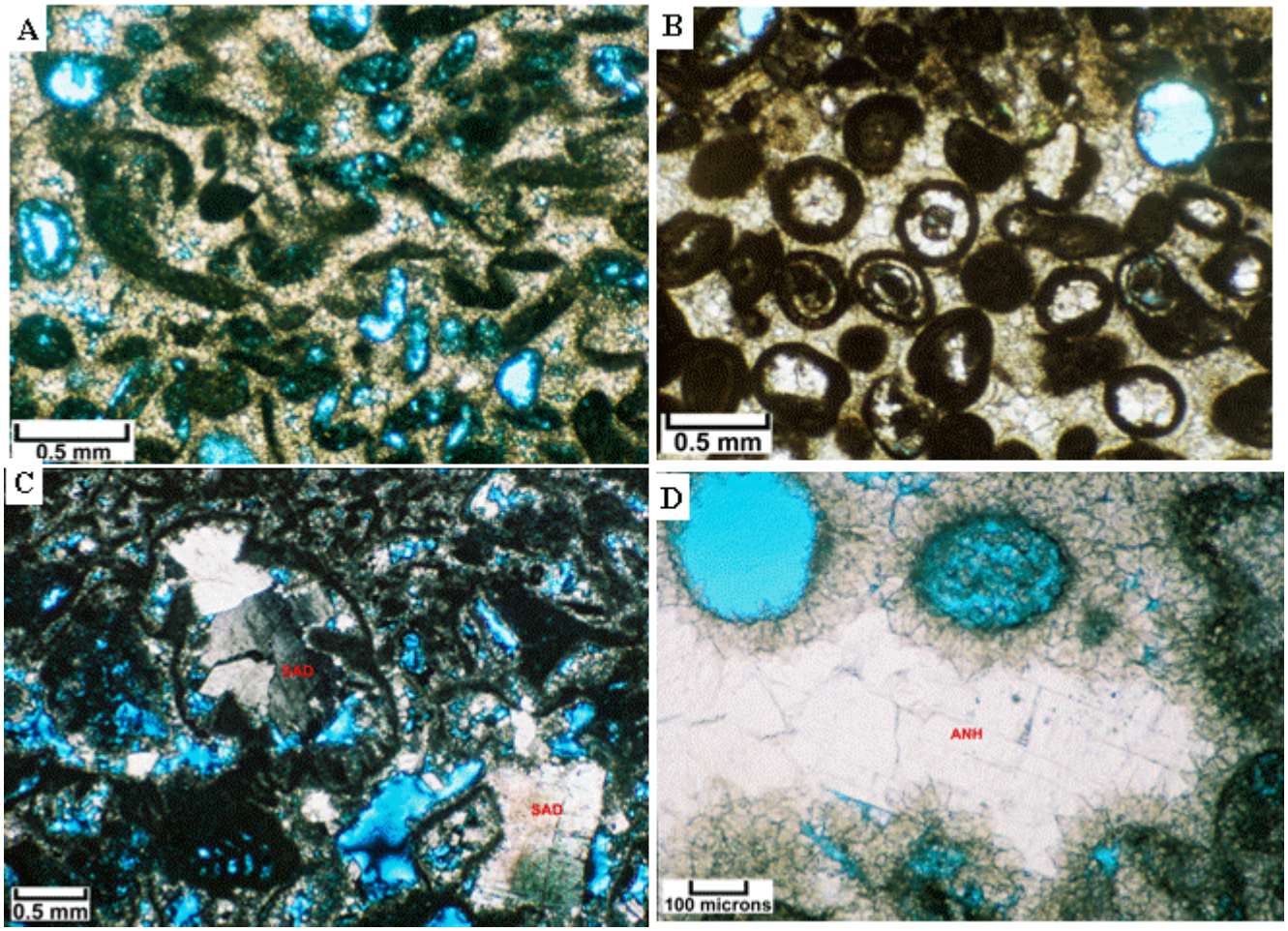

Figure 8. Photomicrographs of post-burial diagenesis. A – "Elephant trunks and tails" texture formed by the compaction of ooid molds (plane light). Aneth Unit No. E-313 well, 5785 feet. B – Late calcite cement completely filling the original interparticle pores between ooids and oomoldic pores (plane light). Aneth Unit No. 27-D-4 well, 5507 feet. C – Saddle dolomite (SAD) within skeletal molds (cross nicols). Note sweeping extinction within the curved saddle dolomite crystal in the center. Aneth Unit No. F-317 well, 5440 feet. D – Closeup of large, late, anhydrite replacement crystals (ANH) within an oolitic grainstone (plane light). Note two large remaining oomolds (blue). Aneth Unit No. H-117 well s, 5413 feet.

The typical early diagenetic events occurred in the following order: (1) early marine cementation, (2) post-burial, replacement, rhombic dolomite cementation due to seepage reflux, (3) vadose and meteoric phreatic diagenesis including leaching/dissolution, and fresh-water cementation, (4) mixing-zone dolomitization, and (5) anhydrite cementation/replacement.

The relatively large number of fractures (Figs. 8 and 9), both horizontal and vertical, suggests fracture-related permeability is significantly higher than matrix permeability but directional flow

anisotropy may not be high. The natural fractures in most cases cut across vertical and horizontal stylolites, which tend to compartmentalize a reservoir, and will enhance conductivity across the stylolites. The low probability of intersecting vertical and near-vertical fractures with near-vertical core, unless the fractures are closely spaced, suggests that Desert Creek reservoir strata are intensely fractured and that fractures are likely to be an important factor in subsurface fluid flow, including directionality and volume of flow. Stylolites may impede flow and influence the directionality of fluid flow.

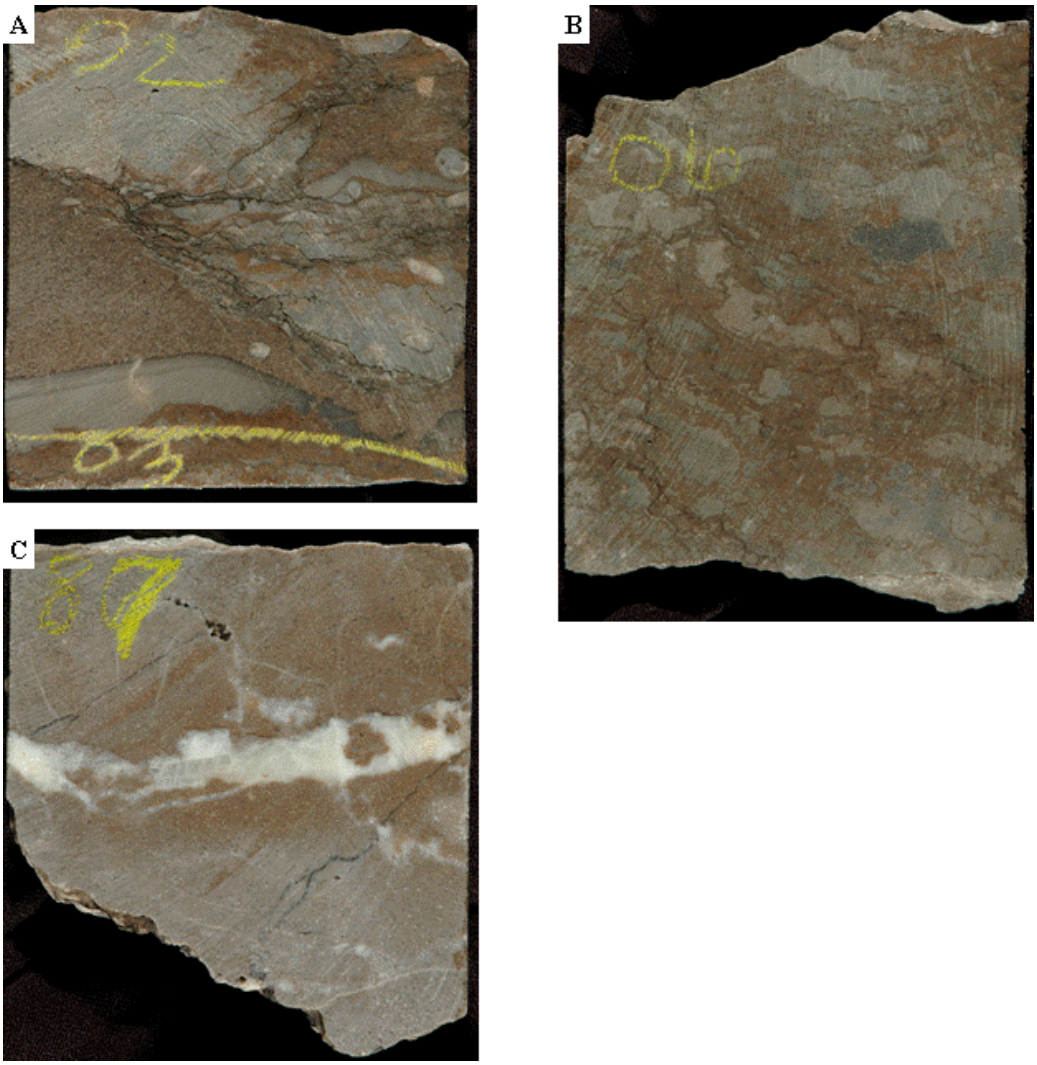

Figure 9. Evidence of possible fault zone near the Aneth Unit No. E-418 well (figure 1-3). A – Dolomite replacement bounded by stylolite and fracture swarms, 6002 feet. B – Breccia with limestone clasts surrounded by stylolites and dolomite, 6006 feet. C – Saddle dolomite hydrothermal alteration replacement and vugs lined with saddle dolomite, well-terminated quartz, and bitumen, 5987 feet.

The most notable and well-documented oil-producing intervals in the Desert Creek zone of the Paradox Basin formed as shallow-water algal buildups. However, they are not significant producers in the Aneth Unit. Grainstones within oolitic shoal lithofacies represent the major reservoir and the best potential CO_2 storage capacity. Dolomite with high porosity identified on geophysical well logs but with unidentified low permeability has led to costly and unwise well completion attempts in these intervals that in reality are baffles to poor-quality flow units.

The Gothic Shale in the Aneth Unit: Seal for Hydrocarbons and CO_2 Geologic Sequestration

The Gothic shale is an effective seal above the Desert Creek reservoir zone within the Pennsylvanian Paradox Formation, Aneth Unit. The Gothic shale ranges in thickness from 5 to 27 feet (1.5-8 m), averaging 15 feet (4.6 m), see example core in Fig. 10.

The core from the Aneth Unit No. H-117 well is an excellent representation of the Gothic shale. The Gothic is remarkably uniform mudstone/shale with grain size ranging between clay and silt. Accessories and biological constituents consist of ubiquitous authigenic pyrite, microfossils, shell fragments, conodonts, and conularoids.

Total organic carbon ranges from 2.2 to 4.4% with type II kerogen.

Lithology consists of argillaceous or calcareous shale and mudstone composed of a clayey to siliceous matrix with weak laminations defined by micas. Within the matrix, calcite crystals, pyrite, quartz, microfossils, flakes of organics, and swarms of intercrystalline micropores are common.

Porosity ranges from 2.7 to 3.4% and pressure-decay permeability is no greater than 0.000146 mD. These and other basic matrix petrophysical parameters indicate the Gothic shale to be a highly effective reservoir seal.

The Gothic shale should support very large CO_2 or hydrocarbon columns based on mercury injection capillary pressure and pore aperture distribution analyses.

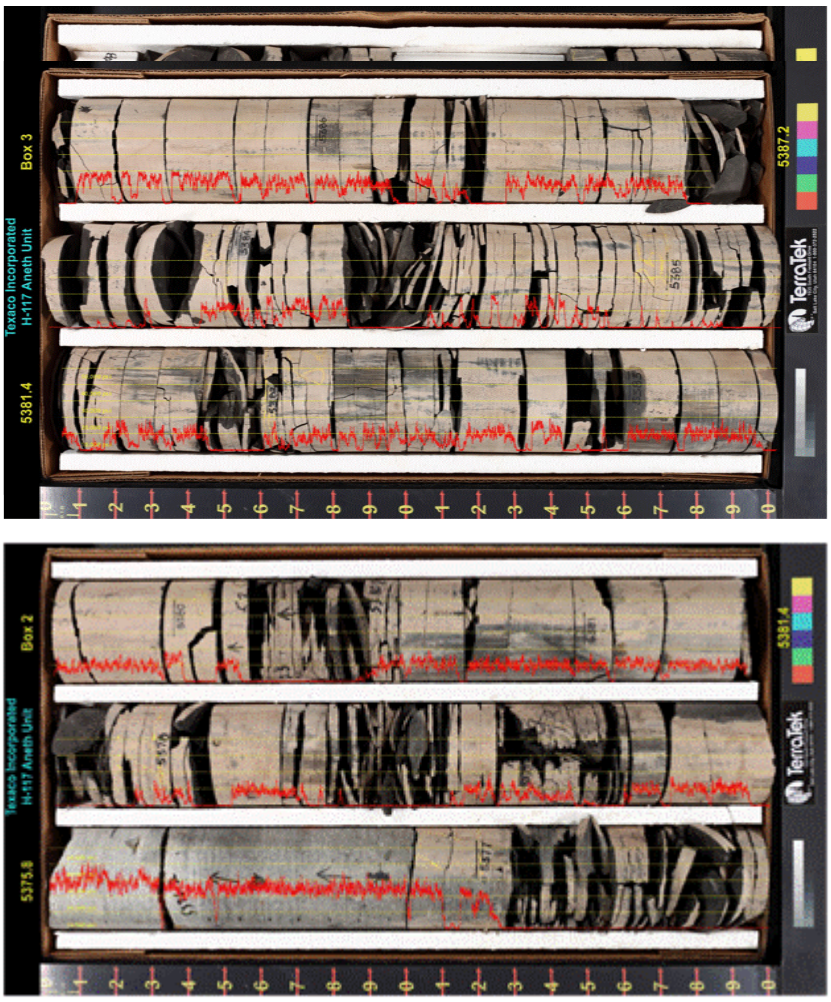

Figure 10. Continuous unconfined compressive strength profile of the Gothic shale core from the Aneth Unit No. H-117 well.

Near the base of the Gothic section, vertical to subvertical extensional fractures are present. Mineralization co-located with these natural fractures is most likely dominated by carbonates and organics.

Continuous unconfined compressive strength profiles show a relatively uniform homogenous shale package. Compressional testing suggests some degree of hydraulic fracture containment.

Evaluation of Production History Curves

Monthly production curves for the sections studied show improved oil recovery resulting from the waterflood. Increasing to flat monthly oil production rates occurred in each section from 2 to 12 years after waterflood operations began. Find in Fig. 11 an example production history. Shown are the monthly oil produced, water injected (1958 – 2006) and gas-to-oil ratio (GOR) for all wells in section 14 (WAG area). Three years after secondary recovery waterflood operations began, the monthly oil production began to increase and the GOR decreased. Horizontal legs were drilled in existing wells and tertiary water-alternating-gas operations began in 1998, resulting in several years of level oil production.

Section 14 (Phase II) had the quickest water breakthrough of all the sections studied. The rapid breakthrough may be due to increased formation water production and not a true breakthrough of injected water. However, if the increased water production is a result of breakthrough of injected water, then this area may experience early breakthrough of injected CO_2 as well. The long period from the onset of water injection to when water breakthrough occurred in section 18 (Phase I) may be due to some of the injected water getting out of zone.

If injected water is going out of zone then some of the injected CO_2 will get out of zone as well. This may not adversely affect the tertiary oil recovery volume, but may require greater volumes of injected CO_2 over time since some of the CO_2 will not be recycled. Oil production from section 14, Township 40 S., Range 24 E., SLBL&M (WAG area) remained steady or increased slightly for about 2.5 years after WAG operations began. A similar response can be expected from WAG operations in Phase I and section 13 of Phase II.

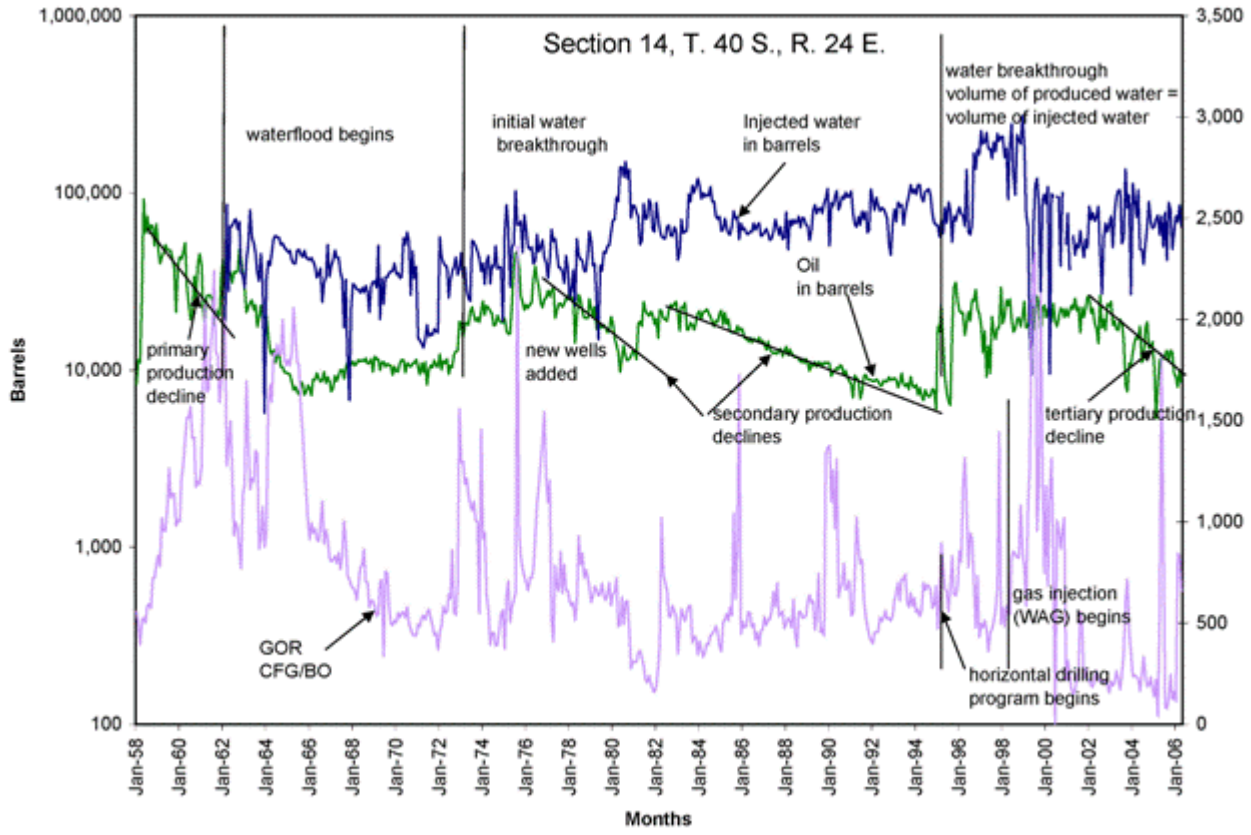

Figure 11. Monthly oil produced, water injected (1958 – 2006) and gas-to-oil ratio (GOR) for all wells in section 14 (WAG area).

Monitoring, Verification, and Accounting (MVA)

Tracer Testing

The primary objective of this research was to characterize waterflood and CO_2-flood tracers in anticipation of their use in CO_2-sequestration applications. This was achieved by using candidate tracers to test fluid-flow patterns within the western portion of the Aneth petroleum field during both a waterflood and a subsequent CO_2 flood.

Comparison of the Performance of the Water- and CO_2-Flood Tracers

On July 19, 2007, 100 kg each of the fluorescent tracers 1,3,5-naphthalene trisulfonate (1,3,5-nts) and 2,6-naphthalene disulfonate (2,6-nds) were injected into Aneth water-injection wells C-214 and D-114, respectively (see Figure 12). Four production wells (B-214, C-314, D-214, and C-114) were subsequently sampled and analyzed. 1,3,5-nts was detected only in well D-214 and 2,6-nds was not detected in any sampled wells. The prominent flow direction appears to be west to east (Figure 12) and no well was sampled east of D-214, thus it is undetermined if 2,6-nds is an effective water phase tracer. The trends are shown in Figure 12 and the results summarized in Table 3.

Following the waterflood, the Aneth field switched to an alternating water and gas (WAG) injection, with CO_2 being the gas. The tracer testing of the CO_2 therefore involved the use of gas-flood tracers, included were two perfluorocarbons (PFT's) and two low-molecular weight alcohols. The PFT's are commonly used as a gas-flood tracer, but the use of low-molecular-weight alcohols has not been reported in the open literature. This gas-flood tracer test at the Aneth petroleum field therefore provided the opportunity to use a well characterized family of tracers (the PFT's) in combination with a novel family of tracers (the alcohols). If the alcohols were to perform well in the gas-flood of a petroleum field, then they would be excellent, cost-effective candidates for CO_2-sequestration tracing applications.

The PFT's selected were soluble in oil and gas and water insoluble. The PFT's were perfluoromethylcyclopentane (PMCP) and 1,3-perfluorodimethylcyclohexane (PDCH). The selected alcohols were gas and water soluble alcohols, n-propanol and iso-propanol (Table 2). The perfluorocarbons provide thermal and biological stability, as well as distinctive mass fragments that are

easily distinguishable from background interference. But, they are relatively expensive and partition moderately into the oil phase. In contrast, the propanols are inexpensive and thermally stable, but would not be stable in systems with significant biologic activity. Like the perfluorocarbons, they partition into the oil phase, but unlike the PFT's partition moderately into groundwater.

The tracer injection was conducted on July 21, 2009. 158 kg of n-propanol and 9.6 kg of 1,3-perfluorodimethylcyclohexane (PDCH) were injected into well C-414. 154 kg of isopropanol and 9.5 kg of perfluoromethylcyclopentane (PMCP) were injected into well B-314. Injection information is summarized in Table 2. Four adjacent production wells were sampled over the following six months. Samples were collected from effluent vapors at the wellheads onto carbon absorption tubes and analyzed using thermal desorption of the carbon absorption tubes, separation of the tracers via gas chromatography, and mass spectrometric detection. The production trends are shown in Figure 12 and values summarized in Tables 4-7.

Table 2. Tracers Used in the Water and CO_2-Flood Tracer Test

Compound	Amount Injected (kg)	Well	Carrier Fluid	Molecular Weight	Boiling Point (°C)	Cost (USD/ kg)
PMCP	9.5	B-314	CO2	300	48	450
PDCH	9.6	C-414	CO2	400	102	300
n-propanol	158	C-414	CO2	60	97	1
isopropanol	154	B-314	CO2	60	83	1
1,3,5-nts	100	C-214	Brine	368		
2,6-nds	100	D-114	Brine	288		

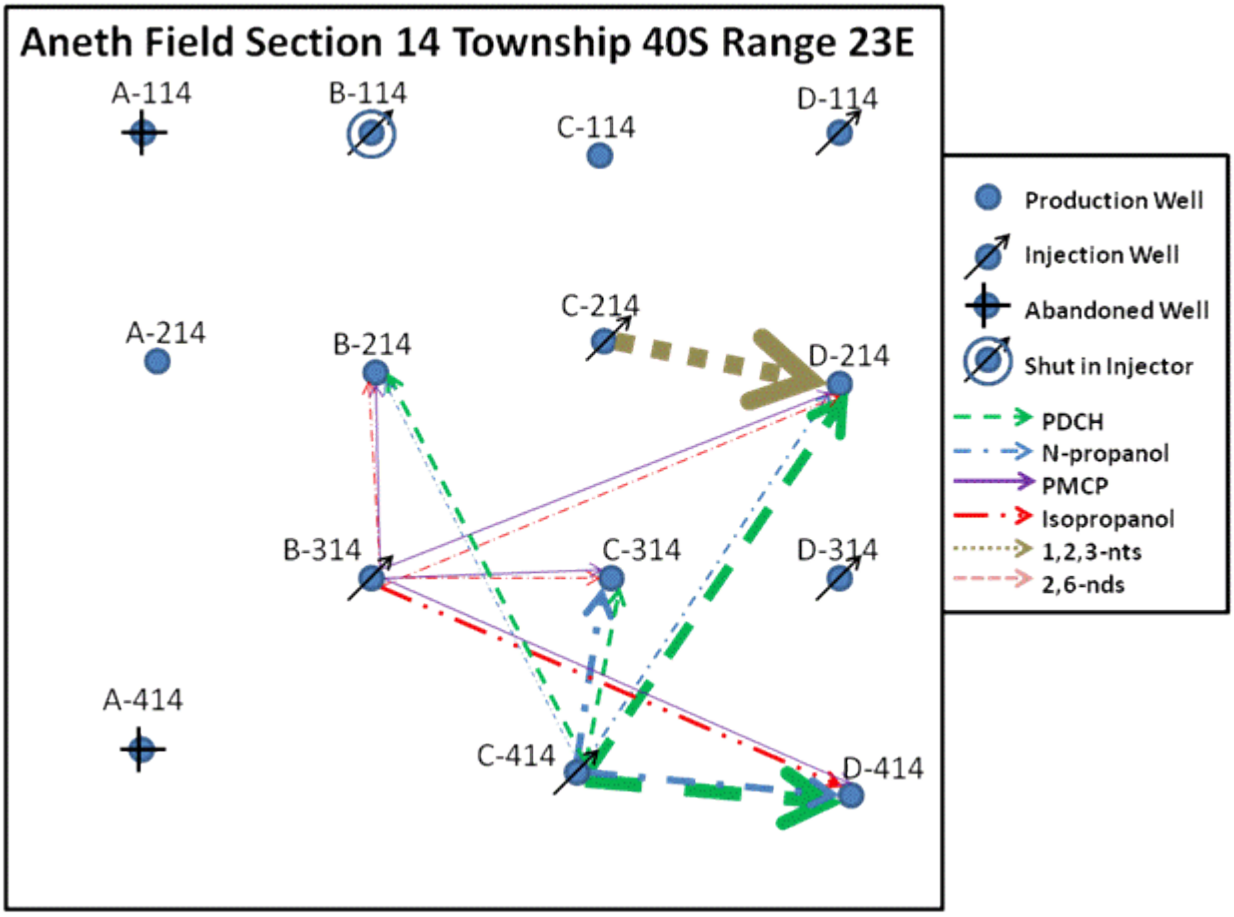

Figure 12. Test site showing the tagged injectors and the breakthrough patterns. The thicknesses of the arrows reflect the relative amounts of tracer produced at each well. Aneth Field Section 14, Township 40S, Range 23E.

Table 3. Measured Concentrations in Parts-per-Billion of the Liquid-Phase Tracers 2,6-Naphthalene Disulfonate and 1,3,5-Naphthalene Trisulfonate injected in the brine at C-214 and measured at the four production wells B-214, C-114, C-314, and D-214("ns" Designates "Not Sampled")

		Well Designation							
Sample Date	Days after Injection	B-214		C-114		C-314		D-214	
		2,6-nds	1,3,5-nts	2,6-nds	1,3,5-nts	2,6-nds	1,3,5-nts	2,6-nds	1,3,5-nts
7/19/2007	0.00	0.00	0.00	*ns*	*ns*	0.00	0.00	0.00	0.00
7/20/2007	1.00	0.00	0.00	0.00	0.00	0.00	0.00	0.00	0.00
7/21/2007	2.00	0.00	0.00	0.00	0.00	0.00	0.00	0.00	0.00
7/22/2007	3.00	0.00	0.00	0.00	0.00	0.00	0.00	0.00	0.00
7/23/2007	4.00	0.00	0.00	0.00	0.00	0.00	0.00	0.00	0.00
7/24/2007	5.00	0.00	0.00	0.00	0.00	0.00	0.00	0.00	0.00
7/25/2007	6.00	0.00	0.00	0.00	0.00	0.00	0.00	0.00	0.00
7/27/2007	8.00	*ns*	*ns*	*ns*	*ns*	0.00	0.00	0.00	0.00
7/28/2007	9.00	0.00	0.00	0.00	0.00	0.00	0.00	*ns*	*ns*
7/30/2007	11.00	0.00	0.00	0.00	0.00	0.00	0.00	*ns*	*ns*
8/1/2007	13.00	0.00	0.00	0.00	0.00	0.00	0.00	*ns*	*ns*
8/3/2007	15.00	0.00	0.00	0.00	0.00	0.00	0.00	*ns*	*ns*
8/5/2007	17.00	0.00	0.00	0.00	0.00	0.00	0.00	0.00	0.00
8/7/2007	19.00	*ns*	*ns*	*ns*	*ns*	0.00	0.00	0.00	0.00
8/9/2007	21.00	0.00	0.00	*ns*	*ns*	0.00	0.00	0.00	0.00
8/11/2007	23.00	0.00	0.00	0.00	0.00	0.00	0.00	0.00	0.00
8/13/2007	25.00	0.00	0.00	0.00	0.00	0.00	0.00	0.00	0.00
8/15/2007	27.00	0.00	0.00	0.00	0.00	0.00	0.00	0.00	0.00
8/17/2007	29.00	0.00	0.00	0.00	0.00	0.00	0.00	0.00	0.00
8/19/2007	31.00	0.00	0.00	0.00	0.00	0.00	0.00	0.00	0.00
8/21/2007	33.00	0.00	0.00	0.00	0.00	0.00	0.00	0.00	0.00
8/23/2007	35.00	0.00	0.00	0.00	0.00	0.00	0.00	0.00	0.00
8/28/2007	40.00	0.00	0.00	*ns*	*ns*	0.00	0.00	0.00	0.00
8/30/2007	42.00	0.00	0.00	*ns*	*ns*	0.00	0.00	0.00	0.00
9/4/2007	47.00	0.00	0.00	0.00	0.00	0.00	0.00	0.00	0.00
9/7/2007	50.00	0.00	0.00	0.00	0.00	0.00	0.00	0.00	0.00
9/10/2007	53.00	0.00	0.00	0.00	0.00	0.00	0.00	0.00	0.00
9/13/2007	56.00	0.00	0.00	0.00	0.00	0.00	0.00	*ns*	
9/17/2007	60.00	0.00	0.00	0.00	0.00	0.00	0.00	0.00	17.46
9/20/2007	63.00	*ns*	*ns*	0.00	0.00	0.00	0.00	*ns*	
9/24/2007	67.00	*ns*	*ns*	0.00	0.00	0.00	0.00	0.00	32.50
9/28/2007	71.00	0.00	0.00	0.00	0.00	0.00	0.00	*ns*	
10/2/2007	75.00	0.00	0.00	0.00	0.00	0.00	0.00	0.00	0.00
10/9/2007	82.00	0.00	0.00	0.00	0.00	0.00	0.00	*ns*	
10/16/2007	89.00	0.00	0.00	0.00	0.00	0.00	0.00	0.00	0.00
10/19/2007	92.00	0.00	0.00	0.00	0.00	0.00	0.00	0.00	34.37
11/1/2007	105.00	0.00	0.00	0.00	0.00	0.00	0.00	0.00	22.47
11/7/2007	111.00	0.00	0.00	0.00	0.00	0.00	0.00	0.00	18.62
11/15/2007	119.00	0.00	0.00	0.00	0.00	0.00	0.00	0.00	21.83
11/21/2007	125.00	0.00	0.00	0.00	0.00	0.00	0.00	0.00	24.84
4/28/2008	284.00	0.00	0.00	0.00	0.00	0.00	0.00	0.00	69.52
7/23/2008	370.00	0.00	0.00	0.00	0.00	0.00	0.00	0.00	35.85
9/10/2008	419.00	0.00	0.00	0.00	0.00	0.00	0.00	0.00	24.60
10/29/2008	468.00	0.00	0.00	0.00	0.00	0.00	0.00	0.00	25.77

Table 4. Measured Concentrations of the CO_2-Phase Tracers Perfluoromethylcyclopentane (PMCP), Perfluorodimethylcyclohexane (PDCH), 1-Propanol (1POH) and 2-Propanol (2POH) Measured at the Production Well D-414 ("nd" Designates "Not Detected")

Tracer injection date and hour	Days since injection	PMCP (ppb)	PDCH (ppb)	1POH (ppm)	2POH (ppm)
7/21/2009 13:00	0.00	nd	nd	nd	nd
7/21/2009 14:30	0.063	nd	nd	nd	nd
7/22/2009 8:10	0.80	nd	nd	nd	nd
7/28/2009 14:20	7.06	nd	nd	nd	nd
8/5/2009 12:30	14.98	nd	nd	nd	nd
8/12/2009 11:30	21.94	nd	nd	nd	nd
8/19/2009 12:10	28.97	nd	0.29	nd	0.0072
8/26/2009 11:50	35.95	nd	0.39	nd	0.0043
9/1/2009 11:15	41.93	nd	7.43	nd	0.0017
9/9/2009 11:30	49.94	nd	nd	40.04	20.70
9/15/2009 13:30	56.02	nd	7.20	19.76	8.61
9/29/2009 11:20	69.93	nd	1.61	nd	0.27
10/14/2009 12:00	84.96	0.93	5.54	nd	0.033
10/27/2009 11:50	97.95	0.11	4.00	nd	nd
12/10/2009 12:40	141.99	0.11	0.10	nd	nd
1/12/2010 12:00	174.96	nd	0.27	nd	nd

Table 5. Measured Concentrations of the CO_2-Phase Tracers measured at B-214 ("nd" Designates "Not Detected")

Tracer injection date and hour	Days since injection	PMCP (ppb)	PDCH (ppb)	1POH (ppm)	2POH (ppm)
7/21/2009 13:00	0.00	nd	nd	nd	nd
7/21/2009 16:05	0.13	nd	nd	nd	nd
7/22/2009 9:05	0.84	nd	nd	nd	nd
8/5/2009 13:00	15.00	nd	nd	nd	0.0011
8/12/2009 12:15	21.97	nd	nd	nd	nd
8/19/2009 12:10	28.97	nd	0.30	nd	1.70
8/26/2009 12:15	35.97	nd	0.31	nd	0.0028
9/1/2009 11:40	41.94	nd	nd	nd	nd
9/9/2009 12:00	49.96	nd	1.02	0.08	0.0012
9/15/2009 14:00	56.04	nd	2.27	0.06	6.84
9/29/2009 11:50	69.95	0.23	1.66	nd	0.59
10/14/2009 12:30	84.98	nd	2.83	nd	0.034
10/27/2009 12:10	97.97	nd	0.89	nd	0.0076
12/10/2009 13:10	142.01	nd	1.11	nd	nd
1/12/2010 12:00	174.96	nd	0.18	nd	nd
2/11/2010 12:15	204.97	nd	0.10	nd	0.0030

Table 6. Measured Concentrations of the CO_2-Phase Tracers measured at D-214 ("nd" Designates "Not Detected")

Tracer injection date and hour	Days since injection	PMCP (ppb)	PDCH (ppb)	1POH (ppm)	2POH (ppm)
7/21/2009 13:00	0.00	nd	nd	nd	nd
7/21/2009 17:05	0.17	nd	0.45	nd	nd
7/22/2009 6:55	0.75	nd	nd	nd	nd
7/28/2009 13:15	7.01	nd	nd	nd	nd
8/5/2009 11:15	14.93	0.17	nd	nd	nd
8/12/2009 13:20	22.01	nd	nd	nd	nd
8/19/2009 10:30	28.90	nd	0.29	nd	nd
8/26/2009 11:00	35.92	nd	0.33	nd	0.0045
9/1/2009 10:30	41.90	0.93	2.00	nd	0.00093
9/9/2009 10:40	49.90	nd	5.50	0.09	0.0019
9/15/2009 21:15	56.34	nd	1.49	15.38	5.54
9/29/2009 10:30	69.90	nd	0.42	nd	0.060
10/14/2009 11:00	84.92	nd	2.27	nd	0.47
10/27/2009 11:15	97.93	0.11	0.20	nd	nd
12/10/2009 11:40	141.94	0.038	0.00050	nd	nd
1/12/2010 12:00	174.96	nd	0.25	nd	nd
2/11/2010 11:10	204.92	nd	1.22	nd	nd

Table 7. Measured Concentrations of the CO_2-Phase Tracers measured at C-314 ("nd" Designates "Not Detected")

Tracer injection date and hour	Days since injection	PMCP (ppb)	PDCH (ppb)	1POH (ppm)	2POH (ppm)
7/21/2009 13:00	0.00				
7/21/2009 15:20	0.10	nd	nd	nd	nd
7/22/2009 7:40	0.78	nd	nd	nd	nd
7/28/2009 13:55	7.04	nd	nd	nd	nd
8/5/2009 13:00	15.00	nd	nd	nd	nd
8/12/2009 11:00	21.92	nd	nd	nd	nd
8/19/2009 10:50	28.91	nd	0.31	0.015	0.0065
8/26/2009 11:20	35.93	nd	0.30	nd	nd
9/1/2009 11:00	41.92	nd	nd	nd	nd
9/9/2009 11:05	49.92	0.68	nd	0.22	0.016
9/15/2009 12:30	55.98	nd	0.16	40.59	10.07
9/29/2009 10:50	69.91	nd	2.59	nd	0.058
10/14/2009 11:30	84.94	0.23	0.16	nd	0.030
10/27/2009 11:30	97.94	0.022	0.34	nd	nd
12/10/2009 12:15	141.97	0.0061	0.42	nd	nd
1/12/2010 12:00	174.96	nd	0.24	nd	nd
2/11/2010 11:40	204.94	nd	0.12	nd	nd

Conclusions

The naphthalene sulfonate 1,3,5-nts aided in characterizing flow patterns between the injector and producers in a water flood at the Aneth petroleum field. In the CO_2 flood, both the perfluorohydrocarbons (PFT's) and propanol performed well in tracing the flow of injected CO_2. Both show generally a prominent west-to-east flow pattern, though there was some flow in all directions sampled. The propanol was produced in relatively higher concentrations. This could be explained by the stronger partitioning of the PFT's into the oil phase as well as the higher. These

tests indicate that various combinations of the naphthalene sulfonates, PFT's, and alcohols could serve as effective tracers in CO_2-sequestration applications.

Soil CO_2 Flux Monitoring at the Aneth Test Site

As CO_2 is injected into reservoirs for storage, several techniques have been developed to verify that the CO_2 remains within the reservoir into which it was injected. One of these methods monitors the soil CO_2 flux. CO_2 naturally exists in the atmosphere and also rises from the soil through biogenic processes, creating a background CO_2 level. This study examines several time series of these measurements to provide a good understanding background CO_2 levels. In the event that the injected CO_2 finds a path to the surface the CO_2 flux from the reservoir will be distinguishable from the background flux due to the higher flux rates.

Results

Site 1 (Phase I area)

During the initial phase at the Aneth field series of soil CO_2 flux measurements, test nodes were placed around two injection wells and one production well during the summer of 2006. The array of nodes was on the far east line of wells in Section 18, Range 24E, and Township 40S between injection wells H-218 and H-418. The production well H-319 was in the center of the array. A set of data was collected during the summer of 2006 and then again during the summer of 2007 prior to injection, for use as a baseline. After these data sets were collected, four more sets were collected at different times of the year and adjoining days to get a better understanding of the change in flux over various conditions. This grid was laid out so that if any leakage occurred, an increasing gradient pattern would be evident as the test nodes approached the injection wells.

Two test nodes were disturbed by trenching for pipelines and were not available for most of the measurements. During measurements in May 2008 a lightning storm approached, making it dangerous to continue the measurements; researchers were not able to return the next day to finish. Also, in March 2010 the last part of the data could not be collected due to technical difficulties with the batteries and equipment. The test nodes of 25a and 25b were only measured once during March 2010.

Site 2 (Phase II area)

This site is in Section 13, Range (R) 23E, and Township (T) 40S between injection wells B-413 and C-313, which involved a single profile line of closely spaced test nodes (15 m) between two wells. At both well pads the test-node spacing was reduced to about 1 meter. The test nodes were also placed closer together to increase the probability of detecting a leak if one actually developed. The first tests were performed during the summer of 2008 prior to injection; after injection started, four repeated sets of measurements were collected.

Flux measurements were measured during the winter, summer and spring as well as different times of the day to gain a better understanding of the magnitude of the variance for an area. The seasonal variations for the two sites are displayed in Figure 13 and an example of the daily variations is illustrated in Figure 14. The season-to-season variance was about the same as the variance that occurs by measuring at different times of the day. The greatest changes occurred during the July 2006 and August 2007 measurements (Figure 13). The July 2006 measurements are particularly low because of the high temperatures in Aneth during that season. Many of the negative readings are within the noise of the analyzer and should be treated as being effectively no flux measurements. In August 2007 the measurements were made shortly after a large rainstorm. These measurements are sensitive to the moisture in the ground because of the increased biological activity in the soil.

In February 2009 two different sets of measurements were made on two successive days with the testing starting at different times (Figure 14). During the morning of February 25 the overall flux was low and had an increasing trend as the day heated up. On the 24th the testing had begun at about the same time the testing ended on the 25th ; each day's respective flux trends were relatively close. Then as the day progressed on the 24th , the flux had gradually decreased, indicating a cyclical pattern. From the trends indicated in the chart it is reasonable to conclude that the flux can be expected to vary by as much as about 0.5 $\frac{\mu mol}{m^2 s}$ each day, which is greater than the average standard deviation for this field.

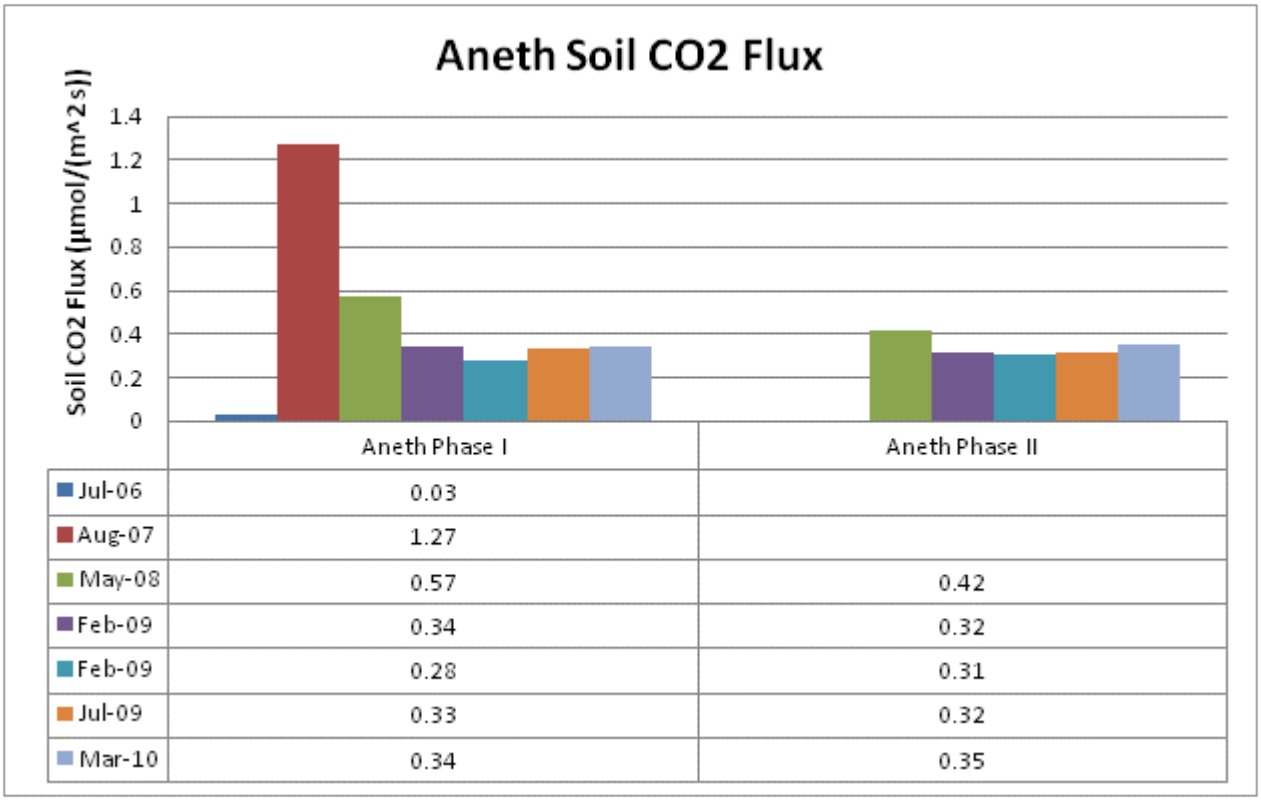

	Aneth											
Location	Phase 1							Phase II				
Date	Jul-06	Aug-07	May-08	Feb-09	Feb-09	Jul-09	Mar-10	May-08	Feb-09	Feb-09	Jul-09	Mar-10
Number	59	47	26	50	50	50	35	37	35	36	36	38
Mean	0.03	1.27	0.57	0.34	0.28	0.33	0.34	0.42	0.32	0.31	0.32	0.35
Max	0.51	4.74	2.41	0.98	1.14	1.05	3.38	1.23	0.76	1.41	3.51	0.59
Min	-0.26	0.11	-0.05	-0.08	-0.14	-0.58	-1.78	0.01	0.11	0.03	-0.22	0.07
StdDev	0.17	0.88	0.45	0.21	0.21	0.34	0.73	0.25	0.14	0.22	0.59	0.14

Figure 13. Summary of mean soil flux data for each acquisition campaign at the Phase I and Phase II sites. Units are µmol/(m^2 s).

Conclusions

Measuring the soil CO_2 flux before and during injection has been successful in establishing a solid background level that can be expected during different seasons and at different times of the day. The average flux for both fields in Aneth was $0.39\frac{\mu mol}{m^2 s}$, which is reasonable for an arid location. For this study it was decided that if a flux consistently remained higher than about two to three times the average value, it should receive additional attention. Several test nodes occasionally tested higher in this range, but after the conditions of the individual test nodes were reviewed, it was found that they had higher concentrations of vegetation.

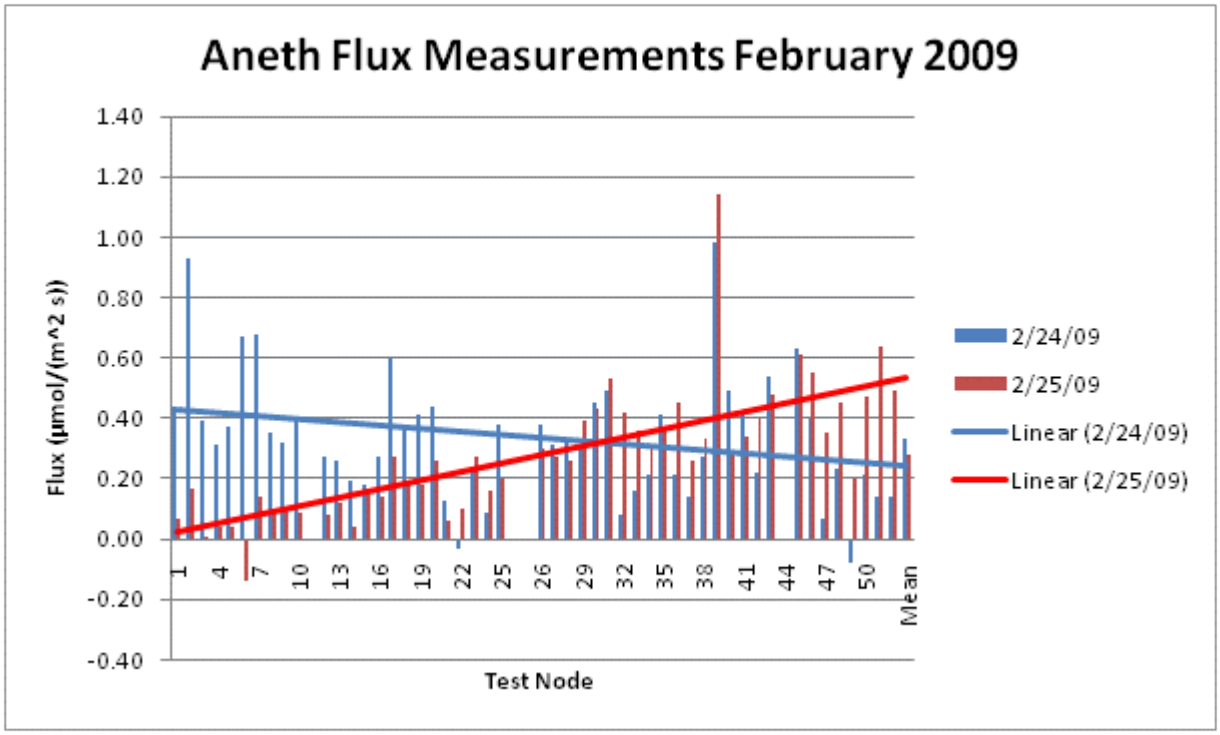

Figure 14. Trends in flux measurements sequenced (left to right). The series of measurements were repeated for two consecutive measurement days.

Self-Potential Monitoring at the Aneth Test Site

Continuous and/or repeat self-potential (SP) measurements were identified as a promising geophysical technique to monitor pressure changes in an aquifer due to CO_2 injection (Ishido et al., 2006). Ishido et al. (2008) carried out numerical simulations of an aquifer system underlying a portion of Tokyo Bay and calculated the temporal changes in geophysical observables caused by changing underground conditions as computed by the reservoir simulation. The STAR general-purpose reservoir simulator (Pritchett, 1995) was used with the CO2SQS equation-of-state package, which treats three fluid phases (liquid- and gaseous-phase CO_2 and an aqueous liquid phase) to calculate the evolution of reservoir conditions, and then used various "geophysical postprocessors" to calculate the resulting temporal changes in the earth-surface distributions of microgravity, apparent resistivity (from either DC or MT surveys), seismic observables and electrical self-potential (SP).

The applicability of any particular method is likely to be highly site-specific. SP measurements can be taken over relatively wide areas, such as monitoring the horizontal extent of a CO_2 plume,

and local SP monitoring is thought to be worthwhile such as monitoring around a deep injector well. SP anomalies of negative polarity are frequently observed near deep wells. These anomalies appear to be caused by an underground electrochemical mechanism similar to a galvanic cell, the so called "geobattery" (e.g. Begalke and Grabner, 1997): the metallic well casing acts as a vertical electronic conductor connecting regions of differing redox potential. Electrons flow upward though the casing from a deeper reducing environment to a shallower oxidizing environment, and simultaneously a compensating vertical flow of ions is induced in the surrounding formation to maintain charge neutrality. If the redox potential in the deeper region is then increased by injecting an oxidizing substance, the difference in redox potential between the shallower and deeper regions will be reduced, resulting in an SP increase near the wellhead.

AIST researchers monitored earth-surface SP during gas injection tests at a few sites in Japan. SP changes were observed at the Yubari test site in Japan, where one well injected CO_2 into a coalbed and the CO_2 content of the fluid produced from a nearby well was monitored (Tosha et al., 2008). SP increased substantially around the injection wellhead, which was believed to be caused by local pH reduction at depth resulting from dissolution of the injected CO_2 in the aquifer fluid. But no significant SP changes attributable to the injection were observed near the production wellhead. This is consistent with the observation that CO_2 did not break through into the production well during the experiment. AIST researchers believe that SP measurements at the earth surface represent a new and promising technique for sensing the approach of CO_2 to well casings deep within the subsurface.

SP Monitoring Network at Aneth

AIST researchers conducted a SP monitoring test in section 13 of T40S., R24E., SLBL&M (Salt Lake Baseline and Meridian) (Fig. 15), focusing on the horizontal injector well C313. Injector C313 was also the focus of the time-lapse VSP monitoring. Considering the depth (~2 km) of CO_2 injection into well C313, a network of electrodes over sufficiently wide area would have been required if they wanted to observe SP changes induced by CO_2 injection through electrokinetic coupling. However, owing to a limit of measurement instruments available for this project, the monitoring network was designed to focus on SP changes expected to appear near a wellhead through the geobattery mechanism.

Sixteen Ag-AgCl non-polarizing electrodes (the drift rate of which has been confirmed very low by more than three years continuous measurements at various fields in Japan) were installed at eight locations shown in Figure 15. At each of four locations near wells C313, C313SE and C413, three electrodes were installed with different distance from the wellhead (see Figure 16); the "near", "middle" and "far" electrodes, denoted with 'n', 'm' and 'f' respectively added to the end of well name, were installed at 2 to 4, 6 to 8 and 14 to 20 meters, respectively from the wellhead. Such an arrangement is suitable to detect change in SP radial profile around the wellhead caused by the geobattery mechanism. Although well C124 had been abandoned and located out of CO_2 injection/oil production area, three electrodes were also installed around its old wellhead location as the above well sites to use one of those electrodes as reference and confirm these electrodes' drift. In addition to these twelve (three times four) electrodes, one electrode was installed at each of four locations, which are more than fifty meters away from any of the wells (Figure 15).

Conclusions

Continuous SP measurements were carried out for more than two years at the Aneth test site (Fig. 17). A local negative SP anomaly was present around wells C313 and C313SE, which is thought to be caused by the geobattery mechanism. Around the C313 CO_2 injection well, a substantial positive change took place during two months starting in May 2008. This change is probably caused by change in the redox potential in the deeper region by pH reduction resulting from dissolution of the injected CO_2 in the reservoir fluid.

At Aneth the SP monitors were installed to detect the arrival of CO_2 plume to the C413 production well or to the C313SE observation well. However, in case of the production well, there was no good quality data due to the presence of severe noise. The SP monitoring technique focusing on the geobattery mechanism is still under development. Further field experiments at CO_2 injection sites are required to improve this unique and supplemental technique for CO_2 geological storage monitoring.

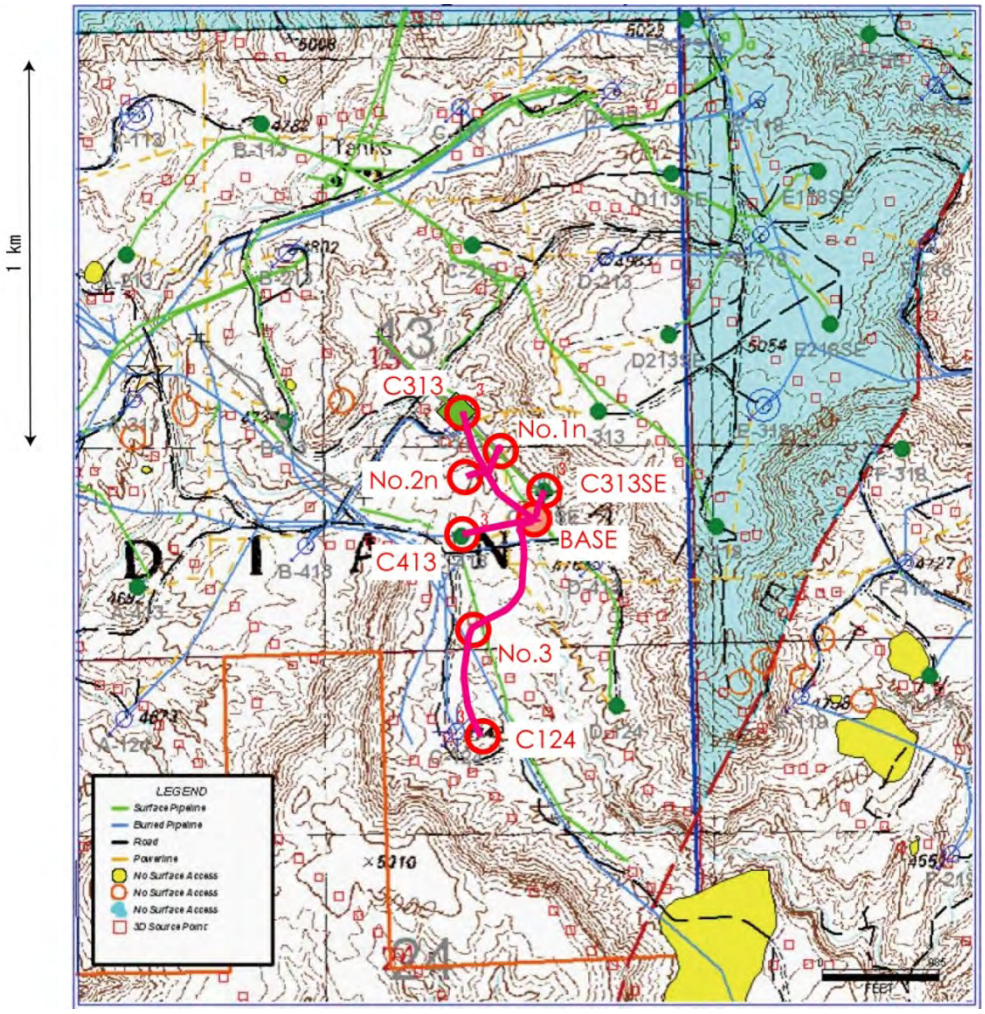

Figure 15. Layout of self-potential monitoring network at the Aneth test site. Three electrodes are installed at each of four locations near the C313, C413, C313SE and C124 wells. A single electrode is installed at each of four locations: "No.1n", "No.2n", "No.3" and "BASE" (where a data logger, solar panel, etc. are also installed).

Figure 16. Photo showing three white-color caps of one-meter holes for electrodes "C313SEn", "C313SEm" and "C313SEf" installed near the C313SE wellhead. An Ag-AgCl electrode itself is set on the bottom of the each hole.

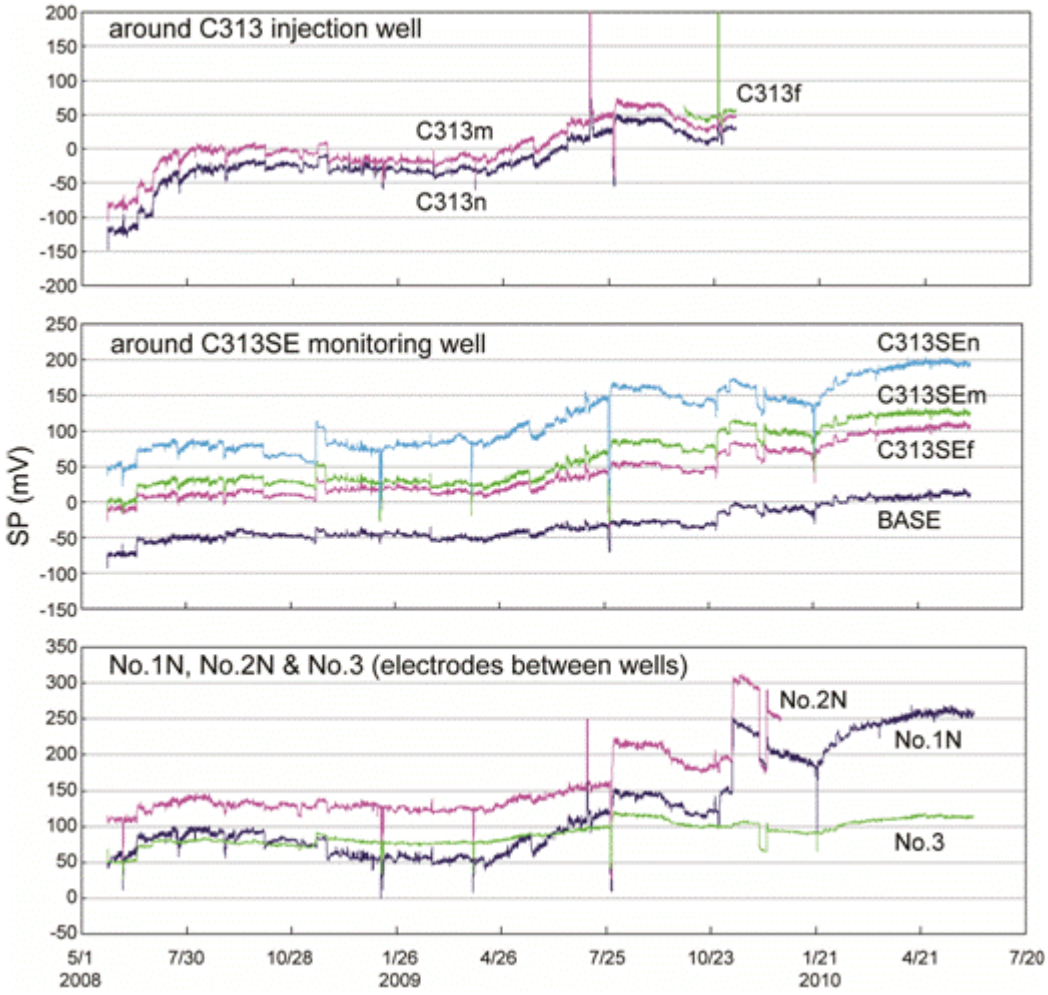

Figure 17. Observed self-potential as a function of time from May 2008 to May 2010 for (top) three electrodes near the C313 injection well, (middle) one electrode at "BASE" and three electrodes near the C313SE well and (bottom) one electrode at each of "No.1n", "No.2n" and "No.3". SP values are relative to electrode "C124m". Time scale division is 90 days and vertical axis range is 400 mV in all plots. Abrupt changes such as those observed in the late July and early December 2009 are correlated with the large changes at "C413m" and "C413f"

Time-Lapse Offset VSP Monitoring of Injected CO_2

Remotely tracking the movement of injected CO_2 within a geological formation is critically important for ensuring safe and long-term geologic carbon sequestration. To study the capability of vertical seismic profiling (VSP) for remote monitoring of CO_2 injection, a geophone string with 60 levels and 96 channels was cemented into a monitoring well C-313SE (in S 13, R 23E, and T 40S, see Fig. 4).

The geophones were placed at depths from 805 m to 1704 m; the oil reservoir is located from approximately 1731 m to 1786 m in depth. A baseline VSP dataset with one zero-offset and seven offset source locations was acquired in October 2007 before CO_2 injection. The offsets/source locations are approximately 1 km away from the monitoring well with buried geophone string. Two time-lapse VSP datasets with the "same" source locations were collected in July, 2008 after five months of CO_2/water injection into a horizontal well adjacent to the monitoring well, and in January, 2009, respectively. The time-lapse VSP data are pre-processed to balance the phase and amplitude of seismic events above the oil reservoir. Because of some uncertainties in the offset VSP source locations, during repeat VSP surveys, researchers used travel times of down going waves and double-difference tomography to invert for the "true" VSP source locations. Wave-equation migration imaging using the pre-processed and balanced time-lapse VSP data and the "true" VSP source locations were conducted. The results shows changes in time-lapse migration images along different offsets are different, indicating CO_2 migration from the injection wells. The repeatability of VSP surveys is essential to make time-lapse offset VSP as an effective tool for monitoring CO_2 injection.

Time-Lapse Offset VSP Surveys

Time-lapse offset VSP monitoring used the same geophone string for microseismic monitoring. The geophone string with 60 levels and 96 channels was cemented into a monitoring well C313SE (Figure 15). Figure 18 is a picture taken when the geophone was cemented into the monitoring well in October, 2007. The geophones are placed at depths from 805 m to 1704 m, and the oil reservoir is located approximately from 1731 m to 1786 m in depth. Figure 19 shows the locations of the monitoring well, injection well, zero-offset VSP source location 1 and offset VSP source locations 2-8. A baseline VSP dataset with one zero-offset and seven offset source

locations was acquired in October, 2007 before CO_2 injection. The offsets/source locations are approximately 1 km away from the monitoring well with buried geophone string. Two time-lapse VSP datasets with the "same" source locations were collected in July, 2008 after five months of CO_2/water injection into a horizontal well (Figure 20) adjacent to the monitoring well, and in January, 2009, respectively.

A number of techniques were required to obtain results from the repeat VSP:

1. These included balancing the time-lapse VSP data because of differences in amplitudes. Thus during data processing the amplitudes of the downgoing and upgoing waves from the different surveys required adjustments.
2. There were differences in the repeat source location from less than one to as many as 25 meters. The adjustments for these were necessary.

Conclusions

The double-difference tomography accurately determined source offsets of time-lapse offset VSP surveys. The double-difference tomography method was successfully applied to time-lapse offset VSP data acquired at the Aneth oil field in Utah for motoring CO_2 injection. The double-difference tomography gives both source offsets of time-lapse offset VSP surveys and velocity profiles between a VSP source offset and the monitoring well. The double-difference tomography results of the time-lapse offset VSP data acquired from the Aneth oil field for monitoring CO_2 injection show that the source locations for different surveys are separated from a few meters to several tens of meters. Accounting for these source location variations during time-lapse offset VSP data analysis can improve reliability of time-lapse offset VSP monitoring.

The spectral analysis method was shown to effectively balance the time-lapse offset VSP datasets. After data balancing, amplitudes of the Aneth time-lapse offset VSP data become comparable to one another. Researchers have performed wave-equation migration of all upgoing waves from Offset 2 to Offset 8 using balanced data and the VSP source locations obtained from double-difference tomography. The time-lapse image differences among different surveys clearly show reservoir changes due to CO_2 injection. Significant changes in migration images are observed along VSP source Offset 2 and Offset 4 from 2007 to 2008, and along Offset 3 and Offset 6 from 2008 to 2009, see Fig. 21. The change along Offset 2 may due to oil production. The other changes are consistent with anticipated reservoir changes due to CO_2 injection.

Figure 18. A picture taken when the monitoring geophone string was cemented into well C313SE in October, 2007 for microseismic and time-lapse offset VSP monitoring.

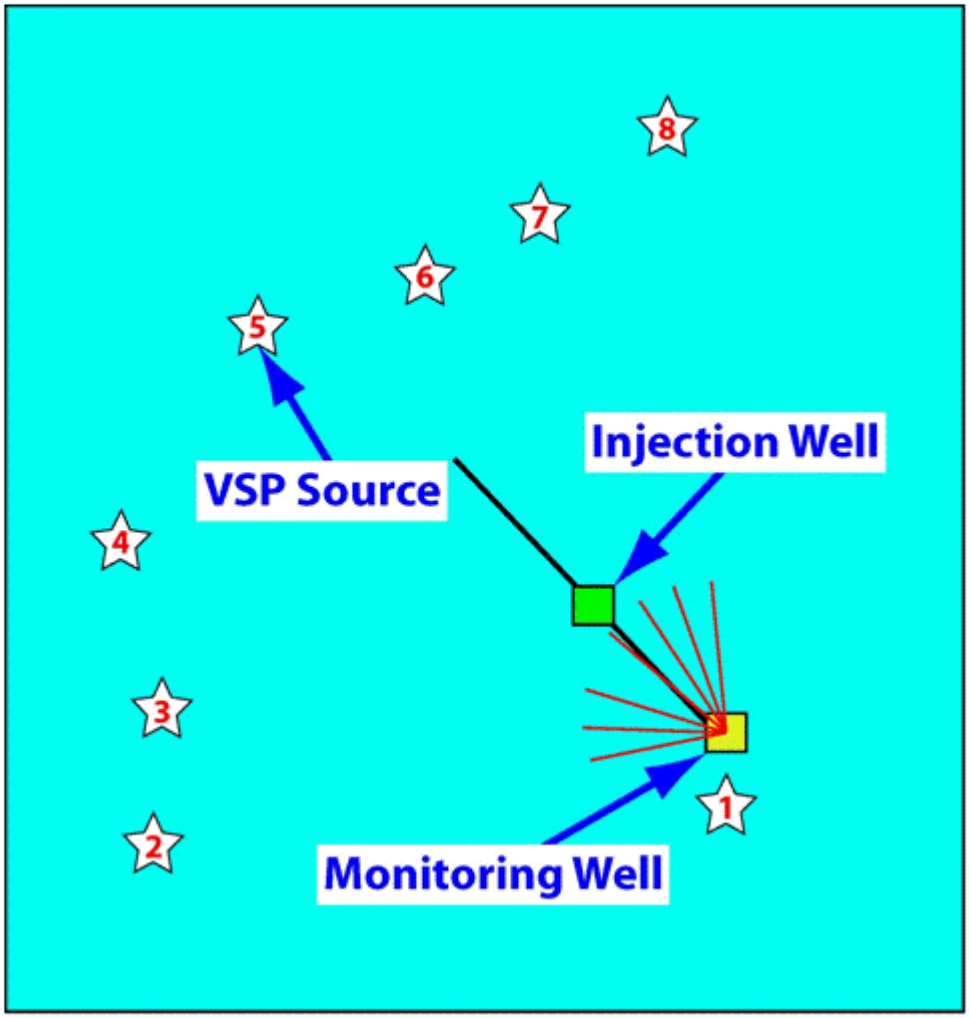

Figure 19. Illustration of the locations of the monitoring well, injection well, the zero-offset VSP source location 1 at well C-313SE about 300 m from the injection well C-313. The offset VSP source locations 2 through 8 are each about 1 km from the monitoring well.

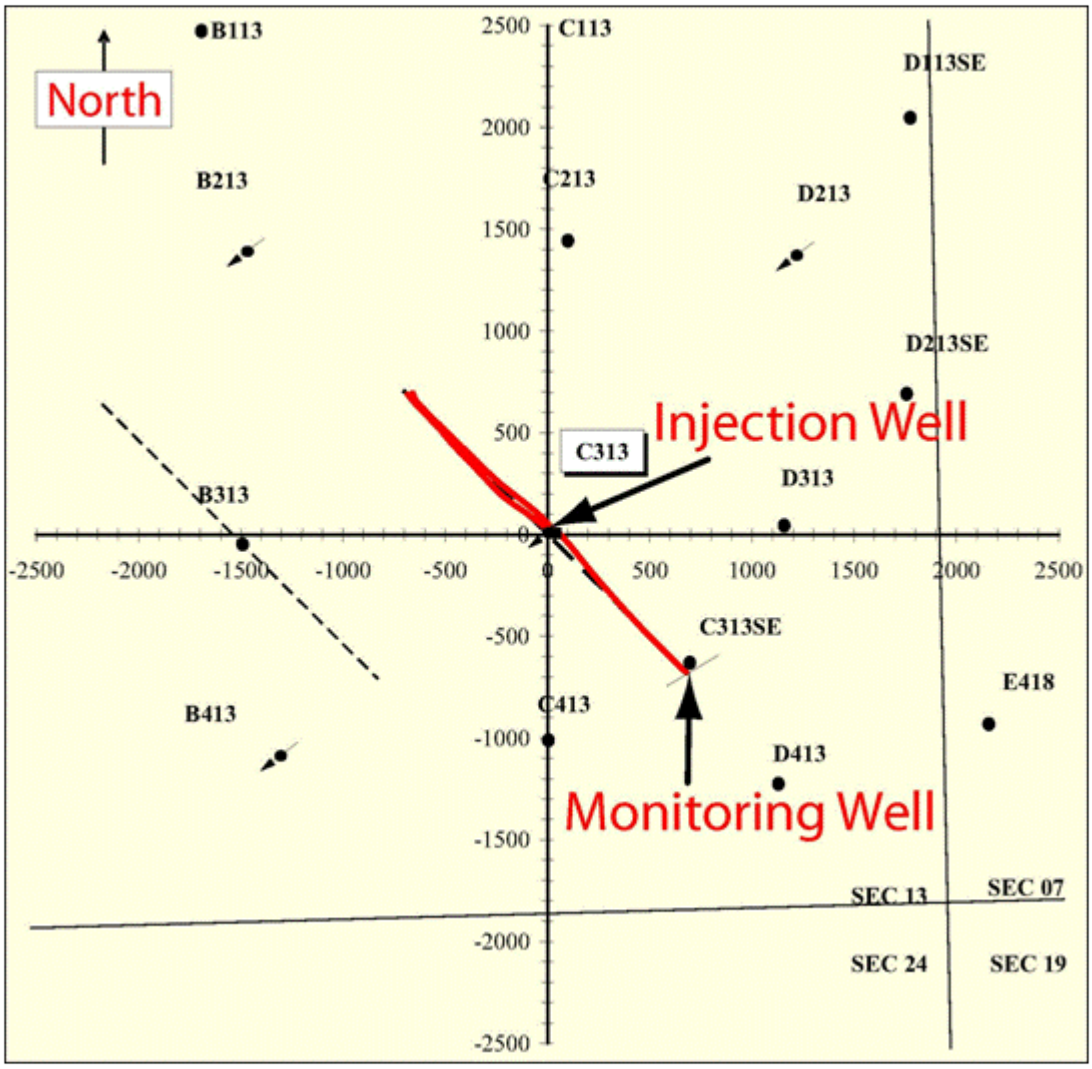

Figure 20. CO_2 was injected into the reservoir through three horizontal laterals within well C313.

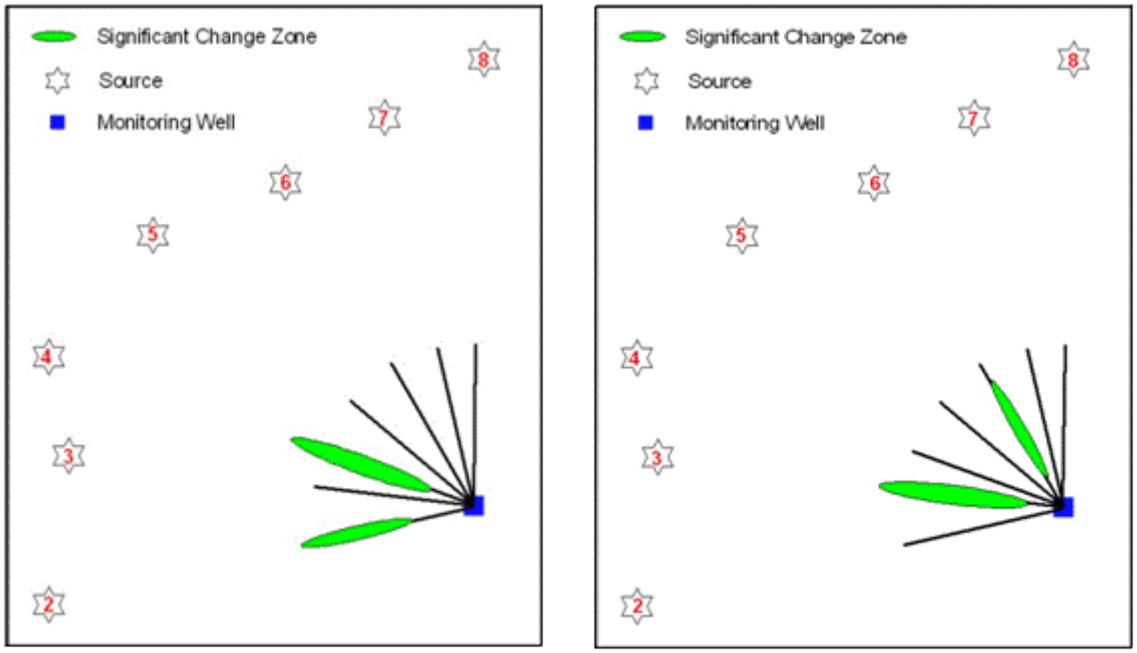

2007-2008 *2008-2009*

Figure 21. Illustration of the profiles along different offset VSP source locations with significant changes in migration images within the reservoir from 2007 to 2008 and from 2008 to 2009.

Passive Seismic Monitoring

Microseismic monitoring should be a useful tool in CO_2 sequestration projects for mapping pressure fronts, detecting and locating fault activation, and identifying potential leakage paths. Slip is likely to be induced on preexisting fractures or faults during CO_2 injection as increased pore pressure reduces the effective normal stresses across such surfaces. Stress changes accompanying larger-scale volume changes can also promote failure within or outside the target storage formations. Deployment of local seismic arrays should be required as part of the site evaluation efforts preceding CO_2 injection and storage projects in order to characterize natural seismicity rates and magnitudes and for assessing the risk of inducing small detectable earthquakes. Evaluating seismic risk should also include measuring stress magnitude and orientations and identifying potentially affected faults via surface mapping and seismic imaging. Once injection operations start, monitoring and characterizing seismicity will be needed to understand the relationship of seismicity to injection and production operations, to evaluate the effect of pressure and stress changes on pre-existing structures, and, if required, to provide some feedback on efforts to mitigate felt seismicity such as changing rates and patterns of injection. On a smaller scale, monitoring microseismicity can be a useful reservoir management tool for delineating fracture flow directions and fracture orientations, and for characterizing the reservoir deformation induced as critical failure.

To monitor microseismicity during the CO_2 injection demonstration at the Aneth field, a 60-level, 2950-ft-length (900 m) geophone array was cemented into a monitoring well with the deepest sonde placed about 90 ft (27 m) above the top of the oil reservoir. During the first year of monitoring approximately 3800 microseismic events with moment magnitude ranging from -1.2 to 0.8 were detected within about 3 miles (4.8 km) of the geophone array. The events delineate two distinct structures active on opposite flanks of the Aneth Unit. Over 96% of events detected occur along a NW-SE trending fracture zone at least 5000 ft long (1500 m) and located about 1100 ft (335 m) beneath the oil reservoir, at a depth of 6950 ft (2120 m), near the top of the Leadville limestone. The time-space evolution of the seismicity and the seismic recurrence (b-value = 2) suggest the structure is composed of a number of discontinuous fault or fracture segments. Researchers found no clear or consistent correlations of the seismicity and moment release rates with injection and production rates in the study area. The high b-value of 2 suggest

that the seismicity is not natural, tectonic seismicity and the source locations on opposite flanks of the Aneth Unit suggest it may be associated with stress changes driven by reservoir volume reduction over the fields 50-plus-year production history.

The western portion of the Aneth Unit that was converted from water to CO_2 injection in 2007-2008 is shown in Fig. 22. The color contours represent the structure at the top of the Desert Creek oil reservoir. A 60-level geophone cable was cemented into the monitor well. The salt-water disposal (SWD) well was drilled about 1 km north of the monitor well and was completed in the underlying Leadville formation with 4 laterals (well C113-SWDW, displayed red)

Figure 23 shows the P-wave sonic log from the SWD well, smoothed with a 100-ft median window (green in Fig. 23). A 7-layer model was selected based on the smoothed log (red). Also shown are the depth locations of the 24-geophone subset used for microseismic monitoring, and the oil reservoir interval.

Event counts for approximately the 1st year of monitoring are shown in Fig. 24. 3825 events were detected over a 376 day monitoring period. The red curve is the cumulative count. The histogram shows the weekly event count. Monitoring effectively started on March 14, 2008 (day 74) after noise associated with poor grounding was removed. Events were detected right away. Monitoring was continuous except for the data gaps marked by the black arrows. The seismicity was intermittent from March 14 to June 6, 2008 (days 74 to 158), after which rates increase and remained at levels averaging about 10 to 20 events per day.

Figure 25 shows areal and vertical microseismic locations occurring over a one-year period. Approximately 1400 events were located (Fig. 25). Reflected and refracted phases were used to help constrain the depths of master event locations. The south group is constrained to the top of the Leadville and Molas formations. The more distant northeast group occurs near the base of the Desert Creek reservoir.

Figure 26 shows the location of the Bluff June 6, 2008 M3.7 earthquake epicenter in relationship to the Aneth test area. Source depth is estimated at 9.5 km. Inset show 8 seconds of vertical

component waveforms from selected geophones of the borehole array. The shake intensity was computed by the University of Utah, but reflects surface geology where areas of greater intensity (hot colors) are areas of basin fill. All production within the yellow curve is co-mingled into a single tank battery. Also shown in Fig. 26 are bi-weekly event count (histogram) and oil production (black, from the area encircled in yellow in the area map in Figure 26). Red dots show the cumulative moment release for the located events shown in Figure 25. The green vertical line marks the occurrence of the Bluff M3.7 earthquake.

The attempts at trying to correlate the seismicity with fluid volume changes are ambiguous and inconclusive. The problems may stem from a monitoring period that is too short, and a production/injection, stress-change history of more than 50 years that preceded this study. Further, correlations in general do not necessarily imply cause-effect relationships and may simply be an indication of processes weakly coupled to some common cause. For example, salt-water-disposal well (SWD) is tied to reservoir production rates, and seismicity and fluid volumes produced will both be affected by pore pressure changes. Interestingly, Ake et al. (2005) found no clear correlation with event occurrence and injection rates in the Paradox Valley study for a continuous 8-year monitoring period except when looking at a small subset of events near the injector. But they were able to correlate event onsets with downhole pressure thresholds.

The high b-values suggest that the seismicity is not natural tectonic seismicity. The source locations on opposite flanks of the Aneth Unit suggest it may be induced by some stress changes associated with the field's 50-plus year history. Segall (1989) and Segall and Fitzgerald (1998) have shown that normal faulting can be promoted on the flanks and outside of a reservoir due to poroelastic contraction of the reservoir. The case studies of induced seismicity that they associate with their model involve pressure depletions of 10s of MPa over decades of sustained production. As a result, small stress changes on the order of 1% of the reservoir pressure drawdown can occur outside of the reservoir where no pore volume changes occur. Such small stress changes could only promote failure on pre-existing, critically stressed structures. Large pressure depletion does not provide a driving mechanism for the Aneth case, where reservoir pressure has been sustained through years of waterflood production, but perhaps some other mechanisms, such as

thermoelastic contraction caused the long-term water injection, could be invoked to explain the seismicity observed.

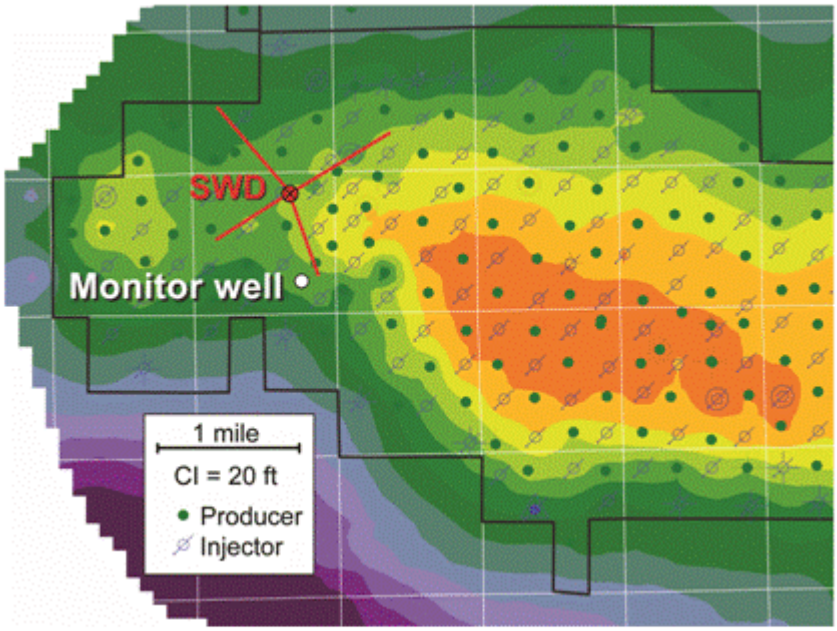

Figure 22. The western portion of the Aneth Unit of the Aneth field that was converted from water to CO_2 injection in 2007-2008.

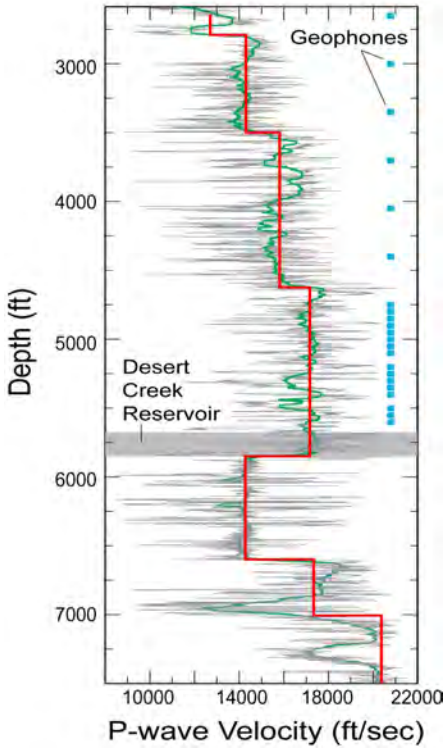

Figure 23. P-wave sonic log from the SWD well (Figure 21).

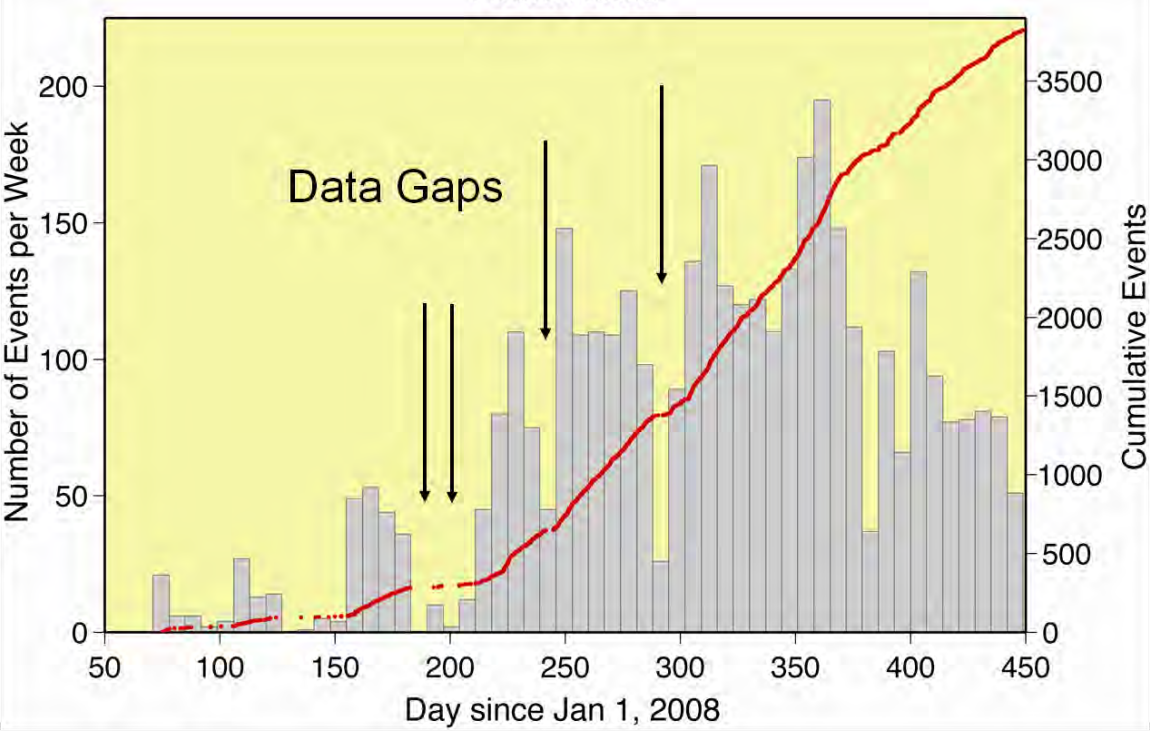

Figure 24. Event count for the first year of monitoring.

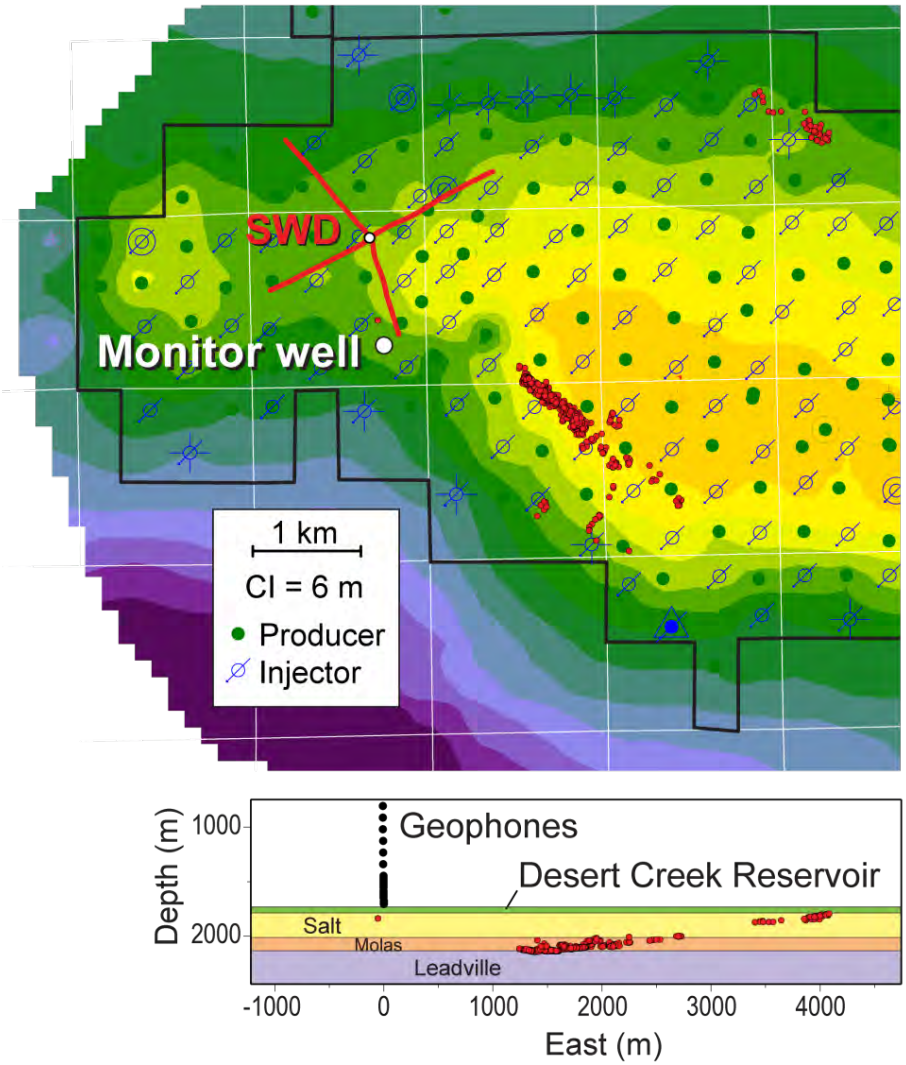

Figure 25. Microseismic locations occurring over a one-year period.

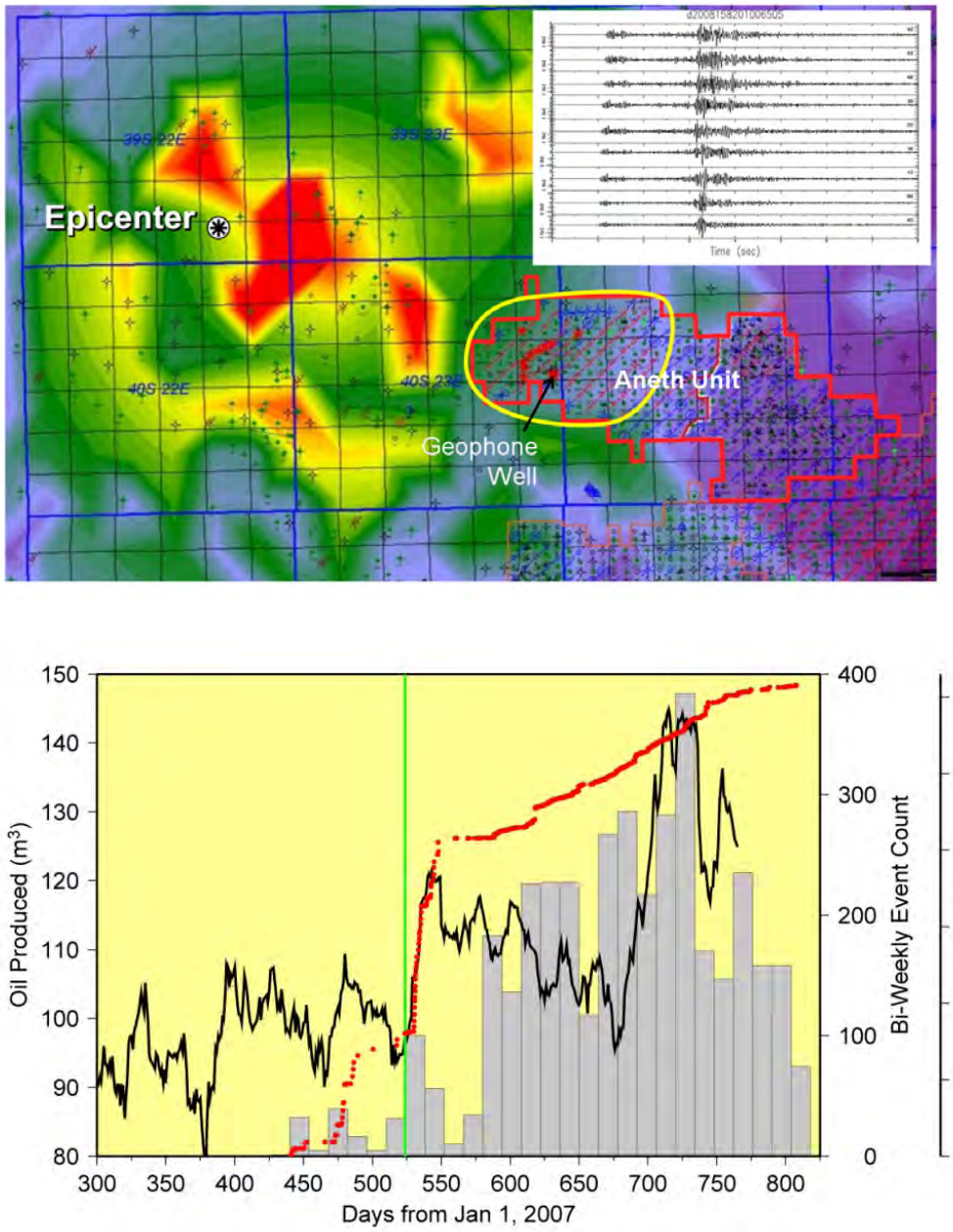

Figure 26. <u>Top:</u> Bluff June 6, 2008 M3.7 earthquake epicenter. <u>Bottom</u>: Bi-weekly event count (histogram) and oil production (black, from the area encircled in yellow in the area map).

Geologic Model Development and Numerical Simulation

SWP researchers developed a geological model of the Aneth field and conducted numerical simulations to demonstrate efficacy of CO_2 sequestration technologies within producing oil reservoirs. The focus was on developing a site-specific geologic model to better understand and design CO_2 storage specifically tailored to oil reservoirs. The research was primarily focused on gathering and using data specific to the Aneth site, but it is anticipated that the results of the Aneth research will be useful in a variety of CO_2 EOR projects and oil fields elsewhere. Geologic sequestration of CO_2 in the Aneth field includes continued injection of up to 150,000 tons/year CO_2 for several years into the future. The major tasks developed and performed in this work include:

- **Data Acquisition**
  - *Digitizing well logs*
- **Petrophysical Properties Estimation**
  - *Estimation of porosity*
  - *Porosity and permeability relationship*
- **Geologic Model Development**
- **Numerical Simulation**

Available stratigraphic, petrophysical, and geophysical information from the Aneth site were collected and compiled from our partners. Acquired well logs were digitized and integrated into the model development, and petrophysical data was reviewed for estimating essential properties such as porosity and permeability. Based on the compiled geologic information/data, a site-specific static geologic model was constructed. Petrophysical properties (porosity and permeability) were populated into the static model using the porosity logs and correlation found from the petrophysical properties. The constructed static model served as an input to the subsequent numerical simulations.

Numerical simulations were conducted on a conceptual model built on geological data from Section 13 and 14 of the Aneth field in southeastern Utah. Investigations on injectivity were conducted on the geological model originally built on the porosity-permeability correlation indicated that the 1MMt/yr injection rate cannot be achieved. Based on that model, the maximal injectivity

is 0.25 MMt/yr. Then the sensitivity of injectivity on the uncertainty of permeability was investigated in several modified geological models by artificially increasing the permeability. The maximal pressure among 14 wells with the injection rate of 1 MMt/yr was evaluated. Moreover, the minimal number of wells for 1 MMt/yr injection was estimated for one geological model.

The effects of hysteresis and WAG schemes were studied with a series of numerical simulations. According to the simulations on the geological model, it was illustrated that the effects of WAG schemes and hysteresis are weak on dissolution trapping mechanisms, and there is no significant effect of a WAG scheme at least for long term residual trapping in the conceptual model.

Data Acquisition

The location of the Aneth Unit of the Greater Aneth oil field is illustrated in Figure 4. The Utah Geological Survey (UGS) collected an extensive set of geologic data, scanned paper, and digital well log images, and petrophysical data from the project site and provided this data to EGI to develop the basis for the initial data acquisition. The following data were assembled for this project:

- Core plug analyses (porosity, density, and permeability)
- Geophysical well log images
- Stratigraphic formation tops data
- Well information
- Injection/production history

These data were catalogued and processed to form an information database for the geologic model development and numerical simulation (Sections 13 and 14 [T40S R23E], respectively). Data is summarized in the Aneth Topical Report.

A total of 1,084 total well log curves from 456 wells in the Aneth Unit are categorized in Table 2. The digitization effort concentrated on Sections 13 and 14 (T40S R23E), where the Phase II project took place. 471 well log curves from 163 wells were digitized in total. Most of these log suites contain both a gamma ray log and a neutron log for each well.

Table 3. Summary of Well Log Digitizing Work

Log Type	Number of Available Logs	Number of Digitized Logs
Gamma Ray	388	163
Caliper	161	66
Bulk Density	25	10
Neutron	254	129
Neutron Porosity	146	55
Density Porosity	43	13
Delta Rho	11	6
CNC	7	4
Conductivity	6	3
Resistivity	11	4
Spontaneous Potential	8	3
Sonic	5	1
Tension	18	12
Photo-electric	2	2
Sum	1,085	471

The vertical sampling interval in the geophysical logs is usually 0.5 feet, which requires an up-scaling step to reduce the total number of cells to a manageable size. We used an arithmetic averaging method to estimate upscaled values. All sample values within each cell were used for averaging without being weighted.

Petrophysical Properties Estimation

Only a few direct petrophysical measurements are available from the site. Ambient porosity and gas permeability data were gleaned from core plug samples of six wells covering three formations (Ismay, Gothic shale, and Desert Creek) and are summarized in Table 4.

Table 4. Summary of Ambient Porosity and Gas Permeability Measurements from Core Plug Samples

Formation	No. of Samples	Porosity (φ)			Permeability (mD)		
		Mean	Median	Std. Dev.	Mean	Median	Std. Dev.
Ismay	10	0.05	0.02	0.06	0.47	0.04	0.78
Gothic Shale	1	0.009	0.009	0	0.012	0.012	0
Desert Creek	81	0.09	0.1	0.07	5.12	0.31	18.92

Most of the samples are concentrated in the Pennsylvanian Desert Creek formation, which exhibits the highest porosity and permeability. The Gothic shale, presumed to be a cap rock formation, shows the lowest porosity (<1%) and permeability (~0.01 mD). Note that only one sample was available for the Gothic shale. Due to the scarcity of data (6 wells), a major concern was how to define porosity and permeability parameters within the rest of the model domain.

Estimation of Porosity and Permeability

Figures 27 is an example plot where the porosity estimates from porosity logs and measured ambient porosities at wells H-117 (API# 43-037-30153). The blue solid line represents the porosity values estimated by taking averages of the neutron porosity and density porosity logs as:

$$\phi = \sqrt{\frac{\phi_n^2 + \phi_d^2}{2}}$$

where ϕ_n and ϕ_d are neutron and density porosities. Pink diamonds represent the measured porosity value from core plug samples. Although there exists a significant difference in a couple of points, overall porosity estimates from well logs match the measured data, which suggest that the estimation of porosity using well logs is appropriate.

Despite the lack of available petrophysical data at the site, the porosity logs showed general agreement with the measured data from the limited core plug samples. Thus, we used digitized

porosity logs to estimate the porosity values where no petrophysical data were available in the Desert Creek formation.

A cross-plot displays the approximate log-linear relationship between permeability and porosity. Considering the scarcity of samples, especially in the Ismay and Gothic shale formations, application of this relationship can be problematic. Since the log-linear relationship is commonly found in the sedimentary rocks, the correlation found in the Desert Creek formation samples was used for assigning the permeability values where no petrophysical data was available in the target formation.

For the static geologic model development formation tops data in the Aneth field were analyzed. This geologic model was constructed to cover the entire Aneth Unit with extensive formation tops data. The software package used for the stochastic reservoir model is Petrel™, Schlumberger's 3-D integrated reservoir modeling tool. First, a detailed geologic model was established based on the formation top picks from 403 wells. The resulting static structural model within the model boundary is shown in Figure 28. The model domain is approximately 15 km by 8 km in the x and y direction. The constructed model contains 11 formations starting with the Jurassic Entrada formation on top to the Pennsylvanian Desert Creek formation at the bottom (Figure 28).

Geologic Model Development

This study used the grid configuration of 150 x 79 x 53 cells in the x, y and z directions, respectively, with a cell horizontal dimension of 100 m by 100m. Vertical cell size is equally spaced into 53 cells along each vertical grid line based on the thickness of the Desert Creek formation. The active cells were allowed to be present only within the model boundary. The average thickness of the Desert Creek Formation within the whole Aneth Unit model area was found to be approximately 53.4 m. The Gothic shale above the Desert Creek was found to be laterally continuous within the model domain and was assumed to work properly as a caprock in this study. The average thickness of the Gothic shale is found to be approximately 4.52 m.

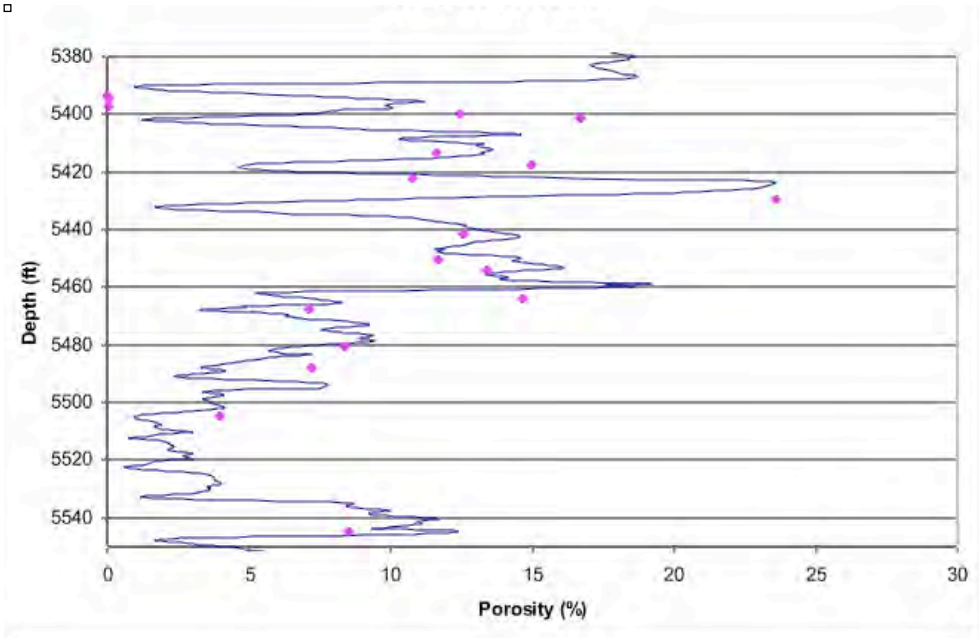

Figure 27. Measured ambient porosity (pink diamond) and porosity estimates (blue solid line) from porosity logs from the H-117 well.

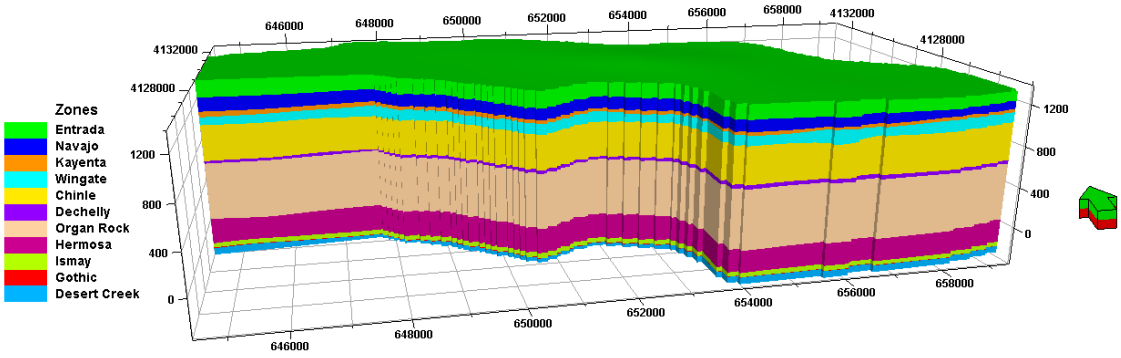

Figure 28. Stratigraphic distribution of geologic formations within the Aneth Unit model boundary.

Having established the 3-D, fine-scale grid model of the geologic formations, the petrophysical properties (porosity and permeability) can be assigned. Assuming the normal distribution in the porosities of each formation, a porosity field was generated using the Sequential Gaussian Simulation (SGS) method to create 3-D equiprobable geological images (Figure 29). Sample variogram from the upscaled neutron porosity logs in the Desert Creek formation were fit to the variogram model with 600 m for the major range, 500 m for the minor range, and 6 m for the vertical rage. Figure 29 shows the simulated porosity fields.

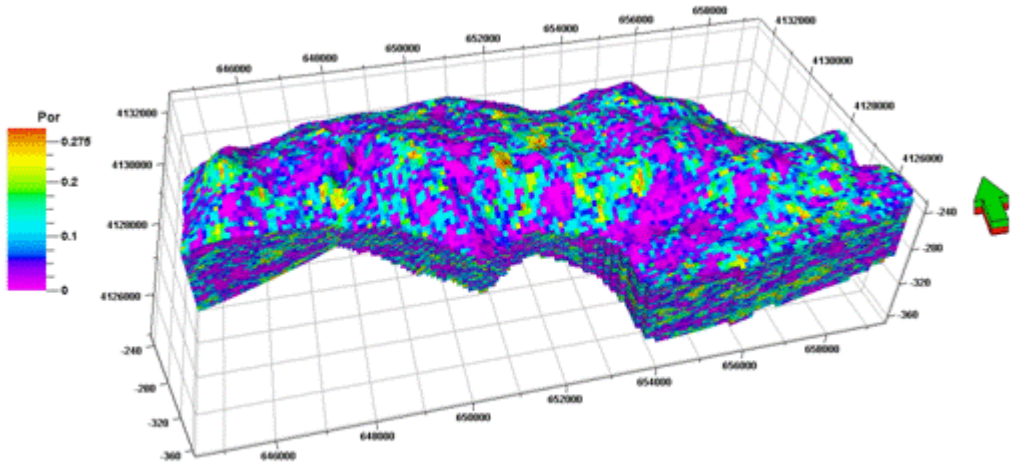

Figure 29. Simulated upscaled porosity fields within the Aneth unit model boundary.

Next, the porosity and permeability relationship ($k = 0.02e^{0.2959\phi}$) was applied from the core plug samples and assigned the permeability values accordingly from the porosity values (see Figures 29 and 30). As a result of this log-linear relationship, the simulated permeabilities exhibit a log-normal distribution. Whereas, the porosity field is normally distributed. Figure 30 illustrates the corresponding permeability field from the porosity field illustrated by Figure 29.

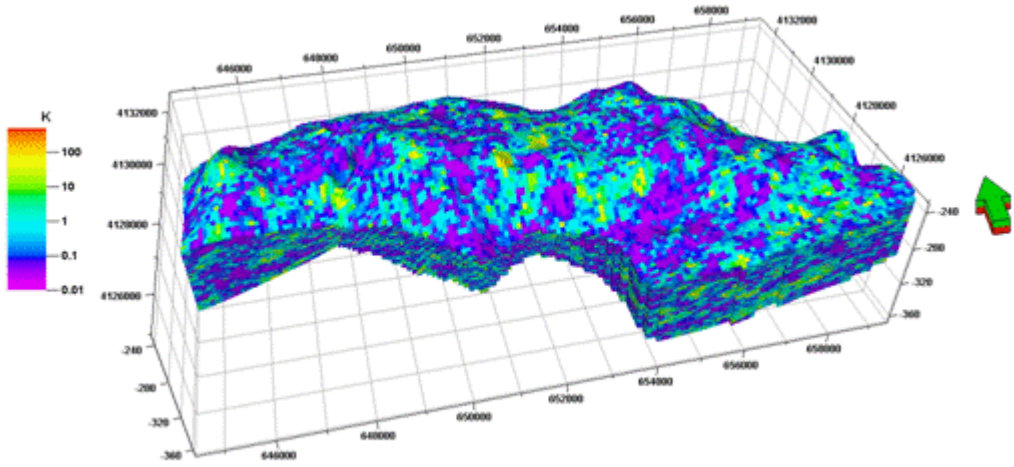

Figure 30. Corresponding permeability (mD) field based on the log-linear relationship between permeability and porosity.

Grid Conversion and Upscaling for PFloTran Simulator

Numerical simulations were performed with PFloTran, a massively parallel subsurface multi-phase, multi-component reactive transport flow simulator based on the PETSc, SAMRAI and MPI packages [Lu and Lichtner, 2006]. PFloTran's capabilities have been adopted to demonstrate the various flow and transport processes in relation to subsurface contaminant and geological CO_2 sequestration [Hammond et al., 2007].

Since PFloTran is restricted to orthogonal grid models ("structured grids"), researchers conducted a grid conversion and remapped the porosity distribution into a new upscaled orthogonal grid by a volume-weighted averaging method to preserve the overall volume between the two grids. Each cell size has been maintained with the same horizontal cell dimension such as 100 m by 100 m in the x and y directions. Vertical grid spacing with the constant Δz value of 2.5 m were used and an additional grid setting with Δz = 7m was created for examining the effect of grid resolution.

Upscaling was accomplished by matching geometry, which involves matching actual z levels. This is typically useful when upscaling from an irregular grid to a regular grid. A simplified method for cell matching was also applied, where all cells with their center inside the upscaled cell were averaged to obtain a property value. The newly-upscaled orthogonal grid maintains the same horizontal cell dimension in the x and y directions. Because of the difference (> 100m) in the structural highest and lowest point of the Desert Creek formation in the Aneth Unit area, the number of layers in the upscaled orthogonal grid (Δz = 2.5 m) did not decrease, totaling 663,600 total cells. Figure 31 illustrates the updated porosity distribution mapped onto the orthogonal grid setting (Δz = 2.5 m) after the volume-weighting method for the PFloTran simulator.

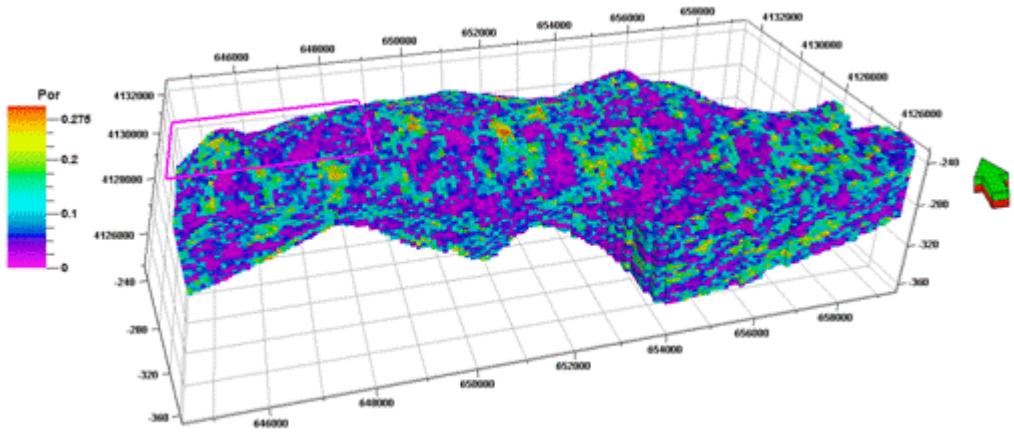

Figure 31. Porosity field after orthogonal grid conversion and upscaling simulator in the Aneth Unit model boundary. Subarea for the numerical simulation work given in the Section 4 is shown with the rectangular boundary.

The constructed static model served as the primary input of subsequent numerical simulations. Since the Phase II project took place in the Sections 13 and 14 (T40S R23E), simulation work focused only on the subarea in/near the Section 13 and 14 shown in Figure 31. Figure 32 illustrates the porosity field in the modeling domain for the numerical simulation on Sections 13 and 14. Each property model consists of 62,608 cells (43 x 26 x 56) for $\Delta z = 2.5$ m.

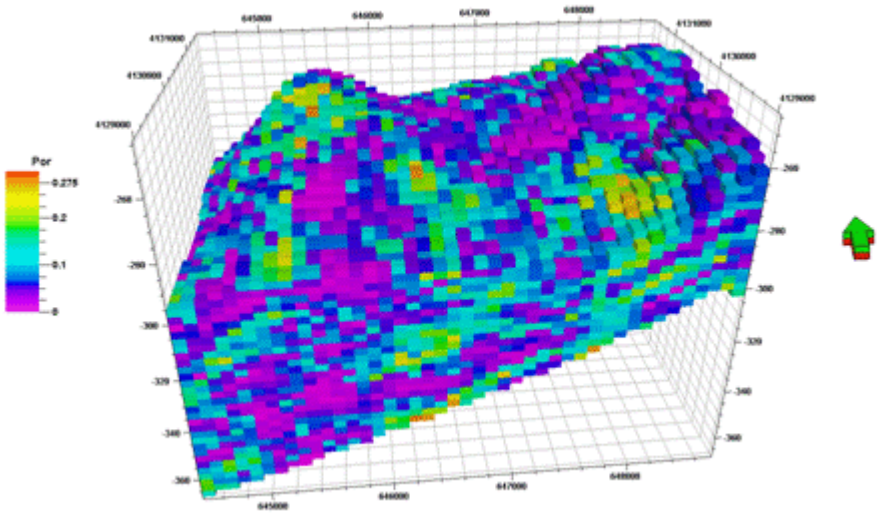

Figure 32. Porosity field prepared for the numerical simulation after orthogonal grid conversion and upscaling in/around the Section 13 & 14 (T40S R23E). Vertical exaggeration is 25 times. $\Delta z = 2.5$ m.

Numerical Simulation

Grid Generation for Numerical Simulation

The computational domain mainly covers Sections 13 and 14, but was extended to include their adjacent regions. Within this domain, only the Desert Creek formation is considered, assuming the Gothic Shale is an effective barrier to prohibit the vertical migration of supercritical CO_2. Two grids with a grid spacing of 100m x 100m x 7m and 100m x 100 m x 2.5 m were generated to test the effects of grid resolution, leading to 43x26x20 (coarse) and 43x26x56 (fine) grids. The porosity profiles represented by these two grids are shown in Figures 33 a) and b), respectively.

The volume averaged porosity and permeability of the coarse and fine grid are listed in Table 5. In order to facilitate numerical simulations, the relative permeability and capillary pressure are arbitrarily assigned as:

$$p_c = \frac{1}{\alpha}\left(s_e^{-1/m} - 1\right)^{1/n} \quad (1)$$

$$k_{rw} = s_e^{1/2}[1-(1-s_e^{1/m})^m]^2 \quad (2)$$

$$k_{rg} = (1-s_e)^{1/2}\left[1-\left(1-s_e^{1/m}\right)^m\right]^2 \quad (3)$$

where the parameters m=0.75, α=0.001. The irreducible water and gas saturation is given as 0.25 and 0.10, respectively.

Since detailed records of bottom hole pressure of the production wells are not available, realistic history matching cannot be accomplished. To facilitate numerical simulations, the model was simplified to a two phase SC CO_2/ brine system and artificially assigned 14 wells in the domain according to the pattern of injection well locations in Section 13 and 14 of the Aneth Field. The initial and boundary conditions are set at hydrostatic conditions with a depth of 1,735m for the formation top. Salinity was assumed to be 1 mol/kg.

Table 5. Volume Averaged Porosity and Permeability

Grid	coarse	Fine
average porosity	0.0820	0.0816
average permeability (mD)	0.7184	1.196

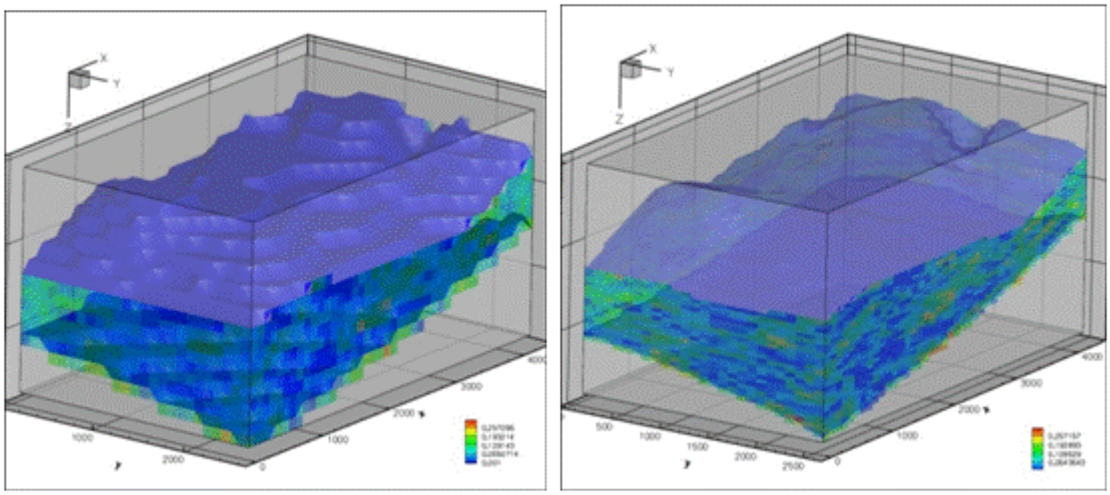

a) coarse *b) fine*

Figure 33. Porosity distribution represented on coarse and fine grid.

Preliminary Simulation Results

According to the injection history, within approximately half a year, the total injection amounts were 907,241and 885,540 mcf (i.e. 5.046E4 and 4.926E4 Tons) in Sections 13 and 14, respectively or a rate of approximately 6.43kg/s. The injections were evenly assigned to 14 wells in the domain. The pressure distributions obtained with coarse and fine grid simulations are similar to each other. The maximum pressures achieved were 33.34 and 34.24 MPa when injection ceased (0.5 years), differing by 2.6%. According to these observations, investigations on pressure distributions were conducted mainly on the coarse grid. Because of low permeability, the CO_2 plume migrated slowly. Figures 34 a) and b) show the saturation profiles calculated on the coarse and fine grid at 100 years. On the fine grid simulation, predicted plume migration in the both vertical and horizontal directions was slightly faster than that with the coarse grid, though the differences were not significant. However, the highest SC phase saturation at 100 years was 0.16 and 0.36, as predicted by simulations on the coarse and fine grids, respectively. Although the maximum saturation differed, the size and shape of SC phase plume are still similar. The simulation results with the coarse grid is acceptable regarding area-of-review and other issues. Simulations for this work were conducted mainly using a coarse grid.

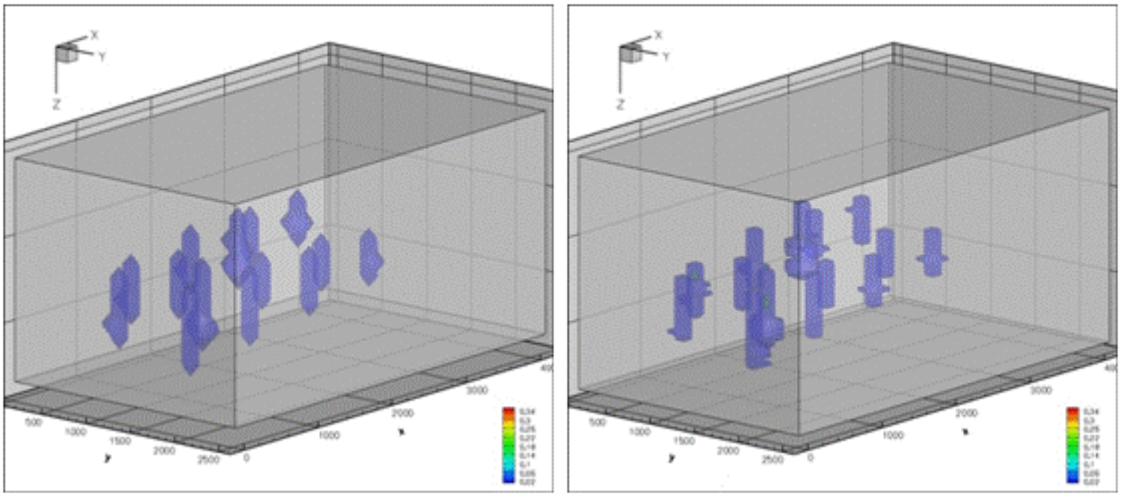

a) coarse ***b) fine***

Figure 34. Saturation profiles at the end of the injection period (100 years).

Optimizations to prevent over-pressuring

Over-pressuring behavior with 1MMt/year: The lithostatic pressure is 44.2 MPa at the depth of the formation top of the Desert Creek (1735m). This was considered the highest allowable pressure. Constrained by this threshold, the attempt to inject 1 MMt of CO_2 within 1 year into Sections 13 and 14 failed even when the injection was distributed among all 14 wells. In the central part of the domain, pressure exceeded the threshold. The iso-surface with the lithostatic pressure envelopes the whole region containing the 14 injection wells, instead of the well vicinities. The highest pressure reached was 118MPa, over double ambient pressure and far exceeding fracture criteria. As a result, the model suggests that it is not advisable to inject 1MMt of CO_2 into Sections 13 and 14 in one year without well stimulation or other advanced reservoir engineering strategies.

From the results, the resulting question is: what is the maximum injection rate if all 14 wells are operational? This issue was addressed with four simulations. The operational conditions of maximum pressure are listed in Table 6.

Table 6. Injection Rate Distributions Among 14 Wells

		Case 1	Case 2	Case 3	Case 4
Injection rate (kg/s)	1	1	0.6	0.6	0.7
	2	1	0.6	0.6	0.6
	3	1	0.6	0.4	0.4
	4	1	0.6	0.4	0.4
	5	1	0.6	0.6	0.6
	6	1	0.6	0.6	0.6
	7	1	0.6	0.6	0.6
	8	1	0.6	0.6	0.6
	9	1	0.6	0.4	0.6
	10	1	0.6	0.6	0.6
	11	1	0.6	0.8	0.8
	12	1	0.6	0.6	0.6
	13	1	0.6	0.8	0.5
	14	1	0.6	0.8	0.6
Total (MMt/yr)		0.4415	0.2649	0.2649	0.2523
Highest pressure (MPa)		62.07	45.77	46.89	40.74

The analysis of maximum sustainable injection rate included several steps:

- The total injection rate was reduced to 0.4415 MMt/year and evenly distributed among the 14 wells. Though the high-pressure zone was much smaller than the 1MMt/year injection rate, it was still continuous and occupied the whole central region of the model.
- The total injection rate was reduced to 0.2649 MMt/year and evenly distributed among the 14 wells. The high-pressure region only exists in the vicinity of 3 wells (Well 3, 4, 9) where the permeability is relatively low. It is possible that over-pressuring can be avoided by re-distributing the injection rate among these 14 wells.
- In order to determine the redistribution scheme, the pressure profile was redrawn as an isosurface at 35 MPa. The larger isosurface dome indicated a higher pressure buildup. The injection rates at Well 3, 4, 9 should be decreased (by 33% in Case 3). Wells 1, 2, 5, 7, and 8 are adjacent to the over-pressured wells, so the injection rate is not changed in Case 3. Instead, the injection rates at Wells 11, 13, and 14 were increased by 33%. As a result, the over-pressurization at Wells 3, 4, and 9 was reduced. However, over-pressuring occurred at Well 11.

- In Case 4, the injection rates at Wells 13 and 14 were reduced to 0.5 kg/s, 0.6 kg/s, while the injection rate at Well 1 was increased to 0.7 kg/s in order to increase the distance between the wells with high injection rates. The highest pressure at year 1 decreased to 40.74 MPa. The total injection rate was 0.2523 MMt/yr. According to these analyses, the suggested total injection rate should not exceed 0.25 MMt/yr, which is about double the injection rate applied in the Aneth Field. Because of the low permeability and relatively small amount of total CO_2 injected, the SC plume did not reach the top of the formation at year 100.

Optimizations on WAG Scheme to Enhance Residual Trapping

It was reported that a WAG injection scheme in CO_2 sequestration processes can enhance the residual trapping mechanism by the hysteresis effect. In order to investigate this aspect, hysteric relative permeability has to be applied. In this work, hysteresis in relative permeability is represented with Land's formulation [Land, 1968], in which the trapped gas saturation is a function of the minimum wetting phase saturation (Sw_{min}) reached in a grid block prior to a increment in aqueous saturation. This model was adopted and further modified by [Kaluarachchi and Parker, 1992].

Four WAG schemes were investigated by simulation, as listed in Table 7. Case 0—3 are set with the injection period in year 1; the total injection amount of CO_2 is 1 MMt and varies with water. The shut-in and timetable of CO_2 and water injection of Case 2—4 is the same, though the water injection rates are different. Case 1 is set as a reference example with hysteric capillary pressure and relative permeability. The simulation case with non-hysteric capillary pressure and relative permeability is referred to as Case 0. Case 5 is set up to test the effect of shut-in and restart frequency. Though the saturation profiles are different, they are quite similar to each other, implying similar behavior of SC plumes.

Within the simulation period, the permeability, residual and solubility trapping mechanism are more important than the mineralization trapping mechanism. Permeability trapping is determined by the formation properties and should have same effect on Case 0-5. The dissolved CO_2 is gathered around the free phase plume; the diffusivity is relatively weak, partly because of the low

porosity, permeability and short simulation period. At 100 years, about 60% of total injected CO_2 remains in the free phase, either being trapped or remaining in the mobile phase, as shown in Figure 35.

The effects of hysteresis and a WAG scheme on the dissolution trapping mechanism are notable in the early stage only, as shown in Figure 36. Generally, the dissolution trapping mechanism is weak in the non-hysteric case because of the relatively low wetting phase relative permeability. The free CO_2 amount in Case 0 is the highest among the six cases investigated. In cases with water injection, the free CO_2 amount decreases once fresh water is injected because of the dilution effect. In all six cases, the total dissolved CO_2 amounts are similar at the end of the simulation period.

Table 7. WAG Schemes Investigated

Case	1		2		3		4	
Month	W	G	W	G	W	G	W	G
1	-	1.1325	0.0	1.69845	0.0	1.69845	0.0	1.69845
2	-	1.1325	0.0	1.69845	0.0	1.69845	0.0	1.69845
3	-	1.1325	0.0	1.69845	0.0	1.69845	0.0	1.69845
4	-	1.1325	0.0	1.69845	0.0	1.69845	0.0	1.69845
5	-	1.1325	0.0	0.0	0.25	0.0	0.5	0.0
6	-	1.1325	0.0	0.0	0.25	0.0	0.5	0.0
7	-	1.1325	0.0	0.0	0.25	0.0	0.5	0.0
8	-	1.1325	0.0	0.0	0.25	0.0	0.5	0.0
9	-	1.1325	0.0	1.69845	0.0	1.69845	0.0	1.69845
10	-	1.1325	0.0	1.69845	0.0	1.69845	0.0	1.69845
11	-	1.1325	0.0	1.69845	0.0	1.69845	0.0	1.69845
12	-	1.1325	0.0	1.69845	0.0	1.69845	0.0	1.69845
Total	-	1	0	1		1		1

(W: water injection rate [kg/s], G: CO_2 injection rate [kg/s], unit of total total injection rate is MMt/yr).

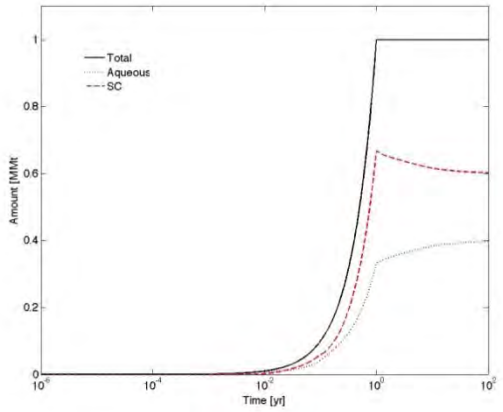

Figure 35. CO_2 phase distribution during simulation period in Case 1.

The residual trapped CO_2 amount of the non-hysteric Case 0 is stronger than the other five hysteric cases within the injection period because of the non-zero irreducible gas saturation impede the migration of SC phase at low saturation. However this effect becomes weaker while SC phase saturation increases by continuous injection. At 100 years, the trapped CO_2 is approximately 0.236 MMt in all five hysteric cases, and is around 0.1 MMt in the non-hysteric case 0, as shown in Figure 37. In Cases 3 and 4, noticeable amounts of CO_2 are trapped within injection period because of the water injection turns regions adjacent to wells from drainage to imbibition status. The more that water injection rate and volume are increased, the stronger the imbibition effect becomes. However, once CO_2 injection is reinitiated, the trapped CO_2 became mobile again. There is no obvious difference in the long-term behavior in this work.

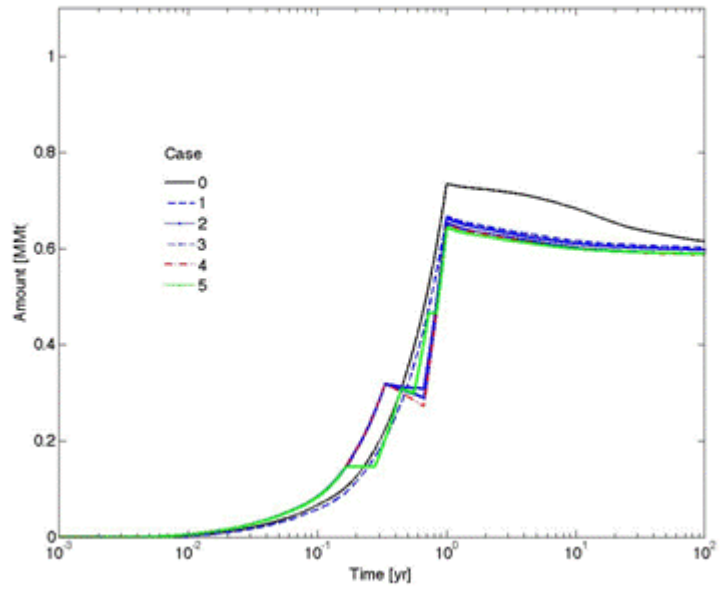

Figure 36. CO_2 mass in the SC phase during simulation period.

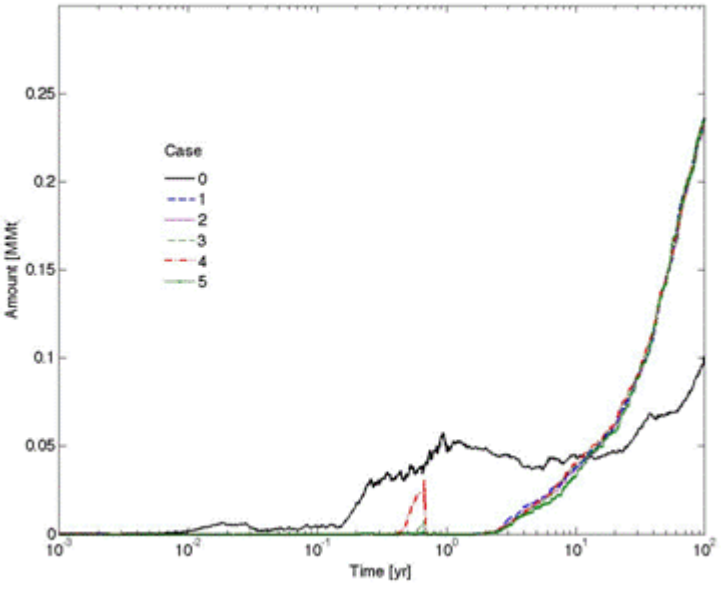

Figure 37. Amount of residual trapped CO_2.

Conclusions

Experiences, discoveries and plans for future work may be summarized as the following:

- More detailed formation characterization is needed. Our empirical porosity-permeability relationship is not accurate enough for flow simulations. Though rock porosity data can be obtained through well logs, related rock permeability data is very sparse.
- According to our estimation of the permeability and resulting numerical simulations, the maximum injection rate should not exceed 0.25 MMt/yr.
- To achieve a 1 MMt/yr injection rate, the permeability should be at least 5 times higher than our estimation, though 10 times higher permeability may be more reasonable.
- The highest pressure induced by injection was investigated according to the number of wells.
- The effects of WAG schemes and hysteresis are weak on dissolution trapping mechanisms. This conclusion is site and model specific and should be investigated using alternative models.
- The hysteresis effect is strong on residual trapping mechanisms. There is no significant effect of a WAG scheme at least for long-term residual trapping in our conceptual model. Differences may be drawn from other sites and models.

Aneth References

Ake, J., Mahrer, K., O'Connell, D., and Block, L., 2005, Deep injection and closely monitored induced seismicity at Paradox Valley, Colorado, Bulletin of the Seismological Society of America, **95**, 664-683.

Babcock, P.A., 1978a, Aneth (Aneth Unit), San Juan County, Utah, *in* Fassett, J.E., editor, Oil and gas fields in the Four Corners area: Four Corners Geological Society Guidebook, v. II, p. 577-579.

Bigalke, J. and Grabner, E. W., 1997, The geobattery model: a contribution to large scale electrochemistry, Electrochemica Acta, 42, 3443-3452

Hammond, G .P., Lichtner, P., and Lu, C., 2007, Subsurface multiphase flow and multicomponent reactive transport modeling using high-performance computing, Journal of Physics: Conference Series, **78** 012025, doi: 10.1088/1742-6596/78/1/012025.

Ishido, T., Nishi, Y., Sugihara, M., Temma, N. and Tosha, T., 2008, Changes in geophysical observables caused by CO2 injection into saline aquifers, Abstract H23D-0993, AGU Fall Meeting.

Lu, C., and Lichtner, P.C., 2006, Numerical investigation of CO_2 sequestration in geologic media using the massively parallel computer code PFLOTRAN, Copenhagen, Denmark, June.

Pritchett, J.W., 1995, STAR: a geothermal reservoir simulation system, Proceedings, 2959-2963, World Geothermal Congress '95, Florence.

Rutledge, J. (2010) Geologic Demonstration at the Aneth Oil Field, Paradox Basin, Utah. Los Alamos National Laboratory, Los Alamos, New Mexico.

Tosha, T., Ishido, T. and Nishi, Y., 2008, Geoelectric monitoring studies for the carbon dioxide geological storage, Abstract H13K-02, AGU Fall Meeting.

Segall, P., 1989. Earthquakes triggered by fluid extraction. Geology, **17**, 942–946.

Segall, P., and Fitzgerald, S.D., 1998. A note on induced stress changes in hydrocarbon and geothermal reservoirs. Tectonophysics, **289**, 117-128.,

Utah Division of Oil, Gas and Mining, 2009.

Pump Canyon CO_2- ECBM/Sequestration Demonstration, San Juan Basin, New Mexico

Introduction and Overview

Unmineable coal seams have significant potential for CO_2 storage with initial estimates of storage capacity equivalent to 12 Gt of CO_2 (at least 12% of nation's current storage). The Pump Canyon CO_2-enhanced coalbed methane (CO_2/ECBM) sequestration demonstration project was planned to demonstrate the effectiveness of CO_2 sequestration in a deep, unmineable coalbed at the Pump Canyon site in the San Juan Basin of northern New Mexico via a small-scale geologic sequestration project (which, though termed small-scale, is the largest volume of CO_2 injected into a coalbed to date). The site is located just within the limits of a high-permeability fairway of prolific coalbed methane production (Figure 38). The study area for the SWP project consisted of 31 coalbed methane production wells located in a nine-section area and the injection well location at the center of section 32, T31N, R8W (Figure 39).

Different monitoring, verification and accounting (MVA) techniques were implemented to track the CO_2 movement within and outside the reservoir. These included continuous measurement of injection volumes, pressures and temperatures within the injection well, coalbed methane production rates, pressures and gas compositions collected at the offset production wells, and tracers in the injected CO_2. In addition, time-lapse vertical seismic profiling (VSP), surface tiltmeter arrays, surface measurements of soil composition, CO_2 fluxes, and tracers were used to help in tracking the injected CO_2. Finally, a detailed reservoir model was constructed to help reproduce and understand the behavior of the reservoir under production and injection operation.

A total of 319 MMscf of CO_2 (or 18,400 tons) were injected in about a 12-month period (July 30, 2008 to August 12, 2009), primarily due to highly permeable coal. However, as expected, the CO_2 injectivity dramatically decreased over the injection period. This was mainly due to matrix swelling and permeability reduction, as a result of the CO_2 being adsorbed onto the coal, while displacing methane, as well as increasing reservoir pressure. It was also determined that injection was predominately into the basal coal, reducing injectivity by 20%.

The CO_2 sensors installed at the three immediate offset wells, as well as the gas sampling from neighboring CBM wells (three immediate offset wells and an additional ring of immediately surrounding wells), suggest that no CO_2 breakthrough occurred at the site. Increase in Nitrogen content in two wells and an increase in the CO_2 content at one of the offset wells, the FC State Com 1, suggest breakthrough was approaching.

Another indication that breakthrough might be approaching is that the perfluorocarbon tracers injected in the CO_2 stream showed up a few months later at the two closest offset wells, the FC State Com 1, followed by the EPNG Com A 300 (where breakthrough is expected to occur first due to its alignment with the face cleats, if it does occur). Again this may also be an early sign of breakthrough.

In addition to monitoring for breakthrough, the project also adopted several ground monitoring techniques to observe any ground deformation. The different ground monitoring techniques used (Tiltmeters, GPS and InSar) all converge to the same conclusion, that no ground deformation is seen. Their effectiveness was probably limited due to the small amount of CO_2 injected and the production of gas at are above the rate injected.

In order to assess the integrity of the site, the project conducted a thorough seismic interpretation of about nine square miles of 3D seismic data centered around the injection well. The seismic interpretation revealed considerable stratigraphic complexity in the Fruitland formation depositional system. Post-stack processing of the 3D seismic suggested the presence of fracturing and minor faulting within the Kirtland Shale caprock, whereas indicators for extensive fracturing and faulting within the Fruitland sequence were much less apparent. However, interpreted faults and fracture zones, with limited vertical extent and major penetrative faults, were not observed at the site, reinforcing the fact that no leakage was expected. Baseline and post injection vertical seismic profiles (VSP) were collected at zero offset and three non-zero offsets. A detailed study of the integrity of the Kirtland Shale caprock has been provided in a topical report, *Natural Tracers and Multi-Scale Assessment of Caprock Sealing Behavior in the SJB Kirtland Formation.*

The simulation work was able to adequately replicate the production/injection profile of the injector and the three immediate offset wells. The model also showed that methane production was enhanced due to the CO_2 injection. While the match is not perfect and predicts breakthrough perhaps a bit too early, the model was successful in tying the results from the field, such as the gas samples (CO_2 content and nitrogen content), to the well performance, lending confidence in the accuracy of the match.

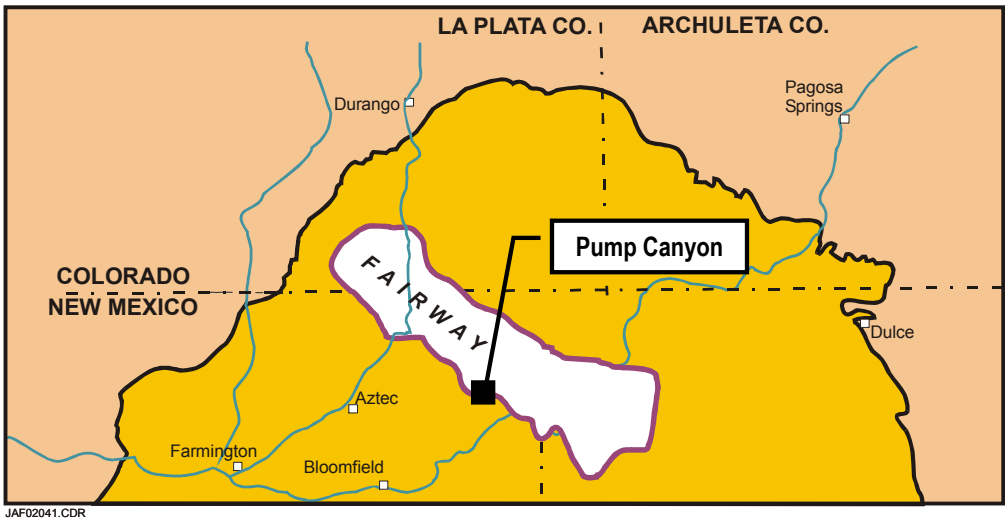

Figure 38. Location of the Pump Canyon Unit, San Juan Basin.

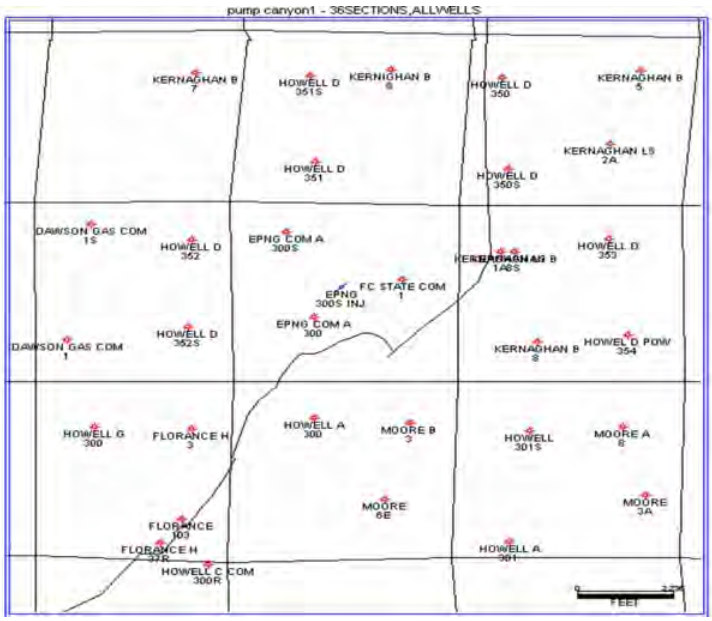

Figure 39. Pump Canyon demonstration area base map.

Permitting and Regulatory

A variety of permitting and other regulatory requirements were necessary to implement the project, including permits for drilling the new CO_2 injection well, installing the pipeline, gaining access to section 32 for the purposes of performing the various proposed MVA activities, and passing a National Environmental Policy Act (NEPA) review by the DOE.

Injection Well: The New Mexico Oil and Gas Conservation Division (NMOCD) was the primary permitting entity for this project and must approve the Application for a Permit to Drill (APD). The State of New Mexico retains primacy over the Federal government for regulating injection operations pursuant to the Safe Drinking Water Act; therefore, the EPA is not required to issue Underground Injection Control (UIC) permits under the Safe Drinking Water Act. Three specific applications were required to obtain permits to drill the new well and inject CO_2 into the Fruitland coal reservoir.

- Application for Permit to Drill (C-101).
- Location and Acreage Dedication Plat (C-102).
- Application for Authorization to Inject (C-108).

These documents were presented to the NMOCD at a hearing on June 21, 2007 in Albuquerque, NM and the permit was subsequently issued.

Pipeline: In order to construct the 2.6-mile pipeline extension, a surface right-of-way had to be obtained. This required both an archeological survey to avoid surface disturbance of sensitive sites, as well as an environmental assessment (EA) study, for traversing both Bureau of Land Management (BLM) and State Trust (State Lands Office - SLO) lands. After all the necessary studies were performed, a finding of no significant impact (FONSI) was received.

Access to the Site: In order for the various project researchers to conduct any activity on the site, primarily in State-held Section 32, permission for site access was required. A Work Authorization Agreement (WAA) between the individual SWP contractors and ConocoPhillips was completed and submitted to the State as evidence of a contractual relationship between the two parties.

National Environmental Policy Act (NEPA): An environmental questionnaire was completed for the project and submitted to the USDOE environmental compliance officer to ensure NEPA compliance. This was completed and the USDOE provided a categorical exclusion, thus fulfilling this requirement.

National Historic Preservation Act (Section 106): When federal funds are involved in a project, proposed surface disturbances must be reviewed by the State Historic Preservation Office (SHPO) and Native American tribes in the area. In this particular area, there are seven tribes with cultural heritage that need to be consulted. Consultation involves preparing detailed descriptions of any proposed disturbances, and their location, providing this information to the SHPO and the Tribes, with sufficient time allowed for any concerns to be raised. The consultation process was initiated in December 2007 and the Tribal approval process took several months to complete. Finally, Section 106 was approved at the beginning of April 2008, which allowed field operations to start.

Site Operations

Steps taken to prepare the injection site included; construction of the pipeline, the drilling of the injection well (including logging and coring) and the installation of the different MVA systems (tiltmeters, CO_2 sensors, etc.) necessary to track the CO_2 plume extension.

Pipeline Construction

The new pipeline section required to reach the injection site was tied to the existing Kinder Morgan-operated Cortez pipeline, which transports CO_2 from the McElmo Dome source in Colorado. Based on a maximum allowable injection rate from the UIC permit and an operating line pressure of 2,000 psig, a 2-inch pipeline diameter was deemed sufficient.

The trenching of the pipeline started in the fall of 2007, but was halted prior to entering State lands, waiting for the Section 106 consultation process to be completed. The trenching was restarted in mid-April 2008 and completed by the end of the month. By mid-May, all sections of the pipeline were hydro-tested to operating pressure and deemed for service.

Surface Deformation Measurements

One of the primary concerns for this project was the possibility of surface deformation due to coal swelling in the presence of CO_2. To monitor and measure any deformation, a unique system of tiltmeters and GPS stations were designed and installed. Pinnacle Technologies installed a total of 36 surface tiltmeters in shallow, 40 ft deep boreholes as well as a data collection enclosure with a satellite link to remotely collect data. All field installation work was completed by April 19, 2008.

In addition to the tiltmeters, two differential GPS stations were integrated into the surface tiltmeter monitoring (STM) array in order to determine absolute changes in elevation and to help constrain the deformation measurements over long periods of time. The layout of the tiltmeter array and GPS stations is shown in Figure 40.

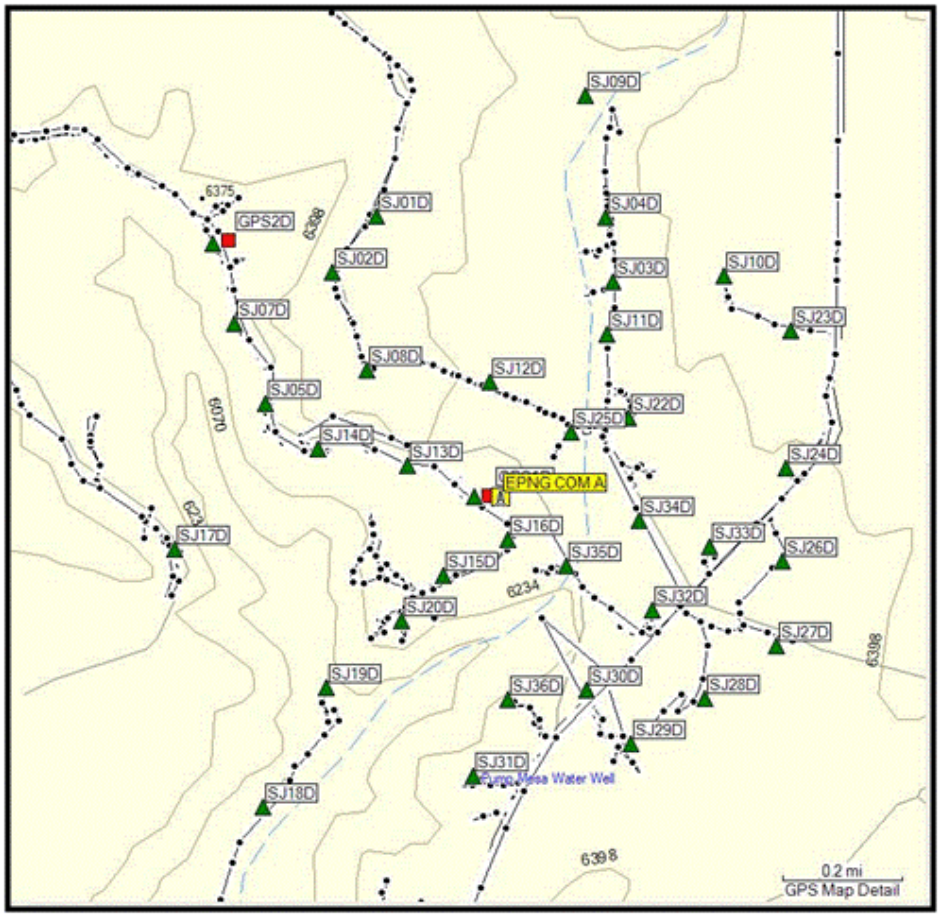

Figure 40. Layout of tiltmeter array showing the 36 sites and GPS system showing the remote and base stations (red squares). Well EPNG Com A.

Surface tilt measurements can be used primarily in three ways:

1) Integrated, using a minimum curvature rule to obtain surface deformation.
2) Inverted, using a poro-elastic model (Segal, Du) to compute reservoir level volumetric strain.
3) Inverted, using a dislocation model (October) to obtain "fracture" parameters provided there is reasonable likelihood of fractures being formed.

For this project, the surface tilt measurements were used primarily to obtain surface deformation by integration. Computation of reservoir strain was also performed for some time-periods when tilt signals were a little more coherent than at other time periods. There were no indications of fracturing from the tilt signals and hence inversion to obtain fracture parameters was not performed.

Logging and VSP

The upper part of the well was logged on May 10, 2008. Logging depths for the different tools varied but extended roughly from 224 ft to 2,933 ft, subsurface. Logs in the upper part of the hole included the Platform Express, Formation Micro Imager (FMI) log and the Sonic Scanner for anisotropy and mechanical properties. FMI log observations provided information on fracturing to within a few feet of the Upper Fruitland Coal, which was encountered at a depth of 2,963 ft, subsurface.

The baseline VSP survey was run on June 3 and 4, 2008. Following the survey, the borehole was then extended through the Fruitland section. Two additional logging runs were made to provide observations from the Fruitland formation. The second logging run extended roughly from 2,846 ft to 3,158 ft and included gamma ray, density, Photo Electric (PEF) and Sonic Scanner runs.

Coring

The success of geologic CO_2 storage depends upon the integrity of the caprock. The Cretaceous Kirtland formation is a regional seal and aquitard, which overlies the Fruitland formation. The Kirtland was cored during the drilling of the injection well in May 2008, and <40 ft of core was collected from the upper and lower members of the Kirtland of the intended 120 ft planned. A variety of analyses to assess seal integrity were conducted on the cores, which included:

1) Mercury injection capillary pressure used to determine seal capacity
2) Petrographic, petrophysical and geologic characterization through X-ray diffraction, total organic carbon content analysis, thin sections, scanning electron microscopy as well as laser scanning confocal microscopy, porosity, permeability, density and fluid saturation measurements
3) Analysis of noble gases to determine the natural helium concentrations, helium gradients, and $^{3}He/^{4}He$ ratios, which are being used to determine transport properties of the Kirtland and concomitant sealing behavior
4) Geomechanical analysis
5) CO_2 sorption tests

Well Drilling

The drilling of the well started mid-May 2008 and was completed by the end of June 2008. The well was drilled to a point just above the Fruitland Coal to a depth of about 3,000 ft, and cored in the overlying Kirtland shale. The first logging suite was then conducted. Casing the well above the coal was done to protect the low pressure (~200 psig) Fruitland formation from the heavier drilling fluids needed to drill the intervals above it.

After casing was set, a smaller hole was drilled through the Fruitland using mist. The coal interval in the wellbore below the casing was then expanded to 9 in. by under-reaming. A perforated liner was placed across the Fruitland formation and attached to the casing above. A flow computer was set up at the well to limit the injection rate to 1,110 psig, a conservative 25 psig below the 1,135 psig permit limit

The low pressure of the formation prevented from using the cavitation process to surge and expand the hole by breaking chunks of the inside of the formation. The high permeability of the coal also made fracturing unattractive.

Drilling Considerations

An important operating fact for the demonstration was that, since ConocoPhillips had the duty to act in the best economic interests of its financial partners in the offset producer wells, had CO_2

breakthrough occurred in one or more production wells, CO_2 injection into the injection zone would have had to stop. At least two potential events could have led to or otherwise accelerated CO_2 breakthrough at an offset well:

- First, the coal face cleat orientation (N35E) is almost precisely aligned in the direction of the offset well directly to the southwest of the injector, the EPNG Com A 300. This well is also the closest offset well, located only 1,100 ft from the injector. These factors represented significant risk of early CO_2 breakthrough in the EPNG Com A 300 well.
- Secondly, due to extremely low reservoir pressures that appeared to exist in the area (about 75–100 psig), fracturing pressures were also expected to be quite low. Since hydraulic fractures in coal also tend to align themselves with the face cleat, this further exacerbated the risk of early CO_2 breakthrough, and again also in the southwest direction towards the EPNG Com A 300 well.

Injection

Injection was performed into the three layers simultaneously in order to inject the volumes of CO_2 required by the demonstration design. The injection started on July 30, 2008 and ended on August 12, 2009. Figure 41 shows the injection rate and wellhead pressure over the course of the injection period. A total volume of 18,407 tons of CO_2 was injected. A loss of injectivity is clearly noticeable as the rate drops from 3,500 Mscfd to 250 Mscfd over the year of injection and is probably due to pressurization of the system and matrix swelling and permeability reduction as CO_2 is being adsorbed onto the coal around the injector.

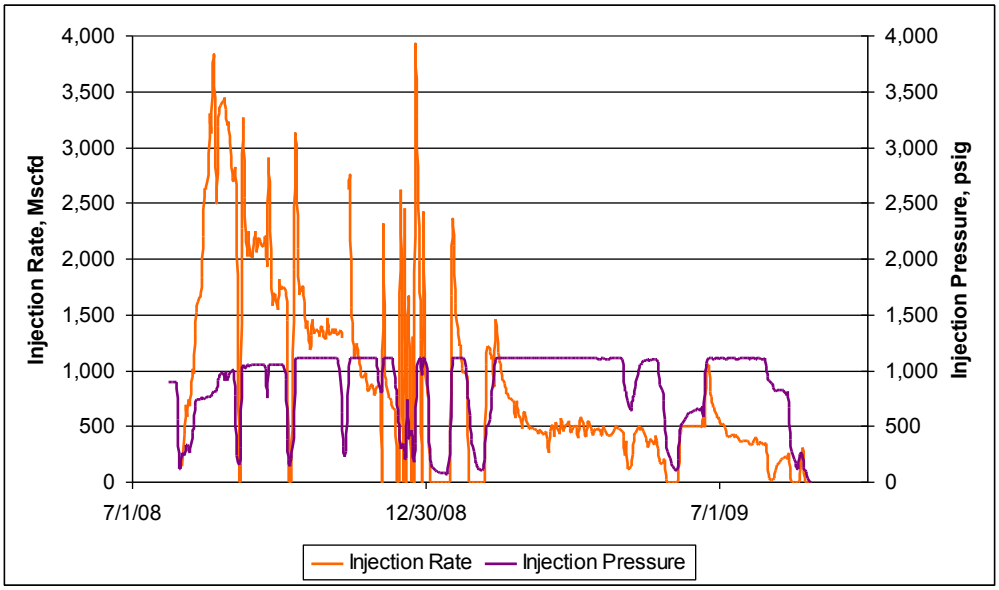

Figure 41. CO_2 rate and wellhead pressure.

Plugging and Abandonment

The injection well was plugged and abandoned using the procedure described in the following steps:

1. Move in and rig up
2. Pressure test blowout preventer equipment
3. Fill hole with 2% KCL and check injection ability at a low pump rate
4. Release packer
5. Trip out of hole with tubing and packer
6. Run in hole with cement retainer and set retainer at 2,900'
7. Trip in hole with workstring and sting into retainer and establish injection
8. Squeeze 5.5 in. liner with 35 bbl cement.
9. Sting out of retainer and circulate tubing and casing clean
10. Pressure test casing and retainer to 500 psig
11. Trip out of hole with work string and lay down pipe
12. Rig down and move off

Reservoir Characterization

Database Development

The Pump Canyon Geodatabase was designed to contain individual feature classes for each type of MVA activity, simulation study, or other testing. These features are all represented on a consistent projection (NAD 83) and allow comparisons to be readily made between activities on a project scale. Features include location of tiltmeters, shallow monitor wells, gas and water sample wells, CO_2 sensor sample wells, soil flux samples, CO_2 pipeline and desalination project.

To complement the Pump Canyon Geodatabase and to provide a context for assessing/integrating MVA, modeling, and risk assessment, the geodatabase also includes basin-scale features that are critical to a larger-scale analysis should commercial application of CCS technology be considered for the San Juan Basin, such as state and county boundaries, townships and ranges, wilderness preservation areas, native Indian lands, federal lands, cities and towns, depositional limits for Lewis Shale, Pictured Cliffs Sandstone, Fruitland formation and CBM Fairway**.**

In addition, well NEBU 77 has been designated as the type well; it is very close to the Pump Canyon project area. Regional dip and strike cross sections have been constructed; dip sections align NE-SW in the basin and strike sections align NW-SE. The focus for the geologic map is the Ojo Alamo Sandstone to the Huerfanito Bentonite within the Lewis Shale. Of particular importance is the relationship of the Ojo Alamo Sandstone to the Fruitland as there is an erosional unconformity that removes the Kirtland Shale caprock along the eastern side of the basin.

The six-township area centered on the Pump Canyon Pilot (Township 30-31 North and Range 7-9 West) is the primary focus of cross-section development. A total of 20 cross sections consisting of 68 wells with raster images were developed. Of these, four cross sections are oriented in the northeast-southwest direction, which parallels depositional dip and eight cross sections parallel depositional strike. An additional seven cross sections were used to ensure all wells with raster images tied correctly with the main dip and strike cross sections.

The correlations being utilized in this geologic model are well described in the *Geologic Evaluation of Critical Production Parameters for Coalbed Methane Resources*, Part 1, San Juan Basin, Annual Report (August 1988 – July 1989), GRI-90/0014.1 and the *Geology and Fuel Resources of the Fruitland formation and Kirtland Shale of the San Juan Basin, New Mexico and Colorado*, U.S. Geological Survey Professional Paper 676 by J.E. Fassett and J.S. Hinds. Figures 42 and 43 are examples of top and isopach maps that were generated for the Fruitland formation and the Kirtland Shale.

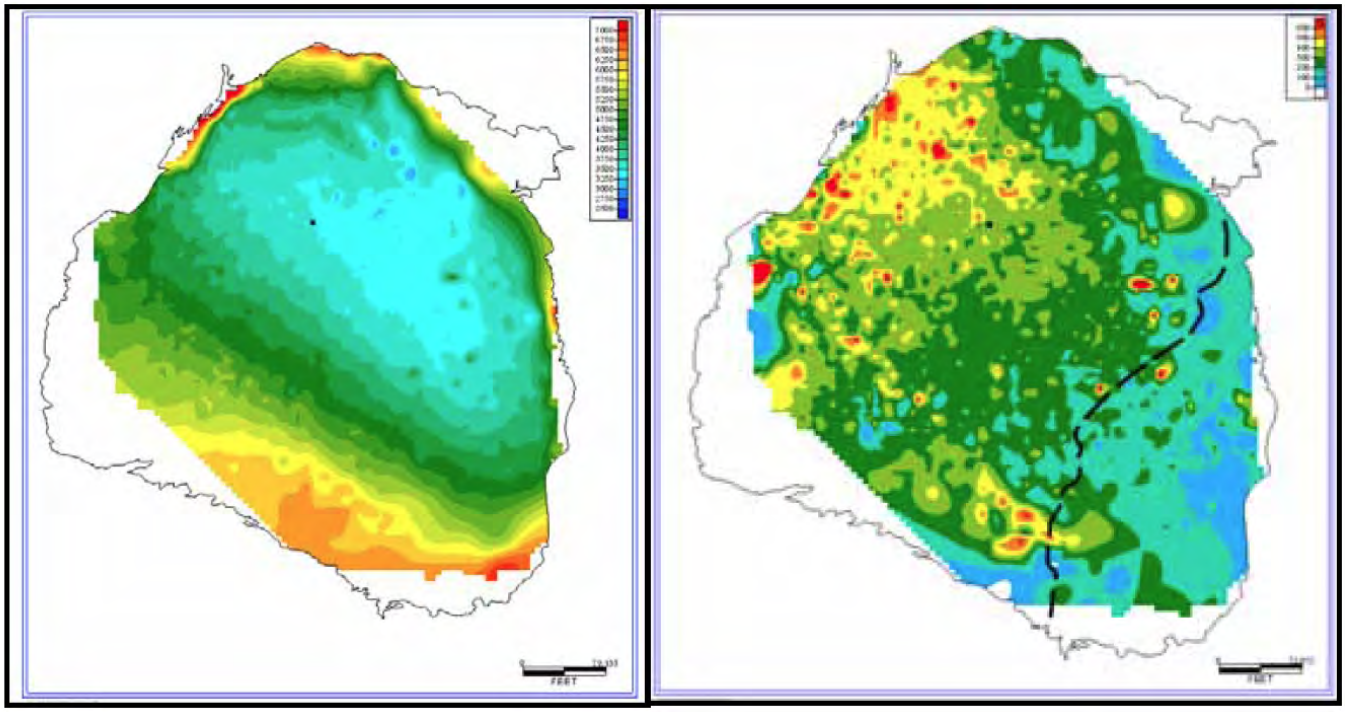

Figure 42. Top and isopach of the Fruitland Formation.

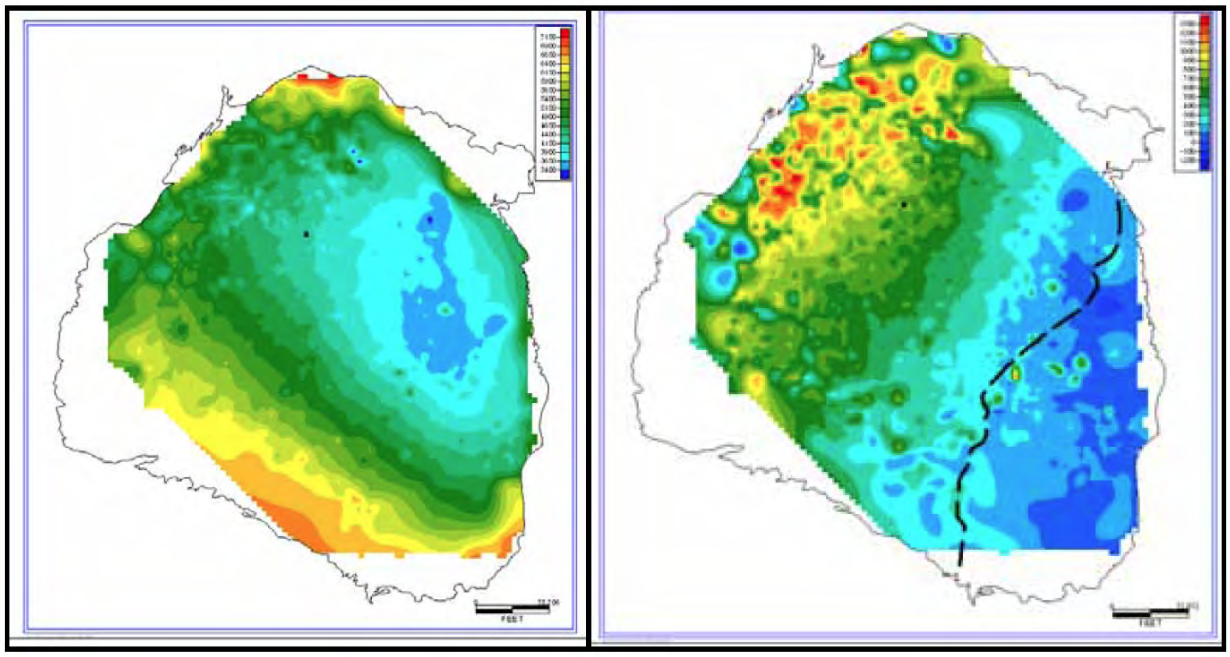

Figure 43. Top and isopach of the Kirtland Shale.

Characterization

Geophysical and geological characterization at the site was undertaken by West Virginia University in support of NETL's tracer and soil gas measurement efforts. Research incorporated independent subsurface mapping, acquisition, processing and interpretation of satellite imagery data (QuickBird, INSAR, and radar), field mapping of surface fracture systems, acquisition, processing and modeling of terrain conductivity data, acquisition and interpretation of comprehensive well logs from the injection well, FMI log analysis of subsurface fracture data, design and specialized processing of the time lapse VSP monitoring survey and 3D seismic interpretation.

3D Seismic study: Seismic interpretation of about 9 mi^2 of 3D seismic data centered around the injection well reveals that the late Cretaceous Fruitland formation forms a well-defined seismic sequence with high amplitude reflections marking the top and base of the sequence. Internal reflection patterns suggest considerable stratigraphic complexity in the Fruitland formation depositional systems. The lower Fruitland coal reflection events are fairly continuous across the site, whereas the middle and upper Fruitland coal events are fairly discontinuous and difficult to correlate through the surrounding area. The detailed seismic view also reveals considerable local

structural complexity not generally observed in well log-derived cross-sections. The overlying Kirtland Shale is considered to represent the effective caprock for Fruitland Formation reservoirs. Variable area wiggly trace displays illustrate the stratigraphic and structural complexity of the Fruitland sequence. Isochore (travel time difference) maps of the Fruitland sequence and lower Fruitland coal intervals reveal considerable variability of thickness throughout the area. Thinning of the Fruitland sequence occurs along a NW-SE trend through the pilot site that coincides with a high in the base of the sequence. Stratigraphic buildup and pinchout are observed in the upper Pictured Cliffs seismic sequence. Researchers speculate that thinning of the Fruitland sequence observed along the NW-SE trend is associated with differential compaction over northwest trending shoreline sand bodies in the upper Pictured Cliffs Sandstone and that differential compaction of the Fruitland may enhance local fracture intensity along this NW-SE trend.

Post-stack processing of the 3D seismic was undertaken to help enhance seismic indicators of fracturing and faulting. The output from specific post stack processing steps is generally defined as a seismic attribute. There are a multitude of seismic attributes including instantaneous phase, instantaneous frequency, envelope, energy, etc. In this study the potential use of a less common attribute was explored consisting of the absolute value of the derivative of the seismic amplitudes. An automatic gain control (AGC) was applied to the output to help equalize attribute amplitude over short time windows. The result of this simple process suggests the presence of considerable fracturing and minor faulting within the Kirtland Shale caprock. Indicators for extensive fracturing and faulting within the Fruitland sequence are much less apparent. The Schlumberger Ant Tracking process, however, does delineate subtle zones of reflection discontinuity that form clusters with approximate N50-55E trend. Similar patterns of discontinuity are observed in the Kirtland and overlying Tertiary intervals (interpreted Ojo Alamo and Nacimiento seismic sequences).

3D seismic coverage is critical to the assessment of site integrity. In this study, 3D seismic analysis reveals numerous details about internal reservoir stratigraphic and structural framework that cannot be inferred from limited borehole correlations. Seismic attribute analysis can be used effectively to enhance subtle features in the seismic response that may be indicative of fracture zones and faults that could jeopardize reservoir integrity. The results of the analysis suggest that

several small faults and fracture zones disrupt overlying intervals and to less extent, the reservoir interval. However, interpreted faults and fracture zones have limited vertical extent and major penetrative faults have not been observed at the site.

EM surveys and model study: Approximately 70 line-kilometers of EM data were collected across the site. Inverse models suggest the presence of a network of low permeability (low conductivity) pathways in the near-surface sandstone at the site that would facilitate atmospheric return of CO_2 should leakage occur.

Injection well logging: Fracture detection and mechanical properties logs helped to extend the understanding of residual stress and fracture distribution from the near surface down through strata overlying the Fruitland coal injection zone. Sonic Scanner observations, unlike those from the FMI log, were available through the injection zone. Drilling-induced breakout orientations of N57W along the length of the borehole suggest invariant in-situ principal compressive stress direction of N33E. The average fast-shear direction obtained from Sonic Scanner measurements over the entire length of the borehole is N43E. The fast-shear direction is associated with stress induced or fracture induced stress anisotropy. The fast-shear direction refers to the shear wave vibration direction. Fracture induced intrinsic anisotropy arises through birefringence of the shear wave into a fast-shear vibration component that parallels the maximum principal compressive stress direction (or the dominant fracture trend) in strata surrounding the borehole; the slow-shear direction is orthogonal to the fast-shear direction. Stress induced anisotropy results from in-situ stress. When the fast-shear direction is evaluated over local intervals above and within the Fruitland coal section, a transition occurs from the average N43E trend to a N14E trend within the coal section. We speculate that this N14E trend observed through the coal bearing intervals may be related to fracture induced anisotropy and also imply a face cleat orientation of N14E.

A variety of open and healed fracture trends are penetrated between subsurface depths of 370 ft to 2,925 ft within the upper Fruitland formation. The distributions are marginally non-random at best. A small set of open fractures in the upper Fruitland (N=5) are significantly non-random with mean trend of N11E with 95% confidence interval of 19 degrees. The occurrence of these

open fractures in the transition zone observed in the fast-shear orientations within the upper Fruitland supports speculation that open fractures and face cleats in the underlying Fruitland coal section may have more northerly trend.

Monitoring, Verification, and Accounting (MVA)

Analysis of Produced Water Chemistry: Implications for CO_2 Movement and the Ultimate Fate during Geologic Carbon Sequestration

Introduction

Water chemistry analysis is an important tool for tracking CO_2 movement and the ultimate fate of injected CO_2. In addition, water chemistry study is crucial to determine the long-term storage mechanism of the geological formation and indicators of potential impact on the receiving environment. In this section the water chemistry of the offset wells of the CO_2 injection site at Pump Canyon in the San Juan Basin is analyzed. Produced water samples from producing wells near the CO_2 injection site were obtained and analyzed to investigate the impact of CO_2 injection on produced water chemistry and to monitor the movement of the CO_2 plume. The main objectives of the water sampling and chemical analysis include:

(1) Investigation of the impact of CO_2 injection on the produced water composition as well as the receiving environment.
(2) Identification of the influences of CO_2 on water chemistry and the movement of the CO_2 plume during CO_2 injection process.

As CO_2 is injected into a reservoir, CO_2 will contact with formation fluid and rocks followed by a comprehensive chemical reaction and movement, which gives crucial indications of the CO_2 movement and its ultimate fate. Potential chemical reactions between injected CO_2 and formation fluid include [Druckenmiller et al., 2005; Raistrick, et al., 2006]:

$$CO_2(g) \Leftrightarrow CO_2(aq)$$

$$CO_2(aq) + H_2O \Leftrightarrow H_2CO_3$$

$$H_2CO_3 \Leftrightarrow H^+ + HCO_3^-$$

$$CO_2(aq) + OH^- \Leftrightarrow HCO_3^-$$

$HCO_3^- \Leftrightarrow H^+ + CO_3^{2-}$

$Ca^{2+} CO_3^{2-} \Leftrightarrow CaCO_3$ (Calcite)

$Mg^{2+} + CO_3^{2-} \Leftrightarrow H^+ + HCO_3^-$ (Magnesite)

$Ca^{2+} + Mg^{2+} + 2CO_3^{2-} \Leftrightarrow CaMg(CO_3)_2$ (Dolomite)

These reactions lead to dissolution of CO_2 and dissociation of H_2CO_3 into formation water. As a result, the pH of formation water and solution alkalinity will decrease. In addition, due to the effects of leaching, ion concentrations of trace metals and isotope contents will vary correspondingly. Many experimental, modeling, and field studies have been conducted to evaluate the implications of fluid chemistry on geological carbon sequestration [Druckenmiller et al., 2005; Johnson et al., 2008]. From the chemical composition studies, the following key issues can be identified, which play crucial roles in quantification of carbon storage mechanisms and tracking the ultimate fate of injected CO_2:

(1) Ultimate fate of CO_2 and long-term storage mechanisms: Several mechanisms are involved in long-term CO_2 storage: dissolution of CO_2 in H_2O followed by dissociation of H_2CO_3 (ionic trapping) and mineral storage of CO_2 through the formation of calcite, magnesite, or dolomite (mineral trapping).

(2) Reactions induced by CO_2 in rocks that were saturated with saline waters include acid hydrolysis of rock-forming minerals and precipitation.

(3) CO_2 movement vertically and spatially.

(4) Potential impact on receiving environment and/or shallow water systems.

This research focused on the investigation of the chemical composition of produced water from offset producing wells and identification of the sources of the CO_2 and its movement in the geologic framework. This information will be an important indicator of CO_2 migration, accumulation, and leakage in heterogeneous coalbed methane formations.

Experimental

Water sampling

Produced water samples were collected from the nearby producing wells of the CO_2 injection site. Water sampling follows a procedure: (1) Select a faucet and run the water to drain the dead volume out to make sure the water sample is a representative sample of in-time reservoir fluid. Clean and leak-proof plastic bottles are used for water sampling. Be careful not to touch the in-

side of the cap and faucet when handling the water sample bottle. An attached sample information sheet must be filled out before sampling. (2) Fill the bottle completely and cap the sample. (3) Label the bottle clearly with the date, and the well name. Fold and wrap the sample information sheet around the bottle, and put them both into a waterproof plastic bag. (4) Keep the sample refrigerated at 5°C and ship to the recipient. (5) Chemical composition of produced water samples will be analyzed in two weeks.

Figure 44 shows the map of CO_2 injection and water sampling sites. The starting time for water sampling was August 08, 2007.

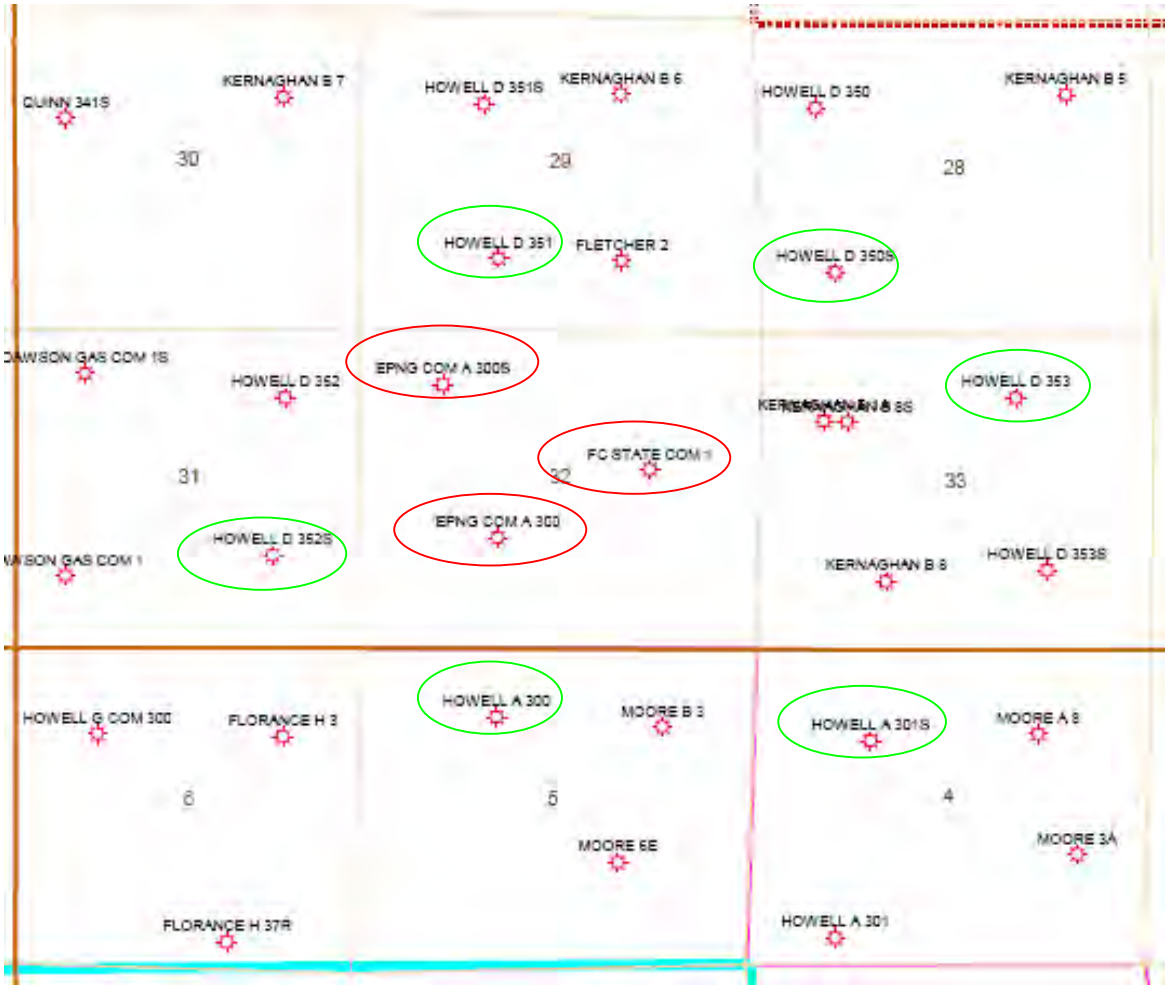

Figure 44. Map of well locations for water sampling.

Table 8 summarizes the production history of all the offset wells, including cumulative water production, gas production, and locations. Early breakthrough was expected to occur at FC State Com 1 and EFNG Com A300.

Table 8. Offset Well Information

Well Name	Spot	Cumulative water production (Bblw)	Gas Cum (MMcf)
HOWELL A 301S (infill)	NW SE NW	135	72.6
HOWELL A 300	SW NE NW	130,281	12944.5
HOWELL G COM 300	NW	310,414	8113.9
HOWELL D 350S	NE SW SW	2,805	167.6
HOWELL D 351	NW SE SW	648,227	9236.2
HOWELL D 352S	SW NE SE	880	634.8
EPNG COM A 300	SW NE SW	9,899	9336.7
EPNG COM A 300S	SE NW NW		189.9
FC STATE COM 1	SE SW NE	147,581	10780.1
HOWELL D 353	SE NW NE	166,179	14198.8

Most of the water samples collected before CO_2 injection contained suspended solid and oil droplets. Physical and chemical properties of the produced water before CO_2 injection were tested as baseline. Dramatic differences in water chemistry from nearby wells or at different time intervals was observed. Figure 45 shows typical produced water samples collected in April 2008.

Figure 45. Typical examples of produced water samples obtained from offset wells of the injection site.

Analysis methods and produced water chemistry

Ion concentration

The ion concentration of the produced water was analyzed by ion chromatography (Dionex DX-120). The Six-Cation-II and Five-Anion standard solutions were used for preparation of the calibration curve. The produced water samples were filtrated with a 0.22 μm filter to remove large particulates and suspensions before ion analysis. All produced water samples were diluted to desirable concentrations (~50 mg/L Na^+) for ion analysis.

Trace metal ion analysis

The trace metals of the produced water were characterized with inductively coupled plasma-mass spectrometry (ICP, ELAN). Water samples were diluted to the desired concentration and introduced into the central channel of the spectrophotometer. As a droplet of nebulized sample enters the central channel of the ICP, it evaporates and any solids that were dissolved in the liquid will vaporize and then break down into atoms. At the temperatures prevailing in the plasma a significant proportion of the atoms of many chemical elements are ionized and then detected by the spectrophotometer. Ion species that were monitored in the produced water include: Ag, Al, Ba, Be, Cd, Cr, Cu, Fe, Mn, Mo, Ni, Ni, C, Sb, Se, SiO2, Sn, Sr, Th, Tl, V.

Dissolved organics

During CO_2 injection, dissolution of CO_2 into the formation water reduces its pH drastically. As a result, the dissolved organics in produced water from the formation will decline correspondingly, due to the diminished solubility of low molecular hydrocarbon at lower pH. Therefore, the organic composition can be tracked throughout the CO_2 injection process. A Shimadzu TOC-5000A analyzer was used to measure the dissolved organic composition of produced water samples. The analysis was carried out by using combustion at 680°C. The accuracy of measured values for TOC was estimated at around 5%.

Results and discussion

Site description for water sampling

Injection of CO_2 into an unmineable coalbed at the Pump Canyon site in the San Juan Basin of northern New Mexico was one of the key field deployment projects for the Southwest Carbon

Sequestration Partnership (SWP). The geologic sequestration was planned in the deep, high-permeability fairway coalbed located in the northern New Mexico portion of the San Juan Basin. The injection well location was at the center of section 32, T31N, R8W, called the Pump Canyon site. Figure 46 shows a map of the injection site location provided by Advanced Resources Inc (ARI).

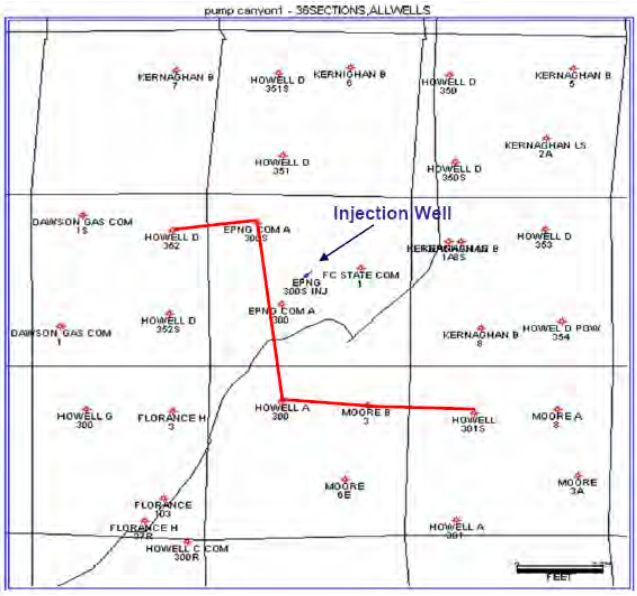

Figure 46. Location of the Pump Canyon CO_2-Sequestration/ECBM site (Diagram from ARI and ConocoPhilips).

From the above geological description, the potential CO_2 breakthrough at the offset wells includes:

a. The coal face cleat orientation is aligned in the direction of the southwest and northeast as shown in Figure 47. Early breakthrough from offset wells was predicted to occur along the southwest to northeast. The EPNG COM A300 well, located 1,100 feet southwest of the injection well, was the most likely offset well for early CO_2 breakthrough.
b. Injection-initiated microfracture usually lies along the cleat orientation.

Therefore, the water samples were collected from wells closest to the injection well. Specifically, the water composition from EPNG Com A 300 well was closely monitored for detection of potential early breakthrough along the cleat orientation. The purpose of the water chemistry analysis was to identify potential early CO_2 breakthrough and to adjust the original injection plan, including sealing off the basal coal formation and reducing injection pressure.

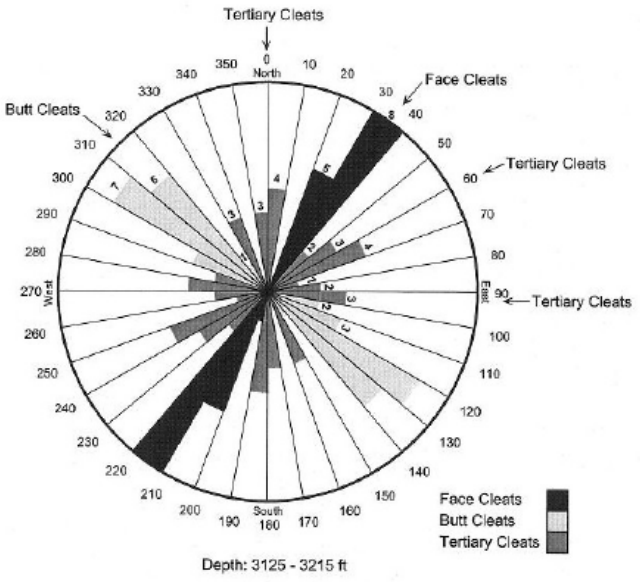

Figure 47. Coal face cleat orientation diagram (from ARI and ConocoPhillips).

Baseline measurement of chemical composition of produced water

The chemical composition of the produced water. including ion species and concentration, total organic carbon, and trace metal ions, was analyzed for a baseline measurement. The chemistry of formation water from the nearby producing well was studied by ion Chromatography (IC). The results are summarized in Table 9.

Table 9. Summary of the Composition of Formation Water from the Nearby Offset Wells

Elements	Ion Concentration, mg/L						
	COM #1	**Howell A 301S**	**Howell A #300**	**Howell D350S**	**Howell D #351**	**Howell G300**	**EPNG A #300S**
CO_3^{2-}	475.1	312.5	175.9	348.3	150.3	393.7	508.5
HCO_3^-	8112.9	6956.6	5870.3	7215	7309.5	8155	10534.2
Cl.	2520.9	3104.9	2389.5	2919.7	3092.3	3211.6	2837.7
F^-	33.2	16.4	28.8	19.6	39.0	18.9	22.9
Na^+	5164.0	5148.5	4169.3	5235.8	4774.1	5727.8	5784
K^+	22.1	18.0	35.0	20.0	55.5	28.0	25
Mg^{2+}	21.2	23.0	19.0	19.0	22.0	23.0	19
Ca^{2+}	14.0	7.3	11.0	9.8	9.1	17.0	7.4
TDS	16363.5	15587.3	12698.8	15787.2	15451.9	17575.0	19738.7

Water Chemistry after Injection

The water chemistry of coalbed methane (CBM) produced waters from nearby offset wells was analyzed. Figures 48–56 give the ion concentration of produced water obtained from the offset wells over a period of two years. Ion species were also monitored during the whole CO_2 injection process. It was observed that the ion concentration varied over the production period. Several spikes of ion concentration in produced water were found to be influenced by the presence of H_2S. Presence of acid gas (i.e., H_2S) in produced water interferes drastically with the detection of CO_2 movement; this mechanism needs to be further investigated.

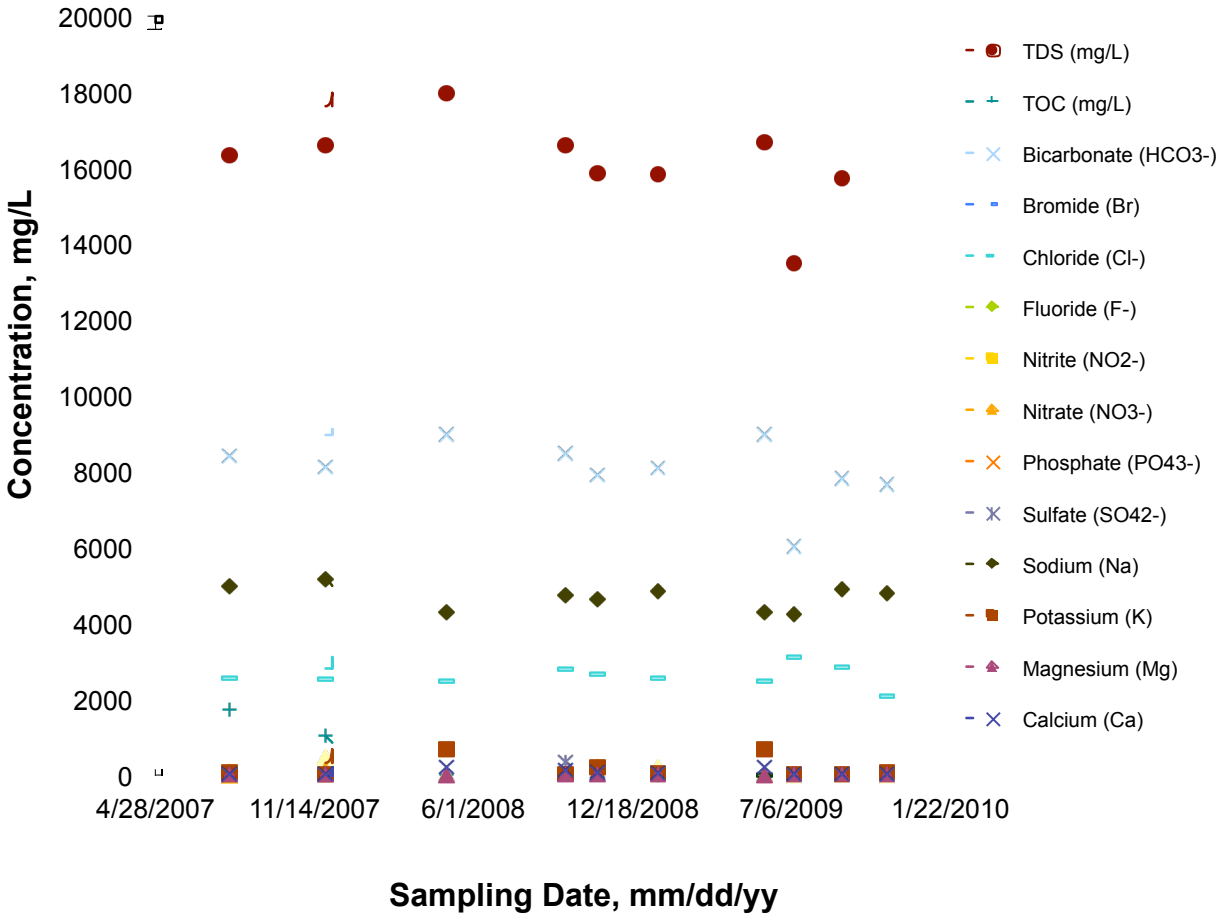

Figure 48. Water chemistry of well FC State COM #1.

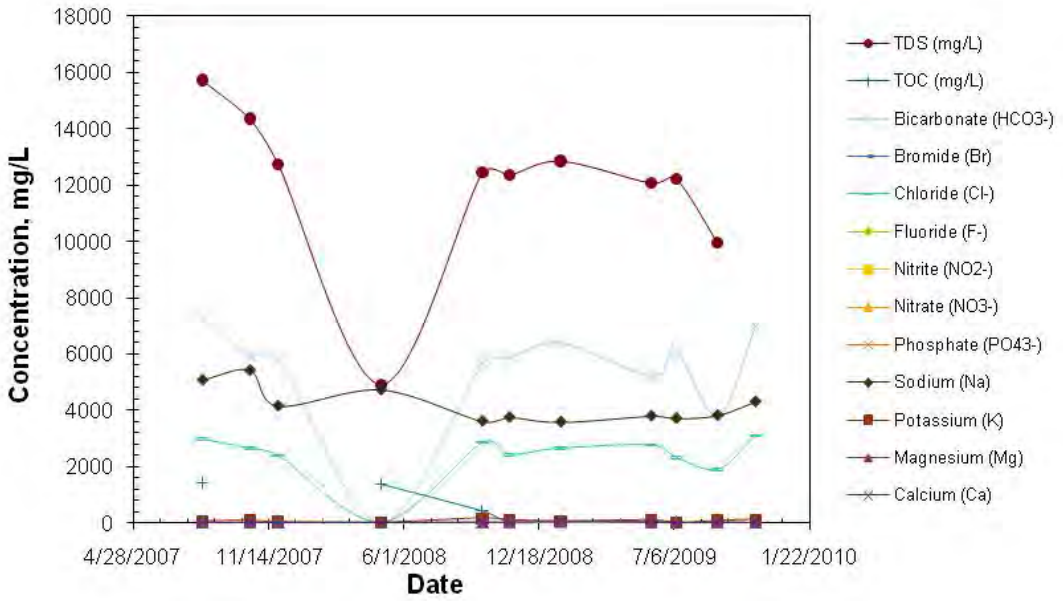

Figure 49. Water chemistry of well Howell A #300.

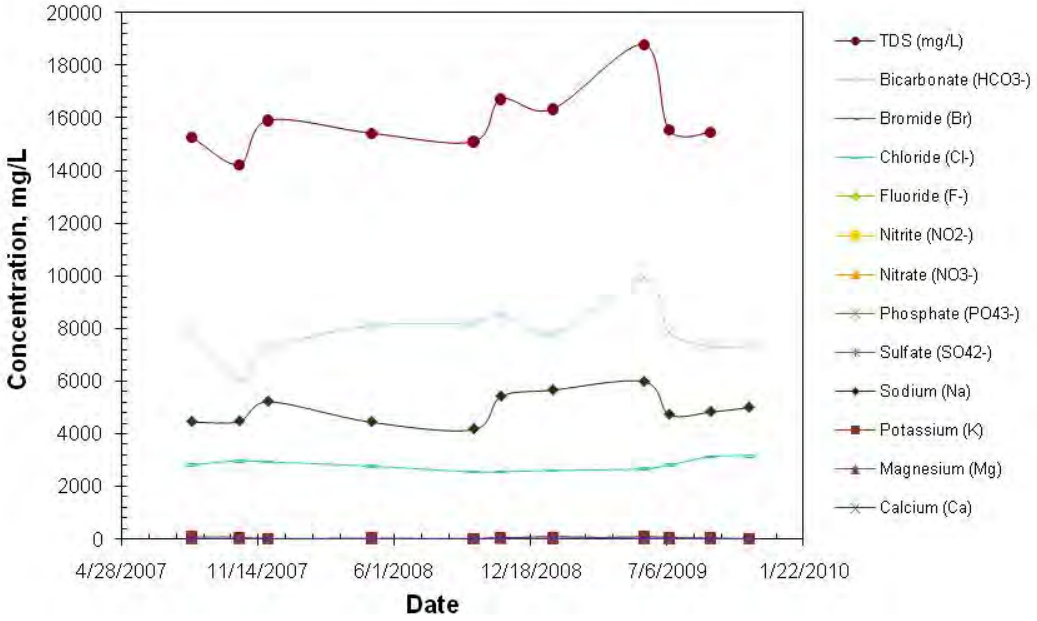

Figure 50. Water chemistry of well Howell D350S.

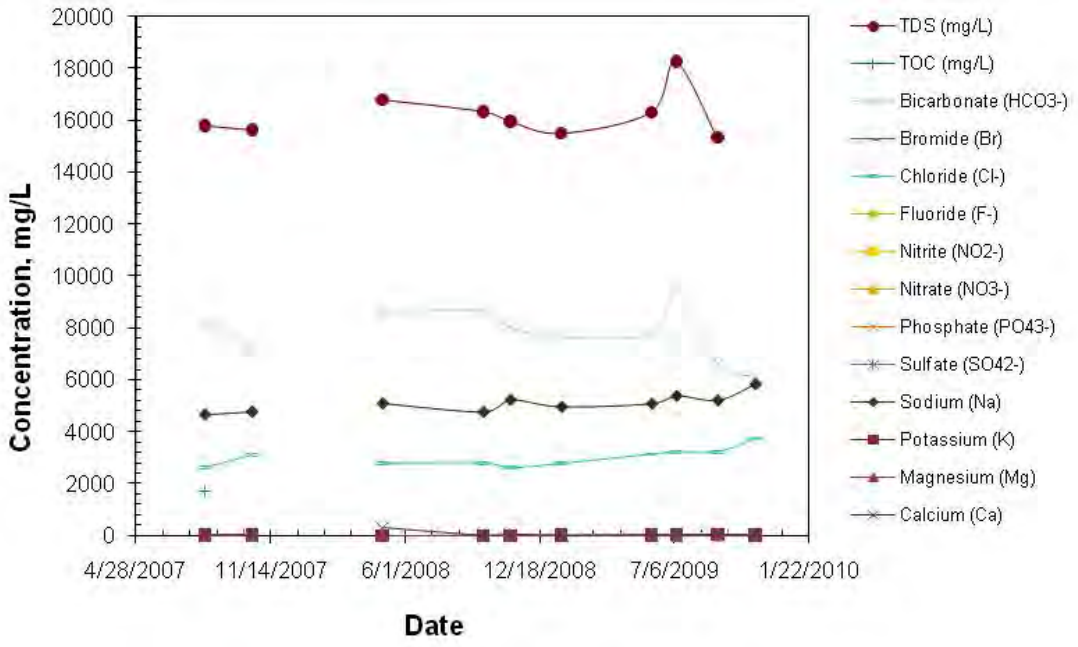

Figure 51. Water chemistry of well Howell D351.

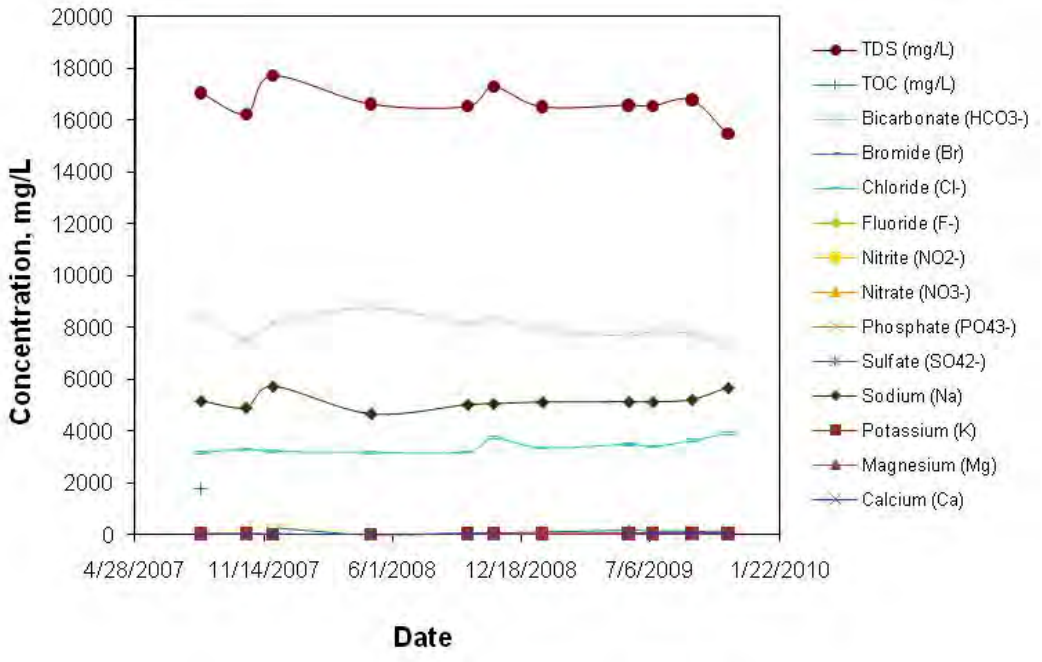

Figure 52. Water chemistry of well Howell G300.

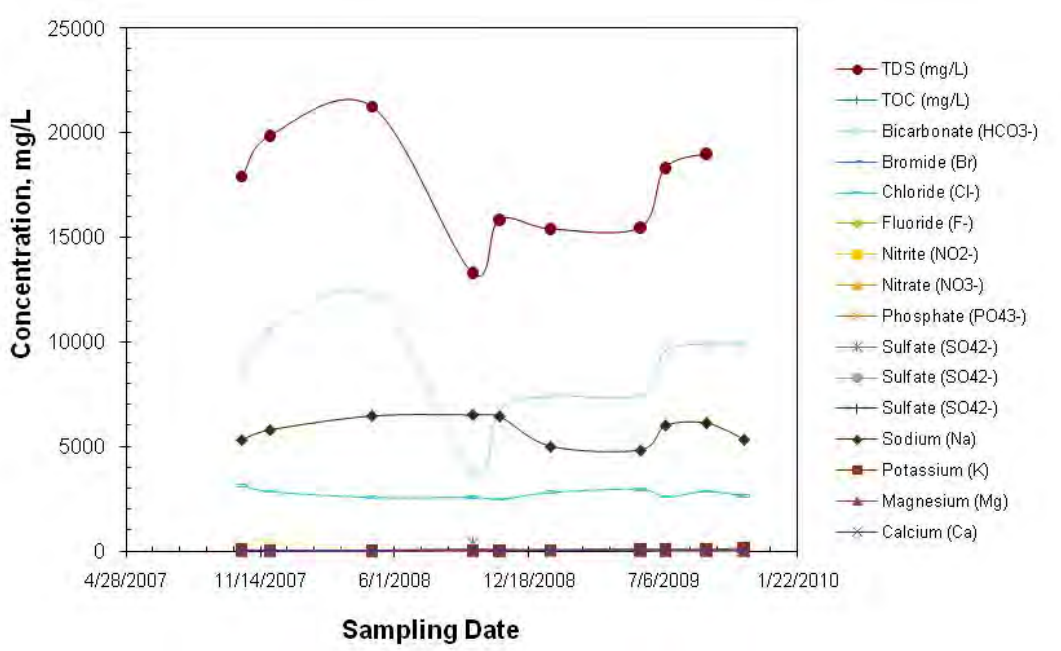

Figure 53. Water chemistry of well EPNG COM A300s.

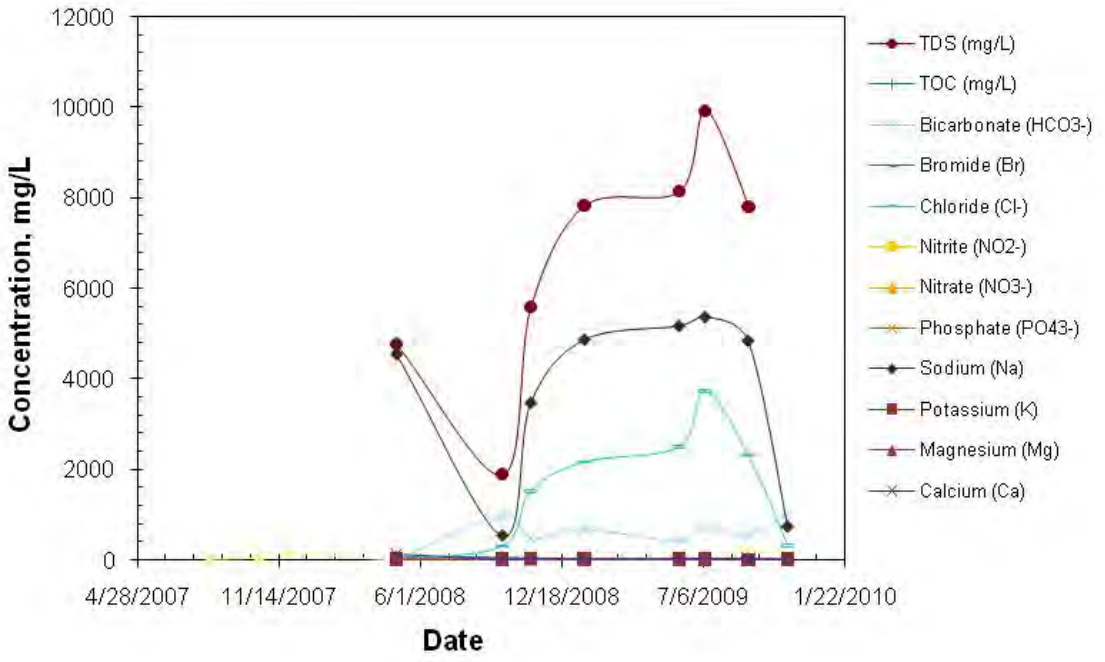

Figure 54. Water chemistry of well EPNG COM A300.

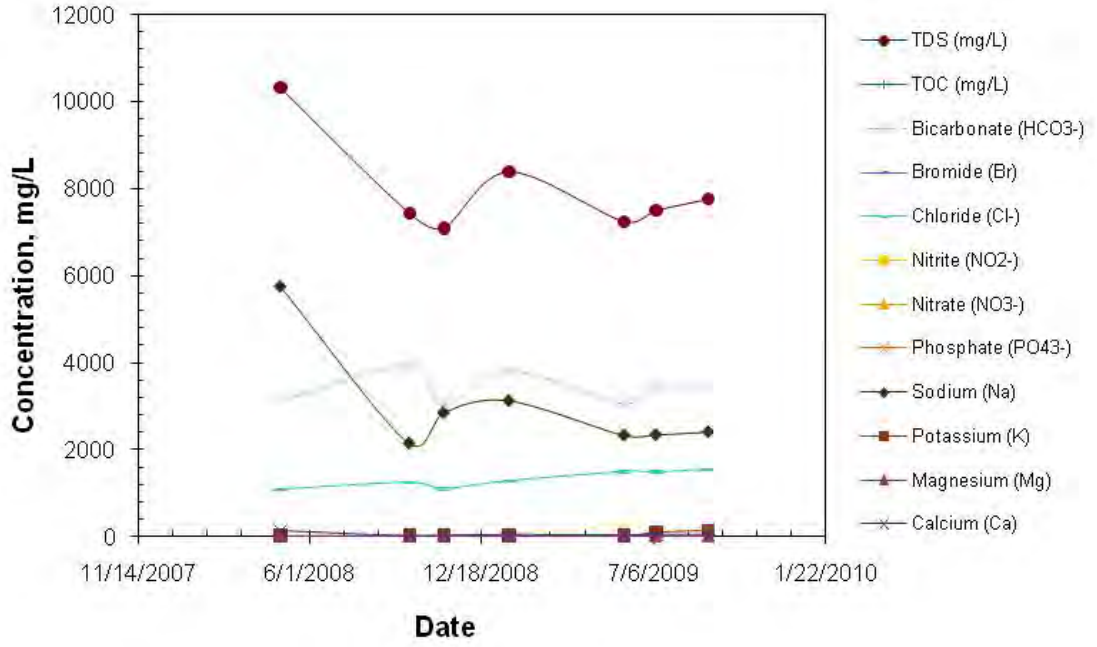

Figure 55. Water chemistry of well Howell D353.

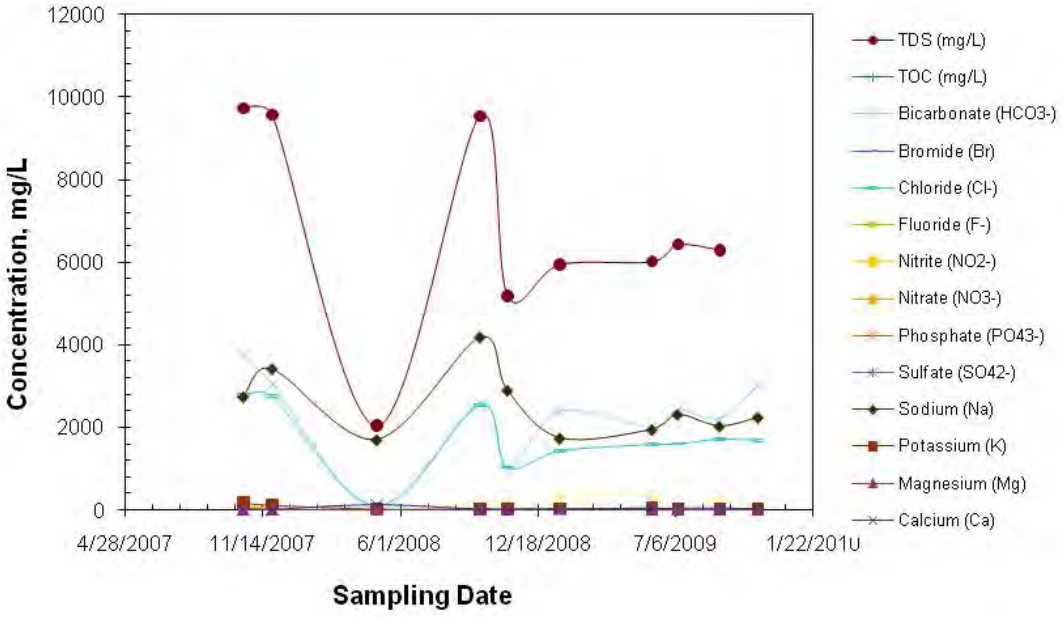

Figure 56. Water chemistry of well Howell D352S.

Figure 57 gives the pH of produced water from the nearby offset wells. The pH of the solutions stabilized at around 8.0 with variations ranging from 7.0 to 9.0. The spike in pH in June

2008 is attributed to a high concentration of H_2S in the produced water. The carbonate and bicarbonate ion concentration could be an important indicator of the front line of the CO_2 plume and thus are carefully monitored during CO_2 injection. Figure 58 gives the HCO_3^- concentration of the produced water and Figures 59–60 give the strontium and barium ion concentration of the produced water. No dramatic change in water chemistry was observed from offset wells during the testing period. Since early breakthrough was expected to occur at the EPNG COM A300 and FC State COM 1, water chemistry and pH values from these two wells were closely monitored.

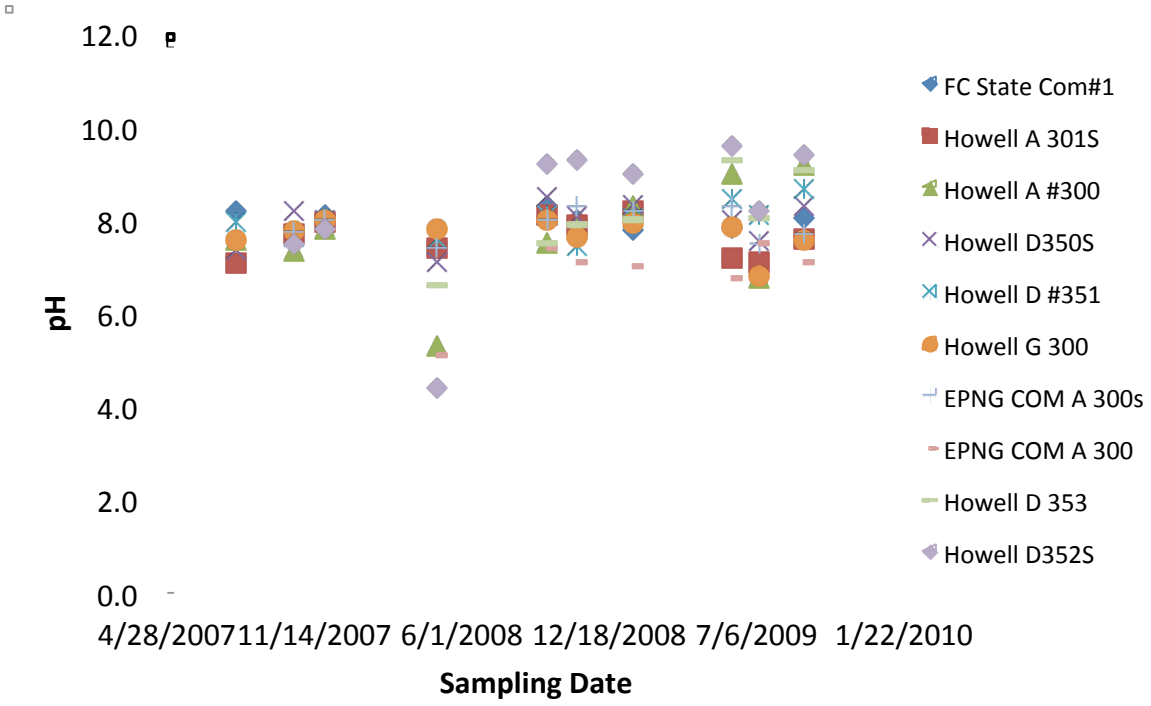

Figure 57. pH of produced water from offset wells.

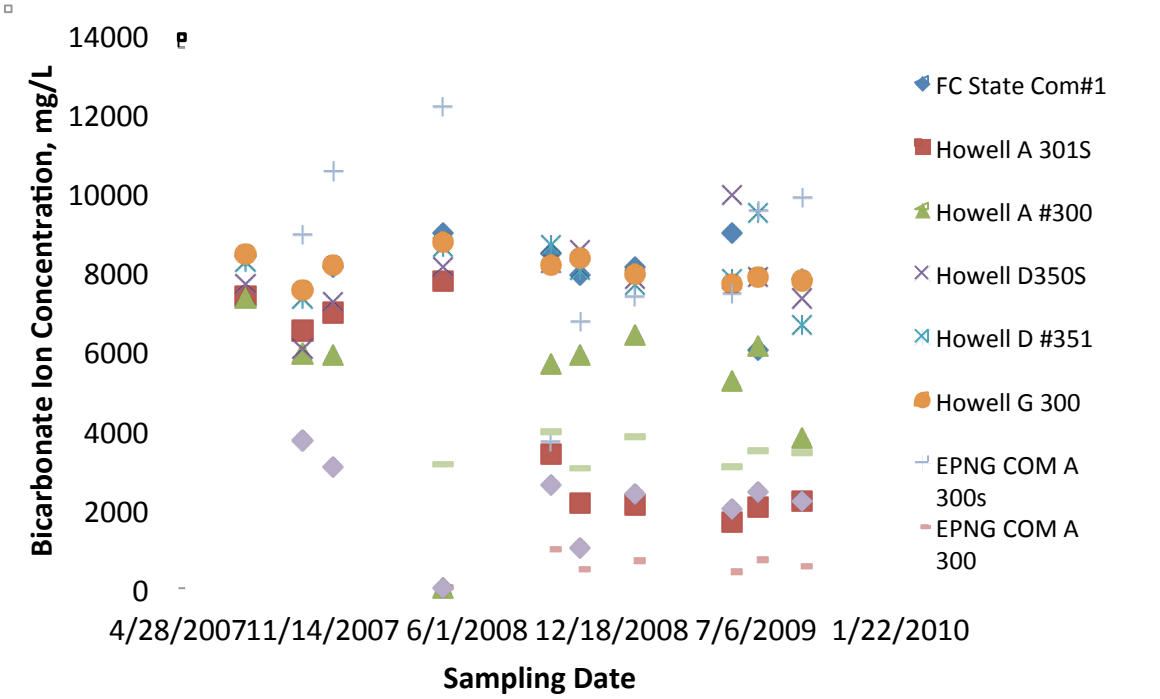

Figure 58. Concentration of bicarbonate ion species in the produced fluid from offset wells.

Figure 59. Strontium ion concentration in the produced water from offset wells.

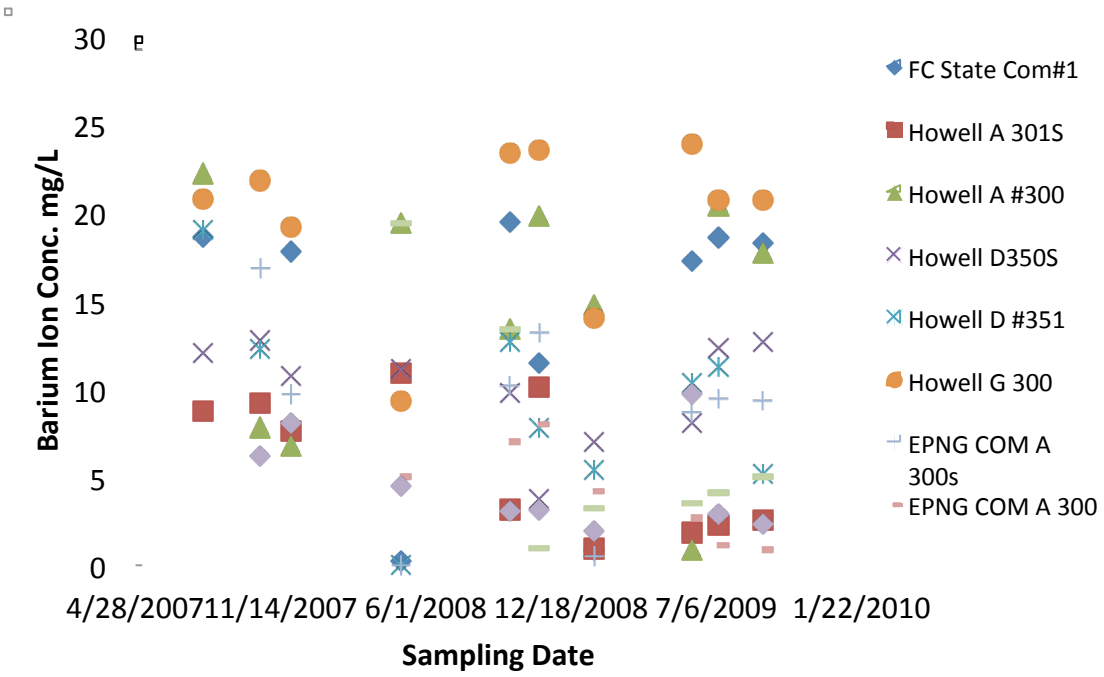

Figure 60. Concentration of barium ion in the produced water from offset wells.

Conclusions and recommendations

About 40 water samples were collected for baseline measurement and over 70 water samples were collected after CO_2 injection for monitoring the movement of CO_2 as well as its impact on the receiving environment. Comprehensive analysis of water chemistry, including ion composition and concentration, dissolved organics, trace metal ion species, carbon isotope, oxygen isotope, and pH values, was carried out and the observations are summarized as:

(1) Presence of other acid gases, such as H_2S, showed a dramatic impact on the water chemistry analysis. The fluctuation of H_2S in produced water was not fully understood.

(2) Though early breakthrough was expected to occur at EPNG COM A300 and FC State COM 1, no breakthrough was indicated from water chemistry changes as a result of CO_2 breakthrough.

(3) A high concentration of bicarbonate ions was detected in the coalbed methane produced water. Since large fluctuations occurred in the pH value of the original produced water and subsequent variations in bicarbonate ions, bicarbonate ion concentration and pH might not be an ideal indicator of the front line of the CO_2 plume in coalbed methane formations. This is not surprising, as CO_2 exists naturally in the coalbed.

Soil Gas Monitoring

Two techniques employed to detect any eventual CO_2 leak were soil-gas monitoring for the presence of tracers, and direct CO_2 flux monitoring at the surface.

Between April 2006 and August 2006, four background sets of sorbent packets were placed and removed from grids set up near the injection site. Average background perfluorodimethylcyclohexane (PMCH) tracer concentrations from these sets were compatible with worldwide distribution concentrations, with soil-gas concentrations about 50% lower than atmospheric background concentrations. Background CO_2 surface flux and soil-gas hydrocarbons (methane and ethane) and CO_2 concentrations were taken from the sampling locations. Four background sets were taken between March and April 2007. The CO_2 soil-gas concentration increased nearly linearly with depth, but showed no clear seasonal trend. The magnitude of carbon isotope shifts correlated to CO_2 concentrations. Hydrocarbon concentrations revealed nine "anomalies", where hydrocarbons increased with depth, indicating the potential for seepage from depth. An example is shown in Figure 61. The magnitude of seepage signatures for the March 2007 survey was much higher than for previous surveys.

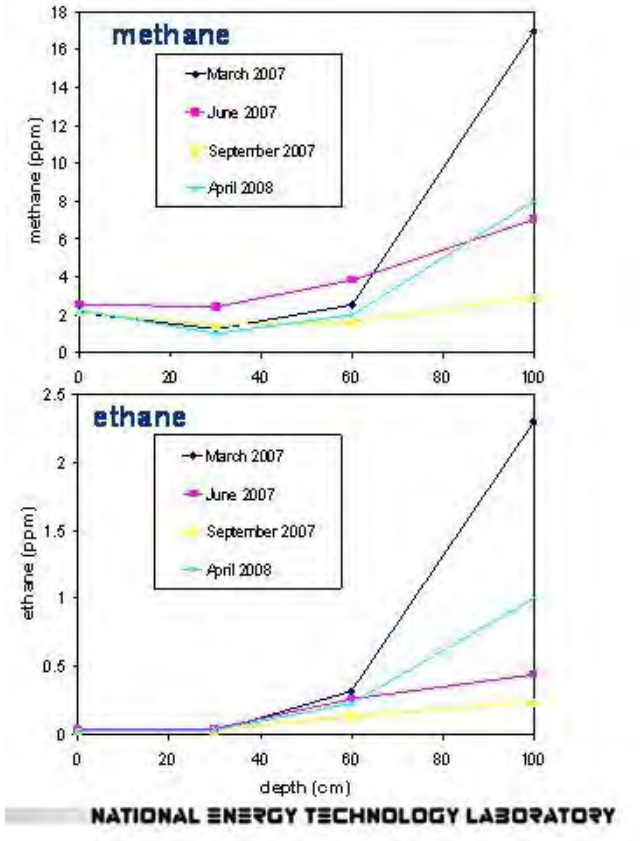

Figure 61. Hydrocarbon anomaly example at Location 24.

Tracer Injection: Two separate, three week-long, sequential tracer injections were conducted shortly after the start of CO_2 injection. The tracers were added directly to the CO_2 from a syringe pump and tracer reservoirs in a van positioned near the injection wellhead. The tracer injections consisted of 20 liters injected continuously at a uniform mixing rate adjusted to the CO_2 flow rate as measured at the wellhead. The first tracer was a mixture of 90% PMCH and 10% ortho-perfluorodimethylcyclohexane (o-PDMCH), with injection beginning on September 18, 2008. The second tracer was 100% perfluorotrimethylcyclohexane (PTCH), with injection beginning on October 9, 2008. Due to the ultra-low detection levels for PFC tracers, rigorous field protocols were observed to prevent cross contamination of samples, and to minimize tracer release to the atmosphere during the injection of tracers.

Grid: The PFC tracer monitoring grid at the San Juan Basin site had a total of 46 permanent installations, and 36 sampling cages to monitor tracer in the atmosphere (Figure 62). All but four of the atmospheric monitors were mounted 4 ft up on steel pipes containing tracer in soil-gas monitors. Of these four, three were mounted 3 in. away from vents to CO_2 sensors. These three locations were distinct from all other sites because they were used as indicators of breakthrough of injected gas to the offset wells *at depth*. It was expected that tracer breakthrough would precede CO_2 breakthrough due to the adsorption of CO_2 on coal. One atmospheric sampling cage (site 68) was not associated with soil-gas monitors or the three off-set wells. A subset of 23 of the tracer monitoring locations were also selected for CO_2 surface flux monitoring, hydrocarbon and CO_2 soil-gas depth profiling, and radon/thoron monitoring.

A rectangular grid was employed with spacing between monitors of 100 meters (Figure 62). In addition, monitors were placed adjacent to six near-by wells to evaluate potential leakage associated with wellbores. Other monitors lying off the main grid were placed to evaluate areas of increased leakage potential based upon the geological assessment, Figure 63.

Results

The breakthrough of tracer at the east and southwest off set wells in shown in Figures 64 and 65 from results of PFC tracer monitors placed directly in front of vents that were releasing a split stream of produced gas from these wells. CO_2 measurements gave no indication of breakthrough, but the conservative tracer breakthrough seemed likely to precede CO_2 breakthrough. ARI and NETL simulations predicted breakthrough in these offset wells, but in reverse order to that found with the tracers.

Soil-gas tracer depth profiles are shown in Figures 66–68 for Sites 36 and 51. These two locations were the only sites to show amounts of PFC tracers beyond background levels. They were located near the injection well and to the south and west of the injection well. An effort underway by Carnegie Mellon University, in collaboration with NETL, to apply a Bayesian Believe Network Analysis to all near-surface results at the San Juan Basin to determine the statistical significance of the results and the techniques employed, was not completed at the time of this report Therefore, the general rule-of-thumb was applied, that significant leakage should be suspected from PFC tracer levels more than two orders of magnitude beyond background level. The

results shown in Figures 66–68 were below this level, but were nonetheless consistent between sets and between tracers. Evidence that the minute levels of tracer detection for sets 18 and 19 might be coming from depth rather than an atmospheric tracer plume reaching the monitors via barometric pumping into the soil included: the generally increasing or level tracer concentrations with depth at site 36 (Figures 66 and 67), the lack of any evidence of an atmospheric tracer plume release after tracer injection (Figure 69), and geophysical measurements (conductivity and lineament analysis) indicating that areas to the south and west of the injection well show at least the potential for near surface expression of migration pathways (Figure 63). Site 36 also showed a hydrocarbon anomaly (Figure 70). It is also interesting to note that Set 18 (14 April – 29 May 2009) revealed an increase in soil-gas tracer above that of Set 17 at both soil-gas arrays and for all tracers. There was also an indication of tracers arriving at sites to the south and to the west of the injection well in Set 18, 1 meter passive grid (Figure 71, bottom left graphic.) There is no known activity at the injection well that would correlate to the time frame of Set 18.

Any potential detection indicated from the results shown here would be exceedingly small. Post injection CO_2, isotope, and hydrocarbon measurements at site 36 did not indicate any significant changes from the pre-injection baseline surveys.

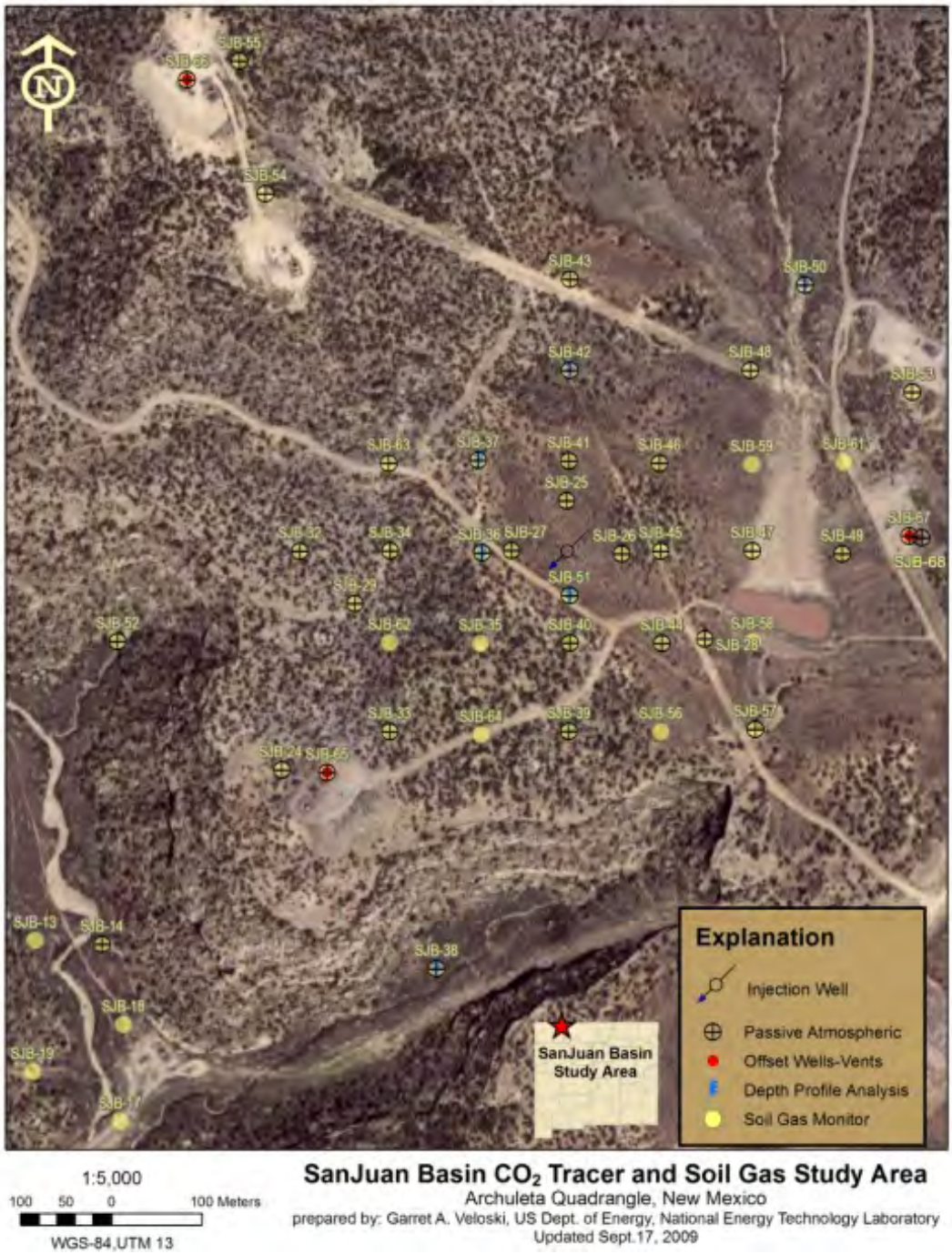

Figure 62. PFC tracer monitoring grid.

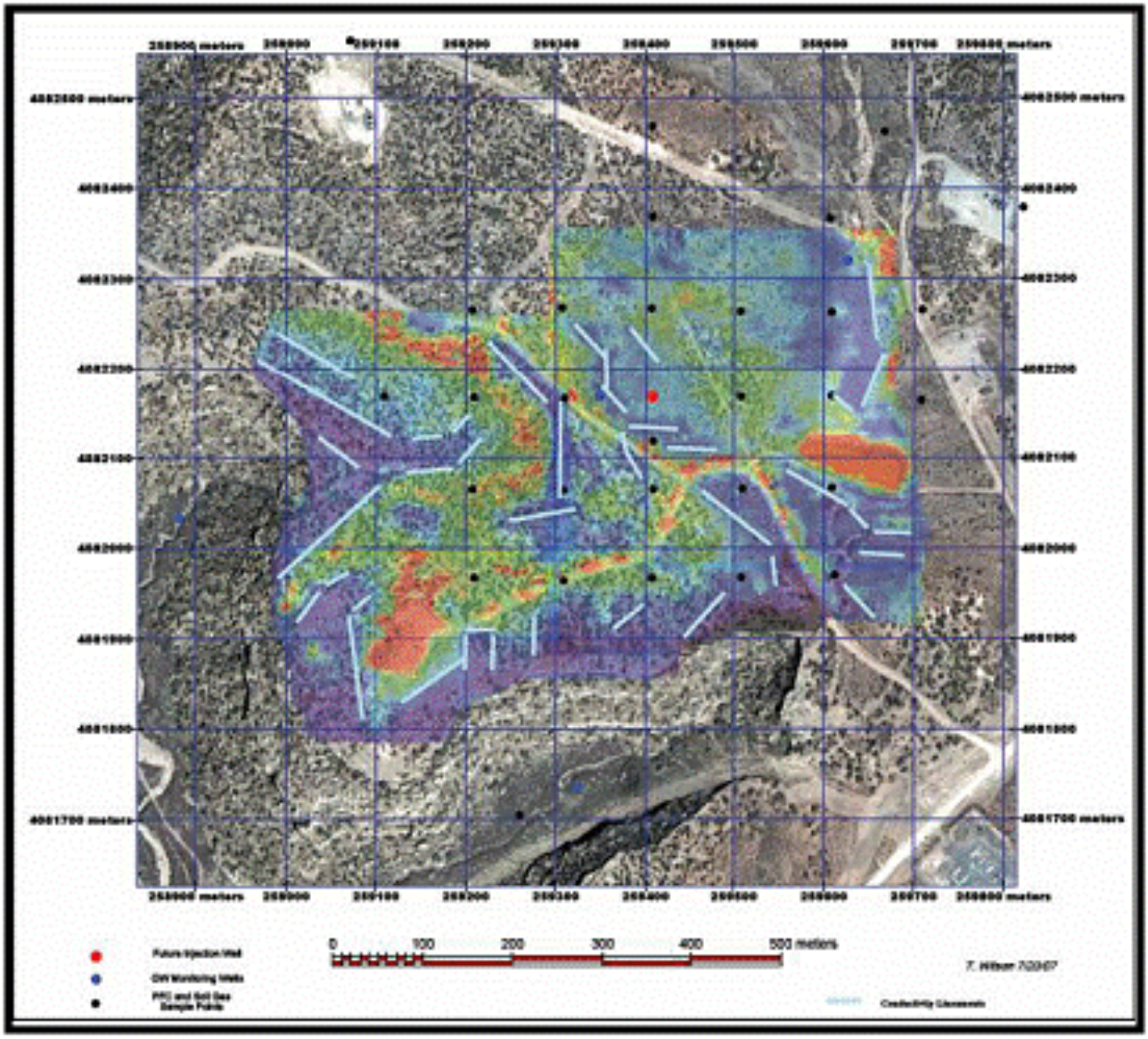

Figure 63. Conductivity survey and lineament.

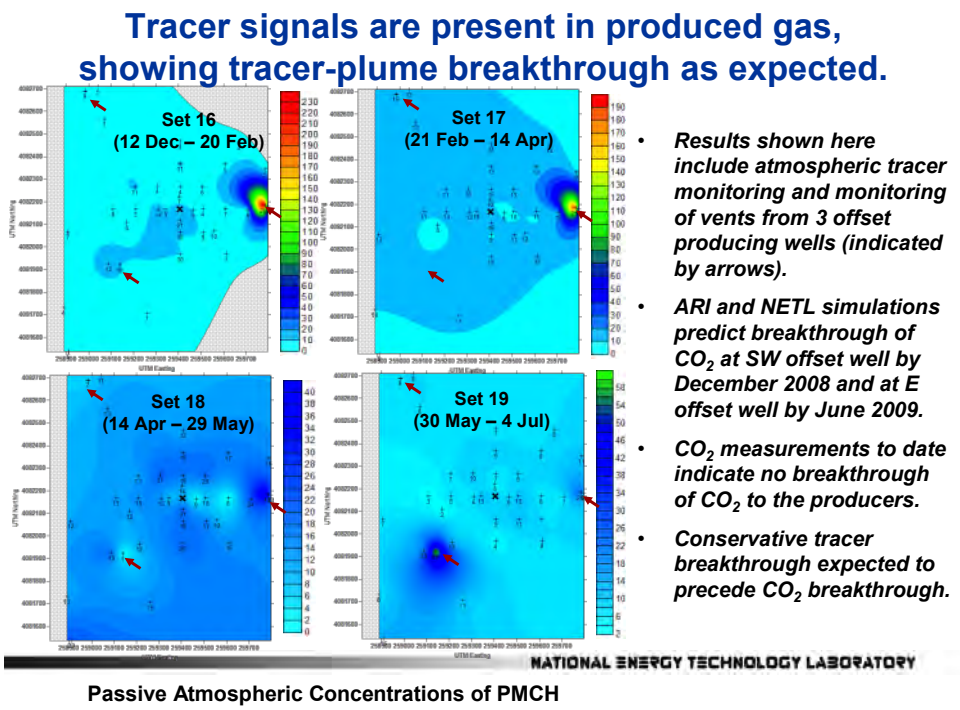

Figure 64. Breakthrough of tracers at the offset well split stream gas vents.

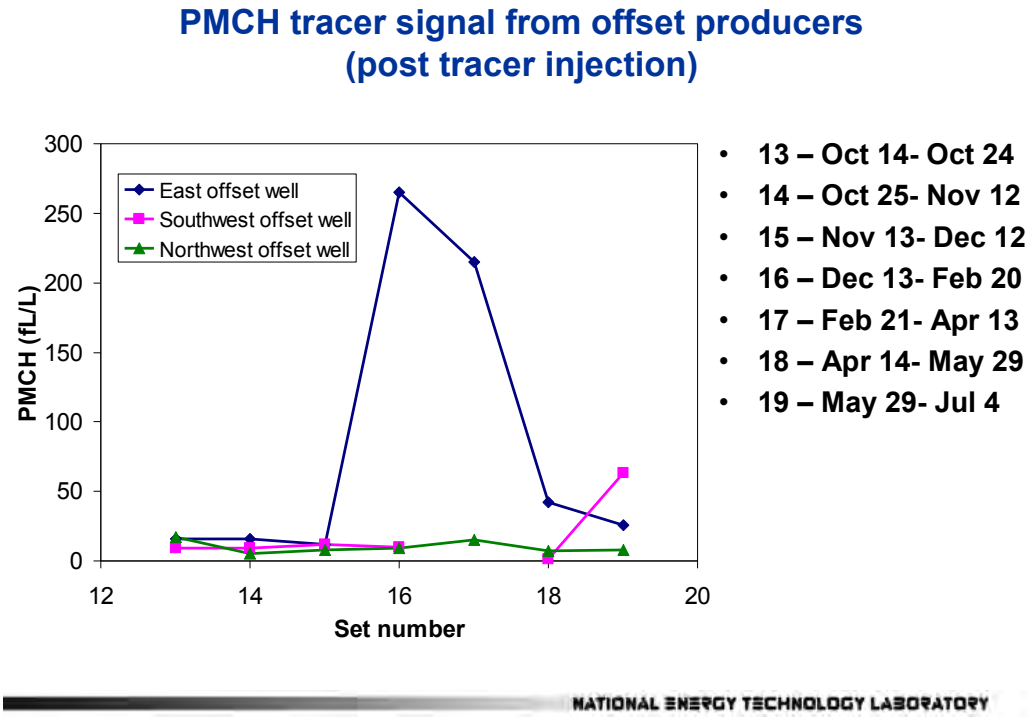

Figure 65. PMCH tracer signal from the offset wells.

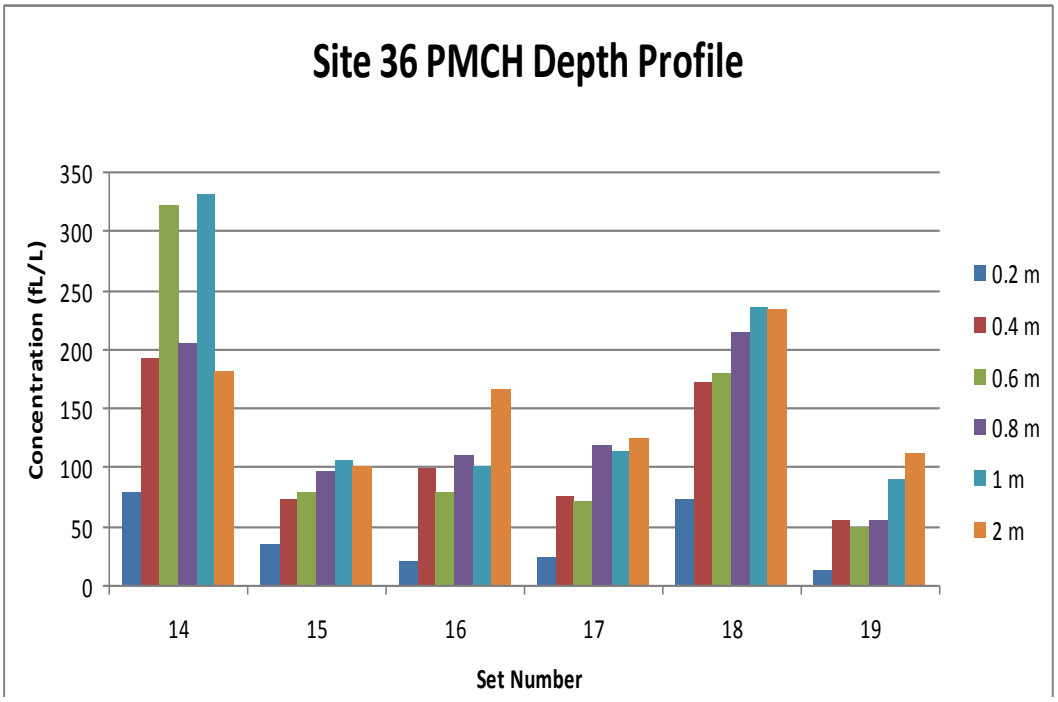

Figure 66. PMCH soil gas depth profile at Site 36.

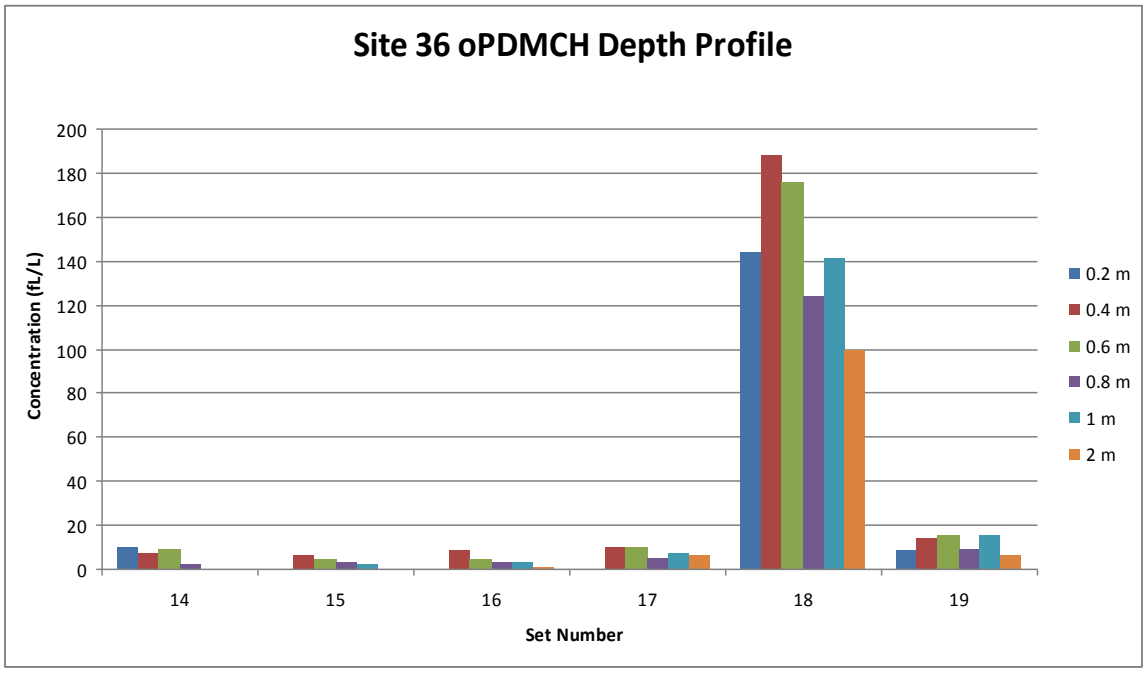

Figure 67. PDCH soil gas depth profile at Site 36.

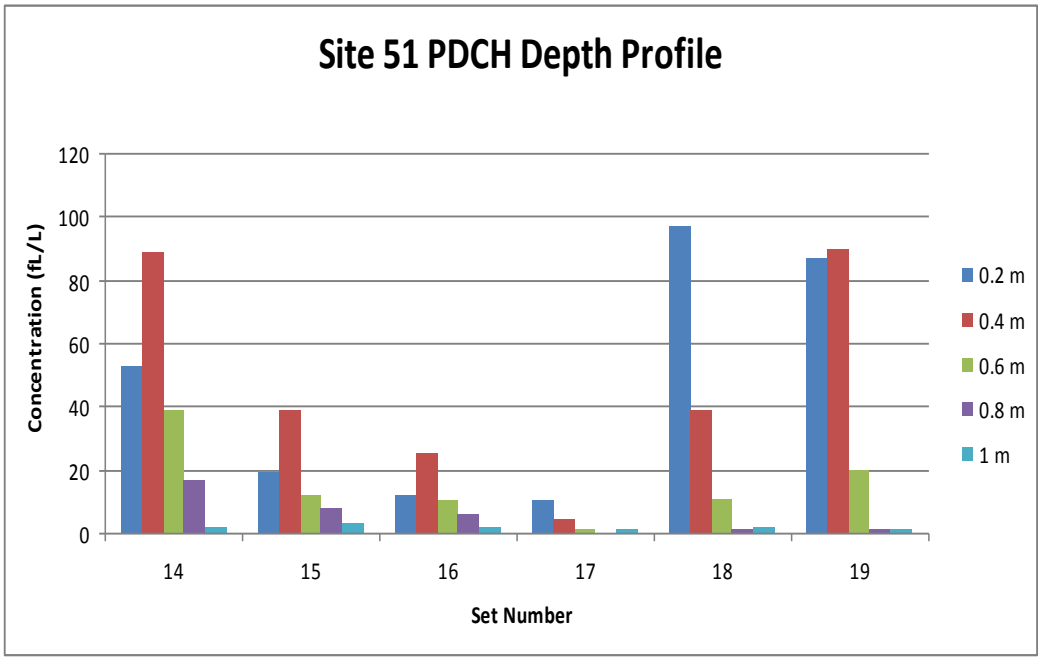

Figure 68. PDCH Soil gas depth profile at Site 51.

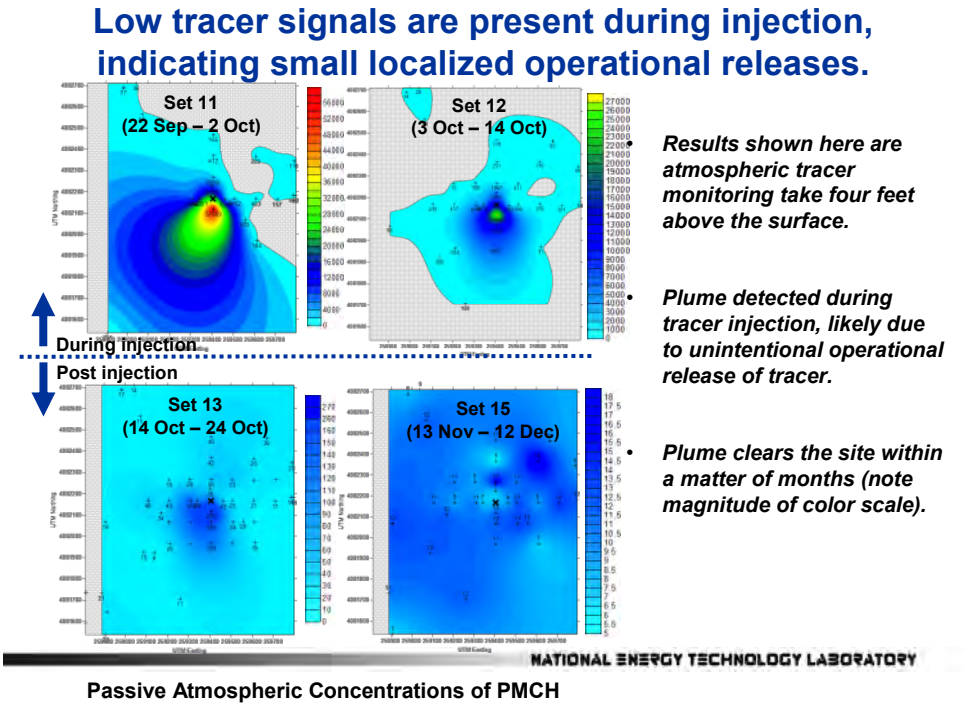

Figure 69. Atmospheric tracer plumes monitored at the San Juan Basin site.

Soil Gas Hydrocarbon Summary

- At majority locations, CH_4 and C_2H_6 decreased with depth.
- Several "anomalies" present where hydrocarbons increase with depth (evidence of possible seepage from depth).
- Magnitude of seepage signatures much higher in March 2007 than other surveys.
- Same nine locations showed hydrocarbon anomalies in all four surveys (Shown in map)

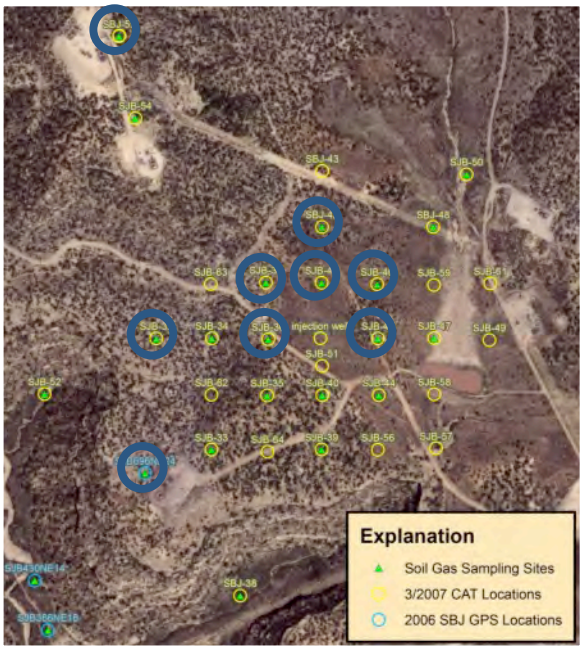

Figure 70. Soil gas hydrocarbon summary at the San Juan Basin site.

Tracer signal is present in soil profile at one site, consistent with tracer migration to surface.

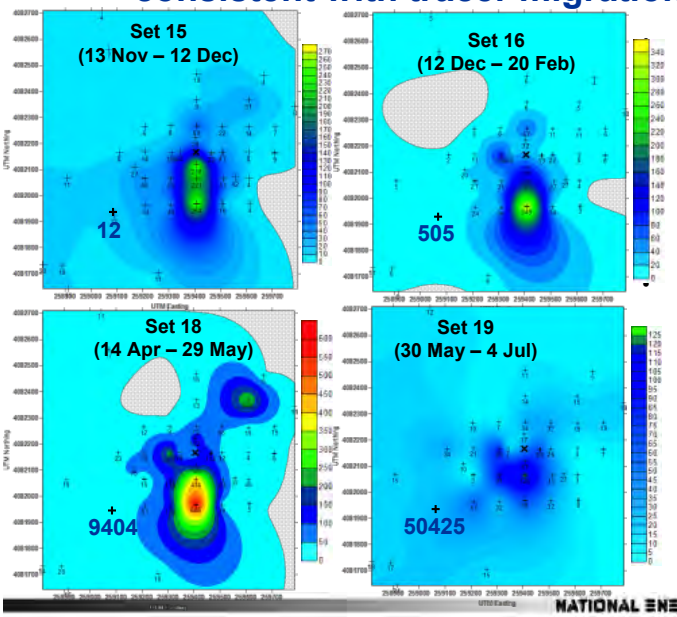

Passive Soil Gas Concentrations of PMCH

Graphs shown here are from soil gas PMCH measurements at a nominal depth of 1 meter.

Tracer signal at a single location near the SW offset well appears in set 16, and is present in 4 most recent surveys.

Signal increases by two orders of magnitude by set 19.

Location of tracer anomaly is one of nine locations reported to have hydrocarbon seepage anomalies.

Detected tracer volume at maximum corresponds to 16 mL of CO_2 leakage at a single point location.

Figure 71. PMCH tracer in soil gas at the San Juan Basin site.

Post-Injection Soil-Gas Surveys

Using a conservative criterion for leakage detection, the criterion employed here for PFC tracers was two orders of magnitude above background levels. Watson et al. (BNL, 2007), suggested one order of magnitude above background levels for quantification of PFC tracers in the atmosphere. Even within the more conservative leakage detection levels, an unambiguous leakage signal was detected at a monitoring location (site 24) just off the well pad at the offset production well ENPG A COM 300. This well is about 0.35 kilometers southwest of the injection well. Tracer levels were evident as early as set 17, exposed from February 21 through April 13, 2009 and remained high through May of 2010.

In an attempt to locate the leakage source, and ascertain the extent of the leakage near site 24, a localized monitoring grid was established and a series of surveys were taken on the well pad and just off the well pad of ENPG A COM 300. On September 26, 2009 active soil-gas depth profiling was employed at these locations using a narrow steel probe, collecting soil-gas samples at depths of 20, 40, 60, 80 and 100 cm as the probe was inserted into the soil. These samples were analyzed for CO_2, methane and ethane (Figures 72B, C and D). Additional samples were actively pumped at the same time through PFC sampling tubes and results are shown for perfluoromethylcyclohexane (PMCH) in Figure 73. Both the levels and trend of increasing concentrations with depth were characteristic of a leakage signal. A second survey at this well pad on October 4, 2009 gave similar results.

Attempts to conduct surveys during the 2009–2010 winter months were not successful due to weather conditions that limited access to the site and created soil conditions that were not suitable for sampling. The next survey at the ENPG A COM300 well pad was conducted on March 28, 2010. A more extensive grid was employed for this survey, with samples collected at 30 and 60 cm. Similar surveys were conducted on May 24, 2010 and on July 20, 2010. The grid area for these surveys was designed to cover most of the well pad and also off the pad to the west where the highest levels were found. To sample on the well pad, the penetrometer was pushed through a compacted layer only a few inches thick, then through into a sandy soil of similar consistency to that of the soil off the well pad. Soil-gas concentrations for all surveys were generally much higher under the well pad.

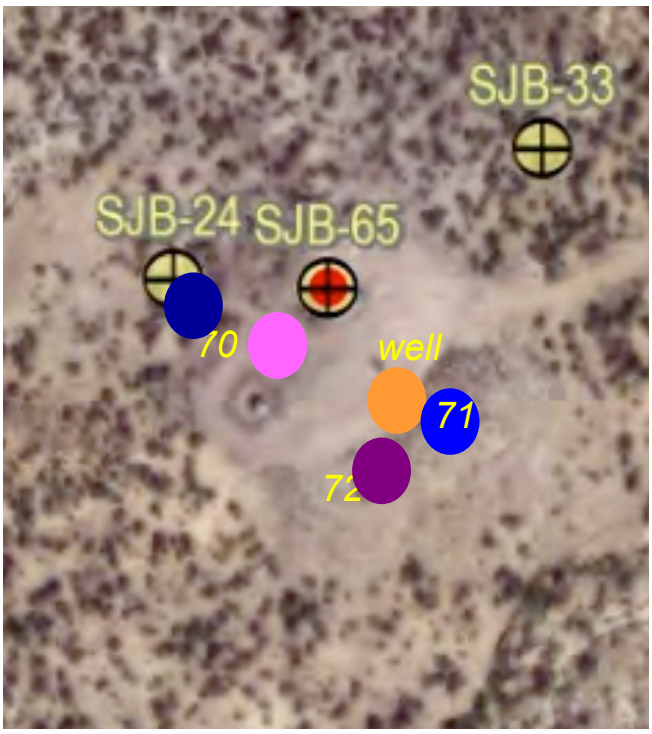

A: Sampling Locations

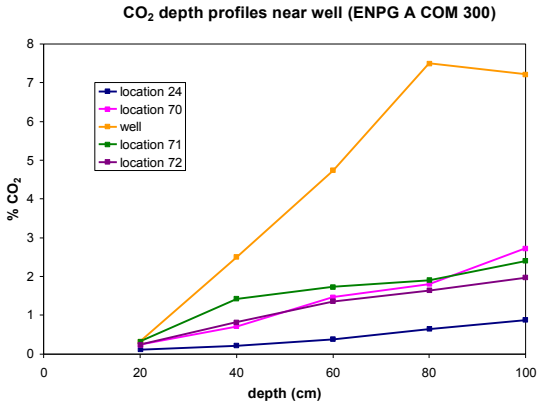

B: CO_2 Depth Profiles

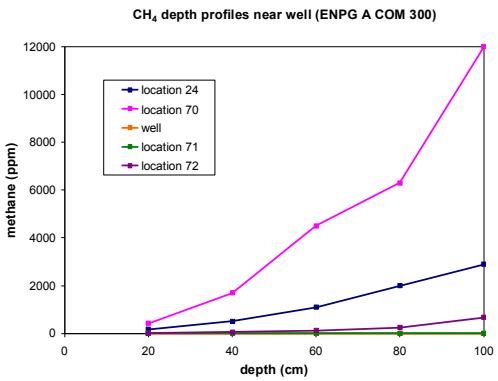

C: Methane Depth Profiles

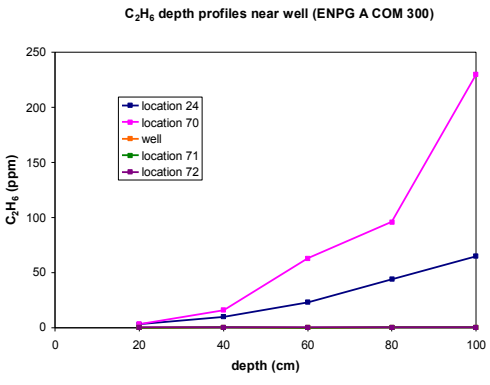

D: Ethane Depth Profiles

Figure 72. Depth profiling grid at southwest offset well, Sept. 27, 2009.

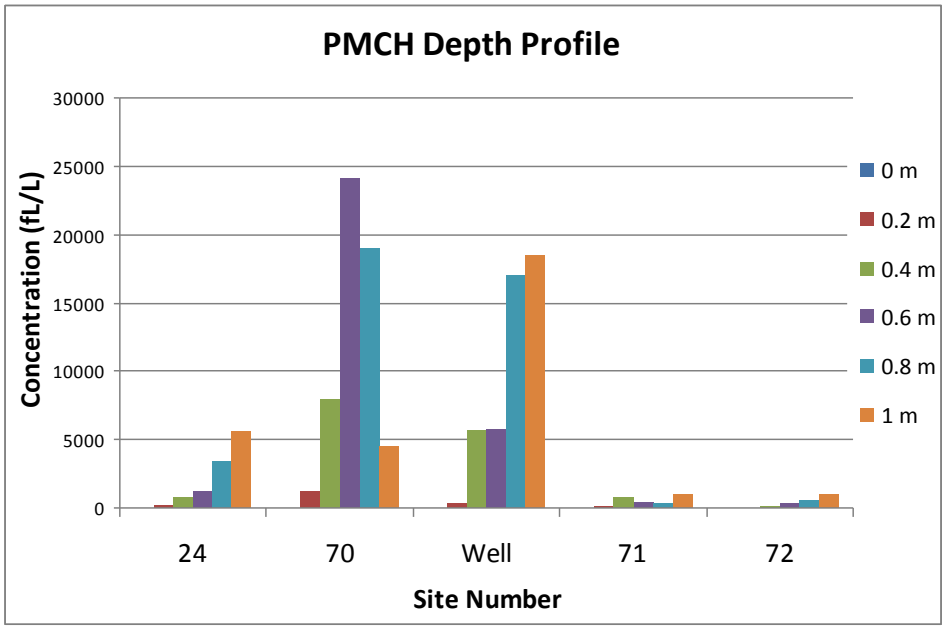

Figure 73. PFC tracer depth profile at southwest offset well, Sept. 27, 2009.

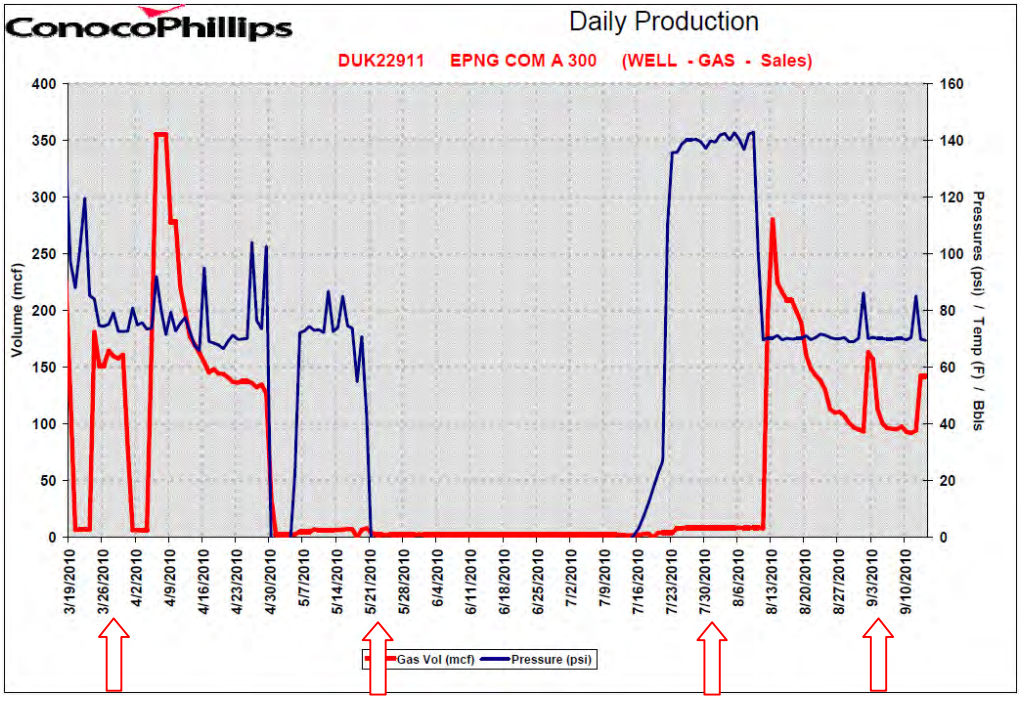

Figure 74. Gas production at the southwest offset well: The approximate dates for soil-gas surveys are indicated with red arrows.

Results under the well pad in March of 2010 were much higher than those found in the 2009 surveys: as high as 16% CO_2, 50% CH_4 and 1,000,000 fL PMCH per liter of soil-gas. These numbers remained high in the survey of May 2010, but fell off significantly with a maximum PMCH concentration of about 300,000 fL per liter of soil-gas. Results for the July survey at the southwest offset well pad were approaching background levels. The production records for this well (Figure 74) help to explain these results. At the May survey, gas production had been shut down for about two weeks, while for the July sampling, the well had been shut down for about two months. The leakage observed under the well pad was clearly related to gas production at the well, and may have been the result of confirmed leakage from a pipe located under the well.

CO_2 Sensors at Offset Production Wells

CO_2 concentration change in the produced gas stream, an important tracking mechanism, was used to determine the subsurface CO_2 movement and the CO_2 breakthrough point. Three CO_2 gas sensors were installed at the three immediate offset production wells. Each sensor, operating at control voltage of 12-24V DC, could measure CO_2 concentrations from 0% to 100%.

Three monitoring wells, EPNG COM A 300S (547m northwest of the injection well), EPNG COM A 300 (499 m southwest of the injection well), and FC STATE COM 1 (386 m almost directly east of the injection well), were selected to monitor changes in CO_2 concentration during the injection process. Figure 75 shows the location of the three monitoring wells and the injection well. The distance of the monitoring wells to the injectors are:

EPNG COM A 300S: 547m northwest of the injection well
EPNG COM A 300: 499 m southwest of the injection well
FC STATE COM: 386 m almost directly east of the injection well

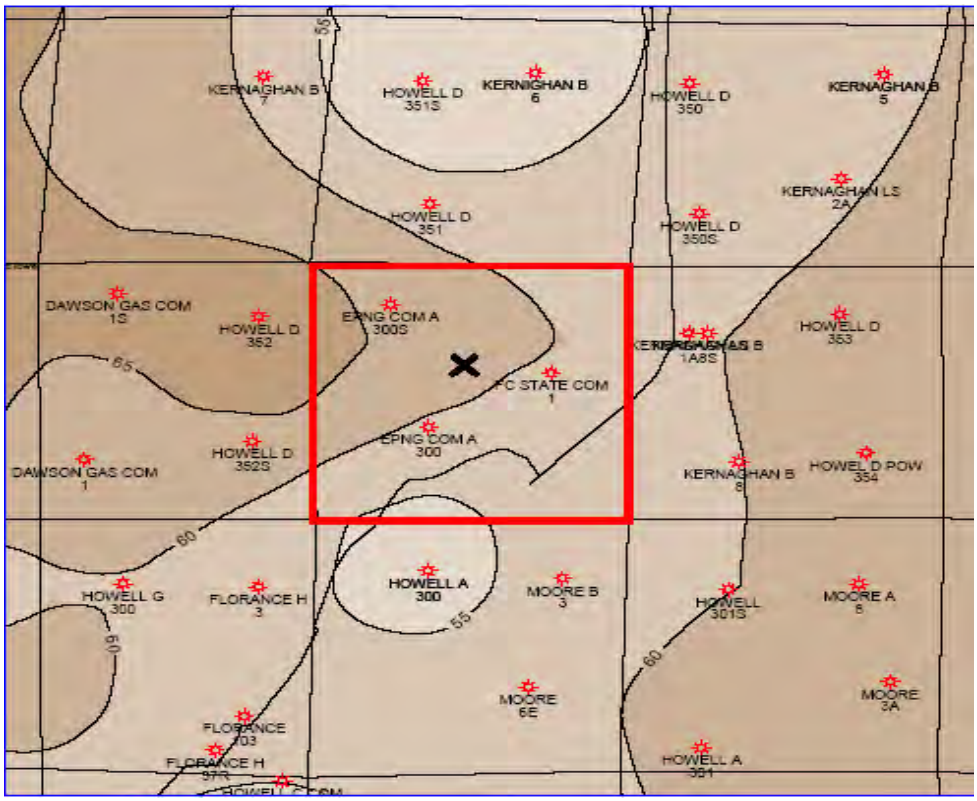

Figure 75. Site map of injection and monitoring wells at the Pump Canyon Site. X indicates the injection well.

Monitoring CO_2 concentration change

Figure 76 shows the results from the CO_2 sensors at well EPNG COM A 300S. CO_2 concentration data from July 1 to July 30, 2008 was regarded as the background data for each well. CO_2 concentration in well EPNG COM A 300S was around 30% in the injection period. A very low CO_2 concentration was observed around August 20, 2008. These low values occurred because the needle valve to control the gas flow rate through the sensor chamber was shut off; thus, no gas passed through the sensor during that time. High CO_2 content fluctuated between November 2008 and March 2009. A desiccant was added during this time to remove water from the gas stream. It was found that the desiccant also adsorbed CO_2 and was sensitive to temperature; thus it would absorb and deabsorb CO_2 on about a 24 hour cycle. On March 11, 2009, the desiccant was removed and the dryer container repositioned to serve as a water drip pod. From that time forward the CO_2 concentration values were much more stable at about 29% CO_2. In August 2009 ConocoPhillips stopped CO_2 injection. The CO_2 concentration in well EPNG COM A 300S remained at ~29% until about December 2009. After December 2009 CO_2 concentration became

erratic and then decreased to ~4%. During this time the well was shut off and thus not dependable. In June 2010 the well was reopened and the CO_2 concentration increased to ~13% by the time the sensors were removed July 22, 2010. There was no evidence of breakthrough.

Figure 77 shows the results of the CO_2 sensor at well EPNG COM A 300. CO_2 content was observed fluctuating before March 2009. After March 11 2009 after the desiccant was removed, CO_2 concentration was quite stable. The average CO_2 concentration in well EPNG COM A 300 was around 20%. Some spikes were observed between March 2009 and May 2010. After discussion with ConocoPhillips, researchers believe that those CO_2 peaks were due to the well operation problem. This well was shut off on May 20, 2010 and reopened on July 15, 2010. The CO_2 concentration in this well was 21% after the well was reopened. The sensors were removed July 22, 2010.

Figure 78 shows the results from the CO_2 sensor at well FC STATE COM. The average CO_2 concentration in well FC STATE COM was 22% before July 2009. CO_2 concentration was observed to slowly increase from 22% to 27.3% from August 1, 2009, to March 4, 2010. After March 4, 2010, CO_2 concentrations in this well fluctuated excessively. It believed that the sensor failed because produced water from the well filled the sensor chamber. When checked and removed on July 22, 2010 the sensor film was corroded and the system filled with water.

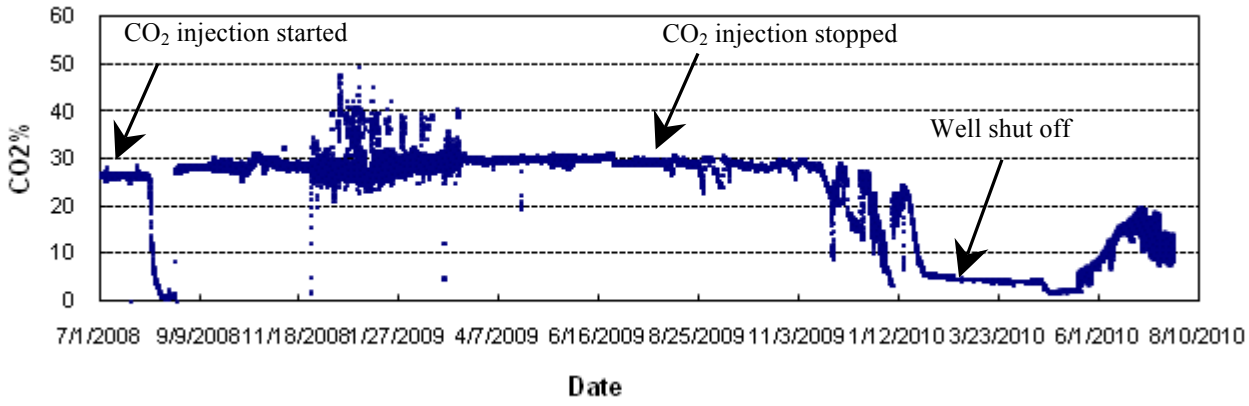

Figure 76. CO_2 concentration change in well EPNG COM A 300S.

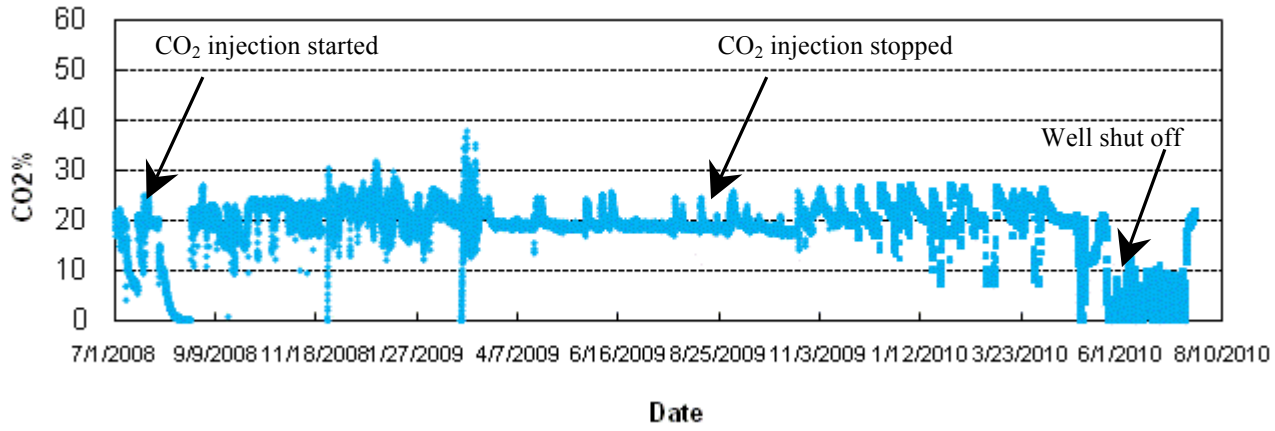

Figure 77. CO_2 concentration change in well EPNG COM A 300.

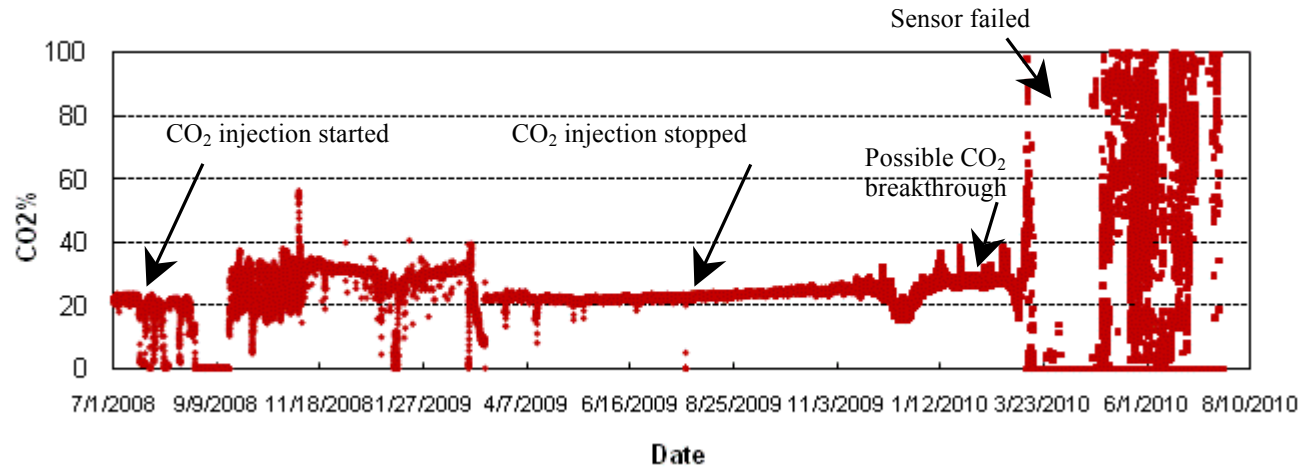

Figure 78. CO_2 concentration change in well FC STATE COM.

Gas sampling data

Gas samples were collected periodically at up to 14 production wells that surrounded the injection well. Tables 10 through 23 show the gas sampling results for each well sampled, including the three monitoring wells. The results confirm that CO_2 concentration did not change for well EPNG COM A 300S and EPNG COM A 300 and increased 8.3% (from 20.2% to 28.5%) for well FC STATE COM between October 24, 2007 and October 20, 2009. In an earlier CO_2 injection into a coalbed it was noted that nitrogen concentration increased a number of months before CO_2 breakthrough. Nitrogen concentration increased from <0.1% to 0.4% from July to September and then to above 1.5% since November 2008 for well EPNG COM A 300. A similar increase from about 0.5% or less to above 1.3% occurred for FC STATE COM (Table 10). Nitrogen may have started to increase in EPNG COM A 300S as of October 2009. Here the

concentration has increased from ≤ 0.1% to 0.476%. In all three cases the nitrogen decreased after peaking and seemed to be returning nearer to normal after more than a year after CO_2 injection ended. It is also interesting to note that the last samples taken over a year after the end of injection showed a decrease of CO_2 and increase of methane for all three of the close production wells. No significant increases in nitrogen content was seen in the wells sampled outside the three monitoring wells. It is known that CO_2 adsorbs and binds tightly onto the coal surface more easily than nitrogen. The nitrogen concentration increase in those two wells was due to the injected CO_2 substituting the adsorbed nitrogen from the coal surface and pushing the released nitrogen out into the reservoir. The last sample data from all the wells showed no breakthrough and the three monitoring wells seemed to be having a decrease in CO_2 and increase in methane concentrations, while there were no significant changes in CO_2 concentrations in the wells outside the three monitoring wells.

Conclusions

Based on the results shown in Figures 76–78 and Tables 10–23, it is concluded that CO_2 concentrations in the monitoring (production) wells of EPNG COM A 300S and EPNG COM A 300 did not change significantly during the injection period July 2008–August 2009. No CO_2 breakthrough was observed from any wells through October 2010. CO_2 concentration in the well FC STATE COM increased slowly from 22% to 27.3% on March 4, 2010, but the sample data from October 2009 and 2010 showed no breakthrough, In fact, the last sample data from all the wells showed no breakthrough; the three monitoring wells seemed to have a decrease in CO_2 and increase in methane concentrations. This could be a small methane bank caused by CO_2 absorption, but since monitoring has stopped on this well no definite conclusion can be postulated.

Table 10. Gas Sampling Results for Well EPNG COM A 300S

SMPL DATE	10/29/2010	10/20/2009	05/20/2009	02/25/2009	11/13/2008	09/11/2008
TEST DATE	11/01/2010	10/28/2009	05/28/2009	03/04/2009	11/18/2008	10/08/2008
RUN NR.	BU100934	BU291439	BU290721	BU290345	BU281523	BU281277
NITROGEN	0.167	0.476	0.110	0.042	0.055	0.063
CO2	21.845	28.609	28.501	27.592	28.692	28.540
METHANE	74.066	69.069	69.469	70.203	69.422	69.628
ETHANE	2.402	1.245	1.281	1.409	1.226	1.203
PROPANE	1.213	0.474	0.506	0.602	0.473	0.447
I-BUTANE	0.148	0.055	0.059	0.070	0.055	0.054
N-BUTANE	0.112	0.043	0.046	0.055	0.043	0.040
I-PENTANE	0.021	0.008	0.009	0.010	0.008	0.008
N-PENTANE	0.008	0.003	0.004	0.004	0.003	0.003
HEXANE +	0.018	0.018	0.015	0.013	0.023	0.014
BTU	836.0	740.0	745.7	758.4	743.5	743.9
GPM	1.0786	0.5070	0.5271	0.5936	0.5040	0.4852
SP.GRAV.	0.7957	0.8471	0.8451	0.8377	0.8463	0.8442

07/28/2008	04/30/2008	01/04/2008	10/24/2007
08/11/2008	05/02/2008	01/09/2008	10/25/2007
BU280992	BU280654	BU280084	BU270877
0.033	0.043	0.048	0.032
28.303	20.790	20.293	28.454
69.987	75.802	74.684	69.960
1.173	2.143	2.897	1.068
0.391	0.987	1.662	0.387
0.050	0.110	0.199	0.047
0.040	0.083	0.158	0.037
0.008	0.016	0.033	0.007
0.004	0.007	0.013	0.003
0.011	0.019	0.013	0.005
745.3	840.8	866.0	742.5
0.4595	0.9238	1.3697	0.4251
0.8409	0.7805	0.7887	0.8415

Table 11. Gas Sampling Results for Well EPNG COM A 300

SMPL DATE	10/29/2010	10/20/2009	05/20/2009	02/25/2009	11/13/2008	09/11/2008
TEST DATE	11/01/2010	10/28/2009	05/28/2009	03/04/2009	11/18/2008	10/08/2008
RUN NR.	BU100933	BU291438	BU290720	BU290344	BU281522	BU281276
NITROGEN	0.525	1.550	1.512	1.724	2.020	0.448
CO2	18.159	23.267	20.011	21.420	23.690	19.384
METHANE	76.583	71.858	74.775	73.704	72.098	76.722
ETHANE	2.716	1.931	2.125	1.838	1.354	1.999
PROPANE	1.516	0.988	1.238	1.026	0.671	1.142
I-BUTANE	0.191	0.115	0.150	0.125	0.082	0.146
N-BUTANE	0.150	0.126	0.123	0.102	0.066	0.110
I-PENTANE	0.029	0.030	0.025	0.020	0.013	0.022
N-PENTANE	0.012	0.021	0.011	0.009	0.006	0.010
HEXANE +	0.119	0.114	0.030	0.032	0.000	0.017
BTU	883.3	804.8	840.2	817.1	778.6	853.8
GPM	1.3214	0.9352	1.0235	0.8719	0.6014	0.9507
SP.GRAV.	0.7701	0.8132	0.7831	0.7932	0.8084	0.7703

07/26/2008	04/30/2008	01/04/2008	10/24/2007
08/11/2008	05/02/2008	01/09/2008	10/25/2007
BU280993	BU280656	BU280083	BU270876
0.078	0.147	0.039	0.051
20.587	19.711	19.446	19.810
77.999	76.295	78.883	75.926
0.969	2.202	1.099	2.375
0.270	1.309	0.418	1.454
0.038	0.160	0.055	0.182
0.030	0.126	0.041	0.147
0.007	0.025	0.008	0.028
0.004	0.011	0.004	0.013
0.018	0.014	0.007	0.014
819.4	858.3	834.8	863.0
0.3674	1.0605	0.4472	1.1624
0.7640	0.7754	0.7548	0.7791

Table 12. Gas Sampling Results for Well FC STATE COM

SMPL DATE	10/29/2010	10/20/2009	05/20/2009	02/25/2009	11/13/2008	09/11/2008
TEST DATE	11/01/2010	10/28/2009	05/28/2009	03/04/2009	11/18/2008	10/08/2008
RUN NR.	BU100935	BU291440	BU290722	BU290346	BU281524	BU281278
NITROGEN	0.599	1.339	1.433	1.482	1.786	0.509
CO2	18.511	28.482	25.419	25.851	24.815	22.485
METHANE	75.646	68.355	71.217	71.081	71.777	74.625
ETHANE	3.023	1.219	1.264	1.090	1.098	1.466
PROPANE	1.762	0.475	0.524	0.391	0.412	0.683
I-BUTANE	0.212	0.056	0.062	0.049	0.051	0.083
N-BUTANE	0.180	0.047	0.052	0.040	0.041	0.075
I-PENTANE	0.033	0.009	0.010	0.008	0.008	0.018
N-PENTANE	0.016	0.004	0.005	0.003	0.005	0.012
HEXANE +	0.018	0.014	0.014	0.005	0.007	0.044
BTU	882.1	732.3	763.8	754.5	762.5	809.6
GPM	1.4455	0.5007	0.5306	0.4339	0.4445	0.6613
SP.GRAV.	0.7759	0.8492	0.8207	0.8224	0.8139	0.7929

07/26/2008	04/30/2008	01/04/2008	10/24/2007
08/11/2008	05/02/2008	01/09/2008	10/25/2007
BU280994	BU280655	BU280085	BU270883
0.352	0.438	0.036	0.238
24.039	24.671	20.235	20.197
73.872	73.134	79.121	77.410
1.173	1.161	0.529	1.326
0.433	0.470	0.059	0.652
0.056	0.058	0.009	0.082
0.048	0.046	0.007	0.065
0.010	0.009	0.001	0.013
0.005	0.004	0.000	0.007
0.012	0.009	0.003	0.010
786.4	779.4	814.6	832.0
0.4772	0.4820	0.1644	0.5932
0.8014	0.8082	0.7546	0.7672

Table 13. Gas Sampling Results for Well HOWELL A #300

SMPL DATE	10/29/2010	10/20/2009	05/20/2009	02/25/2009	11/13/2008	09/11/2008
TEST DATE	11/01/2010	10/28/2009	05/28/2009	03/04/2009	11/18/2008	10/08/2008
RUN NR.	BU100936	BU291441	BU290723	BU290347	BU281525	BU281279
NITROGEN	0.340	0.117	0.102	0.038	0.102	0.063
CO2	15.973	18.596	25.707	25.515	24.253	23.627
METHANE	79.007	77.648	73.396	73.703	74.707	75.426
ETHANE	3.268	2.532	0.641	0.618	0.702	0.686
PROPANE	1.161	0.903	0.110	0.098	0.178	0.151
I-BUTANE	0.143	0.106	0.014	0.012	0.021	0.021
N-BUTANE	0.081	0.060	0.012	0.011	0.020	0.016
I-PENTANE	0.015	0.012	0.002	0.002	0.004	0.003
N-PENTANE	0.006	0.004	0.000	0.000	0.002	0.000
HEXANE +	0.006	0.022	0.016	0.003	0.011	0.007
BTU	898.0	863.4	761.0	762.7	777.5	783.3
GPM	1.2762	0.9949	0.2179	0.2016	0.2570	0.2411
SP.GRAV.	0.7421	0.7600	0.8094	0.8066	0.7967	0.7897

04/30/2008	01/04/2008
05/05/2008	01/09/2008
BU280649	BU280086
0.801	0.056
17.020	24.286
78.225	74.818
2.735	0.666
0.999	0.136
0.122	0.018
0.071	0.014
0.014	0.003
0.006	0.000
0.007	0.003
875.4	776.0
1.0790	0.2283
0.7494	0.7959

Table 14. Gas Sampling Results for Well HOWELL A #301S

SMPL DATE	10/29/2010	05/20/2009	02/25/2009	11/13/2008
TEST DATE	11/01/2010	05/27/2009	03/04/2009	11/18/2008
RUN NR.	BU100937	BU290724	BU290348	BU281526
NITROGEN	0.098	0.125	0.035	0.097
CO2	18.744	8.691	19.146	8.690
METHANE	76.112	81.483	76.548	82.127
ETHANE	3.148	5.617	2.774	5.358
PROPANE	1.484	3.308	1.195	2.787
I-BUTANE	0.177	0.367	0.144	0.338
N-BUTANE	0.137	0.283	0.115	0.264
I-PENTANE	0.025	0.052	0.021	0.051
N-PENTANE	0.011	0.023	0.009	0.023
HEXANE +	0.064	0.051	0.013	0.265
BTU	881.4	1,037.8	867.0	1,036.3
GPM	1.3931	2.6723	1.1709	2.5390
SP.GRAV.	0.7738	0.7117	0.7704	0.7106

Table 15. Gas Sampling Results for Well HOWELL D #350S

SMPL DATE	10/29/2010	10/20/2009	05/20/2009	02/25/2009	11/13/2008	09/11/2008
TEST DATE	11/01/2010	10/28/2009	05/28/2009	03/04/2009	11/18/2008	10/08/2008
RUN NR.	BU100938	BU291443	BU290725	BU290349	BU281527	BU281281
NITROGEN	0.113	0.178	0.075	0.036	0.095	0.029
CO2	25.114	24.662	25.192	25.056	20.402	22.596
METHANE	72.001	72.556	72.254	72.624	75.852	74.635
ETHANE	1.784	1.668	1.612	1.499	2.187	1.766
PROPANE	0.766	0.739	0.688	0.623	1.167	0.766
I-BUTANE	0.090	0.083	0.078	0.071	0.128	0.100
N-BUTANE	0.077	0.071	0.067	0.062	0.115	0.078
I-PENTANE	0.013	0.013	0.012	0.011	0.020	0.015
N-PENTANE	0.007	0.006	0.006	0.006	0.010	0.008
HEXANE +	0.035	0.024	0.016	0.012	0.024	0.007
BTU	790.2	792.1	786.0	785.4	848.8	815.6
GPM	0.7646	0.7168	0.6808	0.6267	1.0058	0.7520
SP.GRAV.	0.8188	0.8132	0.8167	0.8138	0.7799	0.7935

04/30/2008	01/04/2008	10/24/2007
05/05/2008	01/09/2008	10/25/2007
BU280651	BU280088	BU270879
0.171	0.037	0.030
25.011	25.192	25.335
72.791	72.868	72.772
1.345	1.271	1.243
0.539	0.498	0.489
0.063	0.060	0.057
0.054	0.054	0.050
0.010	0.010	0.009
0.005	0.005	0.005
0.011	0.005	0.010
781.6	779.6	777.9
0.5561	0.5213	0.5110
0.8123	0.8125	0.8134

Table 16. Gas Sampling Results for Well HOWELL D #351

SMPL DATE	10/29/2010	10/20/2009	05/20/2009	02/25/2009	11/13/2008	09/11/2008
TEST DATE	11/01/2010	10/28/2009	05/27/2009	03/04/2009	11/18/2008	10/08/2008
RUN NR.	BU100939	BU291444	BU290726	BU290350	BU281528	BU281282
NITROGEN	0.149	0.109	0.045	0.034	0.720	0.027
CO2	25.355	8.819	24.507	17.442	12.553	16.088
METHANE	72.327	85.725	73.580	79.908	83.010	82.950
ETHANE	1.445	3.101	1.298	1.694	2.308	0.698
PROPANE	0.543	1.724	0.407	0.691	1.057	0.169
I-BUTANE	0.071	0.220	0.059	0.098	0.148	0.024
N-BUTANE	0.056	0.177	0.048	0.081	0.124	0.019
I-PENTANE	0.011	0.037	0.011	0.017	0.026	0.004
N-PENTANE	0.006	0.020	0.006	0.010	0.022	0.002
HEXANE +	0.037	0.068	0.039	0.025	0.032	0.019
BTU	780.6	987.7	786.6	867.0	922.8	861.1
GPM	0.5995	1.4827	0.5171	0.7218	1.0275	0.2577
SP.GRAV.	0.8167	0.6814	0.8060	0.7427	0.7070	0.7172

01/04/2008	10/24/2007
01/09/2008	10/25/2007
BU280089	BU270880
0.050	0.035
10.692	24.294
85.074	73.946
2.570	1.174
1.219	0.422
0.173	0.056
0.138	0.044
0.030	0.010
0.016	0.005
0.038	0.014
954.0	786.8
1.1567	0.4740
0.6898	0.8024

Table 17. Sampling Results for Well HOWELL D #352S

SMPL DATE	10/29/2010	10/20/2009	05/20/2009	02/25/2009	11/13/2008	09/11/2008
TEST DATE	11/01/2010	10/28/2009	05/27/2009	03/04/2009	11/18/2008	10/08/2008
RUN NR.	BU100940	BU291445	BU290727	BU290351	BU281529	BU281283
NITROGEN	0.185	0.156	0.069	0.022	0.063	0.079
CO2	16.564	18.548	20.908	20.544	19.561	19.714
METHANE	81.691	80.611	78.382	78.845	79.778	79.559
ETHANE	1.006	0.605	0.565	0.538	0.540	0.570
PROPANE	0.360	0.066	0.054	0.042	0.038	0.063
I-BUTANE	0.043	0.010	0.009	0.007	0.007	0.010
N-BUTANE	0.032	0.004	0.003	0.001	0.002	0.005
I-PENTANE	0.007	0.000	0.000	0.000	0.000	0.000
N-PENTANE	0.002	0.000	0.000	0.000	0.000	0.000
HEXANE +	0.110	0.000	0.010	0.001	0.011	0.000
BTU	864.8	831.1	807.9	811.2	821.1	819.7
GPM	0.4448	0.1846	0.1743	0.1584	0.1627	0.1747
SP.GRAV.	0.7288	0.7390	0.7616	0.7571	0.7481	0.7499

04/30/2008	01/04/2008	10/24/2007
05/02/2008	01/09/2008	10/25/2007
BU280652	BU280090	BU270881
0.037	0.034	0.022
20.595	21.307	21.652
78.822	78.100	77.783
0.505	0.513	0.504
0.032	0.038	0.031
0.007	0.006	0.006
0.002	0.002	0.002
0.000	0.000	0.000
0.000	0.000	0.000
0.000	0.000	0.000
810.1	803.0	799.5
0.1467	0.1503	0.1458
0.7576	0.7645	0.7676

Table 18. Gas Sampling Results for Well HOWELL D #353

SMPL DATE	10/29/2010	10/20/2009	05/20/2009	02/25/2009	11/13/2008	09/11/2008
TEST DATE	11/01/2010	10/28/2009	05/28/2009	03/04/2009	11/18/2008	10/08/2008
RUN NR.	BU100941	BU291446	BU290728	BU290352	BU281530	BU281284
NITROGEN	0.129	0.188	0.037	0.014	0.032	0.042
CO2	21.841	21.151	21.956	23.794	25.149	25.007
METHANE	76.437	76.681	76.103	74.725	73.451	73.510
ETHANE	1.192	1.476	1.438	1.172	1.108	1.143
PROPANE	0.275	0.393	0.367	0.240	0.213	0.229
I-BUTANE	0.031	0.044	0.041	0.028	0.023	0.026
N-BUTANE	0.023	0.031	0.029	0.019	0.015	0.020
I-PENTANE	0.005	0.006	0.006	0.003	0.003	0.005
N-PENTANE	0.003	0.003	0.003	0.000	0.002	0.003
HEXANE +	0.064	0.027	0.020	0.005	0.004	0.015
BTU	809.5	818.8	811.0	787.4	772.4	775.0
GPM	0.4432	0.5423	0.5203	0.3979	0.3707	0.3931
SP.GRAV.	0.7783	0.7736	0.7800	0.7946	0.8070	0.8065

05/08/2008	01/04/2008	10/24/2007
05/08/2008	01/09/2008	10/25/2007
BU280653	BU280091	BU270882
0.088	0.024	0.014
24.777	25.169	23.309
73.723	73.445	75.251
1.131	1.102	1.122
0.221	0.213	0.244
0.026	0.025	0.029
0.016	0.016	0.019
0.003	0.003	0.004
0.001	0.000	0.002
0.014	0.003	0.006
776.4	772.2	792.2
0.3845	0.3689	0.3876
0.8042	0.8071	0.7897

Table 19. Gas Sampling Results for Well FLETCHER 2 (BP)

SMPL DATE	10/29/2010	10/20/2009	02/25/2009	11/13/2008
TEST DATE	11/01/2010	10/28/2009	03/04/2009	11/18/2008
RUN NR.	BP100001	BP290028	BP290006	BP280015
NITROGEN	0.403	0.939	0.600	0.525
CO2	24.487	26.479	30.504	30.490
METHANE	73.673	71.226	68.163	68.256
ETHANE	0.990	0.969	0.646	0.639
PROPANE	0.339	0.304	0.070	0.073
I-BUTANE	0.042	0.035	0.009	0.008
N-BUTANE	0.034	0.030	0.007	0.007
I-PENTANE	0.006	0.005	0.000	0.001
N-PENTANE	0.003	0.002	0.000	0.000
HEXANE +	0.023	0.011	0.001	0.001
BTU	778.2	751.0	705.9	706.8
GPM	0.3961	0.3712	0.1975	0.1965
SP.GRAV.	0.8040	0.8244	0.8572	0.8568

Table 20. Gas Sampling Results for Well FLORANCE H3 (BP)

SMPL DATE	10/29/2010	10/20/2009	02/25/2009	11/13/2008
TEST DATE	11/01/2010	10/28/2009	03/04/2009	11/18/2008
RUN NR.	BP100002	BP290029	BP290007	BP280014
NITROGEN	0.102	0.177	0.028	0.080
CO2	23.255	22.761	22.600	22.744
METHANE	75.397	76.036	76.280	76.114
ETHANE	0.992	0.841	0.875	0.856
PROPANE	0.206	0.151	0.173	0.168
I-BUTANE	0.025	0.019	0.022	0.021
N-BUTANE	0.017	0.013	0.015	0.014
I-PENTANE	0.004	0.002	0.003	0.003
N-PENTANE	0.000	0.000	0.000	0.000
HEXANE +	0.002	0.000	0.004	0.000
BTU	789.8	791.7	795.8	793.3
GPM	0.3379	0.2774	0.2963	0.2876
SP.GRAV.	0.7882	0.7823	0.7806	0.7821

Table 21. Gas Sampling Results for Well KERNAGHAN B8 (BP)

SMPL DATE	10/29/2010	10/20/2009	02/25/2009	11/13/2008
TEST DATE	11/01/2010	10/28/2009	03/04/2009	11/18/2008
RUN NR.	BP100003	BP290030	BP290008	BP280013
NITROGEN	0.106	0.085	0.100	0.460
CO2	17.750	18.107	18.368	18.255
METHANE	79.015	78.771	78.630	78.540
ETHANE	2.084	1.992	1.914	1.811
PROPANE	0.806	0.818	0.767	0.729
I-BUTANE	0.108	0.107	0.100	0.094
N-BUTANE	0.072	0.072	0.069	0.065
I-PENTANE	0.017	0.018	0.017	0.016
N-PENTANE	0.008	0.008	0.007	0.007
HEXANE +	0.034	0.022	0.028	0.023
BTU	868.2	863.7	859.5	855.2
GPM	0.8615	0.8349	0.7985	0.7549
SP.GRAV.	0.7493	0.7519	0.7538	0.7531

Table 22. Gas Sampling Results for Well KERNAGHAN B8S (BP)

SMPL DATE	10/29/2010	10/20/2009	02/25/2009
TEST DATE	11/01/2010	10/28/2009	03/04/2009
RUN NR.	BP100004	BP290031	BP290009
NITROGEN	0.100	0.164	0.019
CO2	19.466	20.896	19.528
METHANE	77.815	76.586	78.750
ETHANE	1.658	1.503	1.140
PROPANE	0.756	0.668	0.444
I-BUTANE	0.089	0.073	0.054
N-BUTANE	0.077	0.062	0.047
I-PENTANE	0.014	0.012	0.009
N-PENTANE	0.006	0.006	0.004
HEXANE +	0.019	0.030	0.005
BTU	845.7	827.8	835.0
GPM	0.7207	0.6492	0.4665
SP.GRAV.	0.7626	0.7750	0.7559

Table 23. Gas Sampling Results for Well MOORE B3 (BP)

SMPL DATE	10/29/2010	10/20/2009	02/25/2009	11/13/2008
TEST DATE	11/01/2010	10/28/2009	03/04/2009	11/18/2008
RUN NR.	BP100005	BP290032	BP290010	BP280012
NITROGEN	0.234	0.364	0.325	0.045
CO2	25.176	22.964	23.820	24.993
METHANE	72.487	75.522	74.967	74.005
ETHANE	0.831	0.846	0.719	0.762
PROPANE	0.153	0.218	0.127	0.146
I-BUTANE	0.019	0.027	0.016	0.018
N-BUTANE	0.016	0.022	0.013	0.015
I-PENTANE	0.000	0.005	0.003	0.004
N-PENTANE	0.000	0.002	0.000	0.005
HEXANE +	1.084	0.030	0.010	0.007
BTU	813.4	790.6	778.6	770.3
GPM	0.7592	0.3178	0.2421	0.2609
SP.GRAV.	0.8361	0.7866	0.7924	0.8033

Tiltmeters, GPS and InSar

Surface Deformation

CO_2 injection was terminated on August 12, 2009. Tilt measurements continued for approximately three months after cessation of injection. The cumulative surface deformation map generated from the tiltmeter data for the period of August 01, 2008 to November 17, 2009 is presented in Figure 79.

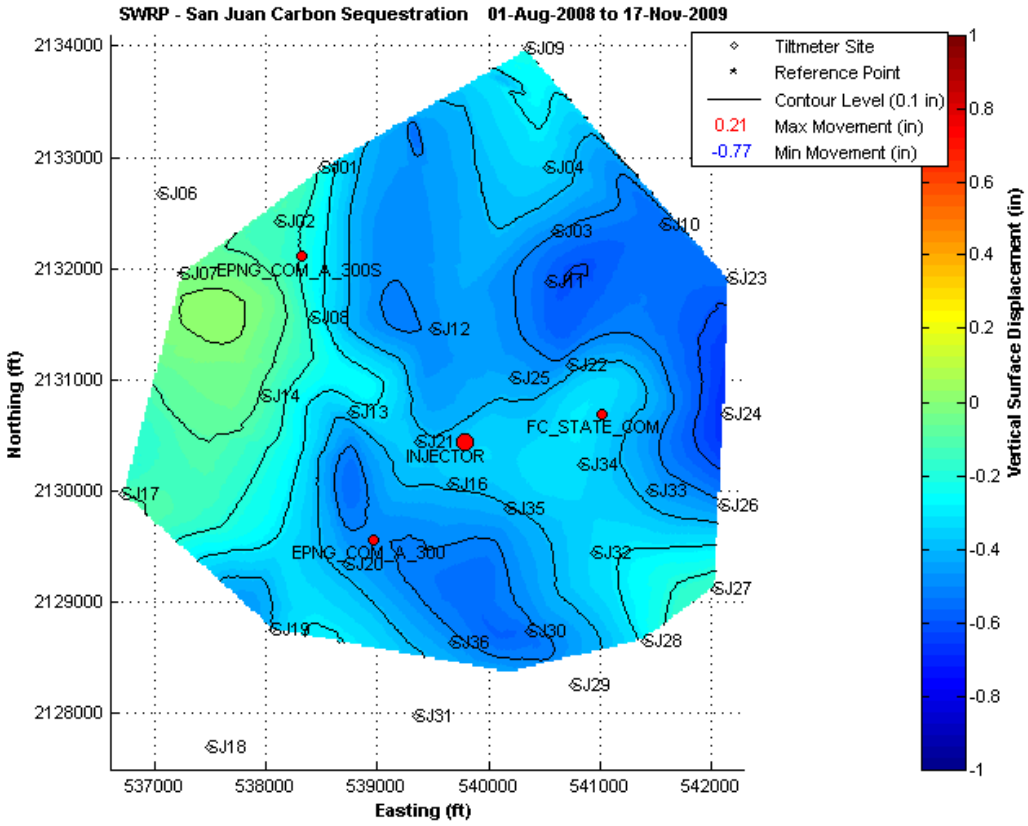

Figure 79. Cumulative surface deformation for August 01, 2008 to November 17, 2009.

From the cumulative surface deformation it is seen that there is an overall subsidence in the field. The subsidence is spread out primarily around the periphery of the tiltmeter array. There is some minimal uplift to the immediate SW of well EPNG Com A 300S but that could be due to the reference tiltmeter(s) (SJ06/SJ07) being located in that region. (Note: All surface deformation is computed with reference to a tiltmeter site, which is assumed to be at constant elevation. For this project, sites 06 and 07 were chosen as the primary and secondary reference sites).

In addition to the production from the three wells producing from the Fruitland coal in Section 32, there are numerous wells producing from the periphery of Section 32 (Figure 80).

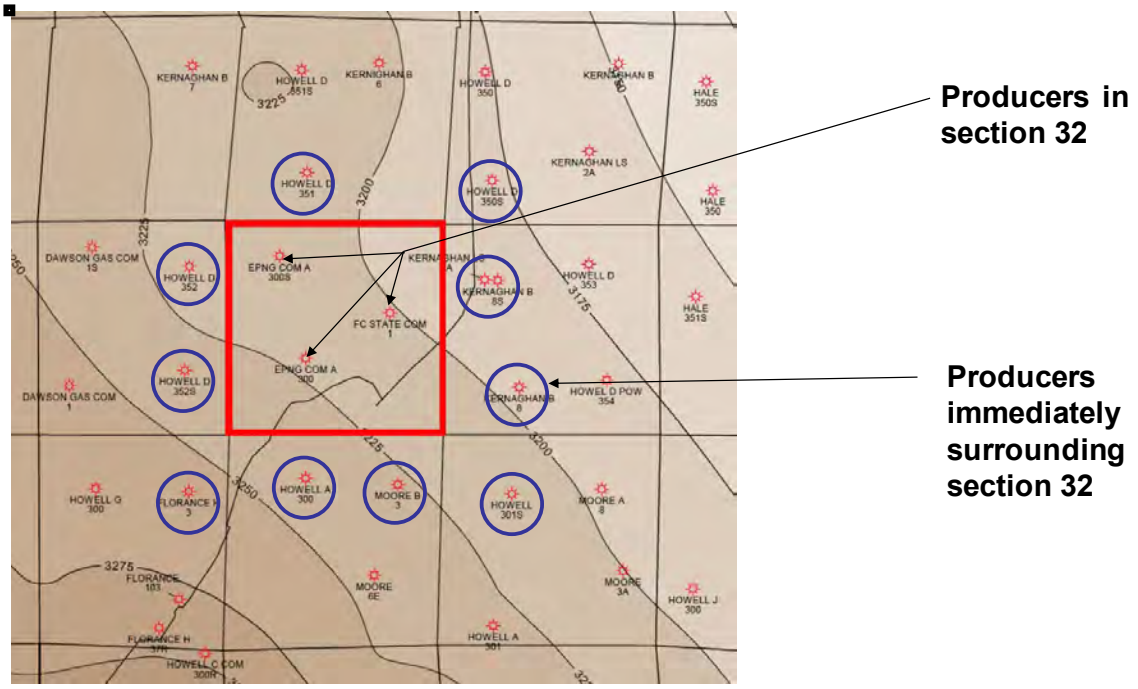

Figure 80. Well layout showing producers from Section 32 and surrounding sections.

In addition to the 13 producers surrounding the CO_2 injector in section 32 and producing from the Fruitland coal at approx 3,000 ft, there were also two wells, EPNG Com A 002 and 002A producing from the Mesa Verde formation in section 32 at approximately 5,500 ft. Production information from these two wells, as well as some of the producers surrounding the injector, was unavailable.

Injection and production rate information are presented in Figures 81 and 82. From Figure 81 it is clear that the injection rate of CO_2 has not been continuous. Initially, the target rate of 3,800 Mscf/day was reached, however it was unsustainable for any length of time, apart from the occasional instantaneous spikes at restart following a period of shut-in with additional periods of shut-in. CO_2 injection ended on August 12, 2009.

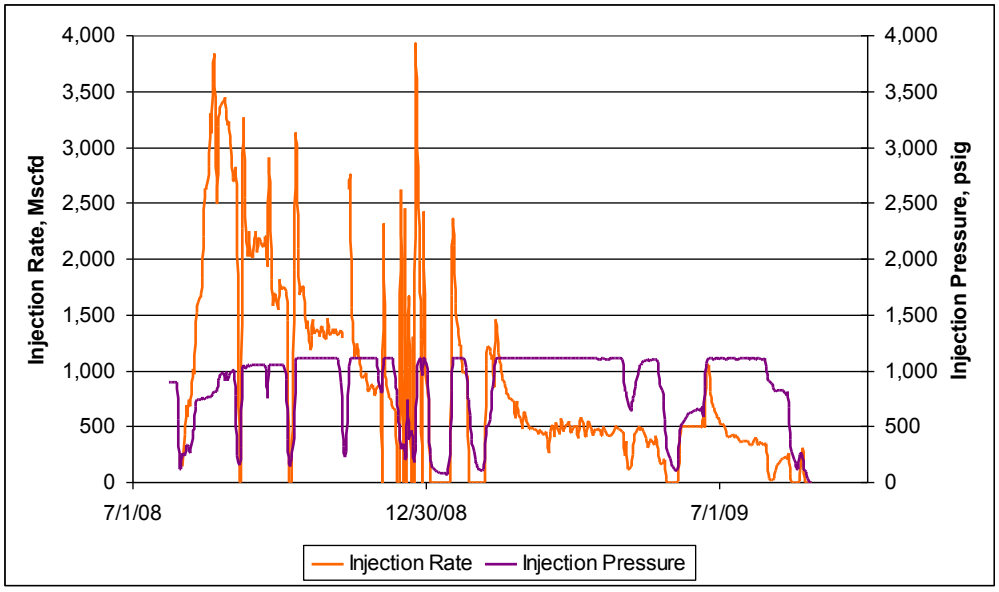

Figure 81. CO_2 injection rate and wellhead pressure.

The production rate from the three producers surrounding the injector has been fairly constant (Figure 82). Although initially there was fluctuation in the production rate, since March 01, 2009 the production rate was constant. Individual wells may have exhibited rate fluctuation but the sum of the three remained fairly constant.

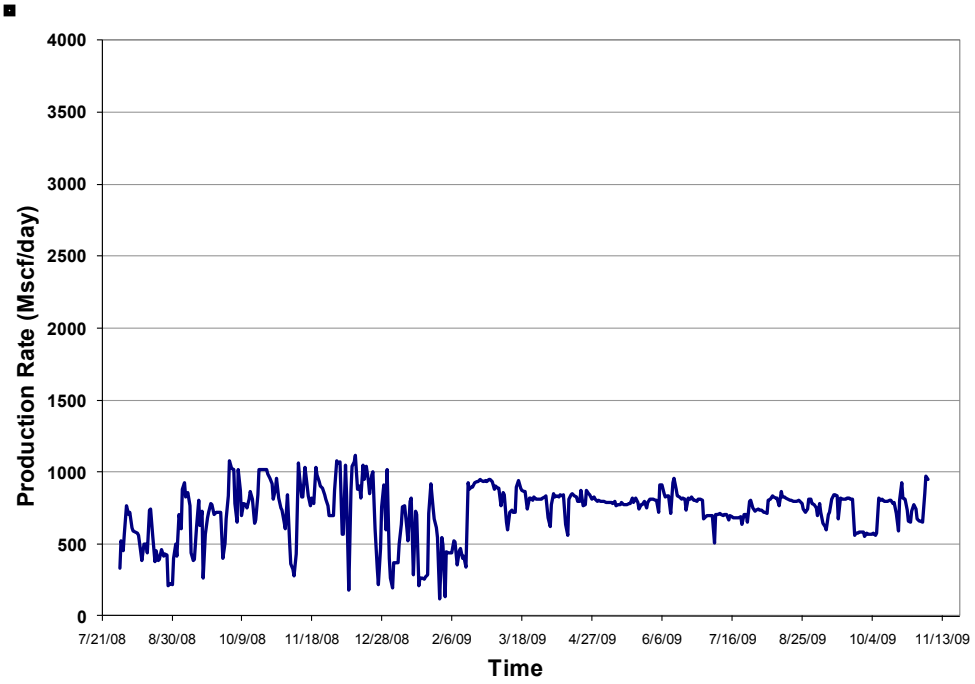

Figure 82. Production rate from the three producers, EPNG Com A 300, 300S and FC State Com 1, surrounding the injector well.

A comparison of the cumulative injected and produced volumes were similar over the injection period for Section 32, Figure 83. If surrounding wells Howell A 300, Moore B3, Howell 301S, Kernaghan BS, Kernaghan B8S, Kernaghan SA, Howell D350S, Howell D351, Howell D352, Howell D352S and Florence H3 are included, production is much greater than the injection, Figure 84.

It is not surprising that little or no uplift was seen; in fact the opposite would have been a surprise.

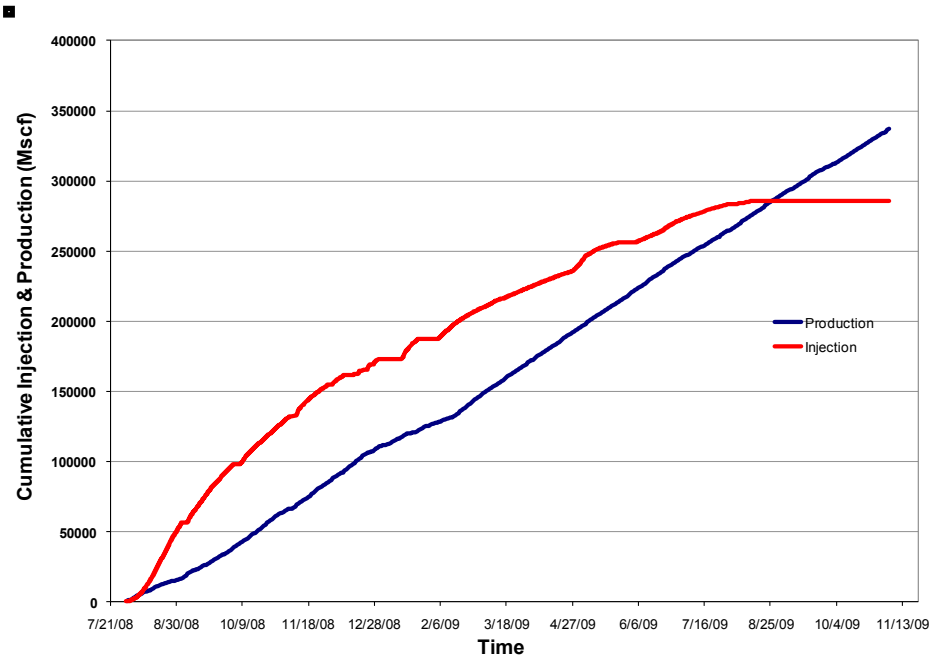

Figure 83. Comparison of cumulative injected and produced volumes (Standard Volume) from Section 32 including three COP Producers, EPNG Com A 300, 300S and FC State Com 1.

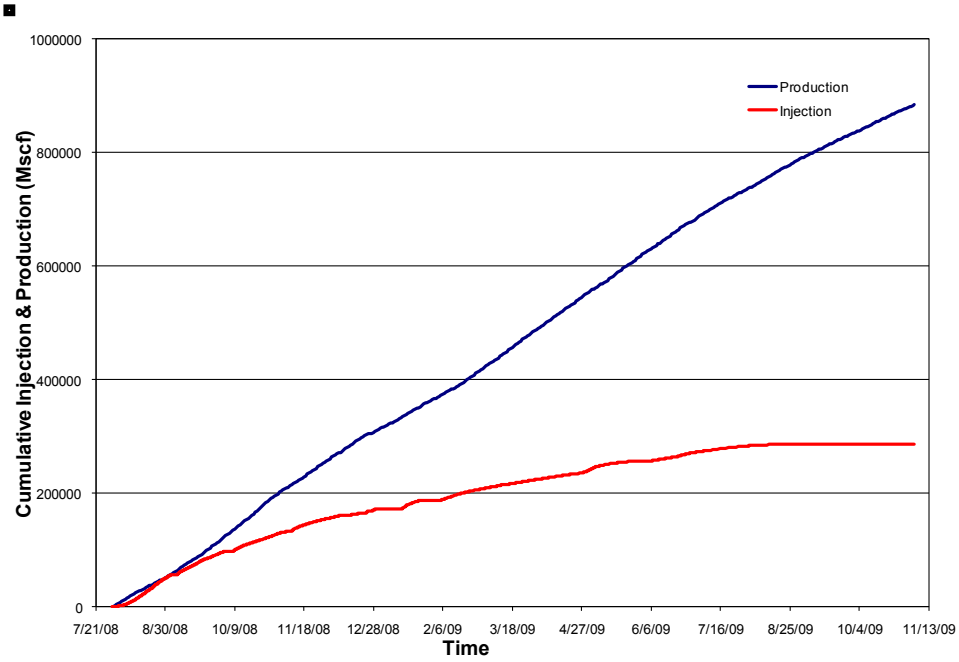

Figure 84. Comparison of cumulative injected and produced volumes (Standard Volume) from Section 32 COP producers and the Howell Wells immediately surrounding Section 32.

GPS Elevation Profile

A differential GPS system was also set up that consisted of one remote and one base station. The base station was located at the far NW section of the tiltmeter array, and the remote station was located approximately 400 ft to the west of the injector. The GPS elevation profile from August 01, 2008 to November 17, 2009 shows that there is no significant cumulative elevation change during this period. There are minor fluctuations inherent with any "natural" data.

Conclusions

There has not been any significant cumulative surface uplift due to CO_2 injection observed. This behavior has been independently verified by the lack of cumulative elevation change in the GPS elevation profile computed at a point 400 feet to the west of injector.

VSP Surveys

A baseline and repeat vertical seismic profiles (VSP) were performed at the San Juan Basin Pump Canyon for the Southwest Regional Partnership on Carbon Sequestration. This was the site of CO_2 injection into a coal formation that is presently considered unminable and is a natural gas production site.

The site layout for the VSP at the San Juan Basin ECBM project is shown in Figure 85. The original plan was to place the offsets at azimuths that were roughly aligned with the identified cleat directions in the coal. However, selecting offset shot point locations proved to be a real challenge at this site given the surface infrastructure, vegetation, and archeologically survey requirements. It had been hoped to place shot point D in a more orthogonal position to Shots C and B.

The cyan squares represent the VSP shot points. Shot point A represents the zero off-set VSP (zvsp). The orange circle represents an offset of 1500 ft. that is the ideal imaging offset given the depth of the target.

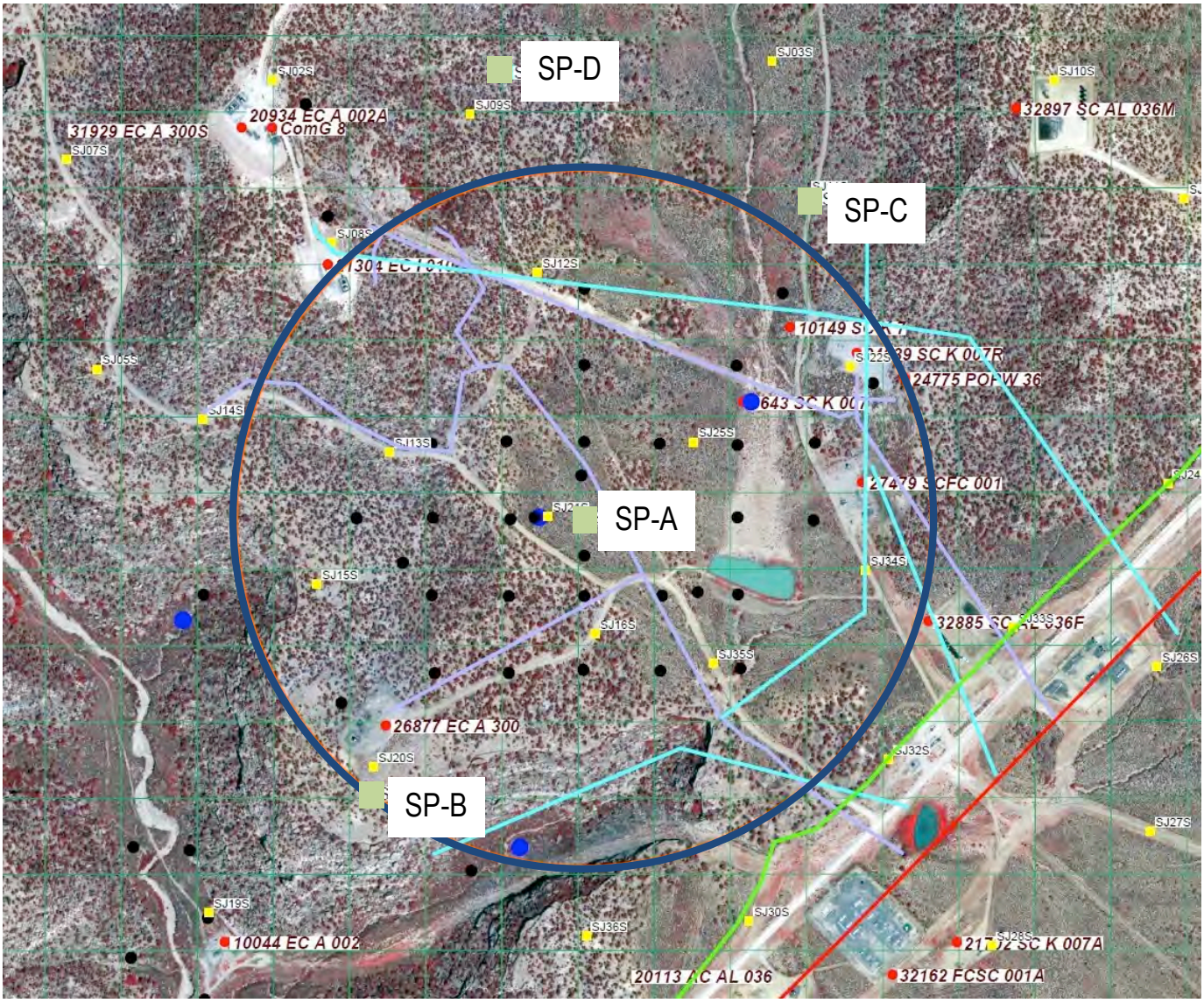

Figure 85. Site layout for the VSP at the San Juan Basin ECBM project.

Figure 86 and Table 24 show the site geometry in feet related to the injection well or zero VSP off-set. The VSP acquisition used 48 levels spaced at 50 ft intervals from 500 to 2850 ft. CO_2 was injected at depths below ~2950 ft. VSP data was not acquired across the Fruitland coal interval because fluid could not be maintained in the wellbore across the coal seam; thus it was not completed for the pre-injection (baseline) test and was plugged off during the post-injection (monitoring) test.

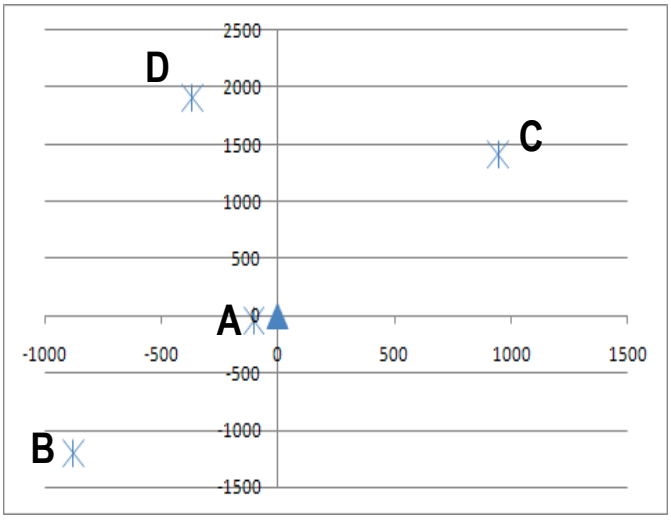

Figure 86. Site configuration.

Table 24. Shot Locations Geometry

SHOT	BASELINE SHOT LOCATION	MONITOR SHOT LOCATION
A (ZVSP)	(-103.32, -48.18)	(-130.51, -60.86)
B (1498 ft OVSP)	(-880.5, -1211.91)	(-880.5, -1211.91)
C (1693 ft OVSP)	(946.71, 1403.56)	(946.71, 1403.56)
D (1942 ft OVSP)	(-370.55, 1906.32)	(-370.55, 1906.32)

Baseline and monitor VSP surveys were acquired in June 2008 and September 2009, respectively. CO_2 injection started July 31, 2008 and ceased August 2009, with 18,400 tons of CO_2 injected over 12 months.

Figure 87 shows the basic concept behind VSP acquisition. Downgoing direct wave arrives first as show in red in the figure. Geophones may also record downgoing multiple energy. Then record reflected upgoing P-wave and convert upgoing shear waves. Upgoing reflections are recorded close to the source. Upgoing and downgoing wavefields need to be separated during processing.

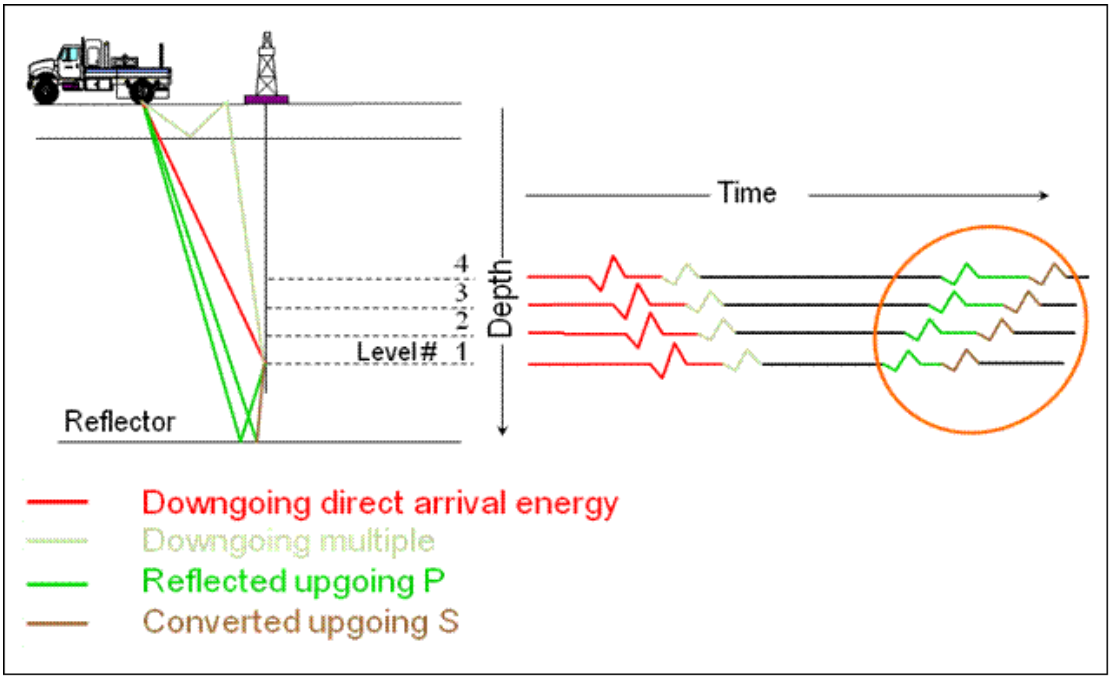

Figure 87. The basic concept behind VSP acquisition.

When a baseline VSP is taken and then followed by an identical repeat, this is considered a time-lapse VSP. The basics of time-lapse seismic are:

- Fluid saturation and pore pressure/stress changes in a formation and the surrounding strata cause time-lapse changes in amplitude and travel times (or time shifts).
- Amplitude differences are caused by changes in velocity, bulk density, bulk and shear moduli. Often indicators of fluid saturation changes.
- Time shifts occur when there has been a change in velocity.
- Repeatability metrics allow quantification of the repeatability of the data.
    - Good repeatability metrics indicate that real timed-lapse changes related to injection or production are being seen.
    - Standard repeatability metrics are NRMS and Predictability.
    - NRMS is sensitive to changes in amplitude, phase, and time shifts.
    - Predictability is sensitive to the amount of noise in the data and changes in reflectivity

Figure 88 shows the processing flow diagram. There were a number of challenges in processing the San Juan Basin VSP that included the following:

- Acquisition conditions were not the same from the baseline to the monitor survey.
    - In particular, wet conditions during the monitor survey had a negative effect on the time-lapse results for Shot C.
- Four receivers in the monitor survey were offset 10 ft from the original receiver depths
    - Interpolation was used to move these traces to the correct depth.
- A velocity model was calibrated for each offset based on the zvsp data.
- A cross-equalization operator was designed over a 100 ms window around the direct arrival in the downgoing wavefield.
- Direct shear arrivals had a negative effect on the repeatability metrics over the course of processing.
    - Shot B and D used receivers 1000 ft and below for final imaging.
    - Shot C used receivers 1500 ft and below for final imaging

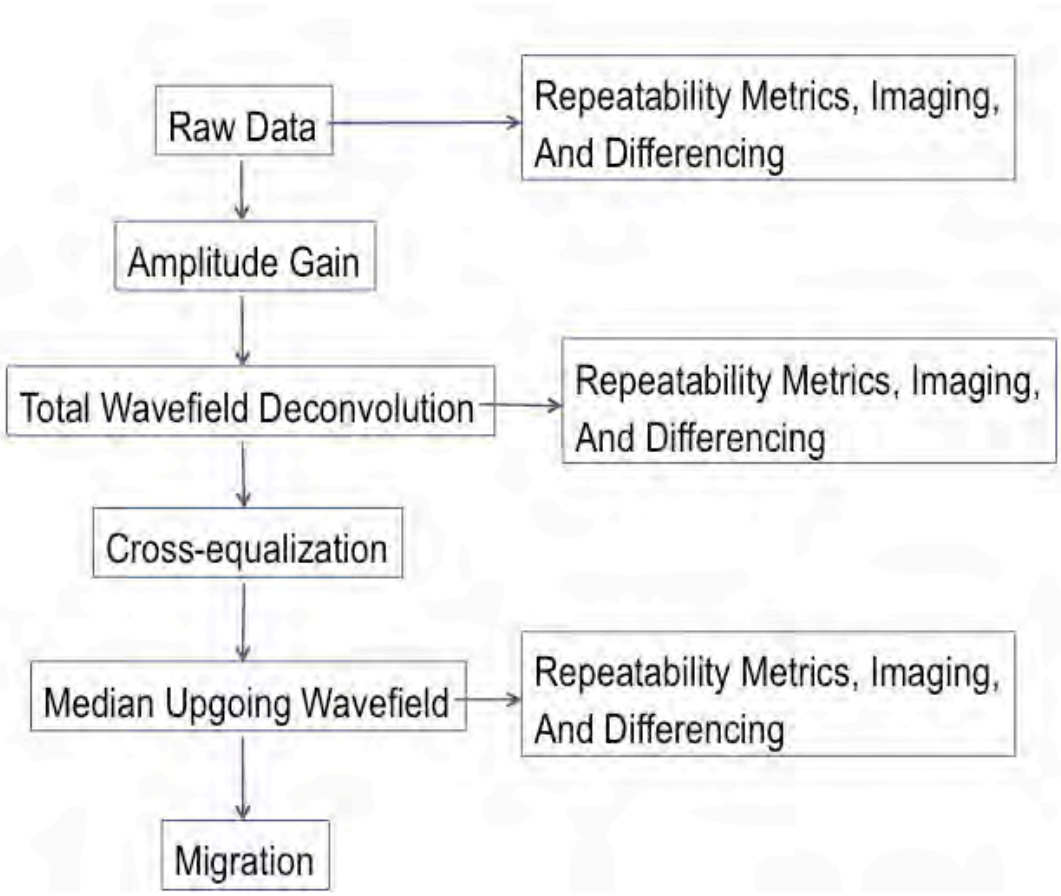

Figure 88. Processing flow diagram.

Figure 89 shows Shot D raw data. The red circles in Figure 89 highlight the direct shear energy that had a negative effect on repeatability in the shallow interval.

VSP Results and Discussion

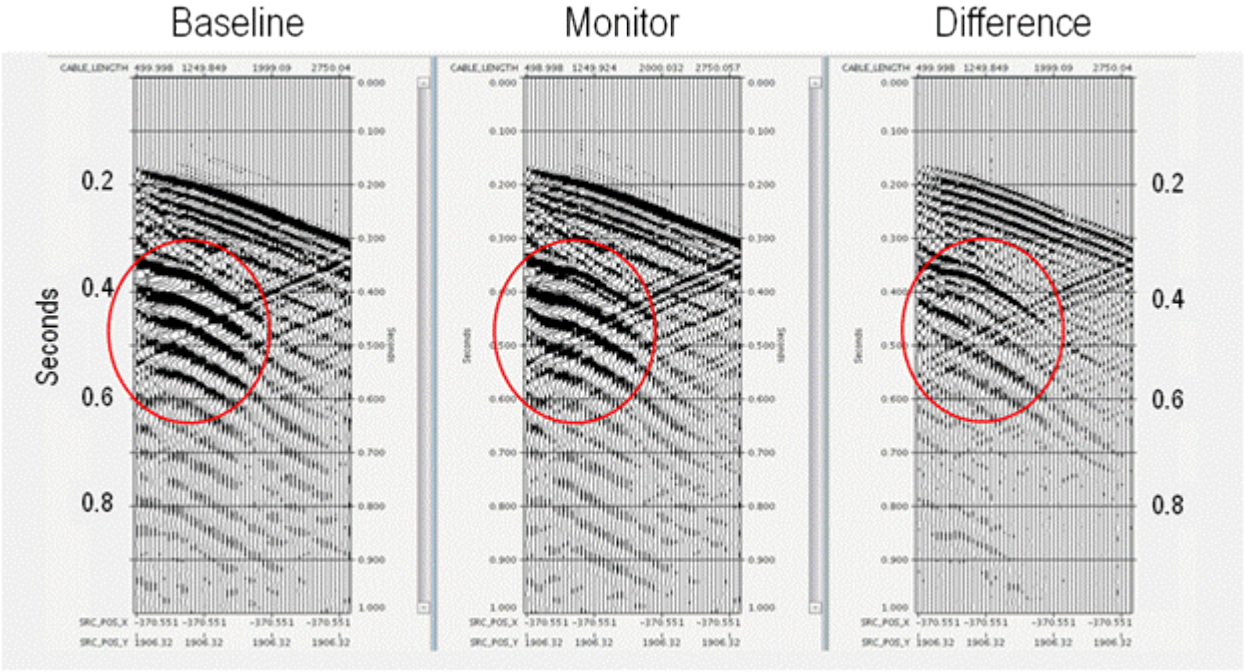

Figure 89. Baseline, monitor, and difference for Shot D.

Figure 90 shows migrated images of the raw data for Shot D. The red circle on the difference display highlights the effects of the four receivers that were 10 ft off-depth for this offset. These caused problems in the processing.

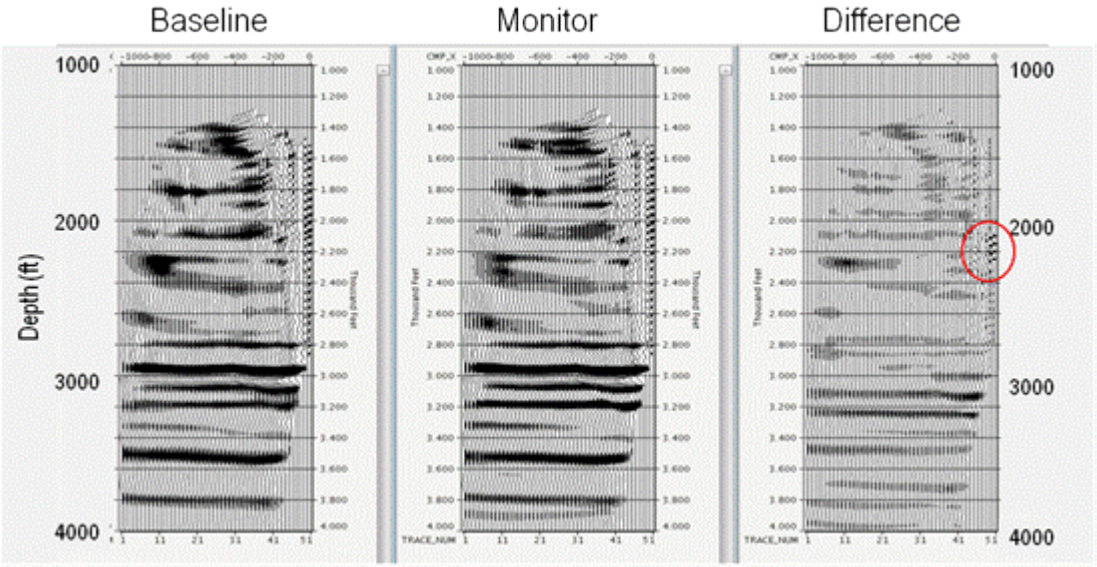

Figure 90. The raw migrated images for Shot D.

Cross-equalization took place after total wavefield deconvolution, shown in Figure 91. The total wavefield decon allowed removal of the effect of source signature on the data early in the processing flow. Then the wavefields were separated using a median filter.

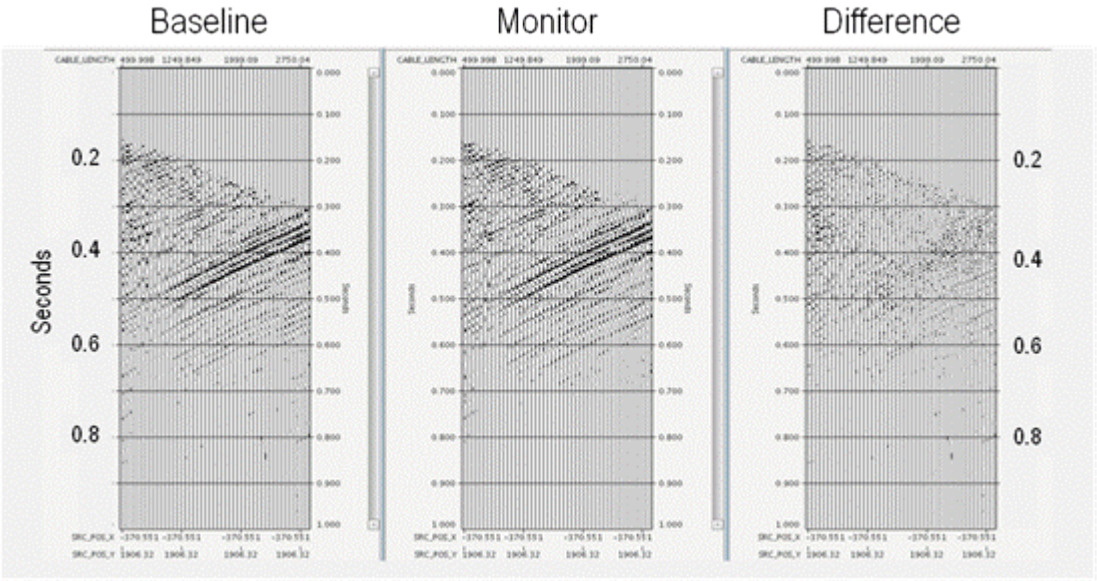

Figure 91. Cross-equalized, interpolated upgoing wavefield.

Figure 92 is a sample of the repeatability metrics calculated for Shot D. The raw and cross-equalized data prior to migration are shown. The negative impacts caused by the direct shear waves in the shallow part of the data can be seen. However, below 1000 ft, small improvements in NRMS and predictability can be seen.

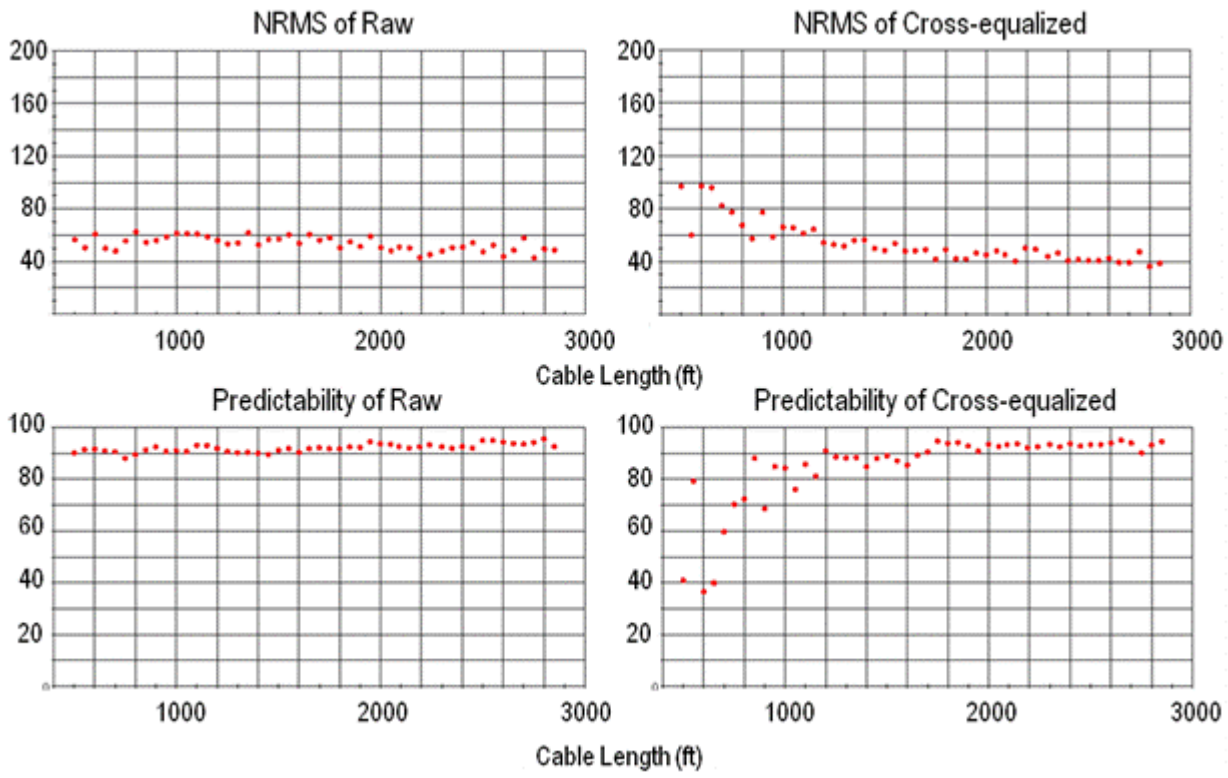

Figure 92. Shot D repeatability metrics.

Amplitudes in the difference display are small and well balanced for the most part as shown in Figure 93. Nothing in particular suggests an anomaly. Circles highlight the location of a possible fault that are not believed to be a processing artifact.

Similarly Figures 94 through 97 show similar raw data. Cross-equalized, interpolated upgoing wavefield, repeatability metrics, and migrated images for Shot B.

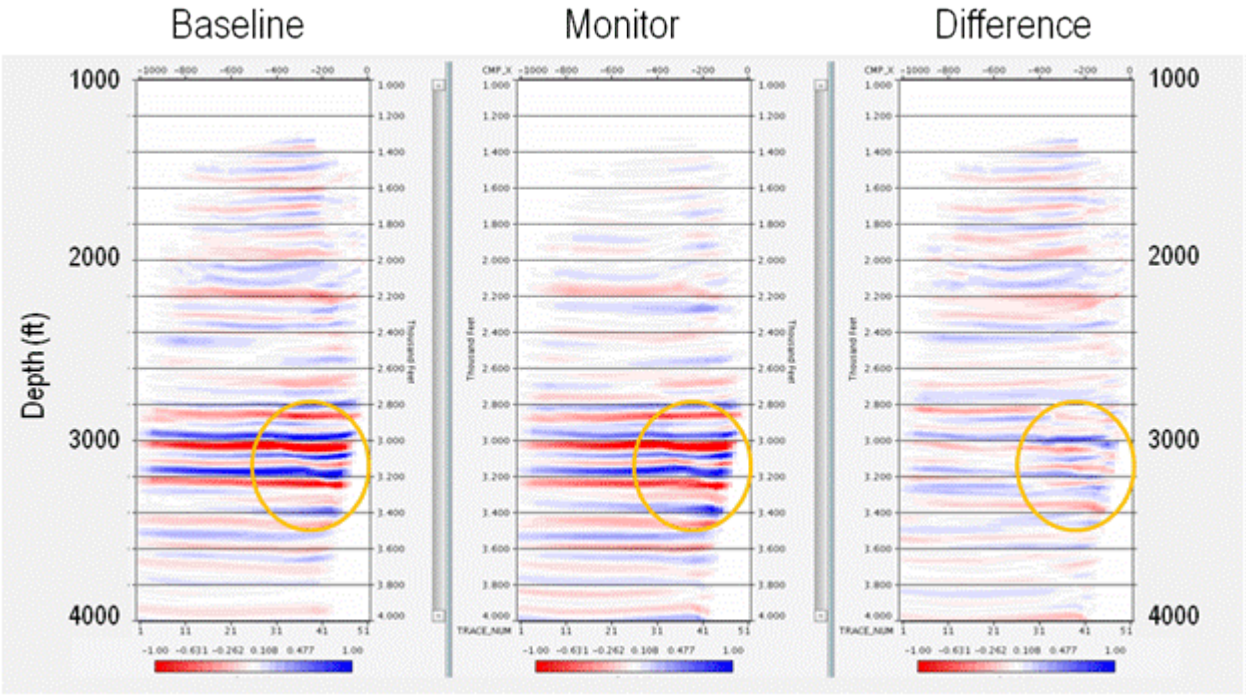

Figure 93. Migrated images for Shot D.

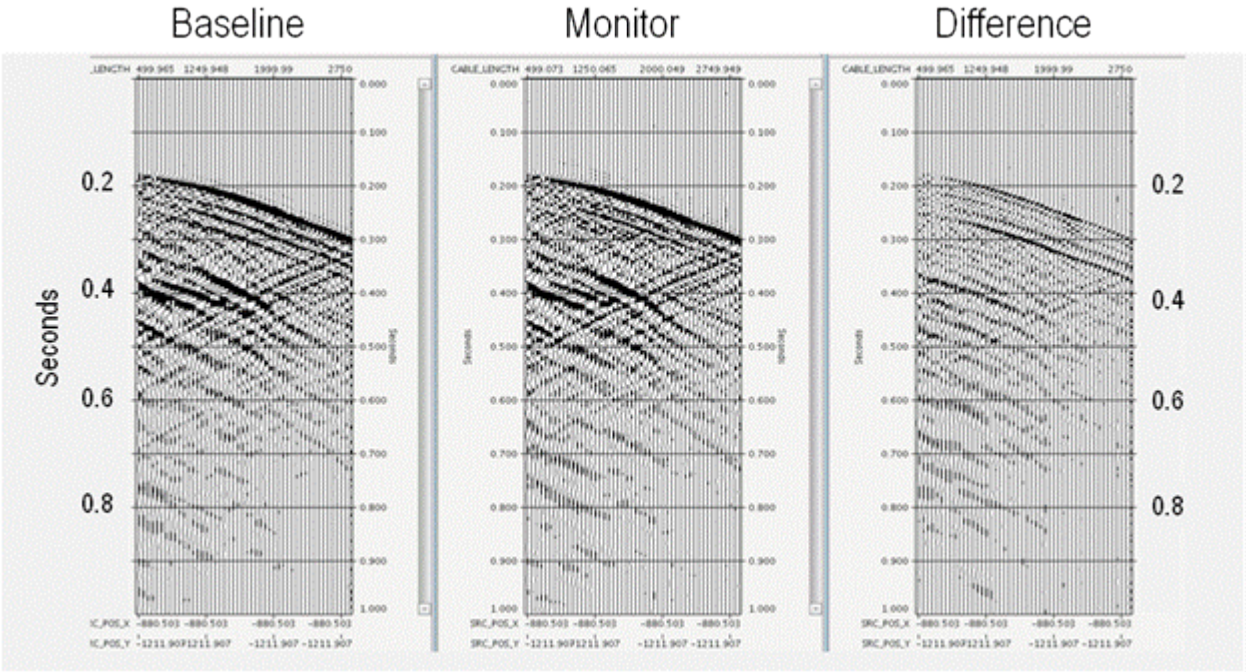

Figure 94. Shot B raw data.

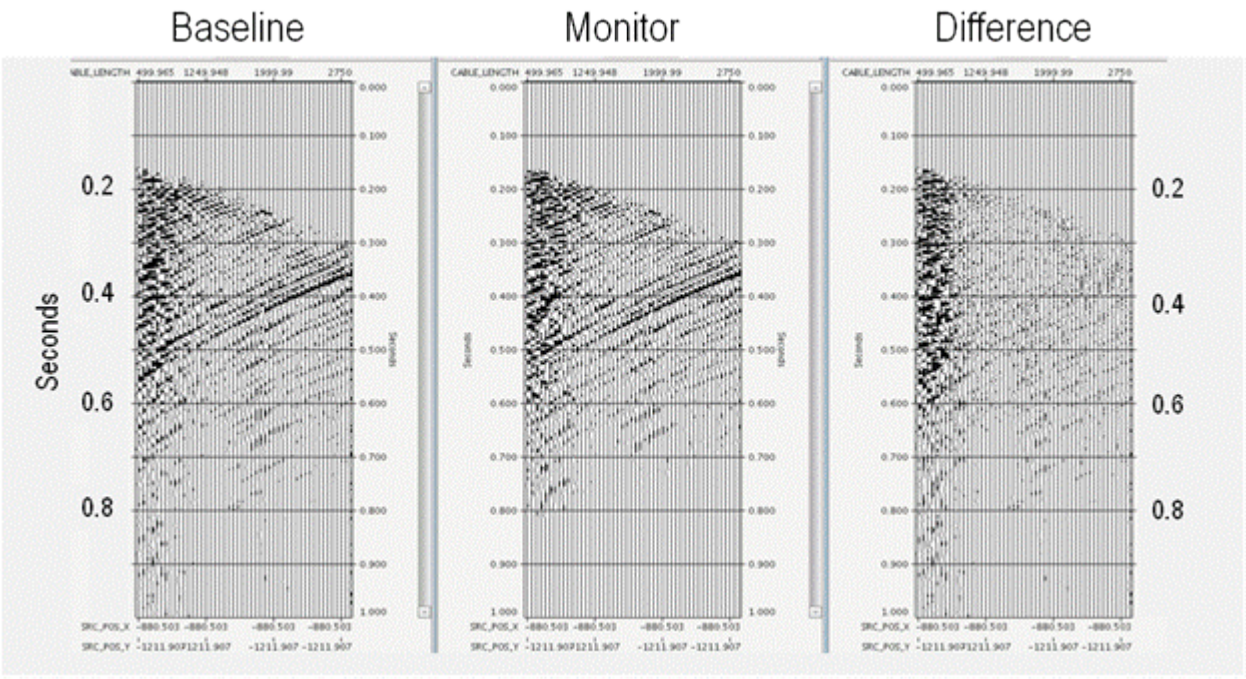

Figure 95. Cross-equalized, interpolated upgoing wavefield for Shot B.

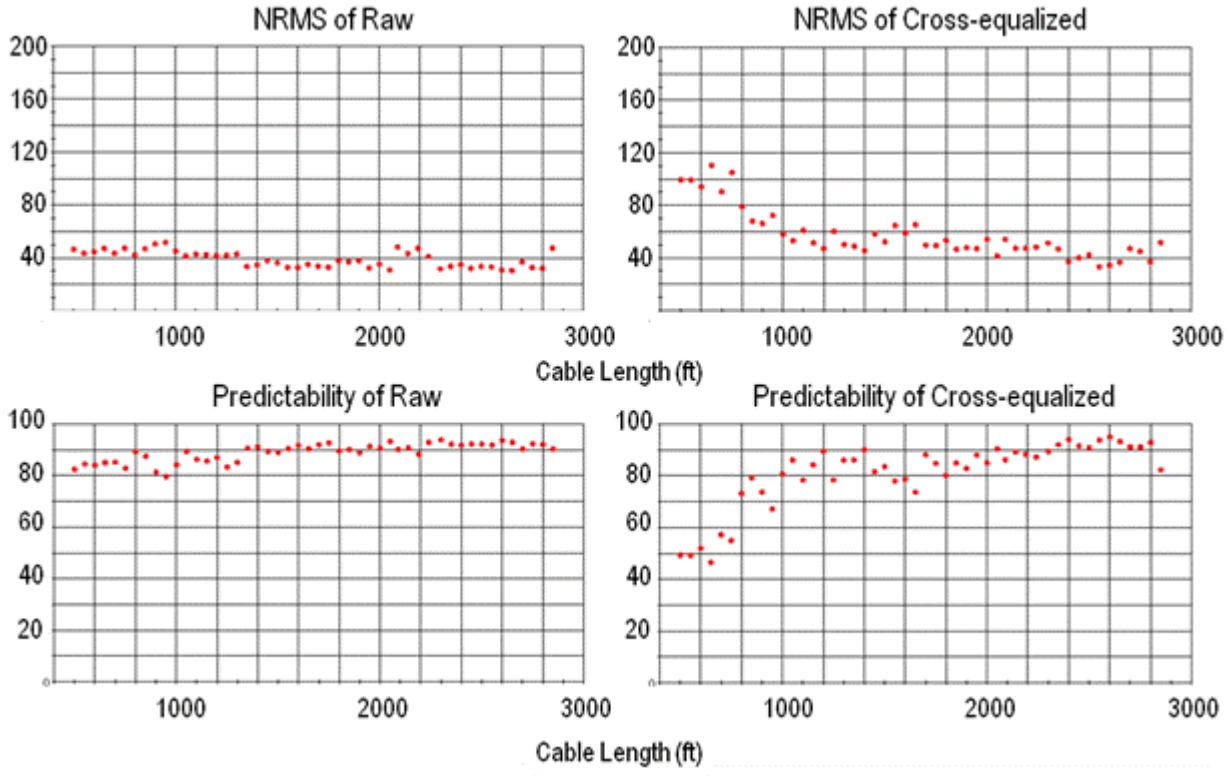

Figure 96. Repeatability metrics for Shot B.

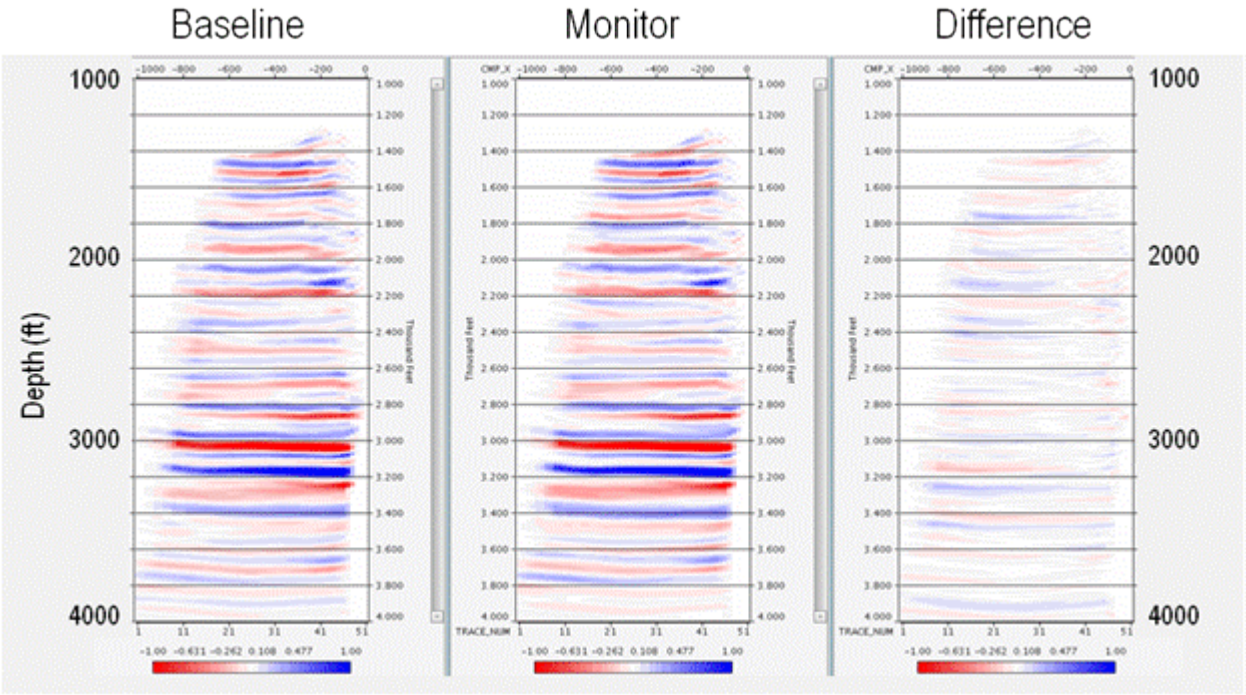

Figure 97. Migrated images for Shot B.

Figure 98 shows the raw data from Shot C. This is the offset that showed the most difference between the baseline and the monitor surveys. It is believed that this is because the ground conditions varied so much from the baseline to the monitor survey, which was much wetter.

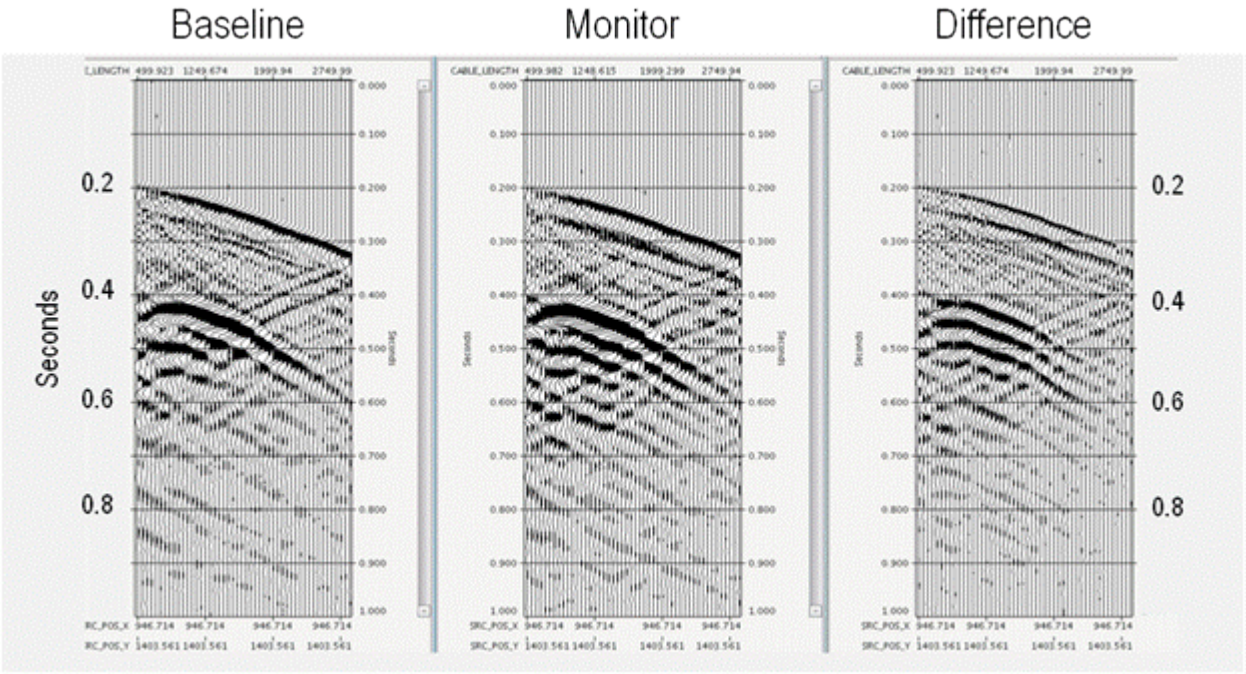

Figure 98. Raw data for Shot C.

Figure 99 shows that the frequency spectra are somewhat different for the baseline and monitor surveys. The monitor survey has lower bandwidths.

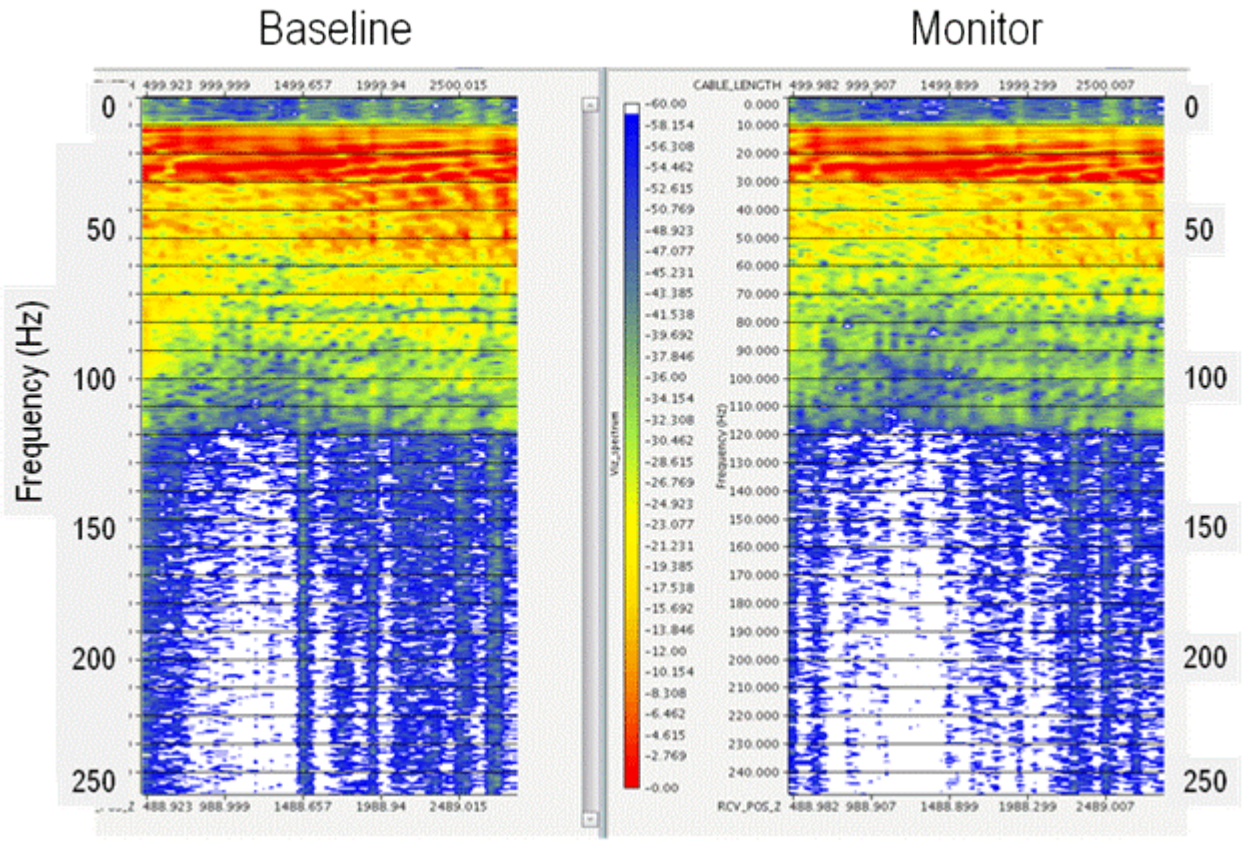

Figure 99. Comparison of the frequency spectra for Shot C.

From Figure 100, it is seen that the repeatability of the data suffered and thus caused problems in the processing.

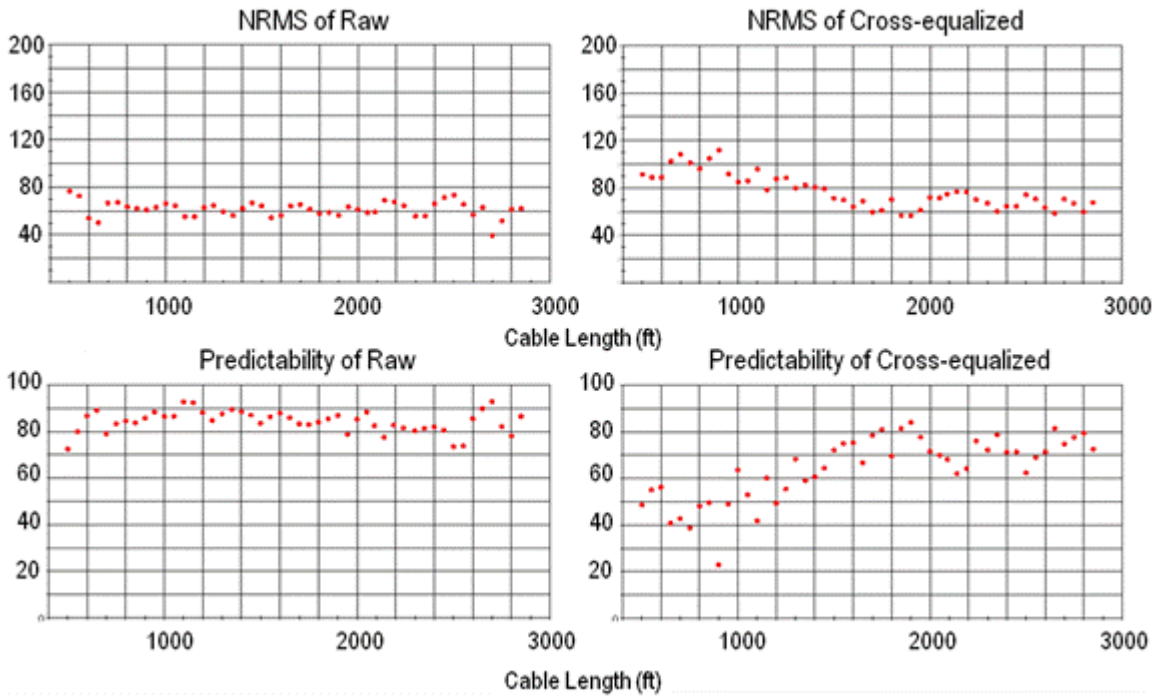

Figure 100. Repeatability metrics for Shot C.

The large differences in the comparison of the baseline and monitor VSP surveys are not related to CO_2 injection (Figure 101).

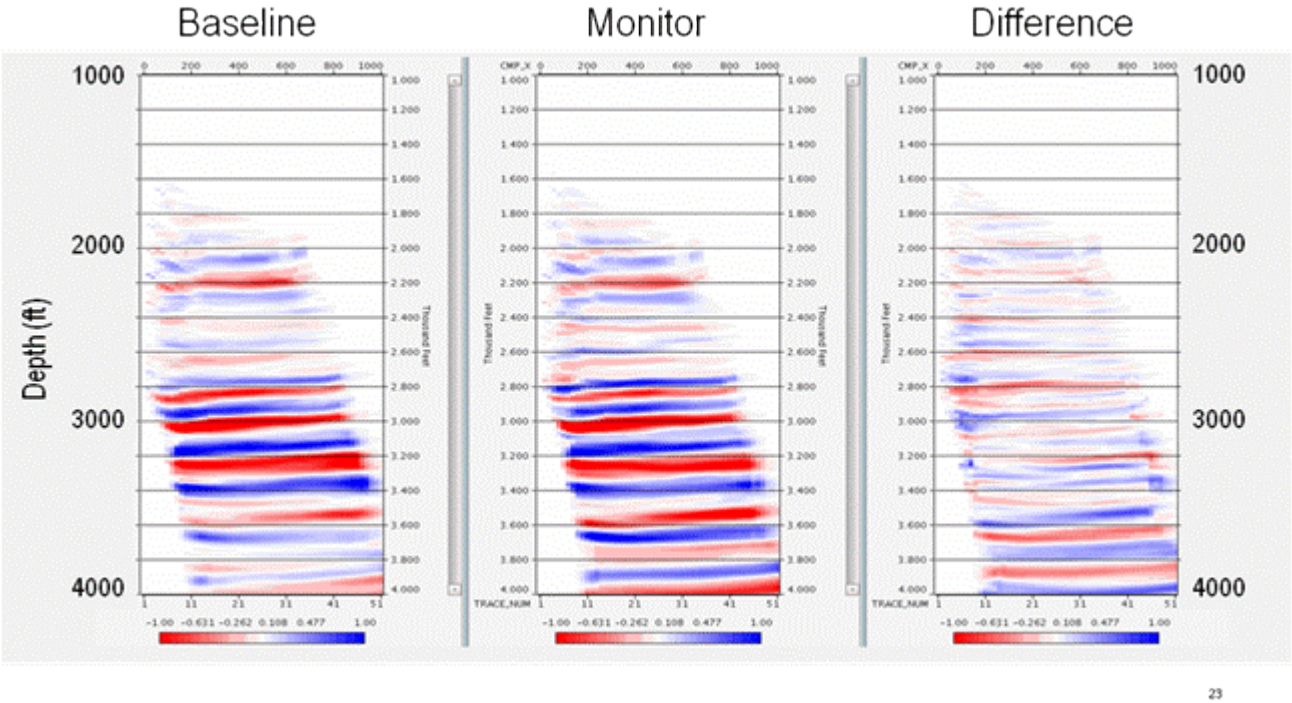

Figure 101. Migrated images for Shot C.

VSP Survey—Conclusions and Recommendations

Conclusions from this study are:

- No significant time-lapse differences were identified on Shots B and D despite good data repeatability.
- Significant differences in ground conditions and source signature have prevented valid time-lapse results from being obtained from Shot C.
- Volume of injected CO_2 may have been too small to identify seismically.
    - It is not currently possible to model the seismic response of the coal given its interactions with CO_2.
- The monitor survey was also acquired after the formation had been allowed to pressure down for a month.
    - There would have been a decrease in the time-lapse effects related to pressure over this time.
- Despite the fact that no significant time-lapse differences were identified, a great deal was learned about processing and analyzing time-lapse VSP data

Recommendations from this study are:

- Offset VSPs for time-lapse monitoring are not recommended, due to the low yield of data collected.
    - For Shot C, the processing was unable to solve issues with non-repeatability because the data was insufficient.
- Acquisition of one or two orthogonal walkaway VSP lines would maximize chances for observing time-lapse effects.
- Complete fluid substitution modeling prior to acquisition of the monitor survey to ensure that enough CO_2 has been injected to image seismically.
- Processing should include:
    - Calculation of repeatability metrics at each major processing step,
    - Imaging and differencing of the data at each major processing step,
    - Cross-equalization of the data to minimize amplitude differences and time shifts in the data outside of the injection zone.

Natural Tracers and Multi-Scale Assessment of Caprock Sealing Behavior in the SJB Kirtland Formation

The assessment of caprocks for geologic CO_2 storage is a multi-scale endeavor. Investigation of a regional caprock—the Kirtland Formation, San Juan Basin, USA—at the pore-network scale indicates high capillary sealing capacity and low permeabilities. Core and well-scale data, however, indicate a potential seal bypass system as evidenced by multiple mineralized fractures and methane gas saturations within the caprock. Interpretation of ^{4}He concentrations, measured at the top and bottom of the caprock, suggests low fluid fluxes through the caprock: 1) Of the total ^{4}He produced *in situ* (i.e., at the locations of sampling) by uranium and thorium decay since deposition of the Kirtland Formation, a large portion still resides in the pore fluids. 2) Simple advection-only and advection-diffusion models, using the measured ^{4}He concentrations, indicate low permeability (~10^{-20} m^2 or lower) for the thickness of the Kirtland Formation. These findings, however, do not guarantee the lack of a large-scale bypass system. The measured data, located near the boundary conditions of the models (i.e., the overlying and underlying aquifers), limit the testing of conceptual models and the sensitivity of model parameterization. Thus, approaches for future studies are suggested to better assess the presence or lack of a seal bypass system at this particular site and for other sites in general.

Multi-Scale Evaluation of Seal Bypass Systems

This section addresses the multi-scale assessment of caprock sealing quality for the Kirtland Formation and other sites in general. This Kirtland Formation-specific investigation involves data collected from the pore, core, well log, and formation scale (i.e., helium data collected at the top and bottom of the Kirtland Formation). The multi-scale assessment is not based on upscaling a variety of data sets, but simply comparing different types of data collected at different scales to determine if the data are coherent.

Mercury intrusion porosimetry (MIP), permeability measured on core, FMI log-based fracture measurements, and other pore-, core-, and well log-scale data do not provide clear indication of the connectedness of transmissive features over the vertical scale of the entire Kirtland Formation. The MIP and core-scale permeability indicate high sealing capacity. However, the core

and well log data indicate potentially transmissive fractures, such as open and mineralized fractures. The mineralization and methane gas saturations within the Kirtland Formation and the overlying Ojo Alamo Sandstone suggest possible large-scale connectivity. Thus, the natural tracer data—helium and neon—are especially important since they are affected by actual transport through the seal. The goal is to determine if the tracer data indicate connectedness and relatively high permeability at the scale of the entire Kirtland Formation. If this is the case, then fractures or other features would have to be invoked as a seal bypass system to explain the data.

The analysis of the noble gas data supports a low fluid flux through the Kirtland Formation. Key findings supporting this statement are: 1) a large percentage of the radiogenically produced ^{4}He is in the pore fluids of the Kirtland Formation, indicating low advective fluid flow from the surrounding aquifers; and 2) simple advection-only and advection-diffusion models estimate low permeability (~10^{-20} m^2 or lower) for the entire thickness of the Kirtland Formation. Thus, following the multi-scale approach, it is proposed that the formation-scale data are coherent with those of the pore-scale (e.g., permeability and MIP). However, the research findings do not guarantee low fluid fluxes and the lack of a seal bypass system. The models rely on restricted conceptualizations (e.g., 1D, fully groundwater saturated fluid flow with homogeneous formation properties). Furthermore, the measured data points are located near the boundary conditions of the models, which are the overlying and underlying aquifers. Tests of different conceptualizations (e.g., lateral flow in the Farmington Sandstone Member) and model parameterization are limited by the location of these data. *In situ* advective transport of a gas phase may also be possible, which we are not able to constrain with only neon and helium data.

The limitations of the analysis in this research indicate the need for careful feasibility studies prior to coring and drilling programs to ensure that the collected natural tracer data will support tests of different conceptualizations. Future studies should tailor data collection programs to the system of interest in terms of flow units, sampling locations, and the types of tracers. Analytical or numerical modeling should be used prior to data collection to optimize the sampling locations. Natural helium and other noble gases were used because they occur in all groundwater systems and reflect transport processes. However, in addition to these tracers, this investigation would have benefited from examining the methane in the system, which may have been an effective

tracer at indicating the degree of large-scale transport. Other sites may have particular, local, natural tracers that would be valuable in addition to the noble gases.

This study is part of the effort, encouraged by the CO_2 research community (DOE, 2007), to develop approaches for large-scale caprock assessment for CO_2 storage. Industrial-scale CO_2 storage may involve reservoir/caprock evaluation at the scale of entire sedimentary basins (Birkholzer and Zhou, 2009). Previous work using noble gases, especially helium, have assessed basin-scale aquifer transport in terms of large-scale permeability and groundwater residence times (Castro et al., 1998; Bethke et al., 1999; Bethke and Johnson, 2008). The goal, however, has not been the diagnosis of seal bypass systems. Future work can build on these studies and the research presented here to assess basin-scale reservoir-aquifer/caprock systems with a focus on identifying and characterizing seal bypass systems.

Well Analysis

On September 8, 2008, two bottomhole memory readout (MRO) gauges were installed within the EPNG Com A Inj #1 well at a depth of 2,865 feet. The gauges were pre-programmed to record high data density pressure and temperature information, which was collected during the injection of CO_2 into the Fruitland coal seams.

Following the termination of injection and in preparation for well abandonment, the MRO gauges were retrieved from the well and the data was downloaded. Figure 102 depicts the raw pressure and temperature data collected from the well. The high-density collection of data stopped on February 17, 2009 due to a full MRO data bank. Nevertheless, sufficient data existed to perform pressure transient analysis on this data set.

In reviewing Figure 102, one can clearly identify the periods of injection that are denoted by bottomhole pressures exceeding 2,000 psia, as well as those periods of interrupted injection where the bottomhole pressure declines in some cases to 100 psia. It is these pressure falloff periods (PFO) that we will investigate further.

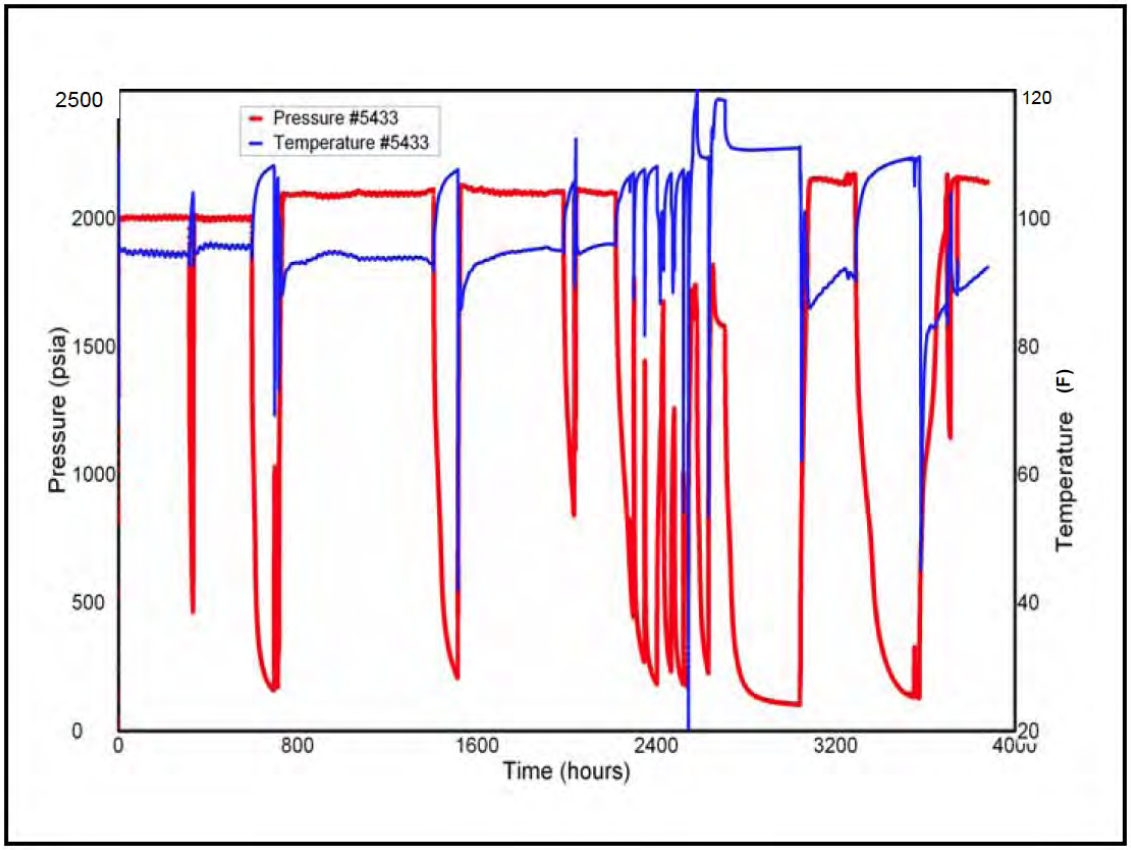

Figure 102. Raw pressure and temperature gauge data.

For the nearly 4,000 hours of collected data, Figure 103 overlays the six PFO periods and the cumulative injection data at each PFO on a plot of pressure and injection rate (note: sign convention is negative for injection). Table 25 depicts the primary input parameters for the well test analysis package. It is important to note that well test software, unlike reservoir simulation software, models the injection reservoir as one discrete formation and not three discrete members of the formation. Thus, the results represent the accumulated formation thickness and are not representative of the discrete coals.

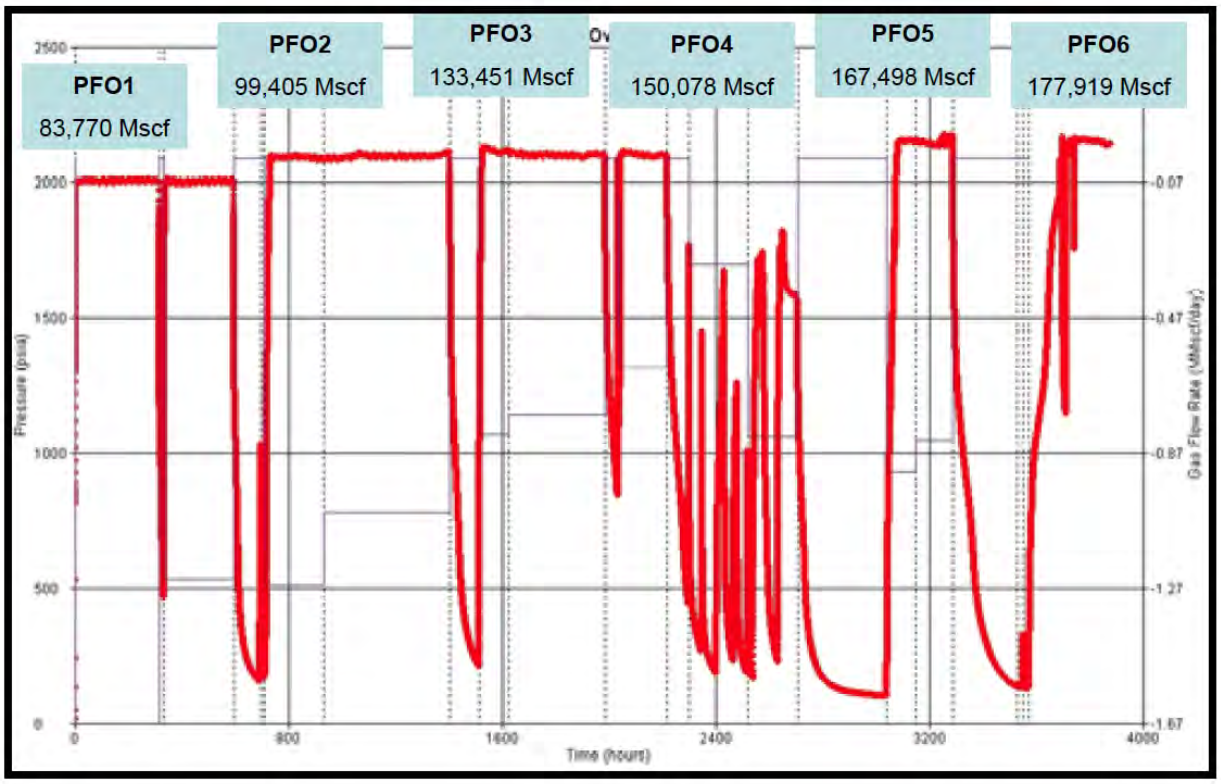

Figure 103. Pressure and injection rate.

Table 25. Well Tests Primary Input Parameters

Parameter	Value	Unit
Thickness	60	ft
Porosity	0.5	%
Total Compressibility	2.70E-02	1/psi
Wellbore Radius	0.375	ft

Figure 104 shows an overlay of each of the six PFOs on the traditional log-log diagnostic plot. An upward shift of the pressure curves from PFO 1 to PFO 6 indicates decreasing permeability, which one might expect to see permeability continue to decline due to coal swelling in the presence of continued CO_2 injection. Interestingly enough, five of the six pressure derivative curves decline rapidly, but at successively longer equivalent times.

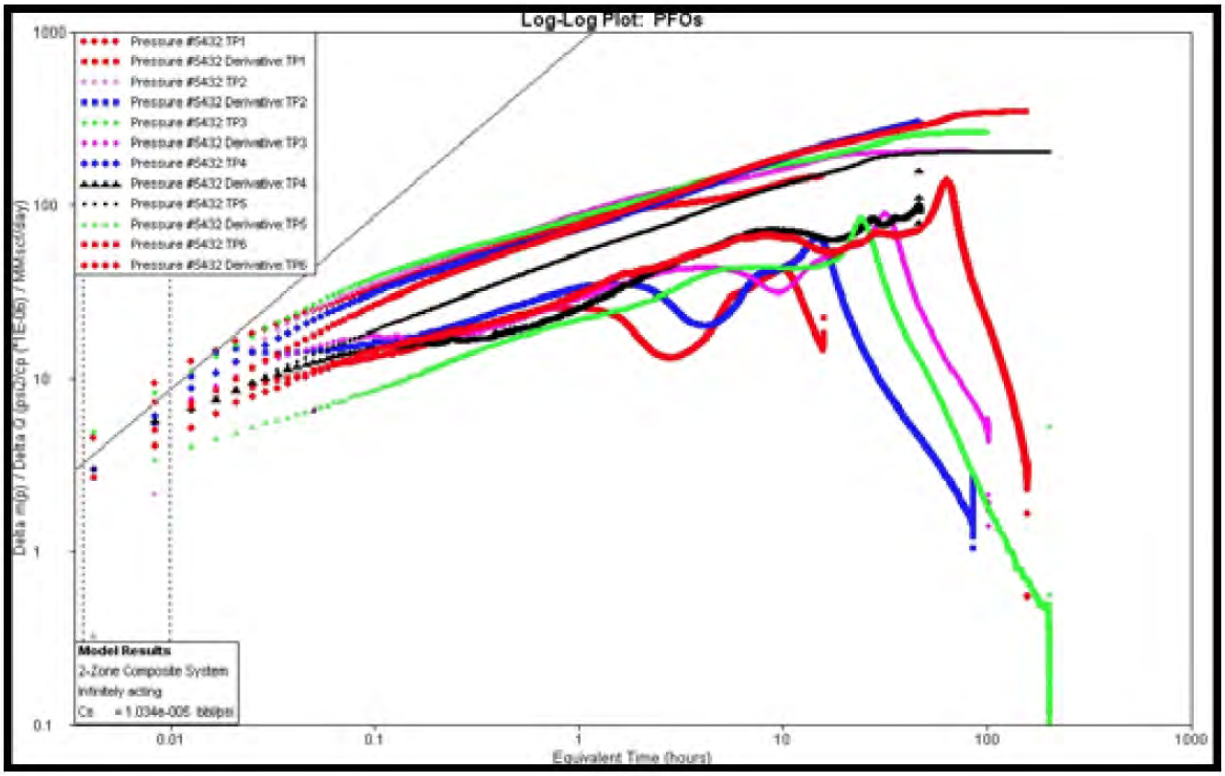

Figure 104. PFOs overlay.

Based on these observations, it was theorized that a radial composite solution may be the most proper way to model this data set. What this model represents is an inner radius of very low permeability (k on the subsequent plots) and skin factor (s) out to a radius (RI2). Outside of this radius, the permeability (K2) increases to a baseline value that is nearly infinite as compared to the inner permeability value. While this has been modeled as 5,000 md, it should be noted that there is little sensitivity in this value above 250 md. As such, this value was fixed and this "increasing" permeability away from the well is believed to be the cause of a steeply declining derivative curve as it attempts to stabilize in radial flow and/or the intersection of highly depleted portions of the Fruitland as the transient approaches the offset production wells.

The log-log plots do not reveal the classic radial flow period (a flattening of the derivative curve that allows the analyst to clearly define permeability and skin factor) in any of the six diagnostic plots. Reasonable best-fit matches were generated that fit the perceived expectation of results for this transient data set. That is, an ever decreasing permeability, near-wellbore, that continues to grow outward as additional CO_2 is injected into the Fruitland coal seams. The results of this analysis are listed in Table 26.

Table 26. Analysis Results

PFO	Cum CO_2 Injected (Mscf)	Perm (mD)	RI (ft)	Skin	Perm 2 (mD)
1	83,770	0.23	34	-1.9	5,000
2	99,405	0.15	33	-2.2	5,000
3	133,451	0.11	39	-2.5	5,000
4	150,078	0.07	57	-3.0	5,000
5	167,498	0.12	39	-2.9	5,000
6	177,919	0.10	50	-2.5	5,000

A plot (Figure 105) of the near-well permeability (k) and its radius of influence (RI2) against cumulative CO_2 injection clearly shows these two behaviors—an increasing radius of influence as permeability declines. Interestingly enough, while a linear fit is suitable for the increasing radius, a power law fit is superior for the permeability decline.

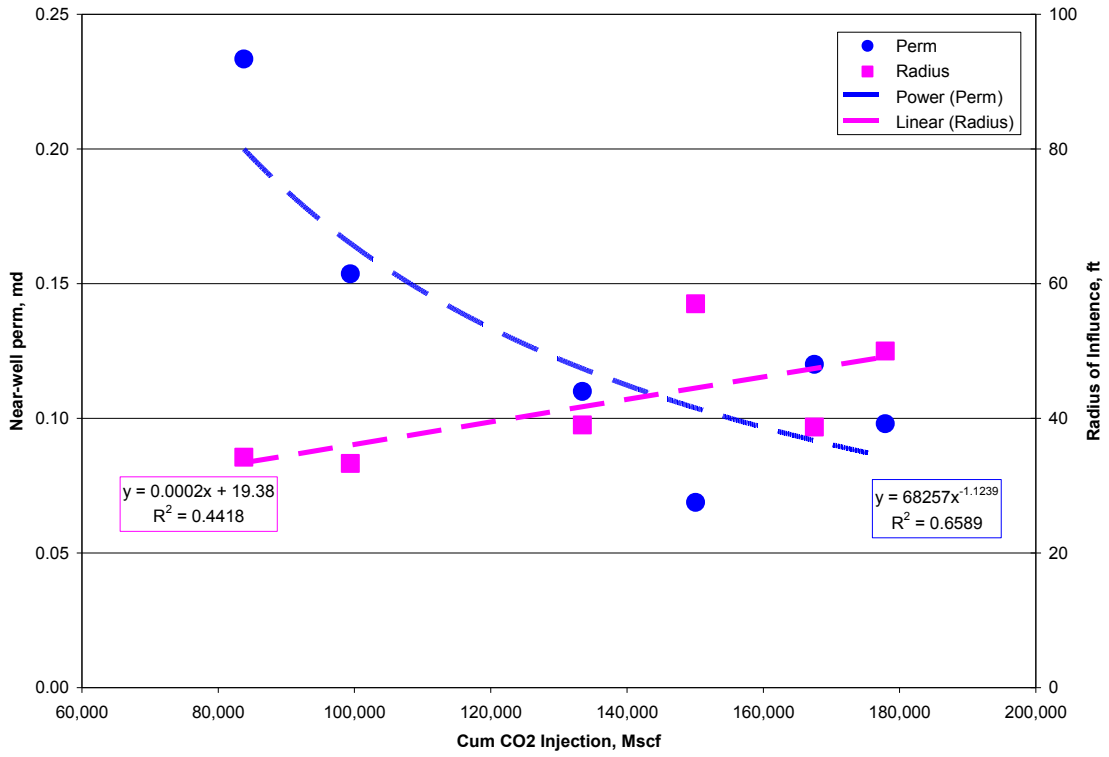

Figure 105. Near-well permeability and radius of influence versus cumulative injected CO_2.

When reviewing these trends, as well as the pressure transient data, itself, it is clear that PFO 4 does not behave like the remaining five PFOs as there is no steeply declining pressure derivative curve. It is unclear, based on available data why this is the case and as a result, this period should be removed as an outlier. Similarly, there is several hundred hours of erratic injection activity following PFO 4 and preceding PFO 5 (Figure 103). Pressure never reaches maximum injection pressure during this time and it is believed that injectivity data or pattern depletion has impacted this PFO period. As such, Figure 106 shows greatly improved correlations without PFO 4 and 5, supporting the basic understanding of coal swelling.

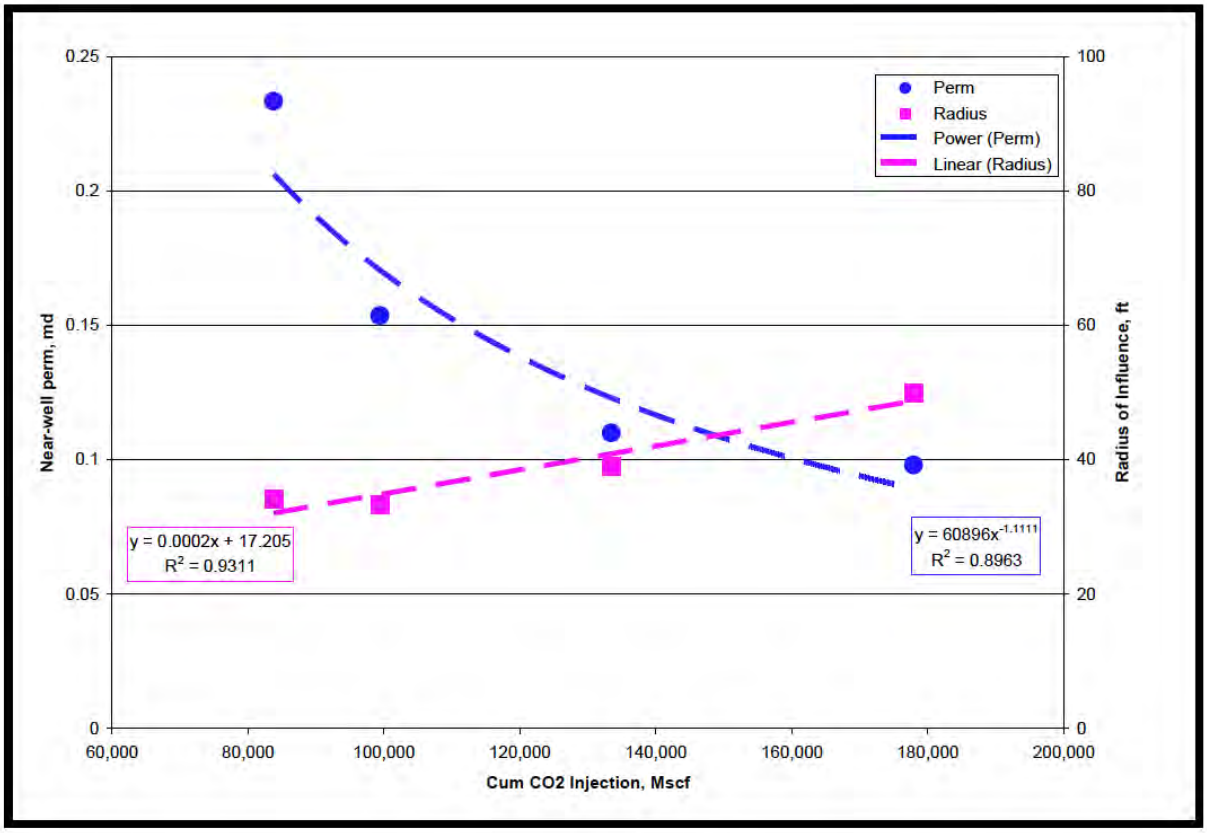

Figure 106. Near-well permeability and radius of influence versus cumulative injected CO_2 (without PFO4 and PFO5).

Since most of the injection is believed to have entered the basal coal, it can generally be said that each of the permeability values may in fact be approximately twice as large, while the radius of influence would be approximately 1.4 times as large (the square root of 2), due to the injection impacting half of the thickness.

Reservoir Simulation

The Pump Canyon site has a considerable amount of reservoir and geologic data available and the infrastructure already in-place. It is located just south of the Allison Unit, the world's first CO_2 sequestration/ECBM field project.

Reservoir properties were obtained from 21 wells drilled in the area to provide input for the model. A refined grid encompassing nine wells plus the injection well was used for comparison to data collected during the field test. Simulations were made of the gas production rates at

nearby wells which were history matched to data collected during the test. A history match was also made between the simulated and measure CO_2 injection pressures.

Offset production wells located roughly 200 meters from the injection well and the produced gas from these wells were monitored for the presence of PFC tracers. Tracer breakthrough was observed at the nearest well to the east of the injection well roughly 90 days after CO_2 injection was started and tracer breakthrough was observed at the southwest offset well around 240 days after injection began. No other production wells produced noticeable tracer signals. Initial simulation results explained pressure increases in Pump Canyon pilot project to be a result of coal swelling. Swelling, however, was limited to a local area around injection well. (The use of lateral wells may reduce impact of coal swelling.)

Tracer information, though only semi-quantitative, provided information on permeability anisotropy. Simulations suggest PFTs are non-conservative in coal, but is retained much less than CO_2. Produced CO_2 was monitored at the same offset wells where PFC tracers in production gas were monitored, but no breakthrough was observed in any well. The most likely explanation would be that the production stream gas in the monitored wells contained roughly 15–30% CO_2, and at the injection rate of about 18,000 tons of CO_2 over a year of injection, it did not raise the concentration of CO_2 in the production gas enough to be detected above background levels.

Reservoir Modeling

Structure and isopach maps of each coal were constructed based on ConocoPhillips log data. The maps were generated using available data from 21 wells. An example structure map for the upper coal is presented in Figure 107, and the total net coal isopach is presented in Figure 108.

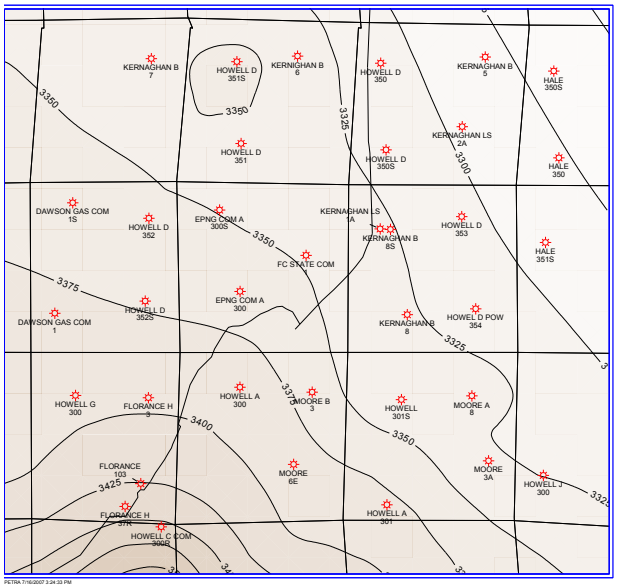

Figure 107. Structure map, upper coal (units in feet above sea level).

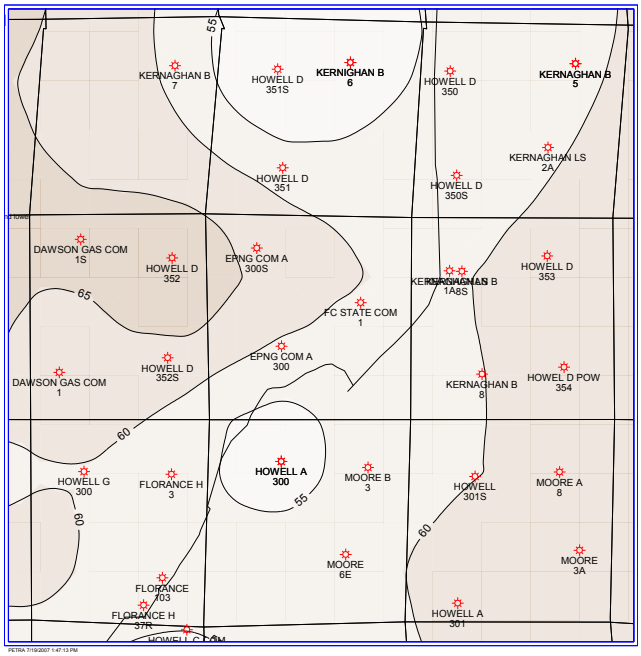

Figure 108. Total net coal isopach (units in feet).

Initial Conditions

Sorption isotherms for both CH_4 and CO_2 were available from five wells in the vicinity of the demonstration. In four wells, two methane isotherms were available for the upper coal, four for the middle coal and four for the basal coal. In two wells, one CO_2 isotherm was available for the

middle coal and two for the basal coal. Due to the lack of information for a CO_2 isotherm for the upper coal, estimations were made based on CH_4/CO_2 Langmuir ratios for the middle and basal coals. These data were then converted from a dry, ash-free basis into in-situ conditions and appropriate units (using coal density) for use in the reservoir simulator, Table 27. No data were available for nitrogen, so CH_4/N_2 Langmuir volume ratios from the Tiffany Unit N_2-ECBM pilot were used to compute nitrogen Langmuir volume from the Pump Canyon CH_4 isotherm data, Table 28.

Table 27. Langmuir Isotherm Constants at In-Situ Conditions

Coal	Average Density[1] (g/cc)	Moisture[2] (%)	Ash Content[3] (%)	Methane		Carbon Dioxide	
				V_L In-Situ (scf/ton)	V_L In-Situ (scf/ft^3)	V_L In-Situ (scf/ton)	V_L In-Situ (scf/ft^3)
Upper	1.51	3.4	31.1	390–503	18–24	809	38
Middle	1.54	3.4	34.6	347–524	17–25	766	37
Lower	1.44	3.4	22.4	419–664	19–30	950–1126	43–50

[1] over nine-section area, [2] average of isotherm samples, [3] using ρcoal=1.3 g/cc and ρash=2.5 g/cc

Table 28. Model Isotherms Inputs

Coal	Methane*		Carbon Dioxide*		Nitrogen	
	V_L In-Situ (scf/ft^3)	P_L (psia)	V_L In-Situ (scf/ft^3)	P_L (psia)	V_L In-Situ (scf/ft^3)	P_L (psia)
Upper	21	546	38	317	12.1	1429
Middle	21	605.5	37	260	12.3	1429
Lower	24.5	519.5	46.5	372	11.5	1429

Initial reservoir pressure data measured in the late 1980s were available for four wells in the demonstration area. Initial pressures range from 1,584 to 1,613 wotj pressure gradients from 0.50 to 0.57 psi/ft.

Cleat orientation was measured in the Northeast Blanco Unit #403 well, approximately seven miles to the east of the demonstration site. These data indicated a face-cleat orientation of N35E, as shown in Figure 109. The simulation grid was oriented in order to respect a higher permeability in that direction.

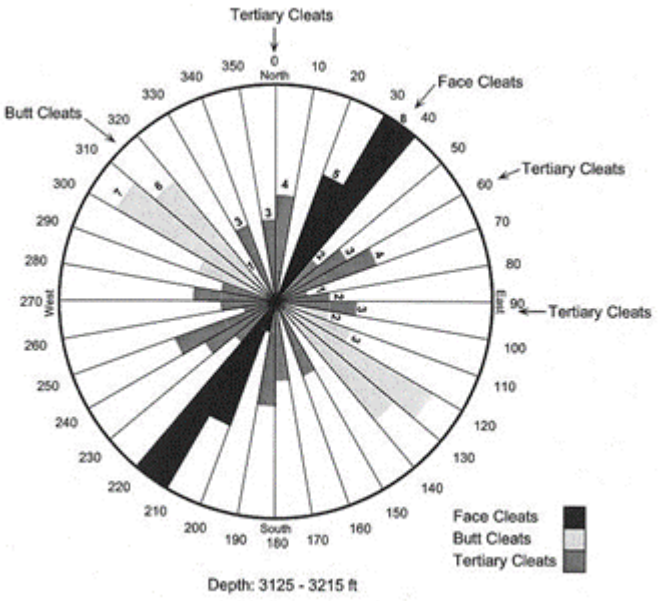

Figure 109. Cleat orientation.

Based on experience in the area (ConocoPhillips) and the review of available logs, the basal coal seems to be of better quality as compared to the upper and middle coals. Based on this information, permeability was allowed to be higher in the basal coal as compared to the middle and upper coals during the history-match process. Porosity was assumed to be correlated with permeability. According to Schwerer and Pavone (1984), permeability can be related to porosity in a fracture through **Equation (1)** where k and ϕ are permeability and porosity with the exponent n typically 3.0.

$$\frac{k}{k_i} = \left(\frac{\phi}{\phi_i}\right)^n \qquad (1)$$

Using this equation, porosity was correlated with permeability using **Equation (2)** where the factor 'a' was allowed to vary during the history-matching process.

$$\phi = a * k^{0.3333} \quad (2)$$

Model Construction

The reservoir simulator used for the study was the *COMET3* (binary isotherm – CH_4 and CO_2) model. Initially, a three-layer (upper, middle and basal), nine-section (Section 32 plus the eight surrounding sections) model was constructed to perform the simulation study. The simulation

grid was oriented in order to respect the face-cleat orientation of N35E. Due to time constraints simulations focused on the middle section, primarily. A 3D view of the model is also shown on Figure 110. A multiplication factor of 20 between the vertical axis and the horizontal axis was used to ease the view of the model.

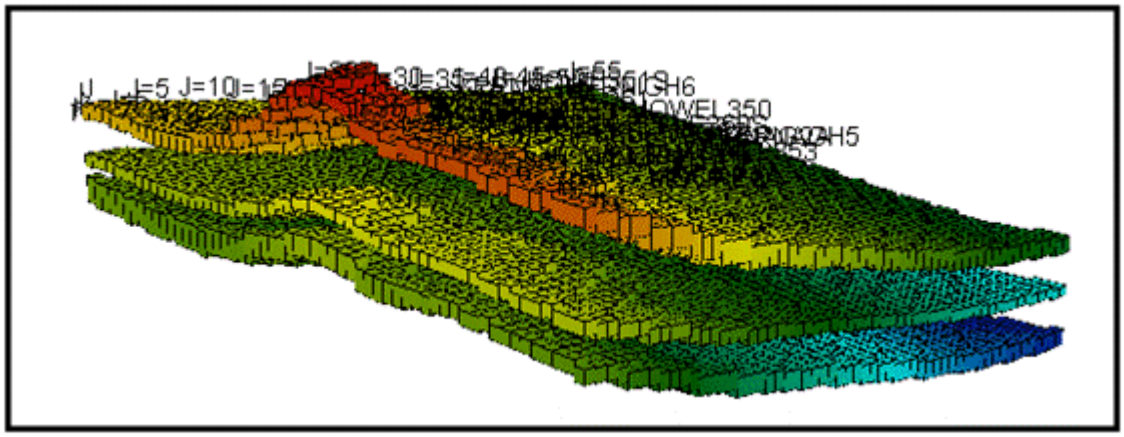

Figure 110. Model 3D view.

History Matching

During the history-matching process, the simulations were run with the wells producing on gas rate, while matching gas rate, gas composition and bottomhole pressure (when available). Water data believed to be unreliable was not matched. The injector was controlled using wellhead pressure while matching gas injection rate (composition of 98.5% CO_2 and 1.5% N_2). The history-match was run until August 2009, corresponding to the end of the injection. Table 29 shows the list of the parameters that were varied and the optimum value.

Figures 111 to 113 illustrate the history match results for the three offset wells (Section 32), EPNG Com A 300, EPNG Com A 300S and FC State Com 1. In general, the results were quite good. The gas rate in late time could not be perfectly reproduced for the EPNG Com A 300S and the FC State Com 1. The nitrogen content increase noticed in the gas samples could be fairly well replicated except for the EPNG Com A 300S well, where an increase in nitrogen content is noticed in the simulation and not in the field.

Table 29. History-Match Optimized Parameters

Parameters	Units	Min	Max	Optimized
Formation Properties				
Porosity Layer 3	-	0.005	0.03	0.023
Initial Water Saturation	fraction	0.75	1	0.99
Absolute Permeability Layer 3	mD	10	1000	582
Permeability Anisotropy	fraction	1	5	1.0
Pore Compressibility	1/psi	5.00E-05	6.00E-04	2.85E-04
Matrix Compressibility	1/psi	5.00E-07	5.00E-06	4.70E-06
Permeability Exponent	-	2	4	3.7
Differential Swelling Factor	-	1	3	2.5
Initial CO_2 Content	fraction	0.01	0.25	0.059
Relative Permeability Relationships				
Irreducible Water Saturation	-	0.05	0.4	0.15
Maximum Krg	-	0.65	0.95	0.85
Krw Exponent	-	1	3	1.6
Krg Exponent	-	1	3	1.9
Well Parameters				
Producer Initial Skin	-	-1	2	1.9
Producer Stimulated Skin	-	-5	0	-3.5

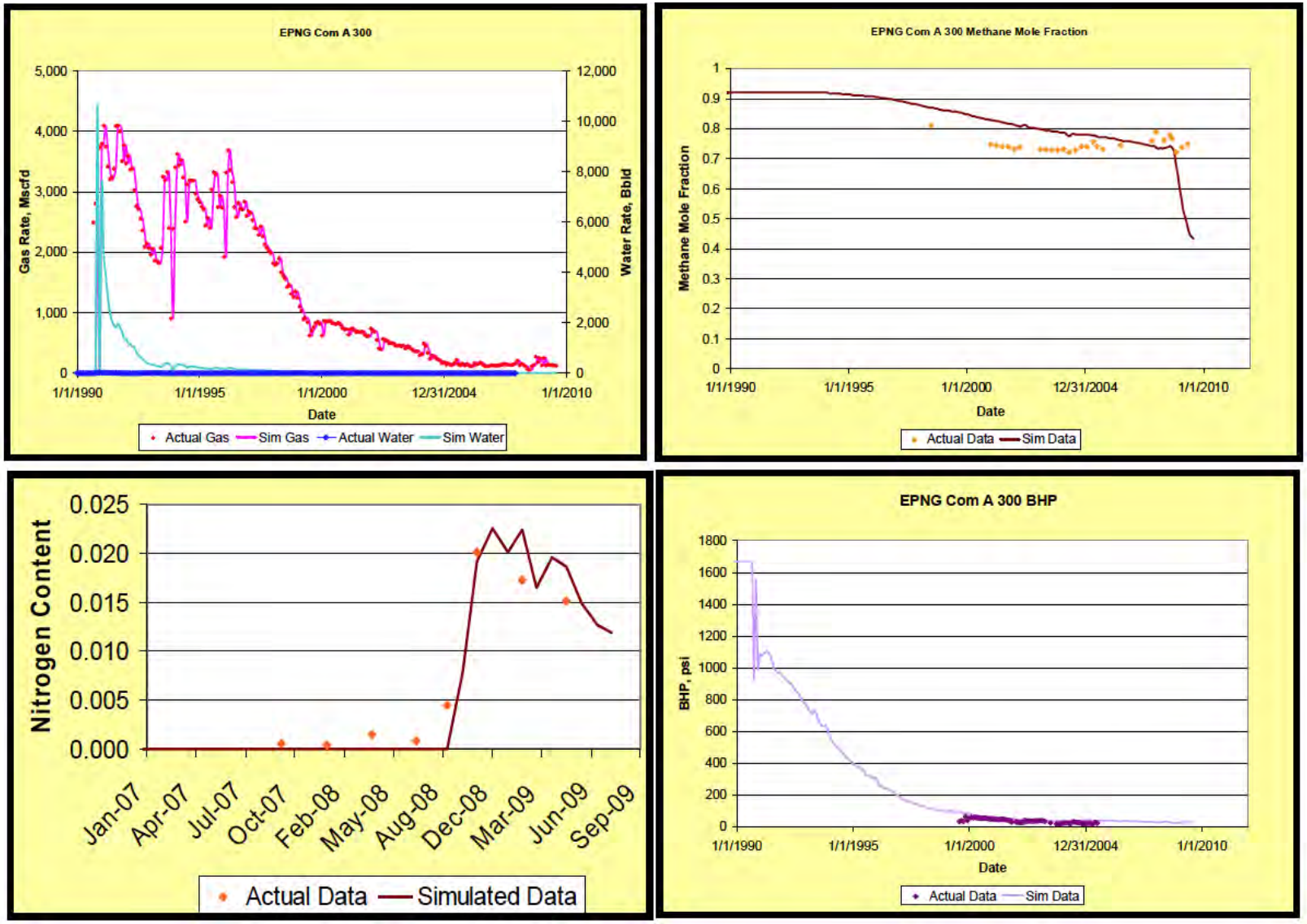

Figure 111. Well EPNG Com A 300 history-match results.

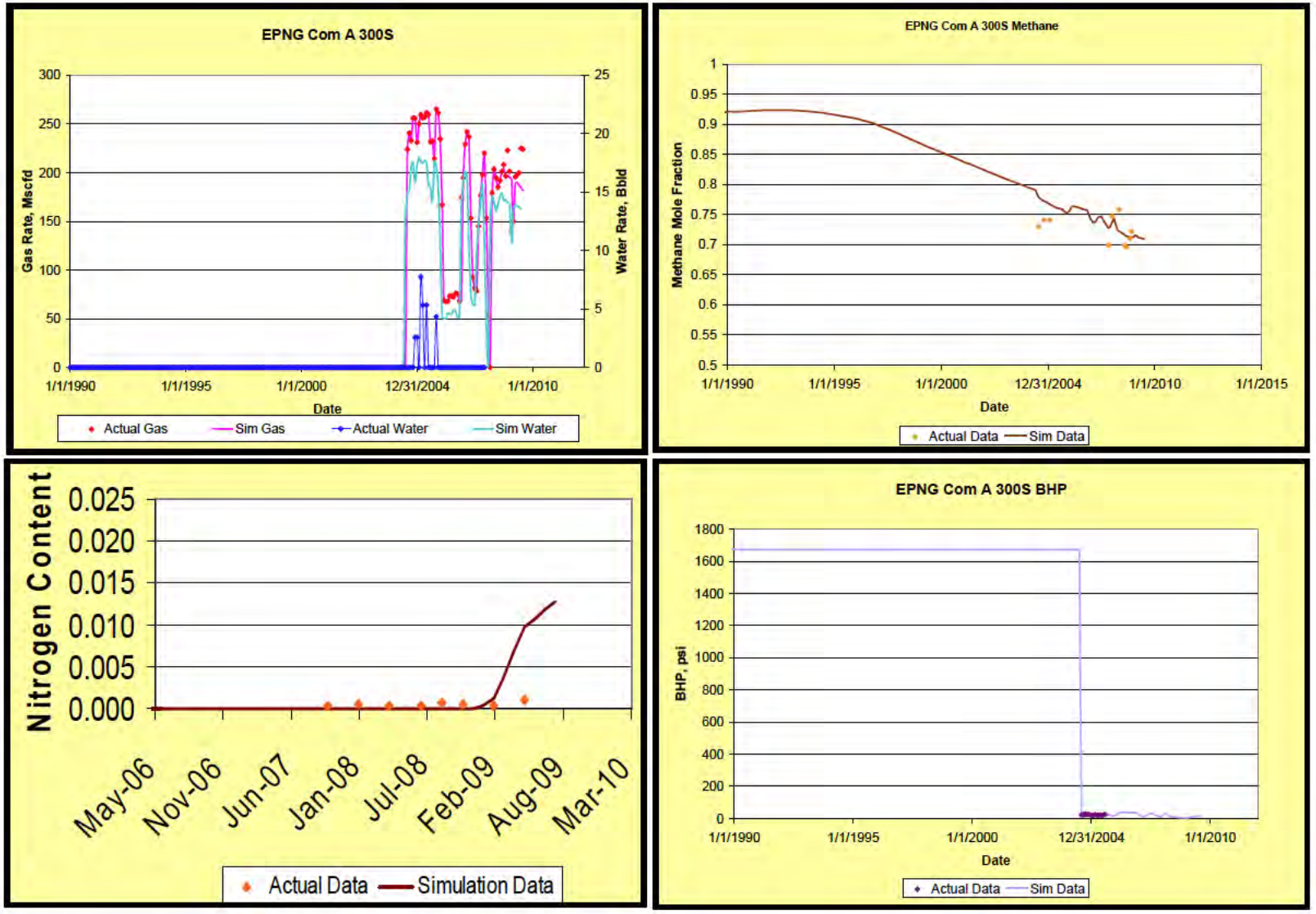

Figure 112. Well EPNG Com A 300S history-match results.

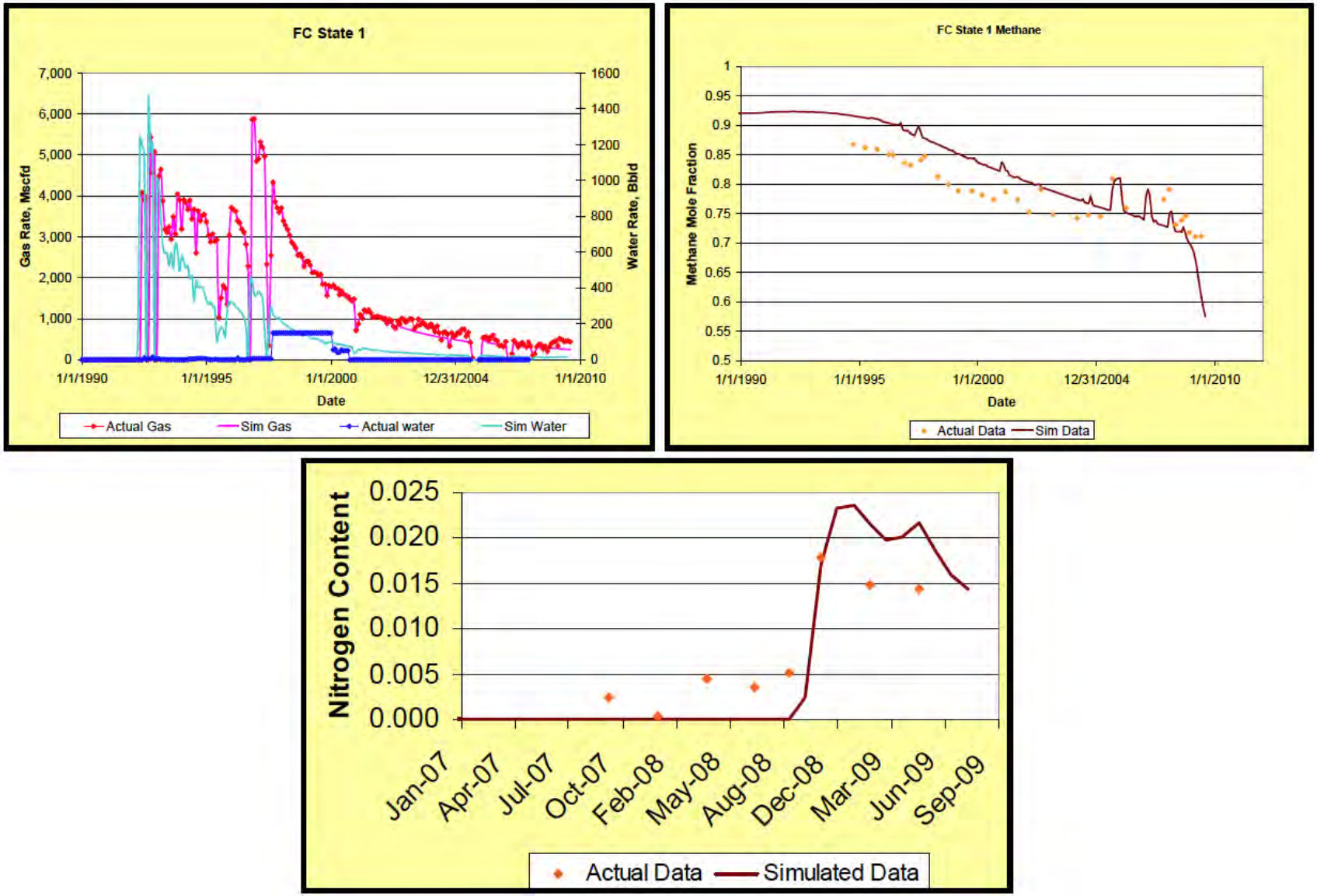

Figure 113. Well FC State Com 1 history-match results.

Figure 114 illustrates the match of both injection rate and injection wellhead pressure. The match is quite good, except for a peak in February 2009, which could not be reduced and as a consequence overestimates the quantity of injected CO_2.

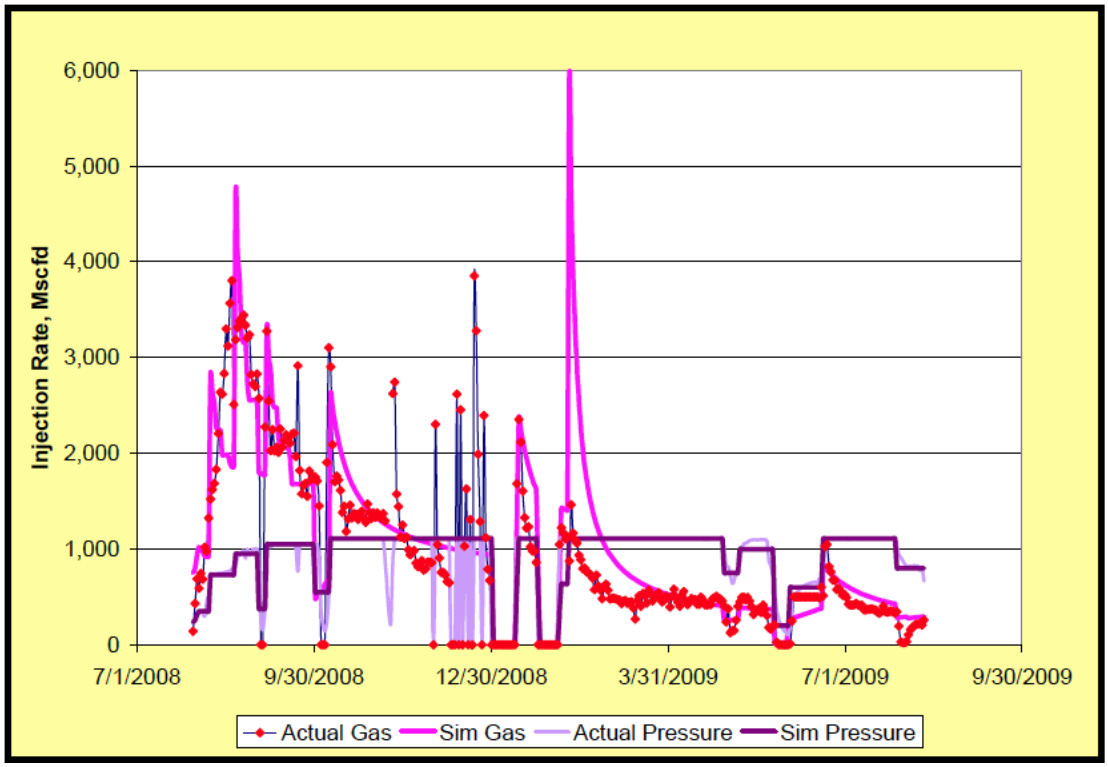

Figure 114. Injector history-match results.

Enhanced Coalbed Methane

In order to assess whether additional production was recovered due to the CO_2 injection, a "no injection" case was modeled. Figures 115–117 show the difference in methane production rate for the CO_2 injection case versus an estimate for the non-injection case for the three offset wells. The results show a total of about 26 MMscf additional methane production over the 12-month injection period or about 17% of the 150 MMscf produced. This scenario does not consider the production after injection, which could have been an increased or decreased production. This 17% increase is also less than 0.15% of the cumulative production of 18,390 MMscf since the start of production until August 2009 (8,604 MMscf for EPNG Com A 300 1990–2009, see Figure 111; 248 MMscf for EPNG Com A 300S, 2004–2009, see Figure 112; and 9,538 MMscf for FC State Com 1, 1992–2009, see Figure 113).

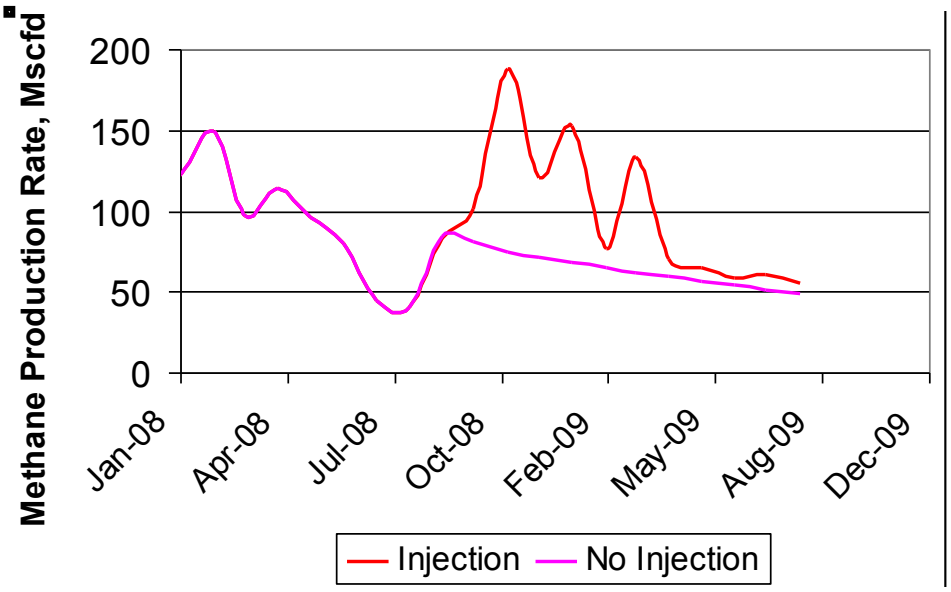

Figure 115. Well EPNG Com A 300 methane production rate – injection versus no injection comparison.

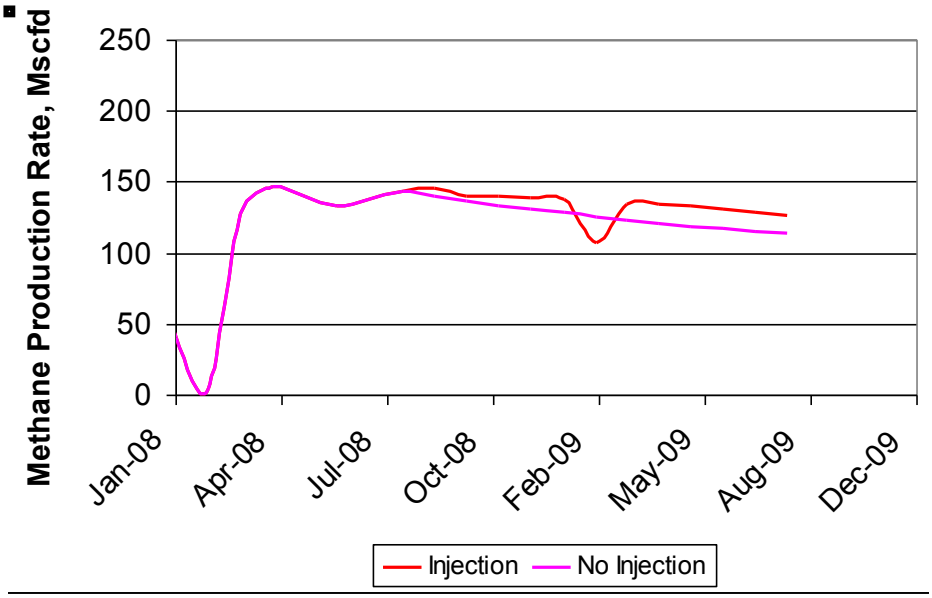

Figure 116. Well EPNG Com A 300S methane production rate – injection versus no injection comparison.

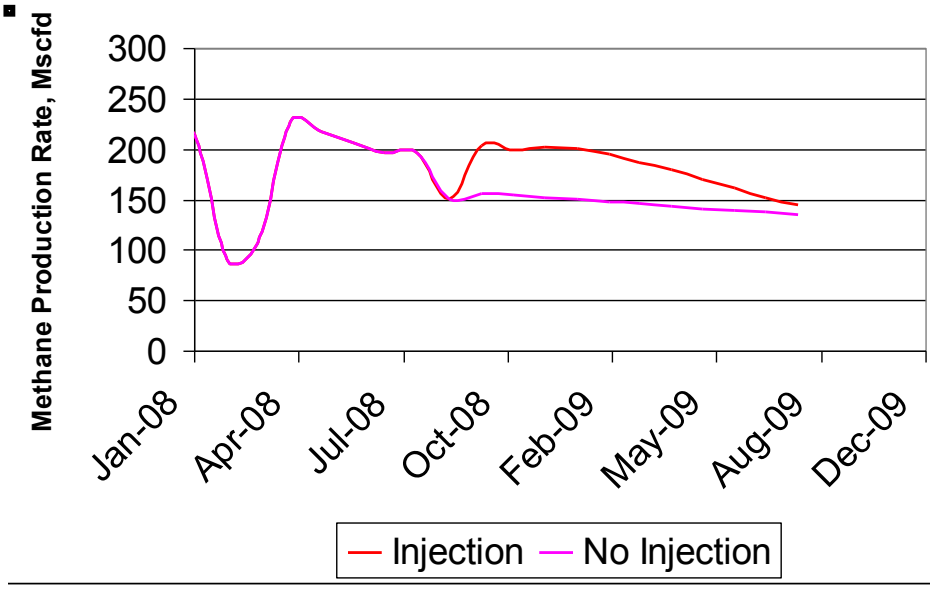

Figure 117. Well FC State Com 1 methane production rate – injection versus no injection comparison.

Pump Canyon Conclusions

The CO_2-ECBM/sequestration pilot project at Pump Canyon is an injection success.

- A total of 319 MMscf of CO_2 (or 18,400 tons) was injected over a 12-month period (July 30, 2008 to August 12, 2009); primarily due to a highly permeable coal.
- However, the CO_2 injectivity dramatically decreased over the injection period due to matrix swelling and permeability reduction as a result of the CO_2 being adsorbed onto the coal while displacing methane and increasing reservoir pressure (pore filling).
- A number of MVA techniques were employed to track the CO_2 plume inside and outside the reservoir. The CO_2 sensors installed at the three immediate offset wells, as well as gas sampling (at the three immediate offset wells as well as an additional ring of surrounding wells), suggested that no CO_2 breakthrough occurred at the site. However, a steady increase in the CO_2 content at one of the offset wells, the FC State Com 1, could have been a sign of imminent breakthrough.
- Perfluorocarbon tracers injected in the CO_2 stream showed up a few months after their injection at the two closest offset wells, the FC State Com 1 followed by the EPNG Com A 300 (where breakthrough was expected to occur first due to its alignment with the face cleats). Teamed with the observed nitrogen increases in these wells, this information indicates the preferential breakthrough path.

- The different ground monitoring techniques used (Tiltmeters, GPS and InSar) all suggested the same conclusion: no ground deformation was seen even though their effectiveness was probably limited due to the small amount of CO_2 injected.
- In order to assess the integrity of the site, a thorough seismic interpretation of approximately 9 mi^2 of 3D seismic data, centered around the injection well, was conducted that revealed a considerable stratigraphic complexity in the Fruitland formation depositional system. Post-stack processing of the 3D seismic suggested the presence of fracturing and minor faulting within the Kirtland Shale caprock, whereas indicators for extensive fracturing and faulting within the Fruitland sequence were much less apparent.
- Interpreted faults and fracture zones have limited vertical extent and major penetrative faults have not been observed at the site, reinforcing the idea that no leakage should occur.
- Baseline and post injection monitor vertical seismic profiles (VSP) were collected at zero offset and three non-zero offsets. The results were inconclusive and would not be recommended for a coal system without significant changes and further testing.
- The simulation work was able to replicate the production/injection profile of the injector and the three immediate offset production wells. The model is also indicating that methane production was enhanced due to the CO_2 injection (~26 MMscf of a total of ~150 MMscf) during the injection period. While the match is not perfect and predicts breakthrough a bit early, the model was able to tie the MVA results to the well performance (production).

Pump Canyon References

Bethke, C.M., and Johnson, T.M., 2008, Groundwater age and groundwater age dating: Annual Review of Earth and Planetary Sciences, v. 36, p. 121-152.

Bethke, C.M., Zhao, X., and Torgersen, T., 1999, Groundwater flow and the He-4 distribution in the Great Artesian Basin of Australia: Journal of Geophysical Research-Solid Earth, v. 104, p. 12999-13011.

Birkholzer, J.T. and Zhou, Q. 2009. Basin-Scale Hydrogeologic Impacts of CO_2 Storage: Capacity and Regulatory Implications. Int. J. Greenhouse Gas Control, v. 3, 745–756.

Castro, M.C., Jambon, A., de Marsily, G., and Schlosser, P., 1998b, Noble gases as natural tracers of water circulation in the Paris Basin 1. Measurements and discussion of their origin and mechanisms of vertical transport in the basin: Water Resources Research, v. 34, p. 2443-2466.

Druckenmiller, M.L., M. M. Maroto-Valer, 2005, Carbon Sequestration using brine of adjusted ph to form mineral carbonates, Fuel Processing Technology, 86, 1599-1614.

Johnson, G., et al., Tracing the fate of injected CO_2 during enhanced oil recovery using stable isotope techniques, CSPG CWLS Convention, 118-122, 2008.

Kharaka, Y.K., D.R. Cole, S.D. Hovorka, W.D. Gunter, K.G. Knauss, and B.M. Freifeld, 2006, Gas-water-rock interactions in Frio Formation following CO_2 injection: Implication for the storage of greenhouse gases in sedimentary basins, Geology, July, 577-580.

Raistrick, M., B. Mayer, M. Shevalier, R.J. Perez, I. Hutcheon, E. Perkins, and B. Gunter, 2006, Using chemical and isotopic data to quantify ionic trapping of injected carbon dioxide in oil-field brines, Environ. Sci. Technol. 40, 6744-6749.

Schwerer, F. C., and Pavone, A. M., 1984, Effect of pressure-dependent permeability on well-test analyses and long-term production of methane from coal seams, paper SPE/DOE/GRI 12857 presented at Unconventional Gas Recovery Symposium, Pittsburgh, PA, May 13–15.

USDOE-BES, 2007, Basic Research Needs for Geosciences: Facilitating 21st Century Energy Systems, Report from the Workshop Held February 21-23, U.S. Department of Energy, Office of Basic Energy Sciences, p. 186.

Watson, T. B., et al., 2007, Florida Tower Footprint Experiments, BNL Report BNL-78032-2007.

SACROC North Platform, Permian Basin, West Texas

Introduction and Overview

The Scurry Area Canyon Reef Operations Committee (SACROC) Field in the west Texas area of the Permian Basin is the oldest continuously operated CO_2-enhanced oil recovery (EOR) operation in the United States, having undergone CO_2 injection since 1972. Currently, CO_2 injection and production continues at the SACROC by the current owner/operator, Kinder Morgan CO_2. This site's CO_2 injection history confirms that injected CO_2 is effectively trapped by a sealing unit

There were two sites in the project scope initially: initially the principle site was the Claytonville field, a nearby field with geology similar to the SACROC unit, which has been acquired by Kinder Morgan, which has never been subjected to CO_2 injection. The Claytonville field was initially slated to be the primary injection MVA test site, but the primary injection MVA test site was later moved to the SACROC unit because CO_2 injection was postponed in the Claytonville field. Pilot scale CO_2 injection testing by SWP researchers began at wells 56-17, 58-2, 56-4, 56-6, and 59-2 in the North Platform SACROC Unit in September 2008.

This chapter on the SACROC test comprises several parts:

- *Site/Reservoir Characterization* provides a concise overview of geology and production history of the SACROC Unit, with an appended section on the production history of the five test wells.
- *Geologic Model Development and Numerical Simulations* describes the development of two models used for evaluating CO_2 storage mechanisms in the SACROC northern platform. The geophysical properties of SACROC were characterized and a geocellular model was built to representing the northern platform at SACROC based on analysis of well logs and 3D seismic surveys. A 3D heterogeneous model of the SACROC site was created to account for CO_2 trapping mechanisms. These simulation models indicate that injecting CO_2 into the reservoir saturated with both brine and oil reduces the amount of free CO_2, which would otherwise likely migrate vertically to the topseal. Based on these re-

sults, researchers recommend CO_2 injection into brine formations that lie below oil reservoirs.

- *Core Testing and Rock Physical Model* details the use of rock physics modeling to quantify the changes in seismic response that occur in the reservoir due to injection of CO_2. Combined microscale, mesoscale, and macroscale information was used to better understand of the various processes at work when CO_2 is sequestered in a limestone reservoir. Samples of SACROC reef limestone were used for ultrasonic velocity measurements, detailed mineralogy and scanning electron microscopy (SEM) characterization, and computed tomography (CT) scanning. Rock physics modeling was performed to quantify the changes in seismic response (velocities, impedances, seismic amplitudes that can occur in the reservoir due to injection of CO_2; the model set up is in a good agreement with the core measurements.
- *Seismic Reflection Data Processing of 3D Surveys Over an EOR CO_2 Injection* presents a detailed 4D reflection seismic imaging project whose results will allow 4D calculation of seismic attributes and change detection related to the CO_2 injection. Two additional small 3-D swath geometry reflection seismic surveys were also collected over the region surveyed; their amplitude differences can be interpreted to represent time variation in pressure and pore filling fluid phases.
- *Time-Lapse Offset and Walkaway VSP Monitoring of CO_2 Enhanced Oil Recovery at the SACROC Unit* presents the results of VSP surveys conducted in July 2008 and April 2009, respectively, in the North Platform of the SACROC Unit in order to study the capability of vertical seismic profiling (VSP) for monitoring migration of CO_2 plume within geologic formations. The VSP surveys detected the changes due to migration of CO_2 plume within geologic formations, which are consistent with the results of a surface reflective seismic survey. The results also indicated that time-lapse walkaway VSP is more reliable than time-lapse offset VSP for monitoring CO_2 sequestration, and that the repeatability of time-lapse VSP surveys is critically important for reliable reservoir monitoring.
- *Interpretation of the Logging Data on SACROC Units #56-4ST and 56-6ST* is a report on the analysis of the data obtained by repeat geophysical borehole logging in two of the three SWP injection experiment site monitoring wells, 56-4ST and 56-6ST.

- *SACROC Field Soil CO_2 Flux Monitoring* demonstrated that measuring the soil CO_2 flux before and during injection was successful in establishing a solid background level that can be expected during different seasons and at different times of the day. Although no leaks were found during the monitoring period, for better detection of leaks, it is recommended to install a system that can monitor CO_2 concentrations in the atmosphere on a more macroscopic level, so that, if the CO_2 concentrations in the soil increase, more localized monitoring can be performed to find the actual source of the leak.
- *SACROC Groundwater Study* showed no impacts to drinking water quality as a result of over 35 years of deep subsurface CO_2 injection. Modeling of stable carbon isotopes ($\delta^{13}C$) of injectate CO_2 gas, DIC in shallow and deep groundwater, carbonate mineral matrix, and soil zone CO_2 suggests that no significant injectate CO_2 has been introduced to the shallow groundwater.

The SACROC field test demonstrates the efficacy of proposed sequestration technologies to reduce or offset greenhouse gas emissions in the region. Risk mitigation, optimization of MVA protocols, and effective outreach and communication were additional, critical goals of these field validation tests. This pilot was an example of a medium-scale validation test in a sink that may host capacity for possible larger-scale sequestration operations in the future. These validation tests also demonstrate multiple value-added benefits for enhanced oil recovery and sequestration.

Site/Reservoir Characterization

The Scurry Area Canyon Reef Operations Committee (SACROC) Unit is the oldest continuously operated CO_2-enhanced oil recovery (EOR) operation in the United States, having undergone CO_2 injection since 1972. Over the past 30 years, about 93 million tons of CO_2 have been injected and about 38 million tons have been produced and reinjected. A simple mass balance suggests that the site has accumulated about 55 million tons of CO_2. Currently, CO_2 injection and production continues at the SACROC by the current owner/operator, Kinder Morgan CO_2. SACROC is found on the eastern flank of the Horseshoe Atoll in western Texas (Fig. 118).

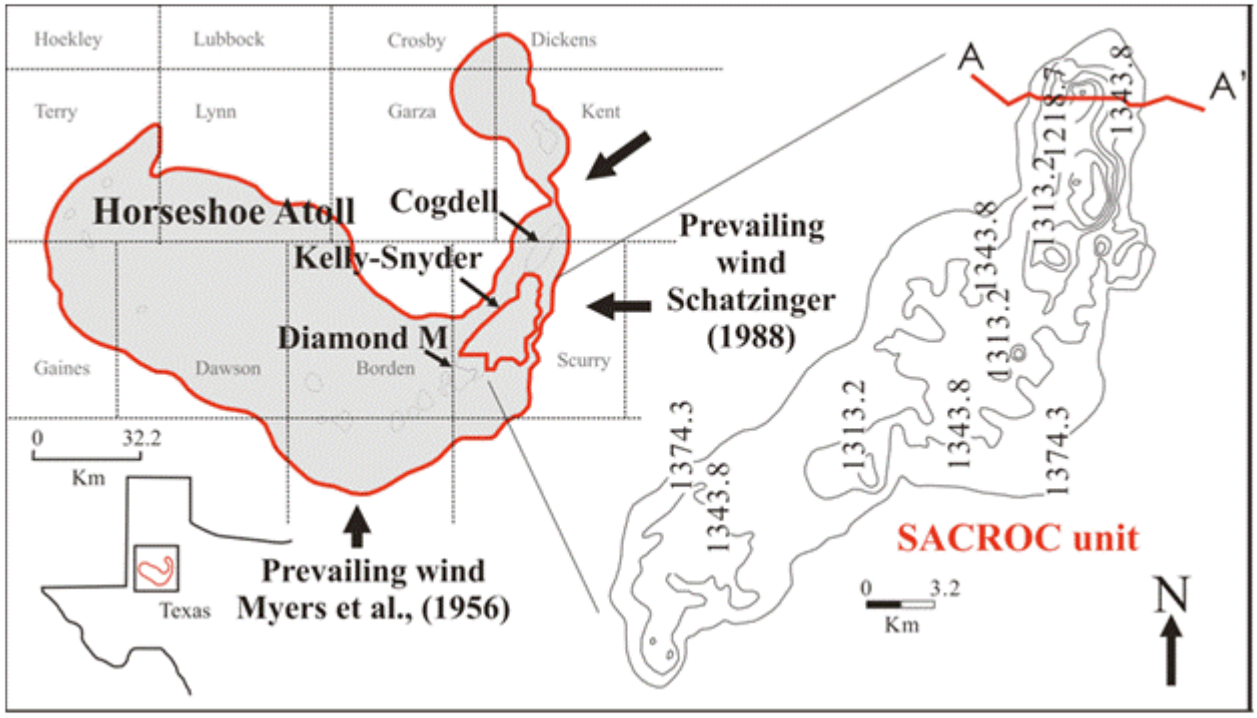

Figure 118. The location of SACROC Unit at the Horseshoe Atoll in western Texas and structural contour map showing subsea depth of the carbonate reef (Stafford, 1954). Contours are on the meter scale.

Initially two sites were in the project scope: the Claytonville field and the SACROC unit. The Claytonville field has never been subjected to CO_2 injection. The Claytonville field was initially slated to be the primary injection MVA test site, but late in 2006 Kinder Morgan decided to delay the building of a CO_2 pipeline to the Claytonville field. In 2007, Kinder Morgan and the SWP moved the primary injection MVA test site to the SACROC unit, where a CO_2 source was immediately available. New injection at SACROC began in fall 2008 in the pilot area.

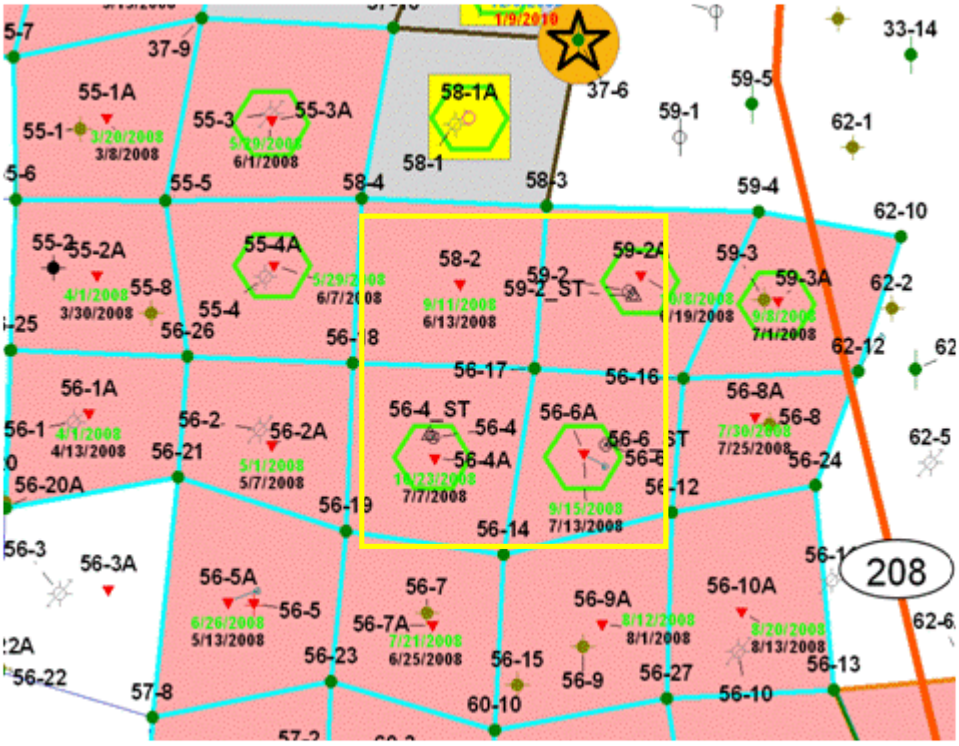

Figure 119. The CO_2 injection pilot site centered on producer well 56-17.

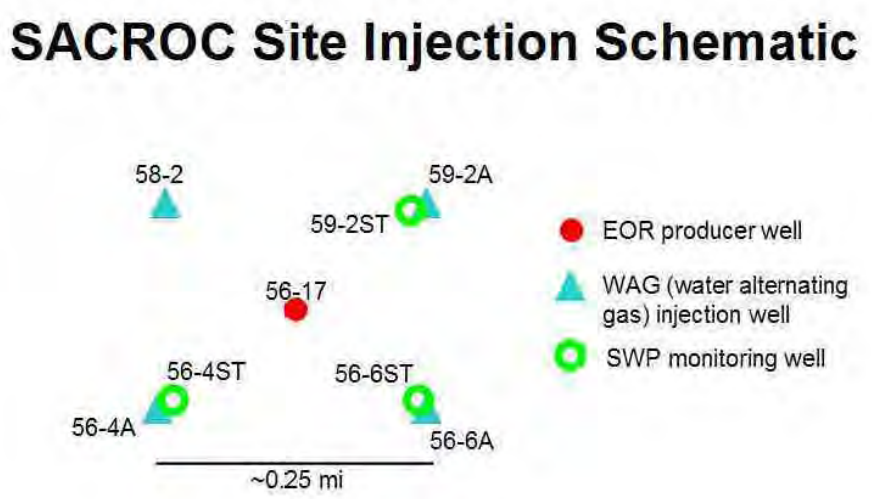

Figure 120. Injection, production, and monitoring wells at the SWP SACROC 56-17 injection experiment site.

CO_2 injection pilot plan

The pilot site for CO_2 injection at SACROC is a five-spot well pattern—one producer (well 56-17) in the center of four injectors (56-4, 56-6, 58-2, 59-2) (Fig. 119). Monitoring wells are located at previous oil well sites 56-4, 56-6, and 59-2 (Figure 120). Injection in wells surrounding 56-17 will be performed over a period of approximately seven years. KinderMorgan drilled three new WAG (water-alternating-gas) injection wells (56-4A, 56-6A, and 59-2A), which are located within 100 to 300 ft of the three injection experiment site monitoring wells (Figs. 98 and 99). The total amount of CO_2 to be injected is the equivalent of 0.57 pore volume (PV) of the reservoir rock. CO_2 re-injection to the trial wells (four injectors 56-4, 56-6, 58-2, and 59-2) was started by the end of 2008. The injectors were used under a WAG injection scenario. CO_2 injection began in each of the four WAG injection wells after 30 days of water injection. The CO_2 was injected below the Cisco formation and within the top of the Canyon formation (Fig. 100). The production of producer 56-17 in the center of the four injectors was monitored. The maximum oil production rate of well 56-17 was 41.16 bbl/d before CO_2 re-injection and 643 bbl/d within one year after CO_2 re-injection. A summary of the injection/production history for these five wells is presented in the SACROC Topical Report, "SACROC North Platform in the Permian Basin, West Texas," (Xiao et al., 2011) with more detail on the entire project.

SACROC geologic description

A cross-section of geologic structure and stratigraphy of the study area is presented in Fig. 121. The carbonate reef complex developed in the early Strawn (Desmoinesian), while the basin was on the equator. During the formation of the Canyon (Missourian) and Cisco (Virgilian), carbonate sedimentation continued. Accumulation of carbonate sediments on the SACROC ended during the Wolfcampian due to the drastic influx of fine-grained clastics. The oil at SACROC is produced from the Canyon and Cisco Formations, which are Pennsylvanian (Vest, 1970). The Wolfcamp shale of the lower Permian acts as a seal above this Pennsylvanian unit representing Canyon and Cisco groups (Raines et al., 2001).

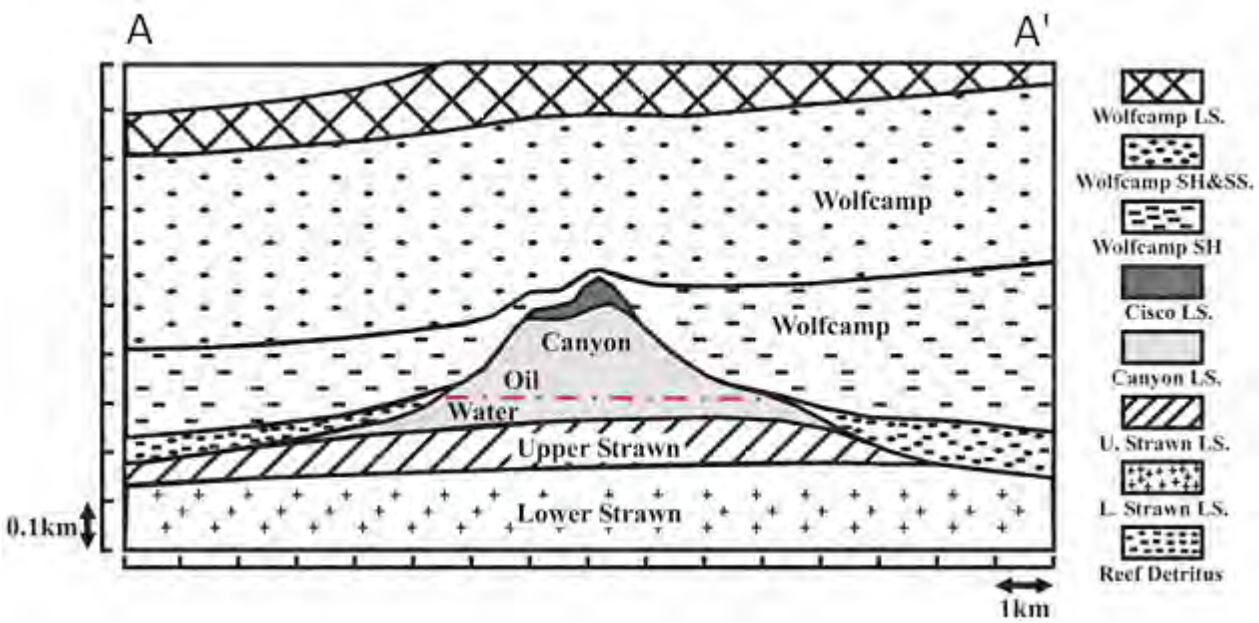

Figure 121. A structural and stratigraphic cross-section of profile A-A', located within the SACROC northern platform (Vest, 1970). for a location of profile A-A'.

The Wolfcamp shale formation that accumulated during the lower Permian age is a low permeability seal above the Cisco and Canyon Groups (Raines et al. 2001). There has been no indication of CO_2 leakage in this field although CO_2 has been injected for the purpose of enhanced oil recovery since 1972. To confirm that the Wolfcamp shale formation is still acting as a perfect seal, water chemistry data was gathered and analyzed. Generally, while most of the brines are Na-Cl types, shallow groundwater shows distribution from Na-HCO_3 to Ca-HCO_3 (Fig. 122).

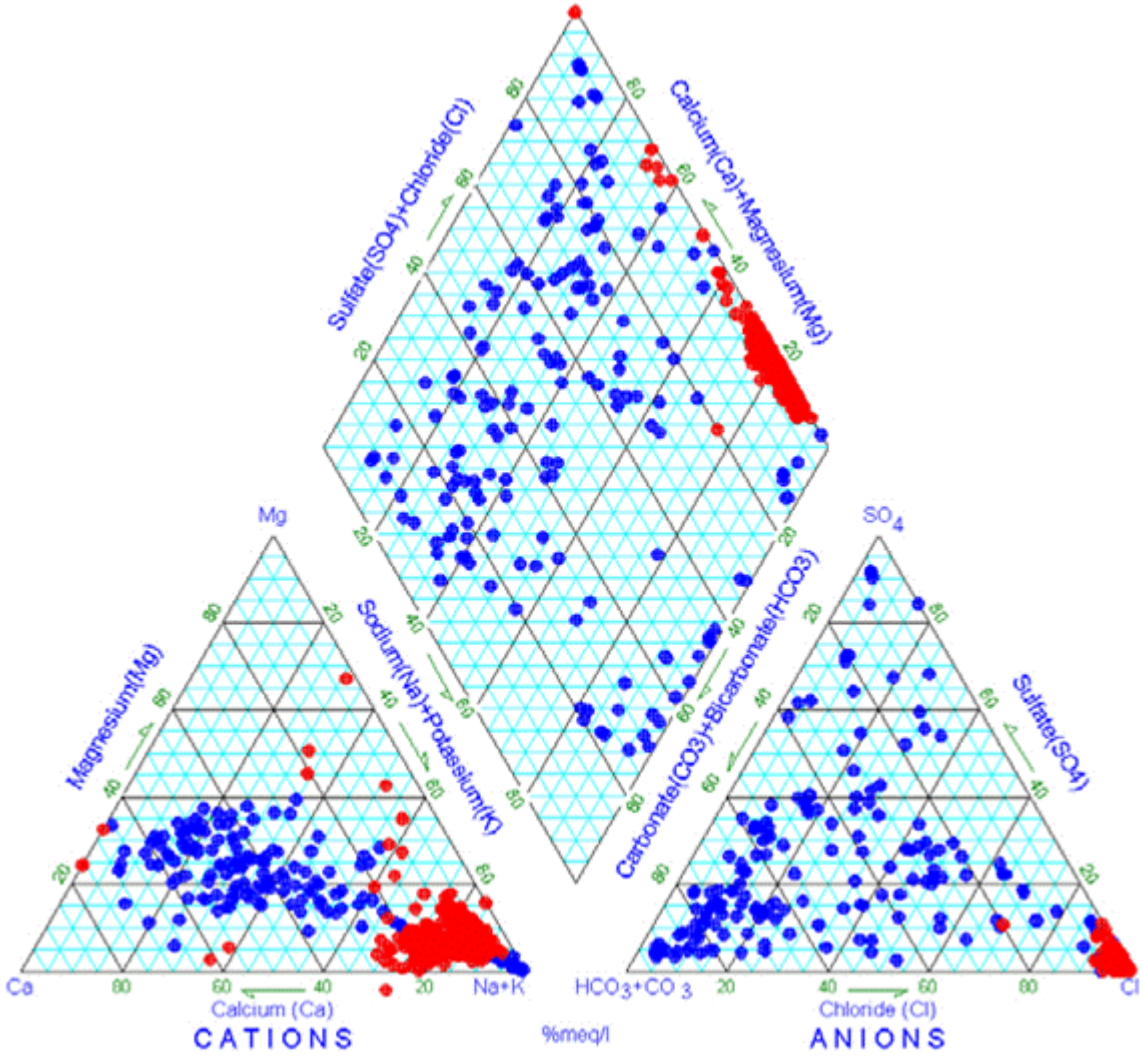

Fig. 122. Hydrogeochemical classification of both brine and shallow groundwater. From Han and McPherson (2007).

Geologically, the carbonate reef complex at SACROC is composed of massive amounts of bedded bioclastic limestone and thin shale beds (mm to cm in thickness) representing the Strawn, Canyon, and Cisco Formations of the Pennsylvanian, and the Wolfcamp Series of the Lower Permian (Vest, 1970). A majority of the Canyon and Cisco formations is composed of limestone, but minor amounts of anhydrite, sand, chert, and shale are present locally (Raines et al., 2001). Recently, Carey et al. (2006) analyzed core samples from wells 49-5 and 49-6 in the SACROC field and indicated that the limestone was mostly calcite with minor ankerite, quartz, and thin clay lenses. X-ray diffraction results indicate that the Wolfcamp shale is mostly illite and quartz

with minor feldspar, carbonate, and pyrite. Based on mineralogical analysis, Carey et al. (2006) indicated that the CO_2 has not interacted with shale.

The changes in depositional environment cause a wide variability of both porosity (0 to 30%) and permeability (0 to 1000 mD) in the Cisco and Canyon Groups. Bergenback and Terriere (1953) megascopically observed porosity and suggested that its range was approximately 0 to 20 %. Similarly, Myers et al. (1956) observed porosity from 0 to 30 % after core analysis. Both found that most porosity was developed during secondary digenesis processes with mineralization evidences such as calcitization, dolomitization, and silicification. Burnside (1959) indicated that open fractures markedly influenced the permeability in this field. Other studies such as Vest (1970), Kane, (1979), Langston et al. (1988), Raines, (2005), and Brnak et al. (2006) also provide detailed discussions of average porosity and permeability.

Reservoir description

The SACROC Unit, comprising about 98% of the Kelly-Snyder field, was discovered in November 1948. Table 30 summarizes SACROC reservoir parameters. The original oil in place (OOIP) in this unit was estimated approximately 2.73 billion stock tank barrels (STB) in the Canyon reef limestone formation (Dicharry et al., 1973). The solution gas content was slightly under 1,000 standard cubic feet (SCF)/STB, with a bubblepoint pressure of 1,805 psi (12.45 MPa) (Dicharry et al. 1973). Later, Kane (1979) estimated the OOIP as 2.1 billion STB and van Everdingen and Kriss (1980) as 2.113 billion STB. Because of the tremendous volume of oil still left in the reservoir after waterflooding, enhanced oil recovery (EOR) techniques were considered to improve oil recovery. Since 1972, CO_2 has been injected to enhance oil recovery. From mass balance analysis, the site has accumulated about 55 million tonnes (55,632,735,360 kg) of CO_2 (Raines, 2005).

Analysis of CO_2 injection/production histories provided by Kinder Morgan CO_2 Inc. show that 97 wells have been used as CO_2 injectors at the northern platform SACROC from 1972 to 2002. Among them, 51 wells were actively used to inject approximately 13 million tonnes of CO_2 (13,048,845,748 kg) into the Cisco and Canyon Formations. Another 219 wells were CO_2 producers during the same period. Among them, 124 wells were used to produce approximately 6

million tonnes of CO_2 (6,104,258,074 kg). A simple mass balance analysis suggests a net of approximately 7 million tonnes of CO_2 (6,944,587,674 kg) were sequestered in the northern platform SACROC from 1972 to 2002.

Initially the nearest CO_2 source was the Ellenburger hydrocarbon gas fields in the Val Verde basin about 220 miles (354 km) south of SACROC Unit. In this gas field natural gas including 18~53% of CO_2, were produced (Newton and McClay, 1977). CO_2 was sold as a byproduct from several gas processing plants. The CO_2 is separated, compressed, and sold for EOR use in the Permian Basin.

Table 30. Reservoir Parameters in SACROC Unit, Estimated by Vest (1970)

Rock Properties	
Porosity (%)	
Net (>3%)	10.03
Gross	7.11
Permeability (mDarcy)	
Net (>3%)	19.4
Gross	30.6
Fluid Properties	
Gravity of oil (°API)	42 (=0.816 specific gravity)
Sulfur (%)	0.183
Formation volume factor (bbl/bbl @SP)	1.500
Viscosity of oil (cp @SP)	0.375 (=0.375x10^{-5} kg/m-s)
Gas cap	None
Gravity of gas	1.13
Solution gas-oil ratio (CFPB @SP)	1000
Water salinity (mg/l)	159000
Water saturation (%)	28.2
Pressure	
Initial reservoir pressure (psig@-4300ft)	3122 (21.53 MPa@-1310.64m)
Bubble point pressure (psig)	1805 (12.45 MP)
Critical gas-saturation pressure (psig)	±1600 (11.03 MPa)
Oil Production Mechanism	
1948 – 1953	Solution gas drive
1954 – 1971	Artificial water injection drive (Center line)
1972 – Current	Pattern waterflood / CO_2 injection drive
Pay Section	
Maximum oil column (ft)	765 (233.17 m)
Average pay thickness (ft)	229 (69.80 m)
Estimated oil in place (billion bbl)	2.73
Estimated total oil recovery (%)	51.7

*SP: Standard pressure, *CFPB: cubic feet per barrel

The CO_2 supply rate was not sufficient or consistent enough to service the entire SACROC Unit simultaneously. This supply rate was equivalent to about one-third of the SACROC Unit's required volume. Therefore, the SACROC engineering committee decided to divide the CO_2 target area into three phases. Each phase had approximately equal hydrocarbon pore volumes (HCPV).

The MMP for CO_2 and SACROC crude is ~1600 psi (11.03 MPa) (Dicharry et al. 1973). A large part of the SACROC Unit was not sufficiently water-flooding (and associated pressure increases), thus the pressures in the targeted area for the WAG project were typically below the MMP.

After performing pre-CO_2 water injection from October 1971 to December 1971 in the Phase I area, CO_2 injection started in January 1972. Although the original reservoir pressure was below MMP, it rose above the MMP (2,400 psi =16.55 MPa) by April 1973 due to water and CO_2 injection (Langston et al. 1988).

As CO_2-WAG proceeded, advanced early CO_2 breakthrough dictated changes in the original plan. Within six months of the initial CO_2 injection in June 1972, CO_2 breakthrough occurred in production wells. The peak CO_2 breakthrough was reached in November 1972 and exceeded the capacity (3,000 MCF/day=84.95 Mm3/day) of the existing CO_2 removal facility (Kane, 1979). Therefore, it was necessary to curtail production rates until the middle of 1973 to complete installation of additional CO_2 removal facilities.

The main causes of the early CO_2 breakthrough were preferential flow paths for the (CO_2) gas, and low pressure, which created an immiscible gas migration. The latter problem was easy to solve by increasing reservoir pressure. Preferential flow paths were not an easy problem to solve. It was determined that increasing the WAG ratio and decreasing the volume of CO_2 could control CO_2 production. Between 1972 and 1985 water-flooding activity increased reservoir pressure above the MMP. However, during this period, the amount of injected CO_2 was relatively small compared to current CO_2 injection rates (Fig. 123) and the CO_2 injection wells were scattered. The CO_2 supply was not continuous because of the discontinuity of CO_2 injection and the difficulty of maintaining the CO_2 supply from the gas plants.

After 1995, Pennzoil, Inc. (Pennzoil), who became the operator of the SACROC Unit, gradually increased the volume of CO_2 injection (Fig. 123). First, Pennzoil injected CO_2 into two project areas as opposed to following the scattered injection patterns over the SACROC Unit. Pennzoil purchased additional CO_2 from McElmo Dome, a natural CO_2 reservoir in Colorado, and thus improved the CO_2 supply (Fig. 123). Even this operation was not as efficient and effective as fu-

ture CO_2 operations. Oil production did not increase dramatically (Fig. 123). One of the reasons for a lack of improved oil production was that the entire production pattern was not above MMP and measures were not implemented to keep oil from migrating outside of the project area.

Since Kinder Morgan CO_2 Inc. (KM) purchased this field oil production rates have increased dramatically (Fig. 123). After KM became the operator of this field, CO_2 injection has targeted residual oil after water-flooding, controlled reservoir pressure through either pre- CO_2 water injection or the operation of water curtain wells, used smaller (~40 acres) patterns, avoided CO_2 flooding where high CO_2 relative permeability is observed, performed CO_2 flooding where successful water-flooding was performed, and significantly increased over all CO_2 injection volumes (Raines, 2001).

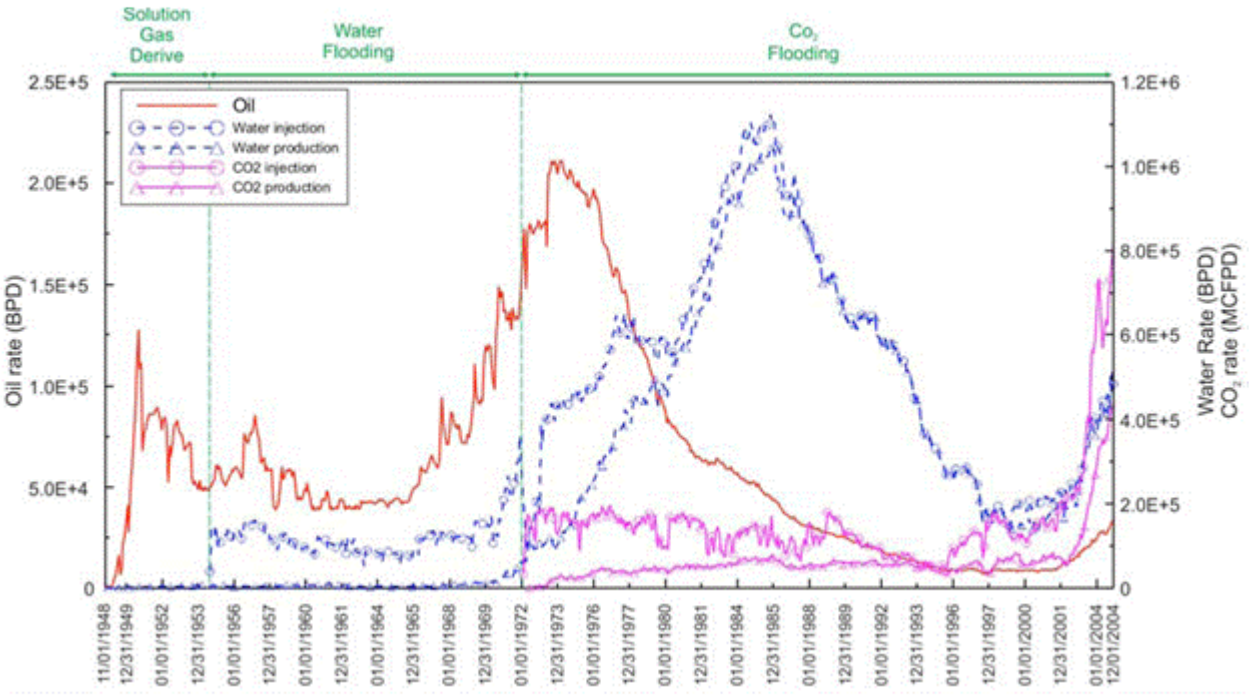

Figure 123. Injection and production history of oil, water, and CO_2 (Raines et al. 2005).

Reservoir Characterization Summary and Conclusions

The SACROC Unit is the oldest continuously CO_2-flooded operation in the US (since 1972). Because of its history and the amount of injected CO_2, the SACROC Unit is regarded as a valuable analogue site for CO_2 sequestration. Extensive records of injection/production history are available and infrastructure for CO_2 injection exists. The SACROC Unit provides direct evidence of

rock property changes associated with CO_2 injection over time, which are difficult to observe in laboratory experiments.

Core Testing and Rock Physics Model

Combining microscale, mesoscale, and macroscale information should lead to a better understanding of the various processes at work when CO_2 is sequestered in a limestone reservoir. Rock physics modeling is a powerful tool to quantify the changes in seismic response (velocities, impedances, seismic amplitudes, etc.) that can occur in the reservoir due to injection of CO_2.

Core samples and 3D seismic surveys from SACROC were acquired in order to better characterize the movement of the CO_2 injection plumes. Ultrasonic velocity, detailed mineralogy and Scanning Electron Microscopy (SEM) characterization, Computed Tomography (CT) scanning, thin section studies, porosity, P and S wave velocities, and permeability at varying pressures, temperatures, and fluid saturations that simulate reservoir conditions, were all performed. Measurements were taken with supercritical CO_2 at in situ pressures and temperatures. Expected velocities for the samples were modeled using the standard Gassmann equations and the Mavko-Jizba equations. Pore volume, area, and connectivity are essential for chemistry experiments that will emulate time exposure of CO_2 to limestone. Further, ImageJ allows pore orientation information to be obtained to understand the anisotropic conditions that may affect seismic data.

SEM and CT Characterization

SEM and X-Ray diffraction analysis revealed a vuggy carbonate with stylolites and abundant ammonoid bioclasts composed of >80% calcite, variable amounts of dolomite, quartz, apatite, and clay minerals. Elemental analysis confirmed the presence of dolomite, (Figure 124).

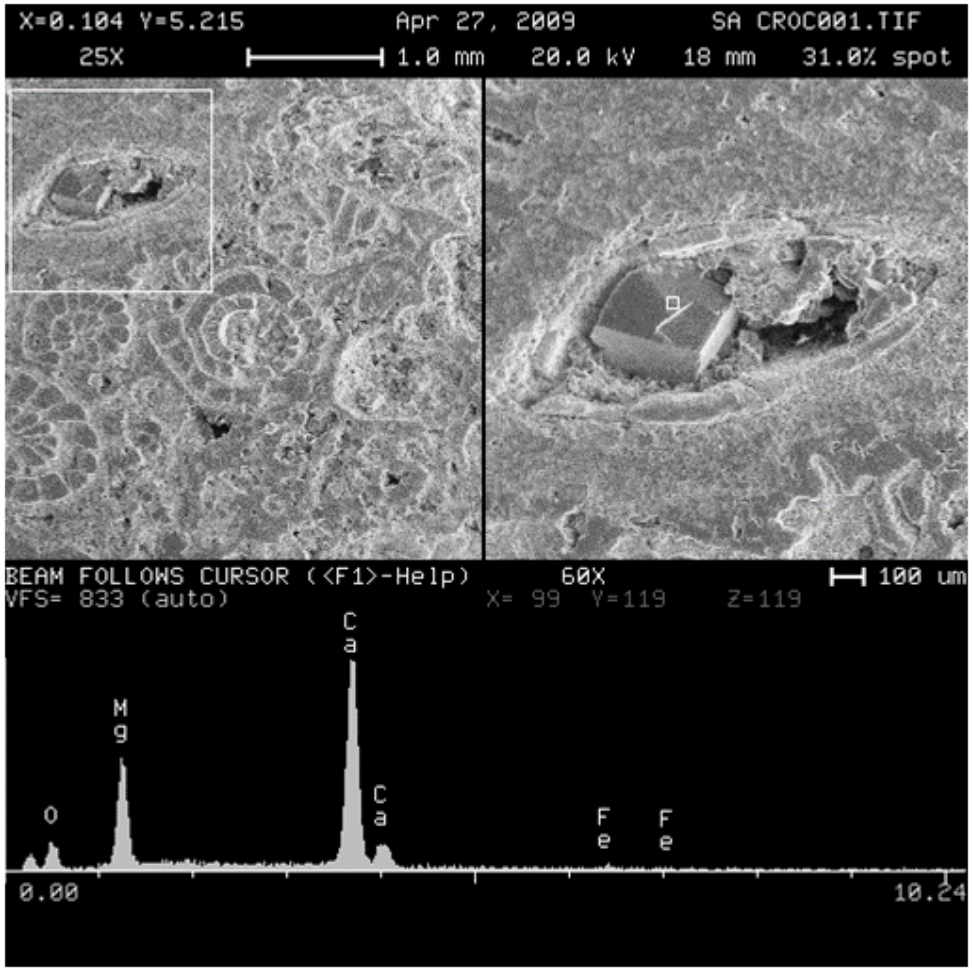

Figure 124. SEM image of a pore from the SACROC core. Note the presence of a dolomite crystal, as shown by the elemental analysis displayed at the bottom of this figure, and geometry of pore. Fossils present in the framework of the rock are also visible.

Numerical Flow Simulation from CT Scans

A portion of the large connected pore network shown in Figure 125 was isolated, converted to a numerical mesh, and used to perform a pore-level computational fluid dynamics (CFD) simulation. By cropping the velocities in the isolated region of the pore network to 0.05 to 0.0012 m/s the primary flow path through this segment was identified, with faster flow in small channels along the percolation backbone.

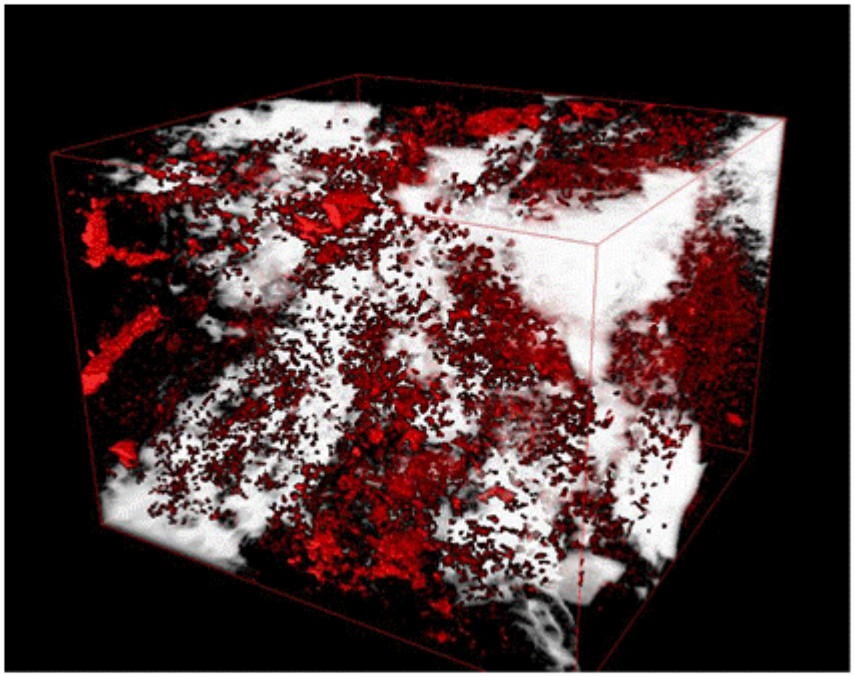

Figure 125. Large connected pore network shown in white and unconnected pores in red. (Volume size 1.54 x 1.40 x 1.12 mm)

Rock Velocity Experiments

Several different types of tests were conducted on one SACROC Core #1. In the first experiments the confining pressure was incrementally raised to 50 MPa. A marked increase in P-Wave velocity was seen, indicating the closure of microcracks in the sample (Shapiro and Kaselow, 2004). Then the core was flooded with CO_2 under varying in-situ conditions, pore pressures between 0 and 30 Mpa, while maintaining a constant confining pressure of 30, 40, and 50 MPa. Increasing pore pressure caused the velocity to decrease rapidly under all confining pressure regimes (Purcell et al. 2010). This agrees well with other studies (Wang and Nur, 1989). Hysteresis experiments on a CO_2 saturated SACROC sample showed little velocity change between pressurization and depressurization (Purcell et al. 2010). Also a higher resolution hysteresis experiment where only confining pressure was changed with no pore fluids show that at high pressures, the velocities agreed well, but at low confining pressures, the velocities on the depressurization curve were found to be higher by ~5%.

An ultrasonic transducer was used to measure one compressional and two orthogonally polarized shear waves and associated waveforms. For each step, the first arrival of P, S1 and S2 were

picked from waveforms. These picks then allowed the determination of VP, VS1, VS2, Young's modulus and Poisson's ratio.

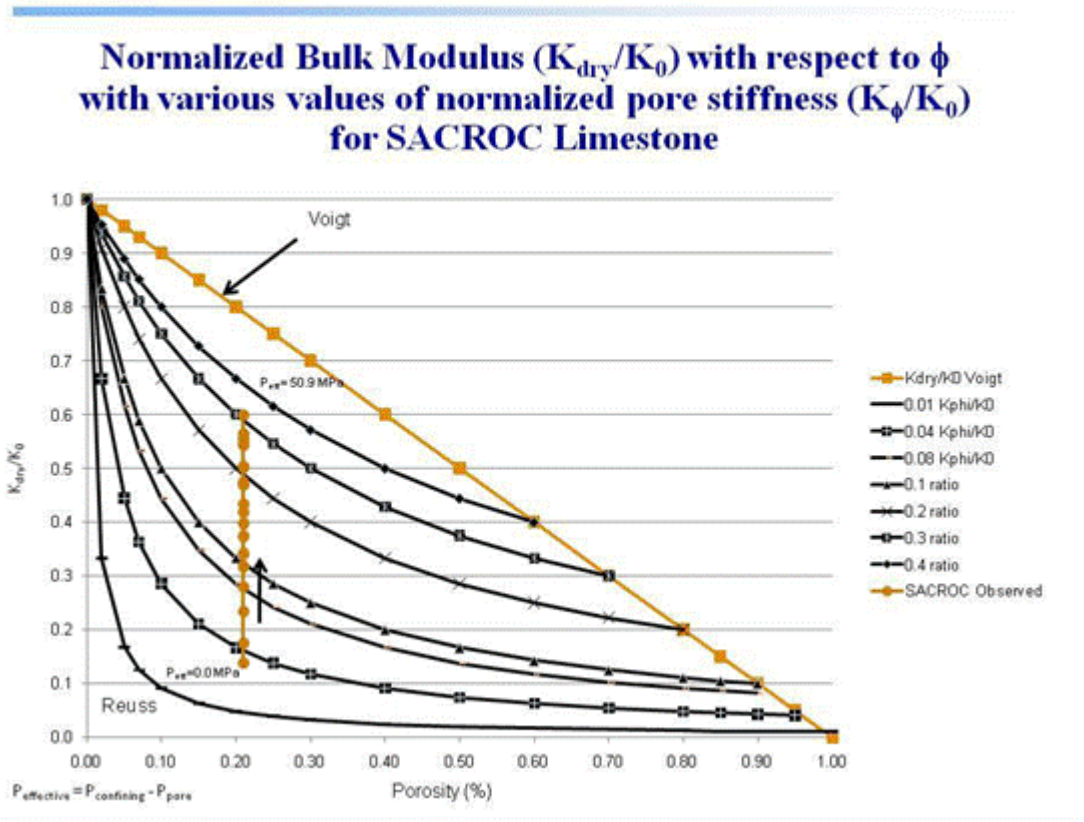

Figure 126. Comparison of Ruess and Voigt expected lower and upper bounds and expected K_{dry}/K_O values for an increasing ratio of normalized pore stiffness values. Our experimental results are shown and show a large variation over the measured P_{eff}. See Mavko et al., (Mavko et al., 2003) for definitions and details.

Gassmann Calculations

Measurements and calculation of standard bounds (Mavko et al., 2003) suggested that the SACROC material was complex (Figure 126). Measurements of SACROC limestone core showed that V_s velocities could be accurately predicted from Gassmann calculations for high effective pressure. However, at lower effective pressures, V_p was not accurately modeled. This is not surprising as earlier studies used models in which the sample pore geometries had spherical stiff porosity and flat cracks compliant porosity, which together produce a pressure and stress dependency on porosity and associated rock mechanical parameters (Shapiro, 2003; Shapiro and Kaselow, 2005).

Anisotropy

Seismic anisotropy is the variation of velocity with direction, and is an indicator of alignment of features that are smaller than the seismic wavelength, such as cracks, pores, or layers, leading to a directional variation in seismic velocity. Anisotropy experiments were performed on two SACROC cores of widely differing porosity (6.6% vs. 19%). The experiments were performed by rotating the core 45 degrees after each set of experiments were completed. Four sets of measurements were completed at 0, 45, 90 and 135 degrees, and confining pressure was varied from 5–60 MPa for each run, with no saturating fluid. Core #1, which has a porosity of 19%, was from a depth of 6500 ft, and Core #2 with porosity of 6.6%, was from a depth of 6180 ft. The results of these experiments show that while Core #1 has only a slight variation in velocity ~1-3%, core #2 has an S-Wave anisotropy of up to 10%, indicating the strong orientation of rock matrix features, perhaps vugs.

Resistivity

A tap water-saturated SACROC core was tested to see if any pressure dependent resistivity could be found varying confining pressure from 5-60 MPa. The resistivity of the sample increased 81% over the pressure range. This increase in resistivity is due to the closing of microcracks, and the cutting off of paths for conductive ion transport.

Conclusions

Predicting the location of injected CO_2 in the reservoir accuracy increased by updating the model from the micro-scale up to the macro-scale. The velocity measurements serve as a test of different rock physics models. Velocity models are more complex and allow for the incorporation of micro-macro pore differentiation, compliant (soft) porosity, and the phase of the pore-filling substance. Results from this study are:

A. The velocity measurements show a marked decrease of velocity when CO_2 is introduced into the pore space. This decrease is large enough to be detectable in a seismic survey, assuming the concentration is high enough.
B. The CT and SEM investigation has produced pore surface and volume values that can be used for chemical modeling as well as pore orientation values that can be used for velocity anisotropy analysis.

C. Testing provides a measure of pore size ranges, and also allows us to determine the relative fractions of micro- and macro-porosity.

Monitoring, Verification, and Accounting (MVA)

Seismic Reflection Data Processing of 3D Surveys

A detailed 4D reflection seismic imaging project was performed for the SACROC Unit injection site. After researchers examined different combinations of AVO coefficents, it was determined that for this limestone reservoir, a high value for ½(A+B) using the Shuey 3 Term approximation is an excellent indicator for CO_2. Related details are presented in Purcell et al., (Purcell et al., 2009 and Purcell, et al., 2010). Such a proxy could be useful in mapping the extent of supercritical CO_2 saturation associated with enhanced oil recovery operations. The swath surveys also shows differences in reflector amplitudes in the target regions.

Amplitude differences between seismic surveys

The seismic processing sequence applied to the two swath 3D surveys of the SACROC were:

- Geometry application
- True amplitude recovery
- Spectral balance
- Surface consistent deconvolution operator length 180 ms white noise .001%
- Refraction statics
- Velocity analyses
- Brute stack
- Surface consistent residual statics
- Velocity analyses
- Normal moveout
- CMP stack
- 3D migration

Comparison of the frequency characteristics of the two surveys showed that replication was excellent. This is probably due to the care taken in geophone and shot location replication by the seismic acquisition contractor and the high quality of reflection seismic processing. A comparison of the two surveys (SACROC-1 and SACROC-2) is shown in Figure 127.

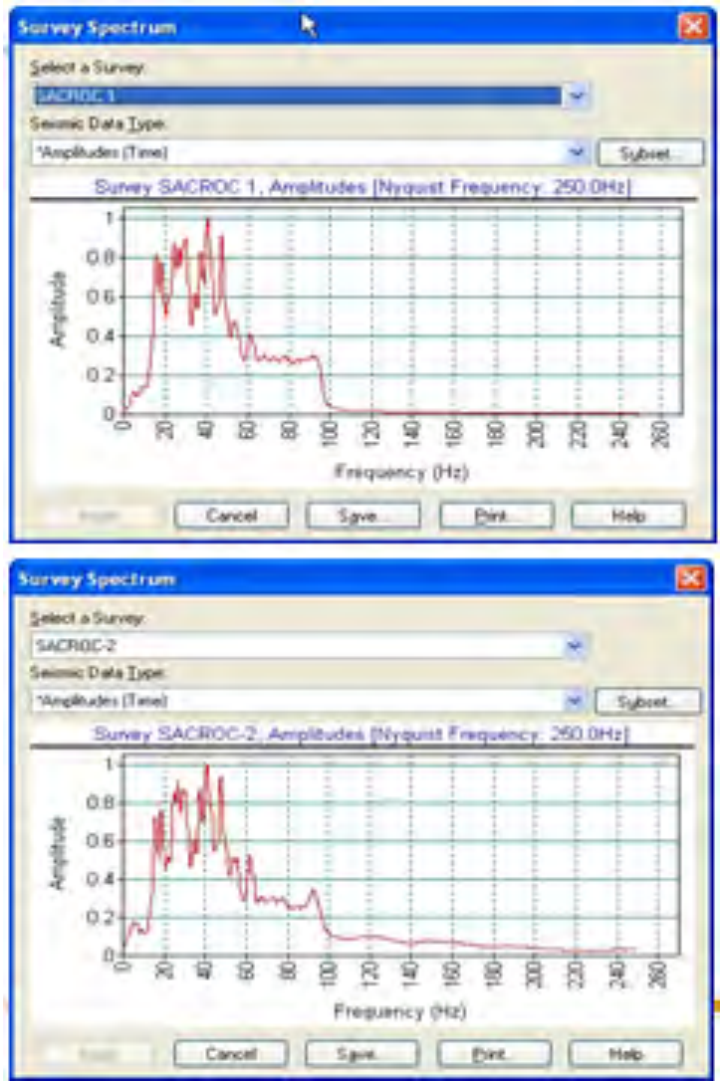

Figure 127. The frequency spectrum comparison of the two surveys (SACROC-1 and SACROC-2).

After processing, the surveys were subtracted from one another to show areas of reflection amplitude variation. Amplitude variations were observed in multiple regions as shown below in

Figure 118; note the location of the wells shown on the reference maps and the corresponding vertical line on the 3D view. In all cases the 3D view shows the difference between reflection seismic amplitudes.

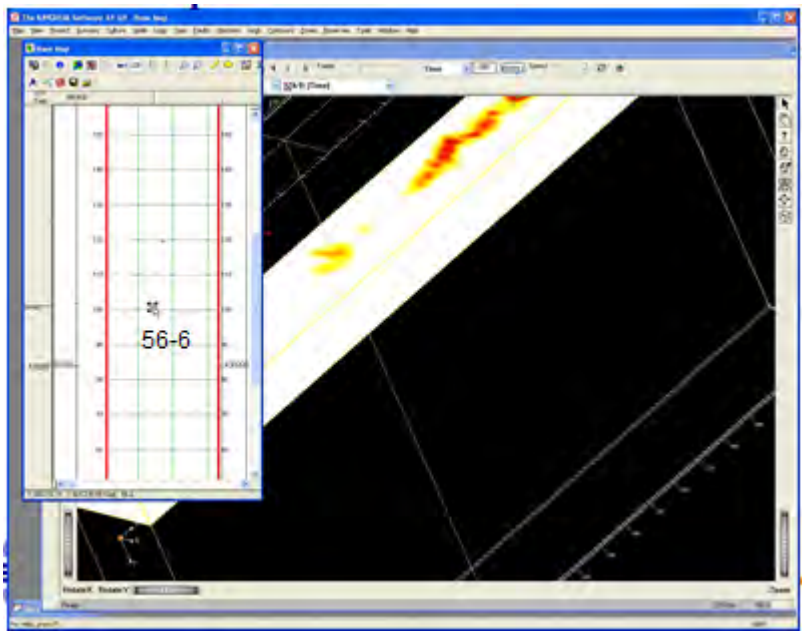

Figure 128. 3D amplitude difference, 1.088 seconds.

Conclusions

After completion and analysis of an AVO study over the survey area, it was found that areas near the injector wells showed an AVO in which:

A. The best results were obtained by using ½(A+B), where A is the intercept and B is the slope. It is believed that a large value for ½ (A+B) indicates the presence of supercritical CO_2 due to the strong positive values near an injector well.

B. The Swath Survey 1 and Swath Survey 2 3D surveys in the SACROC field have been completed. The data quality of both surveys are excellent and consistent. These results allowed 4D calculation of seismic attributes and change detection related to the CO_2 injection. This technique has the advantage of being repeated as many times as needed, and is able to track sequestered CO_2 over a large area. This technique can be combined with other methods, such as surface monitoring, VSP, isotope based geochemical monitoring of water, electromagnetics and other methods to most effectively monitor sequestered

carbon dioxide in order to minimize any potential impacts to the shallow subsurface from deep CO_2 injection.

C. Two additional small 3-D swath geometry reflection seismic surveys have been collected over this region and their amplitude differences can be interpreted to represent time variation in pressure and pore filling fluid phases.

Time-Lapse Offset and Walkaway VSP Monitoring

To study the capability of vertical seismic profiling (VSP) for monitoring migration of CO_2 plume within geologic formations, one baseline and one repeat walkaway and offset VSP surveys were conducted in the monitoring well 59-2ST in July 2008 (before CO_2 injection) and April 2009 (about six month after start of CO_2 injection), respectively. The zero-offset VSP source location was near the monitoring well. The walkaway source line consists of 101 vibrator points and crosses the monitoring well along the north-south direction. The monitoring well is located approximately at the center of the walkaway source line. The total length of the source line is 3660 m. Fifteen-level three-component geophones are used to acquire the time-lapse VSP datasets. The geophones are placed at depths from 1524 m to 1737 m, and the oil reservoir is located approximately from 1820 m to 2100 m in depth where CO_2 is injected. We applied statics corrections and amplitude balancing of the preprocessed time-lapse VSP data to address the repeatability issues of the time-lapse VSP surveys, and conduct VSP-CDP mapping and reverse-time migration imaging. The results demonstrate that time-lapse walkaway VSP is more reliable than time-lapse offset VSP for monitoring CO_2 sequestration.

Time-Lapse VSP Surveys

Figure 129 shows the offset and walkaway VSP source locations and the position of the monitoring well 59-2ST. After removing bad shots, there were 95 of the 101 shot gathers in the 2008 walkaway VSP data and 94 gathers in the 2009 walkaway VSP data. The monitoring well was drilled to a depth of 1758 m, and the walkaway VSP data were recorded at a depth range from 1554 to 1737 m (13 levels) measured in the 2008 survey, and from 1524 to 1737 meters (15 levels) in the 2009 survey.

Time-Lapse Image Differences from VSP-CDP Mappings

VSP-common-depth-point (CDP) transformation is a conventional VSP mapping approach. VSP-CDP mapping was conducted for the time-lapse walkaway VSP data, and obtain the time-lapse image differences by subtracting one image from the other. Figures 130 and 131 show the image differences of VSP-CDP mappings of the time-lapse walkaway VSP data, as well as the results before and after data balancing. Both figures display significant image differences at the two-way time from 0.95 seconds to 1 second, which corresponding to the CO_2 injection zone. Figure 131 contains some notable image differences within the upper oval, which corresponds to a region above the CO_2 injection zone. After data balancing, the image differences within the upper oval in Figure 131 almost disappear completely as expected.

Figure 132 shows image differences of reverse-time migration of the time-lapse walkaway VSP data after the statics corrections and amplitude balancing. It clearly indicates that image differences within the oval in Figure 132, or within the CO_2 injection zone, occur within 200 m from the monitoring that is at the horizontal position of 0 m. Within the oval in Figure 130, the reservoir changes on the right side (or the North side) of the monitoring well are more significant than those on the left side (or the South side) of the well.

The arrows in Figure 129 point to the regions within the CO_2 injection zone where significant image differences are obtained from the time-lapse offset and walkaway VSP data acquired from the SACROC EOR field.

Conclusions

The analyses of the time-lapse VSP data from the SACROC EOR field for monitoring CO_2 injection/migration have demonstrated that the repeatability of time-lapse VSP surveys is critically important for reliable reservoir monitoring.

A. Statics corrections are essential for time-lapse land data due to near-surface irregularities and time-lapse changes in the weathering zone.
B. Data balancing using the spectral analysis method is an effective approach for time-lapse VSP data analyses.

C. Both VSP-CDP mapping and migration imaging of time-lapse VSP data can detect changes due to CO_2 injection.
D. Reverse-time migration can handle multiple scattering that is useful for detecting subtle reservoir changes.
E. Migration imaging can reliably detect where reservoir changes occur.
F. Major reservoir changes inferred from the time-lapse walkaway VSP data at SACROC occur at depth around 2100 m, and within 200 m to the north and south of the monitoring well.
G. Some reservoir changes along the profile from the monitoring well to the VSP source offset 2 were observed. No significant changes were found along the profile from the monitoring well to Offset 3. These observations are consistent with the results of time-lapse surface seismic monitoring.
H. These results show that time-lapse walkaway VSP is more reliable than time-lapse offset VSP for monitoring CO_2 sequestration.

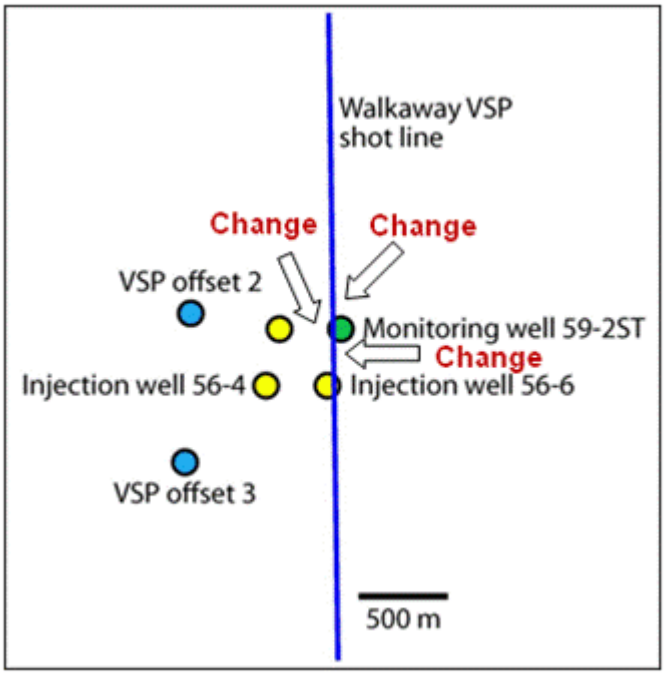

Figure 129. Offset and walkaway VSP source locations. The walkaway VSP source line is along the South-North direction crossing the monitoring well 59-2ST. The arrows point to areas where significant migration image differences in the CO_2 injection zone were observed.

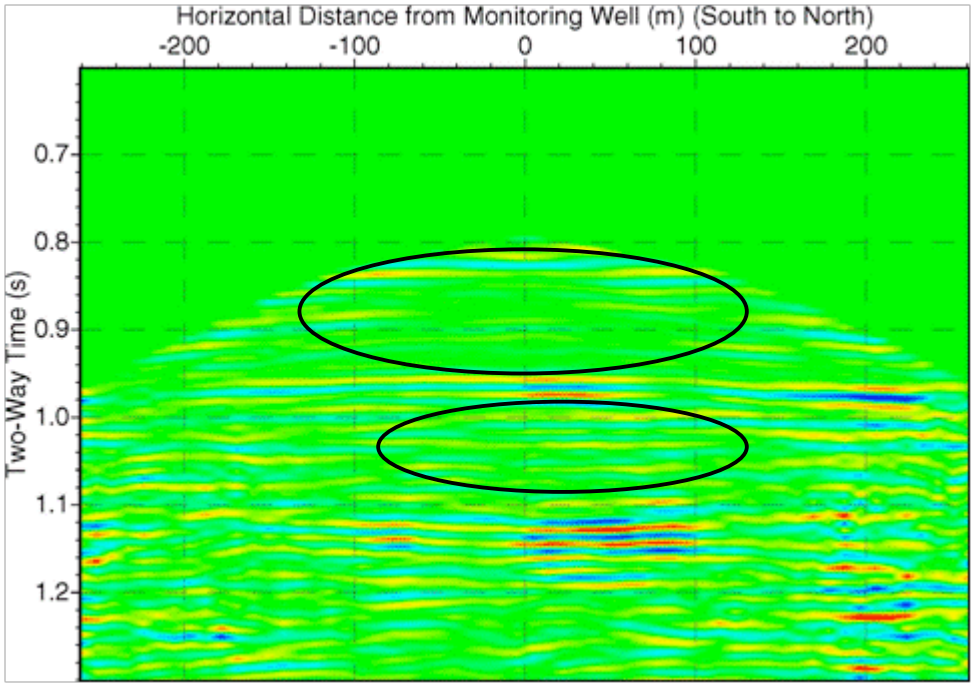

Figure 130. The differences of VSP-CDP mappings of the time-lapse walkaway VSP data before data balancing.

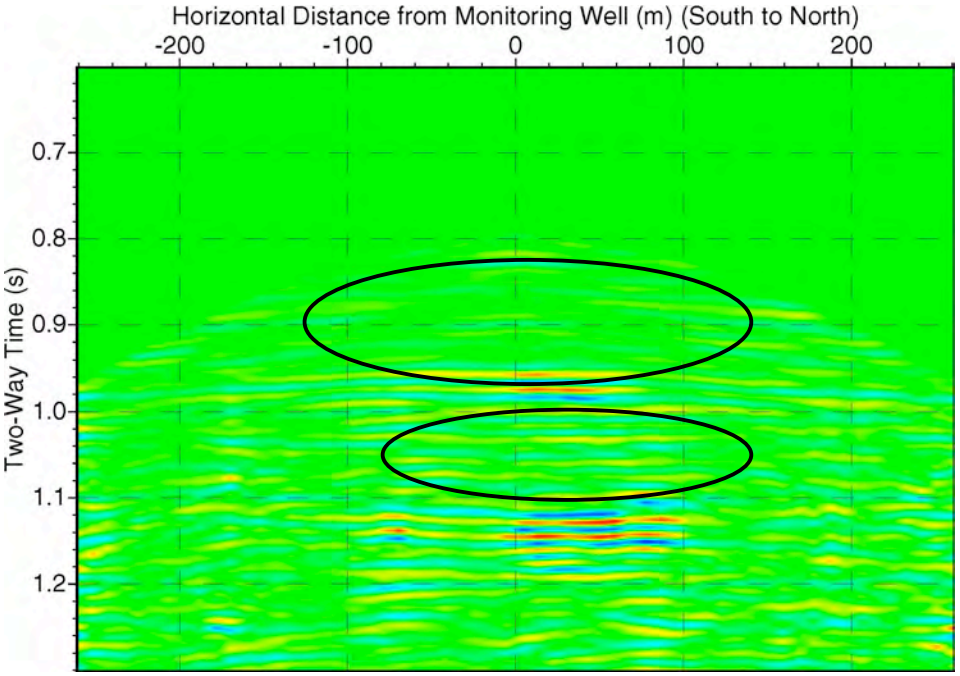

Figure 131. The differences of VSP-CDP mappings of the time-lapse walkaway VSP data after data balancing.

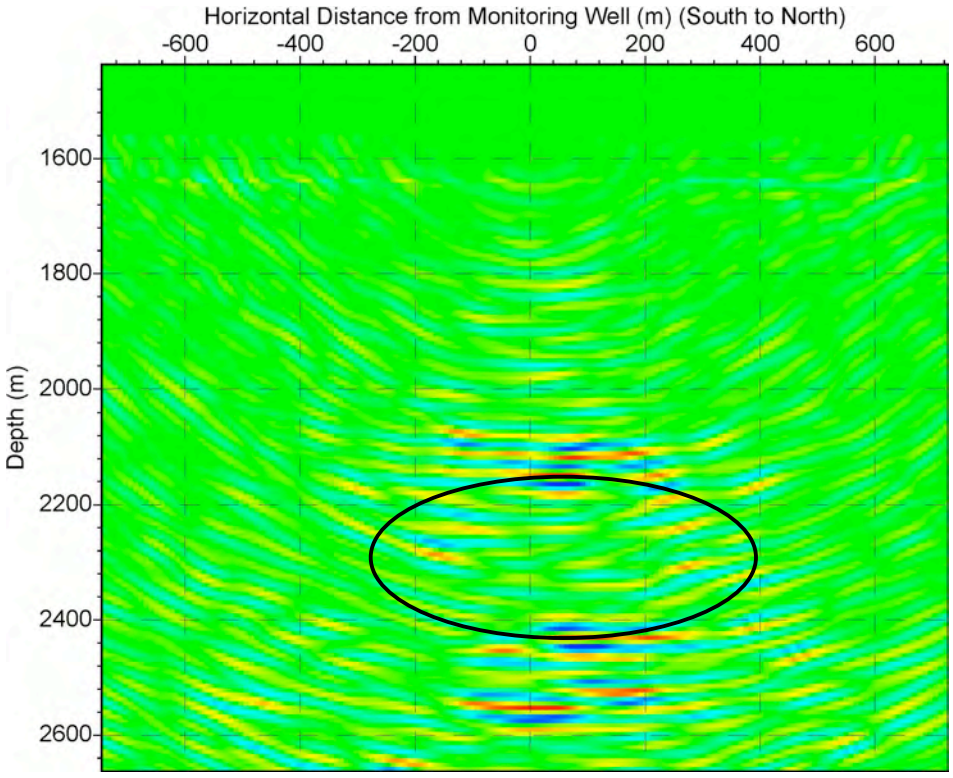

Figure 132. Image differences of reverse-time migration of time-lapse walkaway VSP data.

Interpretation of Logging Data

Repeat geophysical borehole logging was completed in two of the three injection experiment site monitoring wells, 56-4ST and 56-6ST. Logging runs were completed in these two wells in July 2008 (before CO_2 injection) and February 2009 (after CO_2 injection). Pre-injection logging was completed in the VSP well, 59-2ST in July 2008, but problems with the well prevented logging in February 2009. The upper and lower perforation zones in the monitoring wells at SACROC correspond to the combined Cisco and Green Zone, and Middle Canyon units, respectively.

Summary

The wireline evaluation program that was delivered at the SACROC Unit #56-4ST was intended to monitor the movement of formation fluids as CO_2 was injected into a nearby well. The open-hole tool selection was limited by the hole size but included all of the logging tools normally associated with a "triple-combo" logging package. After casing was cemented into the well a sonic log was run in casing to provide a formation slowness thru-casing. Reservoir Saturation Tool

(RST) logging runs were made prior to injection as well as after injection to monitor the changes in the formation fluids. The logging services included:

- Openhole GR, resistivity, density, neutron and caliper logs
- Sonic Log run after casing cemented into well
- RST (Pulsed Neutron Capture) – before injection
- RST Pulsed Neutron Spectroscopy) – before injection
- RST (Pulsed Neutron Capture) – after injection
- RST Pulsed Neutron Spectroscopy) – after injection

After making all of the logging passes the data was analyzed and interpreted. In general it was concluded that while the CO_2 moved some oil, much of the oil remained in place. There are several reasons for this, but the primary reason is that the CO_2 was not being injected into all perforations. Most of the CO_2 entered the upper perforations in each injection interval, with very little getting to the deeper perforations. The radioactive tracer log supports this conclusion. It can also be noted that, in this well, not all of the higher porosity intervals are perforated.

Wireline logging services

- **Openhole Logs:** The openhole logs run included HRLA (High Resolution Laterolog Array) for resistivity, HGNS (Highly Integrated Gamma Ray Neutron) to provide neutron porosity, SLDT (Slim LithoDensity Tool) to provide a formation bulk density measurement as well as a caliper measurement, and Gamma Ray to provide measurement of the gamma rays from the formation.
- **Cased Hole Sonic Log:** The cased hole log SSLT (Slim Sonic Logging) to provide the compressional and shear formation slowness. Only some of the data from the sonic log was usable as the cement quality was not as good as desired. The cement is needed to provide acoustic coupling between the casing and formation.
- **Reservoir Saturation Tool (RST) – Pulsed Neutron Spectroscopy (PNS):** Spectro-LITH (to process for lithology). The primary elements measured are formation elements silicon, iron, calcium, sulfur, titanium, gadolinium, chlorine, barium and hydrogen. Matrix properties and quantitative dry-weight lithologies are calculated from the dry-weight

elemental fractions using the SpectroLith empirical relationships derived from an extensive core chemistry and mineralogy database. The second tool C/O (Carbon/Oxygen ratio) yields carbon and oxygen based on neutron-induced inelastic gamma ray spectroscopy as well as the energy windows for carbon and oxygen.

- **Reservoir Saturation Tool (RST) - Pulsed Neutron Capture (PNC):** The RST can also be referred to as the "Sigma mode." In the capture mode the tool is measuring the rate at which thermal neutrons are captured by the formation. This measurement is called SIGM (Sigma) and is the macroscopic capture cross section. Chlorine has the greatest ability to capture thermal neutrons and hydrogen has the greatest ability to slow the high energy neutrons to the thermal level, this measurement is very responsive to the saltwater in the porosity. If the amount of saltwater decreases and is replaced by oil then the capture cross section of the formation will decrease as oil has a low sigma value compared to saltwater. CO_2 also has a very low sigma value that will cause the sigma measurement to decrease if it replaces saltwater in the porosity. Because of this the Sigma measurement and the porosity measurement from the RST tool can be combined in an analysis to determine the volume of saltwater, oil and gas/ CO_2 in the formation porosity. Gas and CO_2 cannot be differentiated.

Interpretation of the logging data on SACROC Unit Well 56-4ST

The data were interpreted with the ELAN-Plus computer program within GeoFrame. The Elemental Log ANalysis (ELAN) evaluation was done by optimizing simultaneous equations described by one or more interpretation models. The initial interpretation model used the data from the openhole logs plus the lithology derived from the RST spectroscopy log. Once the analysis of the openhole data was complete, the lithology and porosity outputs were used to build the interpretation model for the RST sigma log interpretation. In this model the lithology and porosity are held constant, matching the openhole analysis, and the SIGM and TPHI from the RST are then used to identify the fluid volumes. By doing this, as additional passes of the RST are made the new SIGM and TPHI can be easily input into the model to identify changes in the reservoir fluids. The change in fluids between the first RST log that was run before injecting CO_2 and the second RST log that was run after the CO_2 was injected identified where the CO_2 went and what

other fluid changes took place. Figure 133 shows a section of the composite ELAN results with a description of the data presented.

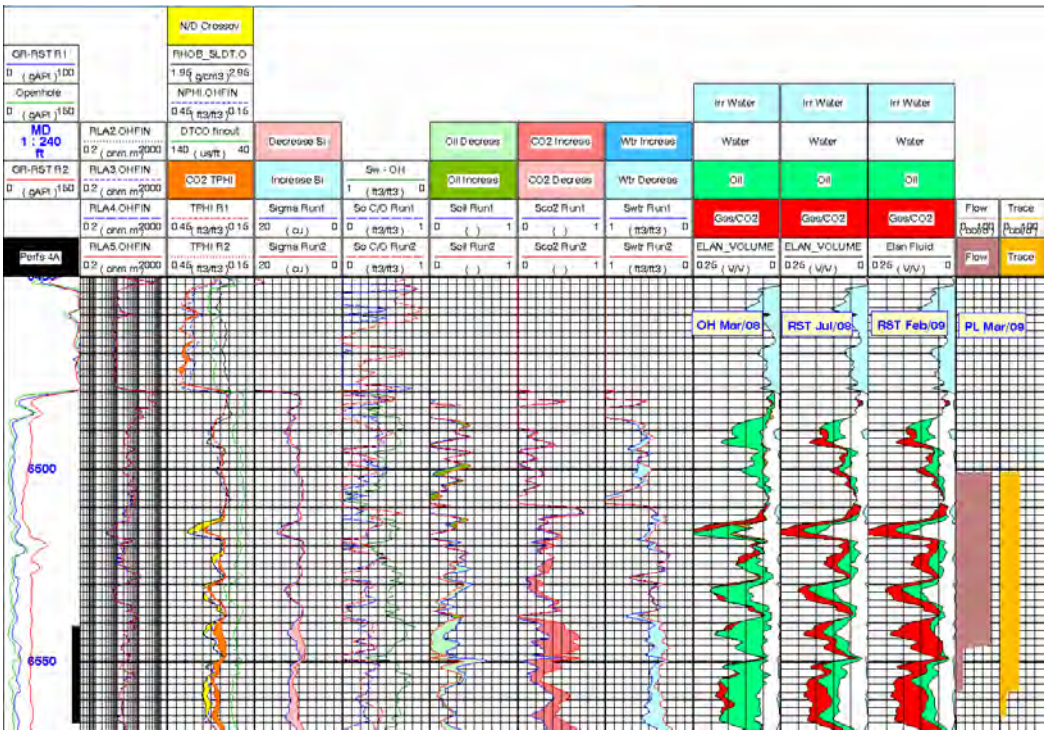

Figure 133. Schlumberger ELAN summary for monitoring well 56-4ST.

Depth Track

- Openhole GR – Gamma Ray from the openhole logging run
- GR-RST R1 – Gamma Ray from the first RST run
- GR_RST R2 – Gamma Ray from the second RST run
- Perfs 4A – These shaded areas indicate the perforation intervals as correlated to the injection well perforations. This well is not actually perforated.

Track 1

- RLA5 – Apparent Resistivity from Computed Focusing Mode 5
- RLA4 – Apparent Resistivity from Computed Focusing Mode 4
- RLA3 – Apparent Resistivity from Computed Focusing Mode 3
- RLA2 – Apparent Resistivity from Computed Focusing Mode 2

Track 2

- RHOB_SLDT – Measurement of the bulk density of the formation. This is used in combination with the neutron and sonic for lithology identification as well as identification of fluids in the porosity.
- NPHI.OHFIN - Measurement of the neutron porosity of the formation from openhole logs. This is used in combination with the density and sonic for lithology identification as well as identification of fluids in the porosity.
- The shading between the RHOB_SLDT and NPHI curves indicate possible gas or CO_2 in the formation porosity (yellow shading)
- DTCO – Compressional slowness from the sonic log
- TPHI R1 – Measurement of the neutron porosity of the formation from the RST first run. This is used in combination with SIGM to determine the fluid volumes in the reservoir at that time.
- TPHI R2 – Measurement of the neutron porosity of the formation from the RST second run. This is used in combination with SIGM to determine the fluid volumes in the reservoir at that time.
- The overlay of the two TPHI curves makes it easy to identify where changes occurred between RST runs (orange shading)

Track 3

- Sigma Run 1 - Sigma from the first RST run. This is used with the TPHI to determine the fluid volumes in the reservoir at that time.
- Sigma Run 2 - Sigma from the second RST run. This is used with the TPHI to determine the fluid volumes in the reservoir at that time.
- The overlay of the two sigma curves makes it easy to identify where changes occurred between RST runs (pink shading)

Track 4

- Sw-OH – Openhole Water Saturation
- So C/O Run1 – Oil Saturation as computed by the analysis of the Carbon/Oxygen data from the RST spectroscopy log first run

- So C/O Run2 - Oil Saturation as computed by the analysis of the Carbon/Oxygen data from the RST spectroscopy log second run

Track 5

- Soil Run1 - Oil Saturation as computed by the analysis of the Sigma and TPHI data from the RST capture log first run
- Soil Run2 - Oil Saturation as computed by the analysis of the Sigma and TPHI data from the RST capture log second run
- The overlay of the two Soil curves makes it easy to identify where changes occurred between RST runs. The dark green shading indicates an increase in oil from RST run 1 to RST run 2 and the light green shading indicates a decrease in oil from RST run 1 to RST run 2

Track 6

- Sco2 Run1 - CO_2 Saturation as computed by the analysis of the Sigma and TPHI data from the RST capture log first run
- Sco2 Run2 - CO_2 Saturation as computed by the analysis of the Sigma and TPHI data from the RST capture log second run
- The overlay of the two Sco2 curves makes it easy to identify where changes occurred between RST runs. The dark red shading indicates an increase in CO_2 from RST run 1 to RST run 2 and the light red shading indicates a decrease in CO_2 from RST run 1 to RST run 2

Track 7

- Swtr Run1 - Water Saturation as computed by the analysis of the Sigma and TPHI data from the RST capture log first run
- Swtr Run2 - Water Saturation as computed by the analysis of the Sigma and TPHI data from the RST capture log second run
- The overlay of the two Swtr curves makes it easy to identify where changes occurred between RST runs. The dark blue shading indicates an increase in water from RST run 1 to RST run 2 and the light blue shading indicates a decrease in water from RST run 1 to RST run 2

Track 8

Volumetric display of the fluids solved for in ELAN analysis of the Openhole data with the RST lithology information. The curve to the far left is the effective porosity with the shading indicating the proportion of each fluid occupying the porosity. Red represents Gas or CO_2, green represents Oil, white represents Water, and cyan represents the Irreducible Water.

Track 9

Volumetric display of the fluids solved for in ELAN analysis of the RST run 1 data. The curve to the far left is the effective porosity with the shading then indicating the proportion of each fluid occupying the porosity. Red represents Gas or CO_2, green represents Oil, white represents Water, and cyan represents the Irreducible Water.

Track 10

Volumetric display of the fluids solved for in ELAN analysis of the RST run 2 data. The curve to the far left is the effective porosity with the shading then indicating the proportion of each fluid occupying the porosity. Red represents Gas or CO_2, green represents Oil, white represents Water, and cyan represents the Irreducible Water.

Track 11

Flow - This data is imported from the Radioactive Production log run in the injector well SACROC Unit 56-4A indicating the velocity profile of the radioactive tracer material in the wellbore.

Track 12

Tracer - This data is imported from the Radioactive Production log run in the injector well SACROC Unit 56-4A indicating where the radioactive tracer material ended up in the formation.

Interpretation Comments

Upper Injection Interval

The porosity in this interval that is correlated to the perforated intervals in the injection well has a range from about 10 to 20 pu with the average being about 17 pu. Examination of the tracks that contain the shadings that would indicate changes in fluid content, shows that the CO_2 has

increased significantly in the interval from 6540 ft to 6574 ft. In this same interval the water volume has decreased throughout and the oil volume has decreased mainly in the top 12 ft. It can also be noted that there is a smaller increase in CO_2 above these correlated perforations up to the high porosity zone at 6515 ft. In the interval from 6574 ft to 6590 ft there is little change in the CO_2 volume but the water volume has decreased and the oil volume has increased. There is very little change in the fluid volumes in the correlated perforation interval from 6598 ft to 6616 ft. It appears that no CO_2 was injected into this interval. The data from the tracer log run in the injector well agrees with much of this in that the CO_2 is being injected into the top set of perforations from 6541 ft to 6566 ft. The tracer also shows that some of the material is moving up to almost 6500 ft. Figure 134 shows the ELAN summary for the upper zone in monitoring well 56-4ST.

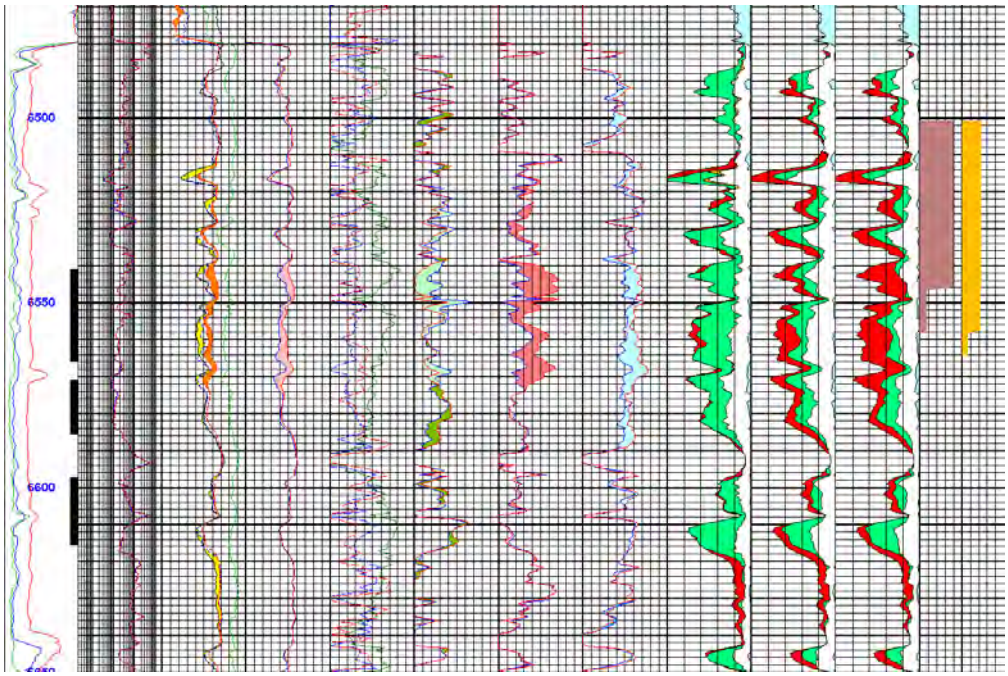

Figure 134. Schlumberger ELAN summary for upper zone in monitoring well 56-4ST.

Lower Injection Interval

The porosity in this interval that is correlated to the perforated intervals in the injection well has a range from about 10 to 20 pu with the average being about 17 pu. Examination of the tracks that contain the shadings that would indicate changes in fluid content shows that the CO_2 has increased significantly in the interval from 6677 ft to 6722 ft. In this same interval, both the water

volume and oil volume have decreased throughout. In the interval from 6733 ft to 6748 ft the CO_2 volume has increased and the water and oil volumes have decreased even though this zone does not appear to be perforated in the injection well. No CO_2 appears to have been injected into the zones correlating to the bottom three sets of perforations starting at 6753 ft down to 6802 ft. There does appear to be some change in the fluid volumes from 6830 ft to 6840 ft. In this interval the CO_2 and water volume decrease and the oil volume increases. This interval may be under outside influences not directly related to the nearby injector well. The data from the tracer log run in the injector well agree with much of this in that most of the CO_2 is being injected into the top two sets of perforations from 6677 ft to 6717 ft. There appears to be some injection in the zone at 6753 ft to 6773 ft based on the velocity fluid measured on the tracer log. There also seems to be some tracer material in the formation that has gone down to 6728 ft from the perforations above. Figure 135 shows the ELAN summary for the lower zone in monitoring well 56-4ST.

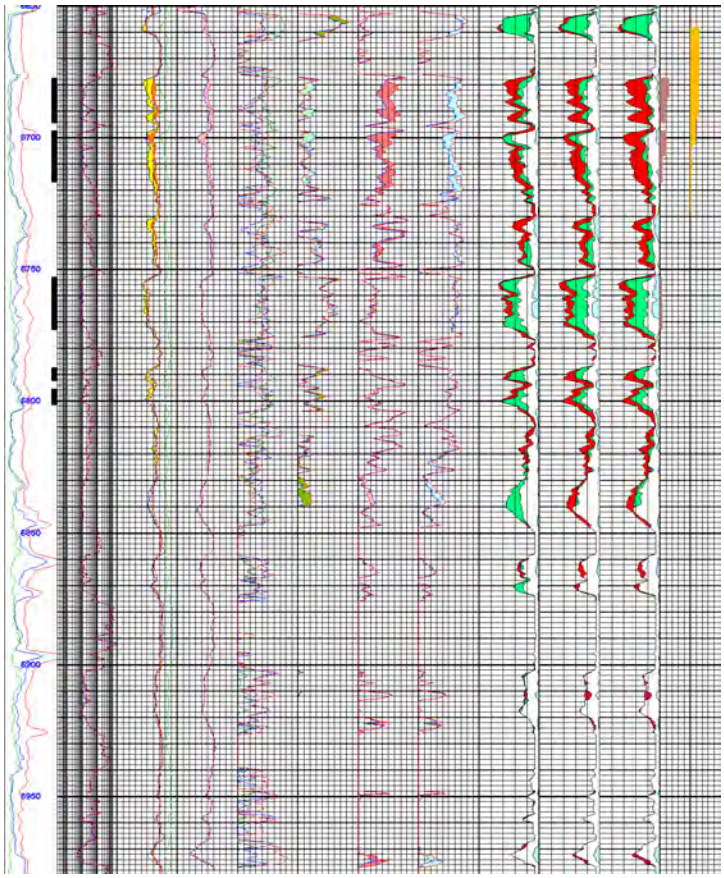

Figure 135. Schlumberger ELAN summary for lower zone in monitoring well 56-4ST.

Interpretation of the logging data on SACROC Well #56-6ST

Monitoring of CO_2 injection for EOR in the SACROC field was performed related to the well logs run on the SACROC Unit #56-6 well to monitor the injection of CO_2 into the nearby injector well SACROC Unit #56-6A using the same approach as in #56-4ST of the previous section. Tracks are similar to well 54-4ST. The ELAN summary for monitoring well 56-6ST is shown in Figure 136.

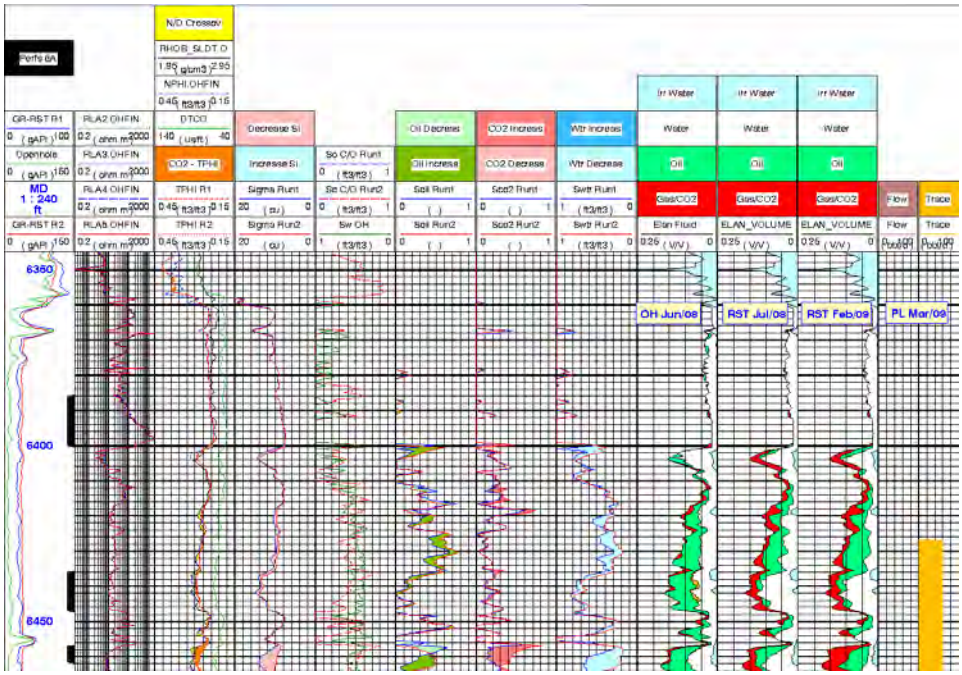

Figure 136. Schlumberger ELAN summary for monitoring well 56-6ST.

Upper Injection Interval

The ELAN summary for the upper zone in monitoring well 56-6ST is shown in Figure 137. The porosity in this interval that is correlated to the perforated intervals in the injection well has a range from about 12 to 18 pu with the average being about 15 pu. By looking at the tracks that contain the shadings that would indicate changes in fluid content it can be seen that the CO_2 has increased significantly in the interval from 6456 ft to 6500 ft. In this same interval the water volume has decreased throughout and the oil volume has increased in some sections and decreased in others. It would appear that most of the CO_2 has entered this zone in the injection well. In the interval above from 6420 ft to 6447 ft there is little change in CO_2 but the water has

decreased and the oil has increase proportionally. It can also be noted that there is a smaller increase in CO_2 in the interval from 6500 ft to 6526 ft. In this interval the water decreases significantly and the oil increases significantly. In this interval it is possible that the initial saturations are being affected by the filtrate from the drilling fluids. The well was drilled with brine water and there is only a month between the drilling and the running of the first RST. The RST has a relatively shallow depth of investigation of only about one foot. Because of this, if the invading fluids from the drilling process have not dissipated the water saturation will be too high. In the zone from 6522 ft to 6600 ft (packer set) there is a significant increase in water and decrease in oil. The CO_2 mostly increases slightly in this interval. This seems to be rather strange behavior in this interval and when this well is correlated to other wells in the project, this section does not correlate well. This interval may need more analysis from a geologist but it would appear that it is being influenced by other wells outside the project area. This also applies to the zone from 6602 ft to 6612 ft. This interval may be considered part of the lower injection interval, but since the response is the same as the zone above it has been included here. The tracer logs from the injector well agree with this analysis.

Note the perforations at 6386 ft to 6400 that do not correlate to a high porosity zone in this well.

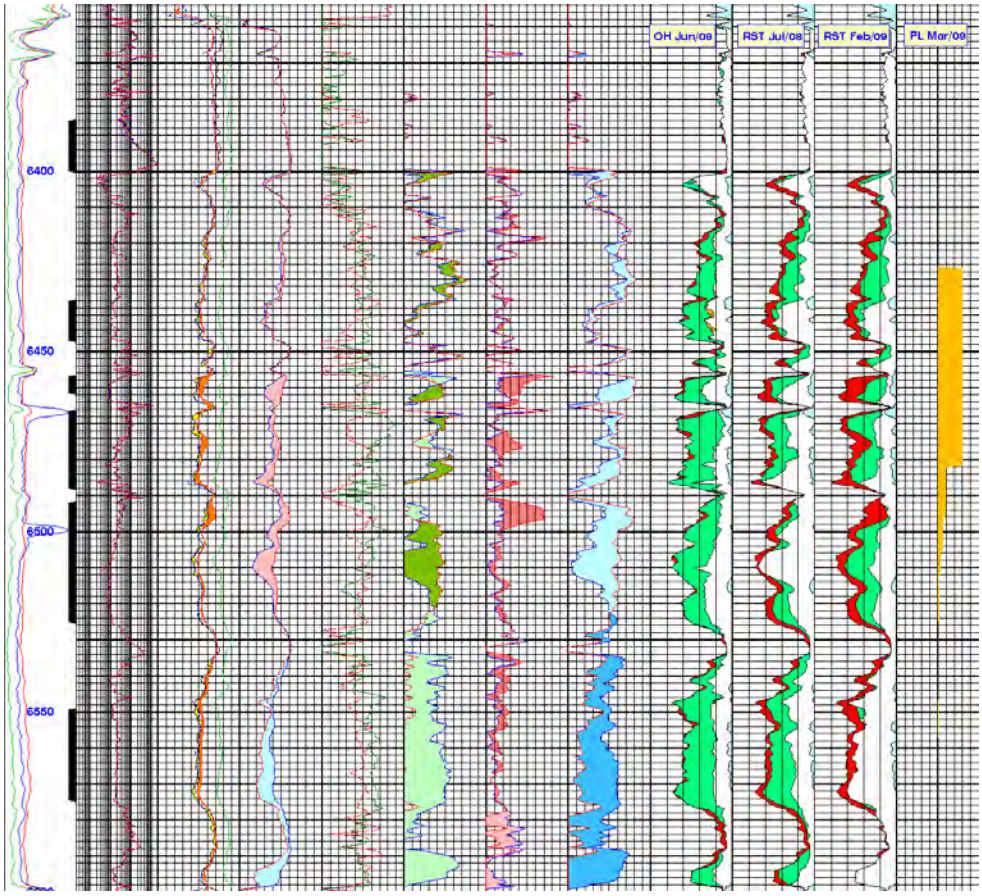

Figure 137. Schlumberger ELAN summary for upper zone in monitoring well 56-6ST.

Lower Injection Interval

The ELAN summary for the lower zone in monitoring well 56-6ST is shown in Figure 138. The The porosity in this interval that is correlated to the perforated intervals in the injection well has a range from about 10 to 18 pu with the average being about 16 pu. By looking at the tracks that contain the shadings that would indicate changes in fluid content it can be seen that the CO_2 has increased significantly in the interval from 6624 ft to 6680 ft. In this same interval the water volume has significantly decreased and the oil volume has increased in some sections and decreased in others. It would appear that most of the CO_2 has entered this zone in the injection well. Below 6680 ft there appears to be only small changes in CO_2. From 6680 ft to 6782 ft there is in general a slight increase in oil with a corresponding decrease in water. In the zone from 6763 ft to 6774 this change is more pronounced. The tracer logs from the injector well agree with this analysis.

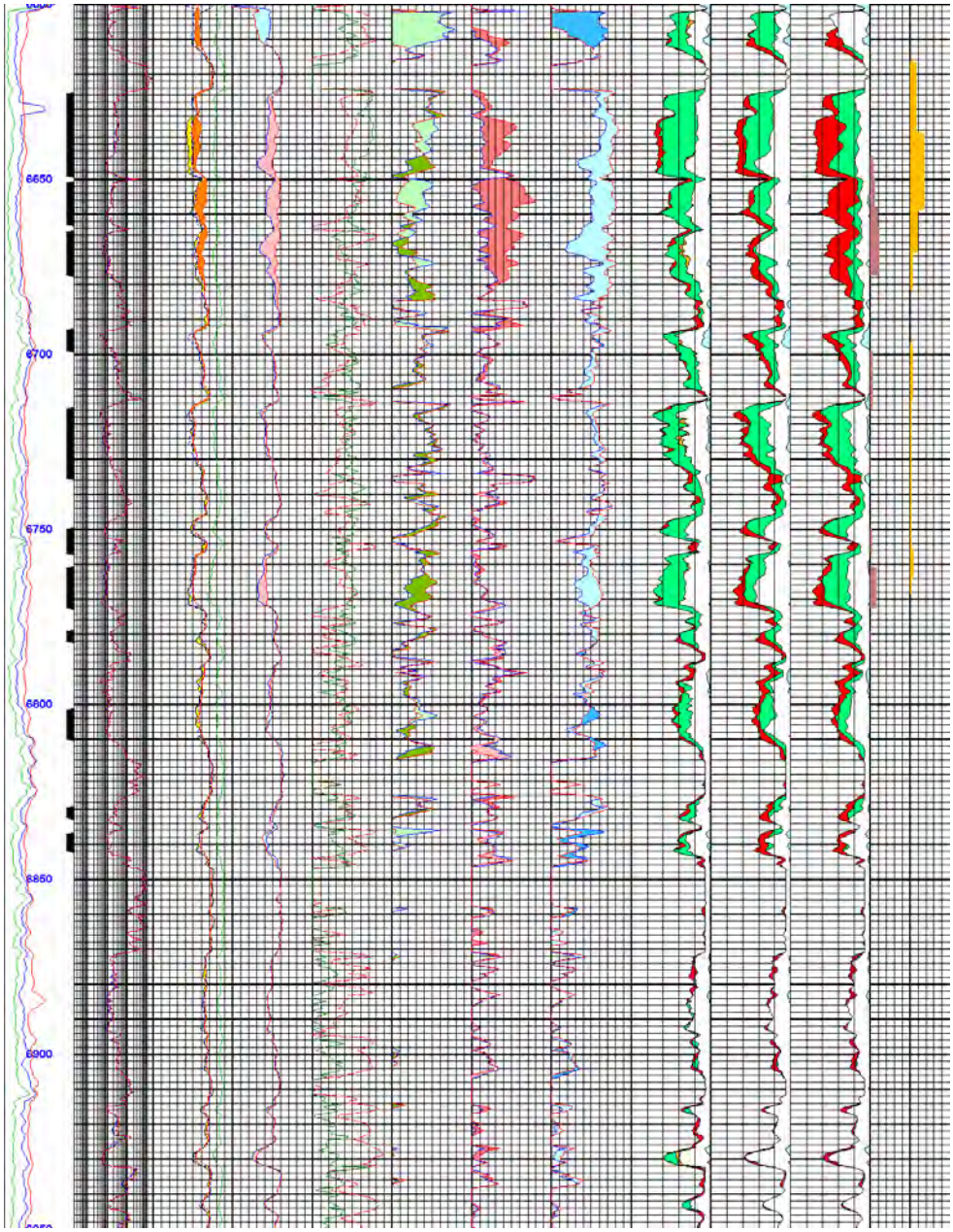

Figure 138. Schlumberger ELAN summary for lower zone in monitoring well 56-6ST.

Soil CO_2 Flux Monitoring

Test nodes were placed in a grid that either spanned an area containing several wells or one that extended radially outward from the well of interest. Soil collars were placed at each of the locations identified as test nodes. Using the LI-COR Automated Soil CO_2 Flux System the CO_2 flux was measured at each node. Because calculations for the flux rely upon the temperature of the soil and large changes in the temperature of the soil during the day and from season to season, the soil temperature probe was used at a depth of approximately one to two inches.

Once the data was received it was reviewed for any increasing trends or unusually high levels of CO_2 flux. If a node had a flux significantly higher than the mean, it was noted and anticipated during the next set of measurements. If a test node consistently had higher levels of CO_2 it was investigated further. Measurements are taken at specified intervals during the test run. Measurements in this case were taken at one-second intervals for approximately two to three minutes.

Offsite Ranch

As CO_2 has been injected into the SACROC reservoirs for many years, it is impossible to measure a natural background level of CO_2 without the risk of measuring injected CO_2 also. To measure the background levels, a site several miles away from the SACROC field was selected. The nodes were placed near a dry well to ensure that there was no CO_2 flux from underground reservoirs (Table 31). The vegetation is similar to that of the sites located within the SACROC field, with the exception that it is slightly less vegetated since it is not directly maintained as pastures for cattle. Figure 139 (an example layout) gives the locations of flux measurements of the test nodes. The dry well is located between S-3 and E-3. The distance between the nodes is 50 feet. The transect pattern in Figure 139 was chosen because it covered the more vegetated areas as well as the less vegetated areas, such as the center area.

The overall mean for the background averages for this site was $1.759\,\frac{\mu mol}{m^2 s}$ during the summer and at $0.79\,\frac{\mu mol}{m^2 s}$ for the winter; standard deviation is $0.55\,\frac{\mu mol}{m^2 s}$.

Production Well 56-17

Production Well 56-17 is located among four injection wells and acts as a monitoring well. It is also adjacent to another well about 70 feet away, which is being used for VSP monitoring. Here the grid for the nodes was chosen to extend radially in four directions to extend toward the locations of the four monitoring wells. Table 32 shows the results tests on Well 56-17.

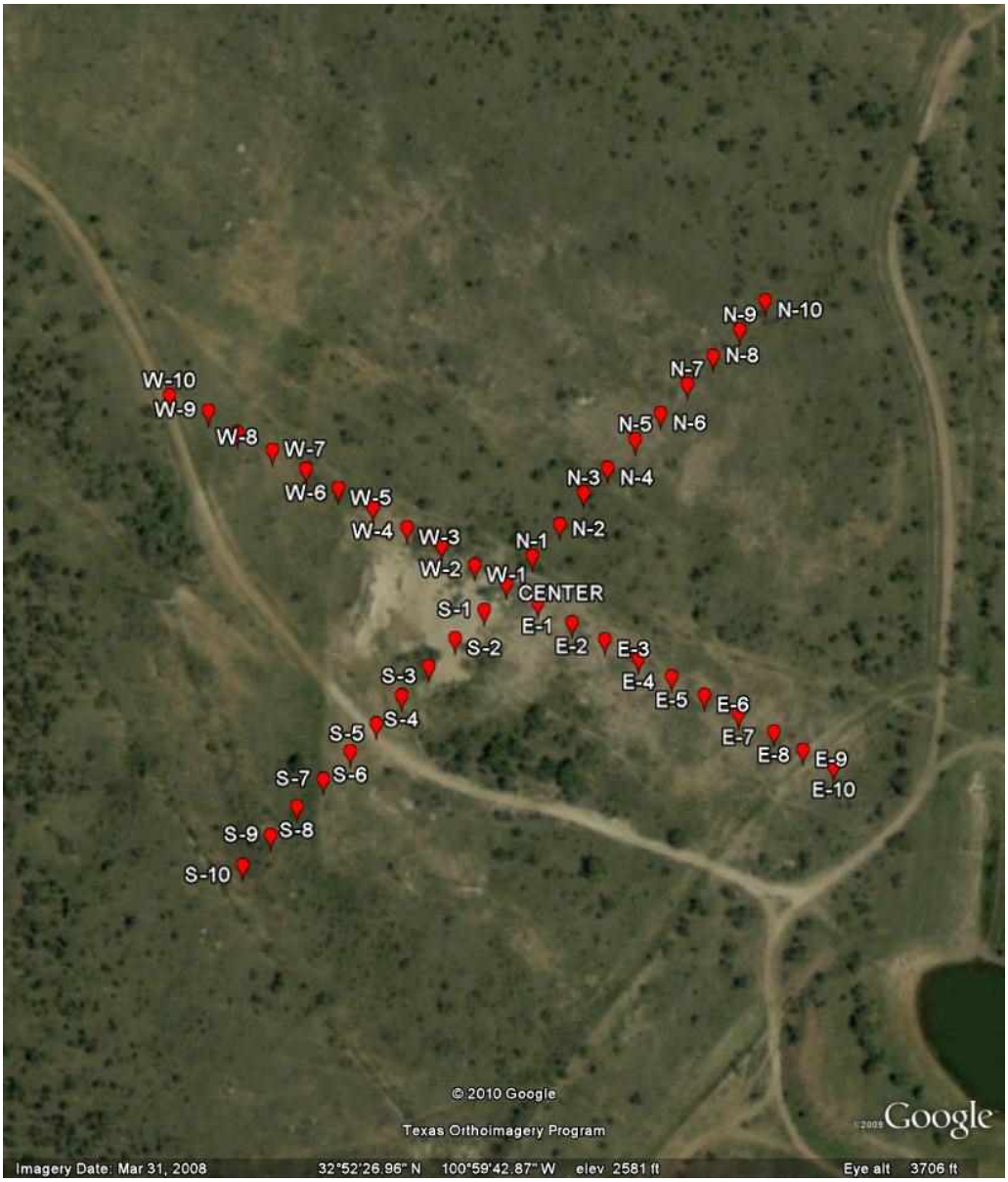

Figure 139. Soil CO_2 background flux measured at off-site ranch.

Table 31. Locations of the Test Nodes for Flux Measurements at Off-Site Ranch

Offsite Soil CO_2 Flux $\left(\frac{\mu mol}{m^2 s}\right)$				
	Jun-08	Jan-09	Jun-09	Mean
Center	3.40		1.62	2.51
N-1	0.27	0.64	1.90	0.94
N-2	2.44	0.92		1.68
N-3	0.07	0.88	1.83	0.93
N-4	3.67	0.73		2.20
N-5	0.46	0.58	1.30	0.78
N-6	0.77	0.80	1.28	0.95
N-7	2.23	0.58	1.26	1.36
N-8	2.35	0.56	1.58	1.50
N-9	1.52	0.94	1.34	1.27
N-10	2.98	1.24	1.52	1.91
S-1	1.15	0.50	1.26	0.97
S-2	0.92	0.00	0.56	0.49
S-3	1.46	0.69	2.49	1.55
S-4	-0.04	0.68	2.99	1.21
S-5	1.30	1.33	2.29	1.64
S-6	1.77	0.80		1.29
S-7	2.68	1.21	2.18	2.02
S-8	5.73	0.87		3.30
S-9	2.13	0.79	1.68	1.53
S-10	2.16	0.64		1.40
E-1	2.11	0.63	1.02	1.25
E-2	2.14	0.51	1.41	1.35
E-3	2.17	0.81	0.40	1.13
E-4	1.79	0.76	0.54	1.03
E-5	1.91	0.79	0.76	1.15
E-6	1.45	0.65	0.81	0.97
E-7	2.12	0.77	1.41	1.43
E-8	2.75	0.94	0.93	1.54
E-9	1.70	0.70	1.01	1.14
E-10	2.07	1.30	1.47	1.61
W-1	1.94	0.36	1.25	1.18
W-2	2.11	0.94	1.62	1.56
W-3	3.00	0.56	1.32	1.63
W-4	2.33		1.14	1.74

W-5	2.55	1.01	2.36	1.97
W-6	4.42	1.00	3.32	2.91
W-7	1.45	0.85	1.14	1.15
W-8	2.62	0.86	2.23	1.90
W-9	2.75	1.14	1.63	1.84
W-10	2.56	0.80	2.37	1.91
Mean	2.08	0.79	1.53	1.51

The overall mean for this location is $2.64\frac{\mu mol}{m^2 s}$ with a standard deviation of $1.81\frac{\mu mol}{m^2 s}$. During the summer the average mean was $3.40\frac{\mu mol}{m^2 s}$ and during the winter the soil CO_2 flux was $1.13\frac{\mu mol}{m^2 s}$. This location had a larger variance because it was being heavily used as a pasture for cattle and horses and, prior to the last test, part of the field was plowed, causing greater change in the soil CO_2 flux.

Table 32. Locations of the Test Nodes for Flux Measurements at Well 56-17

Well 56-17 Soil CO_2 Flux $\left(\frac{\mu mol}{m^2 s}\right)$				
	Jun-08	Jan-09	Jun-09	Mean
C-1	3.09	1.05	1.67	1.94
C-2		0.30	1.51	0.91
C-3		0.26	0.72	0.49
C-4	0.11	0.29		0.20
C-5	0.50	0.03	0.32	0.28
C-6	0.69	0.37	0.08	0.38
C-7	0.54	0.11	0.51	0.39
C-8	1.27	0.10		0.69
C-9	5.01	1.37		3.19
C-10	3.32	0.84		2.08
S-3	5.25		5.82	5.54
S-4	14.49	2.04	5.96	7.50
S-5	9.17	1.77	6.31	5.75
S-6	2.25	2.60	7.25	4.03
S-6	2.53			2.53
S-7	7.68	2.87	4.15	4.90
S-8	3.04	2.51	0.83	2.13
E-2	1.17	1.21	1.50	1.29
E-3	6.02		-0.04	2.99
E-4	4.48	1.27	1.70	2.48
E-5	6.75	1.66	4.20	4.20
E-6	6.86	0.84	11.97	6.56

E-7	4.52	1.36	3.53	3.14
E-8	4.64	1.48	6.62	4.25
E-9	0.57	2.09	7.79	3.48
E-10	5.95	1.03	7.43	4.80
N-1	0.35	0.30	0.46	0.37
N-2	0.35	0.57	0.92	0.61
N-3	0.52	1.03	-0.04	0.50
N-4	1.81	1.44	0.20	1.15
N-5	3.60	1.50	3.13	2.74
N-6	0.73	0.93	1.75	1.14
N-7	4.75	0.99	5.17	3.64
N-8	1.10	1.20	2.05	1.45
N-9	0.70	0.94	2.13	1.26
N-10	4.84	1.68	0.91	2.48
W-3	2.27	0.40	1.25	1.31
W-4	8.47	1.09	5.30	4.95
W-5	3.69	0.90	1.18	1.92
W-6	4.89	1.04	2.51	2.81
W-7	4.53	1.63	5.80	3.99
W-8	3.25	1.71	6.07	3.68
W-9	1.30	0.43	3.61	1.78
W-10	3.52		2.90	3.21
Mean	3.59	1.13	3.21	2.64

Abandoned CO_2 Injection Well

This well was chosen because CO_2 had been injected here in the past. The well has lain dormant for many years. When this well was measured, there were two specific objectives:

1. Whether any large CO_2 leaks resulted from the past injection.
2. Whether this site could be used as an onsite background level.

Two separate measurements were made at this site. Table 33 shows the test results on the abandoned CO_2 injection well. During the third measurement the site was under construction and access was not permitted. The flux for this area during the summer was $2.88\frac{\mu mol}{m^2 s}$ with a standard deviation of $1.24\frac{\mu mol}{m^2 s}$; during the winter it was $0.44\frac{\mu mol}{m^2 s}$ with a standard deviation of $0.23\frac{\mu mol}{m^2 s}$.

Table 33. Locations of the Test Nodes for Flux Measurements at Abandoned Well

Abandoned Soil CO_2 Flux $\left(\frac{\mu mol}{m^2 s}\right)$			
	Jun-08	Jan-08	Mean
C-1	3.24	0.57	1.91
C-2	0.34	0.19	0.27
C-3	1.16	0.17	0.67
C-4	0.26	-0.02	0.12
C-5	1.54	0.24	0.89
C-6	0.66	0.17	0.42
N-1	3.80	0.84	2.32
N-2	2.20	0.77	1.49
N-3	1.97	0.59	1.28
N-4	1.53	0.71	1.12
N-5	1.52	1.13	1.33
N-6	2.52	0.32	1.42
N-7	5.52	0.51	3.02
N-8	2.24	0.47	1.36
N-9	3.52	0.69	2.11
N-10	3.35	0.86	2.11
E-1	2.31	0.25	1.28
E-2	4.20	0.65	2.43
E-3	3.00	0.16	1.58
E-4	3.79	0.33	2.06
E-5	3.20	0.26	1.73
E-6	2.76	0.14	1.45
E-7	1.83	0.27	1.05
E-8	3.99	0.14	2.07
E-9	5.75	0.42	3.09
E-10	4.45	0.26	2.36
S-1	1.42	0.55	0.99
S-2	2.41	0.55	1.48
S-3	1.70	0.47	1.09
S-4	2.29	0.39	1.34
S-5	3.28	0.44	1.86
S-6	3.21	0.13	1.67
S-7	1.95	0.50	1.23
S-8	4.33	0.42	2.38
S-9	3.40	0.35	1.88
S-10	4.78	0.41	2.60
W-1	3.91	0.71	2.31
W-2	3.88	0.54	2.21

W-3	3.27	0.60	1.94
W-4	3.93	0.48	2.21
W-5	2.93	0.71	1.82
W-6	4.14	0.39	2.27
W-7	2.09	0.62	1.36
W-8	2.64	0.30	1.47
W-9	3.12	0.37	1.75
W-10	3.07		3.07
Mean	2.88	0.44	1.69

Well 138-5 with Blown-Out Pipe

Several months prior to the testing in SACROC a pipe ruptured near Well 138-5, leaving a crater the size of a truck in the ground. This site was measured to see if the concentration of CO_2 was elevated due to the blowout. After the area was measured, it was determined that the flux here was approximately the same as that in the rest of SACROC and that, as expected, the CO_2 dissipated quickly. For a more detailed analysis an isotopic test could be performed to determine the origin of the CO_2 that was present. The results of flux measurements at Well 138-5 (Blowout Site) are shown in Table 34**.**

Table 34. Locations of the Test Nodes for Flux Measurements at Well 138-5 (Blowout Site)

Offsite Soil CO_2 Flux $\left(\frac{\mu mol}{m^2 s}\right)$	
	Jun-08
CENTER	0.69
E-1	1.14
E-2	0.36
E-3	1.19
E-4	3.58
E-5	2.53
N-1	1.69
N-2	1.92
N-3	0.63
N-4	7.42
N-5	2.12
N-6	
N-6	2.07
W-1	1.19
W-2	6.13
BO-1	2.01
BO-2	4.07
BO-3	5.37
W-3	6.81
W-4	0.79
W-5	2.80
W-6	2.37
S-1	0.61
S-2	1.47
S-3	2.64
S-4	3.38
S-5	4.69
S-6	5.10
Mean	2.77

Flux measurements were measured during the winter, summer and spring as well as at different times of the day to gain a better understanding of the magnitude of the variance for an area. A significant difference was observed in flux between summer and winter, due to the increased bio-logic changes that occur during the summer.

As shown in Figure 140, the flux for the offsite well located at the ranch was significantly lower during the summer months and approximately the same during the winter. This clearly shows that a baseline flux exists in the $0.75\frac{\mu mol}{m^2 s}$ range when the vegetation is in its slowest growing season. When Google Earth maps of the different sites are compared, there is less vegetation at the ranch compared to the three onsite locations. Because of this, the soil CO_2 flux is lower for the offsite well during the summers.

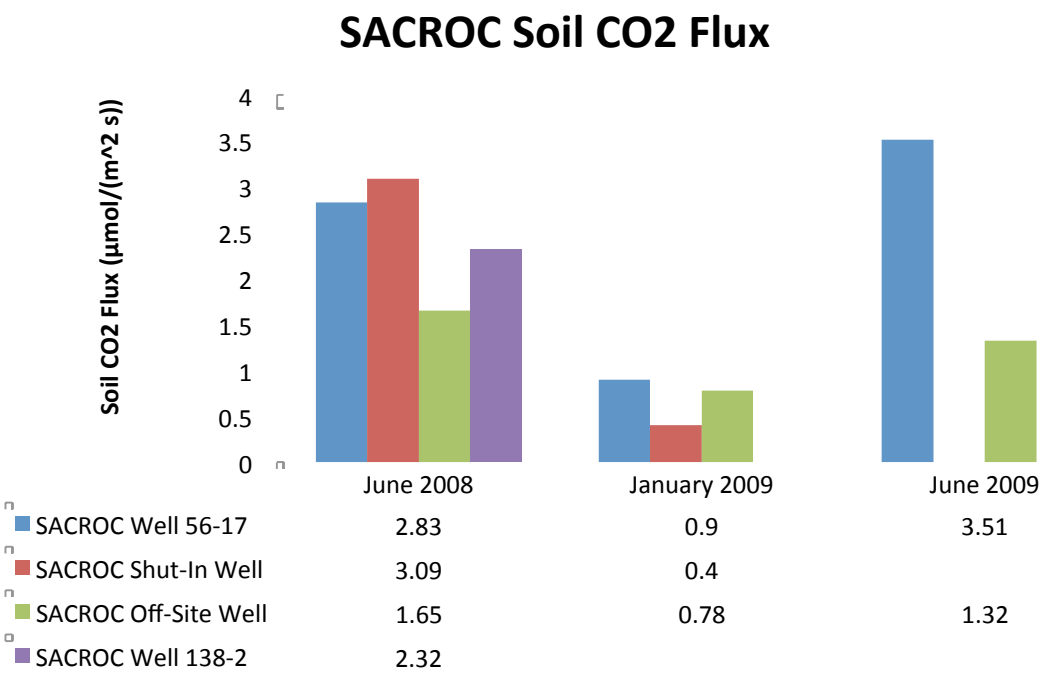

	SACROC								
Location	Well 56-17			Aband. Inj. Well		Offsite Dry Well			Well 138-2
Date	Jun-08	Jan-09	Jun-09	Jun-08	Jan-09	Jun-08	Jan-09	Jun-09	Jun-08
Number	43	46	39	47	48	42	41	36	28
Mean	2.83	0.9	3.51	3.09	0.4	1.65	0.78	1.32	2.32
Max	9.17	2.64	32.72	24.98	1.06	4.08	1.76	1.96	5.77
Min	0	-0.01	1.17	0.22	-0.01	-0.04	0.02	1.18	0
StdDev	2.27	0.58	6.66	3.46	0.23	0.98	0.28	0.15	1.66

Figure 140. Summary flux data (µmol/(m^2 s)).

Conclusions

A. Measuring the soil CO_2 flux before and during injection has been successful in establishing a solid background level that can be expected during different seasons and at different times of the day. The average flux for the fields in SACROC was $2.15\,\frac{\mu mol}{m^2 s}$, which is reasonable for a dry grassy location.

B. For this study it was determined that if a flux consistently remained higher than about two to three times the average value, it should receive additional attention. Because of the consistency of concentration of the vegetation in the grassy fields, there were no areas for special consideration.

During the previous several years, one of the main concerns with taking the soil flux measurements has been the possibility of missing a leak due to the small area measured by the soil flux system. If the CO_2 leaks from the reservoir and diffuses through the ground and eventually spreads out, then a leak will be recognizable by a slowly increasing flux over a wide area. On the other hand, if a leak occurs near a fracture then it may escape to the surface in a small area only detectable if the CO_2 sensors are placed directly over the leak. For future applications, it would be advisable to install a system that can monitor CO_2 concentrations in the atmosphere on a more macroscopic level. Then if the CO_2 concentrations increase more localized monitoring can be performed to find the actual source of the leak.

Monitoring the soil CO_2 flux before and during injection in the SACROC field did not identify any CO_2 leaks. A good background soil CO_2 flux value was obtained and can be used in the future to help in distinguishing between the background biological CO_2 flux and any anomalous soil CO_2 flux.

Groundwater Study

Monitoring groundwater resources over CO_2 geologic sequestration (GS) sites is needed to protect potable water supplies and insure that CO_2 is adequately sequestered with respect to the biosphere. The value of the SACROC groundwater study lies in the long history of CO_2 injection in an oilfield with thousands of active and abandoned wells. According to SWP industrial partner, Kinder Morgan (KM), over 175 million metric tons of CO_2 from natural sources in Colorado and gas processing plants in Texas, were injected at SACROC for EOR between 1972 and 2010. The fact that the quality of shallow drinking water over SACROC has not been impacted by CO_2 injection is strong evidence that it is possible to safely sequester CO_2 in deep subsurface reservoirs. Obtained were 113 ground water samples from 34 domestic/stock, 12 abandoned, and 8 irrigation wells and 1 spring within a ~1,000-mi^2 area containing SACROC and surrounding areas between June 2006 and November 2008. The datasets were augmented using an online historical database from the Texas Water Development Board (TWDB), a State agency that studies groundwater resources in Texas. The primary source of drinking water in the SACROC area is the Triassic-age Dockum aquifer.

The Dockum serves as the source for local public water supply, irrigation for farming, livestock management, and oilfield operations (Bradley and Kalaswad, 2003). Groundwater in the Dockum Group is fresh to brackish (total dissolved solids < 5,000 mg/L) and is locally impacted by dissolution of evaporite deposits in underlying Permian formations (Bradley and Kalaswad, 2003; Dutton, 1989). This impact is due to interaction between two regional aquifers in the Southern High Plains and Rolling Plains. These aquifers include: 1) the Southern High Plains aquifer (SHP) residing primarily in the Tertiary sediments of the Ogallala formation, but also including the Dockum group down to the evaporite-bearing Permian Quartermaster Formation and Whitehorse Group (Richter and Kreitler, 1986); and, 2) the more regionally extensive underlying Paleozoic “deep basin brine” aquifer (DBB) that is separated from the SHP by the Permian layers which comprise an evaporite aquitard of halite, anhydrite, carbonate and mudstone (Bassett et al., 1981; Jorgensen et al., 1988).

Dockum aquifer wells range from ~50–500 ft depth; water samples contain ~400-2,300 mg/L total dissolved solids (TDS). The oil production/CO_2-injection zone lies at 6,000-7,000 ft depth

and contains brine with 50,000-200,000 mg/L TDS. A widely posited hypothesis is that carbonate parameters alone can be used to monitor groundwater quality over a GS site. This is not the case for the Dockum aquifer and likely many others around the world. Dedolomitization caused by mixing with Permian water, and not calcite dissolution, is the geochemical process that dominates the Dockum groundwater system. In an analysis of calcium (Ca^{2+}) versus bicarbonate (HCO_3^-), The data fit modeled curves for dedolomitization, and do not follow a calcite dissolution trend. Instead, data follow increased dedolomitization trends toward higher Ca^{2+} and lower $HCO3^-$, but migrate toward higher PCO_2 values with increased water-rock interaction. The increase in PCO_2 is explained through stable carbon isotope ($\delta^{13}C$) modeling (using PHREEQC code combined with mass balance equations) to be a result of dedolomitization and microbial degradation of organic material.

It is widely recognized that introduction of CO_2 into groundwater will mobilize ions and increase total dissolved solids (TDS). However, our results do not support the hypothesis that contamination of aquifers by increased concentrations of arsenic (As), lead (Pb), or zinc (Zn) will be a likely result of CO_2 GS. Analysis of the data over time for TDS, As, and Zn indicate that these parameters have not increased over time or are not significantly higher in wells inside versus outside of SACROC. Pb was measured above a detection limit of 0.0002 mg/L in 11 of the 59 wells sampled. Of these 11, six are outside and five are inside SACROC. The range of values of Pb detected in wells is between 0.0002-0.00105 mg/L, which is below the drinking water standard (DWS) of 0.01 mg/L. Interestingly, most of the Pb detections are from samples collected in July 2007, with repeat results from the same wells at other sampling trips being below detection limits.

More wells outside than inside SACROC had detections of analyte concentrations in excess of DWS values. Exceptions to this are NO_3^-concentrations, which are higher over SACROC from agriculture, and Cl^- concentrations, which are believed to come from past oilfield practices over SACROC (i.e. brine evaporation pits that used to be maintained on the surface, or leaking brine disposal pipelines and wells).

Methods of SACROC groundwater study

Because data on groundwater quality prior to CO_2 injection at SACROC are spatially and temporally limited, there is not a good "background" dataset against which to compare post-CO_2-injection groundwater quality. For this reason, and to understand why Dockum groundwater is chemically heterogeneous, our study covered ~1,000-mi^2). In lieu of sampling before and after CO_2 injection, BEG sampled both inside and outside SACROC during two consecutive years to assess spatial variation in groundwater chemistry.

During the SWP SACROC groundwater study researchers:

- compiled historical (dating back to 1936) to recent (2008) groundwater chemistry data for eight counties from the TWDB online database (TWDB, 2009);
- collected multiple freshwater samples from 60 private water supply wells (113 samples) and one spring (1 sample), and brine from eight production/injection wells (10 samples);
- compiled chemical data from SACROC production/injection zone brine analyses;
- conducted a study of shallow subsurface stratigraphy;
- measured water levels to construct potentiometric surface maps and identify groundwater flow paths in the Dockum aquifer;
- assessed water quality of potable drinking water zones overlying SACROC;
- performed geochemical modeling to identify controlling processes aid interpretation of groundwater systems overlying SACROC.

Researchers completed six water quality sampling and water level monitoring trips between June 2006 and November 2008. Measured were: Al, Ag, As, B, Ba, Be, Br, Ca, Cd, Cl, CO_3, Co, Cr, Cs, Cu, $\delta^{13}C$, dD, $\delta^{18}O$, F, Fe, HCO_3, Hg, K, Li, Mg, Mn, Mo, Na, Ni, NO_3, Pb, PCO_2, PO_4, Rb, Sb, Se, Si, Sn, SO_4, Sr, TDS, Th, Ti, Tl, U, V, Zn, dissolved inorganic carbon (DIC), dissolved organic carbon (DOC), methane (CH_4), and CO_2.

Analysis of the chemical controls on SACROC groundwater chemistry evaluated processes that include:

- Systematic changes in major element and isotopic chemistry along flow paths away from or across SACROC

- Systematic changes in groundwater chemistry with depth
- pH trends inside vs. outside of SACROC
- chemical trends related to stratigraphic unit
- variation of calcite and dolomite saturation indices with other geochemical parameters
- variations in all other analytes inside versus outside SACROC
- Chemical trends with Ca, Na, Cl, SO4, and
- Oxygen and deuterium trends.

Multiple phases of geochemical modeling can be summarized as follows:

1. Modeling of major ions shows mixing (Permian, Dockum, Ogallala, and produced waters), cation exchange, and dedolomitization are the major geochemical processes. Three samples "representative" of end members are used; however, the chemical variability of the samples precludes choosing discrete end members. This model only gives an idea of the basic carbonate geochemical processes.
2. The carbonate system is dominated by dedolomitization, not calcite dissolution, and is a consequence of mixing, not CO_2 input. Assume that more "evolved" samples have higher P CO_2 due to either:
    i. degassing during dedolomitization in a closed system
    ii. input of exogenous CO_2
    iii. input of microbial CO_2

3. Carbon isotope variations result mostly from dedolomitization reactions, which are slightly degassing. Major assumptions are in the end member carbon isotope variability and the values used for modeling. Calcite and dolomite are not distinguished. The same 13C is used for calcite as for dolomite. Also, average values are used for injectate and microbial CO_2. Variability in these values is not shown in the model.

Results of SACROC Groundwater Study

Ranges and median values of 40 chemical analytes, total dissolved solids (TDS), and well depths for freshwater samples are shown in Table 35. Results from other studies show that pH will decrease and dissolved solids (TDS) will increase when CO_2 concentration is in groundwater is in-

creased. However, this study does not reveal anomalous pH or TDS values associated with SACROC over time (1956-2008), see Figures 141–142.

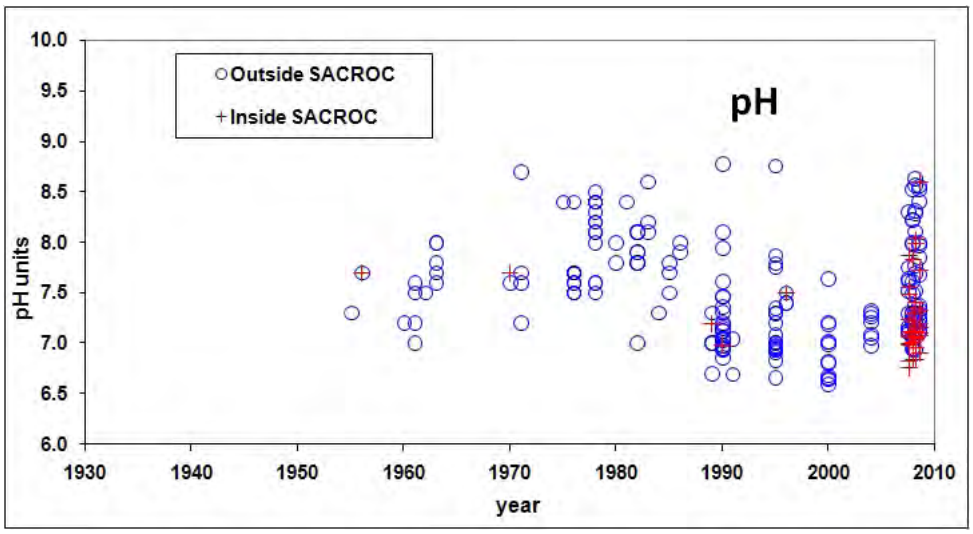

Figure 141. TWDB (1956-2008) and BEG (2007-2008) pH data from Borden, Fisher, Howard, Kent, Mitchell, Nolan, and Scurry Counties, TX.

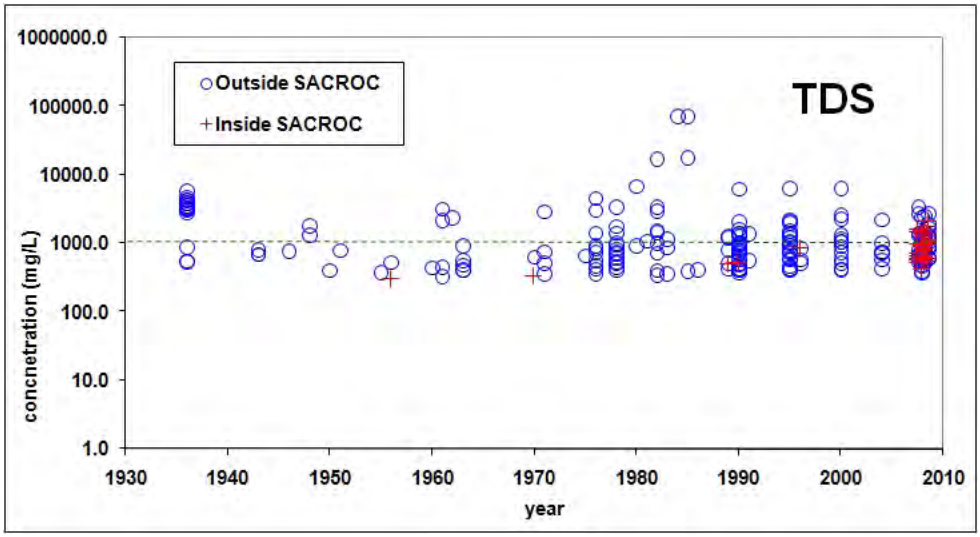

Figure 142. TWDB (1936-2008) and BEG (2007-2008) total dissolved solids (TDS) data from Borden, Fisher, Howard, Kent, Mitchell, Nolan, and Scurry counties, TX

Freshwater samples were obtained from wells constructed in the Ogallala Formation, Dockum Formation, Permian-age units, and combinations of these geologic units. Figure 143 shows the wells classified by geologic formation in which they are completed.

Table 35. Chemical Analyte Ranges and Median Values for 113 BEG Freshwater Samples Collected from Private Wells in Fisher, Garza, Kent, and Scurry Counties

Analyte	range (mg/L)	median (mg/L)	# nd
Silver (Ag)	all nd	na	113
Aluminium (Al)	0.0005 - 0.2439	0.01	25
Arsenic (As)	0.0004 - 0.0278	0.004	6
Boron (B)	0.03 - 2.17	0.26	0
Barium (Ba)	0.01 - 0.54	0.07	1
Berilium (Be)	all nd	na	113
Bromide (Br)	0.05 - 3.64	0.46	2
Calcium (Ca)	1.28 - 596.56	77.96	0
Cadmium (Cd)	0.87	0.87	112
Chloride (Cl)	8.43 - 1129.08	115.68	0
Chromium (Cr)	0.001 - 0.029	0.002	49
Cupper (Cu)	0.0006 - 0.0238	0.0029	21
Cobalt (Co)	0.001	0.001	112
Fluoride (F)	0.586 - 7.750	1.598	3
Iron (Fe)	0.008 - 0.277	0.028	34
Bicarbonate (HCO_3)	19.86 - 795.69	312.00	0
Mercury (Hg)	0.0001 - 0.0004	0.0001	102
Potassium (K)	0.63 - 10.72	3.44	0
Lithium (Li)	0.021 - 0.199	0.070	1
Magnesium (Mg)	0.43 - 396.72	21.17	0
Manganese (Mn)	0.001 - 0.677	0.008	30
Molybdenum (Mo)	0.001 - 0.025	0.004	20
Sodium (Na)	7.38 - 985.88	87.83	0
Nickel (Ni)	0.0008 - 0.1800	0.0041	19
Nitrate (NO_3)	0.07 - 206.34	8.10	7
Lead (Pb)	0.0001 - 0.0123	0.0006	99
Phosphate (PO_4)	0.17 - 0.25	0.21	111
Rubidium (Rb)	0.001 - 0.004	0.001	55
Antimony (Sb)	all nd	na	113
Selenium (Se)	0.001 - 0.082	0.005	17
Silica (Si)	2.98 - 29.63	21.27	0
Sulfate (SO_4)	11.51 - 2931.02	97.37	0
Strontium (Sr)	0.05 - 14.58	1.34	0
Thorium (Th)	all nd	na	113
Titanium (Ti)	0.003 - 0.007	0.003	110
Thallium (Tl)	all nd	na	113
Uranium (U)	0.0002 - 0.0624	0.0067	7
Vanadium (V)	0.001 - 0.140	0.020	28
Zinc (Zn)	0.003 - 0.476	0.018	7
pH	6.73 - 8.63	7.23	0
TDS	358 - 6194	825	0
well depth (ft bgl)	30 - 500	na	na
nd - below analytical detection limit; na - not applicable			

Geologic units present at the surface within our study area range from Permian to Quaternary in age. Two significant water-bearing units crop out at the surface within the study area. The Triassic-age Dockum Formation (Fm.) (TrD in Figure 143 hosts the Dockum aquifer. The second significant water-bearing unit is the Ogallala Fm. (P-EOg in Figure 143). This erosional outlier of the Ogallala Fm. is isolated from the Ogallala aquifer of the Texas High Plains but provides significant freshwater resources in Scurry and surrounding counties. Smaller quantities of fresh groundwater are produced from Permian-age units in the east parts of the study area.

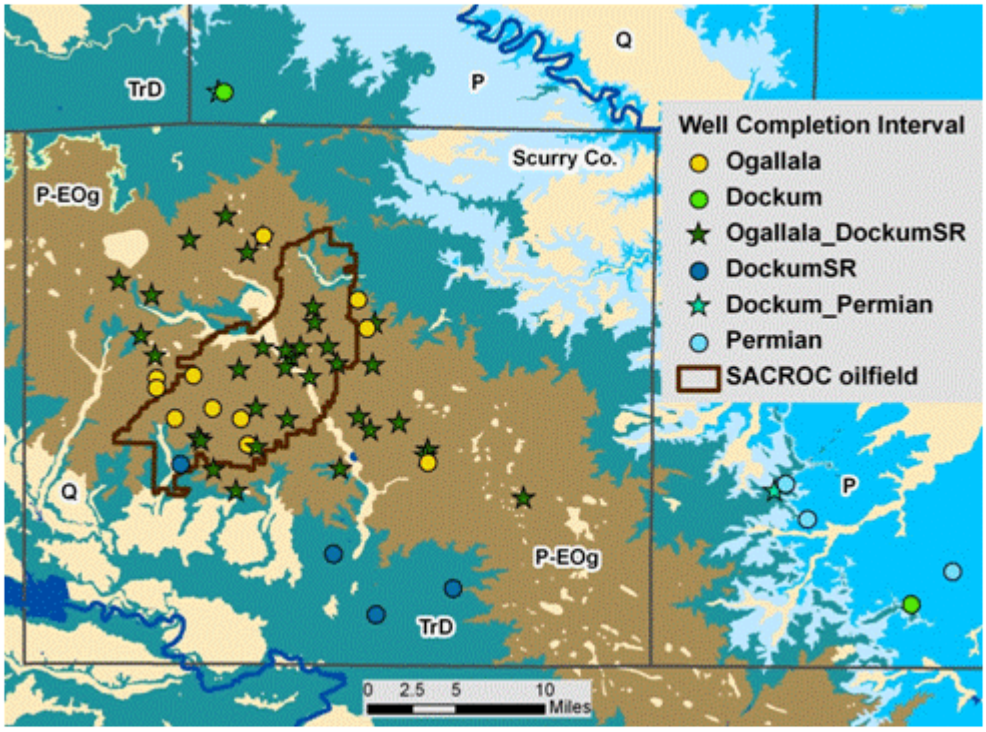

Figure 143. Locations of wells monitored for SWP SACROC groundwater study superimposed on surface geologic units. Geologic unit abbreviations: Q- undifferentiated Quaternary units; P-EOg – Paleocene-Eocene Ogallala Fm.; TrD – Triassic Dockum Fm.; P – undifferentiated Permian units.

Chemistry of Dockum aquifer groundwater is highly heterogeneous because the formation is heterogeneous. The history of oil and gas activity in the region is long, and wells designated as Dockum aquifer by TWDB are completed in different stratigraphic intervals. Wells completed within the Ogallala outcrop are designated by TWDB as Dockum aquifer wells even though not all of them extend into the underlying Dockum Formation, which is subdivided into different depositional units with depth (McGowan et. al., 1979), not all of which are hydraulically con-

nected. A few Dockum aquifer wells penetrate multiple Dockum subunits and extend into underlying Permian-age strata.

A Piper diagram is a graphical display used to show variations in large groundwater chemistry datasets. Milliequivalent percentages of major cations (Ca, K, Mg, and Na) and anions (Cl, HCO_3, and SO_4) are plotted on trilinear diagrams, and combined values are projected onto a central quadralinear plot. The Piper diagram in Figure 144 shows no clear distinction between samples collected inside versus outside the SACROC oil field.

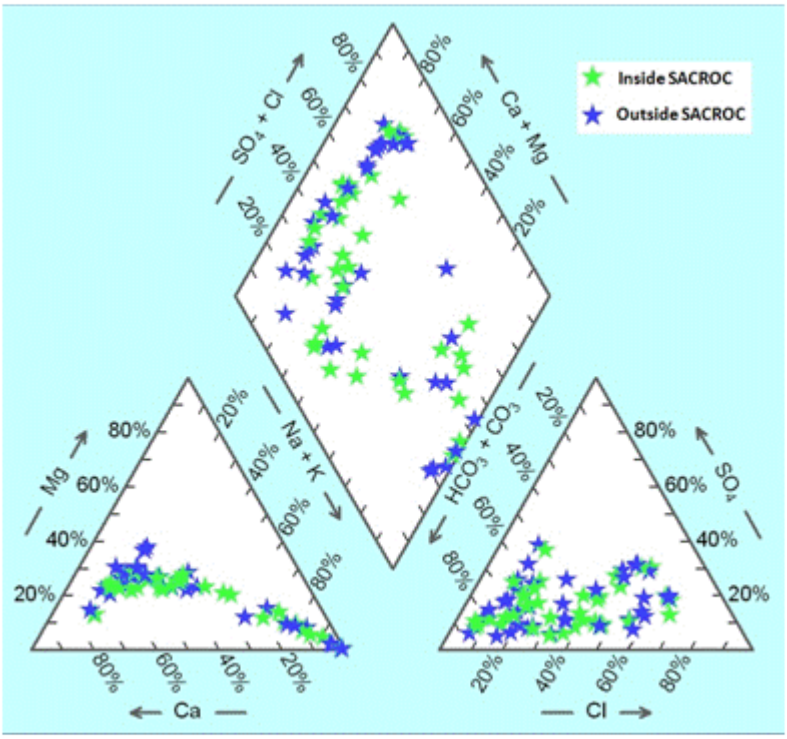

Figure 144. Piper diagram of BEG-sampled wells only, showing no clear distinction between BEG groundwater samples collected inside SACROC versus outside SACROC.

A plot of sulfate (SO_4) versus chloride (Cl) anions (Figure 145) shows a more distinct grouping of samples from inside versus outside SACROC. Samples from inside have higher Cl values than those collected outside SACROC. Samples with higher Cl and SO_4 concentrations (e.g., Permian and produced water samples) have much higher total dissolved solids (TDS) than BEG freshwater samples. Trends of major element concentrations suggest mixing of Dockum aquifer groundwater and water with Permian and production-zone geochemical signatures. Mixing models tested using PHREEQC code predict that <1% produced oil field brine or 12% Permian water could

be mixed with the lowest TDS Dockum freshwater sample to produce the highest TDS Dockum sample.

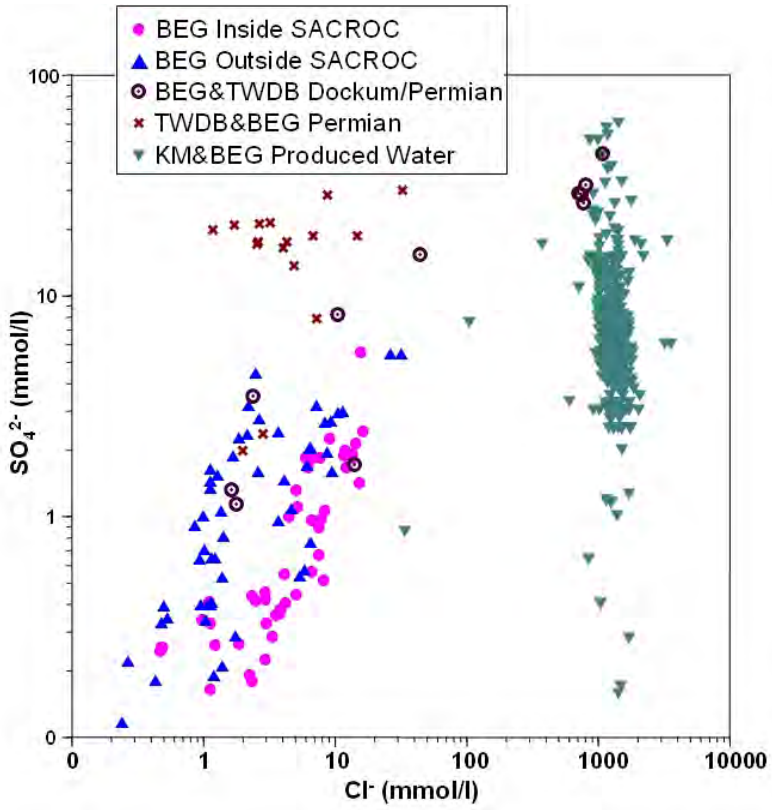

Figure 145. Sulfate vs. chloride concentrations of all BEG samples (five sampling periods, inside and outside of SACROC) and BEG and KM produced water samples.

The main question pertinent to this study remains: Has Dockum aquifer water been impacted by the long history of CO_2 injection at SACROC? If conduit flow along leaking wellbores is responsible for increased TDS in Dockum aquifer water overlying SACROC, we would also expect to see impacts from high CO_2 concentrations. Given the complexity of the natural system and the likely signal from early oilfield activities, it is unrealistic to try to prove that no upward vertical communication of fluids has occurred in the SACROC oilfield. Evidence presented here allows us to say that no obvious impacts to groundwater are found, and that the impacts observed are not a result of interaction of freshwater with large volumes of injected CO_2.

More detailed description of the shallow subsurface stratigraphy underneath SACROC allowed us to construct a potentiometric surface map using water levels from only those wells completed in the Dockum Santa Rosa subunit of the Dockum aquifer. This map reveals a groundwater mound over SACROC (insert with cross section location lines in Figure 146. One way to assess if shallow freshwater resources have been impacted by CO_2 injection at SACROC is to look at profiles of chemical constituents along Dockum aquifer groundwater flow paths in vicinity of SACROC (Figure 146). There are no clear trends of lower pH, higher TDS, or higher concentrations of other analytes over SACROC versus areas downgradient from SACROC.

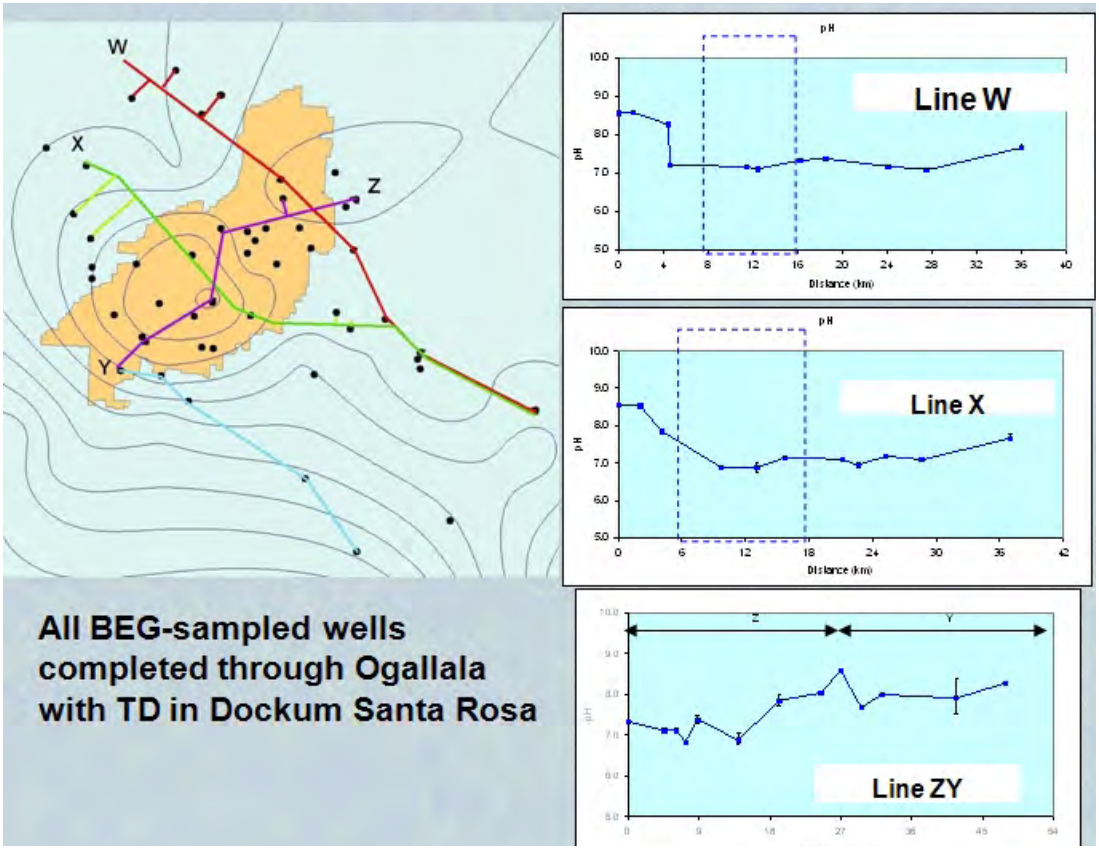

Figure 146. (a) Locations of transect plots relative to SACROC and potentiometric surface contours of Dockum Santa Rosa and (b) pH along gradient-parallel transects W, X, and ZY.

Another way to evaluate data from Dockum groundwater samples is to assess degradation of water quality by comparing analyte concentrations with EPA drinking water standards. Data summarized in Table 36 are from BEG samples that were filtered (0.2 to 0.45 µm) in the field. Cati-

on samples were preserved with nitric acid to pH below 2. No preservative was added to anion samples. Some Dockum freshwater samples have constituents that exceed drinking water samples. The percentage of Dockum aquifer samples taken from 60 wells and one spring with analytes exceeding EPA primary maximum contaminant levels (MCLs) and secondary drinking water standards are highlighted in yellow in Table 36. Without exception, the percentage of samples with analytes in excess of EPA standards is higher outside than inside SACROC.

As and Pb are listed as contaminants of particular concern in the July 2008 EPA proposed rule. The concern is that such constituents will be leached from rocks in the appropriate GS reservoir and mobilized to impact USDWs. Of the 9.8% of wells with As levels above MCLs, only 1.6 percent of these are inside SACROC (Table 36). Only ~12% of the filtered BEG Dockum samples had Pb levels above a detection limit of 0.002 mg/L. Forty-two percent of these samples are from wells inside SACROC.

Table 36. Comparison of EPA Drinking Water Standards with BEG Dockum Aquifer Well Data

Analyte	EPA/TCEQ Primary Drinking Water MCL (mg/L)	BEG Wells Exceeding EPA Standards	BEG Wells Exceeding EPA Standards - Inside SACROC	BEG Wells Exceeding EPA Standards - Outside SACROC
Primary Maximum Contaminant Level (MCL)				
Arsenic (As)	0.01	9.8%	1.6%	8.2%
Cadmium (Cd)	0.005	1.6%	0.0%	1.6%
Fluoride (F^-)	0.4	4.9%	1.6%	3.3%
Nitrate (NO_3-N)	10	13.1%	4.9%	8.2%
Selenium (Se)	0.05	4.9%	1.6%	3.3%
Secondary Drinking Water Standard				
Aluminum (Al)	0.05	34.4%	13.1%	21.3%
Chloride (Cl^-)	250	32.8%	14.8%	18.0%
Fluoride (F^-)	0.2	37.7%	14.7%	23.0%
Manganese (Mn)	0.05	14.7%	4.9%	9.8%
Sulfate (SO_4^{2-})	250	26.2%	1.6%	24.6%
Total Dissolved Solids (TDS)	1000	50.8%	18.0%	32.8%

Geochemical modeling results

Sediment reactivity in the Dockum

Dockum aquifer sediments are predominantly siliciclastic with small amounts (1%) of diagenetic and detrital calcite. Visual inspection of Dockum well cuttings collected from SACROC indicate a general composition of 60–80% quartz, 10–20% feldspar, 15% dark rock fragments and minor carbonate cements. SEM aided by an energy dispersive X-ray system shows mineralogical content of the following: quartz > K-feldspar > albite > dolomite > calcite. Quartz grains show no evidence of overgrowth or corrosion; however, feldspars show limited dissolution features. Clay, mostly smectite, coats most mineral grains. Dolomite (5 %) occurs as ubiquitous rhombic crystals that often exhibit corrosion suggesting dissolution.

The degree of influence of carbonate minerals in the predominantly siliciclastic Dockum aquifer was assessed using co-variation of SiO_2 and HCO_3^- after Hounslow (1995). Data collected inside and outside SACROC, and from the TWDB database show that in spite of the volumetric dominance of silicates in the Dockum, samples are geochemically dominated by carbonate weathering. Regional data also indicate the same importance of carbonate geochemistry with a relatively minor influence of silicate weathering, most likely representing feldspar dissolution. Overall, these geochemical covariations suggest that small amounts of carbonate in an aquifer (1 to 5 % in this case) may yield a geochemistry receptive to changes in CO_2, supporting the hypothesis that carbonate parameters may be useful indicators of leakage. This conclusion is in direct opposition to the assumption of Wilkin and Digiulio (2010) who argue that a quartz-rich aquifer would be non-reactive.

Major element trends

A classic Piper diagram displaying normalized values for cations (lower left triangle), anions (lower right triangle) and a combination of the two (central diamond) was used to graphically indicate water type, mineral reactions, mixing, and ion exchange (Figure 147). Dockum samples plot in all quadrants of the Piper diagram, indicating a geochemical environment with many influences but little distinction between samples collected inside and outside SACROC. As expected, Permian waters that reside in evaporite-containing formations plot in the gypsum field indicating $CaSO_4$-type waters. Waters co-produced with oil are predominantly NaCl-type. Gen-

eral trends on the anions triangle indicate two types of mixing: the majority of samples outside SACROC appear to trend towards Permian compositions, while a majority of samples inside SACROC (and a few outside SACROC) appear to trend towards produced water compositions. The suggestion is that variable amounts of mixing of Dockum water with Permian and co-produced brines affect the geochemistry of the Dockum at SACROC.

A trend stretching from Na^+ to Ca^{2+} on the cation triangle further suggests that input of NaCl brines into the Dockum results in the exchange of Na^+ for Ca^{2+} on exchange sites. In the case of SACROC, the exchange of Na^+ in solution for Ca^{2+} sorbed to clays is fueled by mixing of Dockum and produced waters. Therefore two mechanisms exist by which calcium ions are added to the shallow groundwater system: one a natural process inherent to the regional system (mixing with $CaSO_4$-type waters in the salt dissolution zone), and the other resulting from land-use practices (mixing with co-produced brines and cation exchange). Evidence that both processes are at work can be seen in relatively weak co-variations between Ca^{2+} and SO_4^{2-} that strengthen significantly when addition of a NaCl component and cation exchange is also considered (Figure 148). A general decrease in Cl^- with depth (not shown) indicates that NaCl input is likely from historical disposal of brine into surface pits rather than from brine migrating from the deep production reservoir.

Strong covariation between Mg^{2+} (an indicator of dolomite dissolution) and SO_4^{2-} (an indicator of Ca^{2+} input) with $Mg^{2+}/Ca^{2+} < 0.8$ should be expected; Figure 149 illustrates these relationships in the Dockum aquifer near SACROC.

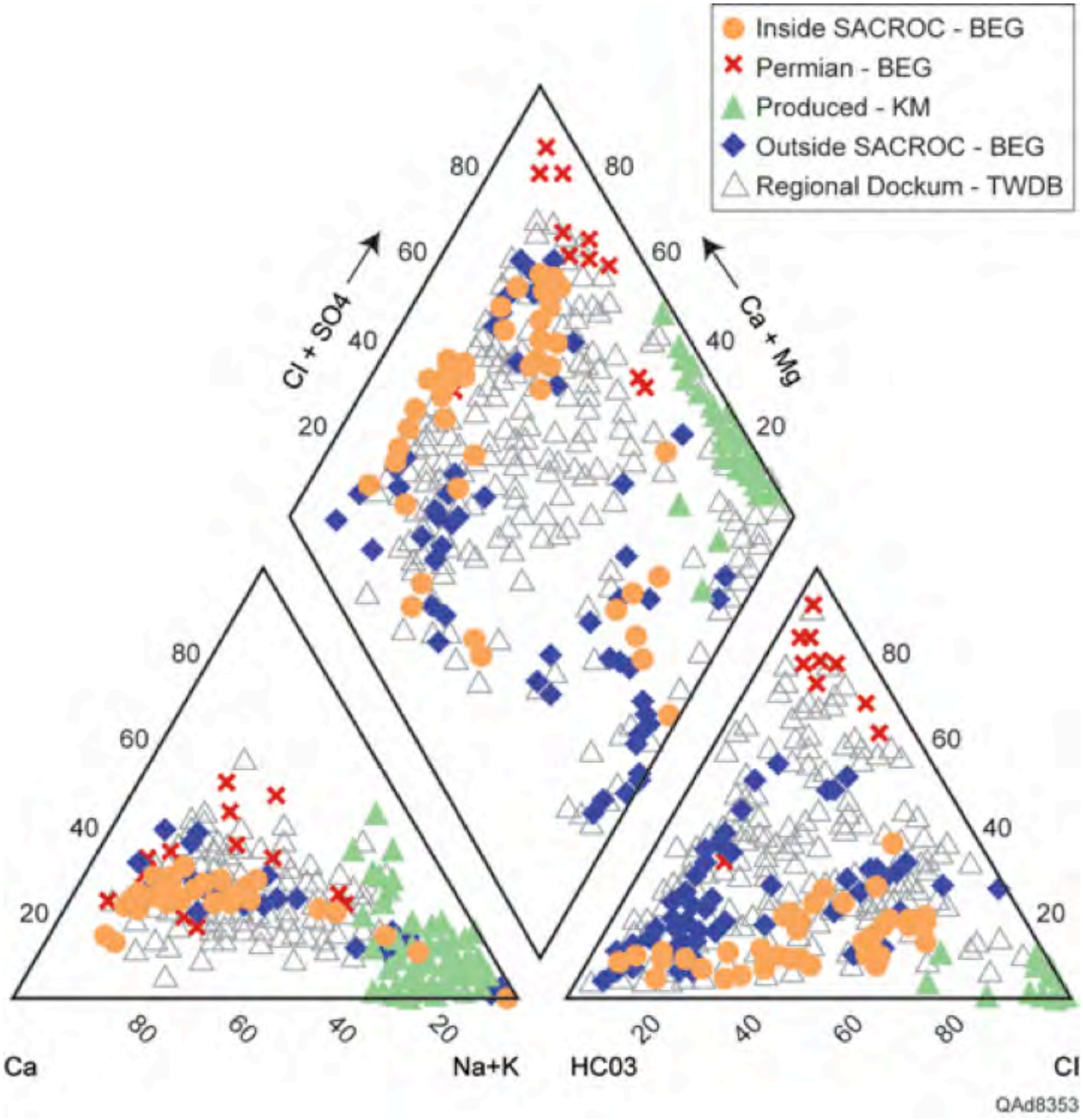

Figure 147. Piper diagram showing compositions of samples from Dockum and Permian formations collected by the BEG during the study. Also shown are analyses provided by Kinder Morgan for produced brines and historical Dockum analyses furnished by the TWDB.

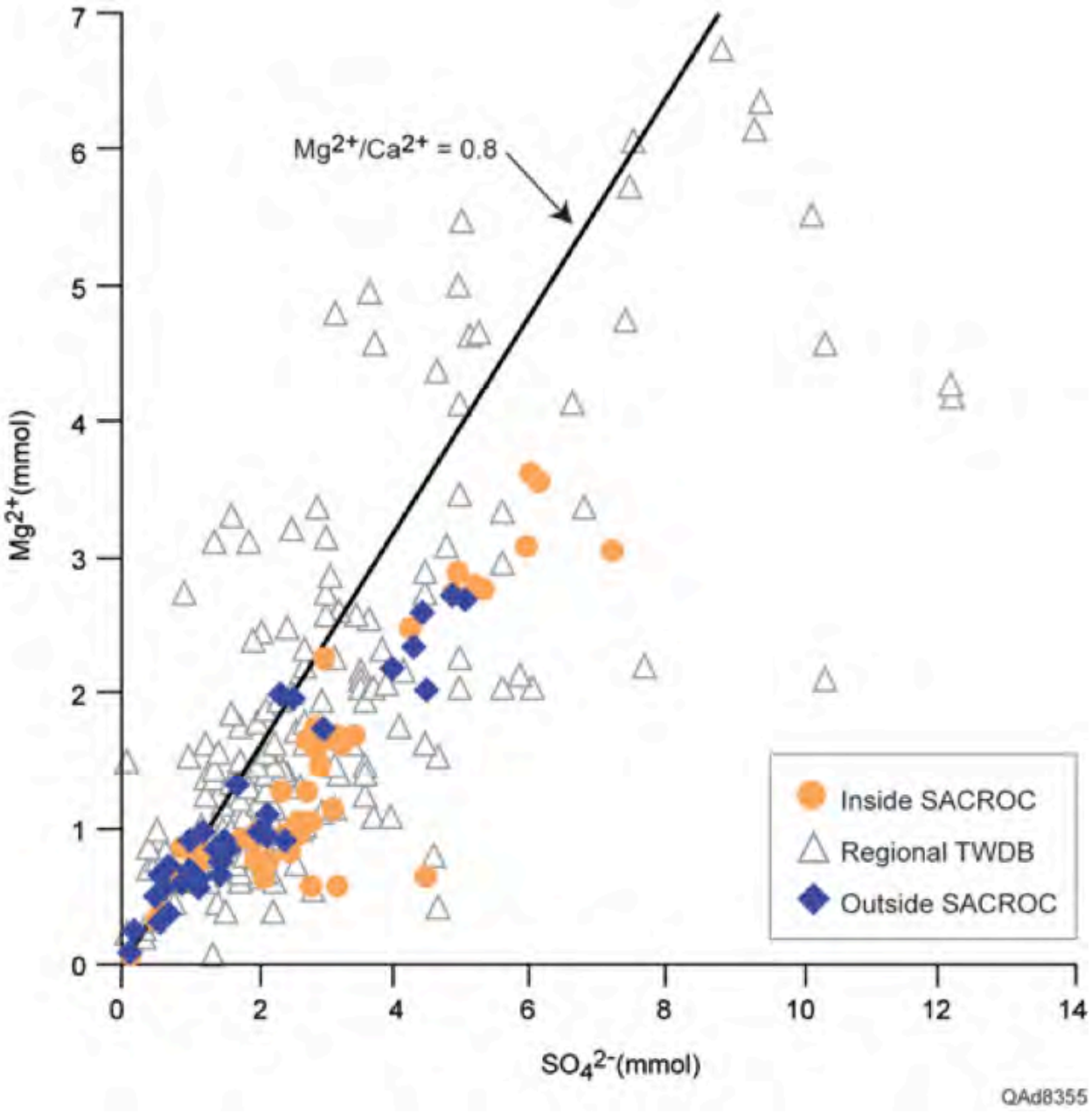

Figure 148. Covariation of Ca^{2+} with SO_4^{2-} (left) is not particularly strong, indicating Ca^{2+} is not solely supplied to the system by mixing with Permian $CaSO_4$ waters. Addition of an NaCl produced water component with cation exchange (right) shows even stronger correlation indicating both processes contribute to the input of calcium ions to the shallow aquifer.

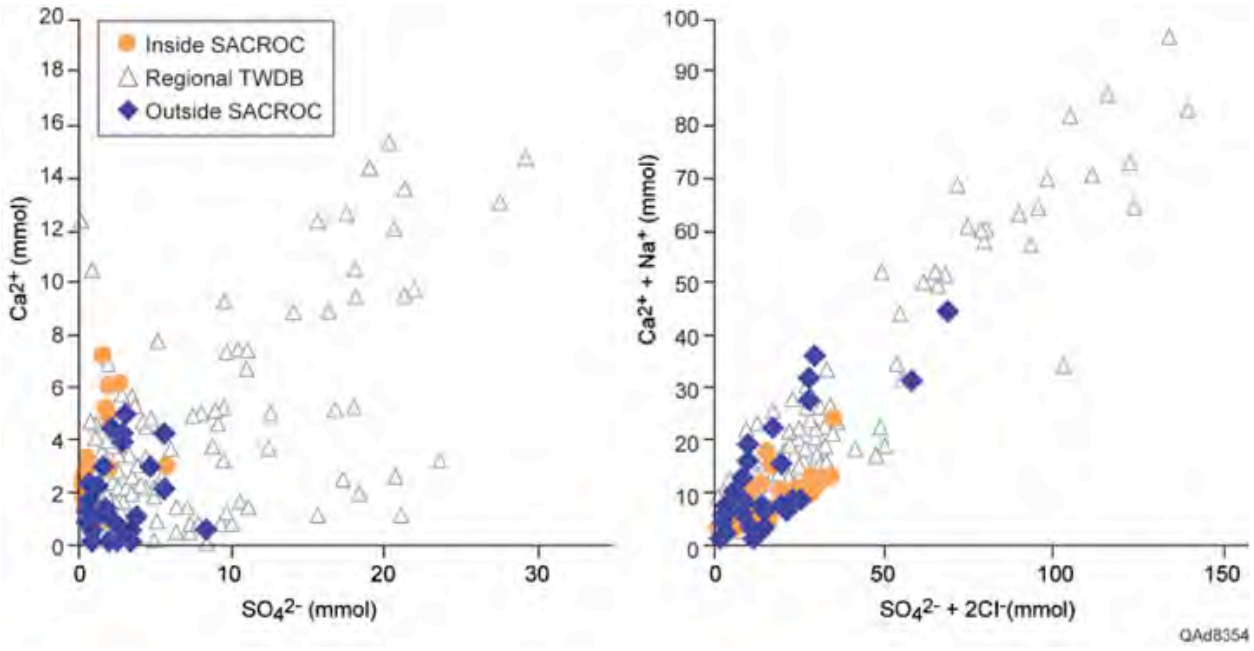

Figure 149. Covariation of Mg^{2+} and Ca^{2+} indicates a chemical driving force for dedolomitization.

Modeling the role of CO_2 in a system undergoing dedolomitization

The conclusion that Ca^{2+} rather than CO_2, is driving the carbonate system is significant because it illustrates that changes in carbonate equilibrium are not necessarily indicators for CO_2 input but can be fueled by mixing. Dedolomitization creates a significantly different carbonate environment than that of simple calcite dissolution. Whereby calcite dissolution is driven by CO_2, dedolomitization is driven by calcium ions, which combine with carbonate supplied by dolomite dissolution to form calcite. The driving forces (products) and the outcomes (reactants) of these two environments are very different illustrating the importance of defining the system before predicting the effects of CO_2.

With the overall system well-defined, the PHREEQC code (Parkhurst and Appelo, 1999) was used to constrain the role of CO_2 in a system dominated by dedolomitization rather than calcite dissolution. During calcite dissolution fueled by CO_2 the data will trend along a line with a slope of 0.5 on a plot of Ca^{2+} versus HCO_3^- (shaded arrow in Figure 150). As expected, data do not follow calcite dissolution trends but rather fall within a range of trends modeled for dedolomitization under several conditions of constant PCO_2. These trends were constructed by mixing 25

mmoles of $CaSO_4$ to Dockum water initially in equilibrium with calcite and dolomite at various fixed PCO_2. Data correspond with these trends and generally lie within the boundaries defined by the range of constant PCO_2 from $10^{-2.7}$ to $10^{-1.5}$ (Figure 150).

During dedolomitization under constant PCO_2, geochemical evolution progresses from high to low HCO_3^- and from low to high Ca^{2+}. This is in contrast to the trend for calcite dissolution which is from low to high HCO_3^- and Ca^{2+}. Numerical modeling shows that dissolved bicarbonate in the initial solution slows dolomite dissolution in the early stages of reaction by supplying some anions necessary for calcite precipitation. As calcite precipitates, dissolved bicarbonate and calcium are quickly used, resulting in decreasing HCO_3^- and relatively steady concentrations. As the dissolved bicarbonate in the initial water is consumed, dolomite dissolves and calcite precipitates and the kinetics of dissolution/precipitation reactions control ion concentrations in the water. If the system re-equilibrates to a higher constant PCO_2 under the normal aquifer conditions observed at the study site (PCO_2 from $10^{-2.7}$ to$10^{-1.5}$), the mass of dolomite dissolution increases, the mass of calcite precipitation decreases, HCO_3^- increases and pH decreases, all at higher constant PCO_2. Without knowledge of the system, it might appear that the high bicarbonate samples, those with HCO_3^- higher than about 10 mmoles, are anomalously impacted by CO_2. However, with the knowledge that the system is undergoing dedolomitization in response to complex mixing and cation exchange relationships, it is apparent that these samples are in fact the least "evolved" or reacted samples in the system.

Sensitivity of the system to CO_2 input

With the geochemical system defined, it is possible to predict the sensitivity of the system to CO_2 input and to identify the geochemical parameters that will best signal this input. When the data in Figure 151 are visually compared to the modeled trends for constant PCO_2 it becomes apparent to the eye that the data trend toward higher PCO_2 with evolution. For example, the majority of samples with relatively low Ca^{2+} of about 2 mmoles cluster near an average modeled PCO_2 trend of about 10^{-2}; however, when these samples have evolved to higher Ca^{2+} concentrations of about 7 mmoles, they cluster near higher modeled PCO_2 of $10^{-1.5}$ suggesting that CO_2 is building in the system.

The observed phenomenon of increasing PCO_2 could result from CO_2 EOR practices; however, no geochemical distinction has been observed between samples collected inside and outside SACROC that would suggest impact from CO_2 injection. In addition, the modern data collected during the study both inside and outside SACROC show no geochemical distinction from historical regional data collected from areas spatially and/or temporally removed from CO_2 injection. Groundwater quality inside SACROC is not significantly degraded compared to EPA drinking water standards (Smyth et al., 2009). Redox reactions producing HCO_3^-, especially sulfate reduction, may play a role; however, aquifer conditions were generally found to be highly oxidizing. It is concluded that, based on PHREEQC model output, increases in PCO_2 represent normal system degassing during dedolomitization.

To simulate the perturbations that would occur if the potable aquifer were to receive CO_2 from the storage reservoir due to a leak, a sensitivity analysis was performed using the system model and the PHREEQC code. In the case of leakage into an aquifer experiencing dedolomitization, two mass transfers into the aquifer occur simultaneously and affect the intricate interplay between HCO_3^- and Ca^{2+}: 1) mass transfer of Ca^{2+} from mixing and/or cation exchange and, 2) mass transfer of CO_2 from a simulated leak. Ca^{2+} input is essentially a function of the hydrodynamic factors producing mixing and can be assumed to be a steady-state process for each environment that is modeled. With a constant rate of mixing and mass flux of Ca^{2+} into the system, a leakage signal can be modeled as an increase in CO_2 input which, when compared to a defined steady influx of Ca^{2+}, manifests as an increase in CO_2/Ca^{2+}. Alternately, this ratio can also be varied and used to represent different conditions of mixing that exist in different aquifers having different hydrodynamics. Because CO_2/Ca^{2+} is independent of absolute fluxes, the ratio can be used to represent a variety of different environmental fluxes and conditions.

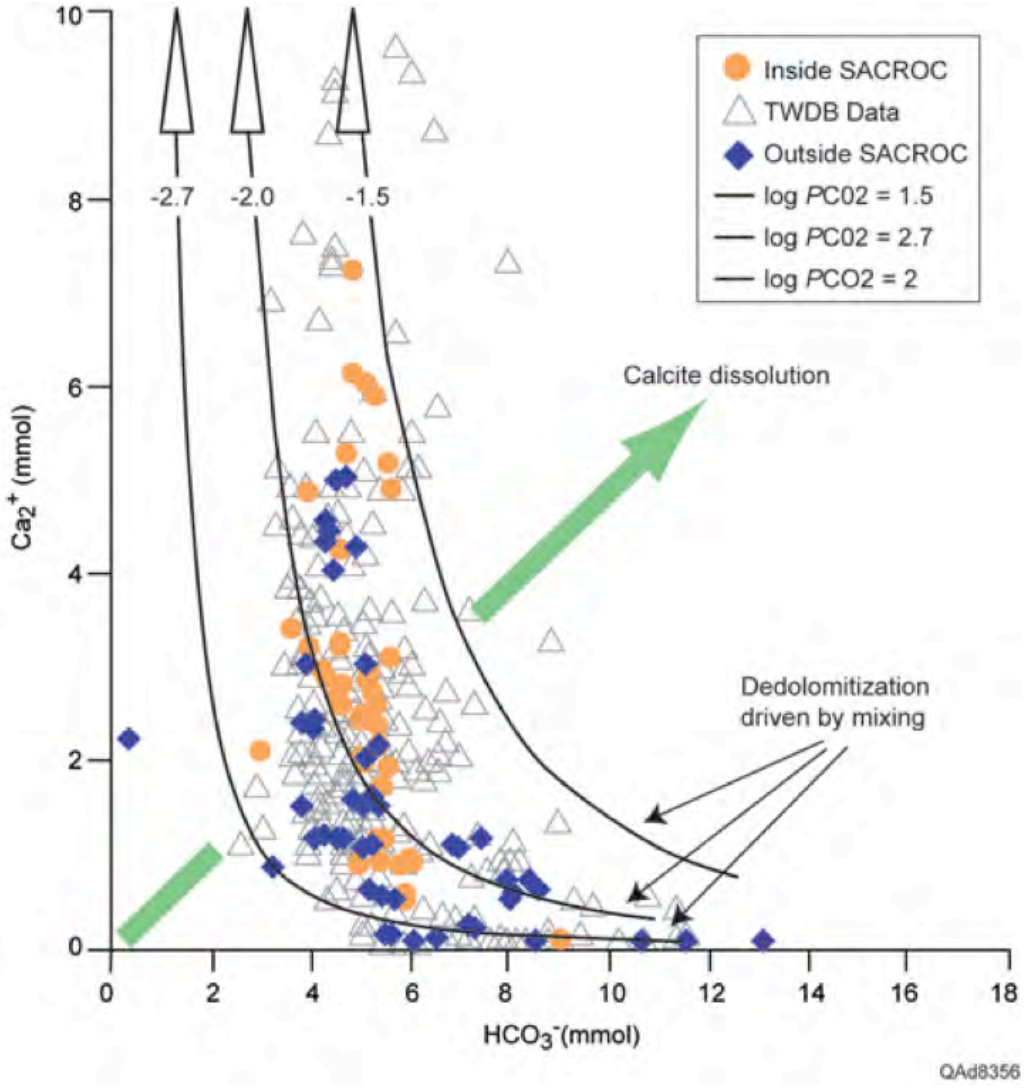

Figure 150. Modeling results for evolution of Ca^{2+} and HCO_3^- during calcite dissolution and dedolomitization. Modeled curves for dedolomitization under constant *P*CO_2 are shown for $10^{-1.5}$, $10^{-2.0}$, and $10^{-2.7}$.

To understand how systems react to CO_2 and to discern the geochemical parameters most useful for monitoring GS sites, two types of analyses are useful: one that addresses how carbonate parameters will respond to different inputs of CO_2 within a given system and one that addresses the range of geochemical responses that would arise from the geologic variability among sites. Both analyses use the response of carbonate parameters such as calcite and dolomite dissolution, DIC, HCO_3^-, pH, and Ca^{2+} to variations in CO_2.

The first analysis determines the sensitivity of a defined system, in this case, the Dockum aquifer above SACROC, to different magnitudes of CO_2 input. This approach achieves two important goals: 1) to illustrate the magnitude of CO_2 input that would be necessary to discern leakage signal from background noise, and 2) to evaluate the sensitivity of individual carbonate parameters to CO_2 within that system. If a system is insensitive to CO_2 input, geochemical parameters will not sufficiently signal a leak in its beginning stages. If a system is sensitive, geochemical parameters may be useful for monitoring because they would signal a leak in its early stages, providing greater options for protecting resources and/or remediation.

The second type of analysis considers the degree to which site-specific factors can affect how carbonate parameters behave in the presence of CO_2. Such an analysis considers the importance of understanding the specific hydrochemical characteristics of each aquifer that exists over a GS site, evaluates the importance of detailed characterization of each aquifer system, and determines the degree to which assumptions can be made based on small data sets. For example, if the magnitude and direction of change of geochemical parameters is similar in any environment, these parameters will be useful for monitoring GS sites. If, however, site-specific conditions create wide-ranging affects and outcomes, their usefulness is decreased because intricate and costly characterizations at each site would be necessary.

The initial sensitivity simulation is structured to define the amount of CO_2 needed to create the observed CO_2 increase shown by the data in Figure 150. A starting water composition is chosen at the point in the system where PCO_2 appears to shift to higher values (about 4.5 mmoles HCO_3^- and 1 mmole Ca^{2+}). The ending composition is chosen to represent the magnitude of the shift that is visually observed in the dataset (about 5 mmoles HCO_3^- and 9 mmole Ca^{2+}). CO_2/Ca^{2+} = 0.1 yields results that represent the spread of regional TWDB data. The model results indicate that the shift toward higher PCO_2 in the data is consistent with the addition of 1.5 mmoles of CO_2 and 15 mmoles $CaSO_4$ at a CO_2/Ca^{2+} ratio of 0.1.

To continue the analyses using the same initial water composition, we then added CO_2 to the system using CO_2/Ca^{2+} ratios of 0.1, 0.5, 1, 2, and 10 to understand how different conditions of mixing would manifest similar CO_2 inputs. The evolutionary trends for the varying CO_2/Ca^{2+} ratios

are shown in Figure 151 (broken lines) along with calcite dissolution (solid line). Results show trends different from the evolution of waters modeled under constant PCO_2 (Figure 150). In systems with less input from mixing (i.e. with greater CO_2/Ca^{2+}), reaction pathways shift to higher HCO_3^- and lower Ca^{2+} and more closely mimic calcite dissolution, although dolomite continues to dissolve and calcite continues to precipitate.

Points of equal CO_2 input are shown by solid triangles in Figure 151 for 1.5 mmoles and 6 mmoles for each environment defined by a specific relative rate of mass transfer (CO_2/Ca^{2+}) and for straight calcite dissolution. Model output for addition of 1.5, 6 and 50 mmoles CO_2. Background geochemical variability at SACROC is represented by the spread of regional data collected in areas devoid of CO_2 injection and those collected outside SACROC as indicated by a shaded area in Figure 151. Sensitivity analysis shows that 6 mmoles of CO_2 is necessary to achieve Ca^{2+} and HCO_3^- compositions outside of background concentrations. Also evident from the simulations is that a system undergoing calcite dissolution is slightly less sensitive to CO_2 input than one undergoing dedolomitization.

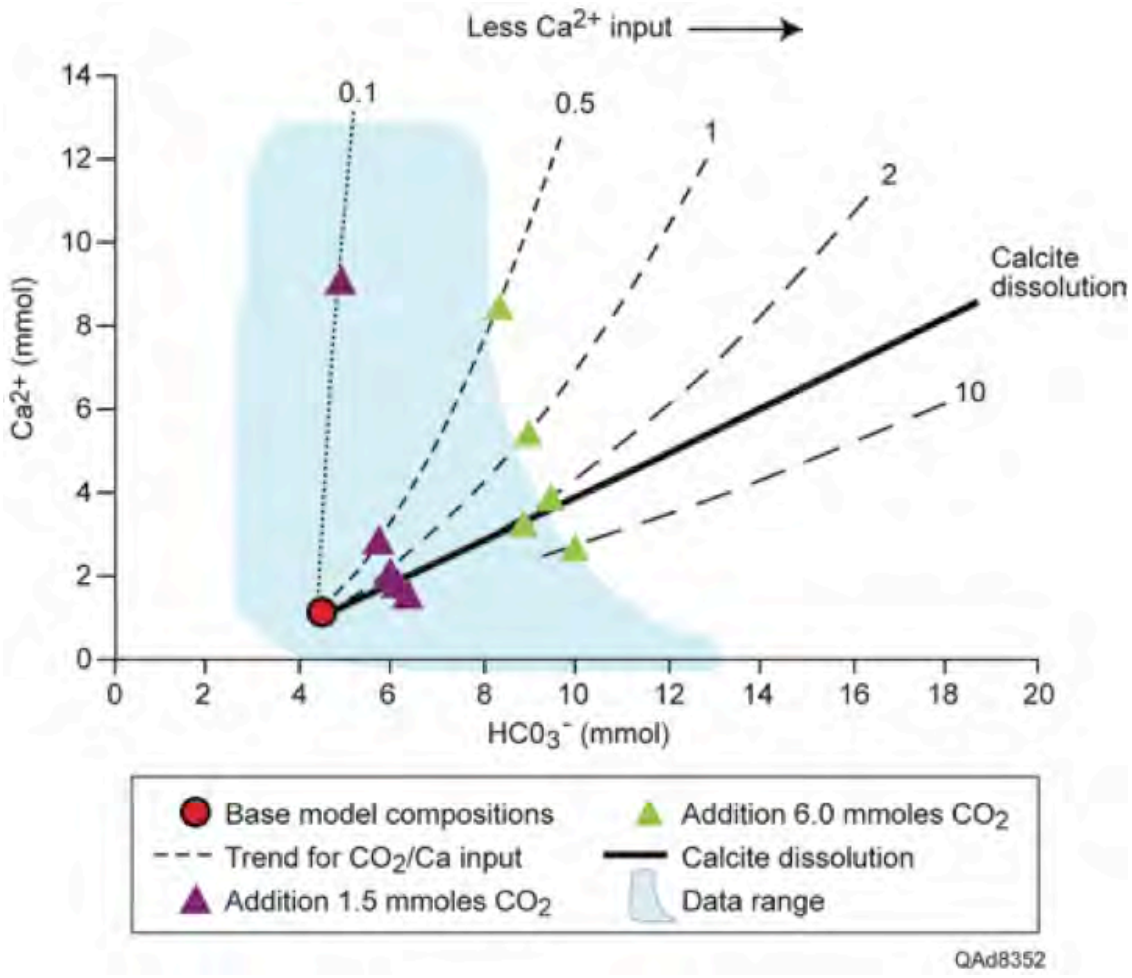

Figure 151. Results of CO_2 sensitivity modeling. Shaded area represents background geochemical variation in the aquifer. Beginning composition for all models is denoted by a red dot. Ending compositions are shown by triangles. Responses of the system to various mass inputs of CO_2 under different mixing conditions are shown.

To understand the significance of 6 mmoles of CO_2 input into an aquifer with regard to leakage rate from a storage formation, a mass balance exercise was performed using the anthropogenic emissions expected from a 500 Megawatt (MW) power plant, which is assumed to produce and store up to 3 million tonnes/year of carbon dioxide (MIT Interdisciplinary Study, 2010). Assumptions are: 1) a saturated aquifer thickness of 60 m with a porosity of 0.30, 2) an area of consideration within the aquifer of 1 hectare; and 3) any CO_2 leaked from the storage reservoir is instantaneously and equally distributed throughout the area of consideration. We have discerned, through careful inspection and modeling of the hydrochemical environment at SACROC, that the CO_2 concentration necessary to produce a geochemical signature above background conditions is

6 mmoles/L. This equates to 4.75 x 10^6 g of CO_2 within the 1 hectare area and represents 0.001% leakage rate of the total yearly output from a 500 MW power plant. The system appears sensitive enough to detect a relatively small leak. However, because the model assumes instantaneous distribution throughout the area of consideration, this is a conservative estimate that depends on the type and areal distribution of the leak. If the leak enters the aquifer as a point source, the geochemical signal will be strong but difficult to locate spatially. If the leak enters the aquifer more diffusely, the geochemical signal will be weaker but easier to locate spatially. The calculation described herein is more applicable to the latter case.

To identify which carbonate parameter is best suited for monitoring at a variety of sites, it is necessary to understand how each parameter responds during carbonate dissolution and under different conditions of leakage versus mixing during dedolomitization. The most desirable parameter will have the highest sensitivity to increasing CO_2 input (i.e the largest variability) and the magnitude and direction of its variability should be similar, and therefore predictable, in any environment. The modeled considered responses of DIC, HCO_3^-, pH, and Ca^{2+} to increasing CO_2 input

Of the four parameters, DIC has the highest sensitivity with the largest and most consistent changes from the starting composition (1171%, 1194%, and 1243% for CO_2/Ca^{2+} = 0.1, calcite dissolution, and CO_2/Ca^{2+} = 10, respectively). Although Ca^{2+} also shows relatively high sensitivity, its variability is large (ranging from 774% to 25,843%) and unpredictable and depends heavily on the flux of Ca^{2+}into the system via mixing. Predicting this outcome necessitates knowledge of mixing relationships which require in-depth characterization of hydrodynamics, therefore disqualifying Ca^{2+} as a useful global monitoring parameter.HCO_3^- exhibits the next greatest sensitivity (ranging from 156% to 420% change from initial composition) but with a highly variable magnitude. This is due to the pH-dependence of the distribution of carbonate species (H_2CO_3, HCO_3^-, CO_3^{2-}) in natural waters, which complicates interpretation of HCO_3^- concentrations with regard to mass of CO_2 that has entered the aquifer. A relatively consistent magnitude and range of variation is shown by the response of pH to CO_2 input (28%, 23%, and 22% for CO_2/Ca^{2+} = 0.1, calcite dissolution, and CO_2/Ca^{2+} = 10, respectively), but sensitivity is relatively small and may be difficult to recognize apart from natural variability.

Errors for calcium concentrations are large (from 971% to 33,813%) and again disqualify this parameter as useful for monitoring. Of the remaining parameters (DIC, HCO_3^-, and pH), errors are bidirectional with some dedolomitization environments yielding parameter concentrations lower and some higher than expected from calcite dissolution. HCO_3^- shows the largest ranges in error (39.03% for 6 mmoles CO_2 input and 58.17% for 50 mmoles CO_2 input). DIC (11.11% and 5.37% for 6 and 50 mmoles CO_2 input, respectively) and pH (6.08% and 8.47% for 6 and 50 mmoles CO_2 input, respectively) exhibit smaller ranges in error. The results indicate that changes due to CO_2 input in an uncharacterized system would be difficult to predict and even more difficult to quantify reliably, illustrating the necessity of understanding the system before correct leakage assessment can occur.

Conclusions

The field-based study of shallow (<500 ft) groundwater overlying and within an ~1,000 mi^2 area of SACROC shows:

1. No impacts to drinking water quality as a result of over 35 years of deep subsurface (6,000-7,000 ft) CO_2 injection.

2. Modeling of stable carbon isotopes ($\delta^{13}C$) of injectate CO_2 gas, DIC in shallow and deep groundwater, carbonate mineral matrix, and soil zone CO_2 suggests that no significant injectate CO_2 has been introduced to the shallow groundwater.

3. Interpretation of groundwater flow regime, and concentrations of major ions and trace metals, indicate mixing of water types and water-rock interaction (i.e. dedolomitization) as major controls on groundwater geochemistry at SACROC.

4. The popular assumption that carbonate parameters alone can be used as indicators of groundwater quality over a GS site is too simple, especially in complex hydrogeologic settings.

5. The importance of defining the regional groundwater system to understand how it might react to introduction of CO_2 and to identify the parameters best suited for monitoring over GS sites.

6. Aquifer sampling and analysis of site-specific conditions may be needed to understand how an aquifer system will react to CO_2 and the parameters best suited for monitoring at sequestration sites.

Geologic Model Development and Numerical Simulation

Heterogeneity greatly impacts the estimation of CO_2 capacity and simulation of CO_2 migration and fate. A 3D heterogeneous model of the SACROC site was developed that accounts for relevant CO_2 trapping mechanisms. A geologic framework model (Figure 152) was built to quantify naturally-occurring porosity and permeability distribution in the northern platform at SACROC. This model is based on analysis of the results of 3D seismic surveys and a database of approximately four hundreds wells. This geologic model presents the Pennsylvanian group, Cisco and Canyon formations, where most of CO_2 was injected. The primary goal was to confirm the estimated 55 million tons of CO_2 storage, and to quantify the different forms of sequestration, or trapping mechanisms of CO_2 injected.

The different mechanisms of sequestration considered include hydrodynamic trapping, residual trapping, aqueous (solubility) trapping, and mineral (precipitation) trapping. Research generally considers hydrostratigraphic (mobile) and solubility trapping mechanisms using either multiphase transport codes (e.g, TOUGH2) or compositional oil simulators (e.g., ECLIPSE, STARS, and others) after coupling appropriate CO_2 equations of state algorithms. Recently, a commercial CMG's GEM multi-dimensional, finite-difference, isothermal compositional simulator, multiphase (oil, water, gas) and multicomponent fluids was expanded into a fully coupled geochemical compositional equation-of-state simulator, CMG's GEM-GHG for aquifer sequestration (Nghiem et al., 2004).

Estimation of Porosity and Permeability

To determine the relationship between rock fabric and petrophysical parameters the method of Lucia (1995, 1999) was used to estimate porosity from seismic data calibrated by porosity logs, then divided pore space into two categories, interparticle porosity and vuggy porosity. Interparticle porosity includes intergrain and intercrystal pore space. The global transforming equation, which calculates permeability from the rock fabric number and porosity, was developed (Lucia,

1999; Jennings and Lucia, 2001; Lucia and Kerans, 2004)). Permeability is estimated from the global transformation using porosity from well logs and the stratigraphically defined rock fabric number (Table 37). In addition, the vertical permeability was calculated from the anisotropy ratio (0.4), which is based on directional measurements taken in SACROC cores (Dicharry et al., 1973).

Table 37. Permeability Estimation Parameters Using Porosity and Rock-Fabric Number (Lucia and Kerans, 2004)

Formation	Sequence	Rock fabric number (λ)	Transforming equations	
Cisco	Late		$k = 2.1625\times10^{6}\times\phi^{3.8844}$	Highest portion of Cisco (Implication of karsting)
	Late	1.7	$k = 1.031\times10^{7}\times\phi^{6.7592}$	Late Cisco (wide variety of rock-fabrics)
	Early	1.9	$k = 2.69\times10^{6}\times\phi^{6.3584}$	Early Cisco (Characterized by fusulinid/crinoidal/peloid grain dominated packstones, grainstones, and wackestones
Canyon	1	2.5	$k = 97628\times\phi^{5.3696}$	Early Canyon: (Characterized by moldic ooid grainstone, grain-dominated packstone, and mud-dominated fabrics)
	2	1.75	$k = 38520\times\phi^{5.0923}$	Late Canyon: (Characterized by crinoidal/fusulinid/peloid, grain-dominated packstones, and mud-dominated fabrics having vuggy porosity)
	3			Below reservoir

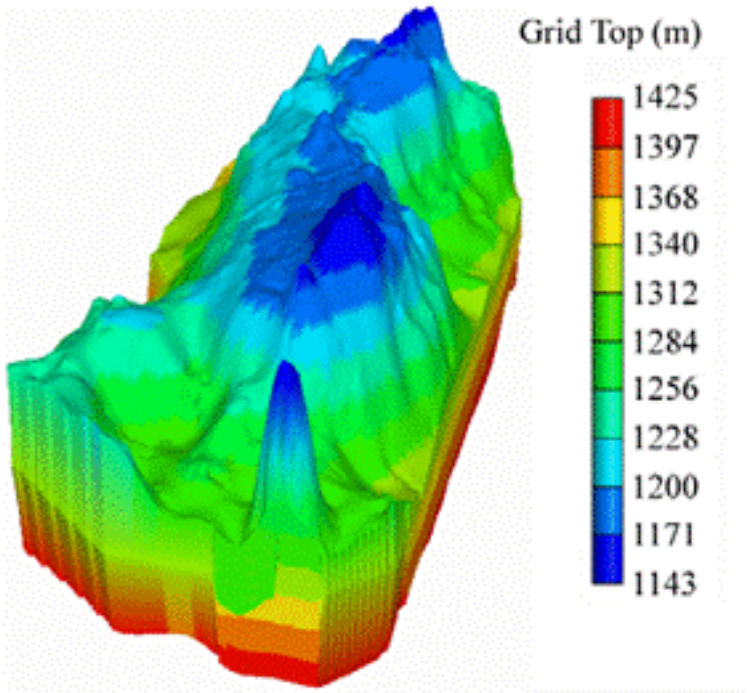

Figure 152. Geologic framework representing the SACROC northern platform (from Han and McPherson, 2007).

Development of Simulation Model

The geocellular model developed by Fred Wang (Bureau of Economic Geology (BEG) of the University of Texas at Austin), describes the Cisco and Canyon groups includes 9,450,623 elements. It was derived from analyzing 3D seismic data and 368 wire-line log data. The SWP modeling group developed a high-resolution numerical model grid from the geocellular model. The new model grid was calibrated by seismic survey data obtained from KM. Figure 103 is a smoothed version of this grid. The approximate size of the model represented is 4000 m wide, 10,000 m long, and 250 m thick. The top of the geologic frame model describes the top configuration of the Cisco formation, which is below sea level ~1150 m, and the bottom of model describes the bottom configuration of Canyon formation, which is below level ~1425 m.

The development of a multi-phase and multispecies reactive transport model is constrained due to the large number of elements. For this reason, it is difficult to directly adapt the geologic frame model without upscaling. Upscaling algorithms were developed through the equivalent resistor network model (King, 1989) that upscales the symmetric grid blocks using self-repetitive geometry until the final block size is reached. Despite its many advantages, this technique has several drawbacks therefore, errors will accumulate during the renormalization process. For the

development of the CO_2 sequestration simulation model, a 15,470 grid model was obtained after three rounds of renormalization.

Model Parameterization

Initial and boundary conditions

From 1954 to 1971 a waterflood was performed to return the pressure above the bubblepoint pressure (12.45 MPa) to improve oil recovery. After CO_2 injection began in 1972, reservoir pressure rose above 16.55 MPa (Dicharry et al., 1973; Langston et al., 1988) and was used as the initial pressure condition in the model. Reservoir pressure in the model is hydrostatically estimated from the formation top (15.73 MPa) to the bottom (17.90 MPa).

Langston et al., (1988) indicates that reservoir temperature is 54.5°C. In the model, reservoir temperature is linearly estimated from formation top (54.35°C) to bottom (59.83°C). The upper boundary, eastern, western and northern boundaries are treated as no-flow boundaries. The carbonate reef complex, the Cisco and Canyon formations, is prism-shaped (Vest, 1970). Therefore, the Wolfcamp shale acts both as the top seal and the side seal. Finally, hydrostatic pressure conditions are assumed at southern boundary because this boundary is connected to the middle part of the reservoir.

The density and viscosity of an aqueous mixture (CO_2–H_2O) with the effect of brine concentration are, respectively, estimated from Rowe and Chou (1970) and Kestin et al. (1981). Brine properties are based or keyed on Cl- concentration. For example, due to the presence of reactions (e.g., $NaCl(aq)=Na^{+}+Cl^{-}$), the concentration of Cl^{-} varies with each time step and is used to adjust brine density, viscosity, and Henry's constant.

When oil was added to the system, the only initial condition change from the previous model is fluid saturation were the initial saturations was then assumed to be brine 0.28 and oil 0.72 (Vest, 1970). The oil phase is regarded as a mixture of 11 different components. The initial oil composition from Dicharry et al., (1973) was used.

Relative permeability and capillary pressure

For CO_2 and brine the fitted relative permeability function were obtained from Bennion and Bachu (2005) that were created after extrapolating data measured in carbonate rock, a low per-

meability carbonate rock collected from Wabamun Lake at 41°C and 22.4 Mpa. To quantify the residual trapped CO_2 depending on residual CO_2 saturation, the hysteresis effect is included in the relative permeability curve using a modified Land equation (Land, 1968). Capillary pressure datasets between gas and brine were available from previous measurements from SACROC cores (Rohan and Haggerty, 1996). Capillary pressure function is extrapolated using Parker's function (Parker et al., 1987).

When oil is added to the system, the fitted relative permeability curves between supercritical CO_2 and liquid are extrapolated relative permeability data measurements of carbonate rocks (Bennion and Bachu, 2005). Hysteretic effects are included in the relative permeability curve using a modified Land equation (Land, 1968). A relative permeability curve for oil measured from SACROC cores (Core128V) at 50°C and 1.4 MPa (Rohan and Haggerty, 1996) was used to calibrate the model oil relative permeability curve. The relative permeability of brine was estimated.

Capillary pressure functions between supercritical CO_2 and liquid were adapted from Parker et al. (1987) and calibrated from data of Bennion and Bachu (2006). Capillary pressure between oil and brine were measured from SACROC cores (Core128V, 136V, and 191V) at 50°C and 1.4 MPa by Rohan and Haggerty (1996). The capillary pressure functions were calibrated by Parker et al. (1987) using the Rohan and Haggerty (1996). However, adapting capillary pressure between oil and brine caused serious convergence problems. Additionally, both Aziz and Settari (1979) and Spiteri and Juanes (2006) pointed out that the effects of capillary pressures are often negligible in field-scale simulation, where the characteristic capillary length is much smaller than the grid resolution. Therefore, the effect of capillary pressure between oil and brine were neglected in this work.

Chemistry data input

The chemical components of the simulation model were constructed using reservoir fluid and core data collected from the SACROC field. The mineralogy is based on XRD analyses by Carey et al. (2006). In their analyses, dolomite and anhydrite was not detected. Previous literature indicates that a reservoir highly altered by calcitization and dolomitization is composed of minor amounts of anhydrite, dolomite, sand, and shale (Bergenback and Terriere, 1953; Mayer et al.,

1956 ; Raines, et al., 2001). Therefore, the mineralogy included dolomite and anhydrite (Table 38). Both siderite and dawsonite were included as secondary minerals. Dawsonite is regarded as a late stage mineral deposited in natural CO_2 reservoirs (Baker et al., 1995; Moore et al., 2005). Furthermore, Carey et al. (2006) detected an X-ray diffraction peak in SACROC core that indicates the possibility of dawsonite precipitation in the SACROC field.

Table 38. Volume Fractions, Surface Areas, and Kinetic Rates

Mineral	Weight percent (Carey, 2006)	Modified weight percent	Volume fraction	Surface area (m^2/g)	Activation energy (J/mol)	$Logk_{25}$ (mol/m^2s)	model kinetic rate	Latest kinetic rate
Calcite	0.82	0.62	0.6063	2.21E-4	41870	-8.80	Svensson and Dreybrodt, (1992)	Lee and Morse, (1999)
Dolomite	0	0.1	0.0933	2.11E-4	41870	-9.22	White, (2005)	Pokrovsky and Schott, (2001)
Kaolinite	0.01	0.01	0.0110	2.49E-3	62760	-13.00	Nagy, 1995	Nagy, (1995)
Anhydrite	0	0.1	0.0892	2.02E-4	41870	-8.80	Same as calcite	Dove and Czank, (1995)
Quartz	0.03	0.03	0.0303	2.29E-4	87500	-13.90	Tester et al., 1994	Tester et al., (1994)
Illite	0.02	0.02	0.0193	2.18E-3	58620	-14.00	Knauss and Wolery, 1989	Knauss and Wolery, (1989)
Ankerite	0.12	0.12	0.1043	1.97E-4	41870	-10.22	Estimated from Dolomite	Estimated from Dolomite
Dawsonite	0	0	0	2.48E-4	62760	-9.09	Hellevang, 2005	Hellevang, (2005)
Sierite	0	0	0	1.52E-4	41870	-10.22	Estimated from Dolomite	Estimated from Dolomite

Since no direct measurements of surface areas are available, the surface area was calculated using grain volume, grain surface area, molar volume, and molecular weight, as detailed in Table 38. The kinetic rate law for the dissolution and precipitation of minerals is from Lasaga (1984) with a temperature-dependent rate constant derived by Arrhenius' law. Uncertainty associated with the selected coefficients is not clear and thus a limitation of this study.

Thermodynamic parameters including equilibrium constants were chosen from the SOLMINEQ.88 and PHREEQC databases (Kharaka et al., 1989; Parkhurst and Appelo, 1999). For the activity coefficient calculation, a B-dot model accounting for the activity coefficient over a wide range of temperatures is implemented (Helgeson, 1969). The initial brine concentration can be obtained after performing equilibrium reactions with an appropriate mineral composition. However with 840 water chemistry data available from this field the quantity of water chemistry

data provides a statistically meaningful representation of brine concentration, the initial concentration was calculated from the average of the brine water chemistry data.

The simulation model with both brine and oil, disregarded some reactions because of the high computation expense of including the oil phase with eleven components. The summary of both aqueous species and minerals in both simulations are listed in Table 39.

Table 39. Chemical Components in the Simulation Model Describing the Reservoir Saturated with Brine Only and Both Brine and Oil

	Simulation describing reservoir saturated with brine	Simulation describing reservoir saturated with both brine and oil
Primary species	CO_2(g),H^+,K^+,Na^+,Ca^{2+},Mg^{2+}, SiO_2(aq), Al^{3+}, Fe^{2+}, Cl^-,SO_4^{2-}	CO_2(g), N_2,C1,C2,C3,I-C4,N-C4, I-C5,N-C5,FC6,C7+,H^+, Na^+, Cl^-
Secondary species	OH-,HCO_3^-, CO_3^{2-},NaCl(aq), $NaCO_3^-$, $NaHCO_3$(aq),$CaCO_3$(aq),$CaHCO_3^+$, $MgCO_3$(aq),$MgHCO_3^+$,$Al(OH)_4^-$, $Al(OH)_3$(aq),$Al(OH)_2^+$,$Al(OH)^{2+}$, $FeCl_4^{2-}$, $FeCl^+$,$Fe(OH)_2$,$Fe(OH)^+$,H_4SiO_4(aq)	OH^-,HCO_3^-, CO_3^{2-},NaCl(aq)
Mineral	Calcite, dolomite, kaolinite, anhydrite, quartz, illite, ankerite, dawsonite, siderite	Calcite, dolomite, kaolinite, anhydrite, quartz, illite, ankerite, dawsonite, siderite

Assignment of CO_2 injection and production wells

More than 300 wells had been used for CO_2 injection and production over 35 years (1972–2007) in the northern platform. Because the dimension ($17 \times 35 \times 26 = 15{,}470$) of the upscaled grid used for this simulation is not large enough to assign the total number of wells, wells were lumped together and uniformly assigned a regular pattern. The total number of producing and injection wells are, respectively, 23 and 22. Injection and production were simulated for a 30 year period, from 1972–2002, and rates were controlled to match an amount of CO_2 net storage with field values (6,944,587,674 kg). The calculation of CO_2 net storage has been detailed elsewhere (Han, 2007). The net storage of CO_2 in the model is 7,059,027,000 kg. Finally, to facilitate calculation of longer-term processes, the total simulation period was 200 years, from 1972 to 2172.

Simulation Results for Reservoir Model with Brine

CO_2 storage in the SACROC Northern Platform under different mechanisms

Figure 153 summarizes the CO_2 mass stored in different forms, with CO_2 storage mechanisms detailed in four stages.

A. Stage I (1972–2002): CO_2 is injected into the reservoir by 22 injection wells and free trapping is dominant. The saturation of CO_2 gradually increases near the injection wells and CO_2 migrates either vertically due to buoyancy-driven forces or horizontally through preferential flow paths. Solubility trapped CO_2 increases in this period because injection-induced high partial pressure makes CO_2 solubility increase. Minerals dissolve mainly near the injection wells during this period.

B. Stage II (2002–2017): This period is immediately after injection is completed. Here residual trapping becomes important. The simulation definition of residual CO_2 is occurs only when no free CO_2 is in a pore space; thus it is under-reported. After stopping injection, the reduction of CO_2 saturation due to the imbibition process occurs at the tail of the CO_2 plume, where brine displaces CO_2. As a result, while CO_2 migrates either vertically or horizontally, some of the free CO_2 becomes trapped in pores. At this point, CO_2 changes its phase from free (mobile) CO_2 to residual (immobile) trapped CO_2. Solubility-trapped CO_2 gradually increases at this stage because injection-induced CO_2 partial pressure decreases after CO_2 injection ceases. Minerals continue to precipitate in this stage, including precipitation at farther distances from the injection well.

C. Stage III (2017–onward): The indefinite time of sequestration. During this time solubility trapping continues to increase because both residual and free CO_2 dissolve in the reservoir brine. Both free and residual trapped CO_2 tend to decrease. Therefore, after several hundred years (not shown in Figure 153), the amount of solubility trapped CO_2 will be greater than both free and residual trapped CO_2. From 2017–2072, the amount of free (mobile) CO_2 slightly increases, corresponding to the reduction of residual trapped CO_2. This occurs because the free (mobile) CO_2 plume at certain injection wells migrates horizontally to neighboring injection wells where residual CO_2 is trapped (again, this is caused by the definition of residual CO_2). When the CO_2 plume arrives at the location

where residual CO_2 is trapped, the saturation of residual trapped CO_2 increases and it becomes free CO_2.

D. Stage IV (~after several thousand years; not shown in Figure 104): Mineral trapping will be greater than any other mechanisms.

Spatial distribution of free (mobile) and residual trapped CO_2

Figure 154 shows the spatial distribution of separate-phase CO_2. Two-dimensional cross-sectional views/slices are presented that indicate that the spreading pattern of separate phase CO_2 is different around each injection well due to heterogeneity.

Separate-phase CO_2 reached the top of the Cisco and Canyon formations (below the Wolfcamp shale) within 30 years (2002) in injection wells I13 and I22 (Figure 154). The simulated spatial distribution of separate-phase CO_2 in this model suggests that both the presence of preferential permeability paths and the geometry of the target formation are important factors that determine how fast separate-phase CO_2 reaches a seal. Additional factors include the injection pressure (and therefore the hydraulic head gradient) and the fluid composition, especially the presence of oil. The presence of oil and its effects on CO_2 migration were evaluated.

By comparing the spatial distribution between CO_2 saturation (Figure 154 (a)) and associated values of relative permeability (Figure 154 (b)), it is easy to distinguish the location of free (mobile CO_2) and residual (immobile) CO_2. When the relative permeability of the separate-phase CO_2 is greater than zero, it becomes mobile. However, when the relative permeability of separate-phase CO_2 is equal to zero, the separate-phase CO_2 becomes immobile and is trapped as residual CO_2. In Figure 154 (a), CO_2 saturation is greater than zero within the CO_2 plumes. However, Figure 154 (b) shows that although certain grid blocks have CO_2 saturation greater than zero, they have zero relative permeability. These grid blocks are where CO_2 is trapped only as a residual form. Finally, the distribution of dissolved CO_2 imitates the distribution patterns of separate phase CO_2, but with wider extent (Figure 154 (c)).

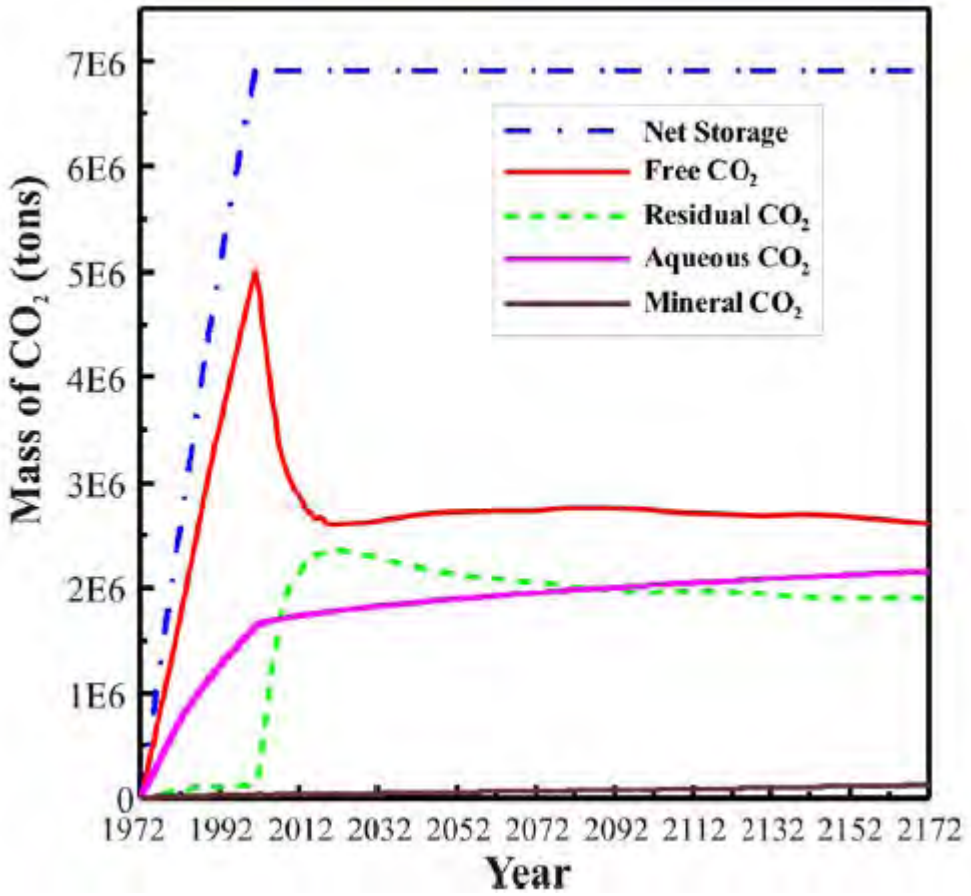

Figure 153. CO_2 storage mechanisms within the reservoir as a function of time.

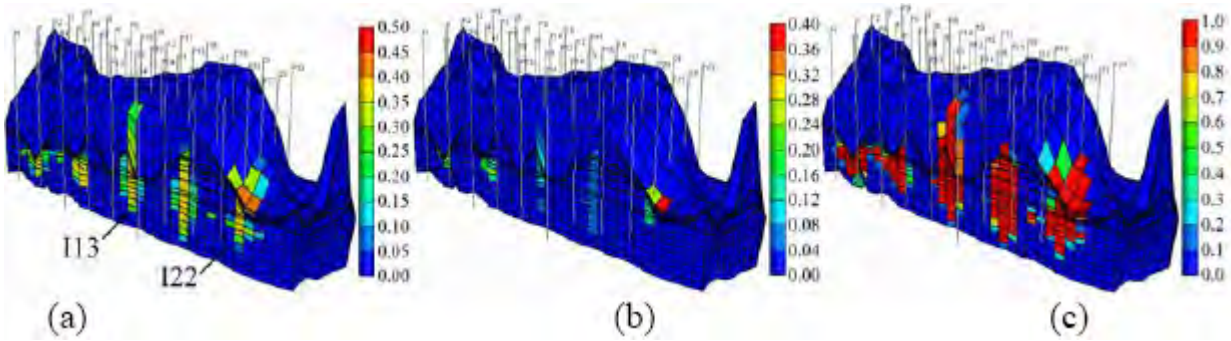

Figure **154.** Two-dimensional cross-section view at year 2002 (30 years after injection starts) (a) **Saturation of separate phase CO_2, (b) Relative permeability of separate phase CO_2, (c) Mole fraction of dissolved CO_2.**

Spatial distribution of aqueous species and minerals

Figure 155 shows representative results describing spatial distributions of aqueous species, such as pH, Ca^{2+}, Mg^{2+}, and, Fe^{2+} at simulation year 2002.

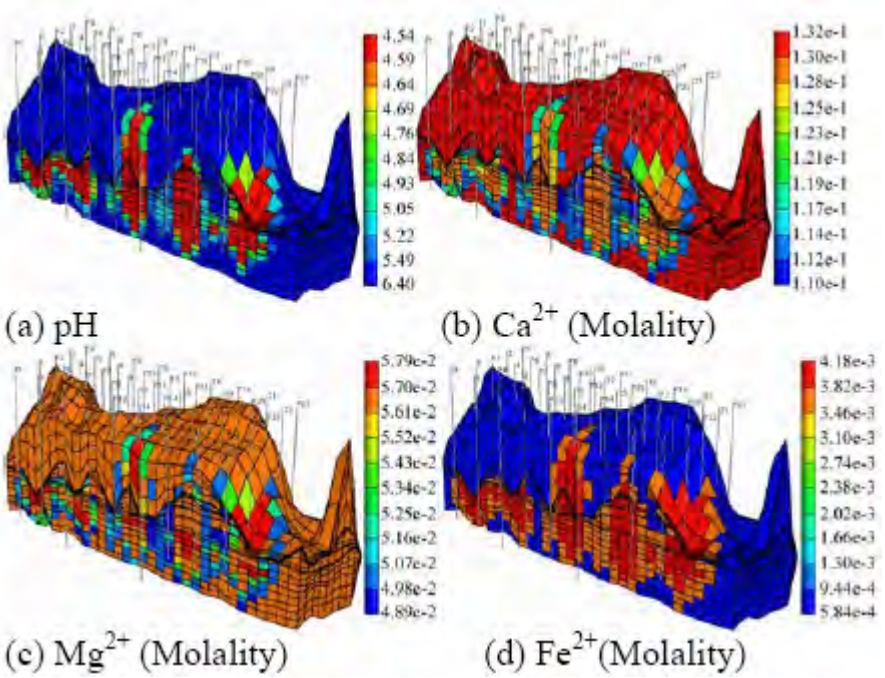

Figure 155. Two-dimensional cross-section view of aqueous species concentrations at year 2002 (30 years after CO_2 injection starts).

Chemical reactions are initiated as the dissolution of CO_2 lowers the pH of brine (Figure 155(a)). pH is controlled by the buffering of carbonate minerals and does not decrease below 4.5. Figure 155(b) shows the spatial distribution of Ca^{2+} ion. Ca^{2+} ion is depleted at the boundary of the CO_2 plumes where the precipitation of calcite, dolomite, and anhydrite are major mechanisms. The depletion of Ca^{2+} ion indicates that the amount of Ca^{2+} ion provided by the dissolution of ankerite is not enough to precipitate calcite, dolomite, and anhydrite at the CO_2 plume boundary. Therefore, Ca^{2+} ions in brine become depleted at the boundary of the CO_2 plume. Figure 155(c) shows the spatial distribution of Mg^{2+} ion, which is closed to the distribution of Ca^{2+} ion. Mg^{2+} ion is also supplied from both the dissolution of ankerite and brine and is mainly consumed by the precipitation of dolomite.

Unlike both Ca^{2+} and Mg^{2+} ions, the concentration of Fe^{2+} ion increases within the CO_2 plume, as shown in Figure 155(d). Fe^{2+} ion is supplied both from the dissolution of ankerite and from the initial brine and is consumed by the precipitation of siderite. Thus, ankerite dissolution exceeds the consumption by siderite.

Mineral precipitation and dissolution are closely related to the spatial distribution of aqueous species. Generally, over 200 years, calcite and siderite were the major minerals precipitated. Both dolomite and dawsonite also precipitated, but minimally. Ankerite was the major mineral dissolved. The changes of mole in clay minerals (kaolinite and illite) and quartz was small.

Ankerite dissolution provides more Ca^{2+}, Mg^{2+}, and Fe^{2+} ions in the brine. As a result, Ca^{2+}, Mg^{2+}, and Fe^{2+} ions become supersaturated in the brine and are triggered to precipitate calcite, dolomite, siderite and anhydrite. Small amounts of kalolinite and illite, respectively, precipitate and dissolve. Although kinetic rates of aluminosilicate minerals are slow (Table 37), the chemical reactions of such aluminosilicate minerals can change the concentration of Al^{3+} ion in brine and cause dawsonite to precipitate (Xu et al. 2004; Hellevang et al. 2005). Through the simulation period, Al^{3+} ion increases from 10^{-11} to 10^{-7} due to the reactions with aluminosilicate minerals. Consequently, the change in Al^{3+} ion concentration indicates in the simulator that there will be precipitation of a small amount (2.5E-3 kg/m^3) of dawsonite by the end of 200 years.

Model results also reveal how much CO_2 is stored as diverse mineral forms. Over 30 years, about 1 kg/m^3 of calcite and 1.2 kg/m^3 of siderite precipitated while about 2.4 kg/m^3 of ankerite dissolved. The model results indicate that about 800 to 2200 tons of ankerite dissolve within each grid block after 30 years of CO_2 injection. The dissolution of ankerite is accompanied by the precipitation of both calcite and siderite. About 400 to 900 tons of calcite and about 400 to 1200 tons of siderite precipitate within each grid block after 30 years of CO_2 injection.

Simulation Results for Reservoir Model including Both Oil and Brine

To save computational expense, the actual oil production history was not included in the simulation, but rather only the presence of oil (after Vest, 1970) and its effects on CO_2 migration and trapping mechanisms.

Figure 156(a) shows the CO_2 mass stored by mechanism in the reservoir initially saturated with brine while Figure 156(b) is with initial saturation of both brine and oil. In the previous brine-only model, there were four distinct CO_2 storage stages. CO_2 storage mechanisms perform clearly different during the brine+oil model (Figure 156(b)). The storage by the different mechanisms does not vary as much with time in the brine+oil model (Figure 156(b)). During the full 200-year simulation period, the dominant CO_2 storage mechanism is oil trapping, with about 4 million

tons of CO_2 dissolved in the oil. In addition, about 2 million tons of CO_2 are stored as a free (mobile) form.

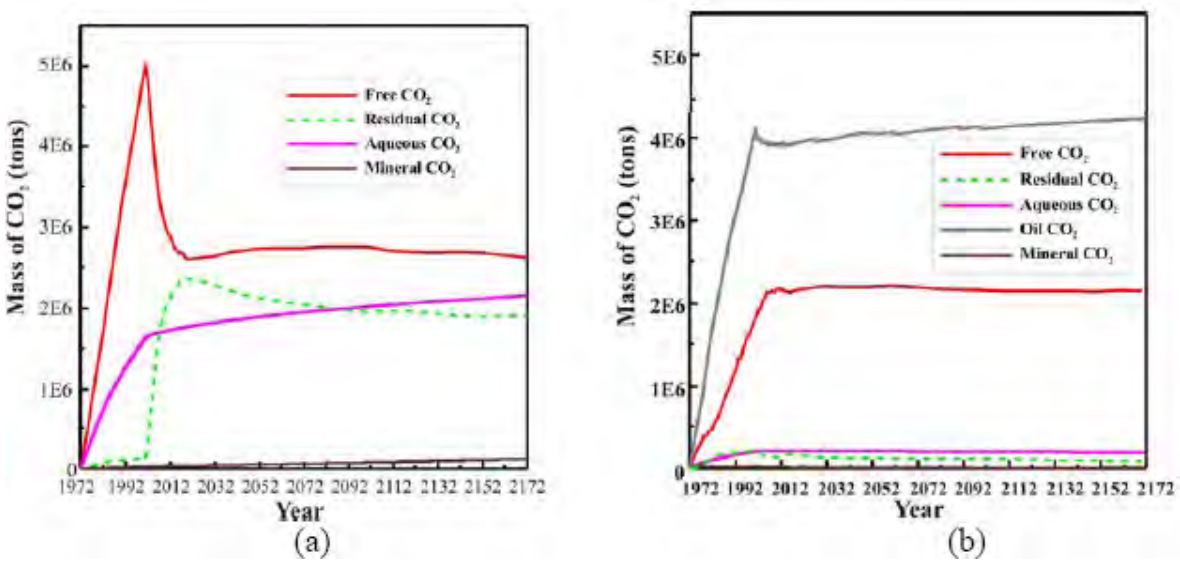

Figure 156. CO_2 storage mechanisms within the reservoir as a function of time: (a) fully brine-saturated reservoir, (b) partially brine- and oil- saturated reservoir.

The simulation results show that CO_2 migration behavior is distinctively different in the two simulated systems. Within 30 years, separate-phase CO_2 in the brine-only model tended to migrate vertically and certain CO_2 plumes were able to reach the top of the Cisco and Canyon formations. The amount of residual trapped CO_2 increased at the tail of the CO_2 plumes while separate-phase CO_2 plumes migrated vertically. However, in the brine+oil model, separate-phase CO_2 did not tend to migrate vertically but stayed near the injection wells with high CO_2 saturation. Physically, separate-phase CO_2 is stored as a free (mobile) form due to its high CO_2 saturation, but it acts like residual (immobile) CO_2.

To evaluate the difference of CO_2 vertical migration behavior between the two models, the density of gas, brine, and oil phases are compared (Figure 157). The density of CO_2 is about 800 kg/m3 at these reservoir conditions (Figure 157(a)). The brine density ranged from 1037 to 1160 kg/m3 (Figure 157(b)). An especially higher density of brine is calculated near CO_2 injection wells because of CO_2 dissolution and the increase of salinity induced by subsequent rock-water interaction. The density difference between CO_2 and brine was approximately 400 kg/m3, which

suggests a significant buoyancy force. Compared to brine density, oil density ranged from 800 to 900 kg/m^3 (Figure 157(c)), similar to the density of both separate-phase CO_2.

In the brine+oil reservoir model, the buoyancy-driven force was lower due to the lower contrast in densities. Consequently, stored CO_2 did not migrate vertically but tended to stay closer to the injection wells. In sum, CO_2 is stored as a free (mobile) form but because of the similarity in density and dissolution in oil, the separate-phase CO_2 behaves like residual trapped CO_2.

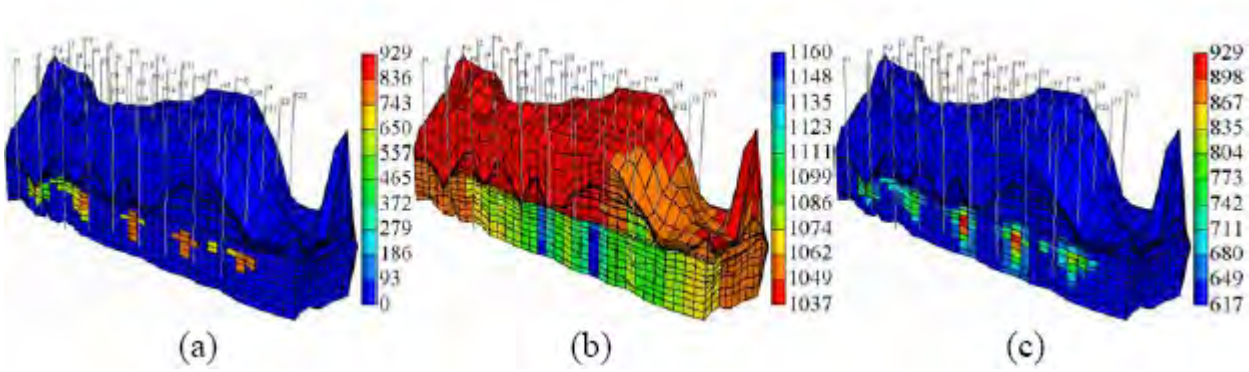

Figure 157. 2D cross-section view at year 2002 (30 years after CO_2 injection starts): (a) gas density, (kg/m^3), (b) brine density (kg/m^3), and (c) oil density (kg/m^3).

Finally, both aqueous and mineral trapping mechanisms in the oil+brine reservoir model are much less active than those in the brine-only model, because most of the CO_2 dissolved in the oil phase due to higher solubility of CO_2 in oil, and because only 28% of reservoir was occupied by brine. Therefore, the subsequent water-rock interactions also decreased.

Simulation Results of the Injected Supercritical-Phase CO_2 Plume

Migration results of the injected supercritical-phase CO_2 plume were plotted at 10, 30, 100 and 500 years (Figure 158). The simulation results at 10 years (1982 in Figure 158(a)) and 30 years (2002 in Fig 158(b)) illustrate the stage when injected CO_2 begins expanding from the injection wells. After stopping CO_2 injection in 2002, buoyancy-driven CO_2 migration becomes dominant (Figures 158(c) and (d)). Simulation results after 500 years (2472) suggest that saturation of supercritical-phase CO_2 become smaller than 0.25 (Figure 158(d)).

Buoyancy-driven CO_2 migration varied spatially in this model. The vertical migration of supercritical-phase CO_2 is greater in the western flank of the SACROC Unit than in the eastern flank

(Figures 158(b) and (c)). To investigate the cause of this spatial variability in buoyancy-driven migration, cross-sections (permeability, porosity, saturation of supercritical-phase CO_2, mass fraction of aqueous-phase CO_2, and the total CO_2 mass) of the eastern and western flanks at 30 years (Year 2002) are plotted (Figures 159 and 160). The cross-section of the western flank shows high porosity zones near the top and bottom of the model, and a low porosity zone (about 0.01) in the middle (Figure 159(a)). The eastern flank shows higher porosity zones in the middle (Figure 160(a)). Figures 159(b) and 160(b) show the corresponding permeability fields of both western and eastern flanks, and higher permeability zones are well connected at the lower part of the model in both western and eastern flanks. CO_2 injection wells in the western flank are generally located at the low porosity and permeability portion of the reservoir (Figures 159(a) and 160(b)) while those in the eastern flank are located in the high porosity and permeability portions of the reservoir (Figures 160(a) and (b)). CO_2 injected into the low porosity and permeability area in the western flanks shows the distinctive buoyancy-driven CO_2 migration (Figures 159(a) and (b)). However, CO_2 injected into the high porosity and permeability portion in the eastern flank is capped below the Wolfcamp Shale (Figures 160(a) and (b)). A comparison of supercritical-phase CO_2 saturation between the western and eastern flanks illustrates that buoyancy-driven CO_2 migration is distinctively dominant in the western flank (Figures 159(b) and (c)). It can be surmised that sequestered CO_2 in the western flank will have greater potential to leak through the caprock because of the greater volume of CO_2 coming into contact with the top-seal.

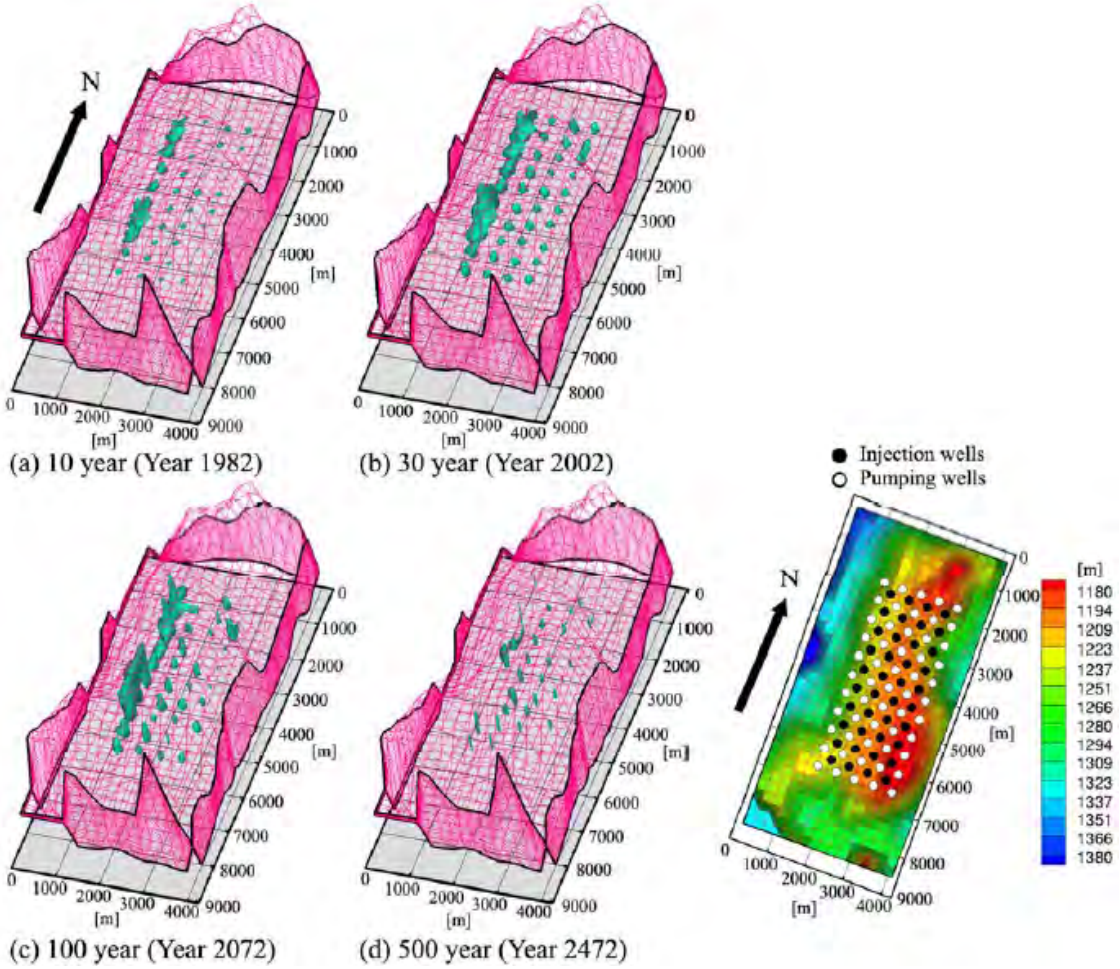

Figure 158. Patterns of supercritical-phase CO_2 plotted with iso-surface contours of 0.25 saturation: (a) 10 years, (b) 30 years, (c), 100 years, (d) 500 years, and (e) the location of the assigned CO_2 injection and production wells are plotted in top layer view. Contours indicate the depth of formation tops.

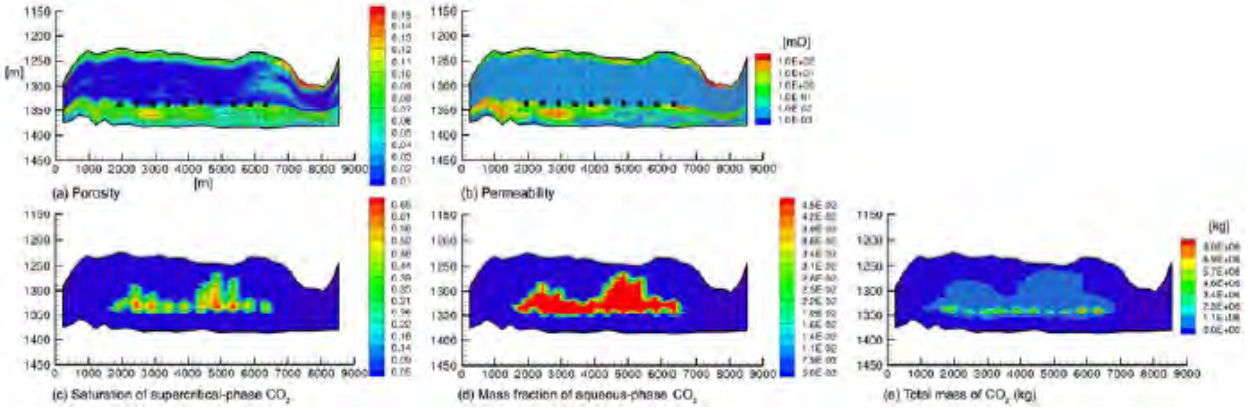

Figure 159. 2-D cross-section in western flank after 30 years: (a) porosity, (b) permeability, (c) CO_2 saturation, (d) mass fraction of aqueous-phase CO_2, and (e) total mass of CO_2.

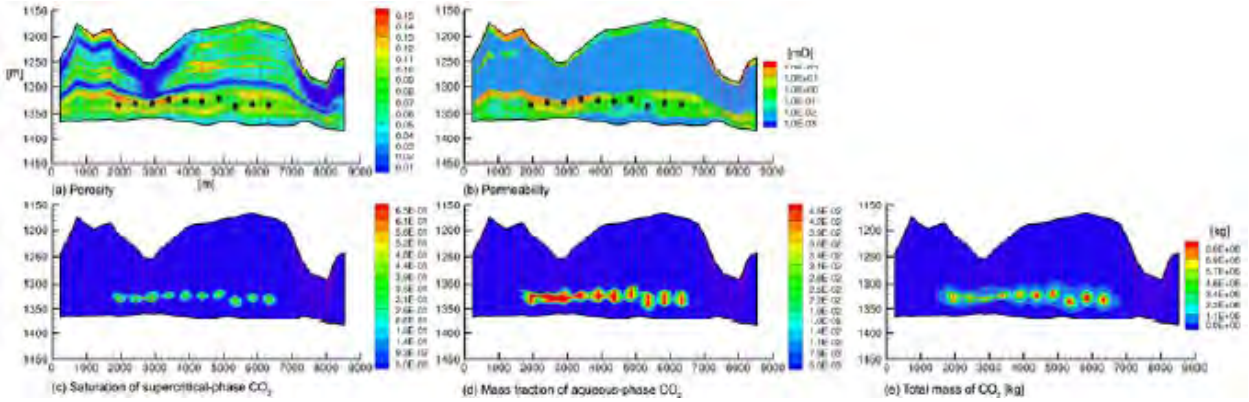

Figure 160. 2-D cross-sections of the eastern flank after 30 years: (a) porosity, (b) permeability, (c) CO_2 saturation, (d) mass fraction of aqueous-phase CO_2, and (e) total mass of CO_2.

Conclusions

Two models evaluating CO_2 storage mechanisms in the SACROC northern platform were developed using GEM-GHG. In a model with brine only, the major CO_2 storage mechanisms were free CO_2, residual CO_2, and solubility trapping during 200 years. During the CO_2 injection period, free trapping was the dominant mechanism. After CO_2 injection stopped, the amount of free CO_2 dramatically decreased and the amount of residual CO_2 suddenly increased. Later, both free and residual CO_2 concurrently dissolved into brine. However, the reservoir model with oil and brine, oil-trapping and free (mobile) trapping became dominant mechanisms over 200 years. The different CO_2 storage mechanisms in the two models were caused by the contrast of thermophysical properties between oil and brine.

Based on the two simulation models, injecting CO_2 into the reservoir saturated with both brine and oil reduces the amount of free CO_2, which would otherwise likely migrate vertically to the topseal. Several advantages of CO_2 injection into reservoir saturated with brine and oil include:

- CO_2 solubility in oil is significantly greater than it is in brine. Therefore, most of the CO_2 will dissolve into oil.

- Although CO_2 exists in a free form, it does not migrate vertically as rapidly because oil density is similar to CO_2 density, causing less buoyancy-driven vertical migration. In simulation results, separate-phase CO_2 in the reservoir saturated with both brine and oil was stored as free CO_2 with higher saturation.

- Although free CO_2 may reach the top of the target formation, an oil reservoir is always covered by a caprock. Therefore, CO_2 cannot escape easily. Although an oil reservoir provides several advantages for minimizing the potential vertical migration of CO_2, its size and volume are limited for CO_2 storage. In comparison, the potential for CO_2 storage in brine formations is immense.

SACROC References

Anderson, K.F., 1954. Petroleum-Engineering Study of Scurry Reef Reservoir, Scurry County, Texas. Petroleum Engineering.

Appelo, C.A.J., Postma, D., 2007. Geochemistry, Groundwater and Pollution: Amsterdam, The Netherlands, AA Balkema.

Apps, J. A., Zhang, Y., Zheng, L., Xu, T., Birkholzer, J.T., 2009. Identification of thermodynamic controls defining the concentrations of hazardous elements in potable ground waters and the potential impact of increasing carbon dioxide partial pressure. Energy Procedia 1: 1917-1924.

Ashworth, J.B., Hopkins, J., 1995. Major and minor aquifers of Texas. Report 345. Austin, Texas: Texas Water Development Board.

Assayag, N., Matter, J., Ader, M., Goldberg, D., Agrinier, P., 2009. Water-rock interactions during a CO_2 injection field-test: Implications on host rock dissolution and alteration effects. Chemical Geology 265(1-2), 227-235.

Aziz, K., Settari, A., 1979. Petroleum reservoir simulation, Elsevier, New York.

Baker, J.C., Bai, G.P., Hamilton, P.J., Golding, S.D., Keene, j.B., 1995. Continental-scale magmatic carbon dioxide seepage recorded by dawsonite in the Bowen-Gunnedah- Sydney basin system, eastern Australia. Journal of Sedimentary Research 65, 522-530.

Bennion, B., Bachu, S., 2005. Relative permeability characteristics for supercritical CO_2 displacing water in a variety of potential sequestration zones in the western Canada sedimentary basin. Society of Petroleum Engineers Journal 95547.

Bennion, B., Bachu, S., 2006. The impact of interfacial tension and pore-size distribution/capillary pressure character on CO_2 relative permeability at reservoir conditions in CO_2-brine systems. Society of Petroleum Engineers Journal 99325.

Bergenback, R.E., Terriere, R.T., 1953. Petrography and petrology of Scurry reef, Scurry County, Texas: American Association of Petroleum Geologists Bulletin. 37(5), 1014- 1029.

Brnak, J., Petrich, B., Konopczynski, M.R., 2006. Application of smartwell technology to the SACROC CO_2 EOR project: A case study. SPE/DOE Symposium on Improved Oil Recovery, 22-26 April 2006, Tulsa, Oklahoma.

Burkett, G.D., 1979. Review of the carbon dioxide enhanced oil recovery project at the SACROC Unit-Kelly-Snyder field, Texas. Chevron Technical Report.

Burnside, R.J., 1959. Geology of part of Horseshoe Atoll in Borden and Howard Counties, Texas. Geological Survey Professional Paper 315-B, 34.

Carey, J.W., Wigand, M., Chipera, S., Woldegabriel, G., Pawar, R., Lichtner, P., Wehner, S., Raines, M., Guthrie, J., 2006. Analysis and performance of oil well cement with 30 years of CO_2 exposure from the SACROC unit, west Texas. International Journal of Greenhouse Gas Control 1, 75-85.

Dicharry, R.M., Pettyman, T.L., Ronquille, J.D., 1973. Evaluation and design of a CO_2 miscible flood project-SACROC Unit, Kelly-Snyder field. Society of Petroleum Engineers Journal 4083.

Gassmann, F., 1951. Elastic Waves Through a Packing of Spheres. Geophysics, 16, 673-685.

Gassmann, F., 1951. Über die elastizität poröser medien: Vierteljahrss-chrift der Naturforschenden Gesellschaft in Zurich, 96, 1-23. (English translation at http://sepwww.stanford.edu /sep/berryman/PS/gassmann.pdf).

Gerling, C.R., 1983. McElmo dome Leadville carbon dioxide field, Colorado. In Fassett, J.E., ed. Oil and gas fields of the four corners area," Four corners geological society, 3, 735-739.

Han, W.S., B.J. McPherson, 2007, Evaluation of CO_2 injection into brine formation below oil reservoir. EOS Trans. AGU, 88 (52), Fall Meet. Suppl., Abstract H12D-04, 2007.

Han, W. the evaluation of CO_2 storage mechanisms at northern platform SACROC in the Permian Basin, site of 35 years of CO_2 injection. M.S. Thesis, New Mexico Institute of Mining and Technology, Socorro, New Mexico (2007)

Helgeson, H.C., 1969. Thermodynamics of hydrothermal systems at elevated temperatures and pressures. American Journal of Science 267, 729-804.

Hellevang, H., Aagaard, P., Oelkers, E.H., Kvamme, B., 2005. Can dawsonite permanently trap CO2? Environmental Science and Technology 39, 8281-8287.

Holtz, M. H., Smyth, R.C., McPherson, B.J., Han, W.S., 2006. Subsurface characterization of CO2 sequestration sites, example from a carbonate reef setting. Proceedings of International Symposium on Site Characterization for CO_2 Geological Storages (CO_2SC), Lawrence Berkeley National Laboratory, Berkeley, California.

Holtz, M. H., and Major, R. P., 2004, Integrated geological and petrophysical characterization of Permian shallow-water dolostone: Society of Petroleum Engineers Reservoir Evaluation & Engineering, Paper No. SPE 87595, p. 47–58.

Holtz, H.M., 2002. Residual gas saturation to aquifer influx: A calculation method for 3-D computer reservoir model construction. Society of Petroleum Engineers Journal 75502.

Juanes, R. Spiteri, E.J., Orr, F.M., Blunt, M.J., 2006. Impact of relative permeability hysteresis on geological CO_2 storage. Water Resources Research 42, W12418, doi:10.1029/2005WR004806.

Kane, A.V., 1979. Performance review of large-scale CO_2-WAG enhanced recovery project, SACROC Unit-Kelly-Snyder field. Journal of Petroleum Technology 31, 217-231.

Kestin, J., Khalifa, H.E., Correia, R.J., 1981. Tables of the dynamic and kinematic viscosity of aqueous NaCl solutionsin the temperature range 20-150°C and pressure range 0.1-35 MPa, Journal of Physical and Chemical Reference Data. 10, 71-87.

Kharaka, Y.K., Gunter, W.D., Aggarwal, P.K., Perkins, E., Debraal, J.D., 1989. SOLMINEQ.88: A computer program for geochemical modeling of water-rock reactions. USGS Water- Resources Investigations Report 88-4227.

Kharaka, Y.K., Cole, D.R., Tordsen, J.J., Kakouros, E., Nance, H.S., 2006. Gas-water-rock interactions in sedimentary basins: CO_2 sequestration in the Frio formation, Texas, USA. Journal of Geochemical Exploration 89, 183-186.

Knauss, K.G., Wolery, T.J., 1989. Muscovite dissolution kinetics as a function of pH and time at 70ºC. Geochimica et Cosmochimica Acta 53, 1493-1501.

Land, C.S., 1968. Calculation of imbibition relative permeability for two- and three-phase flow from rock properties. Society of Petroleum Engineers Journal 1942.

Langston, M.V., Hoadley, S.F., Young, D.N., 1988. Definitive CO_2 flooding response in the SACROC unit. Society of Petroleum Engineers Journal 17321.

Lasaga, A.C., 1984. Chemical kinetics of water-rock interaction. Journal of Geophysical Research 89, 4009-4025.

Jennings, J. W., Jr., and Lucia, F. J., 2001, Predicting permeability from well logs in carbonates with a link to geology for interwell permeability mapping: Society of Petroleum Engineers, SPE Paper No. 71336, 16 p.

Lucia, F. J., 1995, Rock-fabric/petrophysical classification of carbonate pore space for reservoir characterization: AAPG Bulletin, v. 79, no. 9, p. 1275–1300. Lucia, 1999

Lucia, F. J., 1999, Carbonate reservoir characterization: New York, Springer-Verlag, 226 p.

Mavko, G. and Jizba, D., 1991. Estimating grain-scale fluid effects on velocity dispersion in rocks. Geophysics, 56(12), 1940-1949.

Moore, J., Adams, M., Allis, R., Lutz, S., Rauzi, S., 2005. Mineralogical and geochemical consequences of the long-term presence of CO2 in natural reservoirs: An example from the Springerville-St. Johns field, Arizona, and New Mexico, U.S.A.

Myers, D.A., Stafford, P.T., Burnside, R.J., 1956. Geology of the late Paleozoic Horseshoe Atoll in west Texas. Bureau of Economic Geology Publication 5607, p.113.

Nghiem, L., Sammon, P., Grabenstetter, J., Ohkuma, H., 2004. Modeling CO2 storage in aquifers with a fully-coupled geochemiscal EOS compositional simulator. Society of Petroleum Engineers Journal 89474.

Parker, J.C., Lenhard, R.J., Kuppusamy, T., 1987. A parametric model for constitutive properties governing multiphase flow in porous media. Water Resources Research 23(4), 618-624.

Parkhurst, D.L., Appelo, C.A.J., 1999. User's guide to PHREEQC (version 2) – A computer program for speciation batch-reaction, one-dimensional transport, and inverse geochemical calculations. USGS Water-Resources Investigations Report 99-4259.

Purcell, C., Harbert, W., Soong, Y., McLendon, T. R., Haljasmaa, I. V., McIntyre, D., and JiKich, J., 2009, Velocity measurements in reservoir rock samples from the SACROC unit using

various pore fluids and integration into a seismic survey taken before and after a CO_2 sequestration flood, Energy Procedia, 1, 2323-2331.

Purcell, C., Mur, A., Soong, Y., McLendon T.R., Haljasmaa, I.V. and Harbert, W., 2010. Integrating velocity measurements in a reservoir rock sample from the SACROC unit with an AVO proxy for subsurface supercritical CO2. The Leading Edge, 29, 192.

Raines, M. A., 2005. Kelly-Snyder (Cisco-Canyon) Fields/SACROC Unit. West Texas Geological Society: Oil and gas fields in west Texas v.8, Publication number 05-114, p.69-78. West Texas Geological Society, Midland, Texas.

Raines, M.A., Dobitz, J.K., Wehner, S.C., 2001. A review of the Pennsylvanian SACROC Unit. In J.J. Viveros and S.M. Ingram, eds., The Permian basin: Microns to satellites, looking for oil and gas at all scales: West Texas Geological Society Publication 01-110, p.67-74.

Rohan, J.A., Haggerty, D., 1996. Carbonate special core analysis study for Pennzoil exploration and production company: Elevated temperature centrifuge study. Technical report, Westport Technology Center International, IIT Research Institute.

Rowe, A.M., Chou, J.C.S., 1970. Pressure-volume-temperature-concentration relation of aqueous NaCl solutions. Journal of Chemical and Engineering Data 15, 61-66.

Shapiro, S. and Kaselow, A., 2004. Porosity and elastic anisotropy of rocks under tectonic stress and pore-pressure changes. Geophysics, 70(5), N27-N38.

Simpkins, W.W., Fogg, G.E., 1982. Preliminary modeling of groundwater flow near salt-dissolution zones, Texas Panhandle, in Gustavson, T. C., and others, Geology and geohydrology of the Palo Duro Basin, Texas: The University of Texas at Austin, Bureau of Economic Geology Geological Circular 82-7, p. 130–137.

Smyth, R. C., Hovorka, S. D., Lu, J., Romanak, K. D., Partin, J. W., Wong, Corinne, Yang, C., 2009. Assessing risk to fresh water resources from long term CO_2 injection—laboratory and field studies: Energy Procedia, v. 1, p. 1957-1964.

Spiteri, E.J., Juanes, R., 2006. Impact of relative permeability hysteresis on the numerical simulation of WAG injection, Journal of Petroleum Science and Engineering 50, 115- 139.

Spiteri, E.J., Juanes, R., Blunt, M.J., Orr, F.M. Jr., 2005. Relative permeability hysteresis: Trapping models and application geological sequestration. Society of Petroleum Engineers Journal 96448.

Stevens, P.R.,1974. Geohydrology of the Upper Brazos River Basin between Lubbock and Possum Kingdom Reservoir, Texas, with special reference to discharge of brine from springs and seeps: Austin, Texas U.S. Geological Survey, Water Resources Division, Open-File Report.

Vest, E.L.Jr., 1970. Oil Fields of Pennsylvanian-Permian Horseshoe Atoll, west Texas *in* Halbouty, Michael T. (ed.) Geology of Giant Petroleum Fields, AAPG Memoir #14. American Association of Petroleum Geologists, Tulsa Oklahoma, p. 185-203.

Wang, S., Jaffe, P.R., 2004, Dissolution of a mineral phase in potable aquifers due to CO_2 releases from deep formations; effect of dissolution kinetics. Energy Conversion and Management 45(18-19): 2833-2848.

Yang, C., Romanak, KD, Smyth, RW, Nicot, JP, Hovorka, SD, Scanlon, B, in review, Water-rock-CO_2 batch experiments and numerical modeling: Implication for potential impacts of geological CO_2 sequestration on potable groundwater resources. International Journal of Greenhouse Gas Control

Wilkin, R.T., DiGiulio, D.C., 2010. Geochemical impacts to groundwater from geologic carbon sequestration: controls on pH and inorganic carbon concentrations from reaction path and kinetic modeling. Environmental Science and Technology, 44: 4821–4827.

Xu, T., Apps, J.A., Pruess, K., 2004. Numerical simulation of CO_2 disposal by mineral trapping in deep aquifers. Applied Geochemistry 19, 917-936.

Zheng L., Apps J.A., Zhang Y., Xu T., Birkholzer, J.T., 2009. Reactive transport simulations to study groundwater quality changes in response to CO_2 leakage from deep geological storage. Energy Procedia 1:1887-1894

Zhang, Y., Oldenburg, C. M., Finsterle, S., Jordan, P., Zhang**,** K., 2009. Probability estimation of CO_2 leakage through faults at geologic carbon sequestration sites. Energy Procedia 1: 41-46.

General Core Studies

The Effect of Pressure and Temperature on Brine-CO_2 Relative Permeability and Interfacial Tension at Reservoir Conditions

A study was conducted on the displacement characteristics of CO_2 injected into deep saline aquifers because they control both the migration of CO_2 and the available pore space in the reservoir at irreducible saturation conditions. This study determined the steady-state brine-CO_2 relative permeability measurements in a Berea sandstone core under CO_2 flooding conditions versus pressure and temperature. The results indicate a strong correlation between pressure and the end-point relative permeability to CO_2. As the pressure increased from 1200 psi to 2600 psi, the end point relative permeability to CO_2 increased from 32.4% to 46.8%. Temperature was found not to strongly affect the relative permeability, although the end point relative permeability to CO_2 decreased with temperature increase from 31.05°C to 38°C. Also studied are the effects of pressure and temperature on the interfacial tension (IFT) between CO_2 and brine. The IFT was observed to decrease as pressure increased and increase as temperature increased. These data will provide useful information to evaluation, analysis, and optimization of CO_2 sequestration in deep saline aquifers. These data are presented in the SPE paper entitled "The Effect of Pressure and Temperature on Brine-CO_2 Relative Permeability and IFT at Reservoir Conditions." (Liu et al., 2010)

Experimental Determination of CO_2 Transport and Breakthrough Pressure in Ultra-Low Permeability Caprock

A laboratory study was performed for quantitative measurement of CO_2 diffusion in a caprock layer. Low-permeability core samples were obtained from the Cretaceous Kirtland Formation which functions as the major seal for the SWP's Pump Canyon injection site. The core samples were characterized by microprobe study, scanning electron microscope (SEM), and BET analysis. The average pore size is 8.83 nm with porosity ranging from 1.02% to 6.56%. In a CO_2/brine two phase flow system, CO_2 diffusion at different pressure gradient was measured with the selected low-permeability core samples. Experiments have revealed that CO_2 transport in caprock is closely relating to pore size distribution, interfacial tension (IFT), overlying formation, and pressure gradient. At low pressure, i.e., below breakthrough pressure, CO_2 permeation is gov-

erned by solution diffusion mechanism with permeance ranging from 1.57×10^{-7} to 2.08×10^{-7} mol/(m^2.h.kPa). After displacement of pore-filled water (breakthrough), CO_2 permeance was increased to 5.23×10^{-4} mol/(m^2.h.kPa) under volume migration. This study, in which the long-term storage security due to upward diffusion is discussed as well as the influences of formation fluid chemistry and reservoir pressure on the overlaying sealing efficacy, is discussed at length by Chukwukere et al. (2009)

Porosity Properties of Core Samples by BET Adsorption Isotherms and CO_2/H_2O Adsorption by Molecular Simulations

SWP researchers performed a study using BET adsorption measurements to determine porosity properties of two series of rock samples, cores and core cuttings from the Pump Canyon injection site; to date, this is the first research to investigate the porosity properties of underground formations and CO_2 sorption capacity in the San Juan Basin. Porosity properties are important parameters that control CO_2 storage in different reservoirs and evaluate a geological site for CO_2 sequestration. This data was used to help define the adsorptive performance of the formation, to further understand CO_2-water-rock interaction in the CO_2-rich dense phase, and how host reservoir rocks influence CO_2 geological behavior.

The BET (Brunauer-Emmett-Teller) technique defines surface area, pore size and pore size distribution, and void structure of solid materials. Surface area is an important factor in determining the activity of adsorbents. Pore size information gives insight into surface area measurements. The parameters are used to obtain information on the adsorptivity, catalytic activity, permeability, filterability and granular compressibility of solids.

Rock Formations Tested

Porosity properties were determined by the BET method for a number of core cutting samples (denoted as “A Samples”) and core samples (denoted as “B Samples”) from the San Juan Basin, EPNG INJ #1 Pump Canyon well, which features Tertiary formations of the Nacimiento and Ojo Alamo Formations and Cretaceous formations of the Kirtland Shale and the Fruitland Formation, as shown in Figure 161. Each A and B sample was originally derived from a specific depth range

and a particular depth respectively, as listed in Tables 40 and 41. The basin encompasses a maximum of >15,000 ft. of Paleozoic to Eocene sedimentary rock and contains economic deposits of natural gas, oil, coal, and uranium. The Ojo Alamo Formation is overlain by and intertongues with the Nacimiento formation. The Fruitland formation is more sandy than the overlying Kirtland Shale, which is subdivided into a lower shale member, the Farmington Sandstone Member, and an upper shale member.

Porosity properties of rocks samples

A large number of core cuttings (A samples) and core (B samples) samples were measured in order to investigate their porosity properties. Tables 40 and 41 summarize the porosity properties measured, including BET surface area, pore volume and pore size for A and B samples. All the A samples show particular characteristics of mesoporous materials with pore sizes around 60-110 Å, the BET surface area 3-14 m^2, and pore volume 0.005–0.030 cm^3/g, which can be also seen in Figure 162 as filled squares. For B samples, the method of obtaining the sample cores is different from the core cuttings, which may result in the differences in porosity data, Figure 161 circles. Figure 162 plots the BET surface area, pore volume and pore size for A and B samples. Filled squares are for A Samples and opened circles are for B Samples.

According to the patterns of BET surface area and pore volume in Figure 162, there are obviously five sections involved, These samples are located in depths approximately: 1530–1680 ft, 1750–1940 ft, 1970–2370 ft, 2460–2698 ft, and 2730–2930 ft. These BET measurements could be explained by the formations present at those depths, namely, the Nacimiento, Ojo Alamo, upper Kirtland Shale, lower Kirtland Shale, and Fruitland formations, respectively. In the Nacimiento and Ojo Alamo formations, the BET surface area and pore volume increase with depth, while porosity properties decrease with depth for the upper Kirtland Shale and Fruitland Formation. There is no significant difference in the porosity properties in the Kirtland Shale. These results are consistent with the data from Advanced Resources International (ARI).

For A samples, the pore volumes and the BET surface area change appear to correspondingly. Figure 163 gives the correlation between the pore volume and the BET surface area. The linear-like results indicate that the pore volume increases as the BET surface area increases.

Comparing the porosity properties of B samples clearly shows that surface area and pore volume of the B samples are different from A samples; however, the pore sizes for A and B samples are close to each other because the pore size is effectively correlated to the slope of the V-S pattern. The differences of pore volume and surface area for A and B samples are probably attributable to the difference in rock composition at different specific depths.

CO_2 adsorption isotherms and heats of adsorption for cores

The CO_2 adsorption capacity was investigated in terms of adsorption isotherms on core samples from depths of 2052 and 2690 ft. Table 42 clearly shows the porosity properties of these two cores. The BET surface area greatly decreases from 14.67 m^2/g to 10.24 m^2/g and the pore volume decreases from 0.041 cm^3/g to 0.028 cm^3/g, which indicates that the intergranular pores are significantly compressed and the particles sizes are apparently enlarged. This would also be seen from the bulk parameters in Table 42, in which the density and porosity indicate the denser behavior of the 2690 ft sample.

Figures 164 (a) and (b) depict the N_2 adsorption-desorption isotherms of the cores at depths of 2052 ft and 2690 ft. The inserts in Figures 164 (a) and (b) show their BJH pore size distributions. The isotherms in Figure 143(a) are typical type IV isotherms, which are generally characteristic of mesoporous materials. The conclusion of mesoporosity can be also confirmed by the pore size distribution as showed in the inserted pictures in Figure 164. For both core samples, the pore size of both cores is found to be about 20 to 300 Å in diameter. For a comparison, Figure 165 shows the BJH pore size distributions of core cuttings from BET measurements. Basically, the pore size has a wider distribution in samples from lower depths.

For CO_2 adsorption capacity measurements, the 2052 ft and 2690 ft samples were both ground to millimeter-level; the isotherms results are presented in Figures 166 (a) and (b). The 2690 ft sample exhibits higher CO_2 adsorption quantities than the 2052 ft. sample, especially at low temperatures. For example, the quantity of CO_2 adsorbed on 2690 ft core particles at 303 K is around 0.050 mmol/g at a pressure of 750 mmHg, while the value for the 2052 ft sample is about 0.040 mmol/g. However, the CO_2 isotherms results are inconsistent with the porosity properties obtained from the N_2 adsorption–desorption experiment, which indicates the stronger adsorption on the core from 2052 ft because of its larger pore volume, greater surface area, and smaller porosi-

ty. This opposing scenario could be caused by the greater amount of organic matter contained in the core from 2690 ft. With regard to this assumption, the total petroleum hydrocarbon (TPH) content was analyzed by infrared absorption measurement. The TPH content was about 240 ppm and 280 ppm for core from depths of 2052 ft and 2690 ft, respectively. Furthermore, ARI obtained a similar result from total organic carbon (TOC) analyses, which showed that the weight percentage of TOC for the cores from 2050 ft and 2698 ft was about 0.1% and 0.3%, respectively.

To further research the adsorption between the CO_2 and the cores, the CO_2 adsorption isotherms observed on the 2052 ft and 2690 ft core samples were applied to calculate isosteric heat of adsorption. The isosteric heats of adsorption is usually used to measured the interaction between adsobate and adsorbent molecules as well as the energetic heterogenity of the adsorbent surface (e.g., pore surface in rock cores). In general, if the adsorbent is homogenous, it exhibits a constant value with increasing adsorbate loading. If it decreases with increasing adsorbate uptake, the energetic heterogenity of the adsorbent surface is revealed; while the heat increases with increasing adsorbate loading, it is due to the stronger lateral interactions between asdorbed molecules. The isosteric heats of adsorption, Q_{st}, at specific adsorption loading of the measured CO_2 were calculated by the Clausius-Clapeyron equation,

$$Q_{st} = RT^2 \left(\frac{\partial \ln P}{\partial T} \right)_N,$$

where P is the pressure, T is the temperature, N is the adsorbate loading, and R is the gas constant. The isosteric heats of adsorption as a function of adsorbed CO_2 on the core samples are shown in Figure 167. The isosteric heats of adsorption for the 2052 ft and 2690 ft samples decrease from 25 to 5 and 33 to 15 kJ/mol, respectively. The general decrease is attributed to strong interactions between the large quadrupole moment of CO_2 and the heterogeneous adsorbent cores. In other words, the pore surfaces of both core samples exhibit energetic heterogeneity. It should be noted that the Q_{st} of the core from 2052 ft is obviously lower than that from 2690 ft. It is possibly due to the presence of organic matter, which adsorbs CO_2 more easily than the minerals in thick cores.

Simulation of CO_2/H_2O adsorption on model rock formations

A number of simulations were performed of CO_2 and H_2O adsorption on model rock formations with and without surface modification at different pressures and temperatures.

Gas adsorption depends not only on operation conditions (temperature, pressure, gas composition), but also on material intrinsic properties. Gas adsorption on different model rock formations were studied, including quartz, calcite, magnesite and dolomite, which have different chemical compositions. In order to obtain an overview of the effect of surface chemistry on gas adsorption, molecular dynamics (MD) simulations were performed. The surface and its modification chemical used in MD simulations are the natural zeolite surface and the surfactant HDTMA (heaxdecyltrimethylammonium), respectively. Prior to MD simulation of adsorption, the packing structure has to be determined. Fortunately, we have studied the packing structure and it can be used in Monte Carlo (MC) simulation of CO_2 and H_2O adsorption.

Figures 168 a and b give the adsorption of CO_2 and H_2O on bare natural zeolite and on the zeolite surface coated with HDTMA, respectively, at 300K and pressures up to 50MPa. The simulation results show that the surface modifier HDTMA decreases the adsorption of CO_2 and H_2O, but the effect varies with adsorption pressure. At lower pressures (<20MPa), the effect of HDTMA on CO_2 adsorption is larger; while the effect of HDTMA on H_2O adsorption increases with adsorption pressure. Analysis of the detailed configurations (see inserts in Figure 168) from MD simulations shows that this effect is attributed to the head group ($-CH_3$) and the molecular chain HDTMA and its local charge interactions with sorbate molecules.

The effect of surface modifier(s) on CO_2 adsorption on rock formations can be obtained by using a similar procedure: (a) find optimal packing structures of the surfactant on these model rock formations (quartz, calcite, magnesite and dolomite), (b) carry out MC simulations of CO_2/H_2O adsorption on these surfaces, and (c) perform MD simulations of the adsorbed gas molecules on surfaces to elucidate the mechanisms of increased CO_2 adsorption (storage) in these formations. These simulation results will provide a guideline for CO_2 injection and possible further treatment during the course of Phase III.

Table 40. Porosity Properties of A Samples (Core Cuttings)

Depth, ft.	BET Surface Area, m^2/g	Pore Volume, cm^3/g	Pore Size, Å
1530-1560	3.78	0.0066	69.78
1650-1580	14.72	0.021	58.02
1740-1770	8.57	0.015	67.86
1840-1860	10.17	0.018	71.96
1930-1940	13.54	0.024	71.99
1970-1975	9.81	0.021	86.28
2048-2054	10.52	0.020	76.34
2130-2160	10.29	0.022	83.73
2220-2250	9.70	0.020	81.91
2340-2370	7.03	0.015	84.44
2460-2490	13.01	0.024	73.05
2550-2580	13.65	0.027	77.72
2610-2630	13.18	0.025	75.37
2690-2698	12.88	0.026	82.05
2730-2760	10.79	0.022	81.86
2790-2820	10.24	0.023	88.38
2920-2930	6.11	0.017	110.79

Table 41. Porosity Properties of B Samples (Cores) from Various Depths

Depth, ft.	BET Surface Area, m^2/g	Pore Volume, cm^3/g	Pore Size, Å
2048.76	22.65	0.050	88.30
2053.50	19.69	0.043	87.92
2055.19	14.36	0.031	85.80
2062.08	16.97	0.039	92.20
2068.14	14.46	0.033	90.19
2692.19	15.01	0.030	78.68
2697.15	12.97	0.027	84.45

Table 42. Porosity Properties of Cores from Depths of 2052 feet and 2690 feet

Depth, ft.	BET Surface Area, m^2/g	Pore Volume, cm^3/g	Pore Size, Å	Bulk Density, g/cm^3	Porosity, Vol. %
2052 ft.	14.67	0.041	111.89	2.28	6.56
2690 ft.	10.24	0.028	110.98	2.38	5.05

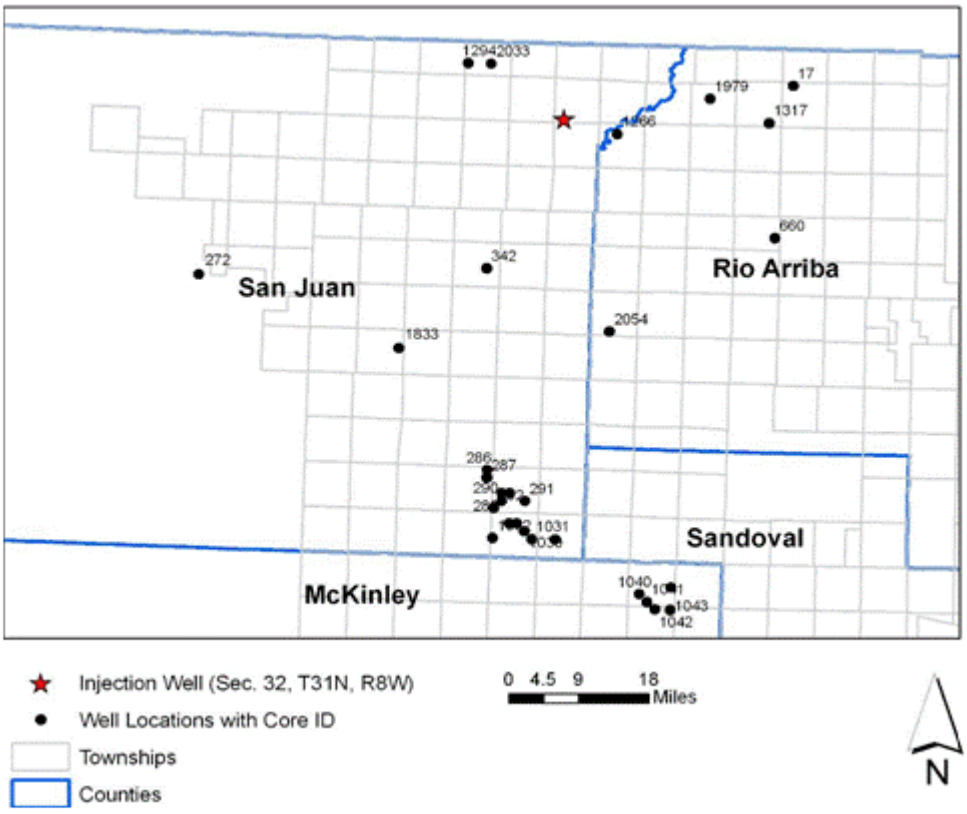

Figure 161. Locations of core samples from wells in northwestern New Mexico. The star indicates the location of A and B Samples (SWP's Pump Canyon injection well).

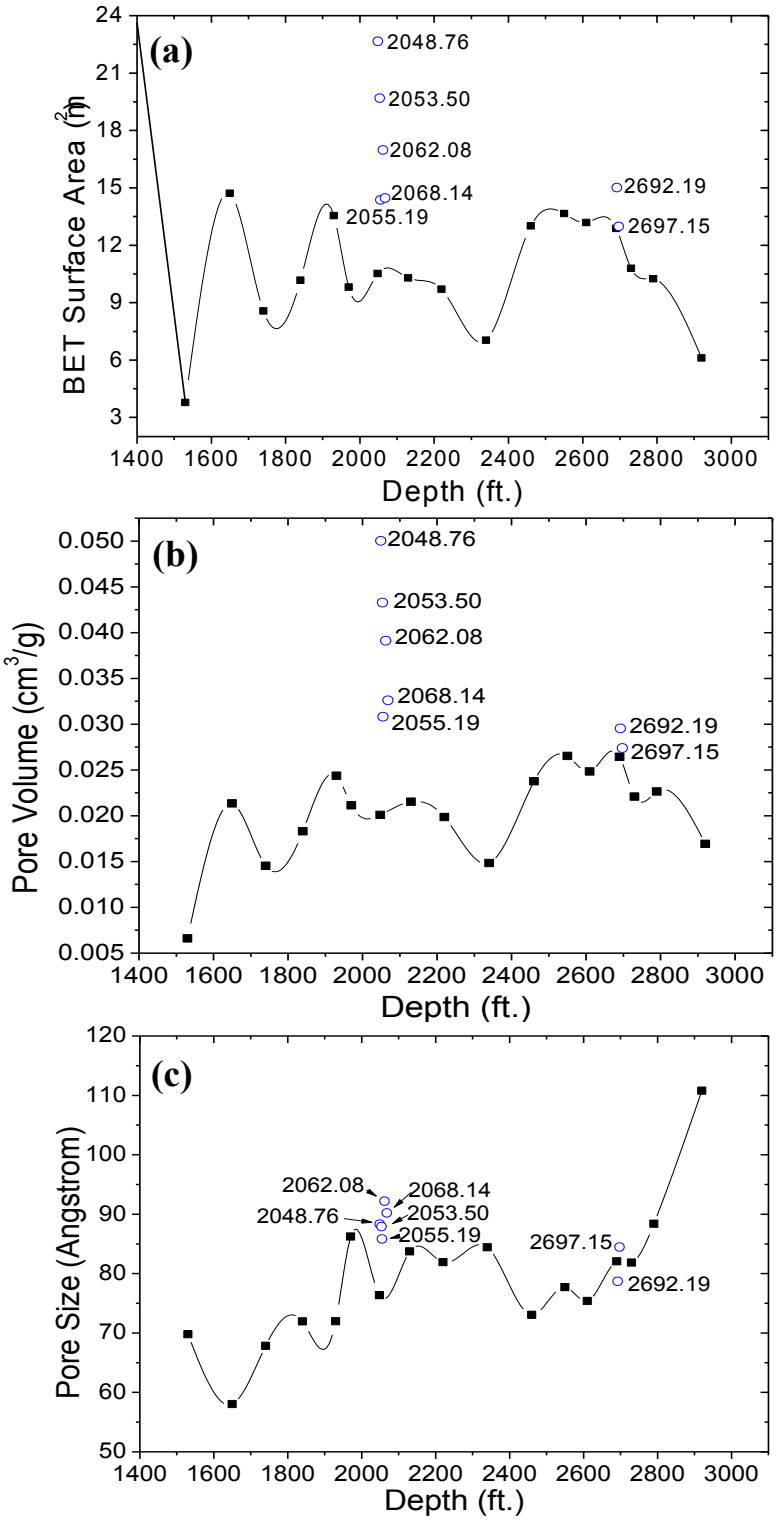

Figure 162. (a) BET surface area, (b) pore volume, and (c) pore size of core samples from various depths. Filled squares are for A Samples (core cuttings); opened circles are for B Samples (cores).

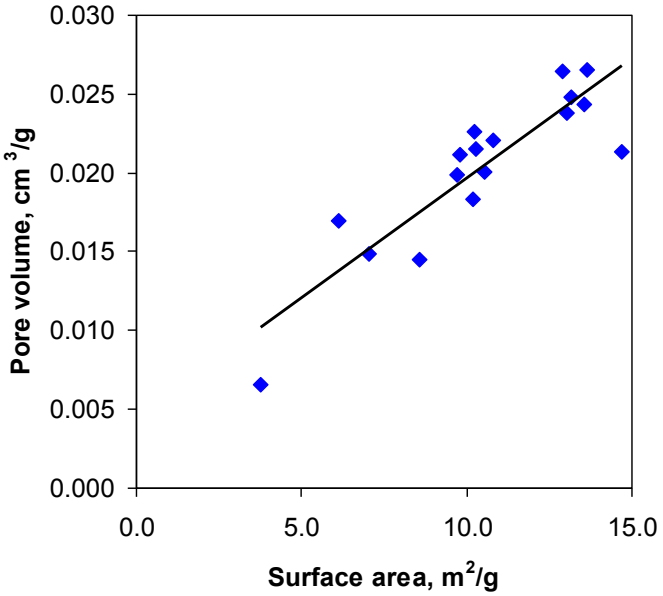

Figure 163. The correlation between the BET surface area and the pore volume for core cutting samples from depths of 1530 ft to 2930 ft.

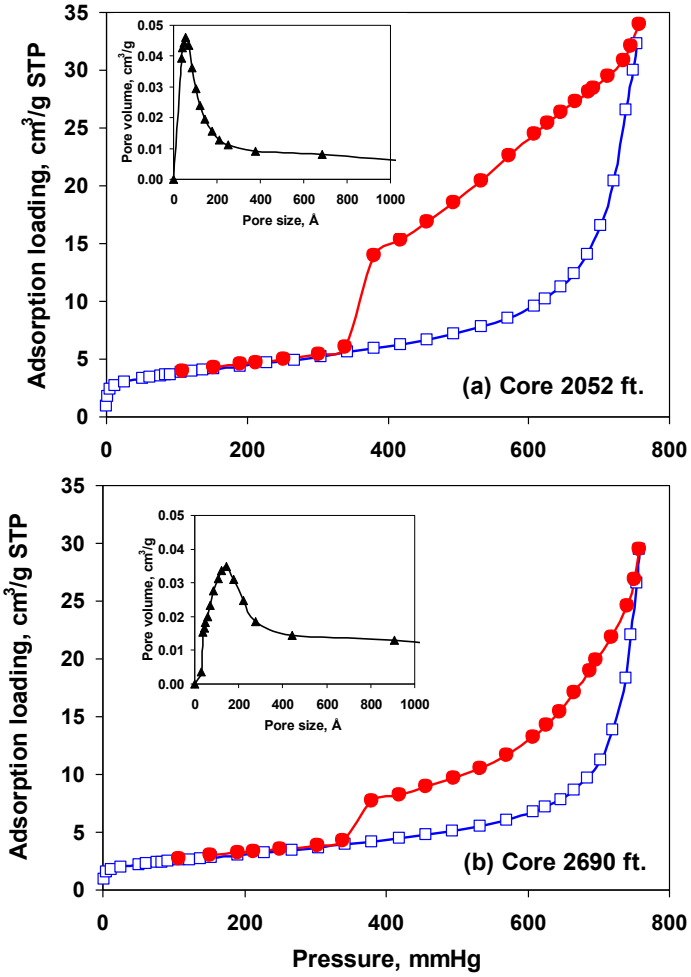

Figure 164. Adsorption–desorption isotherms of N_2 on cores from depths of 2052 ft. (a) and 2690 ft. (b). The insertions are BJH pore size distributions for these two cores.

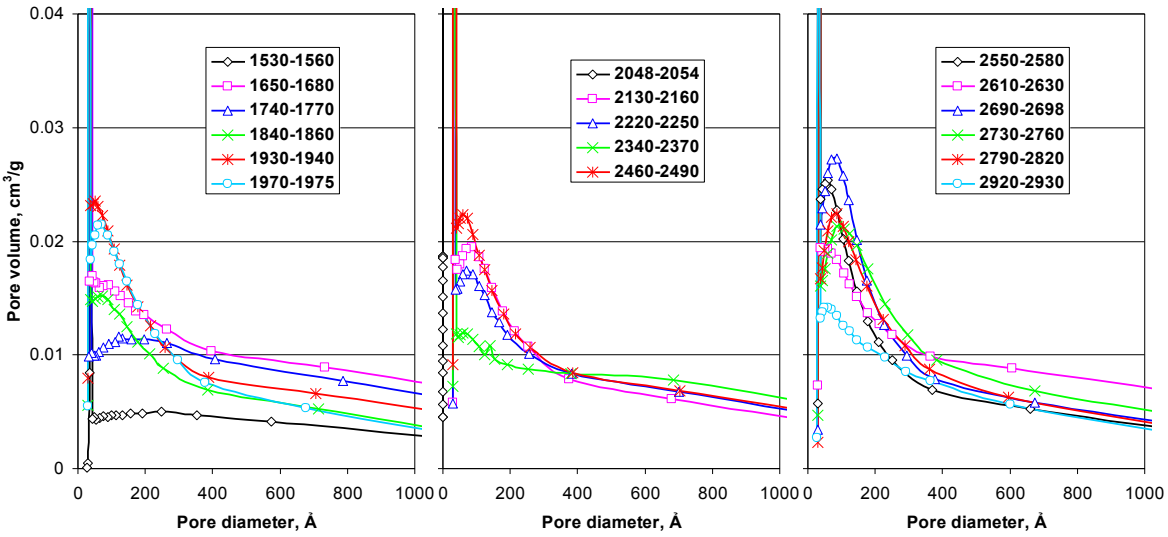

Figure 165. BJH pore size distributions of core cuttings from various depths from 1530 ft to 2930 ft.

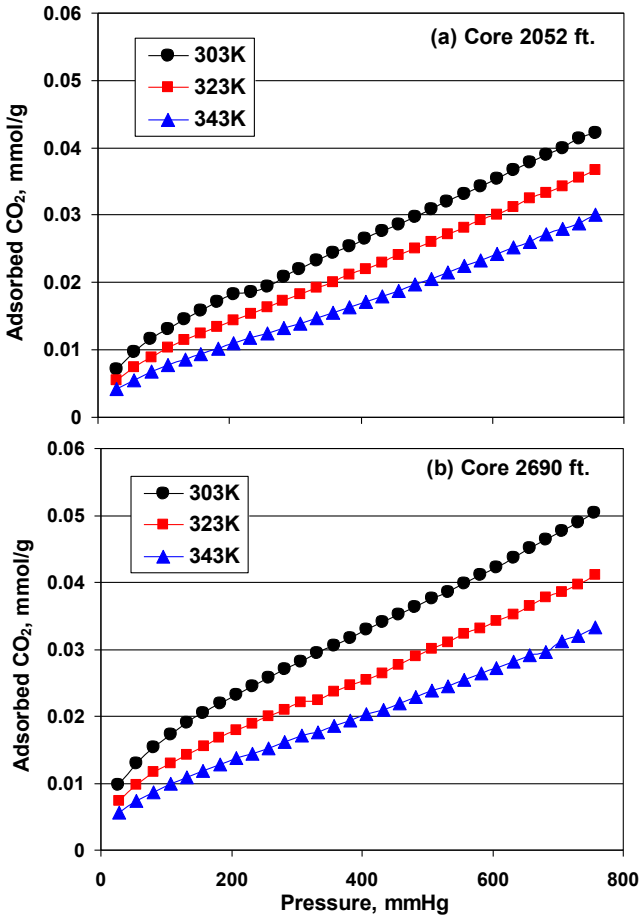

Figure 166. Adsorption isotherms of CO_2 on cores from depths of 2052 ft. (a) and 2690 ft. (b) at temperatures 303K, 323K, and 343K and pressures up to 750 mmHg.

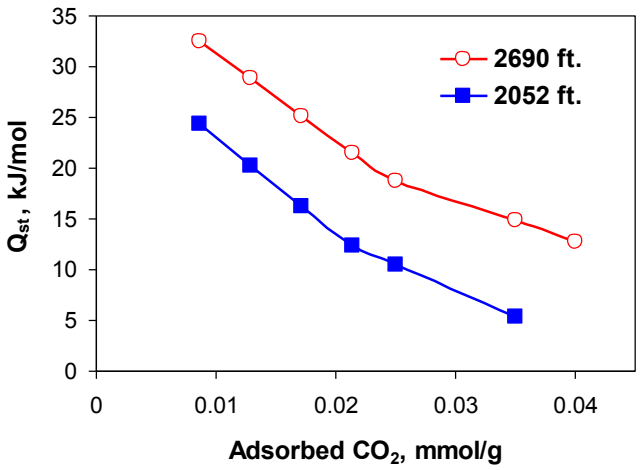

Figure 167. Isosteric heats of adsorption for CO_2 on cores from depths of 2052 ft and 2690 ft.

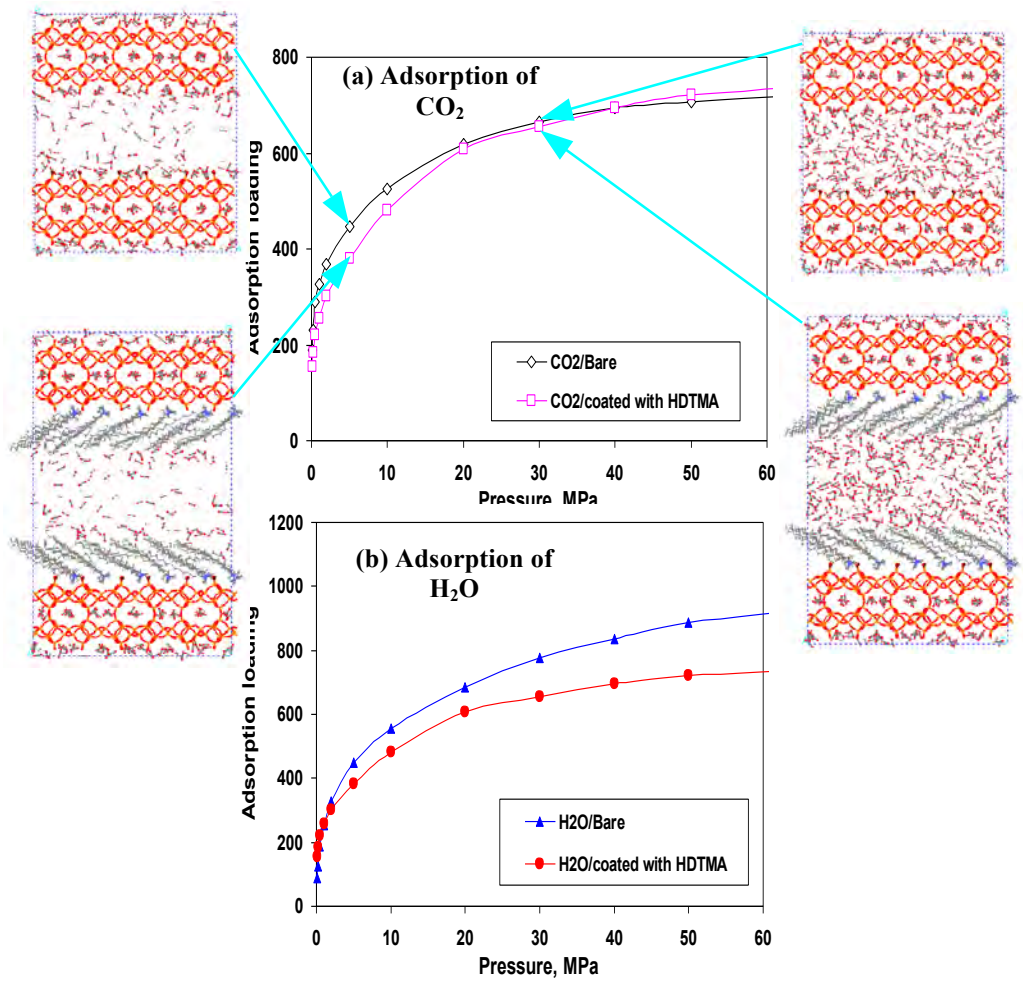

Figure 168. Adsorption of (a) CO_2 and (b) H_2O on bare natural zeolite surfaces and those coated with surfactant HDTMA. The insertions are snapshots from simulations.

Validation and Comparison of Carbon Sequestration Project Cost Models with Project Cost Data Obtained from the Southwest Partnership

A study was performed that developed an estimation tool, using the information and data available from several projects either completed, in progress, or conceptualized by the SWP, to determine the best approach to estimate a geologic sequestration project's cost. The data presented highlights calculated versus actual costs. Several models for carbon compression, transport and/or injection are employed that are designed to aid in determining the cost of sequestration projects. This data is compared to the results obtained by applying several of these models for the projects studied with actual cost, including those by J. Ogden, MIT's Carbon Capture and Sequestration Technologies Program Model, and the Environmental Protection Agency. This estimation process also offers methods to systematically apply the models to future projects of a similar scale. Cost risks associated with a project of this scope are discussed, along with ways that have been and could be used to mitigate these risks.

The resulting tool should enable users to develop a project cost estimate having to supply only a few basic parameters (Table 43), as well as some basic assumptions and "guesstimates" as indicated throughout the process. Most of the values for these parameters should be available from surface measurements and well logs.

Table 43. Basic Parameters for Establishing a Project Budget

Input Parameters	Output Results
Permeability	Capital Cost of the Pipeline
Thickness of Reservoir	Capital Cost of the Heating System
Depth to Reservoir	Capital Cost of Compression
Distance from Source to Sink	Capital Cost of the Dehydrator
Input Pressure to Pipeline	• Capital Cost of the Injection Well
Surface Temperature	Overall Cost
Mass Flow Rate	
Reservoir Pressure	

This procedure is a streamlined process, which will allow a manager, scientist or engineer to quickly calculate the cost of installing a CCS site, determining a range of initial capital costs for a project in just a few hours using the fewest parameters possible. It is completely self-

contained; all conversions have already been done, making the equations and all variables internally consistent. Aside from the required parameters and some assumptions about the field in consideration all other data is supplied. The end result of following this procedure will be a set of ranges for each of the main components of Carbon Capture and Storage (CCS), which will give a good approximation of what the initial capital cost of a future project might be.

The three dominant capital costs included in a Carbon, Capture and Sequestration (CCS) project are compression, the pipeline system and the injection well. Two significant but smaller costs are for line heaters and dehydration units. Three methods are presented for calculating each of the dominant costs as well as a method for heating and dehydration.

A number of dominant risks that have been recognized by the Southwest Partnership during its field tests are addressed. To quantify these risks and to recognize their potential to increase the cost of the projects a contingency fund or "fudge factor" was added to the overall cost of the projects.

The initial capital cost of a case study employing a hypothetical setup was calculated and the resulting cost range and its implications were explored for illustrative purposes.

Finally, three projects were considered. The first project was actually completed and the final costs were accounted for. Two other projects were conceptualized and cost estimates for the initial capital costs were calculated by an engineering firm. The cost estimates by line item are presented in the Appendix to the report. All of the methods in the report were applied to each of the three projects, giving a range of costs and an average. The estimates from the conceptualized projects as well as the final cost of the completed project were then compared to the results. In each case the estimated or actual cost falls within the range of the models' cost estimates.

Conclusions

The method developed in this research has been applied to one actual project, two conceptualized projects and one case study. The following conclusions were drawn:

- Though most of the models are well recognized and widely, used they still produce a fairly wide cost range; about +/-10-15% from the mean value.

- All of the actual or estimated data fit within the calculated cost ranges.
- The cost range can be reduced by having more accurate data and precise design.

References

Full presentation of this study, the tool developed, and the results are contained in:
Harris, M. (2010). Validation and Comparison of Carbon Sequestration Project Cost Models with Project Cost Data Obtained from the Southwest Partnership. M.S. Independent Study, New Mexico Institute of Mining and Technology, Socorro, New Mexico.

Regional Terrestrial Pilot

Overview and Results

The analyses conducted in Phase I of the Southwest Regional Partnership (SWP) clearly showed that there is tremendous potential to increase carbon storage in soils and vegetation through changes in land use and management within the southwest region. However, several factors constrain this potential including low rates of carbon accumulation per hectare due to low rainfall and soil fertility, large variations in the climate make local prediction of sequestration difficult, and cost effective carbon measurement systems are lacking. The complex combination of land use, land management and natural conditions in the SWP region offered the opportunity to build upon and expand the work conducted in the Phase I efforts in order to develop methodologies and analytical tools that would provide the basis for a carbon reporting and monitoring system that could function consistently across hierarchical scales and could assist stakeholders in participation in terrestrial carbon sequestration programs. The main objectives in developing and implementing this system were to 1) develop improved technologies and systems for direct measurements of soil and vegetation carbon; 2) develop remote sensing and classification protocols to improve mesoscale (km2) soil and vegetation carbon estimates; 3) construct ecological process models that reflect soil/vegetation changes resulting from current land use and land use associated with carbon sequestration programs; 4) develop a regional carbon inventory and decision sup-

port tool and 5) explore restoration technologies/strategies that could be used for carbon sequestration on lands near geological sequestration sites.

Some results include:

1. Direct measurements of soil and vegetation carbon using Laser Induced Breakdown Spectroscopy (LIBS) and Near Infrared Reflectance Spectroscopy (NIRS) can provide accurate measurements of soil carbon and can be used to help reduce the cost and time require for soil sampling.
2. Normalized Difference Vegetation Index (NDVI) imagery for monitoring compliance in carbon sequestration programs has potential for monitoring large (e.g., doubling or vegetation biomass) changes, but does not appear to be able to detect subtle changes in management.
3. The use of ecological process models (i.e., state and transition models [STMs]) for representing the range of soil/vegetation combinations associated with carbon management practices and land uses within the region indicate a strong link between ecological states and soil carbon levels in rangelands within the SWP region.
4. Uncertainties associated with model estimates of rangeland carbon sequestration were generally high across the region, though delineating areas where additional data can be collected to reduce uncertainty.
5. A web-based decision support tool with a map-driven user interface was developed.
6. An examination of restoration technologies/strategies that could be used for carbon sequestration was conducted at La Manga Canyon in the San Juan basin.

For direct measurements of soil and vegetation carbon, we examined the capabilities of Laser Induced Breakdown Spectroscopy (LIBS) and Near Infrared Reflectance Spectroscopy (NIRS) instruments for rapid measurement of soil carbon in soils commonly associated with arid and semi-arid rangelands and in landscape changes associated with energy infrastructure development. Results indicated that the LIBS and NIRS instrument can provide accurate measurements of soil carbon and confirm that these technologies can be used to help reduce the cost and time require for soil sampling, see Figures 169 and 170.

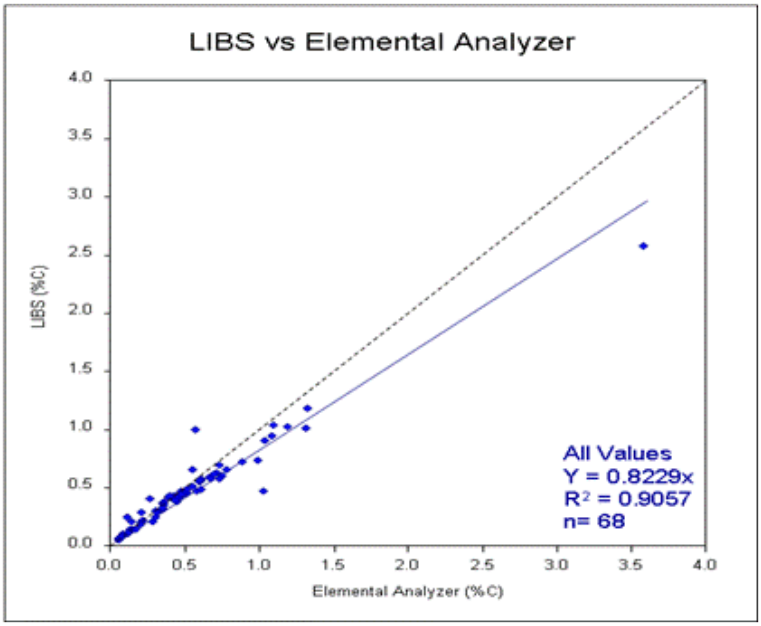

Figure 169. Elemental carbon as detected by Laser Induced Breakdown Spectroscopy (LIBS) vs. an Elemental Analyzer for 68 soil samples from arid rangelands.

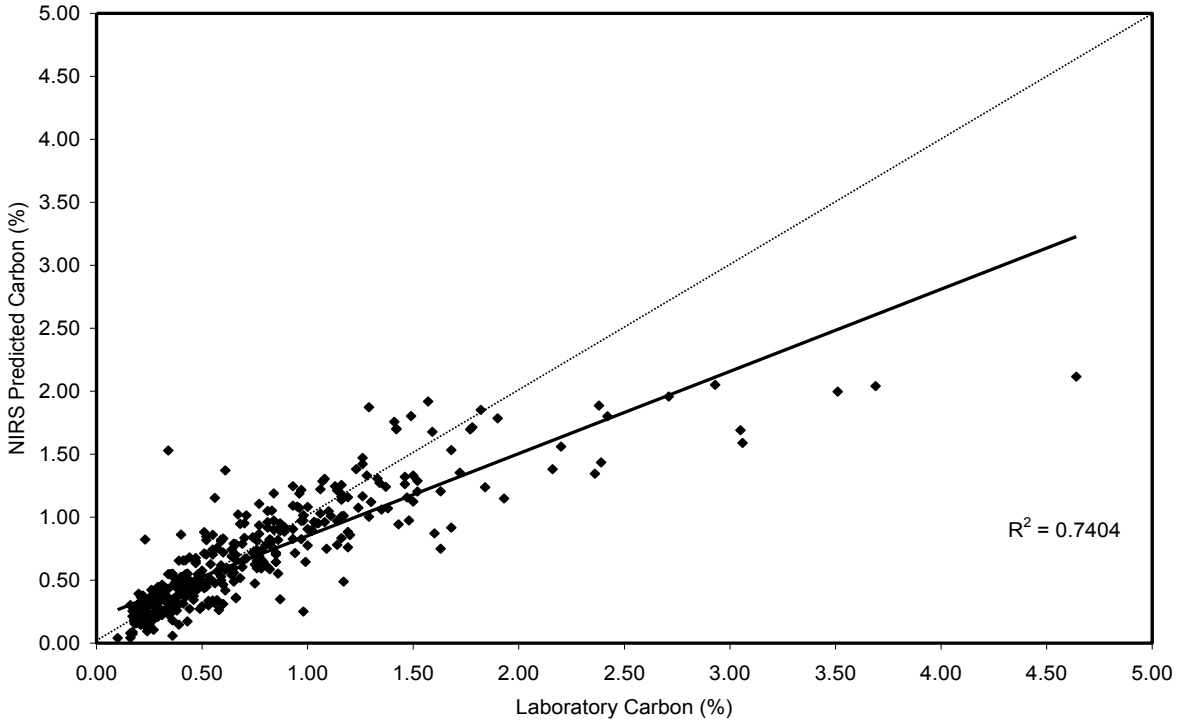

Figure 170. Validation results for the NIRS carbon equation developed for SWP. The x axis represents actual carbon in the soil samples as measured by standard laboratory analysis. The y axis represents the NIRS predicted carbon. Dashed line represents a hypothetical 1:1 correspondence between observed and predicted carbon. The robustness of the validation was reduced by the large number of samples at the lower end of carbon amounts in the soil and by several large outliers with high carbon contents.

In the examination of remote sensing and classification protocols to improve mesoscale (km2) soil and vegetation carbon estimates, we evaluated the use of Normalized Difference Vegetation Index (NDVI) imagery for monitoring compliance in carbon sequestration programs and the use of moderate to high resolution imagery for classifying ecological sites and the associated carbon change from changes in ecological state. Results of the NDVI evaluation indicated that the use of NDVI for monitoring compliance in carbon sequestration programs has potential for being a reliable method of monitoring vegetation biomass changes that would influence rates of carbon sequestration. The method would likely be able to detect large changes in management (e.g., doubling or tripling stocking rates), but does not appear to be able to detect subtle changes in management (e.g., a 10% reduction in stocking rate). The use of high and moderate resolution imagery as a means of inferring carbon levels from changes in ecological state is a valid and doable methodology. However, the correlation of satellite imagery to site dynamics requires an increase in the availability of ecological site descriptions for much of the southwest region.

The use of ecological process models was used (i.e., state and transition models [STMs] for representing the range of soil/vegetation combinations associated with carbon management practices and land uses with the region). Results indicate a strong link between ecological states and soil carbon levels in rangelands within the SWP region. The continued efforts by federal government land management agencies and technical assistance agencies to increase the availability of Ecological Site Descriptions that describe state and transition models for land areas within the region should greatly improve the availability of soil and vegetation information necessary to link soil carbon changes to ecological state.

As part of the regional carbon inventory, an analysis of uncertainty in carbon sequestration estimates for land areas within the SWP region was conducted. Results indicated that management practices involving conversion of row crops or small grains to perennial grass cover had the lowest uncertainty. However, uncertainties associated with model estimates of rangeland carbon sequestration were generally high across the region. This makes credible inventories of carbon sequestration on rangeland problematic for the region. However, our ability to map these uncertainties has assisted in delineating areas where additional data can be collected to reduce uncertainty.

A web-based decision support tool with a map-driven user interface was developed to allow users to examine carbon sequestration practices for a user-defined area (see http://swcarbon.tamu.edu). The tool has live connections to soil and weather databases provided by government agencies, thus insuring that the most recent and relevant data are used by the system. The tool also allows users to define management practices for carbon sequestration and provides a report based on the entire area of interest or by individual soils.

An examination of restoration technologies/strategies that could be used for carbon sequestration was conducted at La Manga Canyon in the San Juan basin. As part of this effort, the extent and density of total energy development in the region was evaluated along with time series analysis of land use change. Based on the extent of the road and well pad development and the temporal dynamics of land use change, we conclude that restoration in La Manga Canyon is not a matter of developing water sources, irrigation technology or adapted species for planting. The alteration of the landscape and changed hydrologic cycle due to the road network has drastically altered the ecology of the area. Restoring drainage patterns in the area would be the most important component for site restoration.

SWP undertook a riparian restoration project in the San Juan Basin. The objectives of this task were to explore restoration technologies/strategies that could be used for carbon sequestration on lands near geological sequestration sites to take advantage of produced water for restoration and improve lands that have been affected by grazing and energy exploration. For this task, the following technologies/strategies were examined:

- New filtration technologies for cleaning produced water to make it suitable for irrigation
- Distribution technologies to enhance survival of planted species used in restoration
- Selection of appropriate species for reseeding
- Landscape scale restoration

Summary and Conclusions

- Existing technologies was adapted (LIBS and NIRS) to the measurement of soil carbon in soils commonly associated with arid and semi-arid rangelands and in landscape changes that reflect the widespread road networks associated with energy infrastructure development. Our results clearly confirm that these more cost effective technologies (~10% of laboratory analytical techniques) can be used to help reduce the cost and time require for soil sampling.

- Results have also demonstrated dramatic changes in soil carbon in response to the change in plant community type associated with livestock grazing and species invasion (*Bromus tectorum*) common across western rangelands. In this region, it is difficult to evaluate the historic changes because there is so little land that has not been grazed and/or invaded. More importantly, our results demonstrate the need to stratify, at an ecological site level, landscapes for sampling in order to determine soil carbon pools and changes over time. Significantly different amounts of soil carbon in each of the ecological site/soil combinations require stratification to develop a credible estimate of landscape scale carbon dynamics.

- The results of the surface soil carbon measurements can also be used to develop statistically valid sampling protocols for determining soil carbon pools in arid rangelands. Our results typically showed standard errors can be reduced to <20% of the mean by increasing sample size to 10 or more samples per ecological site. Because of the amount of disturbance and mixing associated with road development, the number of samples can be substantially reduced.

- The remote sensing of carbon dynamics for arid rangelands using satellite imagery as a means of inferring carbon levels from changes in ecological state is a valid and doable task. However, the correlation of satellite imagery to site dynamics requires an increase in the availability of ecological site descriptions. A surrogate for the input of carbon into soils, seasonal plant production is tractable with the use of NDVI imagery and can be

used to make valid inferences regarding both carbon dynamics and performance in the context of carbon offset programs.

- The use of NDVI for monitoring compliance in carbon sequestration programs shows signs of being a reliable method of monitoring biomass changes across a region. It would likely be sensitive to large changes in management (e.g., doubling or tripling stocking rates), but does not appear to be able to detect subtle changes in management (e.g., a 10% reduction in stocking rate).

- The widespread availability of Ecological Site Descriptions as a part of the federal government land management agencies and technical assistance agencies should greatly improve the availability of soil and vegetation information necessary to link soil carbon to ecological state. In this project, we have shown the link between ecological states and soil carbon levels in arid rangelands.

- An analysis of uncertainty in carbon sequestration estimates for land areas within the SWP region indicated that management practices involving conversion of row crops or small grains to perennial grass cover had the lowest uncertainty. However, uncertainties associated with model estimates of rangeland carbon sequestration were generally high across the region. This makes credible inventories of carbon sequestration on rangeland problematic for this region. However, our ability to map these uncertainties has assisted in delineating areas where additional data can be collected to reduce uncertainty.

- An examination of land cover changes provided an indication of the dynamics in land cover and how this may influence carbon sequestration programs. During a 10 year period, total land cover changes represented less than 2.5% of the total land area in the region. However, in the case of cropland conversion to rangeland and vice-versa, the amount of conversion for these types was nearly identical during the 10-year period. This provides an indication that these land use changes may need to be considered for proper accounting during carbon inventories.

- A web-based decision support tool with a map-driven user interface was developed to allow users to examine carbon sequestration practices for a user-defined area. The tool has live connections to soil and weather databases provided by NRCS and NOAA respectively, thus insuring that the most recent and relevant data are used by the system. The tool allows users to define management practices for carbon sequestration and provides a report based on the entire area of interest or by individual soils.

- Based on the extent of the road and well pad development and the temporal dynamics, we conclude that restoration in La Manga Canyon is not a matter of developing water sources, irrigation technology or adapted species for planting. The alteration of the landscape and changed hydrologic cycle due to the road network has drastically altered the ecology of the area. Revegetation may be a challenging task, but restoring the hydrology without restoring drainage patterns is impossible.

Publications

Refereed Journal Articles

Havstad, K.M., D.P.C. Peters, R. Skaggs, J. Brown, B. Bestelmeyer, E. Fredrickson, J. Herrick and J. Wright. 2007. Ecological services to and from rangelands of the United States. *Ecological Economics*
Brown J.R. and B. T. Bestelmeyer. 2008. Resolving critical Issues for the development of ecological site descriptions: summary of a symposium. *Rangelands*: 30: 16-18.

Brown, J.R. and J. Thorpe. 2008. Climate change and rangelands: responding rationally to uncertainty. *Rangelands*30: 3-6.

de Steiguer, E., J. R. Brown and J. Thorpe. 2008. Contributing to the mitigation of climate change using rangeland management. *Rangelands* 30: 7-11.

Bestelmeyer, B.T., A. J. Tugel, G. L. Peacock Jr, D. G. Robinett, P. L. Shaver, J. R. Brown, J. E. Herrick, H. Sanchez and K. M. Havstad. 2009. State-and-Transition models for heterogeneous landscapes: a strategy for development and application. *Rangeland Ecology & Management*: Vol. 62: 1-15

Brown, J.R., J. Angerer, S. W. Salley, R. Blaisdell and J. W. Stuth. 2010. Improving estimates of rangeland carbon sequestration potential in the US Southwest. *Rangeland Ecology & Management* 63:147-154.

Book Chapters

Bestelmeyer, B.T., J.R. Brown, K.M. Havstad and E.F. Fredrickson. 2006. A holistic view of an arid ecosystem: A synthesis of research and its applications. pp 354-368. In: Structure and Function of a Chihuahuan Desert Ecosystem (eds. K.M. Havstad, L.F. Huenneke and W.H. Schlesinger). Oxford Press. New York, NY USA.

Bestelmeyer, B. T., Havstad, K. M., Damindsuren, B., Han, G., Brown, J. R., Herrick, J. E., Steele, C., Peters, D. C. 2009. Resilience theory in models of rangeland ecology and restoration: the evolution and application of a paradigm. In: Hobbs, J.J., Suding, K.N., editors. New Models for Ecosystem Dynamics and Restoration. Washington, D.C., Island Press. p. 78-95.

Havstad, K. M., Peters, D. C., Allen-Diaz, B., Bestelmeyer, B. T., Briske, D., Brown, J., Brunson, M., Herrick, J. E., Johnson, P., Joyce, L., Pieper, R., Svejcar, A. J., Yao, J., Bartolome, J., Huntsinger, L. 2009. The western United States rangelands: a major resource. In: W.F. Wedin and S.L. Fales, editors. Grassland: Quietness and Strength for a New American Agriculture. Madison, WI. Published by the American Society of Agronomy, Crop Science Society of America, and Soil Science Society of America. 256 p.

Brown, J.R. 2009. Climate Change and Ecology in Rural Lands. pp 39-56. In: A.X. Esparza, G. McPherson (eds.), *The Planner's Guide to Natural Resource Conservation*. Springer. New York, NY.

Brown, J. R., and N. Sampson. 2009. Integrating terrestrial sequestration into a greenhouse gas management plan. pp 317-324. In: B. McPherson and E. T. Sundquist [EDS]. *Carbon Sequestration and Its Role in the Global Carbon Cycle*. Geophysical Monograph Series, American Geophysical Union, Washington DC, USA.

Legal and Regulatory Environment for the Storage of Carbon Dioxide in Geologic Structures

A summary of the status of state and provincial efforts to develop laws and promulgate regulations concerning the geologic storage of CO_2 was prepared by the Interstate Oil and Gas Compact Commission (IOGCC) Carbon Capture and Geologic Storage (CCGS) Task Force. The IOGCC is a multi-state government agency that promotes the conservation and efficient recovery of domestic oil and natural gas resources while protecting public health, safety, and the environment. This report, pertaining to all the Regional Partnerships, is a result of the collaborative efforts of states and provinces to develop a viable CCGS legal and regulatory infrastructure and provide an overview of the importance states and provinces continue to place on the development of CCGS rules and regulations.

It is anticipated that a state or province adopting a regulatory framework for CO_2 geologic storage will make changes to the model framework developed in Phase I (IOGCC Model Statute and Rules) as necessary to conform to the state's unique circumstances. The Task Force therefore continues to envision that the end-product will be a substantially consistent system in the United States and Canada for the geologic storage of CO_2 regulated at the state and provincial level in conformance with national and international law and protocol.

The data for the study were gathered through informal surveys, letters, personal interviews, site visits, and published reports. Sources include government officials, regulatory agency employees, private oil and gas company owners and employees, oil and gas service-industry owners and employees, academics, trade publications, and government documents. Necessarily, much of the information is anecdotal and somewhat subjective. Statistics cited are identified by source. Estimates are based on published statistical evidence with the methodology and source identified.

In addition to state and provincial utilization of the IOGCC Model Statute and Rules, the U.S. Environmental Protection Agency (EPA) also referenced the statute and rules in development of the proposed CCGS rules under the UIC Program.

The rules the states and provinces have developed recognize the dual nature of carbon dioxide. While it is a major contributor to increasing greenhouse gases in the atmosphere, it also has commercial viability in enhanced oil recovery (EOR) operations. This report recognizes this dichotomy. To facilitate CCGS as a climate mitigation strategy and as a commercial resource the IOGCC task force has urged a resource management approach to the development of a CCGS legal and regulatory framework as opposed to a 'waste disposal' framework.

Lessons Learned by Partnerships in Phase II

"Lessons Learned" represents the efforts of the IOGCC Carbon Capture and Geological Storage (CCGS) Task Force review of the work of the seven Department of Energy-sponsored Regional Carbon Sequestration Partnerships' pilot projects. In working with the RCSPs, the IOGCC Task Force on Carbon Capture and Geological Storage compiled challenges—along with recommendations to address the challenges—reported by the Partnerships. Legal and regulatory hurdles faced during the pilot projects were highlighted and key areas where improvements can be made were identified. In addition to the recommendations of the Partnerships, the IOGCC CCGS Task Force created a set of recommendations that identify actions that should be taken in the future to make licensing and permitting of CCGS projects more streamlined and efficient, thus guiding government and business through the initial phases toward commercialization.

Challenges Encountered and Lessons Learned by the Partnerships

The IOGCC, through surveys, identified and the principal challenges encountered and the lessons learned by the Partnerships in seeking licenses and permits for 22 CO_2 geologic storage pilot projects during Phase II. What the partnerships were ultimately seeking from government regulators were the rights to drill and inject CO_2 into geologic formations.

Each license or permit had the potential to involve multiple state regulatory agencies, federal departments, agencies, and regional offices as well as local governments. Most of the pilot projects involved a different amalgam of research partners, many with little or no experience in seeking regulatory approval; the challenges that were encountered by the seven partnerships were numerous and varied. These challenges have been synthesized into five principal categories, with each challenge accompanied by "Lessons Learned" and recommendations.

Challenge #1: Technical Capacity of the Regulator

There were a number of both state and federal regulatory organizations with insufficient technical expertise to grant the licenses or permits requested in a timely and efficient manner.

One of the most common experiences of the Partnerships in their development phase work was working with state and/or federal regulatory personnel with an inadequate understanding of the subject matter of the request.

One clear observation or lesson learned was that at both state and federal levels of regulatory oversight, there was a great deal of difference among the states and EPA regions in terms of the organizational capacity to license these development phase pilot project wells.

In states with active oil and natural gas regulatory programs in place (such as the Southwest Partnership, where all the pilot injection projects took place in areas already under development), the regulators were much less daunted by the licensing and permitting of CO_2 geologic storage wells and were able to issue permits and licenses in a more timely manner. States with little or no oil and natural gas regulatory experience had a great deal more difficulty.

Similarly, concerning administration of the UIC program, states and EPA Regional Offices with experience licensing Class II (oil and natural gas waste) wells under the UIC program had much faster and more efficient processes. This lesson learned supports a recommendation contained in the IOGCC 2007 *Legal and Regulatory Guide for States and Provinces* that the state oil and natural gas regulatory agency, by virtue of its experience licensing and regulating similar wells, should be given first consideration by a state legislature as the most appropriate state agency to designate as the lead regulator of the geologic storage of CO_2.

Another lesson learned is that there are states and EPA regional offices with significant experience licensing these kinds of wells. That expertise could be leveraged to train and support capacity-building in states and regions with less or no experience.

- ***Recommendation:*** Training programs should be created and conducted at the state, federal, and local levels where regulators do not possess the necessary technical expertise to permit and license CO_2 geologic storage wells in an efficient and timely manner. (Modeling analysis expertise in particular was noted as a common technical deficiency in regulatory offices.)

- ***Recommendation:*** In some states, in addition to training, it may be necessary to add staff to license and permit these new wells in a timely matter, especially when commercial-scale development begins.

Challenge #2: Regulatory Infrastructure and Systems

The partnerships encountered a number of state and federal regulatory systems where deficiencies, at times very minor, in systems and procedures for permitting and licensing CO_2 storage wells led to significant delays in issuing the permit/license.

On example of this would be a state where the rules specify that a particular agency may issue a permit only when the application is "complete." The problem is that the rules do not adequately define what constitutes an adequate or "complete" application. This leads to uncertainty and delay.

Another common observation of the partnerships was that the projects for which permits were being sought were small-scale "pilot" projects, designed to allow all parties, regulated and regulator, to learn from the experience. The problem was that the rules and systems in place didn't recognize the "pilot" nature of the project and forced the permit applicant to comply with rigid and inflexible permitting requirements that were inappropriate for small-scale "test" projects.

An additional observation of the partnerships was that overly prescriptive regulations, state and federal, were observed to have had the effect of encouraging inefficiency and unnecessary delay.

Based on their development phase experience, partnerships were generally of the opinion that principle or performance-based regulatory frameworks would be much more efficient and timely for the oversight of CO_2 geologic storage projects. Overly prescriptive regulations for project development, and particularly for research projects, were not flexible enough to account for the unknowns that will inevitably be encountered during project development.

- ***Recommendation:*** EPA and state regulatory agencies should develop a streamlined permit process for small-scale (validation phase) projects for the evaluation of geologic properties at potential CO_2 storage sites.
- ***Recommendation:*** States should tighten up on the definition and/or explanation as to what constitutes a "complete" or adequate permit application.

- ***Recommendation:*** States should implement principle or performance-based regulatory frameworks for CO_2 geologic storage. Additionally, a "waste-disposal" orientation in the regulatory frameworks likely will be more prescriptive and inflexible.
- ***Recommendation:*** States should pursue the adoption of legislation and the promulgation of regulations for the geologic storage of CO_2 along the general lines of the IOGCC model regulatory framework issued in 2007 and updated in 2009.

Challenge #3: Regulatory Jurisdiction

In a number of states the partnerships encountered uncertainty as to which state agency had jurisdiction over the permitting and licensing of pilot project wells. In some states with primacy under the UIC program this manifested as uncertainty between state agencies over which had the lead responsibility for different classes of wells and/or different components of a project. The net result was delay in the ability of a partnership project to acquire a permit to drill or inject.

- ***Recommendation:*** Relevant state agencies should be encouraged to work together to clarify, via interagency agreement or otherwise, agency jurisdiction with respect to the licensing and permitting of CO_2 storage wells. This will be especially important once a final EPA rule for the underground storage of CO_2, expected in late 2010 or early 2011, is promulgated.
- ***Recommendation:*** In states with agencies that regulate oil and gas operations and have UIC primacy, the oil and gas agencies should be given authority to regulate CO_2 injection into saline formations for non-EOR projects.

Challenge #4: Cooperation and Coordination among Regulatory Entities (State/State, State/Federal, State/Local, Federal/Federal)

The partnerships experienced a number of instances where cooperation or coordination among federal, state, and/or local authorities (with a role to play in the process of license/permit issuance) was lacking, resulting in a delay in permit/license issuance.

In the course of securing licenses and permits for their validation phase CO_2 pilot projects, the partnerships often had to deal with multiple layers of government, all with a role to play before a license or permit could be issued. There was also the potential for the involvement of more than

one agency at each level of government (federal or state), each operating under its own statutory authority. As noted earlier, because of the fact that all of the partnership pilot projects were federally funded, there was always the necessity of complying with NEPA. State NEPA equivalents also potentially came into play. Given the particular circumstances, there also could be issues pertaining to endangered species, fish and wildlife, cultural and heritage sites, wetlands, and air emissions, all potentially requiring the involvement of different federal and state agencies. In some cases there was the need to work with local (municipal or county) agencies on issues such as building codes, storm water runoff and noise. If the project was on tribal lands, there were tribal authorities with which the partnerships had to work.

The problem was that there rarely was coordination or cooperation among the various regulatory entities involved. This translated into delay in securing the ultimate approval to drill or inject.

Among the lessons learned by the partnerships from their experiences was that they needed to be much more proactive in communicating with and encouraging communication and cooperation among the government agencies and affected stakeholders. Additionally, it was clear to the partnerships that this work needed to begin early --- as early as the planning process.

- ***Recommendation:*** Efforts should be undertaken to encourage standardization of permit response times at state and federal levels.
- ***Recommendation:*** Joint task forces should be formed to encourage interagency collaboration and streamlining of permit processes with the aim of developing a "one-stop-shopping" approach where feasible.
- ***Recommendation:*** States should be encouraged to designate a single state agency to act as the lead agency for CO_2 storage-related licenses and permits.
- ***Recommendation:*** Encourage state and federal agencies to incorporate into their processes and systems expedited permitting/licensing procedures for small-scale research projects. Agency personnel need to better understand the goal of such research projects in the timely collection of knowledge so as to better educate federal and state policymakers.
- ***Recommendation:*** Partnerships going forward should establish timelines and communicate expectations as to those timelines with government counterparts.

Challenge #5: Achieving Stakeholder Buy-In

Lack of stakeholder buy-in has the potential to delay or prevent the permitting and/or licensing of an underground CO_2 storage project.

The IOGCC CCGS Task Force has previously noted the importance of active public and other stakeholder involvement in the process of developing both the laws and the regulations for CO_2 geologic storage and throughout the CCGS regulatory process. The experience of the Partnerships in the validation phase work continues to make clear that lack of public education, knowledge, and acceptance will continue to pose significant barriers to CCGS development nationally. It is a clear lesson learned or at least "lesson reiterated" that stakeholders need to be included in the process from development of the legislation through implementation of the projects. Without adequate efforts in this regard, even small-scale research projects can be delayed or "vetoed" by an unsupportive public.

- ***Recommendation:*** Incorporate stakeholder input in statute, rule, and regulation development and throughout the development of CCGS projects.
- ***Recommendation:*** Even if there is no formal process, stakeholders need to be engaged from the earliest stages in the planning of even small-scale research projects. This will certainly be true of the Phase III development phase projects.
- ***Recommendation:*** Stakeholder education is essential in building knowledge and acceptance. Misinformation needs to be neutralized with unbiased, scientifically based information. The participation of public utilities and public utility commissions in the dialogue needs to be encouraged.

Risk Assessment

Risks

"Risk is most commonly defined as the probability of an event that causes a loss and the potential magnitude of that loss. By this definition, risk is increased when either the probability of the event increases or the magnitude of the potential loss (the consequences of the event) increases." The risks considered in this report are directly related to the potential increases to the capital cost when beginning a project. These are risks that the managers of the SWP have recognized and have worked with. Here, a number of risks are discussed and some possible solutions to mitigate or prevent the loss posed by the risks are suggested.

Environmental Risks

Environmental risks are the risks that are specific to a location and can be posed by natural conditions, local manmade hazards, and local regulations. For example the losses as a result of these risks can be increased labor cost due to extended construction time, missed deadlines, delayed project start times, broken equipment and supplies and harm to personnel and the local residents and their property. Each of these losses can contribute to additional costs.

Environmental risks may include weather, wildlife restrictions, unlabeled or mislabeled pipelines, poorly maintained roads, and local regulations. The weather risks include flash floods, lightning, high winds, snow, ice and heat. Because of rain and snow causing the dirt roads to become very muddy the SWP found that there were regulations preventing or restricting travel to their sites because of wet conditions on the roadways. They also found that they were restricted from access to their sites during big game closures (elk mating season, in this case). Because of the regulations regarding the depth of rut formations in the road and the elk mating season, the project could be delayed. Lightning and the threat of flash floods delayed or interrupted work. Another risk they learned about was the potential of having mismarked or unmarked pipelines, which could be hit during excavation for new pipelines, or other buried equipment. There are also archeology sites that are protected and cannot be disturbed. Due to these factors, pipelines, well pads, road, and other construction may have to be rerouted.

Ways to address and work with environmental risks include asking specific questions about the wildlife, weather and any restrictions that they pose or that might be imposed by local agencies because of the wildlife and weather. The questions need to include changes due to different seasons in the behavior patterns of wildlife or regulations. When digging and constructing the pipeline and well close attention needs to be paid to plans and contingencies, and emergency plans need to be in place in case a loss or emergency does occur.

Legislative Risks

These are local, state, and federal policies that are present or that might change during a project. Policies can change that are helpful or less so during a project. These can be on a federal, state, or local levels.

Permitting Risks

The greatest risk posed by the permitting process is not filing for the permit early enough to allow sufficient time for approval, thus resulting in project delays. The SWP filed for all of the necessary permits except for one section of a permit of which SWP was unaware. Parts of the work had to be postponed, which caused some scheduling conflicts.

The best way to mitigate this risk is to be aware of all the necessary permits. This can be done by determining all local, state, and federal the permits that are required for similar projects. In addition to this, it is also important to know of any laws or regulations that have changed since the similar project was performed, creating a need for additional permits. Also sequestration is relatively new and in many locals the government authorities are not certain which organization will administer regulations for geologic sequestration and what these regulations are. For example whether a state's Oil and Gas Division or Environmental Division will oversee these activities. Thus time must be given to allow them to determine some of these items.

Contract Risks

Contracts are an essential binding agent that makes it possible for companies and individuals to work with each other. Contracts that are formed without proper preparation can have serious consequences.

The problems of this risk can be avoided. Time and effort for an adequate contract must be taken to ensure that requirements of the company as well as what they offer coincide with what is required by the DOE and the SWP. Additionally, clear specifications must be in the contract so issues can be worked out.

Equipment and Facilities Risks

The risks associated with the equipment and facilities are damage caused by accident, vandalism and adverse weather and also the failure of the materials forming the equipment and facilities. The best ways to mitigate these risks is to have policies in place that will ensure that safe practices are followed when working on the equipment and within the facilities. Policies should also be in place that ensures that the equipment and facilities are regularly inspected to identify early signs of failure.

Cost Escalation Risks

Costs can rapidly escalate due to a number of causes. One cause is the natural changes in the economy that can have large unexpected spikes. For example the 2007–2008 crude oil price shock increased the competition for limited resources for projects competing with oil and gas related items and work. Also at that time, China, the main supplier of work steel, had a massive construction projects related to the 2008 Olympics to be held in China, resulting in a spike in construction steel. Both were significant factors in escalating field construction costs. A second example is cost escalations due to unexpected losses resulting from the other risks. To mitigate these risks it is especially important to recognize that unexpected risks or losses can occur as a result of not being prepared for the outcome. With proper planning and preparation most risks can be identified and can be prepared for. The risks must be estimated so that contingency can be built into the project.

Scheduling Risks

When a schedule is being developed, a significant risk is scheduling conflicts that can then create other conflicts in a snowball effect. A realistic and somewhat conservative estimate of the time required for each step and a constant reevaluation of timing can significantly mitigate these conflicts. Some examples include:

- Correct estimates of lead time for equipment
- Permitting
- Obtaining construction crews
- Obtaining large work equipment such as drilling rigs

Specific Risks That Were Encountered by the SWP during Phase II

Public Perception

Perception of sequestration as a response to climate change. Many are very confused with this concept of climate change and how this has evolved from global warming and are skeptical. It is critical that scientific facts are used and to allow the audience to draw their own conclusions. It is also critical to establish that the sequestration projects are for proof of concept of sequestration, not to prove or disprove issues related to climate change, or even to demonstrate that sequestration is required. The purpose, which should be clearly relayed to the public, is to test the concept, develop sound engineering, estimate cost, and determine what additional resources are required.

Perception of CO_2 as a toxic substance. The publicity about the effects of increased CO_2 levels in the atmosphere has distorted perception of the toxicity of CO_2. The EPA has had much discussion of how to designate CO_2. Thus, the public does not adequately understand the benefits of CO_2 and the concentrations at which CO_2 has adverse health effects, versus the problems related to concentration in the atmosphere and climate effects. The designation of CO_2 as a toxin is potentially detrimental to the credibility of climate change control.

Surface disturbance. Any form of energy recovery requires surface disturbance for the exploitation of the resource or technology. The surface disturbances that will be incurred by geologic sequestration projects need to be understood and outlined.

Seismic activity. Passive micro-seismicity is a useful tool in tracking subsurface changes. The reporting of seismic events seems to be difficult for the public to understand. These events are perceived as earthquakes and thus are related to the large destructive events in the public's mind, instead of the below human detectable levels that are being seen.

Understanding information. The foregoing problematic areas point out the necessity to present facts, data and events in a manner the general public understands. It is important to present engineering and scientific facts without bias or distortion. Many people can rapidly detect whether facts are being presented in a manner to try to sway the public in a certain direction.

Financial

Operator related. While each of the operators in Phase II provided great support to the project, each had unique situations that affected the finances of the project. It was noted that the smaller companies could react to situations faster, but did not have the financial backing to be able to soak up price changes as well.

Economics. Through the experience of working with three hydrocarbon production companies (Resolute Energy, ConocoPhillips, and Kinder Morgan) covering a wide range of sizes, significant experience in project economics at a variety of scales has been obtained.

Aneth Field (UT) Risks and Outcomes

Earthquakes versus microseismicity. During the Aneth Field project the SWP monitored passive microseismicity. The area near the geophones was relatively quiet. This area had been waterflooded for a number of years. The injection/production of CO_2 and brine/oil, gas, CO_2, and brine over the time period of SWP tests was essentially a 1:1 volume ratio. The long history of injection and extraction at a near equilibrium input/output ratio is believed to be the cause of minimal microseismic activity near the geophones. At the onset of monitoring, there was activity

near the edges of the reservoir in area locations. This activity approximately doubled for a time (about one year) after a seismic event about 10 miles west of the reservoir on the order of 5 on the Richter scale. The events within the reservoir were in the -1 to -3 range on the Richter scale. This demonstrated the sensitivity of the geophones. The detected events at the edge of the reservoir occured where the producing formation is pinched off and thus may be a stress point that is more sensitive to changes in the oil formation or in the waste brine injection lower zone.

This also demonstrates the difference between microseismic activities in the reservoir and those caused by a significant geological event. It was also interesting to note that activity increased within the reservoir including oil production for about one year.

Characterization. It is interesting that, even with an oil reservoir that has been extensively studied for decades, there are surprises. It should be noted that an aquifer that will not have had extensive characterization and probably no injection or production history initially, should be expected to have additional surprises.

Change of heart by the operator on aquifer injection. The original proposal included an injection into the Leadville formation, a saline aquifer that had a well with several laterals for disposing of excess produced brine from the Aneth CO_2 EOR project. This is brine in excess of that required for injection into the oil reservoir alternating with CO_2 (WAG). Due to operational reasons, Resolute selected to curtail the CO_2 injection into the saline aquifer to about 100 tons. SWP did not believe the cost justified this small of an injection for the amount of information that would be provided, and thus this part of the project was cancelled.

Site selection (surface rights: Navajo nation vs State land vs Federal land). There were several considerations when the SWP was selecting the final site within the Aneth Field. The first was a location that had never been CO_2 flooded. There had been an earlier pilot in the area to test the concept and the first stage that Resolute referred to as Phase I had started. Resolute's Phase II on the western edge had not started nor was it near any previous flooding and thus was selected. The final location was also not on Navajo Nation lands and thus would have one less entity to required approval of all aspects of the tests and thus was selected.

Previous disturbance, production, waterflood, and brine disposal. As mentioned, the site was selected because it had not previously had CO_2 injection and thus the CO_2 plume would be more obvious. The passive microseismicity interpretation was not as straightforward because the area had previously been depressurized during primary production, repressurized during waterflooding, and was having brine injected in a lower formation (as indicated previously).

Operator: Resolute Natural Resources. Overall, Resolute was easy to work with. It is a relatively small company and decisions were made rapidly. The field and engineering personnel that SWP usually worked with were very helpful and responsive.

SACROC (TX) Risks and Outcomes

Change of site. Initially the project was planned to take place in the Claytonville field in the Permian Basin of west Texas. The operator determined it best to delay CO_2 injection, and thus it appeared this would not occur within the time frame of Phase II. The decision was made to move the project to the SACROC CO_2-EOR project. This had several advantages and disadvantages that required some rescoping of the project.

Advantages included:

- Thirty-plus years of CO_2 flooding, thus a good test for leak detection analysis.
- Tests for wellbore integrity
- Established infrastructure
- Could be completed within desired time frame of Phase II

Disadvantage included:

- Had previously had some CO_2 flooding in the pattern selected, thus more ambiguous to determine location of new CO_2 plume.
- Site already disturbed, years of injection of water and CO_2, 50 years of production.
- Private surface landowners. In Texas most of the land is privately owned, as are the mineral and probably the pore space ownership. Because of private ownership projects such as injection and laying pipeline involves many more parties, complicating things somewhat due to the increased number of contracts involved and the individual preferences of

each landowner. Additionally, in order to access a well or other facilities that are on private land, permission must first be given by the landowners.

Operator: Kinder Morgan. Kinder Morgan (KM) has been a big asset to our projects. Not only were they the operator for the Permian Basin project, but they provided CO_2 for the San Juan and Paradox Basin projects. In one case they provided CO_2 as about 70% cost share. There was a period where KM had provided a number of items/information to the EPA or another federal organization to aid in determining parameters for Cap-and-Trade. Something had happened that caused KM to believe this information was misused or misrepresented and used against the petroleum industry. Thus, because of this occurrence, KM management seemed cold toward the project and limited any additional tests at the site. The SWP had intended to run another CO_2 soil flux test series and probably another round of near-surface water sampling. These were either cancelled or no longer considered.

San Juan Basin (NM) Risks and Outcomes

Injectivity. Initially the injection planned by the project was supposed to be ~1.3 bcf (75,000 tons) over the life of the project. Due to several factors, the SWP was only able to inject 0.32 bcf (18,407 tons). These factors included the well not being initially stimulated, swelling of the coal as the CO_2 passed through, and the increased near-wellbore pressure.

Permitting

Injection well: The injection well, EPNG Com A INJ, was reported by the State of New Mexico to the EPA as a UIC Class V well, using the conditions (AOR, etc.) that they would use with a typical Class II CO_2 injection well.

Pipeline: The pipeline was over two miles long from an existing line to the injection site.

Well pad: The injection well was placed in a new location requiring permitting with the appropriate surveys.

MVA work: There were a number of items that had to be looked at for surveys, especially archeological surveys to make sure there were not disturbances of archeological items. These included the pipeline, well pad, VSP source locations, and tiltmeter installations.

Section 106: While laying the pipeline we became aware of Section 106 which requires that any project funded by federal money and carried out on lands Native Americans have used be reviewed and approved by any affected Native American tribes in a timely manner. This approval assures that no historical or cultural artifacts will be disturbed during the project. In this case seven tribes had passed through this area and needed to be contacted. Receiving approvals from each tribe took several months during which time the project could not continue forward.

Big Game and Weather Closures: During the winter of 2007, while the CO_2 pipeline was being laid from the main CO_2 line to the injection well, construction had to halt due to an unexpected routine closure of the BLM land due to the elk mating season (Dec. 15 through April 15). Shortly after this closure, an uncommon winter storm came through and precipitated several feet of snow. In order to reduce the damage to the roads caused by trucks creating deep ruts (> 6 inches deep), the BLM closed the area to non-essential work for a time.

Geology – 3 coal seams: Initially the plan for this project was to inject first into the lower coal seam and find out what kind of injectivity it would allow. Due to the late start because of the Section 106 and BLM land closures, it was decided to inject into all three seams simultaneously in order to reach the injection goal. Eighty percent of the injected fluids went into one coal seam (the lowest seam).

Stimulation: Typically, when drilling into coal, the formations are stimulated by allowing the pressure differential between the coal seam and the wellbore to cause the coal to slough off, creating a larger volume wellbore with a greater surface area for injectivity. This allows the fluid to flow into and out of the well more easily. Because this pressure in this coal seam had been depleted during gas production, there was not sufficient pressure to properly stimulate the well.

COP: The initial negotiations were with Burlington Energy, which then was purchased by ConocoPhillips. The transition was fortunately smooth, but this is a common occurrence in industry and is a potential risk and contract must be accordingly designed. Also as mentioned below due to promotions, retirements, etc. the personal changes frequently and leaves some memory voids.

Change of personnel

Promotions/reassignments. Within organization, especially corporations, promotions often entail assignment changes and locations. As an example COP changed the person in charge of the site at least three times in three years.

Employer change. There were a couple of cases of this. In one case, the individual changed employment and moved to Europe and thus did not have any association with the project. Another case was Dr. Brian McPherson, PI for SWP. He transferred to University of Utah, but maintained a part-time employment with NMT. Thus he was still involved, but his situation changed and the scope of work sufficient that NMT felt bringing on a Co-PI (Dr. Reid Grigg) would be advantageous.

Retirement. We had one individual retire from a company after another had died and the small company subsequently no longer had the capability to function and even closed their Albuquerque office. Thus their tasks were moved to another partner.

Death. As indicated in Retirement, a death can remove a capability from an organization and leave a void.

Family conflicts. One case occured where some deliverables (final report, data delivery) took a few months longer then expected because one of the primary researchers at one of the SWP partner institutes had a daughter in an accident, father hospitalized, and suffered a personal injury that required time off for an extended period. This was unusual, but not unprecedented.

Liability

Short Term. In any operation, liability during the operation must be accepted by someone. In oil, gas, and coal operations this is a normal practice of the operating company. In the cases for the Phase II geological sequestration projects, these were each a part of a large hydrocarbon extraction operation. In the two EOR projects CO_2 was or would be injected and there was nothing novel except maybe more extensive monitoring of the surface and subsurface. Thus the liability was taken by the operators. Even though CO_2 injection was not being done in the production of natural gas from coalbeds in the Pump Canyon area, the operators were interested in determining

if the injection of CO_2 into unminable coalbeds would be a good sequestration prospect and if it would increase methane production or, at minimum, not decrease or significantly contaminate the methane steam. They took on the liability.

In the case of injecting CO_2 into aquifers or depleted oil and gas fielda that will not have associated production, there will need to be sufficient financial incentive to cover the liability or at least, government taking on this liability.

Long Term. For CO_2 sequestration projects, even with EOR and ECBM taking place long after the production of hydrocarbons has ended, there is a question on how long liability will be required, to ensure there is sufficient proof that the CO_2 is staying in place to drop liability concern. How will this liability be covered? In the case of EOR and ECBM the operators have taken this liability, but the question exists, if something should occur in one hundred years, when the properties have passed through several hands and are no longer claimed by a company who will take the liability. At this time the liability should be low, but probably not zero. This will probably have to have some type of governmental oversite and a type of superfund financed by some funding set aside during the injection by those who were financially benefitted.

General Risk Procedures

During Phase II, the SWP developed a comprehensive risk assessment strategy, which it will continue to refine it during Phase III. Its primary components are:

- "Adaptive" - iterative modeling-monitoring approach for assessment of uncertainty
- Performance assessment: healthy/safety risks, economic and programmatic risks, and otherwise (Figure 171):

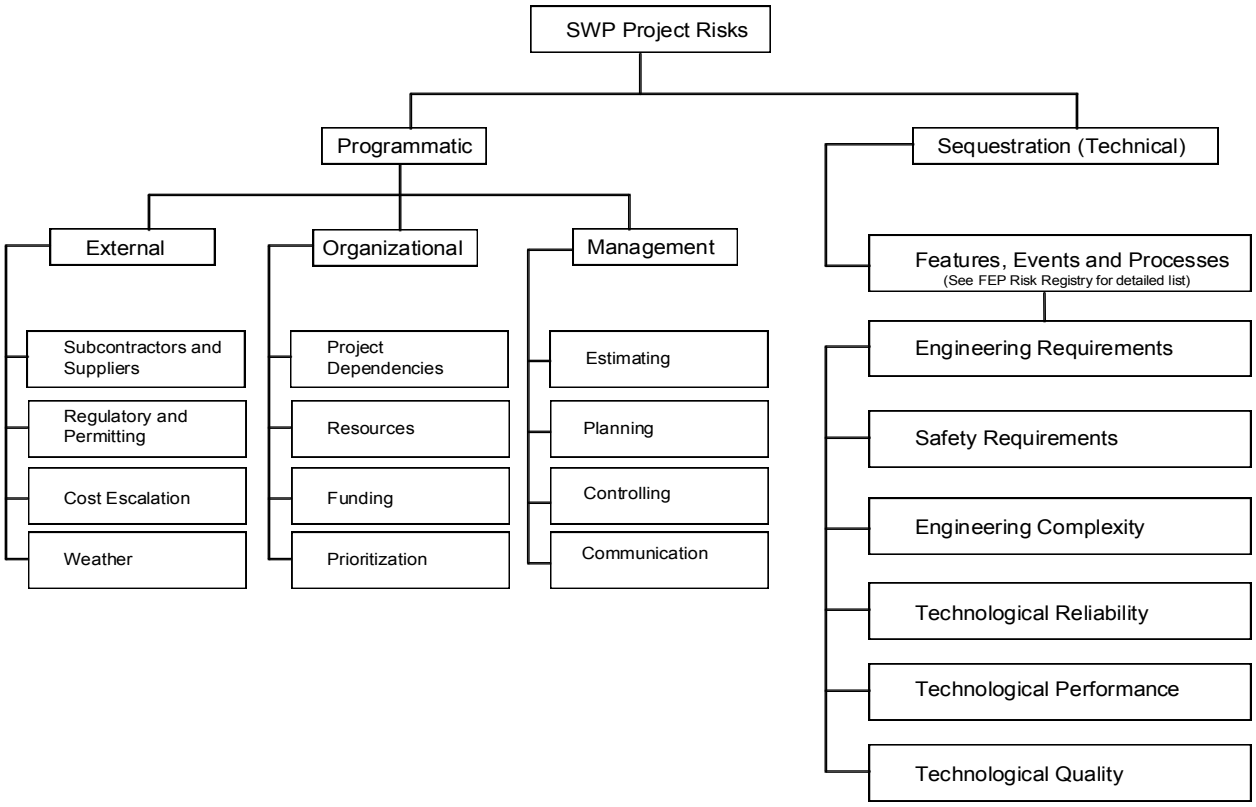

Figure 171. SWP Project Risk Tree

- Early "qualitative" risk assessment
  - site selection,
  - communicating project aspects to the public, and
  - aiding regulators in permitting projects.
- Quantitative risk assessment:
  - quantify risks (e.g., HSE, environmental, GHG emissions)
  - aid in developing monitoring and modeling plans for a sequestration site, and
  - to help evaluate additional information once project is started, in conjunction with monitoring and modeling.
- Features, events, and processes (FEPs)
  - leaky wellbores or faults for features,
  - injection pressure increases or microseismicity for events, and
  - gravity-driven CO_2 movement or residual saturation trapping for processes.
- From FEPs, consequences are identified, in conjunction with monitoring and modeling;

- We will quantify FEPs via probability density functions (PDFs) (Figure 172);
- RA is being conducted in close collaboration with NETL, EPA, and other RCSPs!

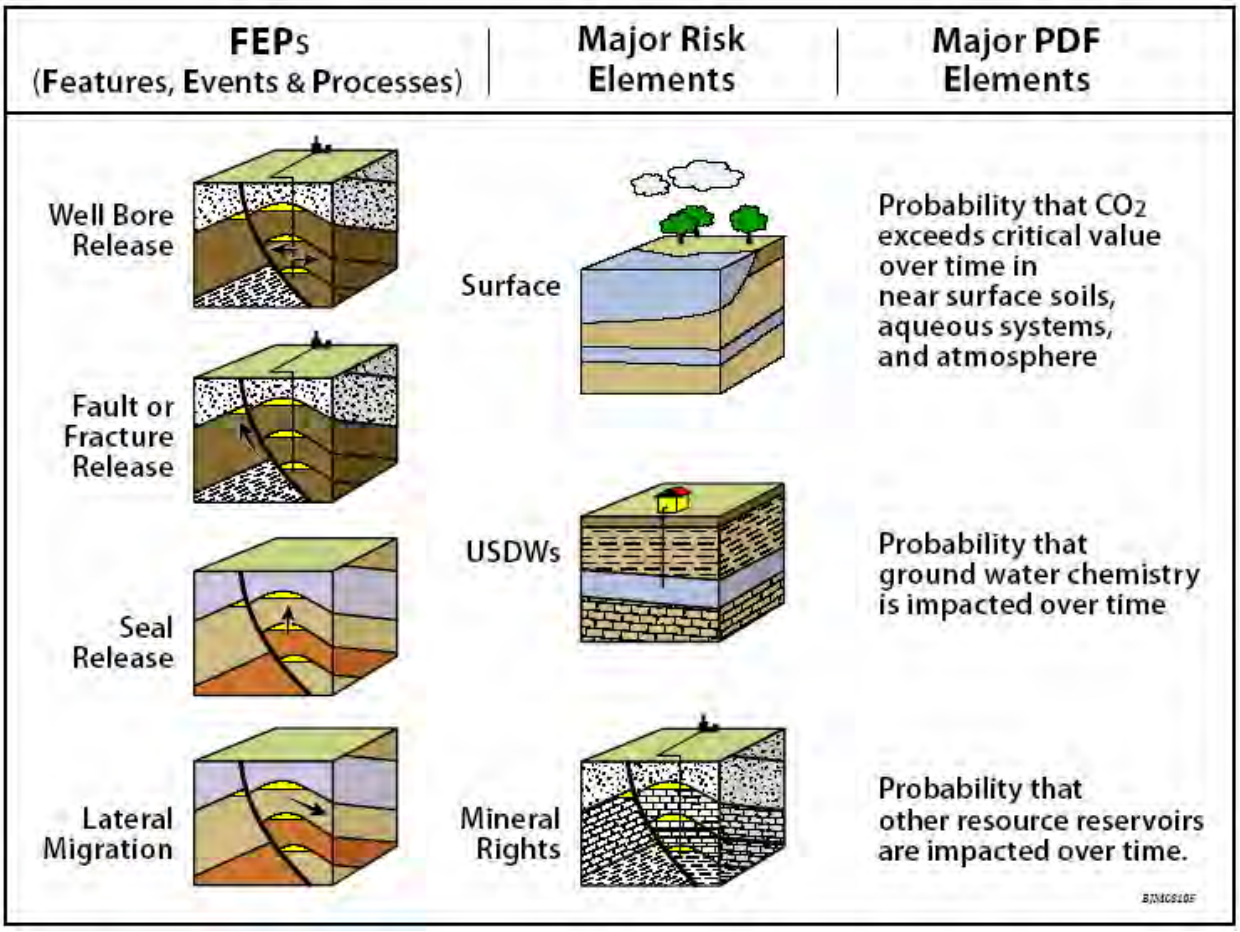

Figure 172. FEPS Risks and PDFs.

From Phase II: Iterative approach with monitoring and models (Figure 173):

- Initial info from site characterization and modeling, used to develop meaningful models
- Monitoring provides feedback
- Updated models provide updated risks

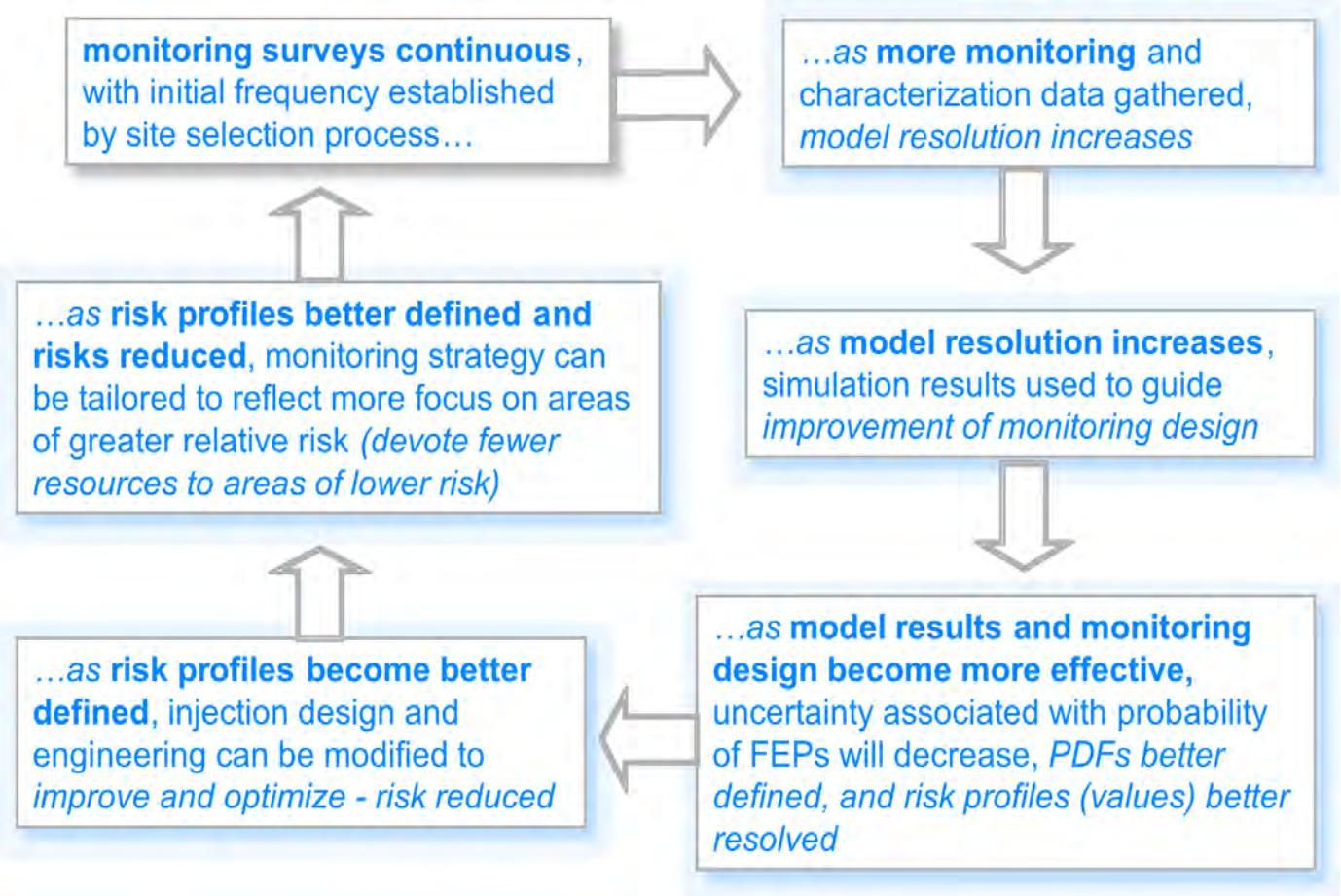

Figure 173. Iterative approach with monitoring and models.

Regional Technology Implementation Plans for Full Scale Deployment of Carbon Sequestration Technologies in the Partnership's Region

It is assumed that the USA will move forward with implementation of CO_2 sequestration to decrease anthropogenic greenhouse gas emissions into the atmosphere during the time of transitioning from a hydrocarbon to a renewable energy based economy. The mass of CO_2 produced even in the relatively sparsely inhabited Southwest Region of the USA is significant and will required extensive infrastructure development and enumerable sites to sequester carbon emissions. This section outlines what has been learned from Phases I and II that will facilitate the implementation of this endeavor.

Method of Project Selection

During Phase I both sources and sinks were identified and this information continues to be defined. During Phase II SWP had three geological and two terrestrial sequestration project sites; from these tests additional information has been gleaned to enable our development of a comprehensive sequestration plan. CO_2 sequestration opportunities are ranked by but not necessarily in this order:

a. Proximity to sources and/or pipeline infrastructure
b. Economics,
c. Safety, and risk mitigation potential.

The most convenient and practical "first opportunities" for geological sequestration lie along existing CO_2 pipelines in the region using oil, gas and/or aquifers below oil and gas fields. The Southwest Region is fortunate to have extensive existing infrastructure that presently has the capacity to transport and inject over 1.7 bcfpd CO_2 (~100,000 tons per day). About 100,000 tons of CO_2 per day are being transported and injected for enhanced oil recovery (EOR) within the SWP. Of this, about 25% is anthropogenic CO_2. This is equal to about 9 million tons per year. There are CO_2-EOR projects presently in Colorado, New Mexico, Oklahoma, Texas, Utah, and Wyoming, all within the SWP. All projects are in depleted oil reservoirs; though there is an abundance of natural gas, coalbed methane, and deep saline aquifers in the region. Though 75% of the existing infrastructure is used for natural CO_2, each of the pipelines are near existing and planned

large point sources of CO_2 emissions that include sources such as power, gas processing, fertilizer, and cement plants. These can be used in the future to replace and augment the natural resources presently being used.

Sequestration Opportunities

These are ranked in order of preference as oil (enhanced oil recovery, or EOR), terrestrial, saline aquifer, gas (enhanced gas recovery, or EGR) and coalbed methane (enhanced coalbed methane, or ECBM) reservoirs.

EOR with sequestration site. EOR is rated highest because of the abundance of location and the maturity of the technology.

- Advantageous geology with large proven sinks with required seals throughout the region
- Reservoirs at pressure and temperature where CO_2 displacement efficiency is high and ease of development of miscible displacement.
- Abundant anthropogenic CO_2 from plants near fields and/or existing infrastructure.
- Local companies with abundant expertise in transport, injection, and monitoring of CO_2 with at least 40 years of experience (first commercial project 1972 with pilots and studies started years earlier).
- Production of oil that will offset cost of sequestration and infrastructure.
- Local acceptance of similar endeavors, i.e. petroleum industry for over 100 years in many cases.

Terrestrial methods. Terrestrial opportunities, second-ranked, are everywhere. Items have been identified (vegetation, rotation, cultivation etc.) that could increase carbon utilization.

- Public acceptance. Improving such elements as vegetation and water drainage are seen as normal and low risk by the public.
- There is a limit to how much CO_2 can be sequestered. In an arid region such as the SWP, there is the danger of range/forests fires that can reverse years of sequestration. If fact, fire is part of the natural cycle, it must be considered, and has been found necessary for a healthy environment in many cases.

Deep saline aquifer sequestration sites. Deep saline aquifers are rated third because of the highest abundance of sites and capacity.

- Advantageous geology with large sinks throughout the region
- Many of the aquifers are situated below oil and gas reservoir that will function as backup sinks and proven seals with required seals throughout the region.
- Using aquifers linked with oil and gas reservoirs, the existing EOR infrastructure can be used and, as with the oil reservoirs, abundant anthropogenic CO_2 is located from facilities near aquifers and/or existing infrastructure.
- Local companies exist with abundant expertise in transport, injection, and monitoring of CO_2 with at least 40 years of experience for oil reservoirs (first commercial project in 1972 with pilots and studies started years earlier).
- A disadvantage for aquifers is that their reservoir characterization is much less mature than oil and gas reservoirs. This disadvantage can be compensated when using aquifers situated below the oil and gas reservoirs.
- Local acceptance of similar endeavors, i.e. petroleum industry, for 100 years.

EGR with sequestration site. EGR is rated fourth because though these reservoirs have proven seals the CO_2 technology has not been proven in the field. It is much less mature than EOR and the resource is less than aquifers.

- Advantageous geology with large sinks with proven seals throughout the region
- Many of the gas fields are situated near oil reservoir with existing infrastructure.
- As with the oil reservoirs abundant anthropogenic CO_2 is located from plants near aquifers and/or existing infrastructure.
- Local companies exist with abundant expertise in transport, injection, and monitoring of CO_2 with at least 40 years of injection experience (first commercial project 1972 with pilots and studies started years earlier).
- A disadvantage for gas fields is that the industry has been hesitant to use gas fields that are not completely depleted, fearing CO_2 will mix with the natural gas and be subsequently produced. The separation of the gases would be cost-inhibitive. Some recent in-

dication is that the mixing within the reservoir might be much less than anticipated; thus additional research and tests are required.

- Local acceptance of similar endeavors, i.e. petroleum industry, for 100 years.

ECBM with sequestration site. ECBM is listed last because the definition of unminable coal is changing with advancing technology and injectivity reduction experienced in Phase II in various partnerships.

- Advantageous geology and abundance in the region.
- Coalbeds with high methane content that could help offset cost.
- Abundant anthropogenic CO_2 from nearby power plants and/or existing infrastructure.
- Local companies with coalbed methane (CBM) and enhanced coal-bed-methane (ECBM) expertise. More detailed reservoir studies of local operators than those that are available in the literature.
- A significant disadvantage at this time is the injectivity reduction seen. This is thought to be caused by reservoir pressure buildup and swelling of the coals from the CO2.

Site Characterization

Any site must be sufficiently characterized before a project can be designed and implemented. A sufficient reservoir size and injectivity must be determined.

- Geological characterization (well logs, core data, pressure-transient data, and any other relevant information for the area).
- Historical hydrocarbon fluids and water compositional data.
- Well locations, completions and stimulation information, and production and operating histories.
- Sink characterization.
- CO_2 sources and pipeline distribution.
- Chemical characterization.
- MVA baseline.

Permitting Requirements

For region-wide implementation of geological sequestration, permitting must be in place and reasonable to facilitate implementation. There are existing oil and gas regulations in each state that can serve as a starting point for these. Some states have determined which organization will oversee permitting for geological sequestration. Also, a number of states have legislation in process to determine items such as pore space ownership.

(1) Colorado, Oklahoma, New Mexico, Texas, Utah, and Wyoming already have existing EOR injection and thus regulatory regimes handling CO_2 injection for EOR projects, which should streamline the permitting process for the geological sequestration projects. The terrestrial project would be permitted in accordance with USDA regulations.
(2) In Texas, CO_2 is currently being injected for EOR, and such activity is classified as Class II injection under UIC. Also, an industry partner for in SWP Phase II projects, Kinder Morgan, has extensive experience transporting and injecting CO_2, and is familiar with the permitting requirements. Converting from Class II to Class V (research) wells or Class VI (the new geological sequestration designation) well will require a significant effort.

Necessary Modeling

At best, field and laboratory data is insufficient for characterization even in reservoirs extensively studied. Core samples and outcrops, seismic data, logs with laboratory core tests, and field production and injection data all provide essential information. Even with the best data interpolation and extrapolation are required for history match. All predictions are extrapolations from what is known. Thus building a model and subsequent simulations are necessary. These include:

- Reservoir geological model,
- Fluid flow model,
- CO_2 injection and distribution,
- CO_2 storage capacity and transportation, and
- Chemical composition and reservoir fluids, injected fluids, and reservoir rock.

Monitoring Required

Surface and Subsurface. Spatial and temporal gaps in monitoring are significant, and our ability to minimize these gaps is a direct function of available budget. We recommend focus on improving ability to monitor the injection interval by optimizing 2-D seismic imaging methods rather than more expensive 3-D methods. It is believed that this offers a great deal of promise for improving plume monitoring. Efficacy of microgravity and other novel geophysical methods are being developed but not proven to this date. MVA used during Phase II, by site, include:

Aneth Field, Utah- EOR with Sequestration

- The testing of repeat vertical seismic profiles, VSP, proved to marginally successful.
- Passive seismic monitoring detected micro seismicity well over a mile from the geophone location. This indicated high sensitivity, but less effective in reservoirs that had had fluids produced and injection for decades.
- Tracers and production data for EOR wells indicated good indicator for EOR or other processed with production.
- Surface potential indicated promise, but not ready for deployment.
- Surface flux is a good indicator of CO_2 leaks, but tests in areas of known CO_2 emissions demonstrated that measurement may need to be at a spacially very high density.

SACROC, Texas-EOR with Sequestration

- Application and testing of 3-D seismic lines are significant in determining baseline data and with a repeat then having a 4-D survey. These should be effective though very expensive.
- VSP provide vertical separation and especially using a walkaway provide good plume identification.
- Water test in an area of almost 40 years of CO_2 injection, 50 years of water injection, and 80 years of oil production provide support of good seals and technology for sequestration exist.
- Surface flux was used to show no detectable CO_2 leaks at the surface.
- Production data is a good indicated for EOR/sequestration projects.

San Juan Basin, New Mexico-ECBM with Sequestration

- For ECBM VSP did not show any indication of a CO_2 plume. The plume was a gas at relatively low pressure, probably around 200 psi at the time of the repeat. This was replacing the natural gas at about the same pressure. It was hoped that he there would be sufficient change of the coal mechanical properties upon absorption of CO_2 to be distinguished from the baseline.
- Repeat logs also did not show much.
- Tiltmeters showed some change, but it was less than 0.5 inches. This was not surprising. Also the simulation indicated the high pressure zone extended less than a 100-ft radius from the injection area. The tiltmeters were on a grid 6 by 6 over a square mile and thus were space about 880 ft apart. Thus the closest tiltmeter to the injection well would be over 600 ft away. To see the changes from the plume, the grid should have been much tighter around the injection well. This area where injection and production were occurring with such low injection was probably too much to expect good resolution.
- Tracers were used and indicated good results. They were ahead of CO_2 breakthrough. This should be expected because CO_2 absorbs on to the coal, displacing natural gas with the tracer moving ahead with the displaced natural gas.
- Compositional changes at the production wells. Continuous CO_2 sensors were placed in the three nearest production wells to the injector. Also gas samples for full compositional analysis were obtained on 14 surrounding wells about every other month.

Outreach

- ***Public acceptance*** has continued to be a vital aspect of sequestration. In areas of present oil, gas, and/or coal production operations, acceptance seems to be good. The public has experience with similar operations, many working in the facilities. Thus they have developed some trust in these operations. In areas without a history of oil, gas, and/or coal more education and the development of trust is required.
- ***Public involvement*** as indicated is required to gain trust in the process. Allow the public to be involved or at least informed during the planning stages.

- ***Education*** is required to develop the understanding of the real risk compared to other risk the public has come to accept in other similar areas of their lives. Also, it is important to understand the process and how it will be mitigated if a problem should arise.

Regulatory, Permitting and Accounting Frameworks

The two EOR projects were in existing oil production field with existing facilities. The ECBM injection well and CO_2 pipelines were new and required a full permitting process. The process went smoothly as SWP learned what permit had to be obtained. There was one delay in complying with Section 106. This was not because it was particularly difficult, but that it had initially been overlooked, so it required slowing down or stopping construction while this was addressed. If Section 106 compliance had been taken into account, its impact on the timing of the project would have been minimal or been completed with the other permits. This demonstrated to SWP the importance of understanding all the regulatory, permitting, and accounting frameworks required early in the process so they all can be completed in a timely faction.

Public Outreach and Education

Improved Partnership Recognition

Logo Development

To improve recognizability for the Southwest Regional Partnership on Carbon Sequestration (SWP), a partnership logo was developed. The logo design is intended to be appropriate for both paper-based materials and electronic materials. Researchers "pilot-tested" several designs on groups of non-science oriented students and other personnel at Texas A&M University. In the end, they selected calming (blue and green) colors to signify the mitigation of global climate change that may be realized through carbon sequestration, and chose simple, cylindrical shapes to create clean lines that signify the value to be gained in joining with others throughout the country (in this case, other partnerships). These elements were combined into a stylized symbol for carbon dioxide.

Public Awareness Measurements

Earlier in 2007, two graduate students traveled to New Mexico to make contacts with residents in Aztec, Bloomfield, and Farmington. Using snowball sampling, they collected contacts throughout the region. Specifically, they inquired about community members who would be interested in participating in a series of focus groups that subsequently took place in the summer of 2007. They met with representatives from San Juan County, the small communities, and from a local NGO called the San Juan Citizens Alliance (a regional environmental and property rights watchdog organization). They also contacted local school districts to determine interest in participating in pilot testing of the educational material to be provided on the SWP website. The Farmington school district provided us with a letter indicating their interest in participating in the project.

A graduate student used GIS analysis to guide the selection of geographically and demographically comparable locations for focus group control locations. Demographic data was obtained from National Atlas and geographic data was obtained from USGS. Sites were chosen for their location, distance to an airport, population, and their designation as a county seat. In cases where multiple options existed, cities were chosen for socio-economic similarities. Focus group locations also were selected as near as possible to the pilot sequestration sites. Sites for focus groups

in Utah were the cities of Blanding, Bluff, Moab, and Monticello. New Mexico sites were Farmington, Bloomfield, Gallup, and Grants, and Texas sites were Midland, Snyder, San Angelo, and Sweetwater. Texas A&M University's Research Compliance Office granted researchers approval to hold focus groups in three states (Utah, New Mexico, and Texas) at the four locations chosen (two study locations, two control). Focus groups were for New Mexico in August 2007 and for Utah and Texas in September 2007.

Focus Group Interview Methods and Analysis

Participants for the focus groups and interviews were recruited through networking with leaders and decision makers of each community. Once interest in the research was established, researchers sent Southwest Regional Partnership on Carbon Sequestration letters of invitation reminding them about the project and explaining the purpose of the focus groups/interviews. Researchers also provided information on the location and dates of the sessions. This letter was followed up by phone calls and emails to ascertain willingness to participate. Sessions were held in publicly accessible locations, such as community centers or university premises, and lasted roughly an hour for individual interviews and two hours for focus groups. Since the focus groups and interviews were to be audio taped for later transcription, those unwilling to be taped were removed from the pool of potential participants without any negative consequences. Food and beverages were provided for focus group attendees. Focus group and interview participants discussed the following topics with a trained facilitator and support team:

(1) Definitions and understandings of climate change and carbon sequestration
(2) Experiences with the energy industry, carbon sequestration, and environmental issues
(3) Opinions of climate change and carbon sequestration
(4) Concerns, knowns, and unknowns about carbon sequestration.

Interview and focus group sessions were audio taped and are in the process of being transcribed and combined with field notes taken during the sessions. Dry-erase boards were also used during the focus group sessions to record group lists of the pros/cons as well as knowns/unknowns of carbon sequestration technologies. These notes were then added to the session's field notes. Surveys were also used to determine opinions about carbon sequestration and obtain demographic information.

To insure confidentiality during the transcription process, numbers were assigned to each speaker. After transcription, audio files of the sessions were destroyed, as dictated by the Texas A&M University Institutional Review Board. Transcriptions were then coded and results reported in aggregate form only.

The report detailing the focus group selection and survey results along with the survey is included in the appendix and is titled "Community Knowledge and Acceptance of Southwest Partnership Phase II Carbon Capture and Storage Projects".

Results from Interviews with Faculty and Graduate Students at Texas A&M University (Technically Literate Public)

This study has demonstrated a lack of consensus between departments as well as within departments on the issue of climate change. In the analysis of three departments within the scientific and engineering community at Texas A&M University, it was found that global warming is a problem viewed through numerous disciplinary as well as social lenses. Faculty and graduate students' fields of study impact how the issue is viewed. People in the Physics department tend to be split on the problem with little impact to their research. Members of Petroleum Engineering feel that their profession is under attack while at the same time they are trying to ensure a reliable energy source for the future. People in Ecosystem Sciences and Management are looking at an unstable future as ecosystems change with unprecedented speed.

Two out of the three departments also have a stake in the cases presented for and against human's impact on the environment, though both are already feeling the pressure of a mobilized society. As mentioned by all of the study participants, global warming has become not only an environmental problem, but also a political, economical, and social one. Our federal government is on the verge of passing climate change regulations limiting the amount of CO_2 that can be released into the air, a federal agency (Environmental Protection Agency) trying to determine how to regulate car emissions, and a handful of states, led by California, are attempting to lower their emissions by 2050. Individuals are choosing to drive hybrids, change their light bulbs to more efficient versions, purchase carbon credits, and work from home to avoid long commutes so as to

lower their carbon footprint. Even with a lack of consensus in the varied disciplines within the scientific and engineering communities, climate change has already created resonance within the United States, and as one participant stated, "We'll just have to see what happens…If there is global warming going on, and it's man-made, then we're in trouble!"

Research Experience in Carbon Sequestration (RECS)

EnTech Strategies, LLC (Pamela Tomski) improved partnership recognition through a variety of activities including the development of the SWP-Team web site and outreach materials targeted to media outlets and the carbon capture and storage (CCS) community.

A significant amount of partnership recognition by was generated by selecting the SWP to collaborate with the Research Experience in Carbon Sequestration (RECS), hosted three consecutive years (2008 – 2010) in New Mexico. RECS is the nation's premier intensive summer CCS education and training experience that fosters and advances education, scientific research, professional training and career networks for graduate students and young professional in the CCS field. The RECS / SWP collaboration offered an opportunity to showcase the SWP. Tomski selected SWP scientists for the RECS faculty and reserved a number of slots for participants from SWP member organizations. Over 30 representatives from the SWP were directly involved in the RECS / SWP collaboration and 100 + people toured the SWP Pump Canyon field site and conducted hands-on field CO2 monitoring with SWP team members. As a result, the SWP Pump Canyon project was featured in America's Power Factuality Tour, a web site dedicated to promoting leading national CCS activities (www.factuality.org). Tomski also produced RECS / SWP promotional materials (i.e. see attached sample poster, brochure and flyer) that were broadly distributed at exhibits in a number of national and regional conferences including:

- National Energy Technology Laboratory's Annual Carbon Sequestration Conference in Pittsburgh, PA (May 2008 – 2010)
- American Geophysical Union's Fall Meeting in San Francisco, CA (December 2008)
- Carbon and Climate Change Conference in Austin, TX (February 2009)

Separately, Tomski provided the PRRC with a number of graphic images from the RECS / SWP collaboration for use in additional SWP promotional materials, monitored news outlets for SWP

recognition and provided copies of articles and links to the SWP web master for inclusion on the SWP web site.

Quarterly Press Releases for Local Commercial Media

Researchers developed positive relationships with electronic and print media in eight communities in the Southwest Carbon Partnership region. Four communities were in West Texas and four were in Southwest New Mexico. A a press contact list was complied, which included electronic and print media sources as well as local television and radio stations in SWP research areas including locations in New Mexico, Utah, and Texas. The contact list was delivered to Pamela Tomski (EnTech Strategies, LLC) for use in producing press releases that were sent out during the quarter.

Methods

The press contact list was compiled by using Google and Yahoo! search engines; searching for press by community (e.g., all focus group communities) and by media type (e.g., newspaper, radio, television station, and community-based web pages) in the Southwest Carbon Partnership Region. Researchers used the website for the Center of Public Integrity (www.publicintegrity.org) to search for media as well. The website allowed searches for press by location, press type, and by ownership. Once media sources per community were identified, the Internet was used to gather contact information for each resource. In most cases, the researcher called the media source to confirm contact information and to introduce the research interests and needs of the partnership. When no phone number was provided online (such was the case with web-based news sources MyWestTexas.com and San Angelo Live!) the researcher made contact via email. Contacts were compiled into an Excel spreadsheet and provided to Outreach researchers, as well as Pamela Tomski at EnTech Strategies.

Results

Print and electronic resources contacted during the quarter included:

- Newspapers:
    - Midland Reporter-Telegram, Midland/Odessa, Texas

  - Sweetwater Reporter, Sweetwater, Texas
  - Snyder Daily News, Snyder, Texas
  - The Daily Times, Farmington, New Mexico
  - Gallup Independent, Gallup and Grants, New Mexico
- Electronic:
  - SanAngeloLive.com
  - MyWestTexas.com
  - GoFarmington.com
- Press release contact information:
  - TX Midland Midland Reporter Lauri Stone: 432.678.8887
  - TX Snyder Snyder Daily Times Wayne: 325.573.5486
  - TX San Angelo San Angelo Times 325.659.8311
  - TX Sweetwater Sweetwater Reporter Coleen: 325.236.6677
  - NM Farmington The Daily Times Leilani Usison: 505.325.4545
  - NM Gallup Gallup Independent Shanna Downey: 505.863.6811
  - NM Los Alamos Los Alamos Monitor Hope or Julie: 505.662.4185
  - NM Albuquerque Albuquerque Journal 505.823.3300
  - NM Aztec The Talon 505.334.1039
  - UT Blanding San Juan Reporter 435.587.2277
  - UT Moab Times Independent 435.259.7741
- E-Media Contact
  - NM Farmington GoFarmington.com chamber@gofarmington.com
  - TX Midland MyWestTexas.com Brian Sales: 325.687.8894
  - TX San Angelo San Angelo Live!
  - Karen@sanangelolive.com
  - Aggregate Media, LLC
  - Blue Mountain Panorama 435.678.3635
- Radio Station Contact
  - NM Gallup KGLP- NPR 505.863.7625 kglpradio@kglp.org
  - NM Farmington San Juan College-KSJE Connie Gotsch 505.566.3377
  - NM Aztec KWYK Sandy Green 505.486.1783

- UT Moab KZMU- Moab Public Radio 435.259.8824
- TV Station NM Farmington KOB-TV 505.326.1141
- UT Bluff KUTV http://www.kutv.com/Default.aspx
- TX Midland KMID Chris Pruitt 432.563.2222

Press Release Information Updated

Tomski updated the media fact sheet, prepared a number of press releases for distribution to regional media outlets (attached) and followed up with targeted media contacts.

Included in the appendix are the following fliers and brochures:

- SWP Media Fact Sheet (updated May 2010)
- SWP Press Release: August 15, 2008 – "CO_2 Storage Project Begins in the Southwest"
- SWP Press Release: July 15, 2009 – "A New Generation of Scientists and Engineers Being Trained in the Southwest to Deploy Carbon Capture and Storage Systems"
- SWP Press Release: April 20, 2010 – "The Southwest is Home to the Research Experience in Carbon Sequestration 2010"

Interactive Website Available to Public

The original website was primarily aimed toward Phase I activities. For Phase II (Fig. 174) new ideas were implemented including restructuring the website to allow easier navigation, providing more information and partnership links, providing web space for technical and site teams, adding information about membership categories, and incorporating educational activities (with supplementary curriculum materials for teachers) and tools (i.e., carbon counter, interactive map). After attending the design meeting, researchers contacted interested parties within and outside of the partnership for assistance in the new website design and interactive programs (e.g., games and interactive models), including the hiring of a software engineer. They also researched national and state science curriculum standards to determine what grade levels would be

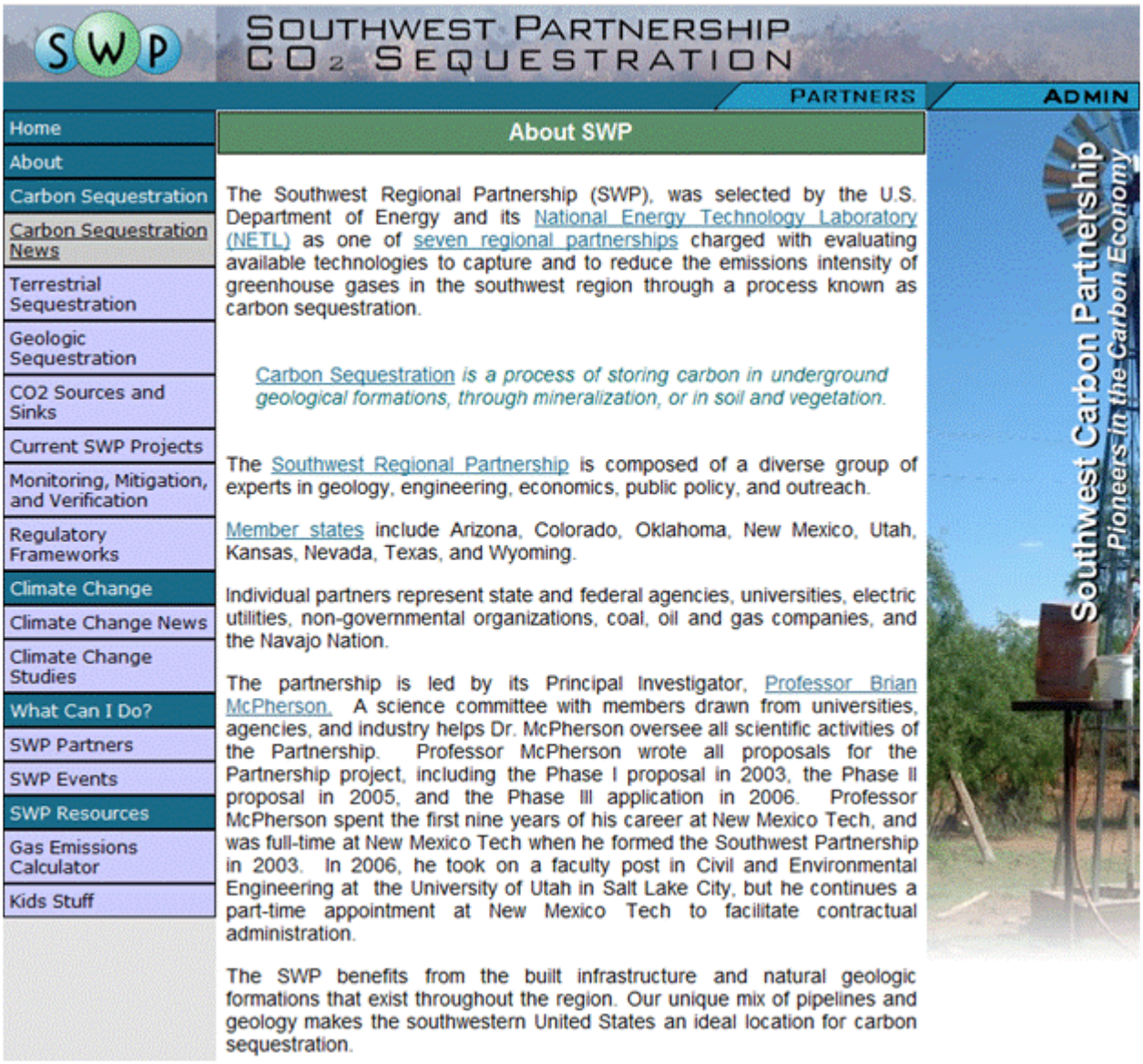

Figure 174. http://southwestcarbonpartnership.org/AboutSWP.aspx

appropriate to target for SWP's educational materials and interactive programs. Researchers corresponded extensively with the website designer via email, and held two teleconferences with him. A later phone conference was held to discuss an appropriate host for the website, as well as issues like capabilities, design, and content. Following this teleconference, the web designer came to Texas for a face-to-face workshop focusing on the new website design, including interactive programs. The first day of our workshop comprised a discussion of revisions to the old website design and layout, which portions of the website should be accessible to the general public, and which should be accessible to partnership members only through the use of password entry. Workshop participants also explored ways partners could update their own sections of the

website, how site managers could update the information regarding their pilot sequestration sites, and how all researchers could share information by uploading and downloading files onto the website.

The second portion of the workshop was held in Austin, TX, where researchers met with Mark Holtz (manager of a partnership site) at Texas BEG to discuss interactive program ideas, including web-based games. This session focused on developing two online games focusing on different sequestration technologies. Each game centers on a different age group, with one game for youth under the age of 12, and the other for youth 12 years and up. The first game had a James Bond theme (Carbon Bond, 00C), taking players through the process of capturing carbon in a factory setting, transporting, and storing the carbon using the EOR method. The second game, called Sim Factory, allows its players to set up their own carbon sequestration systems and maintain them through one simulation to determine success of their efforts, which are valued in carbon credits. Besides working on the games, researchers revised some of the interactive graphics our web designer had developed, and incorporated appropriate text to explain each step of the process.

A graduate student designed and developed GIS figures and maps of the SWP region and for the three carbon sequestration test sites located near Aneth, Utah; Midland, Texas; and Aztec, New Mexico. Data were collected from http://seamless.usgs.gov and other organizations. Email correspondence with Emily Love at DOE provided shapefile data for site-specific location information, The maps were sent to the web designer for posting on the newly designed website.
All presentations from SWP meetings were provided to the web designer for posting to the web site.

SWP Team Website

To supplement the SWP website and offer recognition to SWP team members, Tomski developed and produced the SWP Team web site: www.swp-team.info (attached). The primary purpose of the web site is to provide biographical sketches of SWP team members that highlight their role and accomplishments in the partnership, list key SWP or CCS publications and presentations. The web site also provides a graphics and image library of the SWP field sites, a master

,SWP publications list from all the team members and a list of news articles that feature the SWP or its team members (attached). Furthermore, the web site includes a list of all SWP partnerships with links to their organizations' web site.

The approach to the web site development was to prepare in draft 54 biographical sketches of SWP members for their review and comment. Of the 54 biographical sketches, Tomski received feedback and approval to post 34 to the swp-team web site. These bio sketches were prepared in both HTML and print format.

Tomski undertook all web site content development, production and hosting and will maintain and update the site *pro bono* for a one-year period.

Basic outline of information included on website

Carbon Sequestration

The need for a large, nationwide-scaled carbon sequestration program is explained. It is explained both in text as well as in two videos which are linked to within this webpage. Frequently asked questions are included which answers basic questions about carbon sequestration including questions about its safety, legality and how it works in general. Several links are also included pointing to many sites explaining in depth the subject of carbon sequestration.

Carbon Sequestration News

Links for over sixty news articles related to carbon sequestration are listed on this page along with summaries of or quotes from each article.

Terrestrial Sequestration

A brief explanation of what terrestrial sequestration is and how it relates to the sequestration projects.

Geologic Sequestration

A brief explanation of what geologic sequestration is and how it works. Also on this webpage is an animated picture showing how CO_2 is injected to produce water and oil.

CO_2 Sources and Sinks

Several maps are included which show the distribution of CO_2 sources and sinks throughout the region covered by the Southwest Regional Partnership. Also maps are also included showing

where the oil and gas reservoirs in the region are as well as the locations most suited for terrestrial sequestration. Charts are shown which show the amount of CO_2 produced in each state, the coalbed methane capacities and oil and gas reservoir capacities along with explanations of each.

Current SWP Projects

A brief introduction to the SACROC, San Juan Basin and Aneth projects are given.

Monitoring, Mitigation, and Verification

How and why the SWP monitors the changes in the formations as the CO_2 is injected is explained.

Regulatory Frameworks

A list of each of the regulatory frameworks that the SWP abides by is listed along with links to the actual regulations and explanations of each of the regulation bodies.

Climate Change

An animated graphic of a chart shows how the average temperature of the planet could change in the next 100 years. The link to a video explaining what global warming is included along with descriptions of what climate change means. Additional links are included which point at sites containing more information on climate change.

Climate Change News

This webpage includes over 15 links to news regarding climate change and regulatory and legal issues relating to it.

Climate Change Studies

Several studies are described relating to climate change as well as links to the reports and related websites.

What Can I do?

Several suggestions are given for reducing the amount of pollution as well as reducing the amount of CO_2 in the atmosphere by individuals.

SWP Partners

This webpage lists the partners of the SWP with links to each of their websites.

SWP Events

This webpage lists the events and upcoming meetings sponsored by the SWP.

SWP Resources

Many resources are available for printing and viewing in this webpage. These include the SWP atlases, brochures, fact sheets, information from the United States Carbon Sequestration Council, the International Energy Agency and the Keystone Center. There are also links to the Intergovernmental Panel on Climate Change and NETL's Carbon Sequestration Technology Roadmap and Program Plan and Atlas of the US and Canada.

Gas Emissions Calculator

Links to carbon emission calculators both for personal carbon footprint calculations and also for vehicle emission calculations are provided.

Kid's Stuff

The Adventures of Carbon Bond and the National Energy Technology Laboratory Entrance Exam were created as an educational experience for youth to learn about the dangers of carbon dioxide and other pollutants. The Adventures of Carbon Bond is a short adventure story written in flash animation.

Library of Interactive CO_2 Sequestration Tutorials Available to Public

Youth Internet Activity. The Adventures of Carbon Bond narrated story and game was designed and posted on the Internet within the website (Fig. 175).

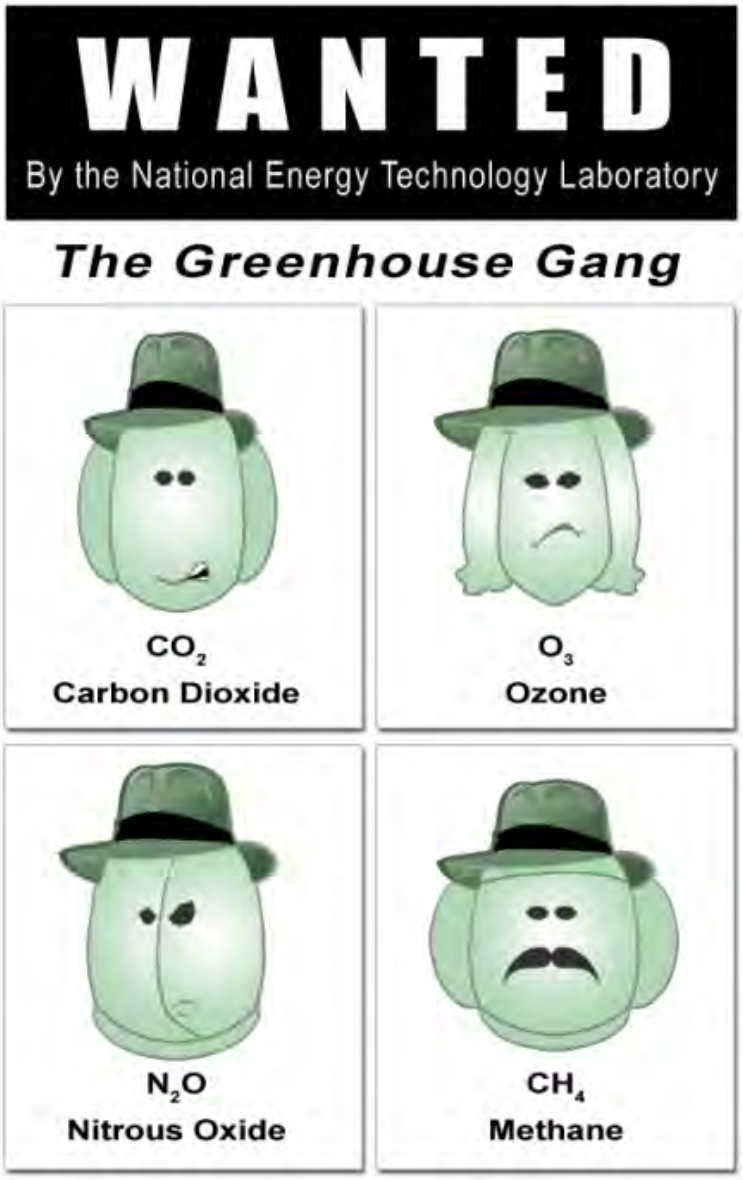

Figure 175. http://southwestcarbonpartnership.org/KidsStuff.aspx

SWP Documentary and NETL Video Projects

Researchers traveled to Aneth, Utah to film VSP survey activities scheduled on July 8, 2008. In addition to VSP, they collected general footage and images of people in the communities of Bluff and Blanding as well as historic cultural sites and landscapes for the partnership documen-

tary and NETL video on MMV. Feldpausch was also able to make connections with members of these communities for the Utah focus groups mentioned above.

Leigh Bernacchi is editing video footage taken by Jodi Minion, Damon Hall, and Feldpausch at the San Juan Basin site with the assistance of Conoco Phillips and the Aneth site with the assistance of Resolute, Los Alamos labs, and Baker Atlas.

New Mexico Teacher Training

SWP Outreach worked with the Keystone Center to arrange for a SWP hosted training course titled "CSI: Climate Status Investigations" on September 25th and 26th of 2008. In addition to materials prepared by the Keystone Center, Feldpausch and Dawn Thorne (University of Utah) gave presentations on the Southwest Partnership. They shared with the science teachers a variety of SWP outreach materials, complete with demonstrations and activities. The training was held in Roswell, New Mexico. The latest version of the Adventures of Carbon Bond story and game is under the *Kids Stuff* button on the SWP website:

(http://www.southwestcarbonpartnership.org/KidsStuff.aspx).

Printed Materials for Distribution at Community Events: Basic Science Brochure and CO_2 Sequestration Brochure

In September 2006, researchers developed a brochure that was presented at the SWP Safety Training and Project Review as part of the Public Outreach Committee review presentation. The brochure cover displayed the SWP logo, and the contents included a brief introduction to the partnership, descriptions of the field validation tests by site, a current membership list, and information on how to become a member. Because the first brochure did not explain the SWP in language that would be generally accessible to a lay audience, and did not use images taken from our region, it was discontinued by the end of 2006 and replaced with a brochure targeting the general public. The new brochure describes carbon sequestration as a practical technology for mitigating global warming, and focuses on the role of the SWP in helping make the technology an economically viable alternative. Researchers pilot-tested the text, revising several times, until a version was produced that the general public could readily understand and found interesting.

Photos from the three pilot sites and other nearby locations were used in the brochure. Final edits were also made to the new SWP brochures, which were printed in time to distribute at the April 18 SWP meeting in Austin, where partnership members (and our advisor) were invited to suggest alterations for the next printing of the brochure.

Earlier in the project, Outreach Group researchers provided text for the SWP section of NETL's North American Carbon Sequestration Atlas. This text was also used as the basis for a set of briefing papers to be distributed to interested stakeholders. One paper was written to attract members of the interested, but not necessarily technically trained, public, informing them of what carbon sequestration is and why it is considered a feasible option for mitigating human-induced carbon emissions. A second paper was directed at people involved in non-fossil fuel related industries to encourage them to consider investment in carbon sequestration technologies.

Other Written Material

- Text and design of three fact sheets on the topics of geologic sequestration, terrestrial sequestration, and the Farnham Dome site, as well as a briefing paper on geologic sequestration for industry.
- Text and design for a Frequently Asked Questions (FAQs) paper and the Southwest Partnership Atlas (with the assistance of the Utah Automated Geographic Reference Center (AGRC) for maps and EGI for pictures and editing).
- Updated content in the SWP Phase II brochure. Fact sheets, briefing papers, FAQs, and brochures were printed at Copy Corner in College Station, Texas and the SWP Atlas was burned to CDs for disbursement.
- Text, pictures, and figures for the second National Carbon Sequestration Atlas. This material was submitted to the Department of Energy.

Mediated Model Constructed Collaboratively With Interested Public

Although an outline was developed for the mediated modeling workshop held earlier in 2007, the modelers with whom SWP researchers had partnered in this effort were not able to engage in

mediated modeling. The workshop was revised and recast as an opportunity for interested stakeholders to view a demonstration of a model that had been developed by SWP researchers, and to provide feedback to the researchers. The workshop also attempted to provide participants with a more systemic view of carbon sequestration by engaging them in a systems thinking game, designed by Jessica Leigh Thompson.

Regulatory Information for State and Local Entities

PacifiCorp, a major utility in the western United States, convened an IGCC Working Group. The purpose of this group is to create a forum for industry, regulators, and citizens to discuss the merits of building an IGCC plant. They asked the SWP to provide an information overview of the partnership's activities, as carbon sequestration is a complementary technology to IGCC. This meeting occurred on July 6, 2006 at PacifiCorp's offices in Salt Lake City with tele- and video-conference links to PacifiCorp's headquarters in Portland, OR. Brian McPherson and David Curtiss attended. McPherson presented an overview of partnership activities followed by ample discussion of CO_2 sequestration and other environmental activities in the region.

Partnership researchers at the University of Utah facilitated a session on regulatory permitting issues at the SWP Farmington meeting in early August. IOGCC provided an overview of IOGCC Phase II Carbon Capture and Geological Storage Regulatory Task Force activities. The discussion then proceeded to regulatory and permitting issues facing the three pilot projects. The operators were currently handling permits covering the wells, but there was a need for assistance to SWP researchers who were conducting tests that require separate permitting. The Partnership participated in a meeting convened by NETL Pittsburgh with the Environmental Protection Agency to review the guidance that EPA is preparing for geologic sequestration activities outside of EOR.

The IOGCC Phase II Carbon Capture and Geological Storage Task Force convened its second meeting in early September 2006 in St. Louis, MO. The task force created three separate work groups to facilitate progress. They include the Alpha Work Group, which focuses on site charac-

terization and operation, the Omega Work Group, which focuses on site closure and abandonment issues, and the Regulatory Group, which is composing specific legal language for the proposed rules. Partnership researcher David Curtiss attended the meeting, participating in the Alpha Work Group and working on the current draft of proposed regulations.

Mr. Curtiss met with John Baza, Director of the Utah Division of Oil, Gas, and Mining, to discuss the IOGCC task force activities, the guidance that EPA is developing for carbon sequestration in saline formations, and the impact of these activities on carbon sequestration in general and specifically on the SWP pilot projects. Actions of the EPA have greatest impact on our saline formation test in the Aneth project. Mr. Baza provided some potential contacts with the appropriate Utah regulatory agency.

Mr. Curtiss also provided the NETL Outreach Group an overview of EPA and IOGCC activities on the September 21, 2006 conference call. Outreach will be critical in the adoption and acceptance of any resulting model regulations.

Finally, SWP collaborators with the Western Governors Association participated with California and Eastern and Midwestern States to implement a Multi-State Greenhouse Gas Registry that can be used to track emissions for voluntary and mandatory state programs. Information from the meeting was shared with the SWP and other western CCS Partnerships.

Summary of the Keystone Center Teacher Training

The Southwest Regional Partnership sponsored Climate Status Investigations; a teacher training at the McGillis School in Salt Lake City. The training was developed and delivered by The Keystone Center. Climate Status Investigations is a curriculum for middle-high school students designed to "broaden the scope and quality of national science education with a balanced, non-biased, comprehensive, and interdisciplinary approach to the study of an issue pivotal to our students' generation - global climate change" (Keystone Center Website). The curriculum was developed in partnership with the U.S. Department of Energy and the National Energy Technology Laboratory. The training course filled to its maximum of 30 teachers quickly with 15 teachers

remaining on the waiting list. Teachers who participated in the training event came from several schools along the Wasatch Front: American Fork (2), Bingham (1), Harrisville (2), Kaysville (3), Kearns (1), Layton (2), North Ogden (1), Riverton (6), Salt Lake City (4), West Jordan (7), and West Valley City (1). They represented the counties of Davis, Salt Lake, Utah and Weber. The training was offered at no cost for the participants, and included covering the costs of transportation, and substitute teachers. All of the teachers received 13 hours of re-licensure points that can be used towards applying for a teaching license renewal in the State of Utah. SWP researchers asked Keystone to investigate ways that teachers could also get University Credit or USOE Credit/Professional Staff Development Credit. As a result, teachers had the opportunity to receive one semester upper level class of University Credit issued from Utah State University for participation in the training at a subsidized rate ($30.00). Eleven teachers chose to receive University Credits. Teachers also received a set of lesson plans and other materials from the Keystone Center that can be used in their classrooms. Out of this training, 18 teachers signed up to be on the Southwest Training Center list serve for K-12 teachers and 13 signed up to participate in the pilot tests for The Adventures of Carbon Bond 2.0 game. Teachers expressed interest in future trainings, field trips with researchers from EGI at Utah sites, and other curriculum materials. Due to teacher interest in and the waiting list for the course, there is high demand for another Keystone training or other training opportunities for teachers in Utah.

SWP Staff Observations on Teacher Training Session

- Many teachers mentioned that they have large class sizes and are teaching multiple subjects within and outside of science.
- Due to limited school resources, teachers are interested in receiving curriculum materials, other teaching materials/equipment, and trainings (especially if offering continuing education credits) from outside sources if made available.
- Though these materials are sought after, there may not always be opportunities to use such materials because of standardized testing demands placed on teachers.
- Teachers are interested in materials that are considered fair and unbiased, referring to the science as well as the social. This applied to the subjects of climate change and carbon sequestration.

- Teachers had a lot of questions about the science behind carbon sequestration and its risks and social ramifications.
- Though carbon sequestration was something new to many teachers, all teachers had some experience with teaching concepts related to the capture and storage of CO_2 in oceanic, terrestrial and/or geologic systems.
- Some teachers found carbon sequestration to be an interesting research topic for their students in the form of classroom activities, field trips, and/or science fair projects.
- Some teachers expressed interest in fieldtrips and other opportunities/materials on the subject of carbon sequestration. This would include interacting with researchers at the University of Utah and Texas A&M University on carbon sequestration activities in the state.
- A few teachers mentioned that their colleagues did not get their paperwork for the training in on time and missed an opportunity to participate. There were teachers on the waiting list for the training (~15 teachers). This demonstrates an interest for having another Keystone Center training or other trainings (the offer of earning continuing education credits is preferred).

Publications and Presentations by Outreach Researchers

Publications

1. Stephens, J. C., E. J. Wilson, and T.R. Peterson. 2008. Socio-Political Evaluation of Energy Deployment (SPEED): An integrated research framework analyzing energy technology deployment. *Technological Forecasting and Social Change* 75: 1224-1246.
2. Feldpausch, A. M., B. J. McPherson, and T. R. Peterson. 2008. SWP CO2 sequestration atlas. Southwest Regional Partnership on Carbon Sequestration.
3. Feldpausch, A. M. 2008. The adventures of Carbon Bond online game. http://www.southwestcarbonpartnership.org/KidsStuff.aspx.
4. Bradbury, J., I. Ray, T. R. Peterson, S. Wade, G. Wong-Parodi, and A. M. Feldpausch. 2009. The role of social factors in shaping public perceptions of CCS: results of multi-state focus group interviews. Energy Procedia, 1: 4665-4672.
5. Wilson, E. J., J. Stephens, T.R. Peterson. 2009. Carbon capture and storage in context: the importance of state policy and discourse in deploying emerging energy technologies. Energy Procedia, 1.

6. Tollufson, L., S. Greenberg, J. Bradbury, D. Daly, S. Hanson, G. Garrett, T. Peterson, A. Parker, R. Myhre, M. Stone and S. Wade. 2009. Public outreach and education for carbon storage projects best practices manual. U.S. Department of Energy National Energy Technology Laboratory. DOE/NETL-2009/1391.
7. Feldpausch-Parker, A. M. 2010. Clean Coal *in* SAGE eReference Green Series. Sage Publications, Thousand Oaks, California, In Press.
8. Feldpausch-Parker, A. M., R. Chaudhry, J. C. Stephens, M. Fischlein, D. M. Hall, L. L. Melnick, T. R. Peterson, C. J. Ragland, and E. J. Wilson. 2010. A comparative state-level analysis of carbon capture and storage (CCS) discourse among U.S. energy stakeholders and the public. Energy Procedia, In Press.
9. Ragland, C. J., A. Feldpausch-Parker, T. R. Peterson, J. Stephens, and E. Wilson. 2010. Socio-political dimensions of CCS deployment through the lens of social network analysis. Energy Procedia, In Press.
10. Daly, D. J. Bradbury, G. Garrett, S. Greenberg, R. Myhre, T. Peterson, L. Tollefson, S. Wade, and N. Sacuta. 2010. Road-testing the outreach best practices manual: applicability for implementation of the development phase projects by the Regional Carbon Sequestration Partnerships. Energy Procedia, In Press.
11. Feldpausch-Parker, A. M. 2010. Communicating carbon capture and storage technologies: opportunities and constraints across media. Unpublished doctoral dissertation, Texas A&M University, College Station, TX.
12. Feldpausch-Parker, A. M., C. J. Ragland, L. L. Melnick, R. Chaudhry, D. M. Hall, T. R. Peterson, J. C. Stephens, and E. J. Wilson. 2011. Spreading the news on carbon capture and storage: a state-level comparison of US media. Science Communication, In Review.

.

Safety Program Development

Based on the safety training conducted at the three geologic sequestration test sites, SWP researchers developed a safety presentation that takes the safety trainings from each of these sites and combines them into one comprehensive training program.

Site operators are responsible for the safety of those who work on their sites and they are also liable if any accidents occur. In order to reduce the number of accidents and to better insure the safety of the workers and visitors that are on their sites the workers and visitors are required to attend safety classes. These safety classes are designed to instruct the workers and visitors in what hazards are present at each site as well as how to mitigate the danger each poses. These classes further teach how to react to different possible emergencies that might arise.

Safety meetings were mandatory and required annually at the Aneth, San Juan Basin and SACROC sites. It was recognized that at some point it may be necessary for the SWP to implement its own safety meetings prior to going out on sites if either the site operator did not have a safety program in place or if the SWP felt that additional training should be given to its members who are not accustomed to working in the field. A safety presentation was developed that takes the safety trainings from each of these sites and combines them into one comprehensive training program.

Several different formats for trainings were used at the SACROC, Aneth and San Juan Basin sites. The most common method was by lecture with PowerPoint slides supplemented by professionally filmed movies about specific topics. In a few cases site specific movies produced by the site contractor were shown in place of the lecture. Also a few of the training courses consisted no more than having the participants read the series of slides usually used during the safety presentation and then signing a roster. The trainings lasted between ten minutes to four hours. The trainings were typically not consistent between visits to the same sites, for example, at one site the training one year lasted about ten minutes, the next year about two hours and then the final year about four hours. Online training was not used by any of the site operators primarily due to the fact that most contractors and visitors were onsite long enough for training.

The safety training developed for the SWP is designed to be used in any setting. A standardized video can be recorded and then watched for the training. PowerPoint slides and lectures can be designed directly from the outlined training. Due to the nature of the SWP's geographical distribution and the added expense of paying for additional accommodations while taking onsite safety classes, online classes have become more promising economically.

Online safety training can be hosted by one of the many safety training hosts online. These hosts typically will help design the safety training in to a slide or video fashion. Once it is designed the students can log in and take the classes. Once the classes are taken a record can be made of the time and class taken. This information can then be supplied to the site operators and SWP supervisors for monitoring and liability reasons.

It is therefore recommended that for future projects three different characteristics be observed when working with future site operators in choosing a safety class for SWP members to take. The first is that there are records kept at a central location with access given to SWP managers and site operators. Second is that a more unified structure for the class be designed so that the length of time and topics covered will be more consistent. And the third, the ability to take a class off-location, is also important due to economic and time constraint reasons.

Requirements for Safety Orientation Courses

These are items that are not site-specific.

Introduction to Site and Area

- This section will give general information of the area, county and other related information

Company

- This section will give general information about the company including:
    - Size
    - Operations
    - Number of wells, pipelines and any other interesting or pertinent facts

Safety Introduction or Credo

- Most companies have their safety code that they live by. This can go here.

Local Hazards

Each area and location presents hazards that are unique and can elevate the risk of harm to personnel and damage to equipment. Before entering new and unfamiliar areas personnel should be aware of local hazards and how to best reduce the hazards to a reasonable and acceptable level. Some of the hazards present in working in desert areas and in an oil or gas field are as follows:

- Snakes
- Lightning
- Flash Floods

Common Hazards

In addition to local hazards there are typical industry hazards that can be expected to exist.

H_2S

- Properties
    - Known as sewer gas, hydrogen sulfide, rotten egg gas and stink damp
    - Invisible
    - Heavier than air
    - Soluble in water, oils and most organic liquids
    - Corrosive
    - Flammable
- Exposure
    - Up to 10 ppm averaged over 8-hour day (NIOSH)
    - Up to 50 ppm for 10 minutes if no other exposure occurs during the day
    - 100 ppm or more is immediate danger to life or health
    - Enters by inhalation
- Symptoms
    - Apnea, coma, convulsions, irritated eyes, conjunctivitis pain, lacrimation, photophobia, corneal vesiculation, respiratory system irritation, dizziness, headaches, fatigue, insomnia, GI disturbances
- Personal Protection and Response
    - Wear and know how to use an H_2S monitor.

  - If alarm goes off or H_2S is smelled evacuate area upwind or uphill.
  - Test air in low laying and enclosed areas before entering.
  - Turn off H_2S supply if safe and possible.
  - Use breathing apparatus if available or hold breath while escaping.
- First Aid
  - Eyes: Flush eyes.
  - Frostbite: Rinse with plenty of water, do not remove clothing.
  - Inhalation: Give victim fresh air and let rest in half upright position. If artificial respiration is needed do not do it mouth-to-mouth.
  - In all cases consult a doctor.

CO_2

- Properties
  - Known as carbon dioxide, carbonic acid gas or dry ice.
  - Colorless gas
  - Odorless
  - Heavier than air
- Exposure
  - Up to 5000 ppm
  - Enters by inhalation and skin or eye contact
- Symptoms
  - headache, dizziness, restlessness, paresthesia; dyspnea (breathing difficulty); sweating, malaise (vague feeling of discomfort); increased heart rate, cardiac out-put, blood pressure; coma; asphyxia; convulsions; frostbite (liquid, dry ice)
  - Targeted organs: respiratory and cardiovascular
- Personal Protection and Response
  - Turn off CO_2 supply if safe and possible.
  - Use breathing apparatus if available or hold breath while escaping.
- First Aid
  - Frostbite: warm exposed area using clean water
  - Breathing: give respiratory support

Other Hazards

- Lead exposure– Primarily in paints and primers. Sandblasting may expose you to lead. Check with operating companies.
- Asbestos may be present in:
    - Gasket material
    - Equipment insulation
    - Koch (ACM/PACM) may be present in blue shed, flooring, doors, & insulation in walls
    - ACM (Asbestos Containing Material)
    - PACM (Presumed Asbestos Containing Material)
- Benzene exposure - found primarily in condensate (oil)
- Pesticides, solvents, CO, and acids may be present
- Fiberglass fiber exposure
- Ergonomics - repetitive motion and awkward body positions
- Noise exposure – Hearing protection shall be worn in all posted areas and areas where the noise level can harm your hearing.
- Welding fumes – Welder and helpers must be aware of welding and cutting fume exposures

Agencies Regulating Site

For improved safety each site operates under standardized regulations. These regulations come from the federal, state, county and city governments as well as from the operating companies responsible for each of the sites. Those working on a site should be aware of and understand the regulations. Some of the regulatory agencies include:

- Department of Transportation
- OSHA
- Others?

Everyone Is Responsible for Safety

Personal Safety

Each person is responsible for their own safety. These responsibilities include:

- Making sure they have had the proper training and has been made aware of the possible hazards and risks associated with the current work duties
- Refusing to work on projects they have not been adequately trained on or that is unsafe

- Asking questions until he/she is fully prepared to perform the required tasks
- Ensuring that prior to beginning work all risks and hazards are managed to an acceptable level
- Being aware of emergency equipment on site and how to use them. The emergency equipment may include:
    - Fire extinguishers
    - Eye wash stations
    - Showers
    - MSDS sheets
    - First aid stations
- Making sure working area is clean and free of tripping hazards
- Learning the Emergency Response Plan

Buddy System

The **buddy system** is a procedure in which two people, the buddies, operate together as a single unit so that they are able to monitor and help each other. In adventurous or dangerous activities, where the buddies are often equals, the main benefit of the system is improved safety: each may be able to prevent the other becoming a casualty or rescue the other in a crisis. When this system is used as part of training or the induction of newcomers to an organization, the less experienced buddy learns more quickly from close and frequent contact with the experienced buddy than when operating alone. This concept is also applicable to minimize tool setup time. (http://en.wikipedia.org/wiki/Buddy_system)

- When working onsite employees are required to be accompanied by another properly trained employee.

Team Safety

A team is a group of two or more people. Working in teams is necessary to reduce job time, increase experience on the job, and increase efficiency. Working in teams can also lend to a safer working environment as each employee acts in the safe interests of others as well as his/her own self.

- Supervisors are responsible for
    - Ensuring employees are properly trained and have been made aware of the potential risks and hazards present in the work place

  - Ensuring that employees comply with industry best practice standards, company standards, and any applicable laws and regulations
  - Ensuring that risks and hazards have been mitigated to an acceptable level
- It is everyone's responsibility to take reasonable action when unsafe practices or conditions are observed. These actions may include:
  - Asking questions, voicing concerns and discussing possible solutions
  - Stopping the work and contacting the appropriate supervisor
  - Correcting the hazardous problem
- Short Service Employees
  - Employee with less than six months experience with the industry and current job functions
  - Short Service Employee must be accompanied by an experienced employee
  - Short Service Employee must be identifiable as such
- Employees must be current on their first aid and CPR training
- Job Safety and Scope Meeting
  - Prior to beginning a job all personnel involved must attend a meeting that discusses the scope of the job, the risks and hazards present and how accidents can be prevented.
  - Change in conditions and risks be discussed and reviewed by all personnel involved
  - Change in job scope or procedures should be discussed and approved
  - This meeting must detail emergency evacuation routes, muster points and cell phone coverage

General Rules

- Non business friends and family should not be allowed on premises during operating hours
- Cutting or gathering firewood is prohibited
- Crossing of private land when not on company business is prohibited
- Picnics or barbeques on field locations without prior approval is prohibited
- Ensure tools are maintained and inspected regularly
- Do not work or drive when fatigued or impaired by alcohol or medications

- Machine guards must be kept in place at all time except during service
- Use the right tool for the job and use it properly
- Defective, damaged, modified or homemade tools shall not be used
- Keep all areas clean and free of obstructions and trip hazards
- Do not open or close wells, open or close valves, change settings on or adjust equipment or instrumentation or operate any facility or equipment unless authorized to do so

Accident Prevention

Accidents happen usually without warning and at any time. With reasonable foresight, thought and proper training nearly all accidents can be avoided. Accidents usually happen when personnel become complacent, lazy, and do not follow proper procedures.

Fire

- Smoke only in designated areas
- Smoking is not allowed within 100 feet of the well or within the rig guy lines
- Use fire extinguisher to put out small fires or to escape a fire
- Make sure that the proper fire extinguisher is used for the type of fire being put out
- Lighters and matches are not permitted on site

Prohibited Items

- Illegal Drugs
- Firearms
- Weapons
- Explosives
- Alcoholic Beverages
- Pets
- Jewelry
- Matches and Lighters

Medical Information

- Medical conditions affecting the ability to properly perform the work must be reported to the supervisor.
- Medical conditions that may affect job performance and especially personnel's safety should also be reported to the supervisor including allergies and using contact lenses.

- Any medications that can potentially impair judgment, cause drowsiness, or affect personnel's work in anyway should be reported to the supervisor.

Vehicle Operation

- Drivers must have the proper licenses.
- Obey laws including wearing seat belts and speed limits.
- If speed limits are not posted a limit of 30 mph will be observed.
- Park were backing up is not necessary. If backing up is necessary park so that the first move is forward.
- When backing up use a spotter or if a spotter is not available visually check the area before backing up.
- Vehicles transporting hazardous substances must have the proper tags and signs and the driver must be properly licensed and trained.
- Cell phones must not be used by the driver when the vehicle is in motion unless a hands-free device is used.
- Avoid contact with power lines.
- Accidents must be reported as soon as possible.
- Do not pick up hitchhikers.
- Respect livestock and other animals in the area.

Permits

Permits are a communication tool. Permits communicate to the worker the type of work that can be performed. They allow supervisors to review and approve the work. And they communicate the type of work that is being performed to any others who are or may become involved with the work.

- Work permits are issued to ensure persons are aware of the scope of the job and hazards and safe operating procedures are identified. Contractors must ensure that operator specific permits and procedures are followed. Additional PPE requirements should be noted on the permits.
- The proper permits for the work must be obtained prior to starting the job. These permits may include:
    - Hot work
    - Confined space entry

  - Lock out/tag out—energy control
  - Lifting
  - Excavation and trenching including One Calls
  - Pressure testing
  - Blinding
  - Equipment opening
  - Cold work permit
- All employees involved with the work should review the work permit and job conditions prior to starting the job.

Personal Protection

- Personnel must wear clothing that is suitable depending on the weather, working conditions, and the environment. Those who work around moving machinery must not wear:
  - Neckties
  - Long hair or beards that are not safely tied back
  - Neck chains
  - Gloves that fasten around the wrist
  - Baggy or loose clothing or anything that could easy be caught in the moving machinery.
- Clothing that becomes saturated in flammable substances or skin irritants should be taken off and cleaned to avoid injury.
- Personal Protective Equipment (PPE)
  - Minimum Requirements:
    - Sleeved shirt and long pants made of natural fibers such as cotton
    - Hard hat
    - Safety glasses with side protection
    - Safety toed shoes
  - Flame retardant clothing (FRC) when appropriate
  - Other PPE that may be required
    - Hearing protection
    - Face Shield
    - Gloves

- Personal H_2S monitor
- Goggles
- Fall protection
- Respiratory protection
- Four Gas Monitor (O_2, H_2S, LEL and CO)

Special Work Clearance

- When digging with power equipment a One Call should be placed to identify buried pipes and wire lines
- Conducting work within 100' of power lines is prohibited unless procedures for safe work are identified and approved by appropriate personnel.

Working around Electricity

- Employees should meet OSHA requirements and be qualified when working around electrical lines or energized equipment
- A minimum of ten feet separation should be maintained when working around power lines
- Vehicles and equipment must maintain at least a four foot clearance from overhead power lines

Material Safety Data Sheet (MSDS)

A **material safety data sheet** (MSDS) is a form containing data regarding the properties of a particular substance. An important component of product stewardship and workplace safety, it is intended to provide workers and emergency personnel with procedures for handling or working with that substance in a safe manner, and includes information such as physical data (melting point, boiling point, flash point, etc.), toxicity, health effects, first aid, reactivity, storage, disposal, protective equipment, and spill-handling procedures. MSDS formats can vary from source to source within a country depending on national requirements.
(http://en.wikipedia.org/wiki/Material_safety_data_sheet)

- Personnel must have an MSDS for each chemical on location
- MSDS books are at the local field office for all chemicals located in the field

Emergencies

Defined

- An **emergency** is an unexpected and difficult or dangerous situation, especially an accident, which happens suddenly and which requires quick action to deal with it.—Google Dictionary
- Typical emergencies might include:
    - A ruptured pressurized pipeline
    - Snake bites
    - Release of hazardous material
    - Fire

Emergency Action Plan

- Site specific plan detailing
    - Muster points
    - Emergency procedures
    - Emergency agencies to contact and how to contact them
    - Evacuation Routes
    - Description of alarm signals
    - Operator contact information
    - Who to report to during an emergency

Reporting an Emergency

- Emergencies should be reported as soon as possible
- They should be reported to both the site supervisor or operator and emergency response personnel
- All incidents including injuries, first aid administered, vehicle accidents, near-misses, thefts, vandalism and spills are to be reported immediately

Muster Points and Evacuation Routes

- A muster point is a safe predetermined location to which all personnel should gather during an emergency
- An evacuation route is the safest and most direct route away from an emergency to a muster point

- Muster points and evacuation routes should be discussed in the safety briefing prior to starting work
- Muster points and evacuation routes may change depending on wind conditions and the nature of the emergency
- Maps or location descriptions should be provided to each employee for the muster areas and evacuation routes

Sign in/out of Facilities

- A central location should be designated for a roster of personnel currently in the facilities
- Prior to working personnel should sign in with the date, time, type of work and location where he/she will be working
- When leaving he/she must sign out
- During an emergency this list will be used to determine where personnel are and if they could potentially need help

Responsibilities for the Environment

The environment the sites are located in include the wildlife, people, land, air, water. When working on a site particular attention needs to be paid to protecting the environment and keeping it clean and safe.

Spills

- All releases and spills must be reported as soon as reasonably possible
- Every effort should be made to prevent releases or spills
- Spills should be cleaned up as soon as possible

Waste

- All waste is the responsibility of the personnel generating the waste and must be disposed of properly
- Anything that is brought onto a site that becomes trash must be taken out

General Environmental Requirements

- Be courteous to land owners
- Respect all right-of-ways
- Keep gates closed even if they were found open
- Do not feed or harass wildlife

- Do not remove nests or harass birds
- Use every reasonable means to prevent wildlife from being trapped in excavations or other facilities

Documentation of Training

- Training documentation should include
    - Name of employee
    - Employer
    - Birth date
    - Date
    - Signature
- Training documentation should be made available to the company that owns or operates the site, the employee taking the training, the training institution and the supervisor of the employee
- This information should be easily accessible
- Reminders should be sent out informing the trainee that the training has expired and that before reentry to the site occurs additional training should be taken

Safety Course Presentation Formats

Lecture

- Lecturing is probably one of the most beneficial forms of training because there is direct student-teacher involvement
- Questions can be directly asked
- It can be expensive because frequently a teacher must be hired as well as more extensive training materials
- Safety training can be contracted out to a local university or safety organization

Video

- Videos are beneficial because they are relatively cheap—ranging from about $100-1000 dollars
- They are usually more entertaining and visually stimulating than lectures
- On the downside they lack the student-teacher interaction and it is more difficult to ask questions

Hands-on Training

- Hands-on training is the most beneficial method, but is typically impractical and expensive

Online

- Online training is good for a number of reasons
    - It is interactive
    - It can show movies
    - It is possible to communicate with teachers online
    - After the initial cost of setting up an online training system the cost of maintenance is minimal
    - Online training can accommodate trainees from across the world
    - The process of keeping records and documentation is automated
    - The cost for additional trainees is minimal
    - Nearly everyone has access to the internet
    - Training can be taken at more flexible times

Other Topics

- JSA Form
- Lone Worker
- Truck flags
- Cameras
- Extension cords

Technology Transfer

Topical Reports Submitted to NETL

Advanced Resources International, Inc. (2010) Pump Canyon CO_2- ECBM/Sequestration Demonstration, San Juan Basin, New Mexico. Houston, Texas.

Angerer, J., and Brown, J. (2010). Regional Terrestrial Pilot. Texas A & M University, Campus Station, Texas.

Chidsey, T.C. (2009) Surface and Subsurface Geological Characterization of the Aneth Unit, Greater Aneth Field, Paradox Basin, Utah. Utah Geological Survey, Salt Lake City, Utah.

Feldpausch, A. (2010) Community Knowledge and Acceptance of Southwest Partnership Phase II Carbon Capture and Storage Projects: Focus Group and Survey Results. Texas A & M University, College Station, Texas.

Han, W-S., Esser, R., Thorne, D., and McPherson, B. (2009) Principal Reservoir Description Associated with Geology and Oil Production History in SACROC, Site of 35 Years of CO_2 Injection. University of Utah, Salt Lake City, Utah.

Harris, M. (2010) Validation and Comparison of Carbon Sequestration Project Cost Models with Project Cost Data Obtained from the Southwest Partnership. New Mexico Institute of Mining and Technology, Socorro, New Mexico.

Heath, J., McPherson, B., and Dewers, T. (2010) Natural Tracers and Multi-Scale Assessment of Caprock Sealing Behavior: Preliminary Findings from a Case Study of the Kirtland Formation, San Juan Basin. Sandia National Laboratories, Albuquerque, New Mexico.

Heath, J., McPherson, B., and Dewers, T. (2010) Natural Tracers and Multi-Scale Assessment of Caprock Sealing Behavior: A Case Study of the Kirtland Formation, San Juan Basin (expanded). Sandia National Laboratories, Albuquerque, New Mexico.

Interstate Oil and Gas Compact Commission Task Force on Carbon Capture and Geologic Storage, Bliss, K., Bengal, L., and Tew, B. (2010) Biennial Review of the Legal and Regulatory Environment for the Storage of Carbon Dioxide in Geologic Structures. Interstate Oil and Gas Compact Commission, Oklahoma City, Oklahoma.

Rutledge, J. (2010) Geologic Demonstration at the Aneth Oil Field, Paradox Basin, Utah. Los Alamos National Laboratory, Los Alamos, New Mexico.

Xiao, C., ed. (2011) SACROC North Platform in the Permian Basin, West Texas. New Mexico Institute of Mining and Technology, Socorro, New Mexico.

Presentations, Workshops, and Publications

Allis, R.G., Bergfield, D., Moore, J.N., McClure, K., Morgan, C., Chidsey, T.C., Jr., Heath, J., McPherson, B. "Implications of results from CO_2 systems for long-term monitoring," Proceedings Volume, Fourth Annual Conference on Carbon Capture and Sequestration, May 2-5, 2005, Alexandria, VA, p. 1367-1388.

Amman, L. Rachel (Project Director, lead research and analyst, lead author) Groundwork interactive state regulatory website, IOGCC, (2009), http://groundwork.iogcc.org/topics-index/carbon-sequestration.

Amman, L. Rachel (Project Director, editor.) IOGCC CCGS Task Force Phase II Biennial Review of the Legal and Regulatory Environment for the Storage of Carbon Dioxide in Geologic Structures, IOGCC, (September 2010).

Amman, L. Rachel (Project Director, editor.) A Policy, Legal, and Regulatory Evaluation of the Feasibility of a National Pipeline Infrastructure fro the Transport and Storage of Carbon Dioxide, IOGCC (January 2011).

Boutt, D. F., Cook, B. K., McPherson B. J. O. L., Williams, J. R. "Direct simulation of fluid-solid mechanics in porous media using the discrete element and lattice-Boltzmann methods," Journal of Geophysical Research, Vol. 112, 2007. B10209, doi:10.1029/2004JB003213.

Bradbury, J., I. Ray, T. R. Peterson, S. Wade, G. Wong-Parodi, A. M. Feldpausch. "The role of social factors in shaping public perceptions of CCS: results of multi-state focus group interviews." Energy Procedia, 1: 4665-4672, 2009.

Bromhal, G. S., Sams, W. N., Jikich, S., Ertekin, T., Smith D. H. "Simulation of CO_2 Sequestration in Coal Beds: The Effects of Sorption Isotherms." Chem. Geol., 217, (3-4), Pages 201-211, 25 April 2005.

Bromhal, G.; Gorucu, F. B.; Jikich, S.; Sams, W. N.; Ertekin, T.; Smith, D. H. "Effects of Gas-Induced Shrinkage and Swelling on Economics for Sequestration of CO_2 in Coal Seams"; 4th Annual Conference on Carbon Sequestration, Alexandria, VA, May 2005.

Bromhal, G. S., W. Harbert, P. Stauffer, H. Visnawathan, D. Wildman, R. Pawar, B. Strazisar, B. Kutchko, G. Guthrie. "Risk Analysis of Sequestration at SACROC" International Geological Congress, Oslo, Norway, Aug. 6-14, 2008

Bromhal, G. S., W. Harbert, B. McPherson, M. Deo, P. Stauffer, W. Carey, B. Strazisar, B. Kutchko, H. Viswanathan, D. Wildman, R. Pawar, and G. Guthrie. "Understanding the impact of the level of characterization on long-term performance predictions at geologic CO_2 sequestration sites" IARU Climate Change Congress, Copenhagen, Denmark, March 9-11, 2009.

Bromhal, G. S. "Lessons Learned in Geologic Sequestration" Plenary talk, SPE E&P Environ-

mental Conference, San Antonio, TX, March 23-25, 2009.

Burcu, G. F., Jikich, S., Bromhal, G. S., Sams W. N., Ertekin, T., Smith, D. H. Effects of matrix shrinkage and swelling on the economics of enhanced coalbed methane production and CO_2 sequestration in coal. SPE Reservoir Evaluation and Engineering, Vol. 10, No.4, Aug. 2007.

Carney, S., Morgan, C., and Vanden Berg, M. "Structural Analysis of Aneth Field, Paradox Basin, southeastern Utah: A Carbon Storage Study site of the Southwest Regional Partnership for Carbon Sequestration [abs.]," American Association of Petroleum Geologists, Rocky Mountain Section Annual Meeting, p. 35, 2007.

Carney, S. "Carbon dioxide sequestration demonstration project underway in Utah!," Utah Geological Survey Survey Notes, v. 41, no. 3, p. 10-11, 2009.

Carvalho, A. and T. R. Peterson, eds. "Discursive Constructions of Climate Change: Practices of Encoding and Decoding;" special issue of Environmental Communication: A Journal of Nature and Culture 3: 2, 2009.

Cheng, A., L. Huang, J. Rutledge. "Time-lapse VSP data processing for monitoring CO_2 injection", The Leading Edge, 29 , no. 2, 196-199, 2010.

Chidsey, T.C., Jr., Allis, R.G., McPherson, B.J., Heath, J., Malkewicz, S.E., Groen, W. "Characterization of Greater Aneth field, Paradox Basin, Utah, for sequestration – influence of risk and mitigation requirements on monitoring strategies [abs.]," Proceedings Volume, International Symposium on Site Characterization for CO_2 Geological Storage, March 20-22, 2006, Berkeley, CA, p. 109-113.

Chidsey, T.C., Jr., Allis, R.G., McPherson, B.J., Heath, J., Malkewicz, S.E., Groen, W. "Aneth oil field, southeastern Utah – demonstration site for geological sequestration of carbon dioxide [abs.]," Briefing Book (ID #046), 5th Annual Conference of Carbon Capture & Sequestration, May 8-11, 2006, Alexandria, VA, non-paginated.

Chidsey, T.C., Jr., Eby, D.E. "Why modelers need to look at the rocks! – examples from the Aneth oil field, Southwest Regional Partnership on Carbon Sequestration demonstration site for geologic sequestration of carbon dioxide, southeastern Utah [abs.]," Briefing Book (ID #013), 6th Annual Conference of Carbon Capture & Sequestration, May 7-10, 2007, Pittsburgh, PA, non-paginated.

Chidsey, T.C., Jr., Eby, D.E., Laine, M.D., Dempster, J.T. "Why modelers need to look at the rocks! – examples from Greater Aneth field, Paradox Basin, Utah [abs]," American Association of Petroleum Geologists, Rocky Mountain Section Meeting Official Program, p. 35, 2007.

Chidsey, T.C. Jr. "Reservoir Properties and Lithofacies of the Pennsylvanian Paradox formation (Desert Creek Zone) from Greater Aneth Oil Field," a mini-core workshop for the Rocky Mountain Association of Geologists and Petroleum Technology Transfer Council Southern Paradox Basin field trip, September 19, 2008. Bluff, Utah.

Chidsey, T.C. Jr. "Petroleum Geology and Potential CO_2 Sequestration in the Pennsylvanian Paradox Formation, Greater Aneth Oil Field", a core workshop for graduate students, Geology 525: Petroleum Systems Analysis, Brigham Young University Department of Geological Sciences, December 1, 2008, Provo, Utah.

Chidsey, T.C. Jr. "Carbonate Sequence Stratigraphy of the Pennyslvanian Paradox Formation, Greater Aneth Oil Field", a core workshop for graduate students, Geology 574: Advanced Stratigraphy, Brigham Young University Department of Geological Sciences, April 13, 2009, Utah Core Research Center, Salt Lake City, Utah.

Chidsey, T.C., Jr., Carney, S.M., Heath, J., and Dewers, T. "The Gothic shale from Greater Aneth oil field, Paradox Basin, southeastern Utah – seal for hydrocarbons and carbon dioxide geologic sequestration [abs.]," American Association of Petroleum Geologists Annual Convention Abstracts, v. 18, p. 42, 2009.

Chidsey, T.C., Jr., Carney, S.M., Morgan, C.D. "Geological site characterization of the Aneth unit, Greater Aneth field, southeastern Utah, for sequestration of carbon dioxide – a project summary [abs]," American Association of Petroleum Geologists, Rocky Mountain Section Meeting Program with Abstracts, p. 43-44, 2010.

Chukwukere, E. S., N. Liu, L. Li, R. Grigg, and R. Lee, "Contribution of Solution-Diffusion and Volume-Migration on CO_2 Transport in Caprock Seal Layer," Eighth Annual Conference Carbon Capture and Sequestration, DOE/NTEL, May 4-7, 2009.

Earman, S., McPherson, B. J. O. L., Phillips, F. M., Ralser, S., Herrin, J. M., Broska, J., "Tectonic Influences on Ground Water Quality: Insight from Complementary Methods," Ground Water, Vol. 46, No. 3, p. 354–371, 2008. http://dx.doi.org/10.1111/j.1745-6584.2007.00402.x

Endres, D., L. Sprain, T. R. Peterson, eds. Social Movement to Address Climate Change: Local Steps for Global Action (Amherst, NY: Cambria Press), 2009.

Esser, R., Levey, R., McPherson, B., O'Dowd, W., Litynski, J., Plasynski, S. "Preparing for a Carbon Constrained World; Overview of the United States Regional Carbon Sequestration Partnerships Programme and its Southwest Regional Partnership. Petroleum Geology: From Mature Basins to New Frontiers." Proceedings of the 7th Petroleum Geology Conferene. London, Vining and Pickering, eds. 2010.

Feldpausch, A. M. "The Role of Social Factors in Shaping Public Perceptions of CCS: Results of Multi-State Focus Group Interviews" – paper presentation at the 9th International Conference on Greenhouse Gas Control Technologies in Washington, D.C, 2008.

Feldpausch, A. M. The adventures of Carbon Bond online game.
http://www.southwestcarbonpartnership.org/KidsStuff.aspx (last updated September 2008).

Feldpausch, A. M. "Southwest Regional Partnership on Carbon Sequestration: Where Are We

Now?" – invited paper presented at the December 15, 2008 Post Kyoto Forum in Lisbon, Portugal

Feldpausch, A. M. "Carbon Bond: Teaching Youth about Carbon Capture and Storage using Internet Games" presented at the 2008 National Agriculture and Natural Resources Extension Professionals (ANREP) Conference in Madison, Wisconsin

Feldpausch, A. M. "Carbon Bond: Teaching Youth about Carbon Capture and Storage using Internet Games" presented at the 2008 National Chapter of the Wildlife Society (TWS) Annual Meeting in Miami, Florida

Feldpausch, A. M. "The Role of Social Factors in Shaping Public Perceptions of CCS: Results of Multi-State Focus Group Interviews in the U.S." presented at the 2009 International Symposium on Society and Resource Management (ISSRM) in Vienna, Austria

Feldpausch-Parker, A. M., R. Chaudhry, J. C. Stephens, M. Fischlein, D. M. Hall, L. L. Melnick, T. R. Peterson, C. J. Ragland, E. J. Wilson. "A comparative state-level analysis of carbon capture and storage (CCS) discourse among U.S. energy stakeholders and the public." Energy Procedia, 4(2011) 6368–6375

Feldpausch, A. M. "Communicating the Science behind Carbon Sequestration: A Case Study of U.S. Department of Energy and National Energy Technology Laboratory Websites" presented at the 2010 International Symposium on Society and Resource Management (ISSRM)

Feldpausch, A. M. "A Comparative State-Level Analysis of Carbon Capture and Storage (CCS) Discourse among U.S. Energy Stakeholders and the Public" presented at the 10th International Conference on Greenhouse Gas Control Technologies in Amsterdam, The Netherlands, 2010.

Feldpausch, A. M. "Socio-Political Dimensions of CCS Deployment through the Lens of Social Network Analysis" presented at the 10th International Conference on Greenhouse Gas Control Technologies in Amsterdam, The Netherlands, 2010.

Ghorpade, S., et al. (2010) "Effects of Pressure and Temperature on Relative Permeability of CO_2-Brine System." Presented at the Ninth Annual Conference on Carbon Capture & Sequestration, May 10–13, 2010, Pittsburgh, Pennsylvania

Grigg, R.B., Svec, R.K., Peter C. Lichtner, P.C., Carey, W., Lesher, C.E.: "CO_2/Brine/Carbonate Rock Interactions: Dissolution and Precipitation," prepared and presented at the Fourth Annual Conference on Carbon Capture & Sequestration, Alexandria, 2-5 May 2005.

Grigg, R.B., Svec, R.K.: "CO_2 Saturations and Transport Mechanisms in Frio Sandstone," Paper 157 presented at the Fifth Annual Conference on Carbon Capture and Sequestration – DOE/NETL, Washington, D.C., 8-11 May 2006.

Grigg, R.B. Svec, R.K.: "Injectivity Changes and CO_2 Retention for EOR and Sequestration Projects," paper SPE 110760 presented at the 2008 SPE Improved Oil Recovery Symposium, Tulsa,

19-23 April.

Han, W. S., McPherson, B.J. "Comparison of Two Different Equations of State for Application of Carbon Dioxide Sequestration." Advances in Water Resources, 31(6), 877-890, 2008.

Han, W. S., McPherson, B.J. "Optimizing geologic CO_2 sequestration by injection in deep saline formations below oil reservoirs." Energy Conversion and Management, 50 (10), 2570-2582, 2009.

Han, W. S., McPherson, B.J. "On using numerical simulation to evaluate CO_2 flow and transport in the subsurface: Uncertainty due to choice of Equations of State algorithms, in Carbon Sequestration and Its Role in the Global Carbon Cycle." B. McPherson, and E. Sundquist, Eds., Geophysical Monograph Series 183, American Geophysical Union, p. 261-278, Washington, D.C., 2009. doi:10.1029/2009gm01308

Han, W. S., Lee, S.-Y., Lu, C. McPherson B.J., "Effect of permeability on CO_2 trapping mechanisms and buoyancy-driven CO_2 migration in saline formations." Water Resources Research, 46, 2010. W07510, doi:10.1029/2009WR007850

Han, W.S., Lee, S.Y., Lu, C., McPherson, B.J., Esser, R.P. "Role of correlation structures of permeability field on residual trapping mechanisms and buoyancy-driven CO_2 migration." Energy Procedia, Volume 1, Issue 1. p. 3493-3498, 2009.

Han, W. S., Greg, A.S., Lu, M., Lu, C., McPherson, B., Park, E. "Evaluation of potential nonisothermal effect and heat transport during CO_2 sequestration" Journal of Geophysical Research-Solid Earth, 2010. doi:10.1029/2009jb006745

Han, W. S., McPherson, B.J., P.C. Lichtner, Wang, F.P. "Evaluation of CO_2 trapping mechanisms at the SACROC northern platform, Permian basin, Texas, site of 35 years of CO_2 injection," American Journal of Science 310, 282-234, 2010.

Harris, M., and Grigg, R. (2010) "Validation and Comparison of Carbon Sequestration Project Cost Estimation Models with Project Cost Data Obtained from the SWP." Presented at the Ninth Annual Conference on Carbon Capture & Sequestration, May 10–13, 2010, Pittsburgh, Pennsylvania

Heath, J., McPherson, B., Dewers, T., Chidsey, T.C., Jr., Petrusak, R., Siriwardane, H., Bromhal, G., Grigg, R., Esposito, R. "Seal analysis of geologic CO_2 storage sites [abs.]," American Association of Petroleum Geologists Annual Convention Abstracts, v. 18, p. 90-91, 2009

Heath, J., Dewers, T.A., McPherson, B.J.O.L., Petrusak, R., Chidsey, T.C., Jr., Rinehart, A.J., Mozley. P.S. "Pore networks in marine and non-marine mudstones – characteristics and controls on sealing behavior," in Advances in 3D imaging and analysis of geomaterials: Geosphere. 2010 (in review).

Huang, L., and Denli, H. (2009) "Differential Waveform Tomography Using Time-Lapse VSP

Data for Monitoring CO_2 Migration." Presented at the Eighth Annual Conference on Carbon Capture & Sequestration, May 4–7, 2009, Pittsburgh, Pennsylvania.

Huang, L., Rutledge, J., Denli, H., and Zhou, R. (2009) "Time-Lapse VSP Surveys for Monitoring CO_2 Migration at the Aneth Oil Field in Utah." Presented at the Eighth Annual Conference on Carbon Capture & Sequestration, May 4–7, 2009, Pittsburgh, Pennsylvania.

Huang, L. et al. (2010) "Time-Lapse Offset and Walkaway VSP Monitoring of CO_2 Injection at SACROC." Presented at the Ninth Annual Conference on Carbon Capture & Sequestration, May 10–13, 2010, Pittsburgh, Pennsylvania

Kobos, P. H., Borns, D. J., Malczynski, L. A., Paananen, O. H. "Southwest regional partnership on carbon sequestration: a test case model in the San Juan Basin". Sandia National Laboratories, Albuquerque, NM,. SAND2005-2481C, May 2005. Fourth Annual Conference on Carbon Capture & Sequestration, May 2-5, 2005 in Alexandria, VA.

Kobos, P. H., Malczynski, L. A., Borns, D. J. "Southwest regional partnership on carbon sequestration: the 'String of Pearls' integrated assessment model". Sandia National Laboratories, Albuquerque, NM. SAND2006-2835C, May 2006. Fifth Annual Conference on Carbon Capture and Sequestration, May 8-11, 2006 in Alexandria, VA.

Koperna, G. J. Jr., Oudinot, A. Y., McColpin, G. R., Liu, N., Heath, J., E., Wells, A. W., Young, G. B. "CO_2-ECBM/Storage Activities at the San Juan Basin's Pump Canyon Test Site." SPE Conference. New Orleans, LA. October 4-7, 2009.

Kuuskraa, V. A., Koperna G. J.: "Assessing and Expanding CO_2 Storage Capacity in Depleted and Near-Depleted Oil Reservoirs" presented at GHGT-8, Trondheim, Norway, June 19-23, 2006.

Li, L., and R. Lee, "Purification of Produced Water by Ceramic Membranes: Material Screening, Process Design and Economics," Separation Science and Technology, 44(15), 3455-3484, 2009.

Liu, N., Y. Li, L.X. Li, R. Grigg, B. McPherson, and R. Lee, "Development of a CO_2 chemical sensor and sensor strategy for CO_2 monitoring in carbon sequestration", Paper presented at DOE-NETL Seventh Annual Conference on Carbon Sequestration, (Seventh Annual Carbon Capture and Sequestration Conference, Pittsburgh, PA. May 5-8, 2008.
Liu, N., L. Li, B. McPherson, and R. Lee, "Removal of Organics from Produced Water by Reverse Osmosis Using MFI-type Zeolite Membranes," J. Membr. Sci. 325, 357-361, 2008.

Lu, C., Han, W. S., Lee, S.-Y., McPherson, B. J. Lichtner, P.C. "Effects of density and mutual solubility of CO_2-brine system on CO_2 storage in geologic formations: "Warm" vs. "Cold" Formations." Advances in Water Resources, 32 (12), 1685-1702, 2009. doi:10.1016/j.advwatres.2009.07.008.

Lu, C., Lee, S.-Y., Han, W. S., McPherson, B.J., Lichtner, P.C. Comments on "Abrupt-interface solution for carbon dioxide injection into porous media" by M. Dentz and D. Tartakovsky.

Transport in Porous Media, 79 (1), 29-37, 2009. doi:10.1007/s11242-009-9362-9.

McPherson, B., L. Li, M. Deo, "Coupled Hydrogeomechanical Impacts of Carbon Sequestration," AIChE Annual Meeting, Salt Lake City, UT, Nov. 04 - 09, 2007.
McPherson, B.J., Han, W. S., Cole, B. "Two Equations-of-State assembled for basic analysis of multiphase CO_2 flow in deep sedimentary basin conditions." Computers & Geosciences, 34(5), 427-444, 2008.

McPherson, B. J., Han, W. S., Lee, S. Y., Lu, C., Esser, R.P. "Mitigation planning for large-scale storage projects: multiple injection zones and reservoir pressure reduction engineering design". Energy Procedia, Volume 1, Issue 1. p. 2595-2597, 2009.

McPherson, B. J. O. L. Sundquist, E. T., 2009, editors, The Science and Technology of Carbon Sequestration, AGU Monograph Series, Publisher: American Geophysical Union, Washington, D.C., 2009.

Oudinot, A. Y., Koperna, G. J., Philip, Z. G., Liu, N., Heath, J. E., Wells, A. W., Young, G. B., Wilson, T. "CO_2 Injection Performance in the Fruitland Coal Fairway, San Juan Basin: Results of a Field Pilot," Paper SPE 127073 presented at the SPE International Conference on CO_2 Storage, Capture and Utilization, 2-4 November, 2009, San Diego, CA.

Pawar, R.J., Warpinski, N.R., Lorenz, J.C. Benson, R.D., Grigg, R.B., Stubbs, B.A., Stauffer, P.H., Krumhansl, J.L., Cooper, S.P., and Svec, R.K.: "Overview of a CO_2 Sequestration Field Test in the West Pearl Queen Reservoir, New Mexico," Environmental Geosciences, V.13, No. 3 (September 2006), pp. 163-180.

Ragland, C. J., A. Feldpausch-Parker, T. R. Peterson, J. Stephens, E. Wilson. "Socio-political dimensions of CCS deployment through the lens of social network analysis." Energy Procedia, 4(2011) 6210–6217.

Romanak, K. D., Smyth, R. C. "Geochemical effects of CO_2-enhanced oil recovery on the shallow Dockum aquifer, west Texas (abs.)," in 7th Annual Conference on Carbon Capture & Sequestration, May 5th–8th, 2008, Pittsburgh, Pennsylvania.

Romanak, K.D., Smyth, R.C., Yang, C, Hovorka, S.D., Lu, J. "Role of dedolomitization in the detection of anthropogenic CO_2 in freshwater aquifers," Proceedings of the 13th International conference on water-rock interaction WRI-13, Guanajuato, Mexico, 16-20 August 2010, p. 887-890.

Romanak, K., Smyth, R., Yang, C., and Hovorka, H. (2010) "Detection of Anthropogenic CO_2 in Dilute Groundwater: Field Observations and Geochemical Modeling of the Dockum Aquifer at the SACROC Oilfield, West Texas, USA." Presented at the Ninth Annual Conference on Carbon Capture & Sequestration, May 10–13, 2010, Pittsburgh, Pennsylvania

Rutledge J. T., "Interpreting Reservoir Microseismicity Detected During CO_2 Injection at the Aneth Oil Field," Eos Trans., AGU 90(52), Fall Meet. Suppl., Abstract U41B-0021, 2009.

Rutledge, J., Zhou, R., Huang, L., and McPherson, B.J. (2009). "Microseismic Monitoring of CO2 Injection in the Aneth Oil Field, San Juan County, Utah." Presented at the Eighth Annual Conference on Carbon Capture & Sequestration, May 4–7, 2009, Pittsburgh, Pennsylvania.

Rutledge, J. (2010) "Mapping and Interpreting Reservoir Microseismicity Detected During CO_2 Injection at the Aneth Oil Field." Presented at the Ninth Annual Conference on Carbon Capture & Sequestration, May 10–13, 2010, Pittsburgh, Pennsylvania

Rutledge, J., Soma, N., and McPherson, B. (2010) "Microseismic Monitoring of CO_2 Injection at the Aneth Oil Field." Presented at the Ninth Annual Conference on Carbon Capture & Sequestration, May 10–13, 2010, Pittsburgh, Pennsylvania

Siriwardane, H., Bromhal, G. S., Gondle, R. "Simulating Pressure response in overburden layers due to fractures" submitted to the 7th Annual Conference on Carbon Capture & Sequestration, Pittsburgh, PA, May 5th - 8th, 2008.

Siriwardane, H., Haljasmaa, I., McLendon, R., Irdi, G., Soong, Y., Bromhal, G. S., "Influence of CO_2 on coal permeability," International Journal of Coal Geology, Volume 77, Issues 1-2, Pages 109-118, 7 January, 2009.

Siriwardane, H. J., Gondle, R. K., Wells, A. W., Bromhal, G. S., Bowes, B. D., Strazisar, B. "Modeling of CBM Production and CO_2 Injection at Pump Canyon CO_2 Sequestration Field Site in San Juan Basin." Ninth Annual Conference on Carbon Capture & Sequestration, Pittsburgh, PA. May 7-10, 2010.

Small, M., Yang, Y., Gray, D., Ogretim, E., Liu, G., Bromhal, G. S., Wells, A. W., Strazisar, B. "Integrating CO_2 and Tracer Transport Models to Predict Leak Detection Probabilities for a Monitoring Network." Nineth Annual Conference on Carbon Capture & Sequestration, Pittsburgh, PA. May 7-10, 2010.

Smith, D. H.; Sams, W. N.; Bromhal, G.; Jikich, S.; Ertekin, T. "Simulating Carbon Dioxide Sequestration/ECBM Production in Coal Seams: Effects of Permeability Anisotropies and Other Coal Properties". SPE Reserv. Eval. Eng. 8, pp.156-163, June 2005.

Smyth, R. C., Hovorka, S. D., Romanak, K. D., Partin, J. W., Wong, C., Meckel, T. A., Nicot, J. P., Holt, R. H. "Assessing risk to fresh water resources from long term CO_2 injection—laboratory and field studies (abs.)," in 9th International Conference on Greenhouse Gas Technologies, November 16–20, 2008, Washington, D.C.

Thompson, J. L., C. B. Forster, C. Werner and T. R. Peterson. "Mediated modeling: Using collaborative processes to integrate scientist and stakeholder knowledge about greenhouse gas emissions in an urban ecosystem." Society and Natural Resources 23: 742-757, 2010.

Tollufson, L., S. Greenberg, J. Bradbury, D. Daly, S. Hanson, G. Garrett, T. Peterson, A. Parker, R. Myhre, M. Stone S. Wade. "Public outreach and education for carbon storage projects best

practices manual." U.S. Department of Energy National Energy Technology Laboratory, 2009.

Wells, A. W., Hammack, R. W., Veloski, G. A., Diehl, J. R., Strazisar, B. R., Wilson, T. H., Rauch, H., White, C. M., "Monitoring, mitigation and verification at sequestration sites: SEQURE technologies and the challenge for geophysical detection" The Leading Edge, October 2006, pages 1264-1270.

Wells, A. W., Diehl, J. R., Bromhal, G. S., Strazisar, B. R., Wilson, T. H., White, C. M. "The use of tracers to assess leakage from the sequestration of CO_2 in a depleted oil reservoir, New Mexico, USA." Applied Geochemistry, 22 (5), 996-1016, May 2007.

Wells, A. W., Nowak, M., Diehl, J. R., Strazisar, B., Hammick, R., Veloski, G., Hamill, P. "NETL Monitors CO_2 Storage," Clean Coal Today, No. 71, Spring 2007.

White, S.P., Allis, R.G., Moore, J., Chidsey, T.C., Jr., Morgan, C., Gwynn, W., Adams, M. "Simulation of reactive transport of injected CO_2 on the Colorado Plateau, Utah, USA," Chemical Geology, v. 217, issues 3-4, p. 387-405, 2005.

Wilson, E. J., J. C. Stephens, T. R. Peterson, and M. Fischlein. "Carbon Capture and Storage in context: the importance of state policy and discourse in deploying emerging energy technologies." Energy Procedia 1: 4519-4526, 2009.

Wilson, T. H.; Wells, A. W.; Diehl, J. R.; Bromhal, G. S.; Smith, D. H.; Carpenter, W.; White, C. "Ground-penetrating radar survey and tracer observations at the West Pearl Queen carbon sequestration pilot site, New Mexico". The Leading Edge. pp.718-722, July 2005.
Wilson, T., Wells, A. W., Koperna, G. "Seismic Evaluation of the Fruitland Formation with Implications on Leakage Potential of Injected CO_2," In the Proceedings of the 2009 International Pittsburgh Coal Conference, Pittsburgh, PA, USA September 21-24, 11p.

Wilson, T. H., Nutt, L., Smith, R., Gulati, J., Coueslan, M., Peters, D., Wells, A. W., Hartline, C., Koperna, G., Akwari, B. "Pre- and Post-injection Vertical Seismic Profiling over the Southwest Regional Partnership's Phase II Fruitland Coal CO_2 Pilot." AAPG Rocky Mountain Section Meeting. Durango, Colorado, June 13-16, 2010

Yang C., Romanak, K.D. Hovorka, S.D., Linder, J., Smyth, R.C., Trevino, R., Paine, J., Holt, B., Smith, L.T., Xia, Y., Lu, J. "Geochemical characterization of shallow groundwater at the Cranfield aquifer and numerical simulation: can pH and carbonate parameters be used to detect potential CO_2 leakage at geological CO_2 sequestration sites?" The 9th Annual Conference on Carbon Capture & Sequestration, May 10 - 13, 2010, Pittsburgh, Pennsylvania.

Yang, Y., E. O. Ogretim, M. J. Small, D. D. Gray, G. S. Bromhal, B. Strazisar and A. W. Wells. "Statistical techniques for incorporating near-surface monitoring and modeling for CO_2 leak detection" presented at the 7th Annual Conference on Carbon Capture & Sequestration, Pittsburgh, PA, May 5th - 8th, 2008.

Young, G. B. C., S. R. Reeves, B. Henthorn, T. H. Wilson, G. S. Bromhal, D. H. Smith, "San

Juan Basin enhanced coalbed methane (ECBM)-carbon storage pilot: role of pre-injection site characterization in project design," Annual Meeting of the American Association of Petroleum Geologists, Long Beach, CA, April 1-4, 2007.

Zhang, Z. and Huang, L. (2010) "Wave-Equation Migration of Time-Lapse Offset VSP Data for Monitoring CO_2 Injection at the Aneth Oil Field in Utah." Presented at the Ninth Annual Conference on Carbon Capture & Sequestration, May 10–13, 2010, Pittsburgh, Pennsylvania.

Zhou, R., Huang, L., Denli, H., and Rutledge, J. (2009) "Double-Difference Tomography Using Microearthquake Data for Monitoring CO_2 Injection at Aneth, UT." Presented at the Eighth Annual Conference on Carbon Capture & Sequestration, May 4–7, 2009, Pittsburgh, Pennsylvania.

Zhou, R., L. Huang, and J. Rutledge, "Microseismic event location for monitoring CO_2 injection using double-difference tomography," The Leading Edge, 29, 208-214, February, 2010.

Zhou, R. et al. (2010) "Coda-Wave Interferometry and Time-lapse Monitoring of Geological CO_2 Sequestration." International Journal of Greenhouse Gas Control, **4** (4), 679–686.

Conclusions

The SWP's Phase II project comprised a series of validation tests of the most promising sequestration technologies for the region. These validation tests demonstrate multiple value-added benefits, enhanced oil recovery and sequestration, enhanced coalbed methane production and sequestration combined with a local terrestrial (riparian restoration) sequestration pilot, and a regional terrestrial sequestration pilot program focused specifically for the Southwest region.

Central to the SWP's strategy was an extensive array of MVA protocols for each field pilot designed to track the movement and fate of CO_2 injected into deep saline aquifers and coalbeds, and oil and gas reservoirs. Additional MVA goals were to monitor CO_2 well injectivity, verify abandoned well veracity, and to assist with risk assessment and mitigation. Baseline MVA activities elucidated the geologic, hydrogeochemical, isotopic and other physical conditions prior to injection. These baseline data were compared to results of repeat and continuous MVA surveys conducted after injection to forecast ultimate fate of CO_2 in the subsurface for different conditions.

All of the SWP's findings, which are extensive, have been reported in the series of Topical Reports and this Final Report produced by SWP Researchers. The broadest conclusions that were drawn from Phase II research can be summarized here.

Program Goal-Related Conclusions

Storage Capacity Verification

The SWP is developing technologies for Phase III that will support our industry partner's ability to confirm CO_2 storage capacity in geologic formations. The uncertainty or tolerance planned is ±30 % (target is ±10 %). Through Phase II project results, we conclude that the most reliable technology for such capacity verification are:

- vertical seismic profiles (VSP)
- direct measurements (e.g., tracers, pH, pressure, fluids etc.)

- 3-D simulation models of the specific geologic storage system

Verification of Containment

The SWP is refining a technological approach to confirm that 99 % of injected CO_2 remains in the injection zones. Based on Phase II project results, SWP considers that the most effective approach for verification of containment is through:

- geophysical (VSP) surveys
- tracer monitoring
- pressure and geochemical monitoring
- detailed numerical modeling calibrated by these data
- fluid sampling

Best Practices

The SWP has contributed significantly to Best Practice Manuals (BPM) development, including:

- *Risk Analysis and Simulation for Geologic Storage of CO_2* (McPherson served as RCSP coordinator for this BPM)
- *Site Screening, Selection, and Characterization for Storage of CO_2 in Deep Geologic Formations*
- *Monitoring, Verification, and Accounting (MVA) of CO_2 Stored in Deep Geologic Formations* (MVA; Fessenden assisted with coordination of this BPM)
- *Public Outreach and Education for Carbon Storage Projects* (Peterson assisted with coordination of this BPM) Geologic Storage Formation Classification: Understanding *Its Importance and Impacts on CCS Opportunities in the United States*
- *Terrestrial Sequestration of Carbon Dioxide*

Injectivity and Capacity

Based on Phase II results, the SWP concludes that the most reliable technology for evaluating and optimizing injectivity is wellbore simulation models calibrated with:

- produced water disposal (injection) data from existing wells
- laboratory analysis of existing cores from the field
- injectivity tests

Storage Permanence

The most reliable methods for confirming storage permanence, according to results of our Phase II field tests, include:

- geophysical (VSP) surveys
- tracer monitoring
- pressure and geochemical monitoring
- detailed numerical modeling calibrated by these data

Risk Assessment

As a result of research in Phase II, the SWP has developed a comprehensive risk assessment strategy:

- "Adaptive": iterative modeling-monitoring approach for assessment of uncertainty
- Performance assessment: healthy/safety risks, economic and programmatic risks, and otherwise.

Outreach and Education

The SWP has developed successful outreach and education methods during Phase II projects, including:

- focus groups with opinion leaders and decision-makers in the communities;
- quarterly press releases about the Southwest Partnership's field progress;
- Continual expansion and revision the partnership web site, with a focus on interactive capabilities;

- efforts developing K-12 and University curricula, as well as professional short courses for industry and other entities, in collaboration with the Southwest CCS Training Center.

Team Selection and Budget

Phase II project experience has proven our Workgroup leader selection to be effective:

- All group leaders led workgroups for previous successful projects
- Budget breakdown also based on this experience:
  - ~28% of federal budget dedicated to field operations
  - ~72% of federal budget dedicated to science (both measurements and analysis)

Key Findings in Phase II

MVA

These outcomes will have significant implications for the Phase III Commercial Scale injection Project.

Surface Flux Measurements

All locations but one at three sites saw small variations that were well within variations due to seasonal conditions and time-of-day. The one exception is where natural gas fluxes increased due to a leak in an underground pipeline, and not due to CO_2 injection.

Simulations

Simulations were used to model, predict, and verify mechanisms of sequestration and flow for each of the three geologic injections. A number of commercial and research models have been used to simulate flow and sequestration in oil, gas, coal, and aquifer reservoirs. We have been successful in modeling initial and changing, various trapping mechanisms, swelling of coal, reservoir pressure and temperature changes, and fluid interactions. Both field and laboratory data have been used to build and verify these results.

Tracers

Tracers, both gas and liquid phase, were tested at two sites. At one location, a test demonstrated that alcohol tracers perform similarly to perfluoro-hydrocarbon tracers but at a significant cost savings. The results provided improved understanding of reservoir flow patterns.

Seismic

Because of cost, vertical seismic profiles (VSP) were used at all three Phase II geologic sequestration sites. The multiple test of a Walkaway VSP test was demonstrated to be more definitive then point tests. Point tests in particular were sensitive to locating the source at precisely the same location each time (within < meters/centimeters versus 10's of meters). 3D done at one location demonstrated the value of this technique, although its use will be limited because of cost. Passive microseismic used at one location indicated sensitivity although, because of previous oil production and waterflooding, the CO_2 injection front was not defined.

Microseismicity

- Microseismicity—both natural and induced—occurs just about everywhere.
- Most seismic/microseismic events are associated with pre-existing faults and/or low permeability zones.
- Microseismicity can aid in identifying geologic features like "critically-stressed" faults
- In some systems microseismicity can detect fluid and/or pressure fronts
- Induced seismicity can be controlled through effective reservoir/injection engineering
- Careful and effective site characterization and selection are keys to successful microseismicity management

GPS and Tiltmeter

In the SWP San Juan Basin Phase II tests, fluid was both injected and produced, so the tiltmeter results did not show much change. The changes were close to background noise, though they did coincide slightly with the injection and production locations.

Electrical Self-Potential

Electrical self-potential monitoring was inconclusive, though it appears a positive change was seen for a few months at the injector.

Groundwater

Assessed baseline and multiple repeat reservoir and groundwater (brine) compositions show no effect of 38 years of CO_2 injection, though results indicate possible effects from early production practices (pre-1950). No CO_2 or contaminants detected at or near the surface that are attributed to CO_2 leakage were found at any of our three sites.

Other Key Findings from Phase II

- Oil/gas fields can play an important monitoring role in deep saline sequestration.
- Oil/gas field can be primary storage sites or are excellent secondary sites (stacked storage), catching any CO_2 leakage from saline aquifers used for carbon storage beneath the hydrocarbon formations.
- In all cases, it is difficult to predict geomechanical processes.
- In all cases, it is difficult to predict induced or triggered seismicity.
- CO_2 diffusivity ≠ hydraulic diffusivity.

For the Future/Phase III

- Confirm the CO_2 source as soon as feasible.
- Refine design of stacked storage monitoring.
- Develop the surface and subsurface baseline for monitoring and characterization.
- Measure baseline CH_4 fluxes (if any) in the field, as a means of evaluating hydraulically any communication of faults with the natural gas-producing Ferron Sandstone (Phase III) and the surface.
- Continue simulation development and increase resolution of risk assessment.

Appendix

Topical Reports Submitted to NETL: The title page and abstract of each of these reports are included in the Appendix.

Advanced Resources International, Inc. (2010) Pump Canyon CO_2- ECBM/Sequestration Demonstration, San Juan Basin, New Mexico. Houston, Texas.

Angerer, J., and Brown, J. (2010). Regional Terrestrial Pilot. Texas A & M University, Campus Station, Texas.

Chidsey, T.C. (2009) Surface and Subsurface Geological Characterization of the Aneth Unit, Greater Aneth Field, Paradox Basin, Utah. Utah Geological Survey, Salt Lake City, Utah.

Feldpausch, A. (2010) Community Knowledge and Acceptance of Southwest Partnership Phase II Carbon Capture and Storage Projects: Focus Group and Survey Results. Texas A & M University, College Station, Texas.

Han, W-S., Esser, R., Thorne, D., and McPherson, B. (2009) Principal Reservoir Description Associated with Geology and Oil Production History in SACROC, Site of 35 Years of CO_2 Injection. University of Utah, Salt Lake City, Utah.

Harris, M. (2010) Validation and Comparison of Carbon Sequestration Project Cost Models with Project Cost Data Obtained from the Southwest Partnership. New Mexico Institute of Mining and Technology, Socorro, New Mexico.

Heath, J., McPherson, B., and Dewers, T. (2010) Natural Tracers and Multi-Scale Assessment of Caprock Sealing Behavior: Preliminary Findings from a Case Study of the Kirtland Formation, San Juan Basin. Sandia National Laboratories, Albuquerque, New Mexico.

Heath, J., McPherson, B., and Dewers, T. (2010) Natural Tracers and Multi-Scale Assessment of Caprock Sealing Behavior: A Case Study of the Kirtland Formation, San Juan Basin (expanded). Sandia National Laboratories, Albuquerque, New Mexico.

Interstate Oil and Gas Compact Commission Task Force on Carbon Capture and Geologic Storage, Bliss, K., Bengal, L., and Tew, B. (2010) Biennial Review of the Legal and Regulatory Environment for the Storage of Carbon Dioxide in Geologic Structures. Interstate Oil and Gas Compact Commission, Oklahoma City, Oklahoma.

Rutledge, J. (2010) Geologic Demonstration at the Aneth Oil Field, Paradox Basin, Utah. Los Alamos National Laboratory, Los Alamos, New Mexico.

Xiao, C., ed. (2011) SACROC North Platform in the Permian Basin, West Texas. New Mexico Institute of Mining and Technology, Socorro, New Mexico.

Advanced Resources International, Inc. (2010) Pump Canyon CO_2- ECBM/ Sequestration Demonstration, San Juan Basin, New Mexico. Houston, Texas.

Southwestern Regional Partnership For Carbon Sequestration (Phase 2)

Pump Canyon CO_2- ECBM/Sequestration Demonstration, San Juan Basin, New Mexico

U.S. DOE Award No: DE-FC26-05NT42591

Final Report

Submitted by:
Advanced Resources International, Inc.
Houston, TX

January 31, 2010



Executive Summary

The Southwest Regional Partnership on Carbon Sequestration (SWP) is one of seven regional partnerships sponsored by the U.S. Department of Energy (USDOE).

Within the SWP, three demonstrations of geologic CO_2 sequestration are being performed – one in an oilfield (the SACROC Unit in the Permian basin of west Texas), one in a deep, unmineable coalbed (the Pump Canyon site in the San Juan basin of northern New Mexico), and one in a deep, saline reservoir (underlying the Aneth oilfield in the Paradox basin of southeast Utah). The Pump Canyon CO_2-enhanced coalbed methane (CO_2/ECBM) sequestration demonstration project plans to demonstrate the effectiveness of CO_2 sequestration in deep, unmineable coal seams via a small-scale geologic sequestration project. The site is located in San Juan County, northern New Mexico, just within the limits of the high-permeability fairway of prolific coalbed methane production. The study area for the SWP project consists of 31 coalbed methane production wells located in a nine section area.

CO_2 was injected continuously for a year and different monitoring, verification and accounting (MVA) techniques were implemented to track the CO_2 movement inside and outside the reservoir. A total of 319 MMscf of CO_2 (or 18,400 tons) were injected over a 12-month period (July 30st, 2008 to August 12th, 2009); primarily due to highly permeable coal. However, as expected, the CO_2 injectivity dramatically decreased over the injection period. This was mainly due to matrix swelling and permeability reduction, as a result of the CO_2 being adsorbed onto the coal, while displacing methane, as well as increasing reservoir pressure. It was also determinded that injection was predominately into the basal coal, reducing injectivity by 20%.

The CO_2 sensors installed at the three immediate offset wells, as well as the gas sampling from neighboring CBM wells (three immediate offset wells and an additional ring of immediately surrounding wells), suggest that no CO_2 breakthrough has occurred at the site. However, a steady increase in the CO_2 content at one of the offset wells, the FC State Com 1, might be a sign of breakthrough. The CO_2 monitoring system has been left in place and the data will be regularly updated to verify whether this is the case.

Perfluorocarbon tracers injected in the CO_2 stream showed up a few months later at the two closest offset wells, the FC State Com 1, followed by the EPNG Com A 300 (where breakthrough is expected to occur first due to its alignment with the face cleats, if it does occur). This may also could be an early sign of breakthrough.

In addition to monitoring for breakthrough, the project also adopted several ground monitoring techniques to observe any ground deformation. The different ground monitoring techniques used (Tiltmeters, GPS and InSar) all converge to the same conclusion, that no ground deformation is seen even though their effectiveness was probably limited due to the small amount of CO_2 injected.

In order to assess the integrity of the site, the project conducted a thorough seismic interpretation of about nine square miles of 3D seismic data centered around the injection well. The seismic interpretation reveals considerable stratigraphic complexity in the Fruitland formation depositional system. Post-stack processing of the 3D seismic suggests the presence of fracturing and minor faulting within the Kirtland Shale caprock, whereas indicators for extensive fracturing and faulting within the Fruitland sequence are much less apparent. However, interpreted faults and fracture zones, with limited vertical extent and major penetrative faults, have not been observed at the site reinforcing the fact that no leakage is expected. Baseline and post injection vertical seismic profiles (VSP) were collected at zero offset and three non-zero offsets, but the preliminary processing is still in progress. A detailed study of the integrity of the Kirtland Shale caprock is provided in an independent report.

The simulation work was able to adequately replicate the production/injection profile of the injector and the three immediate offset wells. The model is also showing that methane production was enhanced due to the CO_2 injection. While the match is not perfect and predicts breakthrough perhaps a bit too early, the model was successful in tying the results from the field, such as the gas samples (CO_2 content and nitrogen content), to the well performance, lending confidence in the accuracy of the match.

Angerer, J., and Brown, J. (2010). Regional Terrestrial Pilot. Texas A & M University, Campus Station, Texas.

Southwest Carbon Sequestration Partnership – Phase II
Major Task Area 5: Regional Terrestrial Pilot

Topical Report

DOE Contract No. DE- FC26-05NT42591

Submitting Organization: New Mexico Institute of Mining and Technology
801 Leroy Place
Socorro, New Mexico 87801

Reporting Period: September 1, 2007 through September 30, 2010

Authors:

Jay Angerer, Texas A&M University
Joel Brown, Agriculture Research Service, Las Cruces
November 15, 2010

ABSTRACT

Terrestrial carbon sequestration is an important component of a comprehensive greenhouse gas (GHG) management strategy in the southwest. The ability to transfer and store atmospheric carbon in soils and vegetation by manipulating the rate and magnitude of naturally occurring processes, such as photosynthesis, humification and aggregation by changing land management is an attractive alternative to reduce GHG levels because 1) results can be achieved quickly, 2) technologies can be implemented without major economic impact and are associated with improved management of resources and more efficient production systems, and 3) delivery infrastructure programs within extension and federal agencies is generally in place.

The analyses conducted in Phase I of the Southwest Regional Partnership on Carbon Sequestration (SWP) showed tremendous potential to increase carbon storage in soils and vegetation through changes in land use and management within the southwest region. Several factors that constrain this potential include low rates of carbon accumulation per hectare due to low rainfall and soil fertility, large variations in the climate that make local prediction of sequestration difficult, and the lack of cost-effective carbon measurement systems. The complex combination of land use, land management and natural conditions in the SWP region offered the opportunity to build upon and expand the earlier work. The main objectives of this study were to: 1) develop improved technologies and systems for direct measurements of soil and vegetation carbon; 2) develop remote sensing and classification protocols to improve mesoscale (km^2) carbon estimates; 3) construct ecological process models that reflect soil/vegetation changes resulting from current land use and land use associated with carbon sequestration programs; 4) develop a regional carbon inventory and decision support tool; and 5) explore restoration technologies/strategies on lands near geological sequestration sites.

Some results include:

1. Direct measurements of soil and vegetation carbon using Laser Induced Breakdown Spectroscopy (LIBS) and Near Infrared Reflectance Spectroscopy (NIRS) can provide accurate measurements of soil carbon and can be used to help reduce the cost and time require for soil sampling.
2. Normalized Difference Vegetation Index (NDVI) imagery for monitoring compliance in carbon sequestration programs has potential for monitoring large (e.g., doubling or vegetation biomass) changes, but does not appear to be able to detect subtle changes in management.
3. The use of ecological process models (i.e., state and transition models [S^TMs]) for representing the range of soil/vegetation combinations associated with carbon management practices and land uses within the region indicate a strong link between ecological states and soil carbon levels in rangelands within the SWP region.
4. Uncertainties associated with model estimates of rangeland carbon sequestration were generally high across the region, though delineating areas where additional data can be collected to reduce uncertainty.
5. A web-based decision support tool with a map-driven user interface was developed.
6. An examination of restoration technologies/strategies that could be used for carbon sequestration was conducted at La Manga Canyon in the San Juan basin.

Chidsey, T.C. (2009) Surface and Subsurface Geological Characterization of the Aneth Unit, Greater Aneth Field, Paradox Basin, Utah. Utah Geological Survey, Salt Lake City, Utah.

SURFACE AND SUBSURFACE GEOLOGICAL CHARACTERIZATION OF THE ANETH UNIT, GREATER ANETH FIELD, PARADOX BASIN, UTAH

FINAL REPORT

Thomas C. Chidsey, Jr., Utah Geological Survey Project Manager
Utah Geological Survey
Salt Lake City, Utah

September 2009

Southwest Regional Carbon Sequestration Partnership-Phase II

U.S. Department of Energy
Contract No. DE-FC26-05NT42591
and
New Mexico Institute of Mining & Technology
DSRP20, CFDA No. 81.089

ABSTRACT

Greater Aneth oil field, Utah's largest oil producer, represents an archetype of a mature western U.S. oil field. Located in the Paradox Basin of southeastern Utah, Greater Aneth is a stratigraphic trap, with fractures and small faults. The field produces oil and gas from the Pennsylvanian (Desmoinesian) Paradox Formation. The Paradox forms a complex reservoir representing a variety of shallow-shelf depositional environments that produce significant heterogeneity. Production from the Aneth Unit in the northwestern part of the field had declined by 50% over the past 20 years. However, the unit has produced 149 million barrels (24 million m^3) of the estimated 450 million barrels (72 million m^3) of oil in place - a 33% recovery rate. The large amount of remaining oil, combined with a nearby carbon dioxide (CO_2) pipeline, made the Aneth Unit ideal to (1) demonstrate both CO_2 storage capability and enhanced oil recovery by flooding the reservoir with the CO_2, and (2) extensively monitor the effects of injection from reservoir to surface. Therefore, the Aneth Unit was selected as a demonstration site for the Southwest Regional Partnership on Carbon Sequestration – Phase II: Field Demonstrations project. The Utah Geological Survey evaluated the surface and subsurface geology of Aneth Unit demonstration site and how it will affect sequestration operations and engineering strategies. The research for the project included (1) mapping the surface geology, (2) describing the local stratigraphy, (3) mapping the reservoir, seals, and overlying aquifers, (4) characterizing the geology of the reservoir, (5) describing the geochemical, petrographic, and geomechanical properties of the seals, and (6) evaluating the production history.

The Montezuma Creek and Navajo Canyon quadrangles, which contain the Aneth Unit, consist of Jurassic Morrison through Cretaceous Dakota Sandstone outcrops and Quaternary sediments. The Recapture Shale and Salt Wash Members of the Morrison Formation are easily eroded and form low-lying hills of red shale and lenticular channel sandstone beds. The Brushy Basin Member of the Morrison Formation and the Burro Canyon Formation form steep variegated slopes beneath the Dakota Sandstone, which caps most of the mesas in the area. Strata in the Aneth area dip <5° to the northeast and are relatively structurally undeformed. No significant faults are found that offset surface strata in the Aneth Unit.

The bedrock surface geologic section exposed in the Montezuma Creek and Navajo Canyon Quadrangles consists of the Recapture Shale Member, Salt Wash and Brushy Basin Members of the Jurassic Morrison Formation, and the Cretaceous Burro Canyon and Dakota Sandstone. The Recapture Shale is dominantly dark red shale with interbedded lenticular sandstones generally a few feet thick. The Salt Wash consists of thicker, stacked, light-gray, channel sandstone deposits with interbedded red and gray-green shale and siltstone. The Brushy Basin is composed of alternating bright colored bands of red, green, and gray swelling mudstones that typically weather to a distinctive popcorn texture. The Burro Canyon Formation has a basal conglomerate overlain by variegated shale. Where the conglomerate is absent it can be difficult to distinguish the Burro Canyon shale from the underlying Brushy Basin shale, although the Burro Canyon shale does not weather to a popcorn texture. The Dakota Sandstone is cross-bedded, medium- to coarse-grained fluvial sandstone that forms the cap for the mesas in the area.

Surface structural analysis of the site was done, in part, to identify possible pathways for CO_2 migration from the oil-producing and potential CO_2 storage reservoir to the surface. Field mapping was directed at identifying faults and fracture patterns, types, and orientations within sandstones of the Jurassic Morrison Formation and the Cretaceous Burro Canyon and Dakota

Formations exposed on the surface. One type of fracture, deformation band, is abundant in the field area. We measured orientations of >1100 deformation bands and identified a few small, localized normal faults within the Jurassic Morrison Formation. Deformation bands in the western part of the field area have a strong northwest-southeast orientation, while those in the east part of the field appear to be more randomly oriented. There is a strong northwest-southeast oriented regional trend of large, open folds in this area of the central Colorado Plateau and the deformation bands could have been produced from localized stress during the same tectonic regime or as a result of compaction during burial. Faults in the area have small, vertical offsets (< 3 feet [1 m]), are likely shallow structures, and are probably a result of gravity-driven, localized deformation. Our study indicates that there are no geologically produced, structural migration pathways between the reservoir and the surface of the Aneth Unit.

A subsurface structural and stratigraphic analysis was done to identify structures within the Desert Creek zone (the reservoir) and the Gothic shale zone (the overlying seal) of the Paradox Formation which could act as potential migration pathways for CO_2 out of the reservoir. Structure contour and isopach maps were created for the Desert Creek and Gothic shale as well as the Ismay zone of the Paradox Formation. Similar maps were also created for the Jurassic Navajo and Permian DeChelly Sandstones, which are shallower fresh and saline water aquifers, respectively, in the Aneth area. Migration and infiltration of CO_2 into either of these aquifers, especially the Navajo Sandstone, could cause problems for the local communities that depend on them for agriculture and culinary use. The structure contour maps show no major structures in the study area, except for one small fault that appears to be localized in the Paradox Formation. Because this fault does not appear to penetrate into the overlying strata, CO_2 migration from the Desert Creek reservoir into the DeChelly or Navajo aquifers is not expected to occur.

Determining the nature, location, and extent of reservoir heterogeneity is the key to determining CO_2 storage potential in the Aneth Unit. Three factors create reservoir heterogeneity: (1) variations in lithofacies and lithology, (2) mound relief and flooding surfaces, and (3) diagenesis. Cores from Aneth Unit wells reveal a complex reservoir consisting of limestone (oolitic, peloidal, and skeletal grainstone and packstone, and algal boundstone/bafflestone) and finely crystalline dolomite. These lithotypes represent a variety of depositional environments that produce reservoir heterogeneity beyond what is determined from well logs. Diagenetic events include early marine cementation, post-burial dolomitization, dissolution, fresh-water cementation, and anhydrite cementation/replacement. Desert Creek reservoir strata may be fractured, which is an important factor in subsurface fluid flow, including directionality and volume of flow. The most notable and well-documented oil-producing intervals in the Desert Creek zone of the Paradox Basin formed as shallow-water algal buildups. However, they are not significant producers in the Aneth Unit. Grainstones within oolitic shoal lithofacies represent the major reservoir and the best potential for CO_2 storage capacity.

The Gothic shale is an effective seal above the Desert Creek reservoir zone within the Pennsylvanian Paradox Formation, Aneth Unit. The Gothic shale ranges in thickness from 5 to 27 feet (1.5-8 m), averaging 15 feet (4.6 m). Within the Aneth Unit, it is remarkably uniform, consisting of black to gray, laminated to thin-bedded, dolomitic marine shale and mudstone. The core from the Aneth Unit No. H-117 well is an excellent representation of the Gothic shale. Accessories and biological constituents consist of ubiquitous authigenic pyrite, microfossils, shell fragments, conodonts, and conularoids. Total organic carbon ranges from 2.2 to 4.4% with type II kerogen. Lithology consists of argillaceous or calcareous shale and mudstone composed of a clay to siliceous matrix with weak laminations defined by micas. Within the matrix calcite

crystals, pyrite, quartz, microfossils, flakes of organics, and swarms of intercrystalline micropores are common. Porosity ranges from 2.7 to 3.4% and pressure-decay permeability is no greater than 0.000146 millidarcies. These and other basic matrix petrophysical parameters indicate the Gothic shale to be a highly effective reservoir seal. The Gothic shale should support very large CO_2 or hydrocarbon columns based on mercury injection capillary pressure and pore aperture distribution analysis. Near the base of the Gothic section vertical to subvertical extensional fractures are present. Mineralization co-located with these natural fractures is most likely dominated by carbonates and organics. Continuous unconfined compressive strength profiles show a relatively uniform homogenous shale package. Compressional testing suggests some degree of hydraulic fracture containment.

Within the Aneth Unit several different production strategies for the Ismay and Desert Creek zones are employed: (1) most wells are vertical and under waterflood, (2) an area slightly larger than 2 square miles (5.2 km^2) has vertical wells in which horizontal laterals were drilled into the Ismay and Desert Creek zones after many decades of production from the vertical well bores, and are currently under waterflood, and (3) an area slightly larger than 1 square mile (2.6 km^2) has vertical wells in which horizontal laterals were drilled into the Ismay and Desert Creek zones after many decades of production from the vertical well bores, and are currently under water-alternating-gas (WAG) flood. Decline curves were constructed to compare the production history of: (1) primary production to waterflood production from vertical wells, (2) primary production to waterflood production from vertical wells and the increased production gained from drilling horizontal laterals, and (3) primary production to waterflood production from vertical wells and the increased production gained from drilling horizontal laterals, and converting from a waterflood to WAG flood. Decline curve analysis was used to demonstrate the production response that can be expected in Phase I and Phase II areas of the Aneth Unit. Phase I is 2 square miles (5.2 km^2) with vertical wells and Phase II is 2 square miles (5.2 km^2) with mostly vertical wells; both areas are currently under waterflood but will be converted to WAG flood. Both areas where horizontal laterals were drilled showed a significant increase in production. After the initial production increase due to the horizontal laterals, the area that was converted to WAG flood showed a slower decline than the area that was returned to waterflood. Both Phase I and Phase II areas experienced a lower production decline as a result of the waterflood. The Phase I area did not have water breakthrough for 39 years, much longer than other areas in the unit. This may be due to a large reservoir volume or injected water flowing outside of the productive zones. A similar loss of CO_2 could occur when the area is converted to WAG. A portion of Phase I had water breakthrough in just four years; a similar early breakthrough of CO_2 could occur when the area is converted to WAG.

Feldpausch, A. (2010) Community Knowledge and Acceptance of Southwest Partnership Phase II Carbon Capture and Storage Projects: Focus Group and Survey Results. Texas A & M University, College Station, Texas.

Southwestern Regional Partnership on Carbon Sequestration (Phase 2)

Community Knowledge and Acceptance of Southwest Partnership Phase II Carbon Capture and Storage Projects: Focus Group and Survey Results

Topical Report

April 1, 2006 – December 31, 2010

November 24, 2010

By:

Dr. Andrea Feldpausch

Texas A & M University

Project Manager: Robert Lee

Principal Investigators: Reid Grigg and Brian J. McPherson

DOE Contract No. DE- FC26-05NT42591

Submitting Organization: New Mexico Institute of Mining and Technology
801 Leroy Place
Socorro, New Mexico 87801

Abstract

This study focused on public perceptions of CCS technologies near phase II pilot projects within the SWP region. We conducted focus groups and surveys to discover how these communities perceive the technology and accept the possibility of deployment. Subject matter for discussion included knowledge, opinions and concerns relating to community issues, climate change and CCS. I found that participants focused their conversations on industry and government knowledge, risks and unknowns of CCS and processes for decision-making. Skepticism and distrust of government entities and corporations influenced participant willingness to accept storage risks to mitigate for CO2 emissions. After open discussion of pros and cons associated with the technology, however, participants were more willing to consider CCS as an option, indicating a need to talk through the issue and come to their own conclusions.

Han, W-S., Esser, R., Thorne, D., and McPherson, B. (2009) Principal Reservoir Description Associated with Geology and Oil Production History in SACROC, Site of 35 Years of CO_2 Injection. University of Utah, Salt Lake City, Utah.

Southwest Partnership Phase II Project Site: Principal Reservoir Description Associated with Geology and Oil Production History in SACROC, Site of 35 Years of CO_2 Injection

Topical Report

Reporting Period Start Date: October 1, 2005
Reporting Period End Date: September 30, 2009

Weon Shik Han[a,b], Richard P. Esser[b],
Dawn A. Thorne[b], Brian J. McPherson[a,b]

August 1, 2009

DOE Award Number: DE-FC26-05NT42591 (Task 2.1)

Submitting Organization: New Mexico Institute of Mining and Technology
801 Leroy Place
Socorro, NM 87801

Prepared by: [a]Department of Civil and Environmental Engineering,
University of Utah
Salt Lake City, Utah 84108 USA
[b]Energy and Geoscience Institute, University of Utah
423 Wakara Way, Suite 300
Salt Lake City, Utah 84108 USA

ABSTRACT

For the past 35 years, CO_2 has been transferred from both gas processing plants and natural CO_2 reservoirs and injected into the SACROC Unit for the purpose of CO_2 enhanced oil recovery (EOR). The calculation of net mass balance based on injection/production performance databases at the site suggest that SACROC Unit has accumulated approximately 55 million tonnes of CO_2 during the past 35 years. Because of the CO_2 injection history and amount, the SACROC Unit has become one of the most important sites for providing the opportunities to study CO_2 sequestration processes at the field scale. In an effort to better understand the CO_2 sequestration processes, pilot scale CO_2 injection tests began at wells 56-17, 58-2, 56-4, 56-6, and 59-2 in the northern platform SACROC Unit on September, 2008 by research groups in the Southwest Regional CO_2 Partnership. The purpose of this research is to gather valuable information associated with site characterization for understanding geology and historical CO_2 injection/production operation. We expect that better understanding SACROC Unit including geology and historical operation will be beneficial to future operation of commercial scale CO_2 sequestration processes.

Harris, M. (2010) Validation and Comparison of Carbon Sequestration Project Cost Models with Project Cost Data Obtained from the Southwest Partnership. New Mexico Institute of Mining and Technology, Socorro, New Mexico.

Southwestern Regional Partnership on Carbon Sequestration (Phase 2)

Validation and Comparison of Carbon Sequestration Project Cost Models with Project Cost Data Obtained from the Southwest Partnership

Topical Report

April 1, 2006 – December 31, 2010

October 2010

By Milton Lee Harris

Project Manager: Robert Lee

Principal Investigators: Reid Grigg and Brian J. McPherson

DOE Contract No. DE- FC26-05NT42591

Submitting Organization: New Mexico Institute of Mining and Technology
801 Leroy Place
Socorro, New Mexico 87801

Abstract

Obtaining formal quotes and engineering conceptual designs for carbon dioxide (CO_2) sequestration sites and facilities is costly and time-consuming. Frequently, when looking at potential locations, managers, engineers and scientists are confronted with multiple options, but do not have the expertise or the information required to quickly obtain a general estimate of what the costs will be without employing an engineering firm. Several models for carbon compression, transport and/or injection have been published that are designed to aid in determining the cost of sequestration projects. A number of these models are used in this study, including models by J. Ogden, MIT's Carbon Capture and Sequestration Technologies Program Model, the Environmental Protection Agency and others. This report uses the information and data available from several projects either completed, in progress, or conceptualized by the Southwest Regional Carbon Sequestration Partnership on Carbon Sequestration (SWP) to determine the best approach to estimate a project's cost. The data presented highlights calculated versus actual costs. This data is compared to the results obtained by applying several models for each of the individual projects with actual cost. It also offers methods to systematically apply the models to future projects of a similar scale. Last, the cost risks associated with a project of this scope are discussed, along with ways that have been and could be used to mitigate these risks. This work was funded by the Department of Energy (DOE) through the National Energy Technology Laboratory (NETL) and the State of New Mexico. It was submitted in partial fulfillment of the requirement for the degree of Masters of Engineering Management to the New Mexico Institute of Mining and Technology, October 2010.

Heath, J., McPherson, B., and Dewers, T. (2010) Natural Tracers and Multi-Scale Assessment of Caprock Sealing Behavior: Preliminary Findings from a Case Study of the Kirtland Formation, San Juan Basin. Sandia National Laboratories, Albuquerque, New Mexico.

Natural Tracers and Multi-Scale Assessment of Sealing Behavior at Geological CO_2 Storage Sites: Preliminary Findings from a Case Study of the Kirtland Formation, San Juan Basin, USA

Topical Report

Reporting period:
September 1, 2007 – February 28, 2010

Authors:
Jason E. Heath[1,2], Brian J.O.L. McPherson[3], and Thomas A. Dewers[4]

Date report was issued:
February 2010

U.S. Department of Energy
DOE Award No.: DE-FC26-05NT42591

Submitting organization:
Sandia National Laboratories
Department of Geophysics
P.O. Box 5800, MS 0750
Albuquerque, NM 87185-0750

Affiliations:
[1]Department of Earth and Environmental Science, New Mexico Institute of Mining and Technology, Socorro, NM 87801
[2]Department of Geophysics, Sandia National Laboratories, Albuquerque, NM 87185-0750
[3]Department of Civil and Environmental Engineering, University of Utah, Salt Lake City, UT 84112-0561
[4]Department of Geomechanics, Sandia National Laboratories, Albuquerque, NM 87185-0751

Disclaimer

U.S. Department of Energy

ABSTRACT

This study investigated the extent to which pore- and pore-throat-scale properties and processes govern sealing behavior of the Kirtland Formation, San Juan Basin, USA, at the site of CO_2 injection into coal seams. The Kirtland is considered a regional aquitard and reservoir seal. Nanometer- to formation-scale data facilitated evaluation of past fluid migration through the Kirtland and potential, future fluid flow. Mercury porosimetry indicates high quality sealing at the plug scale (~2.54 diameter by 2.54 cm long). However, image well logs and fracture analysis of core found open and mineralized fractures. The mineralization indicates multiple fluid-flow events through the Kirtland. Natural noble gas tracers evince stagnant, diffusion-dominated transport in the upper Kirtland, thus supporting the matrix-scale evidence of a high quality seal. The lower Kirtland has more log-based fractures than the rest of the Kirtland, and helium data indicates less diffusion-dominated transport than the upper Kirtland. Thus, the lower Kirtland, although it had the highest sealing capacity in terms of MICP data and has low matrix permeability (i.e., $\sim 8 \times 10^{-20}$ m^2), needs further investigation to determine if it indeed behaves as a significant barrier to fluid flow.

Keywords: seal or caprock, CO_2 or carbon dioxide, noble gases, isotopes, leakage, preferential flow path

Heath, J., McPherson, B., and Dewers, T. (2010) Natural Tracers and Multi-Scale Assessment of Caprock Sealing Behavior: A Case Study of the Kirtland Formation, San Juan Basin (expanded). Sandia National Laboratories, Albuquerque, New Mexico.

Natural Tracers and Multi-Scale Assessment of Caprock Sealing Behavior: A Case Study of the Kirtland Formation, San Juan Basin (expanded)

Topical Report

Reporting period:
September 1, 2007 – November 15, 2010

Authors:
Jason E. Heath[1], Brian J.O.L. McPherson[2], and Thomas A. Dewers[3]

Report issued:
December 2010

U.S. Department of Energy
DOE Award No.: DE-FC26-05NT42591

Submitting organization:
Sandia National Laboratories
Department of Geophysics
P.O. Box 5800, MS 0750
Albuquerque, NM 87185-0750

Affiliations:
[1]Department of Geophysics and Atmospheric Sciences, Sandia National Laboratories, Albuquerque, NM 87185-0750
[2]Department of Civil and Environmental Engineering, University of Utah, Salt Lake City, UT 84112-0561
[3]Department of Geomechanics, Sandia National Laboratories, Albuquerque, NM 87185-0751

ABSTRACT

The assessment of caprocks for geologic CO_2 storage is a multi-scale endeavor. Investigation of a regional caprock—the Kirtland Formation, San Juan Basin, USA—at the pore-network scale indicates high capillary sealing capacity and low permeabilities. Core and well-scale data, however, indicate a potential seal bypass system as evidenced by multiple mineralized fractures and methane gas saturations within the caprock. Our interpretation of ^4He concentrations, measured at the top and bottom of the caprock, suggests low fluid fluxes through the caprock: 1) Of the total ^4He produced *in situ* (i.e., at the locations of sampling) by uranium and thorium decay since deposition of the Kirtland Formation, a large portion still resides in the pore fluids. 2) Simple advection-only and advection-diffusion models, using the measured ^4He concentrations, indicate low permeability (~10^{-20} m^2 or lower) for the thickness of the Kirtland Formation. These findings, however, do not guarantee the lack of a large-scale bypass system. The measured data, located near the boundary conditions of the models (i.e., the overlying and underlying aquifers), limit our testing of conceptual models and the sensitivity of model parameterization. Thus, we suggest approaches for future studies to better assess the presence or lack of a seal bypass system at this particular site and for other sites in general.

Interstate Oil and Gas Compact Commission Task Force on Carbon Capture and Geologic Storage, Bliss, K., Bengal, L., and Tew, B. (2010) Biennial Review of the Legal and Regulatory Environment for the Storage of Carbon Dioxide in Geologic Structures. Interstate Oil and Gas Compact Commission, Oklahoma City, Oklahoma.

Southwest Partnership Phase II: IOGCC CCGS Task Force Phase II Biennial Review of the Legal and Regulatory Environment for the Storage of Carbon Dioxide in Geologic Structures

TOPICAL REPORT

Principal Authors:

IOGCC Task Force on Carbon Capture and Geologic Storage

Kevin Bliss, Esq., Interstate Oil and Gas Compact Commission, Washington, D.C.

Lawrence E. Bengal, Director, Arkansas Oil and Gas Commission

Berry "Nick" Tew, Jr., Oil & Gas Supervisor/Geologist, State Oil and Gas Board of Alabama

September 30, 2010

DOE Award Number: DOE-FC26-05NT42591

Reporting Period: September 1, 2007 through September 30, 2010

Submitting Organization: New Mexico Institute of Mining and Technology
801 Leroy Place
Socorro, NM 87801

Prepared by: Interstate Oil and Gas Compact Commission
PO Box 53127
Oklahoma City, OK 73152-3127

Disclaimer

This material is based upon work supported by the Department of Energy award number DE-FC26-05NT42591.

Abstract

This report is the product of the Interstate Oil and Gas Compact Commission (IOGCC) Carbon Capture and Geologic Storage (CCGS) Task Force. It is the penultimate deliverable of Phase II of the IOGCC CCGS Task Force under a cooperative agreement with the Southwest Regional Partnership on Carbon Sequestration. The report constitutes a "biennial review" that both updates the CCGS Task Force's 2007 guidance document for U.S. states and Canadian provinces and summarizes the status of state and provincial efforts to develop laws and promulgate regulations as concerns the geologic storage of carbon dioxide. As with the IOGCC CCGS Task Force's 2007 guidance, it is anticipated that a state[1] adopting a regulatory framework for CO_2 geologic storage will make changes to the model framework as necessary to conform to the state's unique circumstances. The task force therefore continues to envision that the end-product will be a substantially consistent system in the United States and Canada for the geologic storage of CO_2 regulated at the state and provincial level in conformance with national and international law and protocol.

[1] Although references throughout this Executive Summary are, for the most part, to "state" or "states", it is the intent of the task force that the comments and provisions are equally applicable to Canadian provinces. Of course, this would not apply to discussions concerning underground storage rights and the Underground Injection Control Program of the U.S. Safe Drinking Water Act.

Rutledge, J. (2010) Geologic Demonstration at the Aneth Oil Field, Paradox Basin, Utah. Los Alamos National Laboratory, Los Alamos, New Mexico.

Southwest Regional Partnership on Carbon Sequestration
Phase II

Topical Report

for the period 09/01/07 through 09/30/10

Geologic Demonstration at the Aneth Oil Field, Paradox Basin, Utah

by
James Rutledge
Los Alamos National Laboratory
DOE Contract No.: DE- FC26-05NT42591

Submitting Organization: New Mexico Institute of Mining and Technology
801 Leroy Place
Socorro, New Mexico 87801

December 2010

Prepared for U.S. Department of Energy's National Energy Technology Laboratory and New Mexico Institute of Mining & Technology

ABSTRACT

The Southwest Regional Partnership (SWP) on Carbon Sequestration designed and deployed a medium-scale field pilot test of geologic carbon dioxide (CO_2) sequestration in the Aneth oil field. Greater Aneth oil field, Utah's largest oil producer, was discovered in 1956 and has produced over 455 million barrels of oil (72 million m^3). Located in the Paradox Basin of southeastern Utah, Greater Aneth is a stratigraphic trap producing from the Pennsylvanian Paradox Formation. Because it represents an archetype oil field of the western U.S., Greater Aneth was selected as one of three geologic pilots to demonstrate combined enhanced oil recovery (EOR) and CO_2 sequestration under the auspices of the SWP on Carbon Sequestration, sponsored by the U.S. Department of Energy. The pilot demonstration focuced on the western portion of the Aneth Unit as this area of the field was converted from waterflood production to CO_2 EOR starting in late 2007. The Aneth Unit is in the northwestern part of the field and has produced 149 million barrels (24 million m^3) of the estimated 450 million barrels (71.5 million m^3) of the original oil in place – a 33% recovery rate. The large amount of remaining oil makes the Aneth Unit ideal to demonstrate both CO_2 storage capacity and EOR by CO_2 flooding.

This report summarizes the geologic characterization research, the various field monitoring tests, and the development of a geologic model and numerical simulations conducted for the Aneth demonstration project. The Utah Geological Survey (UGS), with contributions from other Partners, evaluated how the surface and subsurface geology of the Aneth Unit demonstration site will affect sequestration operations and engineering strategies. The UGS' research for the project are summarized in Chapters 1 through 7, and includes (1) mapping the surface geology including stratigraphy, faulting, fractures, and deformation bands, (2) describing the local Jurassic and Cretaceous stratigraphy, (3) mapping the Desert Creek zone reservoir, Gothic seal, and overlying aquifers, (4) characterizing the depositional environments and diagenetic events that produced significant reservoir heterogeneity, (5) describing the geochemical, petrographic, and geomechanical properties of the seal to determine the CO_2 or hydrocarbon column it could support, and (6) evaluating the production history to compare primary production from vertical and horizontal wells, and the effects of waterflood and water-alternating-gas flood programs.

The field monitoring demonstrations were conducted by various Partners including New Mexico Institute of Mining and Technology, University of Utah, National Institute of Advanced Industrial Science and Technology, Japan, Los Alamos National Laboratory and Cambridge Geosciences. The monitoring tests are summarized in Chapters 8 through 12, and includes (1) interwell tracer studies during water- and CO_2-flood operations to characterize tracer behavoirs in anticipation of CO_2-sequestration applications, (2) CO_2 soil flux monitoring to measure background levels and variance and assess the sensitivity levels for CO_2 surface monitoring, (3) testing the continuous monitoring of self potential as a means to detect pressure anomalies and electrochemical reaction due to CO_2 injection, (4) conducting time-lapse vertical seismic profiling to image change near a CO_2 injection well, and (5) monitoring microseismicity using a downhole string of seismic receivers to detect fracture slip and deformation associated with stress changes.

Finally, the geologic modeling and numerical simulation study was conducted by researcher at the University of Utah. Chapter 13 summarizes their efforts which focused on developing a site-specific geologic model for Aneth to better understand and design CO_2 storage specifically tailored to oil reservoirs.

Xiao, C., ed. (2011) SACROC North Platform in the Permian Basin, West Texas. New Mexico Institute of Mining and Technology, Socorro, New Mexico.

Southwestern Regional Partnership on Carbon Sequestration (Phase 2)

SACROC North Platform in the Permian Basin, West Texas

Topical Report

April 1, 2006 – December 31, 2010

January 31, 2011

Compiled By:

Chongwei Xiao

Project Manager: Robert Lee

Principal Investigators: Reid Grigg and Brian J. McPherson

DOE Contract No. DE- FC26-05NT42591

Submitting Organization: New Mexico Institute of Mining and Technology
801 Leroy Place
Socorro, New Mexico 87801

Abstract

The Southwest Regional Partnership on Carbon Sequestration (SWP) carried out a field pilot test at the SACROC Field in the west Texas area of the Permian Basin. The objective of this project was to demonstrate enhanced oil recovery combined with geologic carbon sequestration and infrastructure concepts. The SACROC field test demonstrates the efficacy of proposed sequestration technologies to reduce or offset greenhouse gas emissions in the region. Risk mitigation, optimization of MVA protocols, and effective outreach and communication were additional, critical goals of these field validation tests. This pilot was an example of a medium-scale validation test in a sink that may host capacity for possible larger-scale sequestration operations in the future. These validation tests also demonstrate multiple value-added benefits for enhanced oil recovery and sequestration.

The geologic sequestration pilot site for CO_2 injection at SACROC is a five-spot well pattern at the northern edge of the SACROC unit. The pilot test included injection of a minimum of ~75,000 tons/year CO_2, with minimum injection duration of one year. The geophysical properties of SACROC were characterized and a geocellular model was built to representing the northern platform at SACROC based on analysis of well logs and 3D seismic surveys. A 3D heterogeneous model of the SACROC site was created to account for CO_2 trapping mechanisms. Samples of SACROC reef limestone were used for ultrasonic velocity measurements, detailed mineralogy and scanning electron microscopy (SEM) characterization, and computed tomography (CT) scanning. Rock physics modeling was performed to quantify the changes in seismic response (velocities, impedances, seismic amplitudes that can occur in the reservoir due to injection of CO_2, and the model set up is in a good agreement with core measurement. The vertical seismic profilings (VSP) detected the changes due to migration of CO_2 plume within geologic formations, which are consistent with the results of surface reflective seismic survey. A good background soil CO_2 flux value was obtained and soil flux monitoring did not identify any CO_2 leaks. The groundwater study indicated that the quality of shallow drinking water over SACROC has not been impacted by CO_2 injection is strong evidence that it is possible to safely sequester CO_2 in deep subsurface reservoirs.